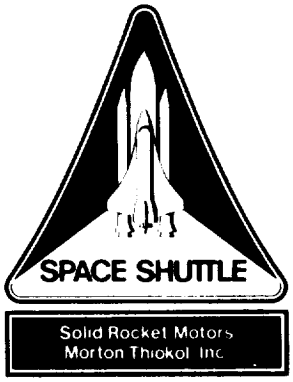

TWR-17272, Vol. XI

FLIGHT MOTOR SET 360L001 (STS-26R) FINAL REPORT (RECONSTRUCTED DYNAMIC LOADS ANALYSIS)

June 1989

Prepared for:

NATIONAL AERONAUTICS AND SPACE ADMINISTRATION
GEORGE C. MARSHALL SPACE FLIGHT CENTER
MARSHALL SPACE FLIGHT CENTER, ALABAMA 35812

Contract No. NAS8-30490

DR. No. 3-5

WBS.No. 4B601-03-08

ECS No. 956

MORTON THIOKOL, INC.

Aerospace Group

Space Operations

P.O. Box 707, Brigham City, Utah 84302-0707 (801) 863-3511

FORM TC 4677 (REV 1-88)

(NASA-CR-183811) FLIGHT MOTOR SET 360L001 (STS-26R). (RECONSTRUCTED DYNAMIC LOADS ANALYSIS) Final Report (Morton Thiokol) 372 p

N90-12656

CSCL 21H G3/20

Unclas 0242995

DOC NO. VOL REV

TITLE TWR-17272, Vol. XI

Flight Motor Set 360L001 (STS-26R) Final Report (Reconstructed Dynamic Loads Analysis)

June 1989

Prepared by:

V. B. Call
Systems Loads and Environments

Approved by:

D. R. Mason, Supervisor
Systems Loads and Environments

for R. Lavery, Manager 8-3-9
Requirements and Certification

B. R. McQuivey 8/9/89
Project Engineer

C. A. Saderholm 8-4-89
C. A. Saderholm
Program Manager

Certification Planning 8-3-9

Reliability 16 Aug 89

Systems Safety

Released by:

P C Tydeck 8-17-89
Data Management
ECS No. 956

MORTON THIOKOL, INC.
Aerospace Group
P.O. Box 524, Brigham City, Utah 84302 (801) 863-3511

CONTENTS

APPENDICES

CONTENTS (Cont.)

FIGURES

CONTENTS (Cont.)

TABLES

1.0 INTRODUCTION

A transient analysis has been performed to correlate the predicted versus measured behavior of the Redesigned Solid Rocket Booster (RSRB) during Flight 360L001 (STS-26R) liftoff, which occurred on 29 September 1988. Approximately 9 accelerometers, 152 strain gages, and 104 girth gages were bonded to the motors during this event. Prior to Flight 360L001, a finite element model of the RSRB was analyzed to predict the accelerations, strains, and displacements measured by this developmental flight instrumentation (DFI) within an order of magnitude (see Reference 1). Subsequently, an analysis has been performed which uses actual Flight 360L001 liftoff loading conditions, and makes more precise predictions for the RSRB structural behavior. Essential information describing the analytical model, analytical techniques used, correlation of the predicted versus measured RSRB behavior, and conclusions, are presented in this report.

A detailed model of the RSRB has been developed and correlated for use in analyzing the motor behavior during liftoff loading conditions. This finite element model, referred to as the "RSRB global model", uses superelement techniques to model all components of the RSRB in detail. The principal objective of the RSRB global model is to accurately predict deflections and gap openings in the field joints to an accuracy of approximately 0.001 inch. The model of the field joint component was correlated

to Referee and Joint Environment Simulation (JES) tests. The accuracy of the assembled RSRB global model was validated by correlation to static-fire tests such as DM-8, DM-9, QM-7, and QM-8. This validated RSRB global model was used to predict RSRB structural behavior and joint gap opening during Flight 360L001 liftoff.

This report presents the results of a transient analysis of the RSRB global model with imposed liftoff loading conditions. Rockwell used many gage measurements to reconstruct the load parameters which were imposed on the RSRB during the Flight 360L001 liftoff. A description of each load parameter, and its application, is presented herein. Also presented are conclusions and recommendations based on the analysis of this load case and the resulting correlation between predicted and measured RSRB structural behavior.

2.0 CONCLUSION

A transient analysis has been performed to correlate the predicted versus measured structural behavior of the RSRB during liftoff conditions. A detailed global model of the RSRB was developed and correlated for use in this analysis. The objectives of this analysis are:

1. To compare the DFI instrumentation measurements to the predicted gage readings on the RSRB during Flight 360L001 liftoff.
2. To predict other structural phenomenon which may have occurred during Flight 360L001 liftoff; i.e., field joint gap opening, axial growth, and twang.

A reconstructed Flight 360L001 liftoff load case was provided by Rockwell to simulate the 29 September 1988 liftoff loadings on the RSRB global model. In general, the predicted structural response of the RSRBs compares very well with the measured, and the measured data are within any allowables imposed for displacement, strain etc.

The results of this analysis indicate that the global model radial growth predictions compare well with the measured data (generally within ±12 percent). A spiking phenomena was exhibited in some of the girth gage measurements, and is believed to be a problem with the gages. Hoop strain predictions also compare very well with the gage measurements (within ±10 percent).

Except for Station 1493.0, the mean predicted axial strains compare favorably with the measured axial strains (on an average, within ± 30 percent). However, the predictions exhibit dynamic effects which are a direct result of the loads input (both in magnitude and damping). These effects indicate axial strain values that are not shown in the measured data. It is recommended that the Rockwell reconstructed loads be evaluated and compared with measured loads (i.e., ET attach and MLP tie-down bolt loads) to determine any differences or conservatisms in the magnitudes, frequencies, and damping values.

Axial strain predictions for Station 1493.0 do not correlate well due to analytical model simplifications in the curved region aft of the field

joint pin centerline. It is recommended that the model be enhanced in this region for future analyses.

Three of the nine accelerometers bonded to the forward skirts were severely compromised by noise (Channels B08D8151A through B08D8153A). For the remaining six accelermometers, a direct comparison of the predicted to measured data at 40 Hz shows that, generally, the predicted acceleration levels are high. However, a comparison of the frequency content shows good correlation between predicted and measured. The accelerometers bonded to the case during liftoff had a frequency range of 5 to 50 Hz. Therefore, any dominant modes below 5 Hz were not detected. It is recommended that accelerometers with a wider frequency range (0.0 to 2000 Hz) be used for future flights.

Calculations were also performed for field joint gap opening, twang, and axial growth of the motor during liftoff. Although the analytical results cannot be correlated with measured data, the results are reasonable, and indicate structural responses which are normally expected in these areas.

3.0 TRANSIENT ANALYSIS METHODS

An advanced method of mode acceleration transient analysis was used to calculate the RSRB response during the liftoff conditions. This advanced mode acceleration method was developed by Structural Dynamics Research Corporation (SDRC), and implemented for MSC/NASTRAN using DMAP sequences

(see References 2 and 3). This method is substantially more efficient than the standard method for certain types of problems. Also, this method will calculate accurate responses for points in upstream superelements.

This advanced mode acceleration method recovers the physical transient responses by combining the static responses caused by the steady-state loads and the dynamic responses of the known modes. The entire model is used to calculate the static responses, so that the steady-state responses of the truncated high frequency modes are included accurately. The static solution is computed only once for each set of transient loads, and these static solutions are scaled by their transient scaling functions. These static solutions are superimposed with the physical responses to the inertia and damping forces to compute the total responses to the transient loads. This computation is expressed by:

$$\{x\} = [\psi]\{p\} - [\phi][\omega^2]^{-1}\{\ddot{q}\}$$

where $\{x\}$ = transient displacements of physical DOFs

$[\psi]$ = static displacements caused by unit steady-state load cases

$\{p\}$ = transient scaling functions for the applied load cases

$[\phi]$ = mode shapes

$[\omega^2]$ = diagonal matrix of eigenvalues

$\{\ddot{q}\}$ = transient accelerations of the modal DOFs

The steps in the advanced mode acceleration analysis method consist of simply calculating each of the matrices and vectors on the right-hand side

of the above equation, and combining them to evaluate the displacement results.

4.0 LIFTOFF TRANSIENT ANALYSES

A transient analysis of the RSRB global model has been completed to predict the behavior or structural response of the RSRB during Flight 360L001 liftoff loading conditions. An actual Flight 360L001 liftoff load case (reconstructed by Rockwell) was used to simulate those loading conditions. The principle objectives of the global model analysis are to predict DFI gage measurements, and to predict opening of the field joint gaps. The following paragraphs describe the transient analysis of the RSRB global model.

4.1 Description of Liftoff Superelement Model

The liftoff RSRB was modeled using superelement methods for the MSC/NASTRAN finite element analysis program. The motor was broken into twelve superelements. Except for the forward skirt and the ET attach ring, the motor superelements were each developed from a primary and several image superelements, taking advantage of the motor symmetry where possible. This superelement approach enables RSRB components, such as the joints, to be modeled in fine detail, while the entire RSRB system is analyzed for critical dynamic load cases. Figures 1 and 2 are computer model plots of the

liftoff motor. Organization of superelements in the RSRB model is shown by the superelement tree in Table 1. Table 2 contains a listing of the material and geometric properties used in this analysis of the liftoff RSRB. A description of each RSRB component is contained in the following paragraphs.

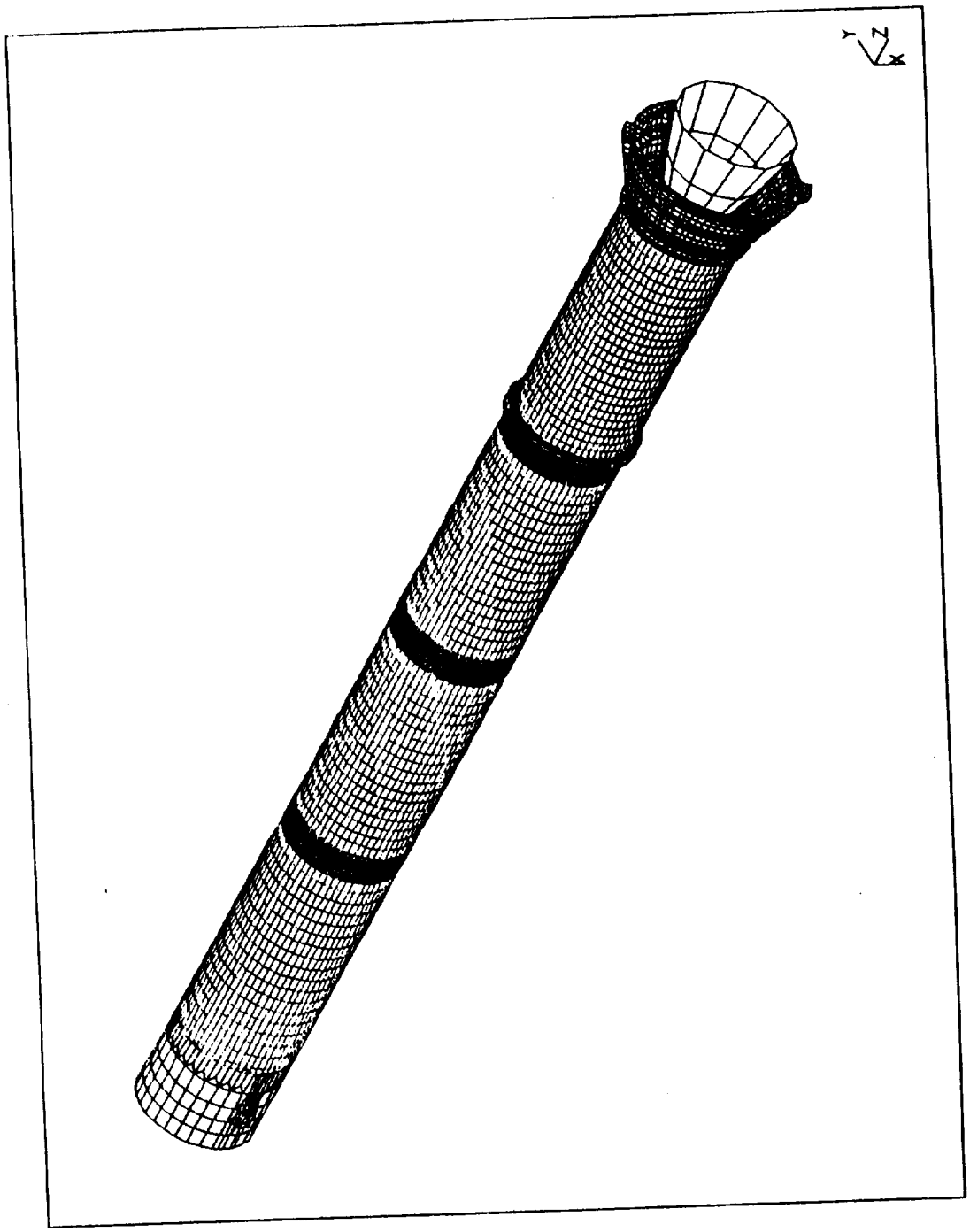

Figure 1
NASTRAN Superelement Model of Liftoff Motor

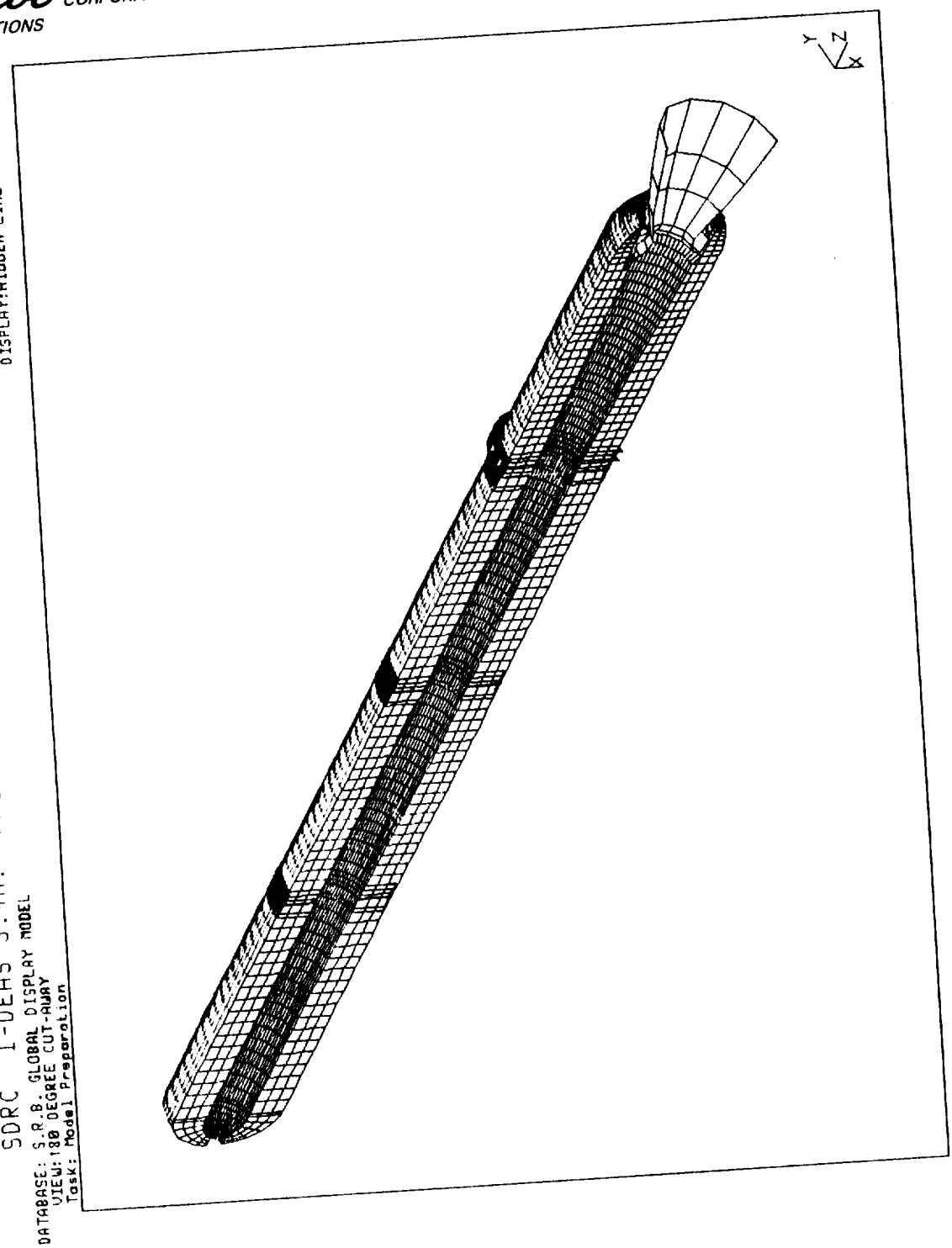

Figure 2
Cutaway View of Liftoff Superelement Model

Table 1
Global Model Superelement Tree

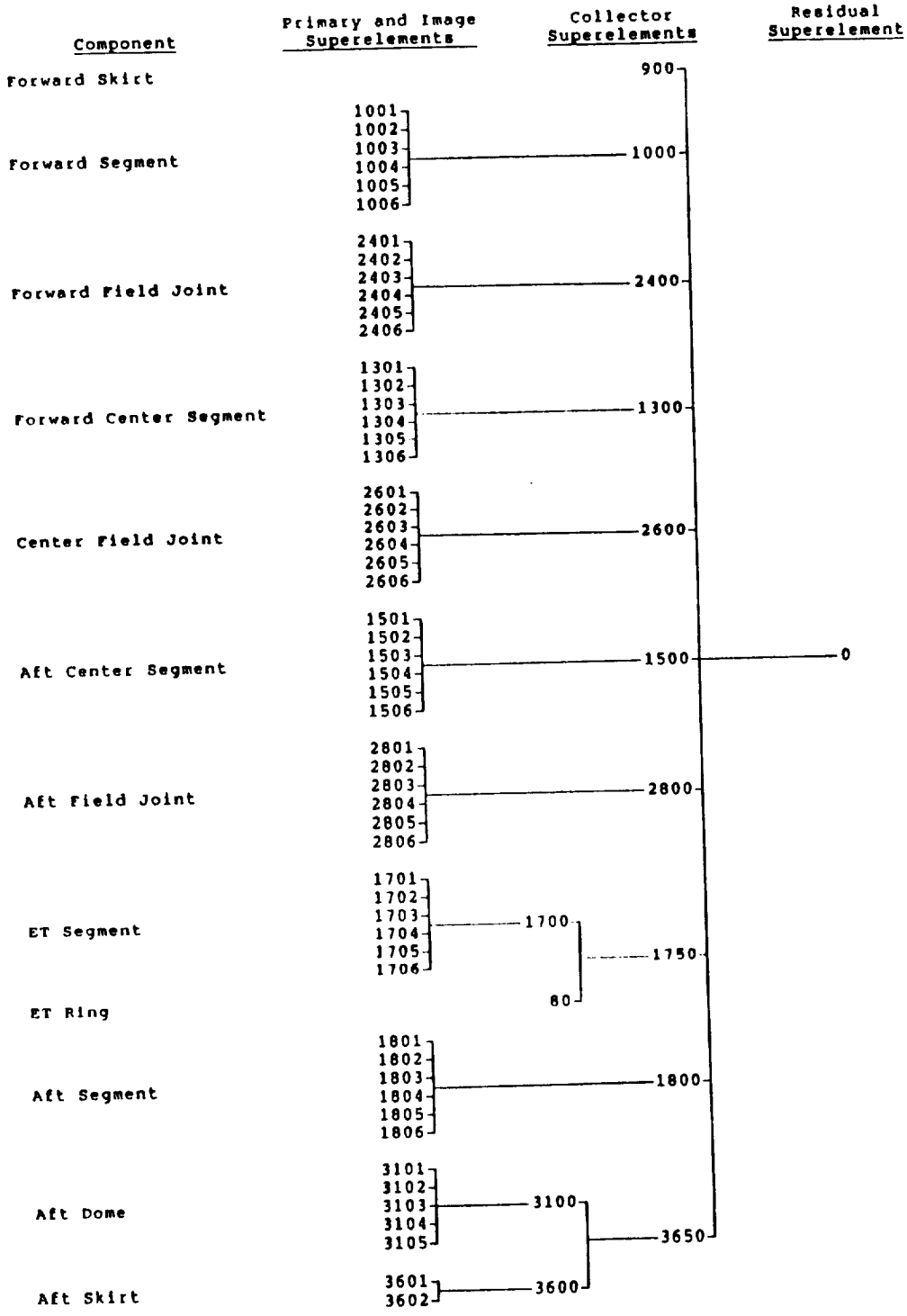

Table 2
Material and Geometric Properties

Material	Elastic Modulus E (psi)	Poisson's Ratio μ	Weight Density ρ (lb /in.^{3})
Steel	29.0E6	0.290	0.283
Aluminum	10.45E6	0.330	0.102
Propellant	5000.	0.499	0.0634

Component	Model Weight (lb)
Forward Field Joint	36,550
Forward Center Segment	261,850
Center Field Joint	35,940
Aft Center Segment	261,850
Aft Field Joint	28,600
ET Segment	66,830
Aft Segment	200,510
Aft Dome	51,450
Total SRM	1,262,390
	Actual Weight = 1,256,125 lb (Model Error = 0.5%)
Forward Skirt	19,190
ETA 360° Ring	1,610
Aft Skirt	11,000

FORWARD SKIRT

The forward skirt was developed by modeling a 360 degree superelement. This might be considered a 'collector' level superelement. Figure 3 shows the 360 degree collector superelement which makes up the forward skirt.

Plate elements were used to represent the skirt, including the stiffening rings and posts. The ET attach point and stiffening posts are located at 270 degrees. The forward frustrum was represented as a rigid body with the entire forward frustrum mass lumped at its center of gravity. Reference 4 contains the listings of the MSC/NASTRAN bulk data files used to analyze the forward skirt, and detailed figures showing the grid and element numbering schemes in the model.

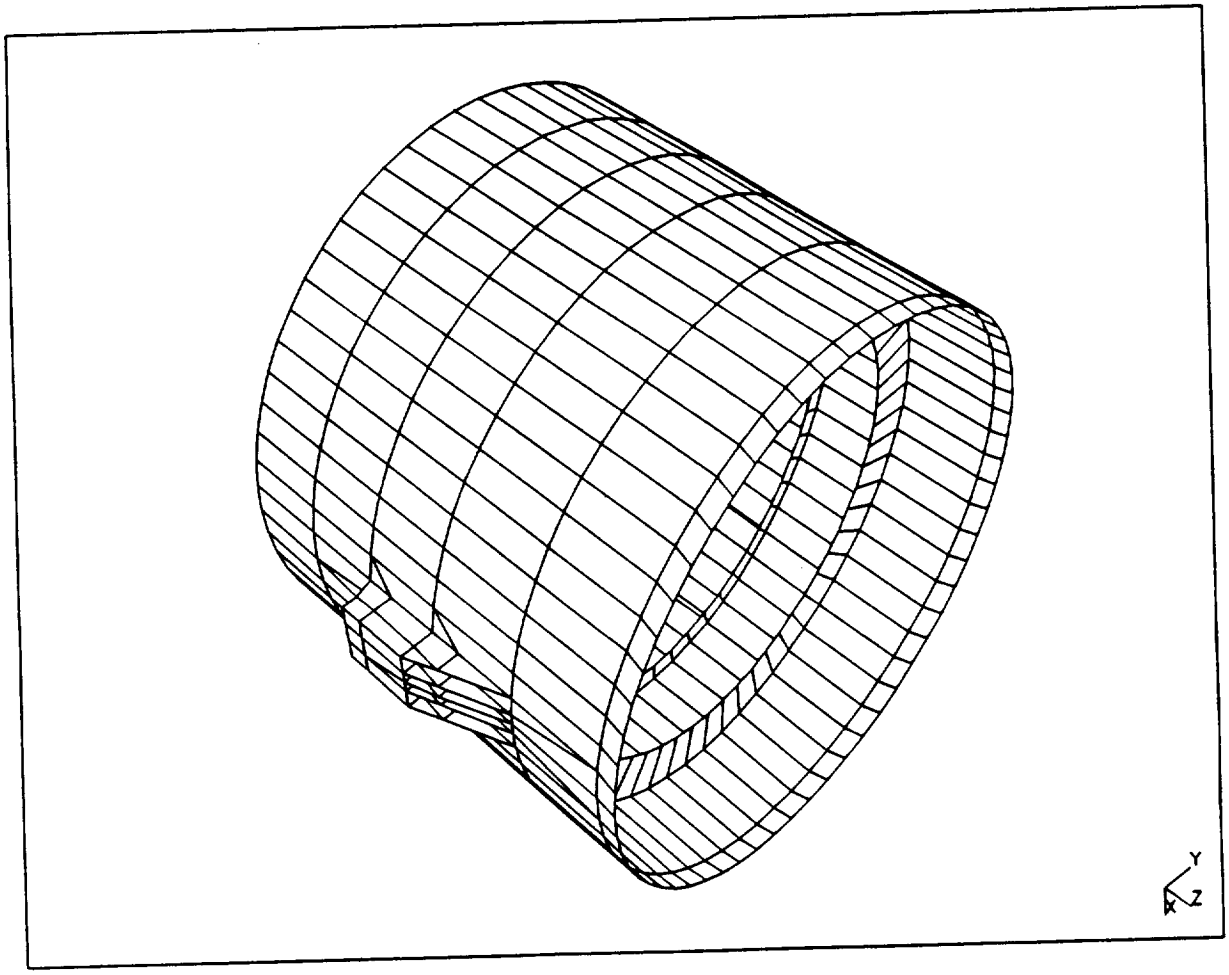

Figure 3
NASTRAN Superelement Model of Forward Skirt

FORWARD SEGMENT

The forward segment was developed by first modeling in detail a 60 degree slice of the segment. This primary superelement was then rotated five times to form five image superelements. The 60 degree primary and image superelements were combined into a collector superelement to represent the 360 degree segment. Figure 4 shows three of the superelements which make up half the segment.

Plate elements represent the steel case and forward dome. The nominal thickness of the standard forward segment case is 0.500 inch (compared with other high performance motor (HPM) segments which are 0.479 inch, nominal thickness). The propellant is represented by solid brick elements. As shown, the star region of the propellant was simply modeled as continuous solid elements circumferentially and axially. As modeled, the total mass and volume of the propellant in the star region is represented. However, this configuration eliminated many of the mode shapes resulting from the movement of the star region alone. The modes of the star region alone are assumed to have insignificant effect on the structural response of the entire motor. Reference 4 contains the listings of the MSC/NASTRAN bulk data files used to analyze the forward segment, and detailed figures showing the grid and element numbering schemes in the model.

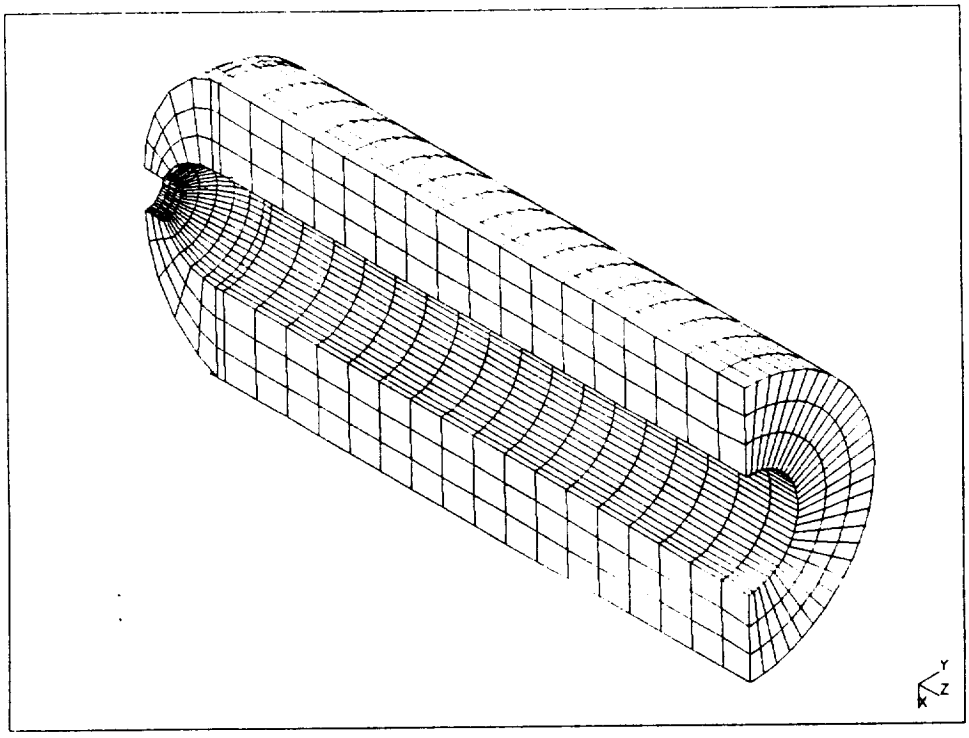

Figure 4
Cutaway View of Forward Segment

FORWARD AND CENTER FIELD JOINTS

The forward and center field joints were developed by first modeling in detail a 60 degree slice of the joint. At the pin centerline, this primary superelement has 180 grid points circumferentially. To interface with other components, the grid points were transitioned down to 60 at both ends of the superelement. This primary superelement was then rotated five times to form five image superelements. The 60 degree primary and image superelements were combined into a collector superelement to represent the 360 degree joint. Figure 5 shows three of the superelements which make up half the joint.

The field joint was modeled using linear plate elements and springs. The axial length of the joint model is approximately 32 inches, and the nominal thickness of the case at the interfaces is 0.479 inch. Connection springs were used between the tang, pin, and clevis. Extremely stiff springs were used to represent a 'rigid' connection, such as contact between the end of the outer clevis leg and the tang. Axial springs were used which correlated the appropriate bending deflection (sag) of the motor in the horizontal static fire configuration. Very soft springs were used to monitor gap opening or closing at several locations in the joint.

The propellant is represented by solid brick elements. Since the forward and center field joints are exactly alike, the forward joint was copied, and renumbered, for the center joint. Reference 4 contains the listings of the MSC/NASTRAN bulk data files used to analyze the forward and center joints, and detailed figures showing the grid and element numbering schemes in the two models.

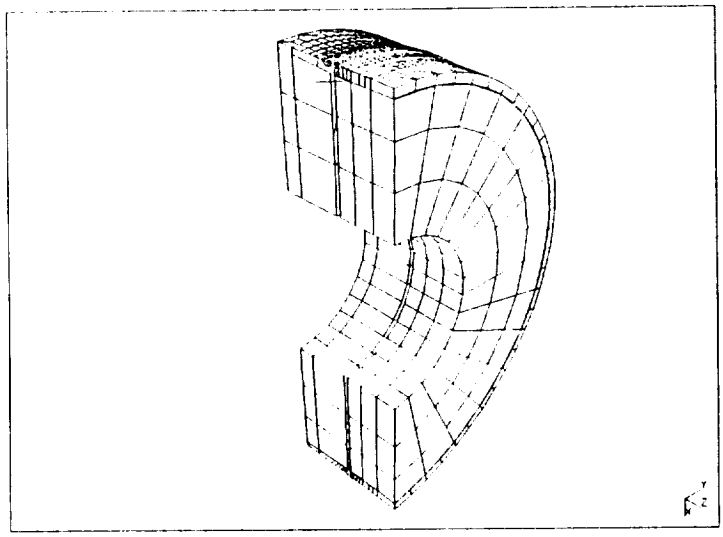

Figure 5
Cutaway View of Forward and Center Field Joints

CENTER SEGMENTS

The forward center segment was developed by first modeling in detail a 60 degree slice of the segment. This primary superelement was then rotated five times to form five image superelements. The 60 degree primary and image superelements were combined into a collector superelement to represent the 360 degree segment. Figure 6 shows three of the superelements which make up half the segment.

Plate elements represent the HPM steel case which has a nominal thickness of 0.479 inch. The propellant is represented by solid brick elements. Since the forward center and aft center segment geometries are exactly alike, the forward center segment was copied, and renumbered, for the aft center segment. Reference 4 contains the listings of the MSC/NASTRAN bulk data files used to analyze the forward center and aft center segments, and detailed figures showing the grid and element numbering schemes in the two models.

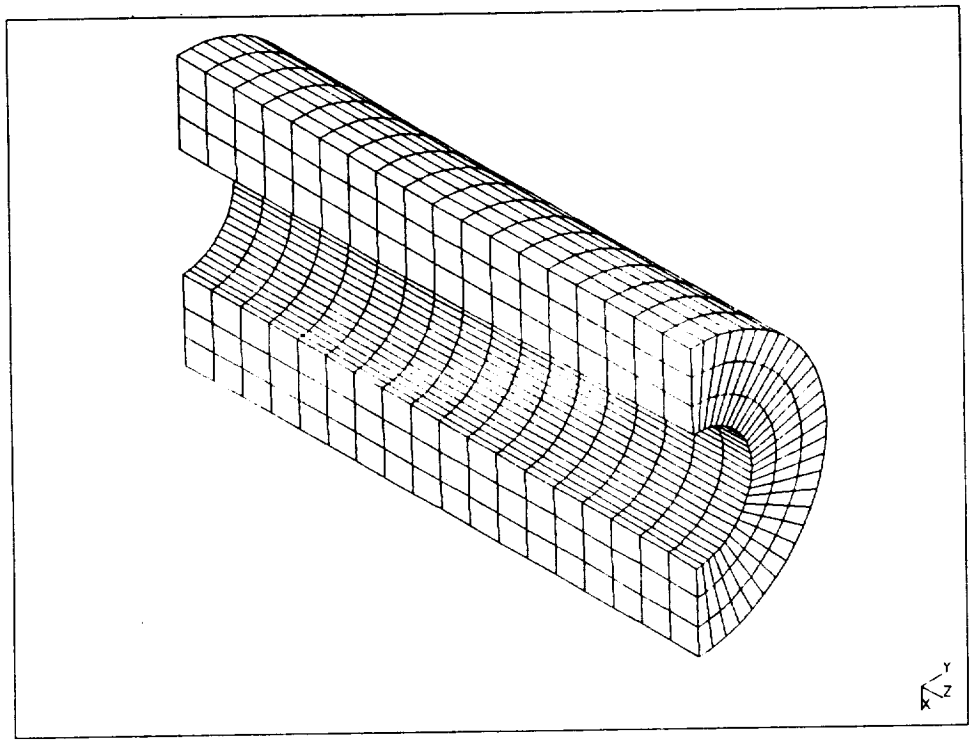

Figure 6
Cutaway View of Center Segments

AFT FIELD JOINT

The aft field joint was developed by first modeling in detail a 60 degree slice of the joint. As with the forward and center field joints, this primary superelement contains 180 grid points circumferentially at the pin centerline. Since the aft center segment has only 60 grid points it was necessary to transition one end of the aft field joint superelement down to 60 grid points to interface properly. However, the other end of the aft field joint interfaces with the ET segment which was also modeled with 180 grid points circumferentially. This primary superelement was then rotated five times to form five image superelements. The 60 degree primary and image superelements were combined into a collector superelement to represent the 360 degree joint. Figure 7 shows three of the superelements which make up half the joint.

The aft field joint was modeled using linear plate elements and springs in the same manner as were the forward and center field joints. The propellant is represented by solid brick elements. Reference 4 contains the listings of the MSC/NASTRAN bulk data files used to analyze the aft field joint, and detailed figures showing the grid and element numbering schemes in the model.

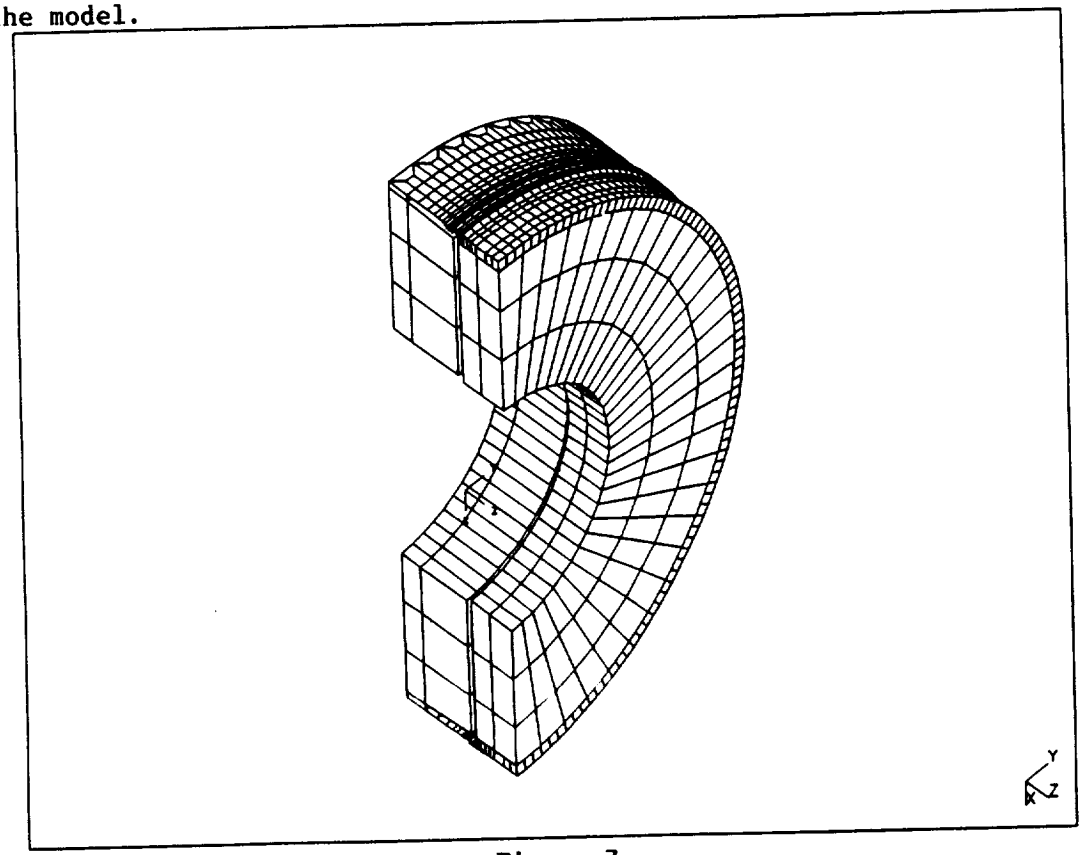

Figure 7
Cutaway View of Aft Field Joint

ET SEGMENT

The ET segment was developed by first modeling in detail a 60 degree slice of the segment. This primary superelement was then rotated five times to form five image superelements. The 60 degree primary and image superelements were combined into a collector superelement to represent the 360 degree segment. Figure 8 shows three of the superelements which make up half the segment.

Plate elements represent the HPM steel case which has a nominal thickness of 0.479 inch. The propellant is represented by solid brick elements. Reference 4 contains the listings of the MSC/NASTRAN bulk data files used to analyze the ET segment, and detailed figures showing the grid and element numbering schemes in the model.

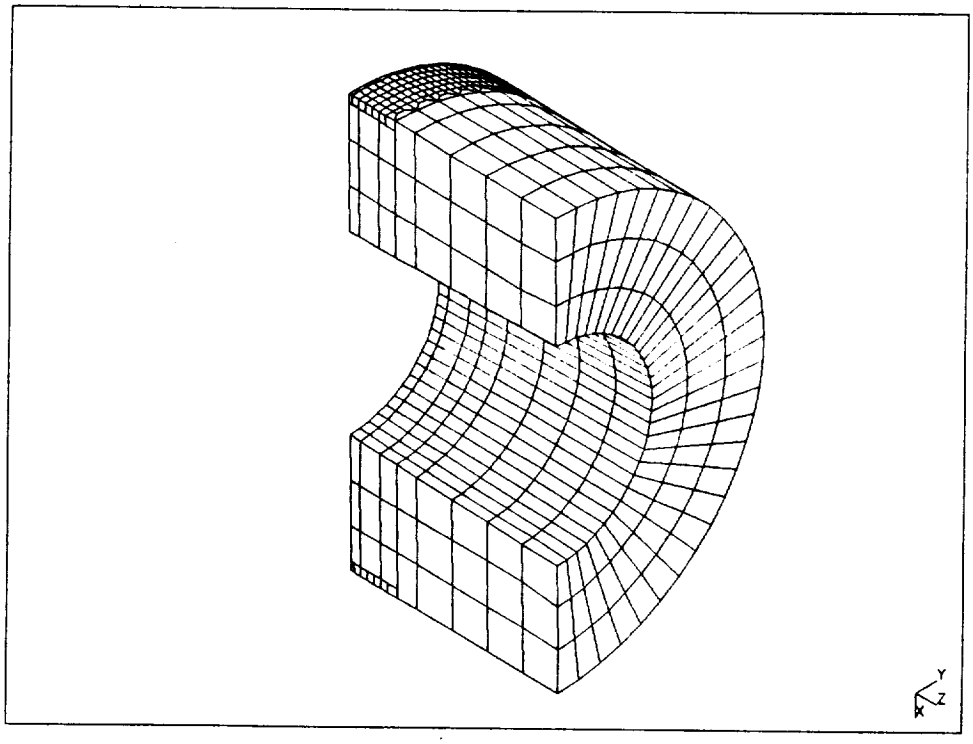

Figure 8
Cutaway View of ET Segment

ET ATTACH RING

The ET attach (ETA) ring used in the liftoff analysis was a 360 degree left hand ring. For this analysis, the ETA ring was modeled as one superelement. As with the forward skirt, this 360 degree superelement might be considered a collector level superelement. Figure 9 shows the entire ETA ring model.

Plate elements were used to represent the ring, including the stiffeners and P8, P9, and P10 strut attach points which are located at approximately 223, 317, and 282 degrees, respectively. Reference 4 contains the listings of the MSC/NASTRAN bulk data files used to analyze the ETA ring, and detailed figures showing the grid and element numbering schemes in the model.

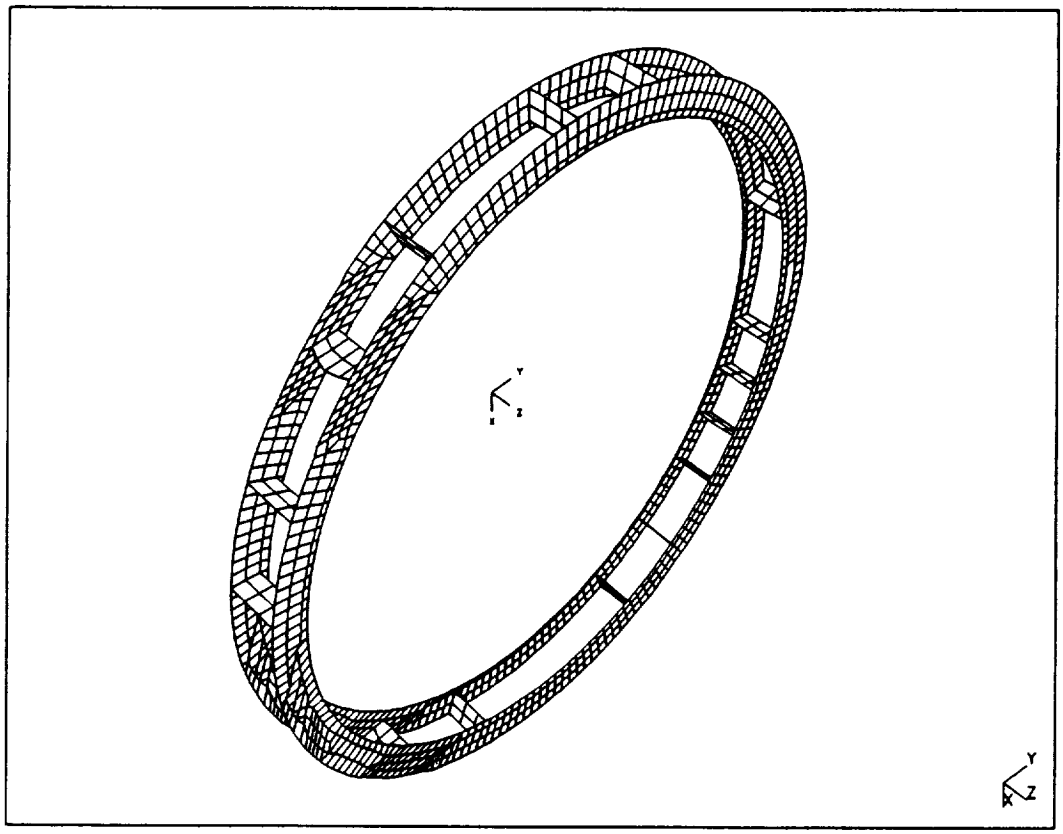

Figure 9
NASTRAN Superelement Model of ET Attach Ring

AFT SEGMENT

The aft segment was developed by first modeling in detail a 60 degree slice of the segment. This primary superelement was then rotated five times to form five image superelements. The 60 degree primary and image superelements were combined into a collector superelement to represent the 360 degree segment. Figure 10 shows three of the superelements which make up half the segment.

Plate elements represent the HPM steel case which has a nominal thickness of 0.479 inch. The propellant is represented by solid brick and tetrahedral elements. Reference 4 contains the listings of the MSC/NASTRAN bulk data files used to analyze the aft segment, and detailed figures showing the grid and element numbering schemes in the model.

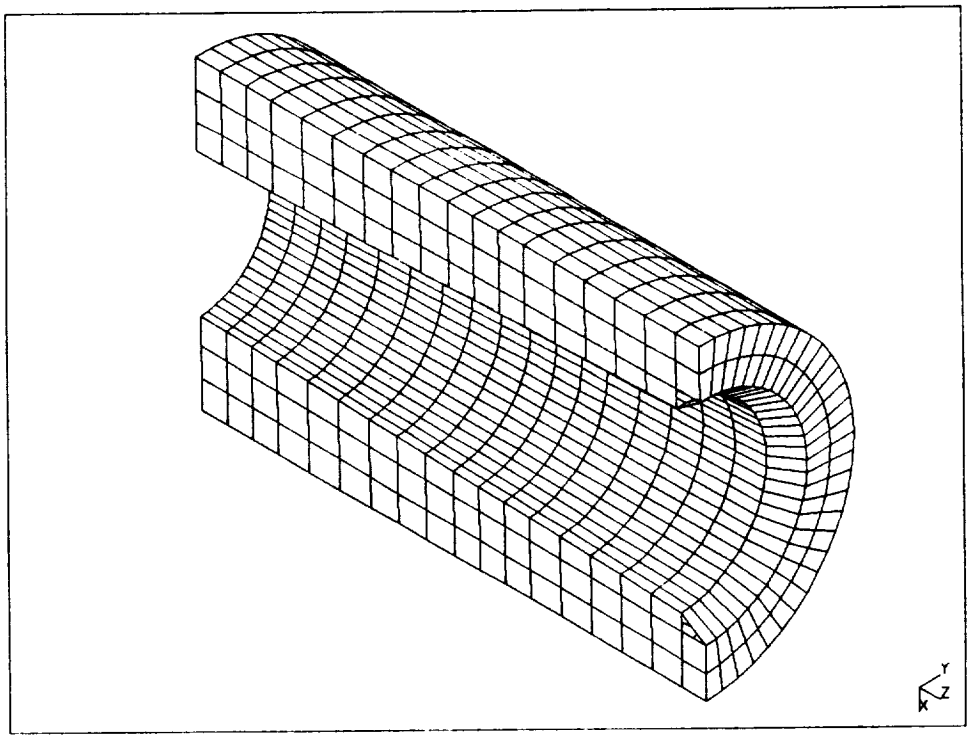

Figure 10
Cutaway View of Aft Segment

AFT DOME

The aft dome was developed by first modeling in detail a 72 degree slice of the dome and fixed housing. This primary superelement was then rotated four times to form four image superelements. The 72 degree primary and image superelements were combined into a collector superelement to represent the 360 degree dome and fixed housing. The nozzle was modeled as a rigid body with the entire nozzle mass lumped at its center of gravity. The rigid body nozzle was connected to the fixed housing model using spring elements which appropriately represent the aft end ring stiffness. Figure 11 shows three of the superelements which make up 216 degrees of the aft dome. The nozzle is shown graphically, although it was not modeled in its entirety for this analysis.

Plate elements represent the steel case and fixed housing. The nominal thickness of the standard aft dome case varies down the length of the dome. The nominal thickness of the fixed housing also varies. The propellant is represented by solid brick elements.

At the nozzle-to-case joint there are 200 bolts, spaced 1.8 degrees apart which alternate in the radial and axial directions. For the RSRB global model, springs were used to represent two bolts (one radial and one axial) at every 3.2 degrees. It is assumed this method of modeling the bolts has an insignificant effect on the structural response of the entire motor. Reference 4 contains the listings of the MSC/NASTRAN bulk data files used to analyze the aft dome, and detailed figures showing the grid and element numbering schemes in the model.

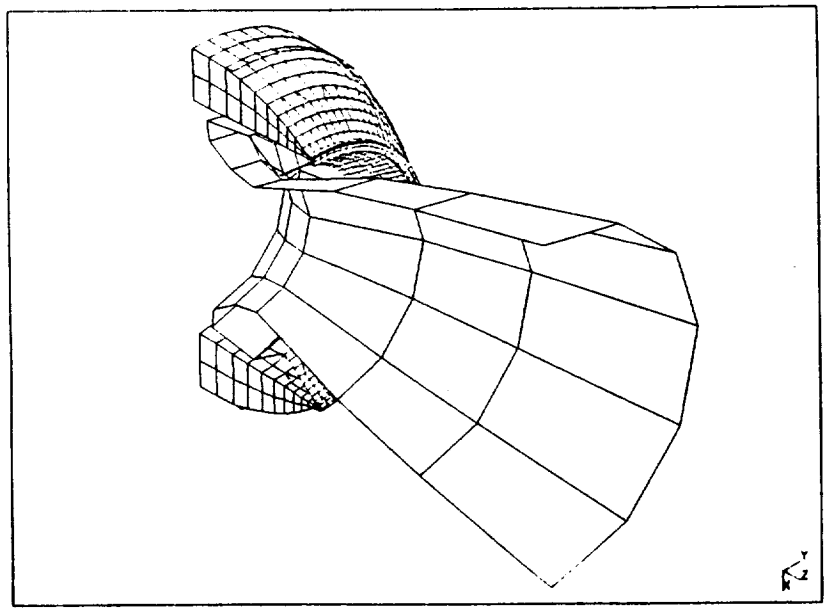

Figure 11
Cutaway View of Aft Dome

AFT SKIRT

The aft skirt was developed by first modeling in detail a 180 degree section of the skirt. This detailed model included the skirt from 90 to 270 degrees. This primary superelement was then mirror imaged to form one image superelement. The 180 degree primary and image superelements were combined into a collector superelement to represent the 360 degree skirt. Figure 12 shows the primary superelement, which represents half the aft skirt.

Plate elements were used to represent the skirt, including the stiffening rings and the bolt tie-downs. The bolt tie-downs are located at 30, 150, 210, and 330 degrees. Reference 4 contains the listings of the MSC/NASTRAN bulk data files used to analyze the aft skirt, and detailed figures showing the grid and element numbering schemes in the model.

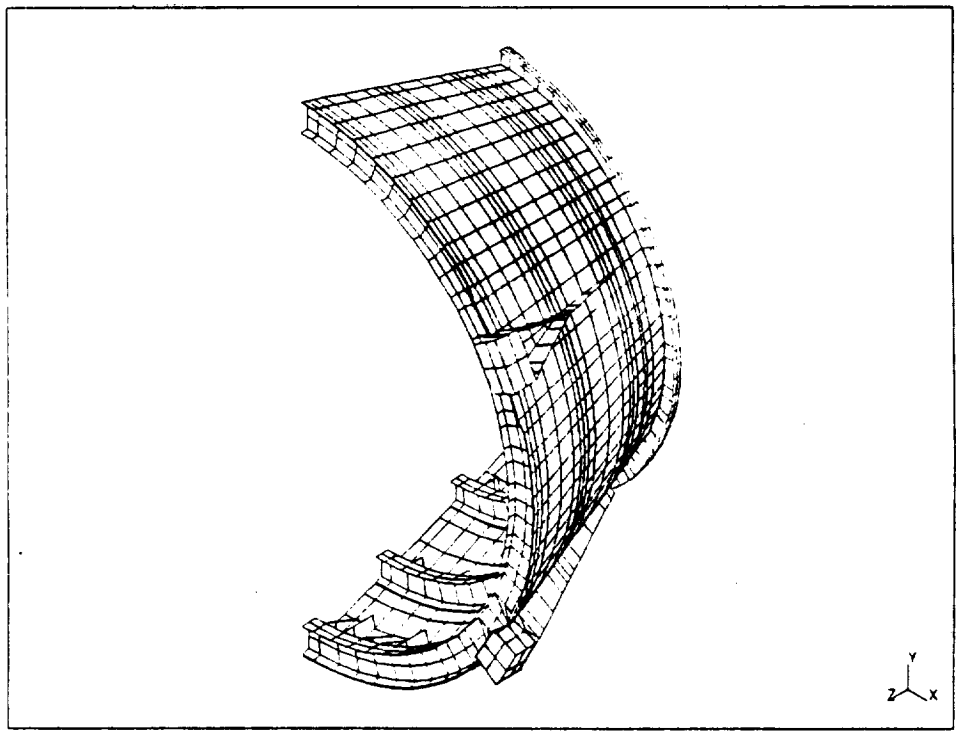

Figure 12
Cutaway View of Aft Skirt

4.2 Normal Modes Analysis of the RSRM Global Model

The RSRB global model was modeled as a free-free structure for the liftoff analysis. A mathematical support which constrained six degrees of freedom (DOF) was added to allow inversion of the stiffness matrix, which is necessary for mode acceleration operations. The base of the aft skirt was chosen for this support location, such that all displacements of the model would be relative to the mobile launch pad (MLP) attach points.

Because of the size of the RSRB global model, it would be very costly and time-consuming to calculate all modes. Therefore, the modal analysis was truncated by specifying a cutoff frequency of 40 Hz for the residual model. In previous analyses of this model, the modal analysis was truncated to 15 Hz (see Reference 1). However, as discussed in Reference 5, there might be significant modes which occur at higher frequencies. There were 162 modes calculated under 40 Hz, six rigid body modes and 156 elastic modes. Table 3 details some of these modes, and Appendix A contains plots of the mode shapes under 20 Hz. All 162 mode shapes are contained in Reference 6. The contribution of the higher frequency modes (up to 40 Hz) includes higher order bending, toothpaste, radial, and axial modes that were not seen in previous analyses.

Table 3
Modes of RSRB Liftoff Model

Mode Shape	Frequency (Hz)
Six Rigid Body Modes	0.0
Nozzle Torsion	3.94
First Bending	4.35
Second Bending	10.47
I=1, J=2 (Toothpaste Mode)	10.80
I=2, J=2 (Toothpaste Mode)	11.21
Torsion	14.06

4.3 Description of the Reconstructed 360L001 Liftoff Load Case

To predict the behavior of the RSRB during Flight 360L001 liftoff, the actual loads imposed on the RSRB during the 29 September 1988 liftoff were analyzed. Rockwell personnel reconstructed that load case using many of the measurements taken during Flight 360L001 liftoff (see Reference 7). These parameters were generated for both the left-hand and right-hand motors, and analyses were performed for each motor. The RSRB global model used in this analysis represents a left-hand motor (as described in Section 4.1 of this report). Therefore, it was necessary to transform each of the right-hand load parameters so they were appropriately applied to the model. A brief description of each load applied to the RSRB global model is given in the following paragraphs, and Figure 13 shows the location of these loads.

GRAVITY

A gravity load was applied to the RSRB to account for any weight effects of the booster itself. As discussed in the following paragraphs, effects of the weight of the ET and orbiter are applied through the ET attach and strut loads, and the CG offset loads.

PRESSURIZATION

The head end pressure transients applied to the RSRB global model are shown Appendix B. As shown, the duration of each transient is 10 seconds. A peak pressure of approximately 915 psi occurs in the left-hand motor, and a peak pressure of approximately 919 psi occurs in the right-hand motor. Since the pressure transient occurs at the head end of the RSRB, it was necessary to factor the transient at each RSRB segment to simulate the pressure gradient down the bore. Figure B-1 of Appendix B shows a comparison of the nominal and actual flight pressure loadings as a function of axial station, as predicted by Thiokol Ballistic Engineers (see Reference 5). Since there is less than a two percent difference between the pressure profiles, the nominal pressure gradient was used in the analyses for both the left- and right-hand motors.

Figure 13
Application of Reconstructued 360L001 Liftoff
Load Case to the RSRB Model

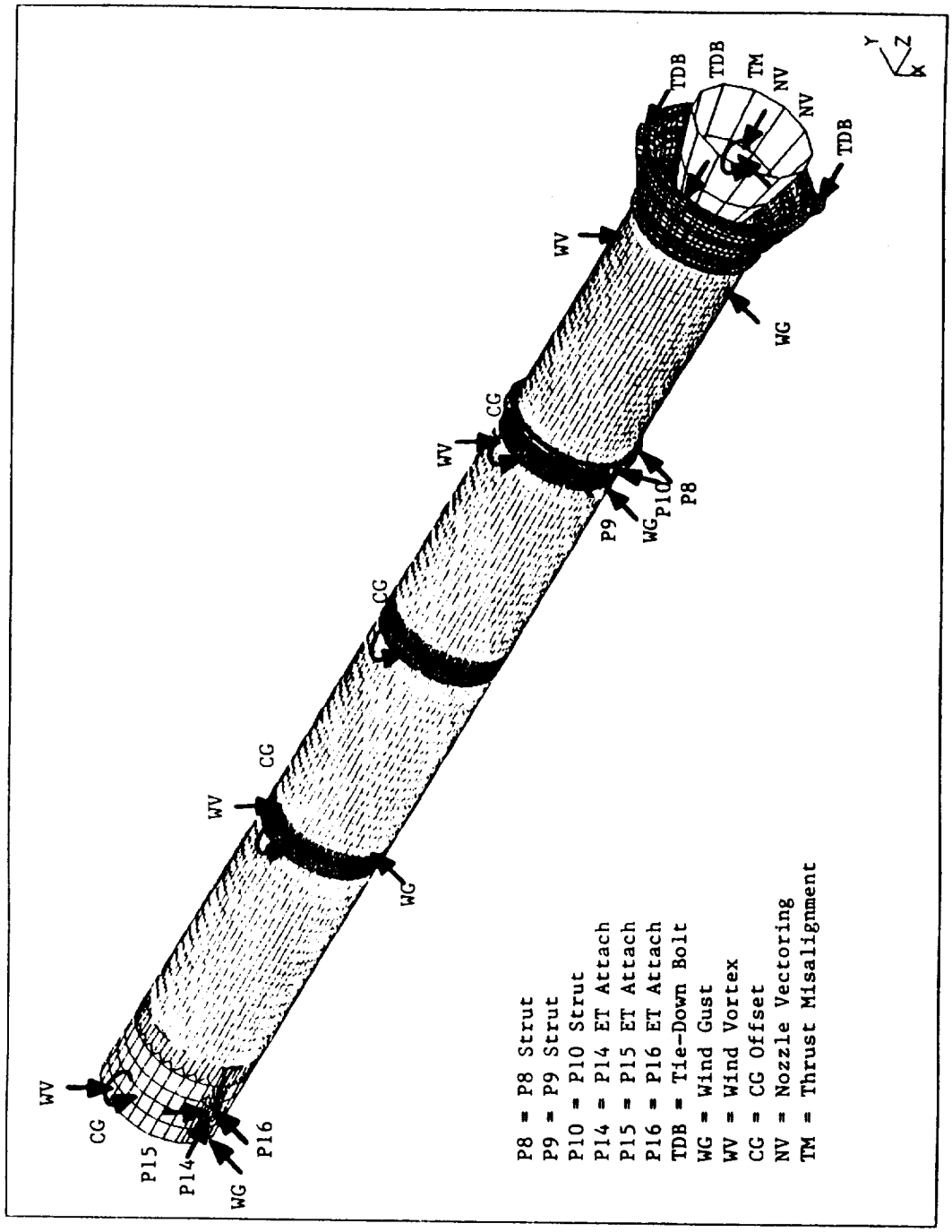

ET ATTACH LOADS

The transient external tank (ET) attach loads applied to the RSRB global model are shown in Appendix B. The forward attach loads (P14, P15, and P16) were applied to the forward skirt at the 270 degree location of axial station 447. The ET struts (P8, P9, and P10) were applied to the ET ring at 317, 223, and 282 degrees respectively. The strut attach points are modeled on the ET ring at axial station 1511. Application of these ET attach loads to the RSRB global model is shown in Figure 13.

MLP TIE-DOWN BOLT LOADS

Prior to pressurization of the boosters, the RSRB is held down to the MLP via bolts attached to the aft skirt. Application of these tie-down bolt loads to the RSRB global model is also shown in Figure 13. The transient loads caused by these tie-down bolts are shown in Appendix B. As shown, when the boosters pressurize at approximately 6.5 seconds, the tie-down bolts disconnect, and the loads go to zero.

WIND LOADINGS

The wind conditions during Flight 360L001 liftoff were considered negligible (see Reference 7). Therefore, no wind gust or vortex loadings were applied to the model for this analysis.

CG OFFSETS

Because of the weight of the orbiter, the center of gravity of the RSRB is slightly shifted during the time it is still attached to the MLP. Rockwell has accounted for this in its CG offset loadings. The transient CG offset loads at four locations on the RSRB are also shown in Appendix B. Rockwell applied these loads to two points at each location to create a bending moment. Since the geometry of the RSRB global model is different from the Rockwell model, it was necessary to calculate an equivalent moment at each of the four locations. In calculating these equivalent moments it was desireable to 1) load all of the grid points at the specified axial stations such that point stresses could be avoided, and 2) load the grid points in the vertical direction such that large shear stresses could be avoided. The location of these CG offset loadings is shown in Figure 13.

MISCELLANEOUS NOZZLE LOADS

Appendix B also contains plots showing the loadings caused by nozzle vectoring. There are three lateral loads representing nozzle rotation under load and flight control command angles. All of these loads were applied at the nozzle pivot point, as shown in Figure 13. Thrust misalignment, which is normally represented by a moment at the nozzle pivot point, was considered negligible.

5.0 TRANSIENT ANALYSIS RESULTS

As detailed in earlier sections of this report, the advanced method of transient analysis was used to analyze the behavior of the RSRB when subjected to liftoff loadings. Version 65A of the MSC/NASTRAN computer code was used to perform this analysis (see Reference 8). A reconstructed Flight 360L001 liftoff load case (generated by Rockwell) was applied to the RSRB global model, and several parameters were studied in an effort to understand the behavior of the RSRB during Flight 360L001 liftoff. These parameters include radial growth, biaxial strains, acceleratons, axial growth, RSRB twang, and field joint gap opening. DFI instrumentation predictions were correlated with actual gage measurements. A discussion of the results is contained in the following paragraphs.

5.1 Membrane and Joint Radial Growth

Radial girth gages were bonded to each of the RSRB steel motor cases at 52 different axial stations. Locations of the girth gages are shown in Appendix C. As stated earlier, pressurization of the RSRBs occurs at approximately 6.5 seconds. Until that time, radial growth in the motor is negligible. At initial conditions, the motor slightly slumps because of the gravitational loads, causing a very small radial growth. The predicted transient radial growths were calculated by taking the average radial displacement of all grid points around the circumference.

Comparisons of the predicted and measured radial growths for each girth gage are shown in Appendix D. These time history plots represent the duration of the liftoff from 0.0 through 10 seconds. In order to get a direct comparison of the predicted and measured radial growths, it was necessary to initialize each set of data, and to shift the curves such that t=0.0 represents SSME ignition. Tables 4 and 5 show the maximum radial growth values over the duration of the liftoff, and the percent difference between each predicted and measured radial growth. Unfortunately, many of the girth gages mounted to the case were lost prior to flight or did not function properly during flight.

In general, the predicted radial growths compare fairly well with the measured radial growth data. Tables 4 and 5 show that the predicted case membrane radial growth is within nine percent of the measured. The predicted field joint radial growths are, generally, within 12 percent of the measured. The aft factory joint radial growth is, generally, within 20 percent of the measured. All the radial growth predictions are lower than the measured, indicating that the radial stiffness of the analytical model may be slightly too stiff.

Table 4
Left RSRB - Comparison of Maximum Measured
to Predicted Radial Growth Values

Gage	Station	Measured (Inches)	Predicted (Inches)	% Difference
Membrane:				
B08G7272A	771.50	0.270	0.251	-7
B08G7282A	1091.50	0.279	0.256	-8
B08G7292A	1411.80	NG	0.242	-
B08G7301A	1637.50	0.248	0.243	-2
Forward Field Joint:				
B08G7273A	847.00	0.172	0.168	-2
B08G7274A	848.75	NG	0.148	-
B08G7275A	850.20	0.148	0.143	-3
B08G7276A	852.80	0.169	0.138	-18
B08G7277A	855.50	0.187	0.158	-16
B08G7278A	857.50	0.208	0.187	-10
Center Field Joint:				
B08G7283A	1167.00	0.170	0.160	-6
B08G7284A	1168.75	NG	0.141	-
B08G7285A	1170.20	0.144	0.136	-6
B08G7286A	1172.80	NG	0.131	-
B08G7287A	1175.25	NG	0.150	-
B08G7288A	1177.50	0.193	0.177	-8
Aft Field Joint:				
B08G7293A	1487.00	0.186	0.155	-17
B08G7294A	1488.75	NG	0.137	-
B08G7295A	1490.20	0.156*	0.132	-
B08G7296A	1492.80	0.142	0.125	-12
B08G7297A	1495.25	0.167*	0.138	-
B08G7298A	1497.50	0.171*	0.150	-
Aft Factory Joints:				
B08G7299A	1574.75	NG	0.142	
B08G7300A	1576.40	0.231*	0.142	-
B08G7302A	1694.75	0.195*	0.132	-
B08G7303A	1696.40	0.193	0.132	-32

* Indicates gages that exhibited the spiking phenomenon

Table 5
Right RSRB - Comparison of Maximum Measured to Predicted Radial Growth Values

Gage	Station	Measured (Inches)	Predicted (Inches)	% Difference
Membrane:				
B08G8272A	771.50	NG	0.252	-
B08G8282A	1091.50	0.280	0.257	-8
B08G8292A	1411.80	0.262	0.243	-7
B08G8301A	1637.50	0.243	0.243	0
Forward Field Joint:				
B08G8273A	847.00	NG	0.169	-
B08G8274A	848.75	NG	0.149	-
B08G8275A	850.20	NG	0.144	-
B08G8276A	852.80	NG	0.139	-
B08G8277A	855.50	NG	0.159	-
B08G8278A	857.50	NG	0.187	-
Center Field Joint:				
B08G8283A	1167.00	NG	0.160	-
B08G8284A	1168.75	NG	0.141	-
B08G8285A	1170.20	NG	0.136	-
B08G8286A	1172.80	0.157	0.132	-16
B08G8287A	1175.25	NG	0.151	-
B08G8288A	1177.50	NG	0.178	-
Aft Field Joint:				
B08G8293A	1487.00	0.163	0.155	-5
B08G8294A	1488.75	NG	0.138	-
B08G8295A	1490.20	0.135	0.132	-2
B08G8296A	1492.80	0.143	0.125	-13
B08G8297A	1495.25	NG	0.139	-
B08G8298A	1497.50	0.152	0.150	-1
Aft Factory Joints:				
B08G8299A	1574.75	0.170	0.142	-17
B08G8300A	1576.40	NG	0.142	-
B08G8302A	1694.75	0.167	0.132	-21
B08G8303A	1696.40	0.159	0.132	-17

It should be noted that several of the girth gage measurements indicate spiking prior to the time of peak pressure. This phenomenon has been investigated and is believed to be a girth gage measurement problem. The results of the spiking investigation are detailed in Reference 9.

5.2 Membrane and Joint Hoop Strain

Strain gages were bonded to the RSRB steel motor cases at seven different axial stations, with up to nine gages around the circumference of the motor at each station. Pairs of strain gages were used to measure both axial and hoop strain at each location. Locations of these biaxial strain gages are shown in Appendix C. Strains were recovered at the element centroid, which was generally at 4 degrees for the elements recovered. Strains in the outer fiber of the plates were calculated for comparison with strain gages mounted to the outside of the motor.

Comparisons of the calculated and measured hoop strains for each strain gage are contained in Appendix E. As with radial growths, it was necessary to initialize each set of data, and to shift the curves such that t=0.0 represents SSME ignition. Tables 6 and 7 show the maximum hoop strain values over the duration of the liftoff, and the percent difference between each predicted and measured hoop strain.

Table 6
Left RSRB - Comparison of Maximum Measured to Predicted Hoop Strain Values

Gage	Station	Degree	Measured (μ in./in.)	Predicted (μ in./in.)	% Difference
B08G7319A	556.5	0	NG	3859	-
B08G7321A	"	98	NG	3817	-
B08G7323A	"	180	3449	3865	12
B08G7325A	"	270	NG	4043	-
B08G7327A	876.5	0	3506	3722	6
B08G7329A	"	98	3489	3646	4
B08G7331A	"	180	3522	3699	5
B08G7333A	"	270	3377	3674	9
B08G7335A	1196.5	0	3160	3459	9
B08G7337A	"	98	NG	3465	-
B08G7339A	"	180	3280	3562	9
B08G7341A	"	270	3313	3503	6
B08G7343A	1466.0	0	3136	3243	3
B08G7345A	"	98	3243	3297	2
B08G7347A	"	180	3313	3419	3
B08G7349A	"	270	3449	3337	-3
B08G7355A	1493.0	0	1954	1731	-11
B08G7353A	"	98	1704	1708	0
B08G7351A	"	180	1825	1804	-1
B08G7367A	"	220	1809	1862	3
B08G7365A	"	255	1910	1778	-7
B08G7363A	"	270	1770	1747	-1
B08G7361A	"	285	1849	1709	-8
B08G7359A	"	300	1705	1833	8
B08G7357A	"	320	NG	1674	-
B08G7391A	1501.0	0	1696	1820	7
B08G7389A	"	98	1833	1895	3
B08G7387A	"	180	1822	2056	13
B08G7403A	"	220	1852	1913	3
B08G7401A	"	255	1869	1942	4
B08G7399A	"	270	1806	1933	7
B08G7397A	"	285	1705	1846	8
B08G7395A	"	300	1737	1895	9
B08G7393A	"	320	1705	1769	4
B08G7405A	1797.0	0	2994	3339	12
B08G7407A	"	98	3200	3612	13
B08G7409A	"	180	NG	3561	-
B08G7411A	"	270	NG	3651	-

Table 7
Right RSRB - Comparison of Maximum Measured to Predicted Hoop Strain Values

Gage	Station	Degree	Measured (μ in./in.)	Predicted (μ in./in.)	% Difference
B08G8323A	556.6	0	NG	3865	-
B08G8321A	"	82	3908	3851	-2
B08G8319A	"	180	3562	3840	8
B08G8325A	"	270	NG	3847	-
B08G8331A	876.5	0	NG	3706	-
B08G8329A	"	82	3538	3655	3
B08G8327A	"	180	NG	3649	-
B08G8333A	"	270	NG	3677	-
B08G8339A	1196.5	0	NG	3569	-
B08G8337A	"	82	NG	3465	-
B08G8335A	"	180	3377	3463	3
B08G8341A	"	270	NG	3510	-
B08G8347A	1466.0	0	3313	3429	4
B08G8345A	"	82	3128	3298	5
B08G8343A	"	180	3104	3247	5
B08G8349A	"	270	3337	3344	0
B08G8351A	1493.0	0	2018	1811	-10
B08G8353A	"	82	NG	1710	-
B08G8355A	"	180	1552	1733	12
B08G8357A	"	220	1608	1673	4
B08G8359A	"	240	1849	1833	-1
B08G8361A	"	255	NG	1702	-
B08G8363A	"	270	NG	1746	-
B08G8365A	"	285	1914	1781	-7
B08G8367A	"	320	1922	1862	-3
B08G8387A	1501.0	0	1914	2060	8
B08G8389A	"	82	1833	1896	3
B08G8391A	"	180	1640	1819	11
B08G8393A	"	220	1748	1893	8
B08G8395A	"	240	1817	1901	5
B08G8397A	"	255	1761	1853	5
B08G8399A	"	270	1761	1944	10
B08G8401A	"	285	1479	1940	31
B08G8403A	"	320	NG	1923	-
B08G8409A	1797.0	0	3256	3577	10
B08G8407A	"	82	3200	3625	13
B08G8405A	"	180	2919	3347	15
B08G8411A	"	270	3112	3657	18

The plots in Appendix E show a very good correlation of the predicted and measured hoop strains. In general, the predicted hoop strains are within ±10 percent of measured data. Prior to RSRB ignition the curves correlate almost perfectly. Following RSRB ignition, however, the predicted hoop strains indicate a higher frequency content than the measured data. This frequency does not dampen out as rapidly as the oscillations shown in the measured hoop strain curves. This phenomenon will be discussed further in following sections of this report.

5.3 Membrane and Joint Axial Strain

Strain gages were bonded to the RSRB steel motor cases at seven different axial stations, with up to nine gages around the circumference of the motor at each station. Pairs of strain gages were used to measure both axial and hoop strain at each location. Locations of these biaxial strain gages are shown in Appendix C. As with the hoop strains, axial strains were recovered at the element centroid, which was generally at four degrees for the elements recovered. Strains in the outer fiber of the plates were calculated for predictions of strain gages mounted to the outside of the motor.

Comparisons of the calculated and measured axial strains for each strain gage are contained in Appendix F. As with the hoop strains, to get a direct comparison of the measured and predicted axial strains, it was necessary to initialize each set of data, and to shift the curves such that

t-0.0 represents SSME ignition. Tables 8 and 9 show the maximum axial strain values over the duration of the liftoff, and the percent difference between each measured and predicted axial strain. On an average, the maximum predicted peaks compare within approximately 45 percent of the measured.

Examination of the plots in Appendix F shows that the measured and predicted axial strains compare very well prior to RSRB ignition. Following RSRB ignition the predicted axial strains contain some dynamic effects which are not exhibited in the measured response. It has been determined that the magnitude and damping of the predicted axial strains are a direct result of the loads input. Tables 10 and 11 show a comparison of the mean values of axial strain following RSRB ignition. On average, the mean predicted axial strain, compares within approximately 26 percent of the mean measured axial strain.

The comparison of predicted to measured axial strains is least favorable for the gages located at Station 1493.0, which is slightly aft of the aft field joint pin centerline. It has been determined that the poor correlation is due to analytical model simplifications in the curved region between the field joint pin and the membrane interface. It is recommended that the model be enhanced in this region for future analyses.

Table 8
Left RSRB - Comparison of Maximum Measured to Predicted Axial Strain Values

Gage	Station	Degree	Measured (μ in./in.)	Predicted (μ in./in.)	% Difference
B08G7318A	556.5	0	530	823	55
B08G7320A	"	98	1515	829	-45
B08G7322A	"	180	769	748	-3
B08G7324A	"	270	832	917	10
B08G7326A	876.5	0	997	1311	31
B08G7328A	"	98	932	1115	20
B08G7330A	"	180	811	989	22
B08G7332A	"	270	830	1001	21
B08G7334A	1196.5	0	1045	1449	39
B08G7336A	"	98	852	1187	39
B08G7338A	"	180	827	898	9
B08G7340A	"	270	650	1000	54
B08G7342A	1466.0	0	1116	1637	47
B08G7344A	"	98	939	1389	48
B08G7346A	"	180	718	938	31
B08G7348A	"	270	779	1121	44
B08G7354A	1493.0	0	674	-465	-
B08G7352A	"	98	935	-508	-
B08G7350A	"	180	1156	-587	-
B08G7366A	"	220	770	-609	-
B08G7364A	"	255	803	-559	-
B08G7362A	"	270	907	-542	-
B08G7360A	"	285	765	-518	-
B08G7358A	"	300	873	-588	-
B08G7356A	"	320	939	-459	-
B08G7390A	1501.0	0	897	1393	55
B08G7388A	"	98	869	1188	37
B08G7386A	"	180	804	908	13
B08G7402A	"	220	785	974	24
B08G7400A	"	255	698	1035	48
B08G7398A	"	270	773	1092	41
B08G7396A	"	285	867	1017	17
B08G7394A	"	300	883	1092	24
B08G7392A	"	320	845	1200	42
B08G7404A	1797.0	0	1382	2544	84
B08G7406A	"	98	612	939	53
B08G7408A	"	180	724	1401	94
B08G7410A	"	270	450	906	101

Table 9
Right RSRB - Comparison of Maximum Measured to Predicted Axial Strain Values

Gage	Station	Degree	Measured (μ in./in.)	Predicted (μ in./in.)	% Difference
B08G8322A	556.5	0	NG	750	-
B08G8320A	"	82	Q	781	-
B08G8318A	"	180	NG	825	-
B08G8324A	"	270	915	940	3
B08G8330A	876.5	0	Q	994	-
B08G8328A	"	82	1055	1110	5
B08G8326A	"	180	NG	1327	-
B08G8332A	"	270	Q	997	-
B08G8338A	1196.5	0	610	905	48
B08G8336A	"	82	NG	1180	-
B08G8334A	"	180	1067	1478	39
B08G8340A	"	270	742	998	35
B08G8346A	1466.0	0	638	947	48
B08G8344A	"	82	851	1377	62
B08G8342A	"	180	1108	1674	51
B08G8348A	"	270	674	1124	67
B08G8350A	1493.0	0	598	-593	-
B08G8352A	"	82	NG	-511	-
B08G8354A	"	180	935	-465	-
B08G8356A	"	220	642	-459	-
B08G8358A	"	240	545	-588	-
B08G8360A	"	255	835	-512	-
B08G8362A	"	270	650	-542	-
B08G8364A	"	285	626	-567	-
B08G8366A	"	320	558	-610	-
B08G8386A	1501.0	0	670	914	36
B08G8388A	"	82	963	1187	23
B08G8390A	"	180	1124	1407	25
B08G8392A	"	220	831	1234	48
B08G8394A	"	240	815	1162	43
B08G8396A	"	255	943	1050	11
B08G8398A	"	270	726	1096	51
B08G8400A	"	285	494	1035	110
B08G8402A	"	320	726	1018	40
B08G8408A	1797.0	0	646	1384	114
B08G8406A	"	82	582	955	64
B08G8404A	"	180	1417	2585	82
B08G8410A	"	270	514	898	75

Table 10
Left RSRB - Comparison of Mean Measured to Mean Predicted Axial Strains After RSRB Ignition

Gage	Mean Axial Strain (μ in./in.) Measured	Predicted	% Difference
B08G7318A	500	775	55
B08G7320A	1500	750	-50
B08G7322A	750	700	-7
B08G7324A	738	738	0
B08G7326A	925	1133	22
B08G7328A	867	1025	18
B708G330A	700	819	17
B708G332A	750	900	20
B08G7334A	975	1200	23
B08G7336A	767	1033	35
B08G7338A	680	640	-6
B08G7340A	588	817	39
B08G7342A	929	1357	46
B08G7344A	873	1160	33
B08G7346A	600	600	0
B08G7348A	720	860	19
B08G7390A	844	1200	42
B08G7388A	833	1022	23
B08G7386A	756	667	-12
B08G7402A	716	654	-9
B08G7400A	663	731	10
B08G7398A	725	863	19
B708G396A	825	888	8
B708G394A	800	933	17
B708G392A	700	960	37
B708G404A	1023	1941	90
B708G406A	600	600	0
B708G408A	713	1027	44
B708G410A	420	573	36

Table 11
Right RSRB - Comparison of Mean Measured to Mean Predicted Axial Strains After RSRB Ignition

Gage	Mean Axial Strain (μ in./in.) Measured	Predicted	% Difference
B08G8322A	---	715	---
B08G8320A	---	745	---
B08G8318A	---	775	---
B08G8324A	693	755	10
B08G8330A	---	825	---
B80G8328A	987	1020	3
B08G8326A	---	1137	---
B08G8332A	---	900	---
B08G8338A	327	687	110
B08G8336A	---	1000	---
B08G8334A	971	1200	24
B08G8340A	683	850	24
B08G8346A	525	625	19
B08G8344A	800	1117	40
B08G8342A	1000	1343	34
B08G8348A	6517	875	42
B08G8386A	600	600	0
B08G8388A	938	969	3
B08G8390A	1085	1192	10
B08G8392A	719	938	30
B08G8394A	746	938	26
B08G8396A	892	877	-2
B08G8398A	708	892	26
B08G8400A	469	742	58
B08G8402A	653	653	0
B08G8404A	622	911	46
B08G8406A	567	617	9
B08G8404A	1080	1880	74
B08G8410A	593	600	1

5.4 Accelerations

Nine accelerometers were bonded to the RSRBs: three to the left RSRB, and six to the right RSRB. All of the accelerometers were bonded on the forward skirts near Station 500. Exact locations of the accelerometers are shown in Appendix C. Three of the accelerometers (channels B08D8151A through B08D8153A, requested by USBI) were severely compromised by noise. Six of the accelerometers were requested by Thiokol Engineers, and a discussion of these six is contained herein. Predicted accelerations were recovered at the grid point nearest to the actual gage location. Plots of the measured accelerations are contained in Appendix G.

Since the modal analysis was truncated to 40 Hz (as discussed in Section 4.2), the measured accelerations for the six good gages were filtered to 40 Hz to get a direct comparison with the predicted values. These plots are also contained in Appendix G. For each of these gages, the frequency content of the acceleration curves was determined by performing a Fourier transform on each set of data. Appendix G also contains a comparison of the measured and predicted curves for both the accelerations and the Fourier transforms, in addition to waterfall plots of the measured data filtered to 40 Hz.

Tables 12 and 13 show a comparison of the measured and predicted peak accelerations and dominant frequencies for each of the good gages. Since the gages can only record frequencies higher than 5 Hz (see Appendix C), the dominant frequencies under 5 Hz for the predicted accelerations were not included in this comparison. As shown, the predicted accelerations do not correlate very well with the measured. However, the dominant frequencies predicted above 5 Hz compare favorably with the measured.

Modal frequencies which represent two structural modes of vibration can be identified in the waterfall plots. In the plot for channel B08D7160A an axial mode is detected at approximately 29 Hz. However, it is very difficult to correlate this mode with the analytical mode shapes because there is not a purely axial mode represented. Channels B08D7161A and B08D8161A indicate a torsional mode at approximately 15 Hz. This correlates to an analytical torsional mode at 14.1 Hz.

Table 12
Comparison of Peak Measured to Predicted Accelerations

Gage	Station	Degree	Direction	Peak Acceleration (g) Measured	Predicted
B08D7160A	500	0	Axial	0.6	1.1
B08D7161A	500	0	Tang	0.3	0.5
B08D7162A	500	0	Radial	1.3	0.4
B08D8160A	500	180	Axial	1.1	1.0
B08D8161A	500	180	Tang	0.3	0.6
B08D8163A	500	0	Tang	0.3	0.6

Table 13
Comparison of Measured to Predicted Dominant Frequencies (Hz)

Gage	t = -5 to 0 sec. Measured	Predicted	t = 0 to 4 sec. Measured	Predicted
B08D7160A	16.2	15.5	28.8	8.5
B08D7161A	7.1	6.2	14.5	17.5
B08D7162A	Noise	8.5	Noise	16.5
B08D8160A	Noise	8.5	Noise	15.5
B08D8161A	6.2	6.2	14.5	17.5
B08D8163A	Noise	6.0	Noise	17.5

5.5 RSRB Axial Growth

Figures 14 and 15 show the predicted axial growth of the left and right RSRBs, respectively, during the liftoff transient. The axial growth was calculated by subtracting the axial motion of the aft dome-to-aft skirt interface from the axial motion of the forward segment-to-forward skirt interface. As the plots show, at initial conditions the motors are slumped because of the gravitational load. As each motor twangs over it becomes less compressed. Then, when the RSRBs pressurize, the motors extend to their peak axial growth. It is predicted that both motors extended approximately 1.03 inches at 7.2 seconds.

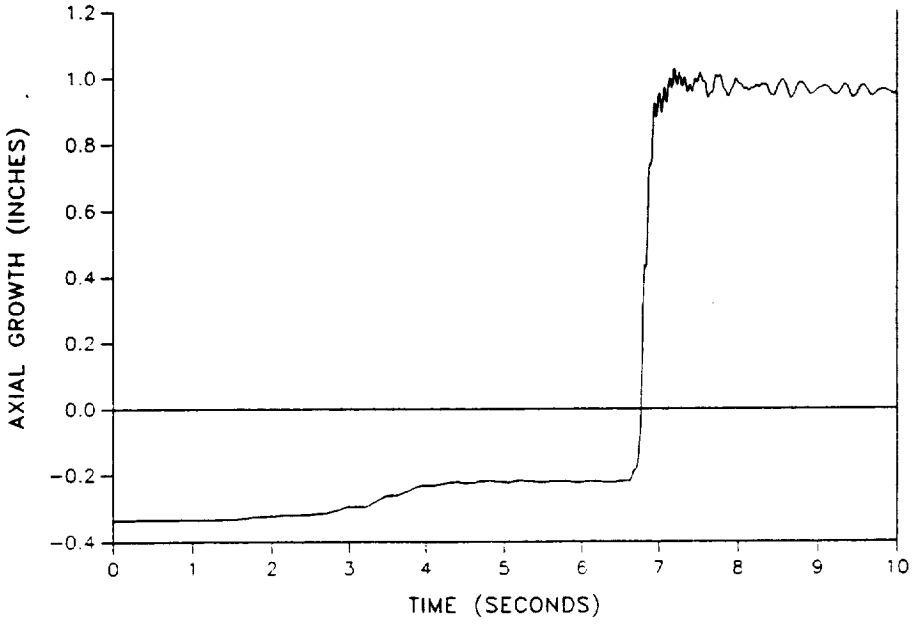

Figure 14
Predicted Axial Growth of the Left RSRB

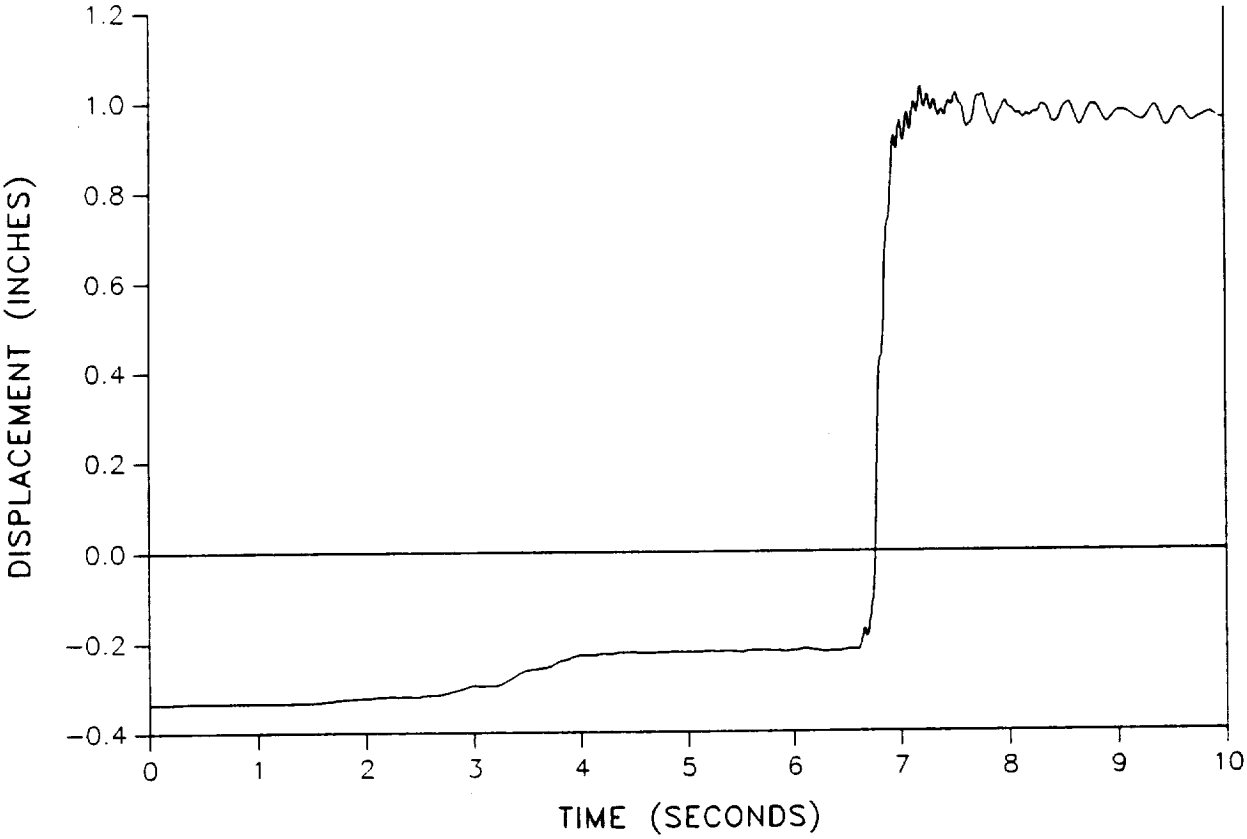

Figure 15
Predicted Axial Growth of the Right RSRB

5.6 RSRB Twang

For Flight 360L001, the main engines of the orbiter ignited at approximately 1.4 seconds. At that time, the RSRBs were still bolted to the MLP, and these bolts did not disconnect until approximately 6.5 seconds. During this elapsed time, the RSRBs twang over in the pitch direction, and then begin to come back to an upright position prior to RSRB

pressurization. It should be noted that at initial conditions, the RSRB is displaced in the opposite direction. This is caused by the weight of the orbiter, making the CG of the RSRB to shift in the direction of the orbiter.

Figures 16 and 17 are plots of the predicted horizontal displacement of the left and right motor igniters, respectively. These plots clearly show that the motors twang over during SSME ignition, and begin to return to vertical prior to RSRB ignition. The analysis predicts that the left motor igniter was initially at 2.7 inches from vertical, and then twanged in the opposite direction approximately 16.5 inches. It is predicted that the right motor igniter was initially at 2.7 inches from vertical, and then twanged in the opposite direction approximately 16.9 inches.

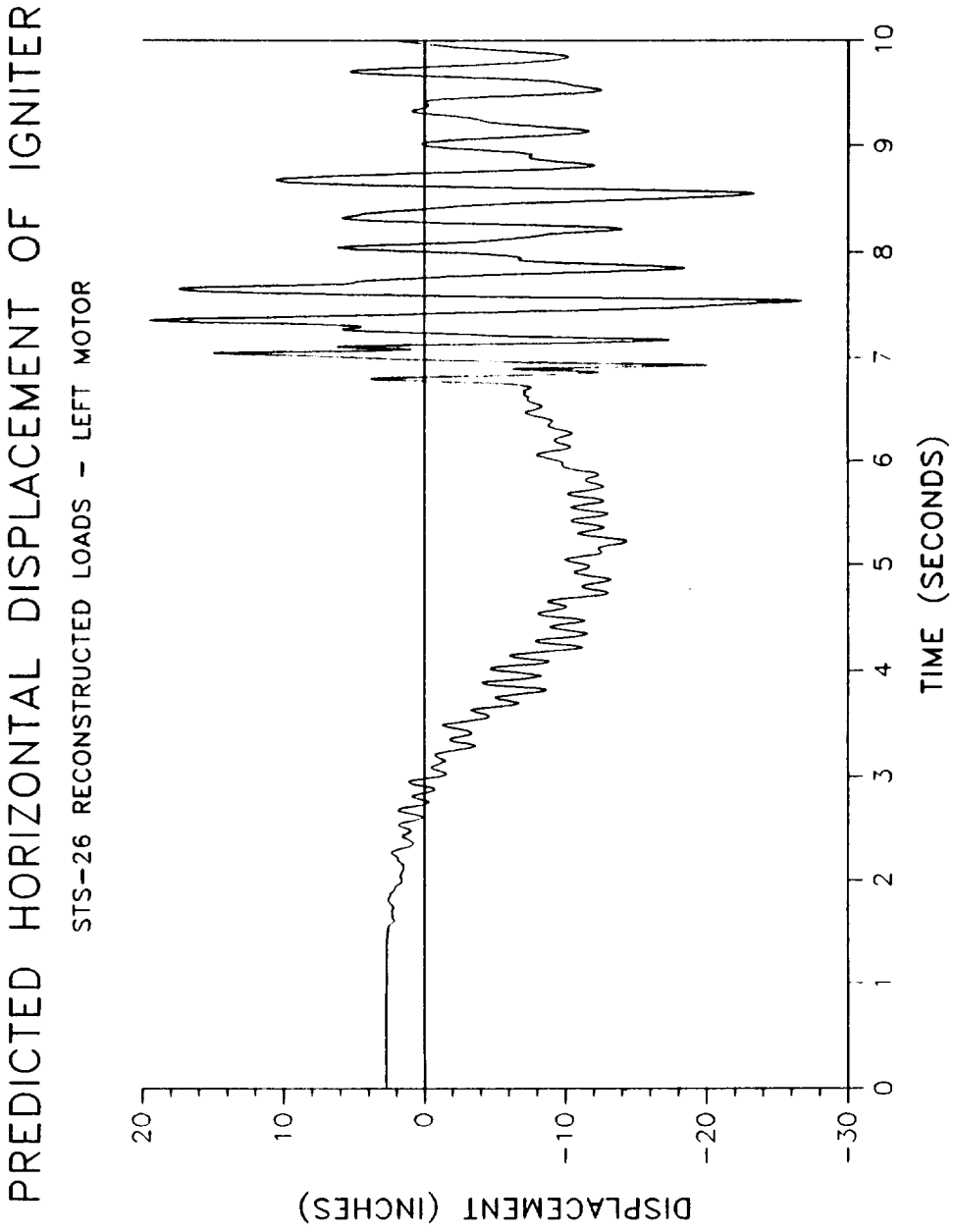

Figure 16
Twang - Predicted at the Left RSRB Igniter

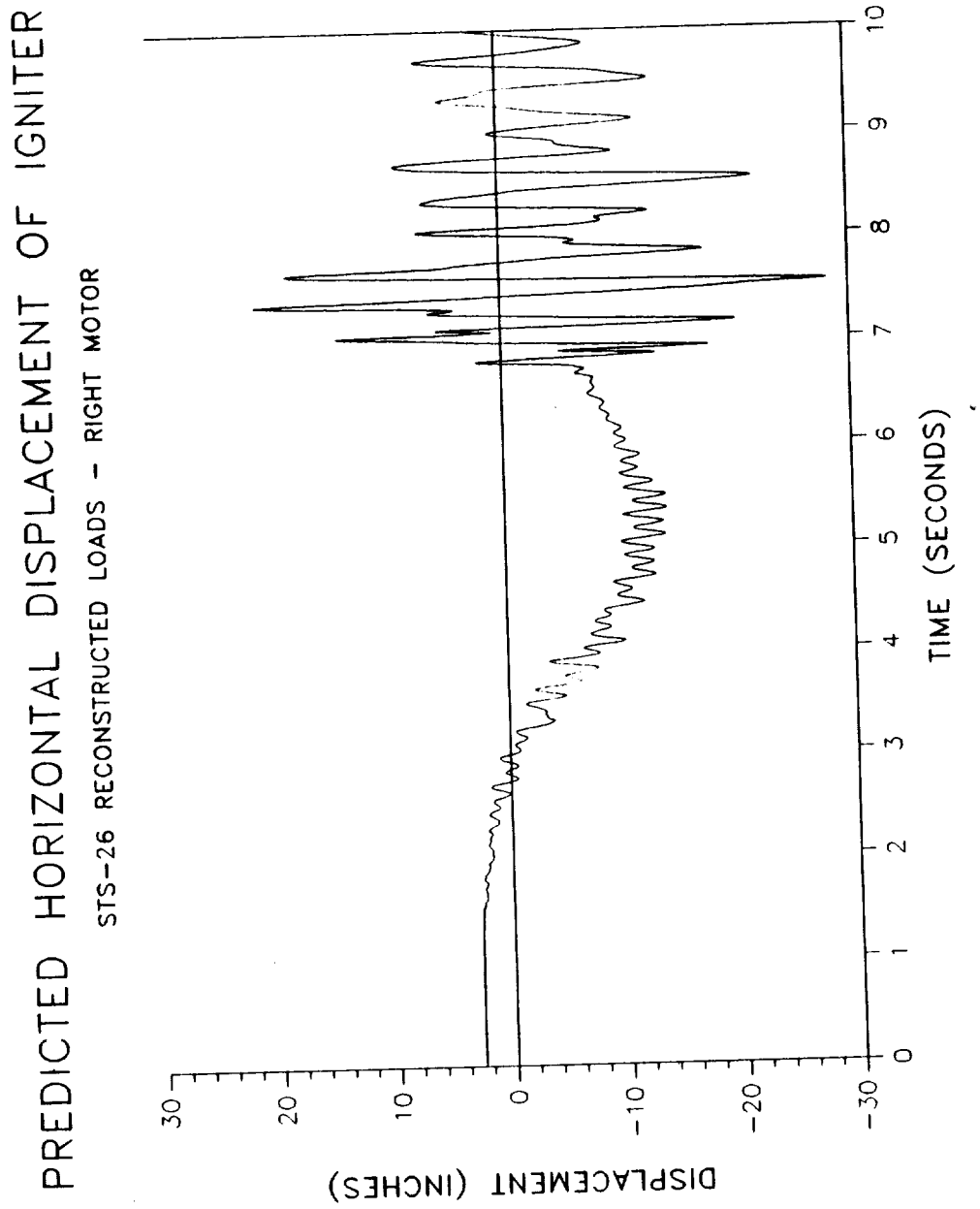

Figure 17
Twang - Predicted at the Right RSRB Igniter

5.7 Field Joint Gap Opening

This was the first flight which included the redesigned capture feature joints. The RSRB global model used for the liftoff analysis contains plate models of the capture feature field joints which have been correlated to Referee test results. Gap opening values were predicted close to the primary and secondary O-ring locations at each field joint. Appendix H contains plots which show the maximum gap opening predictions for each field joint. The maximum gap opening predicted for the left motor occurs at the forward field joint at approximately 56 degrees circumferentially. An opening of 5.93 mils is predicted for the land between the O-rings. The maximum gap opening predicted for the right motor also occurs at the forward field joint at approximately 56 degrees circumferentially. An opening of 5.94 mils is predicted for the land between the O-rings.

6.0 REFERENCES

1. V. B. Call, "Predicted Structural Behavior of the RSRB Due to FRF and Liftoff Loading Conditions Using the Launch Configuration RSRB Global Model", Morton Thiokol, Inc. TWR-18212, September 1988

2. C. C. Flanigan, "Accurate and Efficient Mode Acceleration Data Recovery for Superelement Models", 1988 MSC/NASTRAN World Users Conference, March 1988

3. V. B. Call, "Modal Transient Analyses with EZTRAN: A User's Guide", Morton Thiokol, Inc., TWR-18939, December 1988

4. L. D. Peel and V. B. Call, "Space Shuttle Solid Rocket Motor Three-Dimensional Global Finite Element Model Description", Morton Thiokol, Inc., TWR-17800, September 1988

5. G. A. Ricks, "Flight Motor Set 360L001 (STS-26R) Final

Report", Morton Thiokol, Inc., TWR-17272, Volume 1, December 1988

6. V. B. Call, "Dynamic Global Model Mode Shapes Up to 40 Hz", Morton Thiokol, Inc., TWR-19751, To Be Published

7. C. E. Ellis Memo to S. B. Medrano, "STS-26 Reconstructed Liftoff Loads", L225:FY89:729, Morton Thiokol, Inc., 24 February 1989

8. The MacNeal-Schwendler Corporation, MSC/NASTRAN, Version 65A, CRAY XMP, Kansas City, MO, 5 February 1987

9. A. W. Macbeth, "Flight Girth Gage Investigation Team Final Report", Morton Thiokol, Inc., TWR-19736, To Be Published

APPENDIX A

Flight RSRB Global Model Mode Shape Plots

	Mode Shape Description	Frequency (Hz)
1.	Rigid Body XY	0.
2.	Rigid Body XY	0.
3.	Rigid Body Rotation (Y)	0.
4.	Rigid Body Axial	0.
5.	Rigid Body Rotation (X)	0.
6.	Rigid Body Torsion	0.
7.	Nozzle Torsion	3.93
8.	First Bending	4.35
9.	First Bending	4.35
10.	Second Bending + Nozzle	10.29
11.	Second Bending	10.47
12.	I=2, J=1 (Toothpaste Mode)	10.80
13.	I=2, J=1 (Toothpaste Mode)	10.81
14.	I=2, J=2 (Toothpaste Mode)	11.21
15.	I=2, J=2 (Toothpaste Mode)	11.22
16.	Nozzle Bending	11.25
17.	I=2, J=3 (Toothpaste Mode)	12.46
18.	I=2, J=3 (Toothpaste Mode)	12.48
19.	Torsion	14.06
20.	I=2, J=4 (Toothpaste Mode)	15.06
21.	I=2, J=4 (Toothpaste Mode)	15.11
22.	Nozzle Bending	15.40
23.	Nozzle Bending	16.60
24.	Third Bending	17.30
25.	Nozzle Bending	17.90
26.	I=2, J=5 (Toothpaste Mode)	18.75
27.	I=2, J=5 (Toothpaste Mode)	18.79
28.	Nozzle Bending + CTR Joint Radial	20.01

FLIGHT DISPLAY MODEL

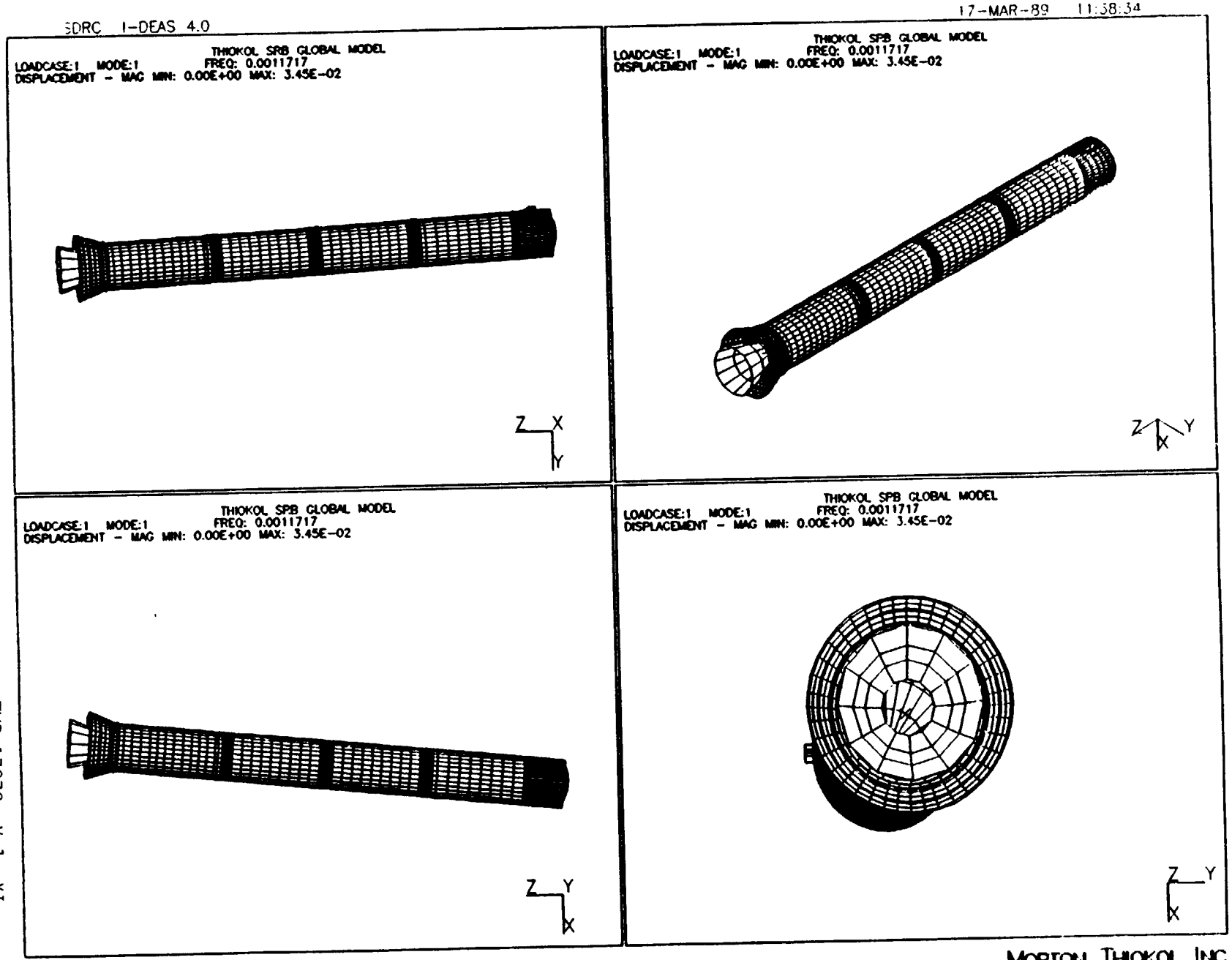

FLIGHT DISPLAY MODEL

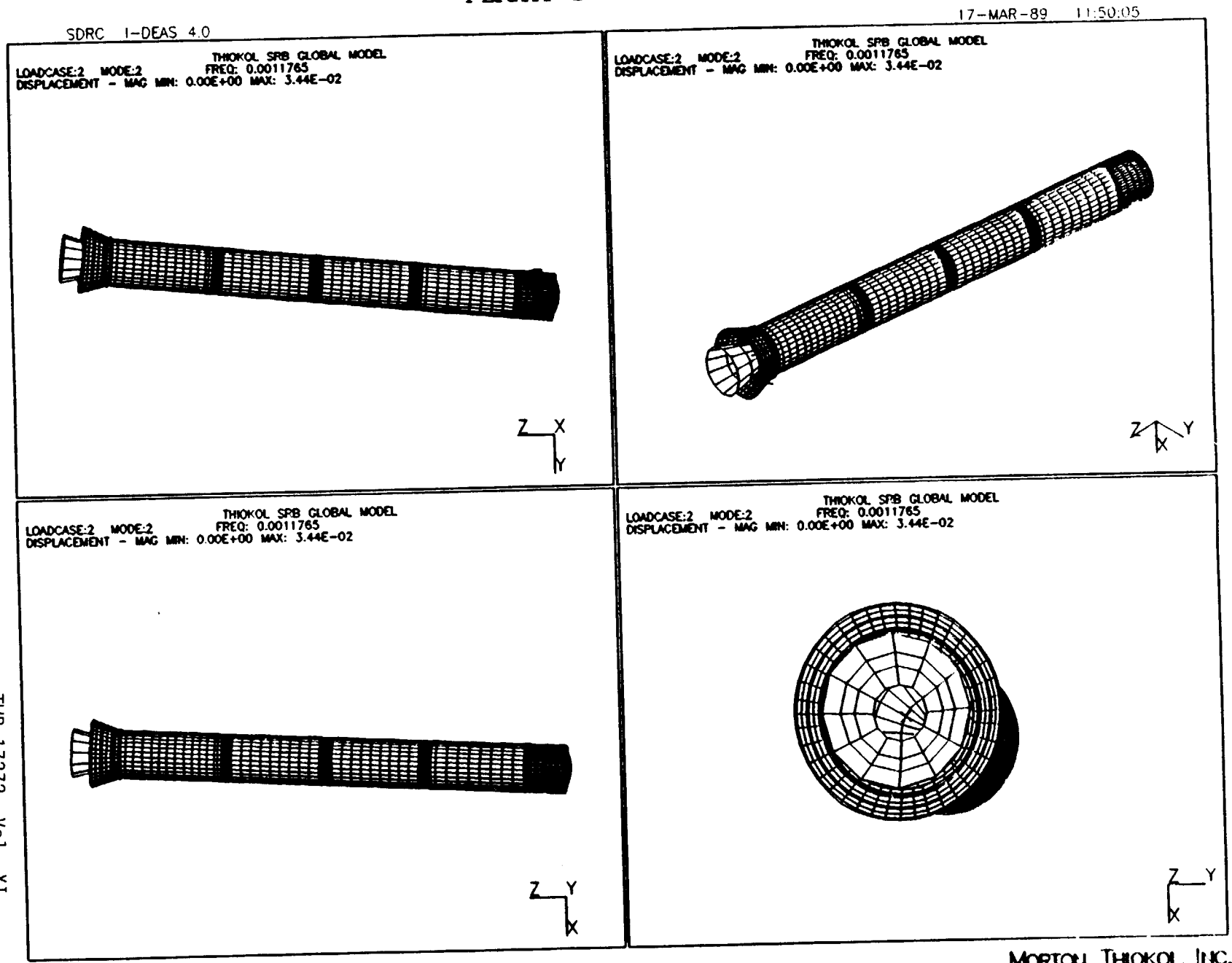

FLIGHT DISPLAY MODEL

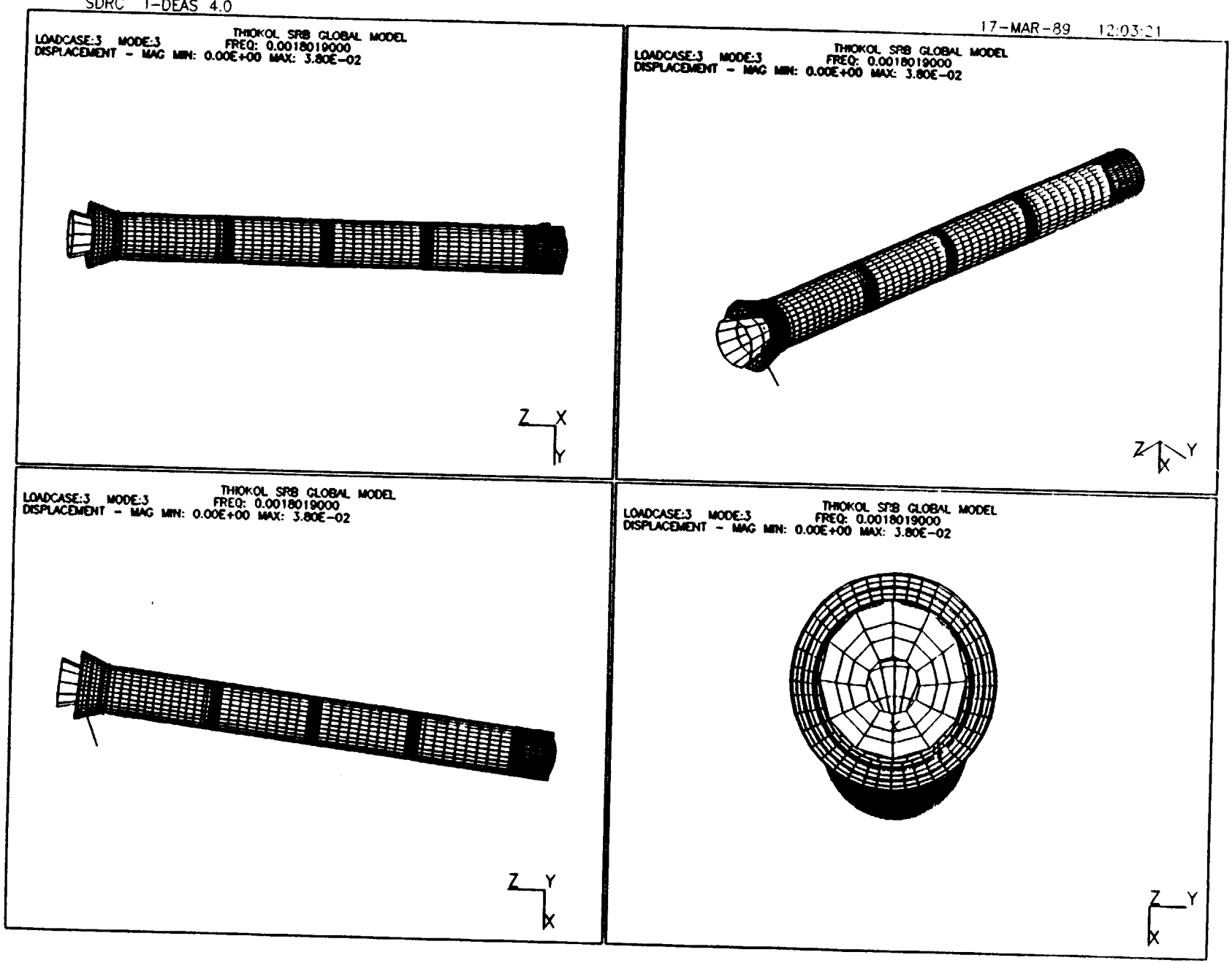

FLIGHT DISPLAY MODEL

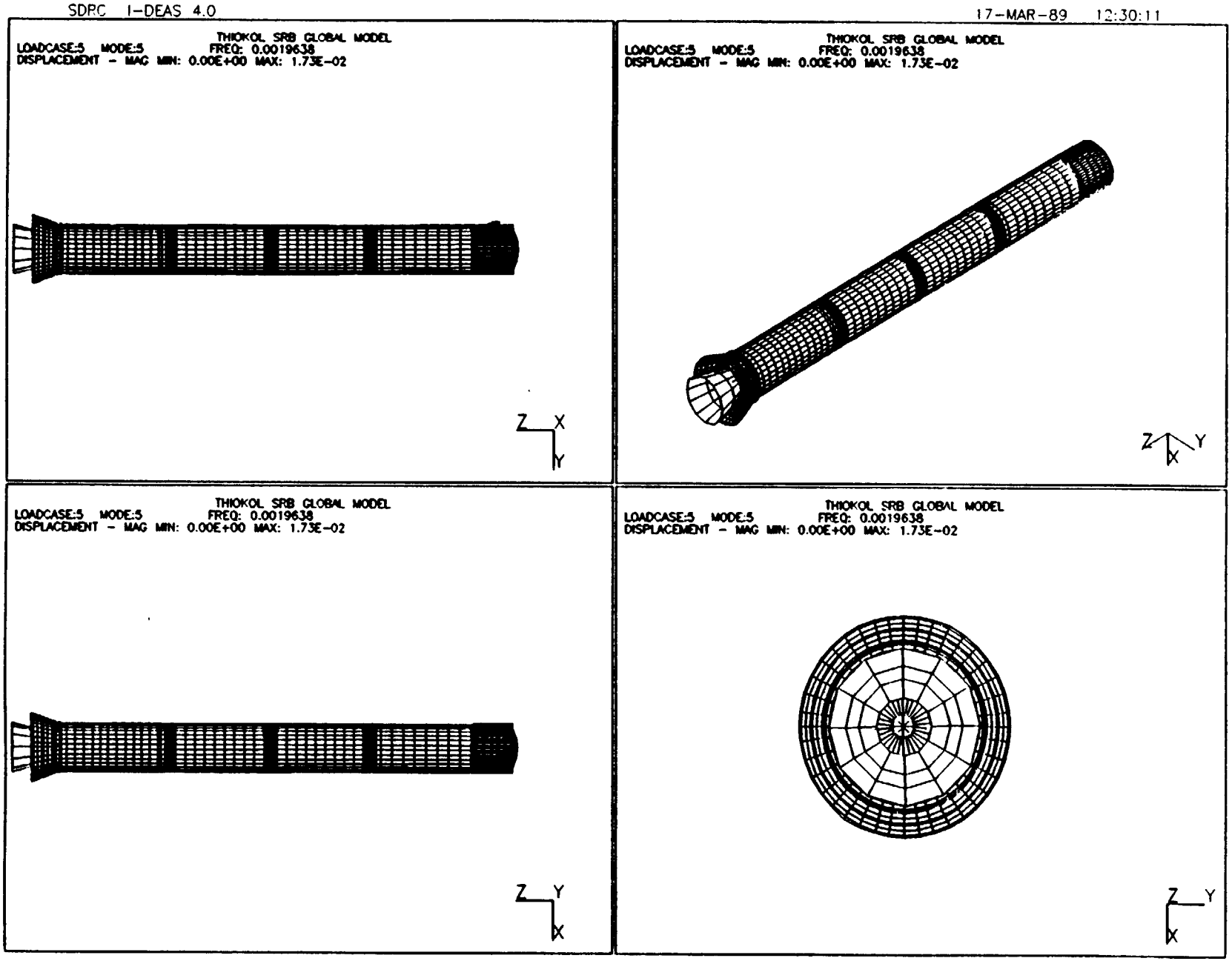

FLIGHT DISPLAY MODEL

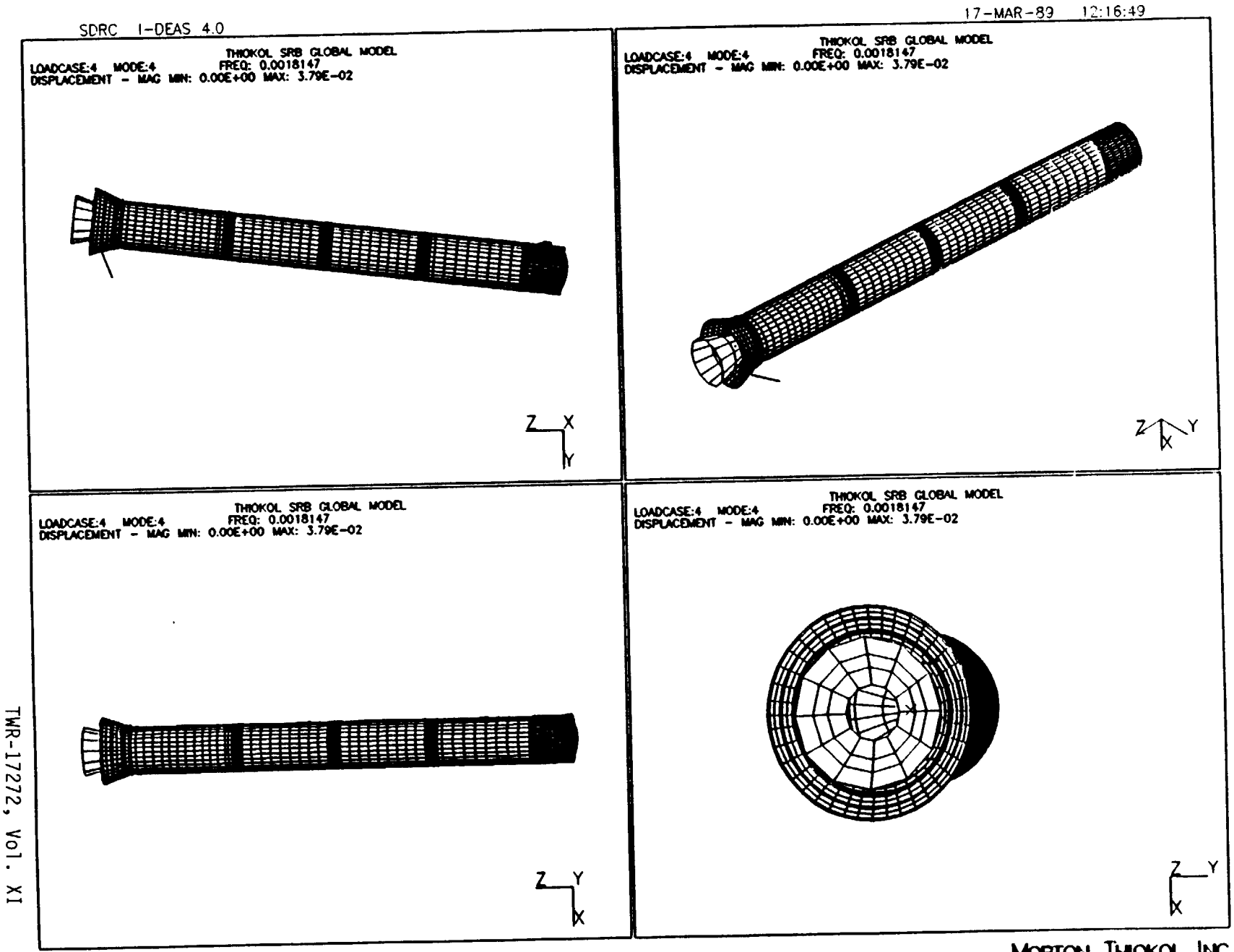

FLIGHT DISPLAY MODEL

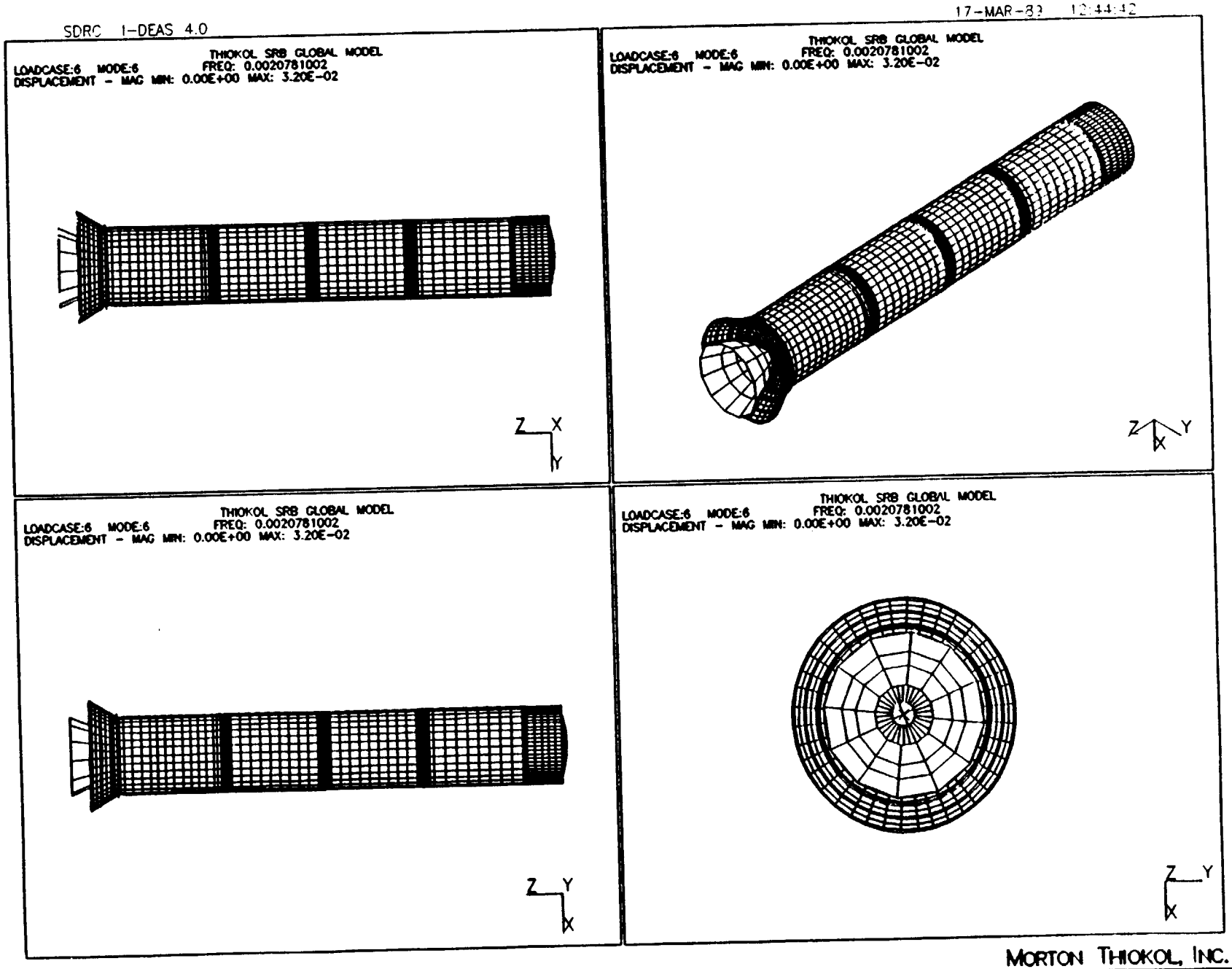

FLIGHT DISPLAY MODEL

SDRC I-DEAS 4.0 17-MAR-89 12:57:47

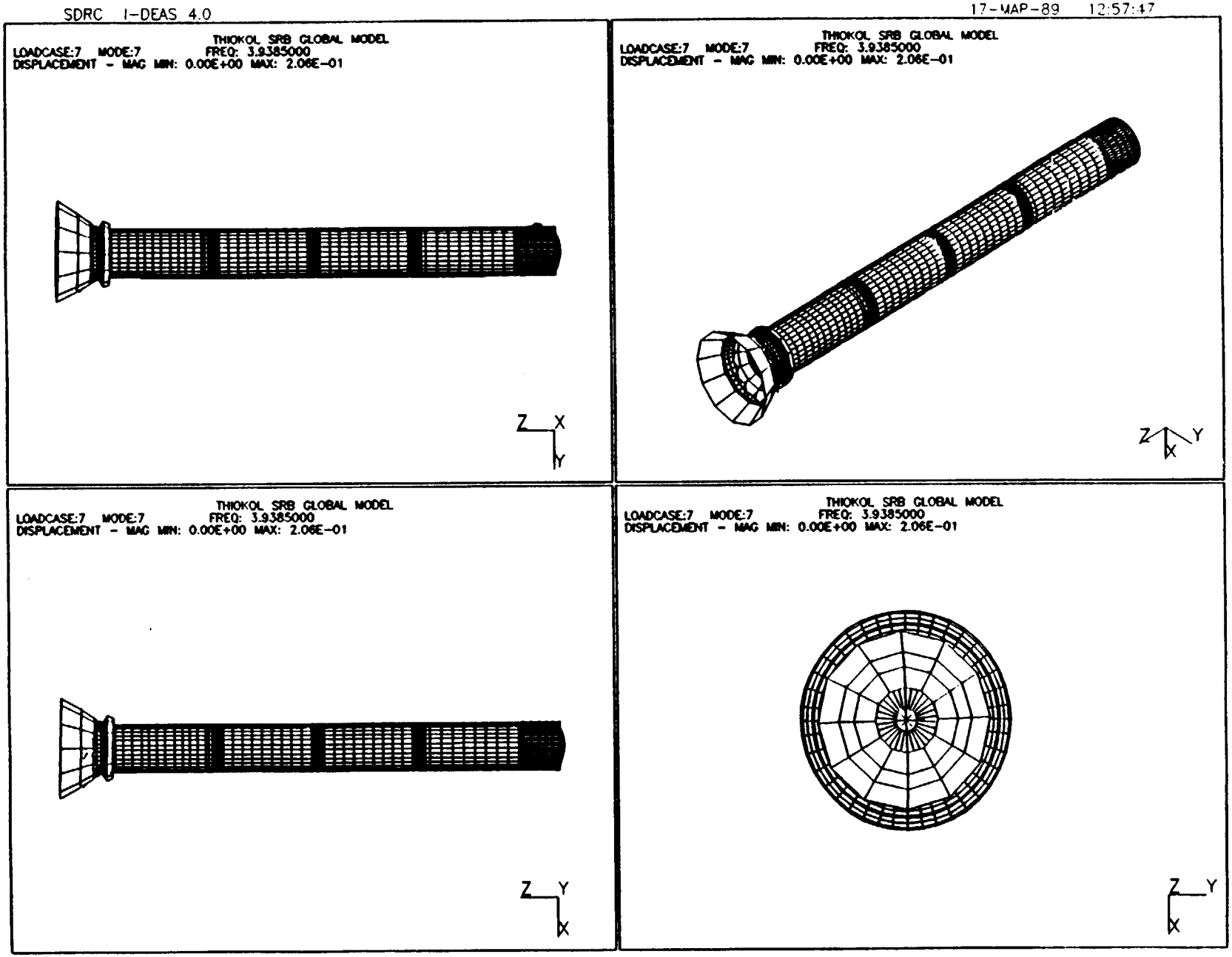

FLIGHT DISPLAY MODEL

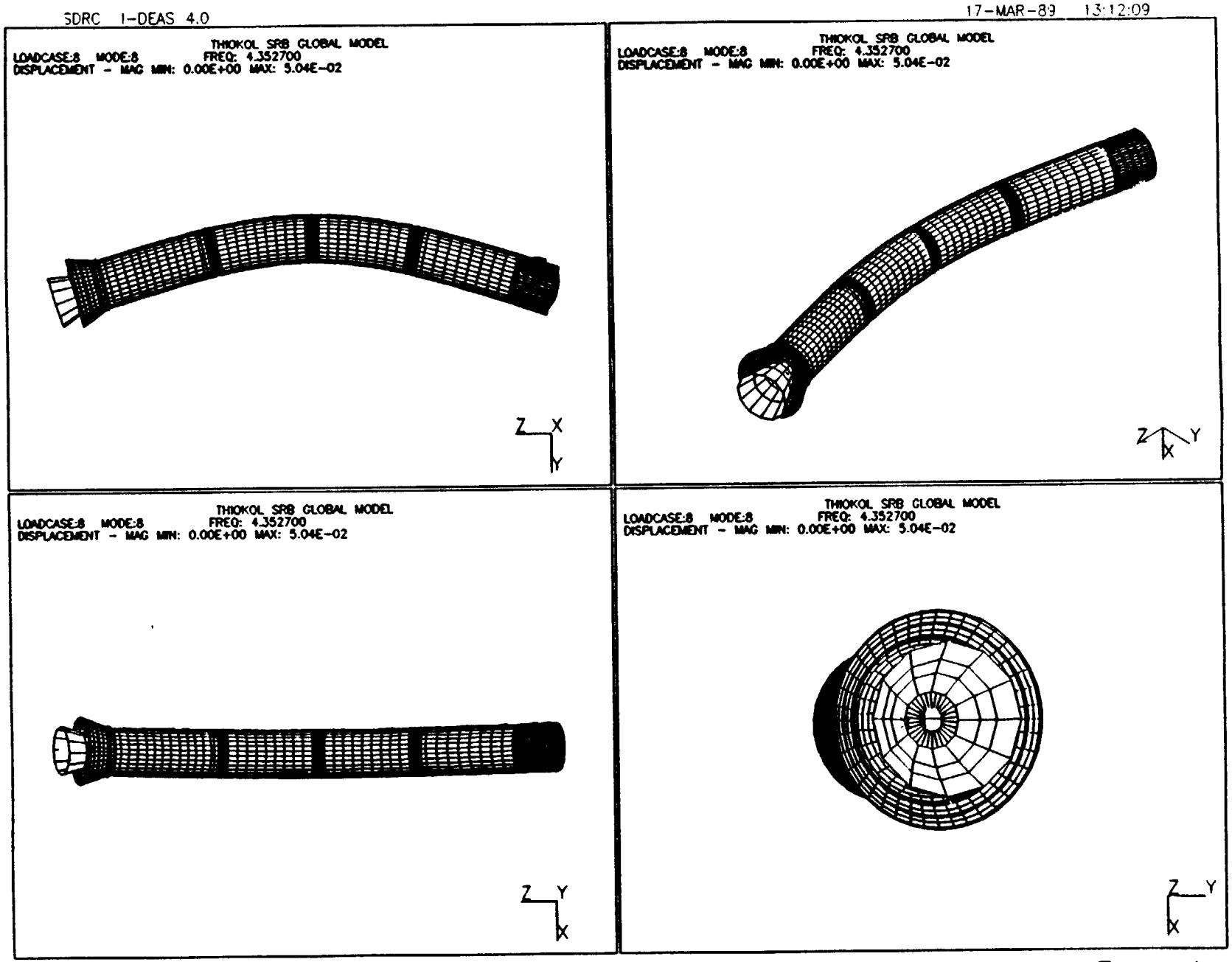

FLIGHT DISPLAY MODEL

SDRC I-DEAS 4.0 17-MAR-89 13:26:07

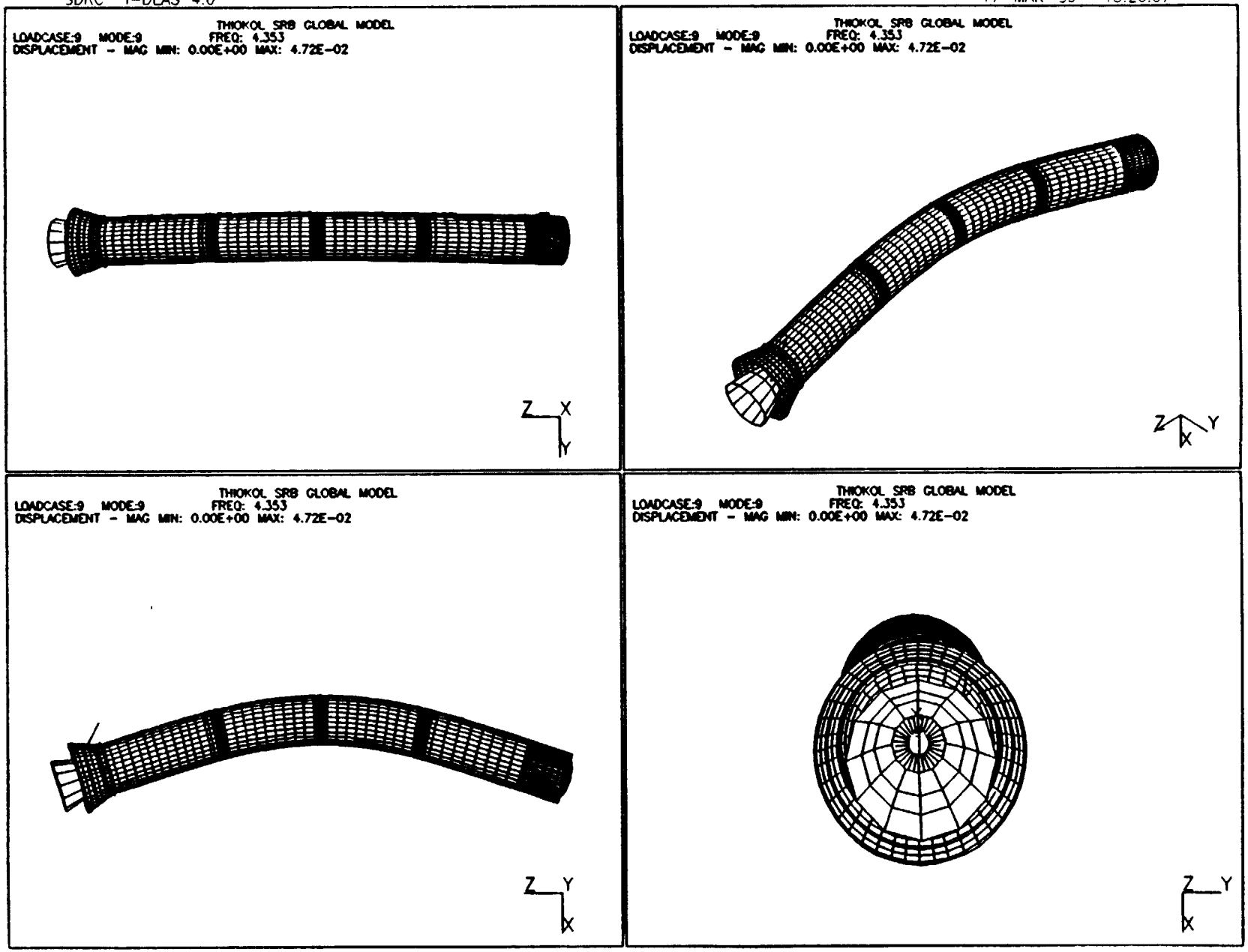

FLIGHT DISPLAY MODEL

SDRC I-DEAS 4.0 17-MAR-89 13:42:12

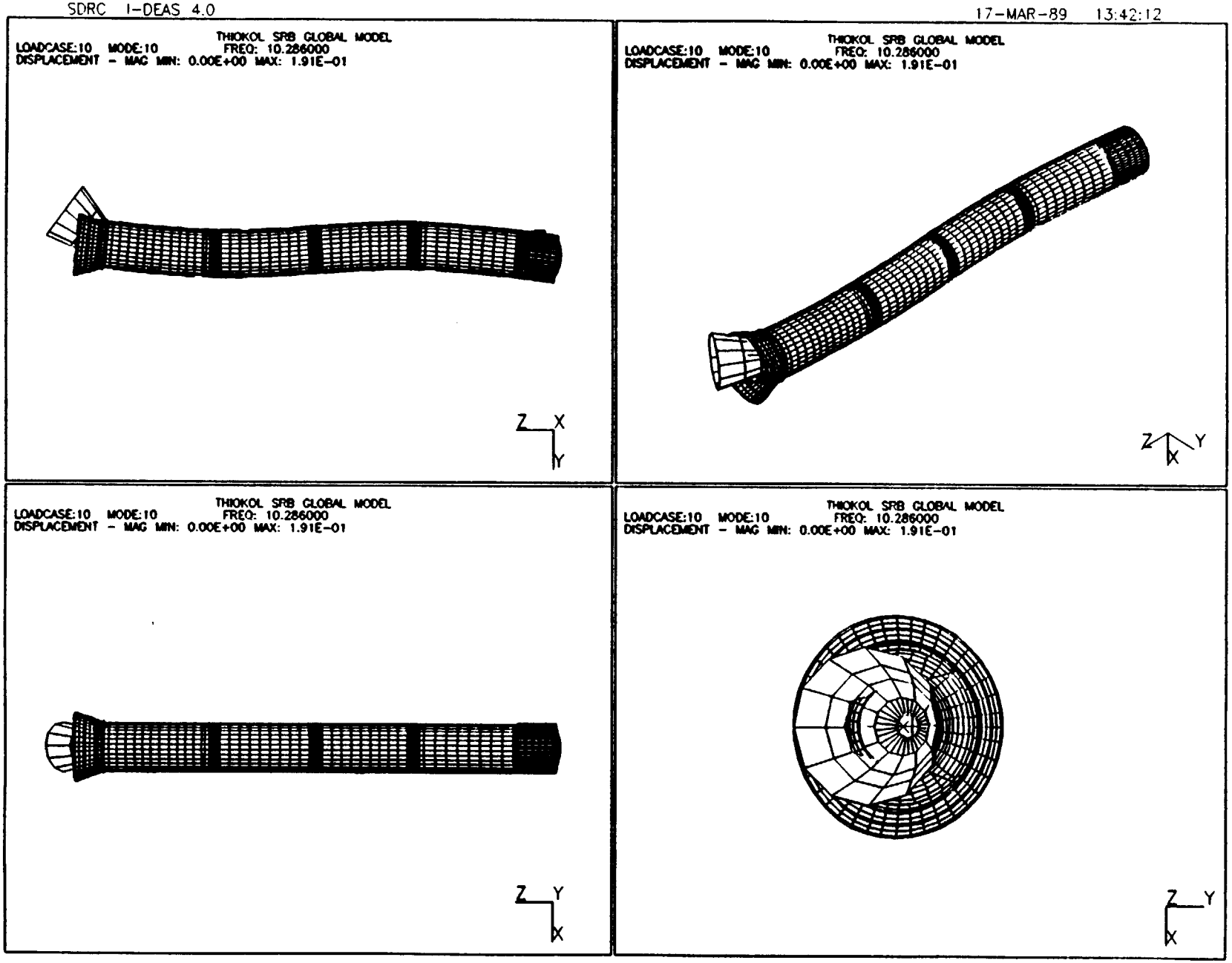

FLIGHT DISPLAY MODEL

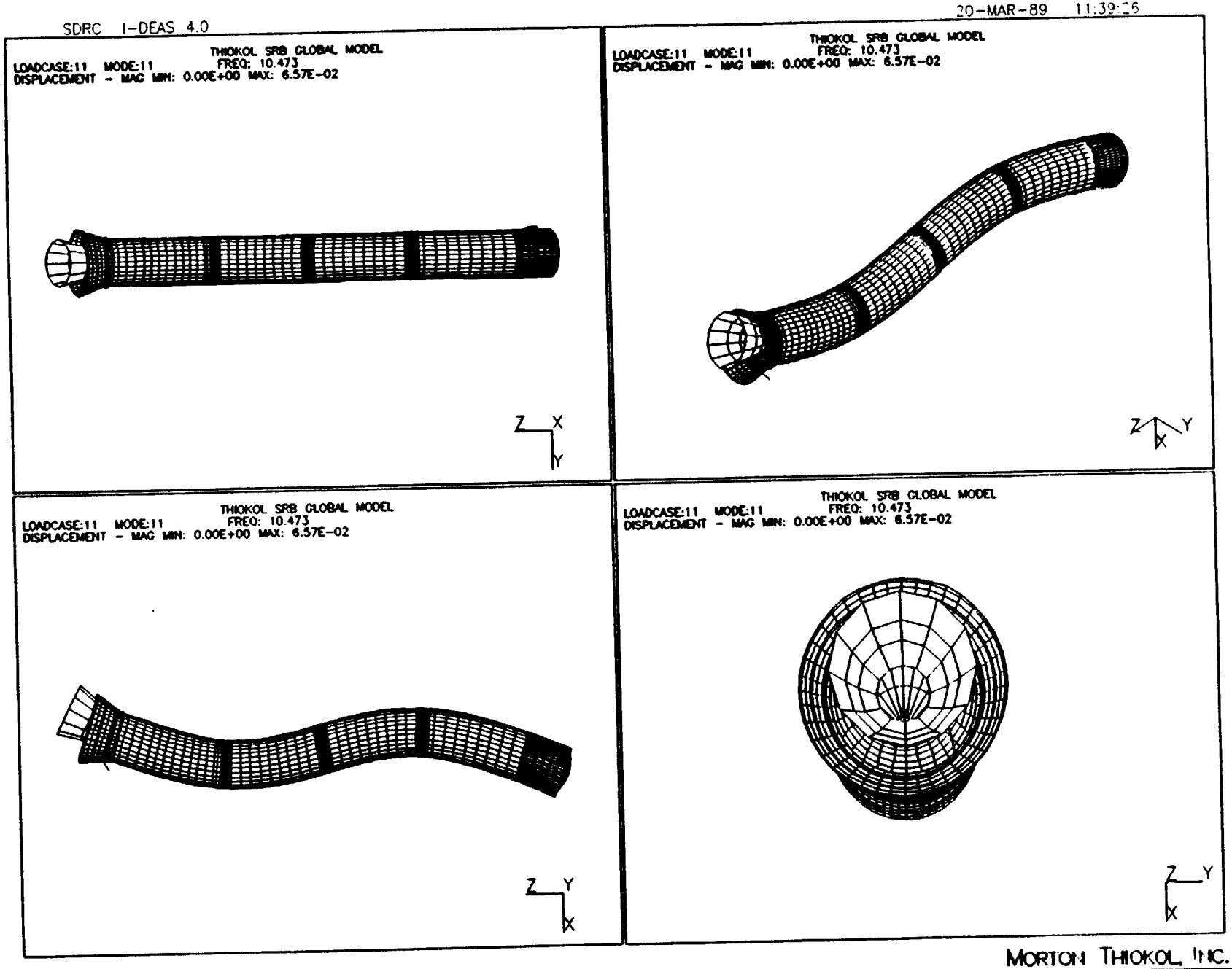

FLIGHT DISPLAY MODEL

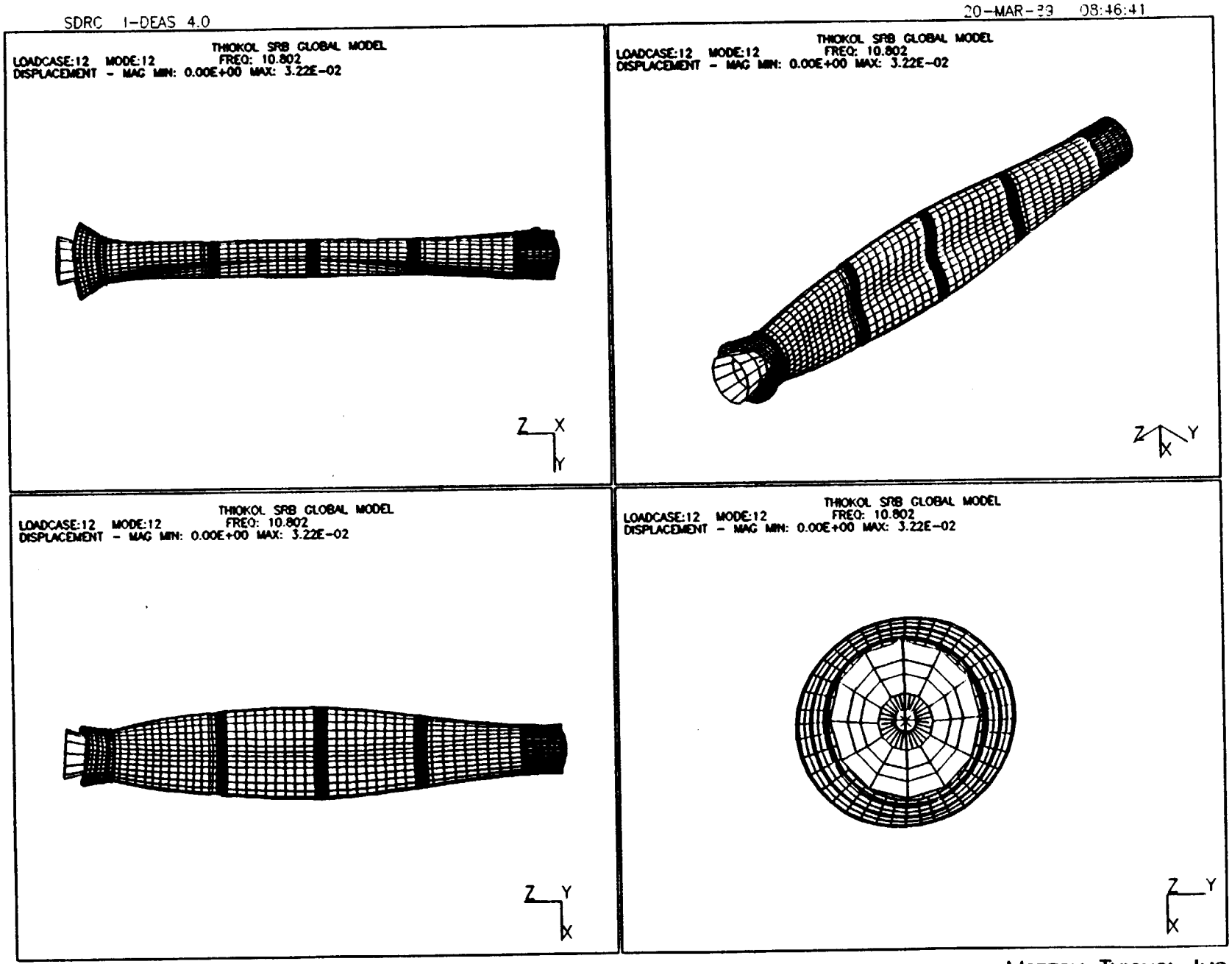

FLIGHT DISPLAY MODEL

20-MAR-89 08:56:01

SDRC I-DEAS 4.0

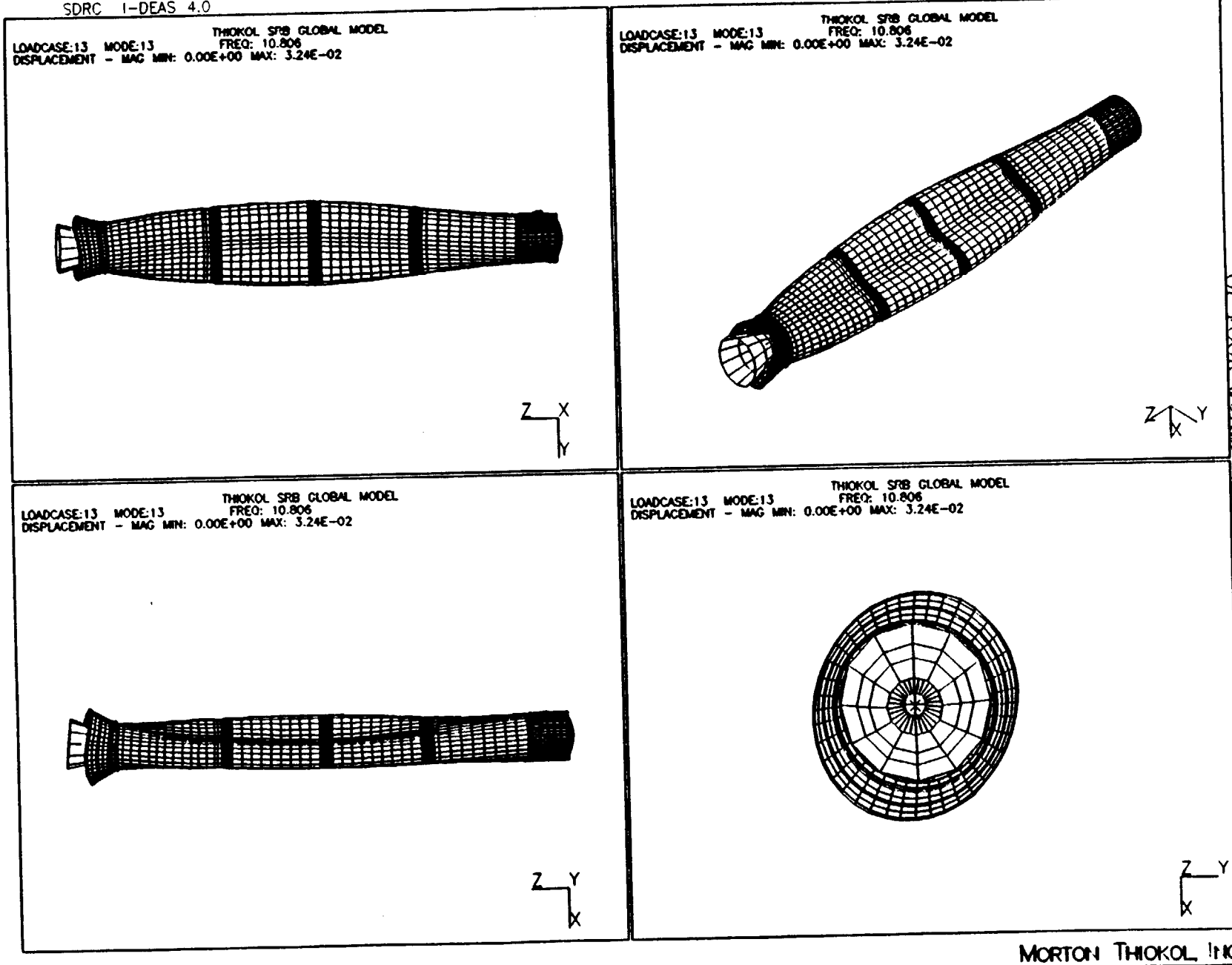

FLIGHT DISPLAY MODEL

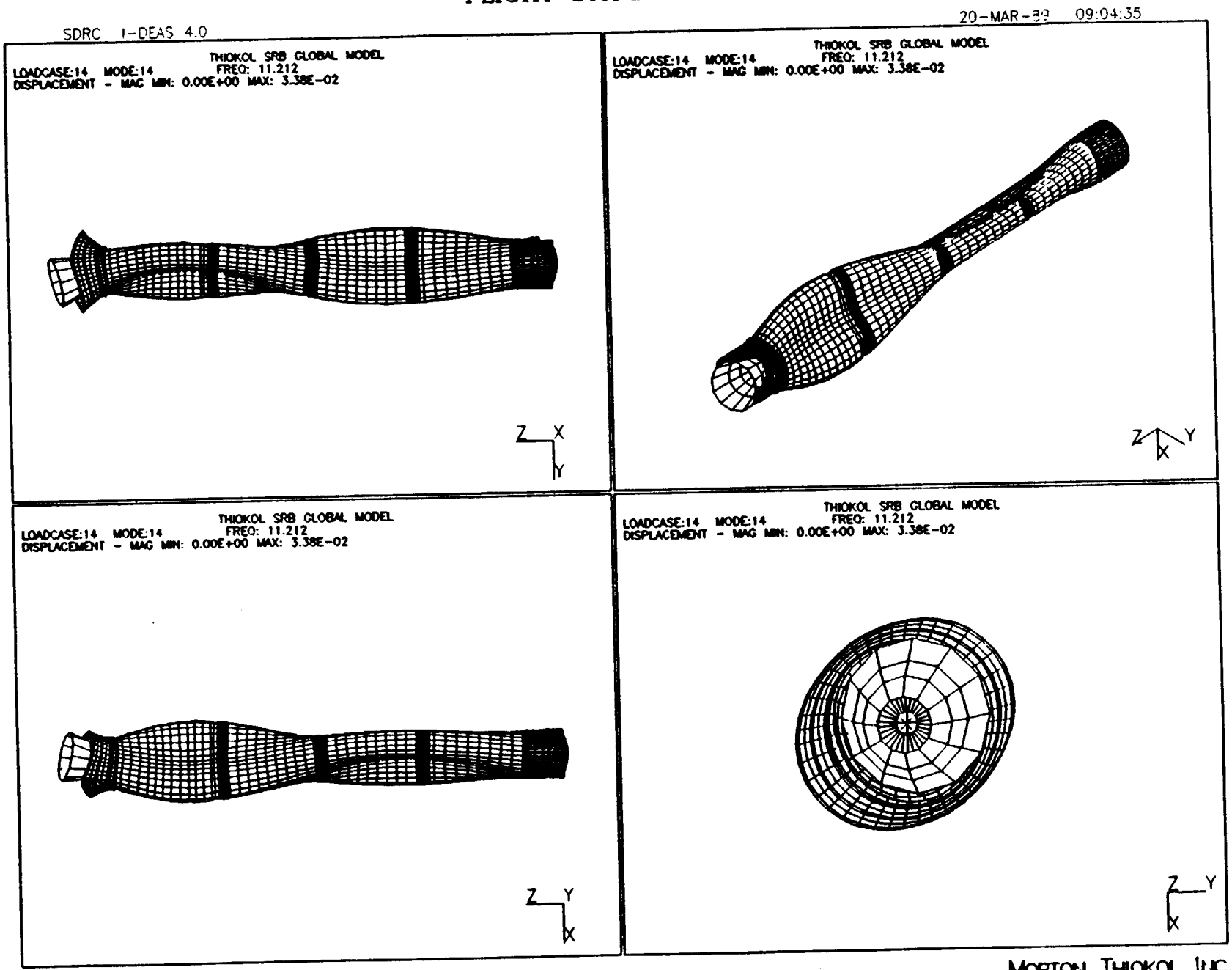

FLIGHT DISPLAY MODEL

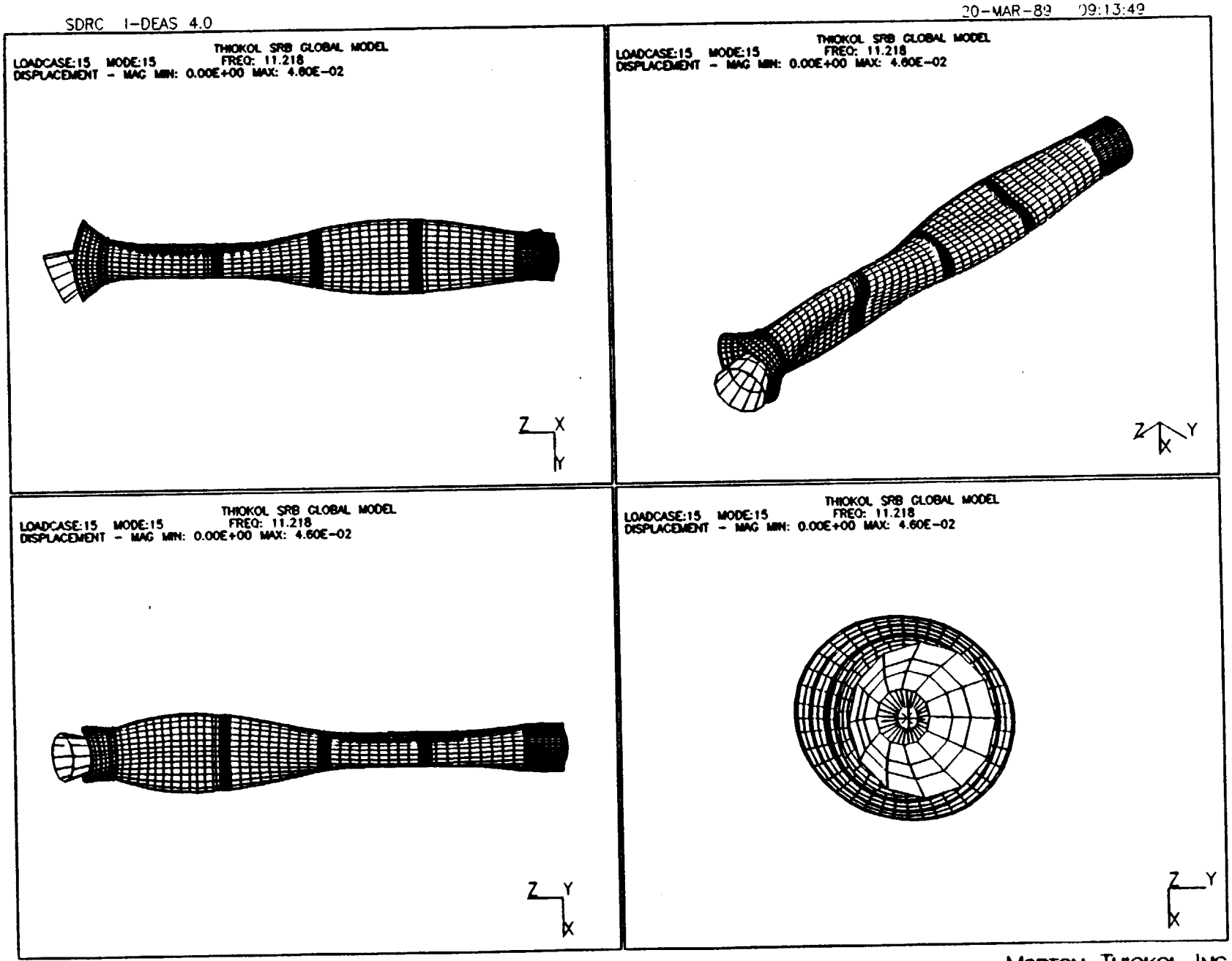

FLIGHT DISPLAY MODEL

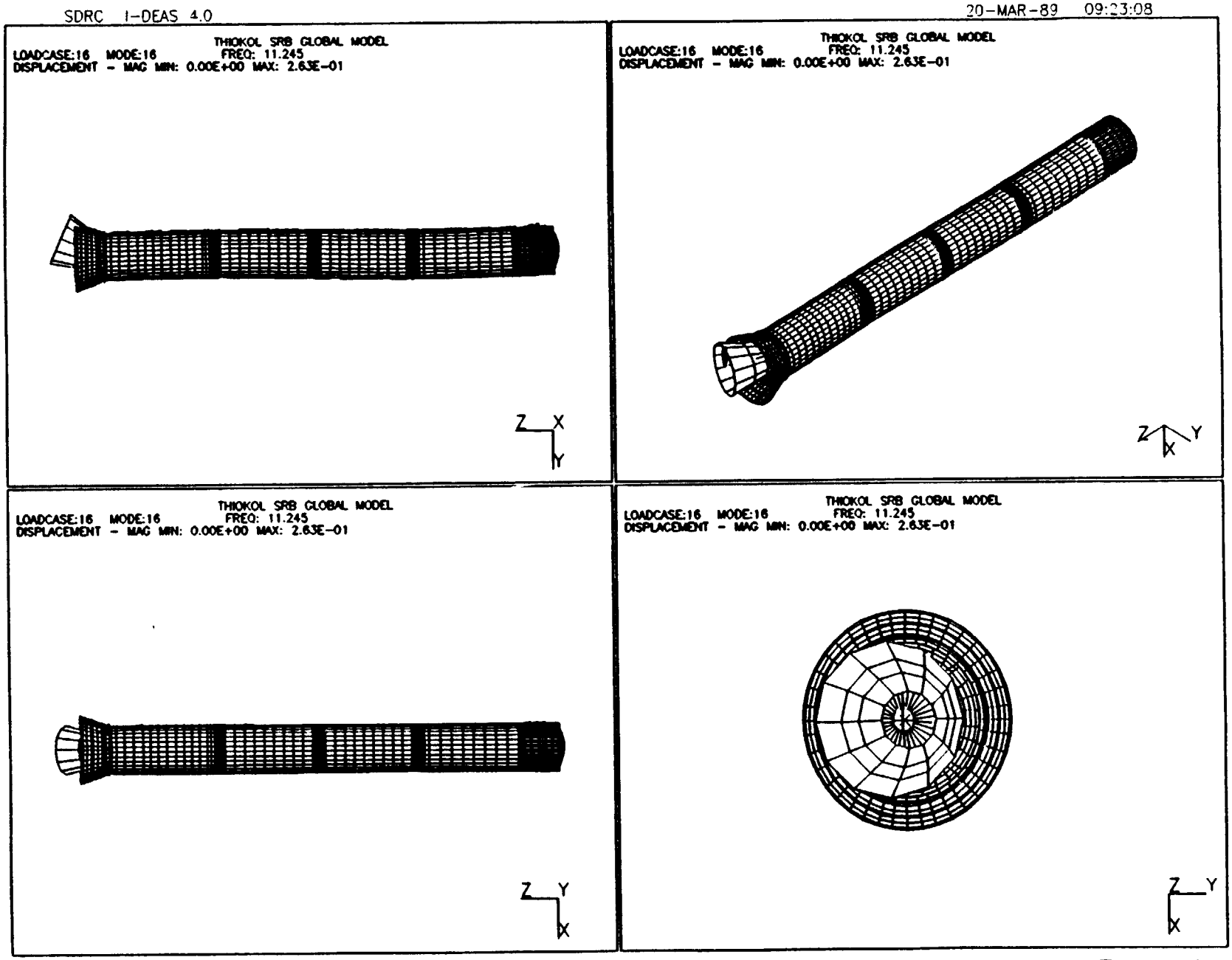

FLIGHT DISPLAY MODEL

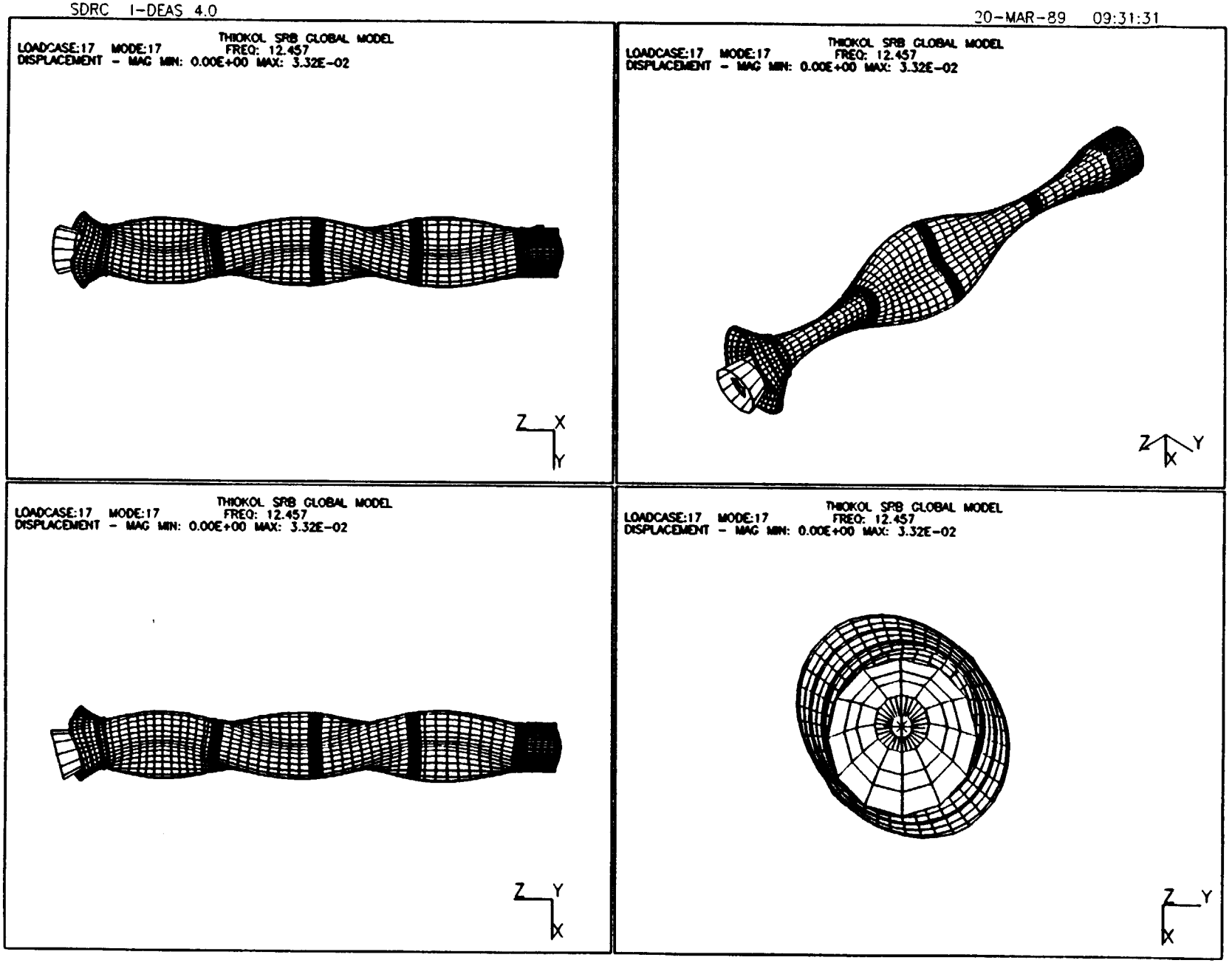

FLIGHT DISPLAY MODEL

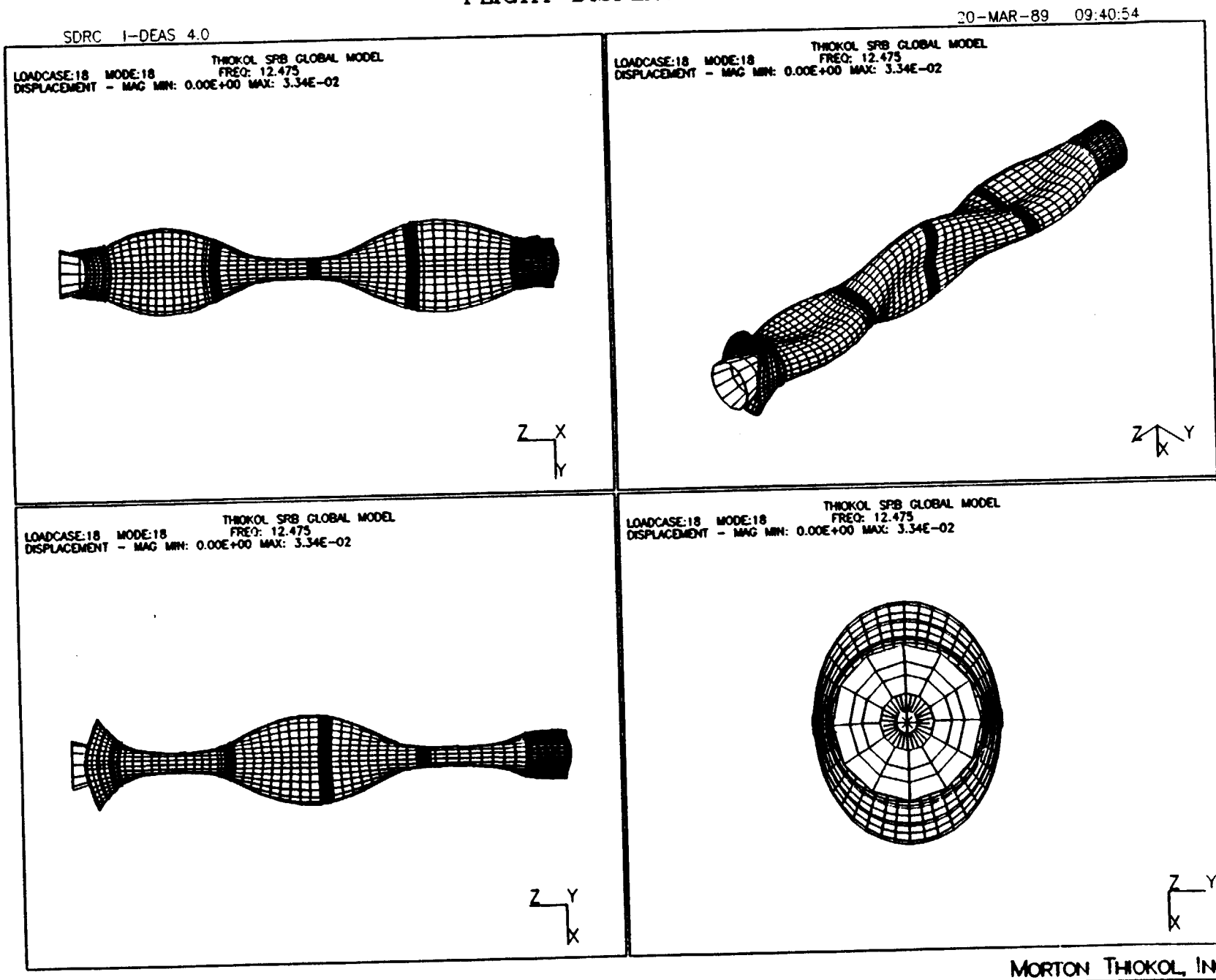

FLIGHT DISPLAY MODEL

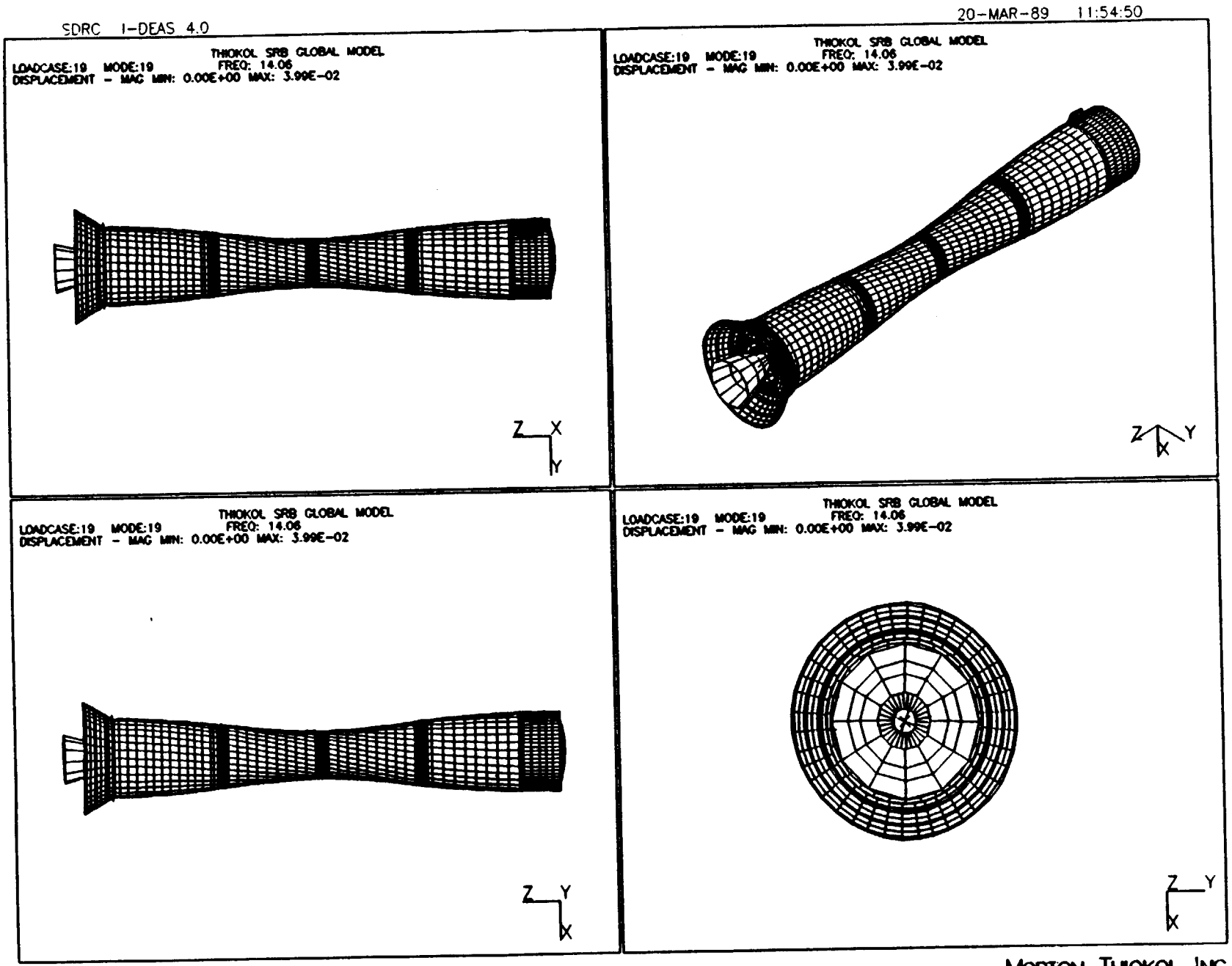

FLIGHT DISPLAY MODEL

SDRC I-DEAS 4.0 20-MAR-89 10:01:52

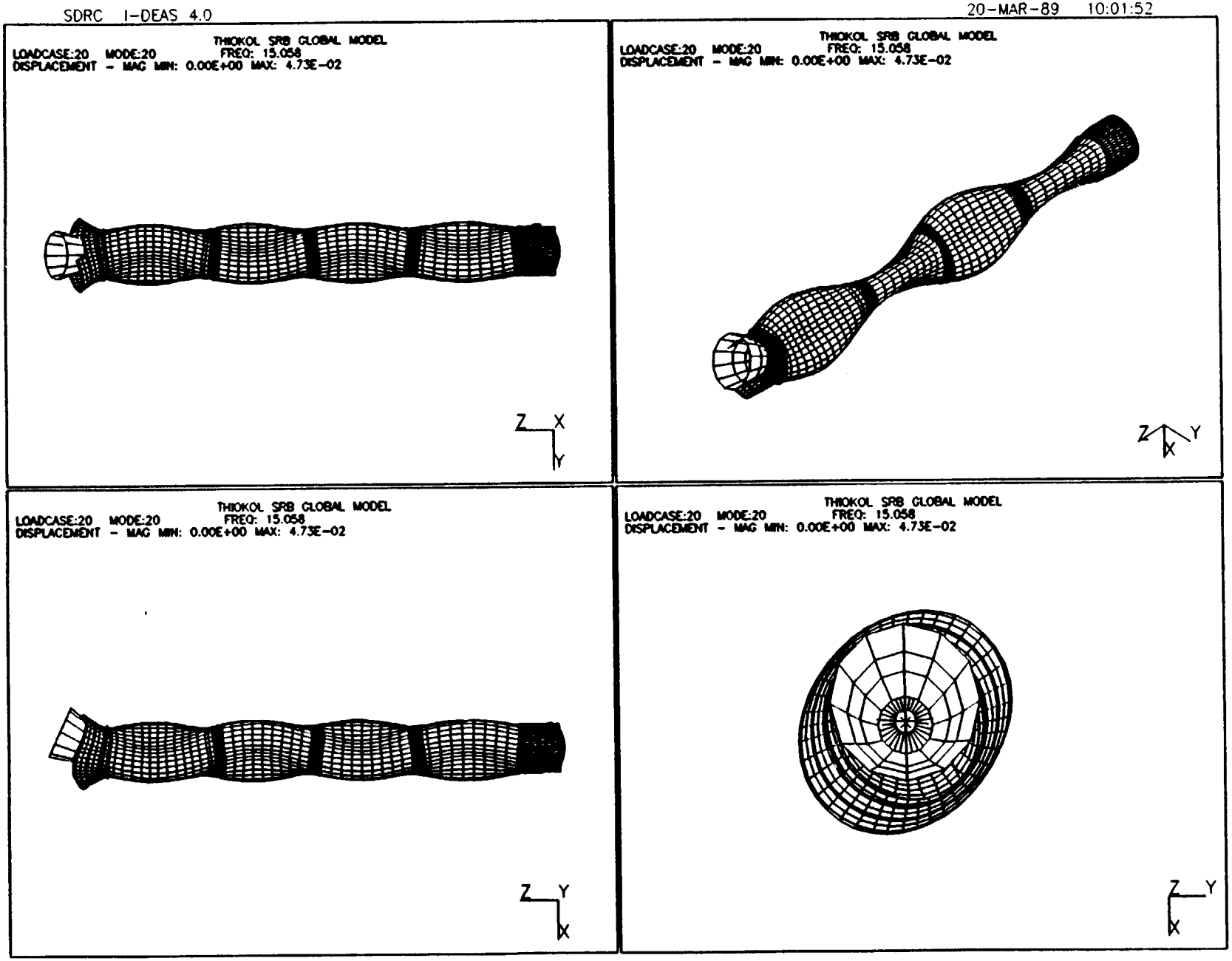

FLIGHT DISPLAY MODEL

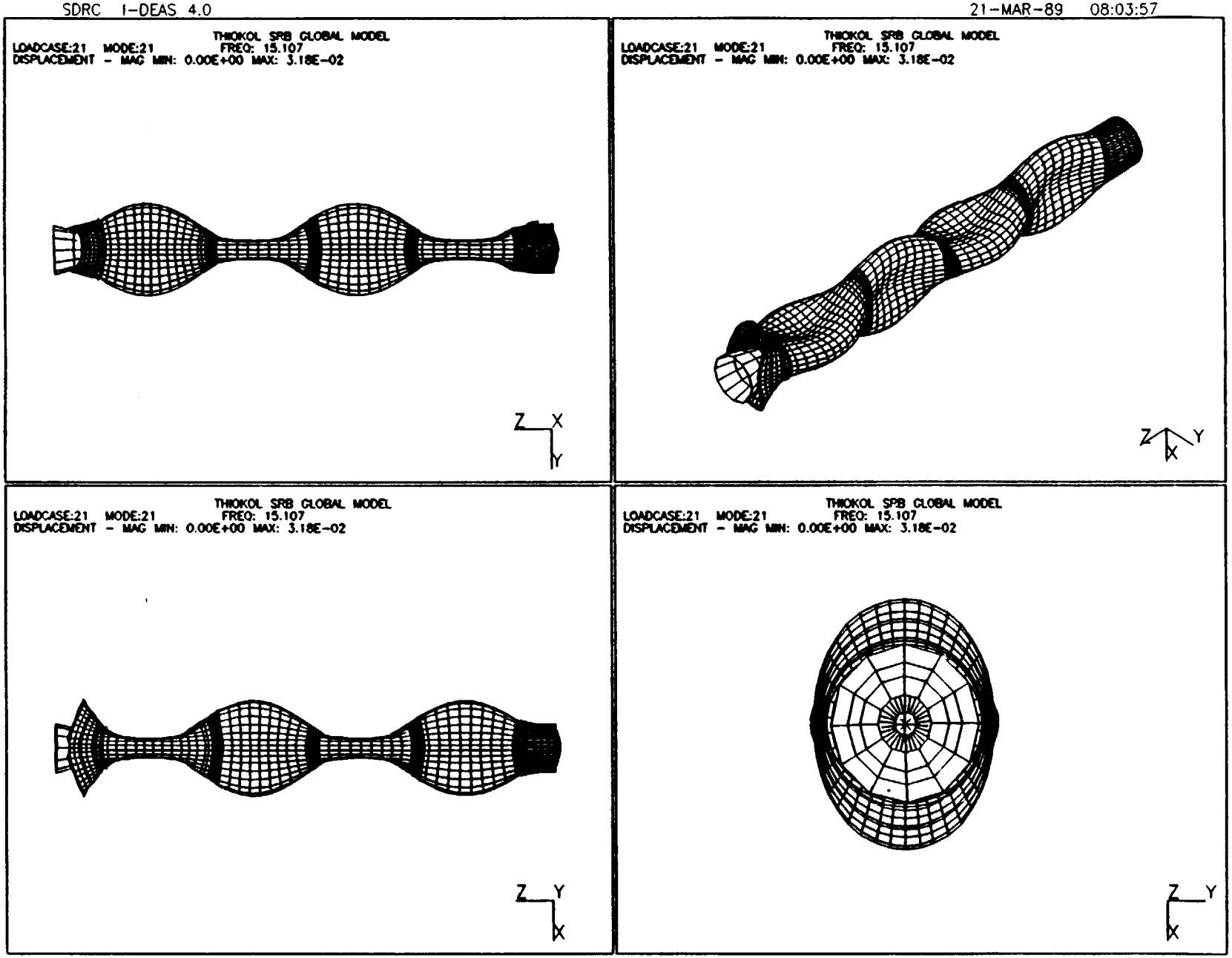

FLIGHT DISPLAY MODEL

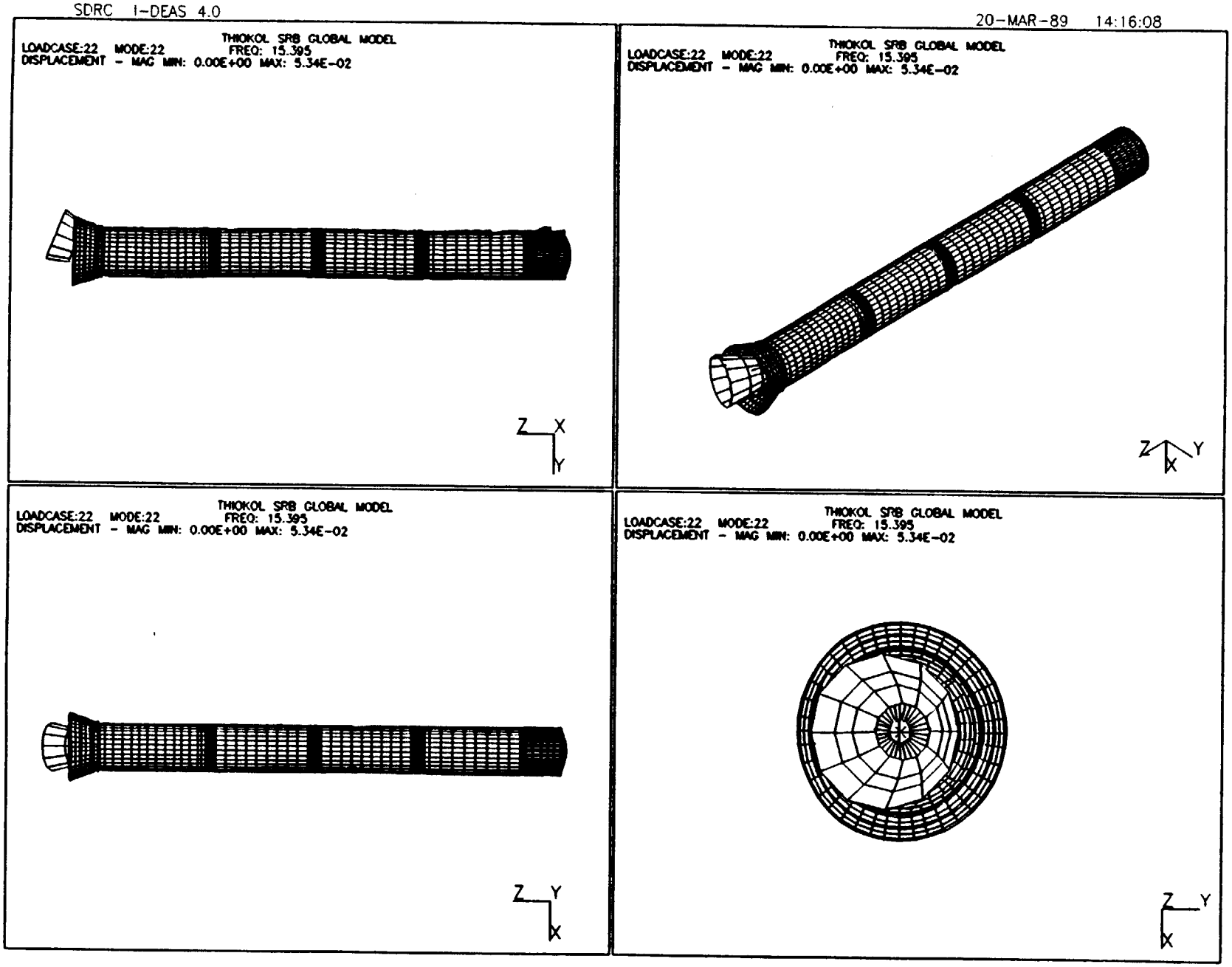

FLIGHT DISPLAY MODEL

SDRC I-DEAS 4.0 20-MAR-89 14:35:09

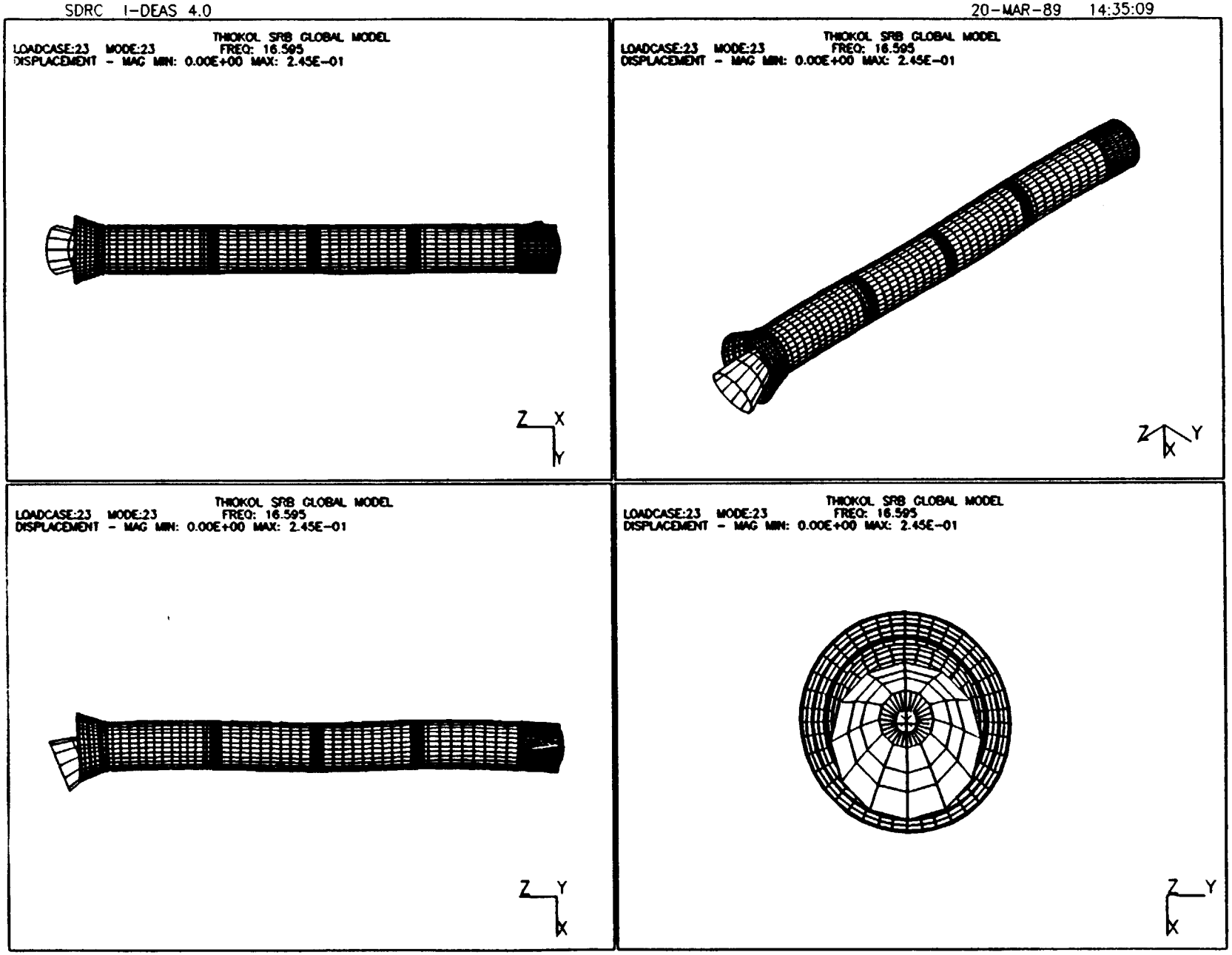

FLIGHT DISPLAY MODEL

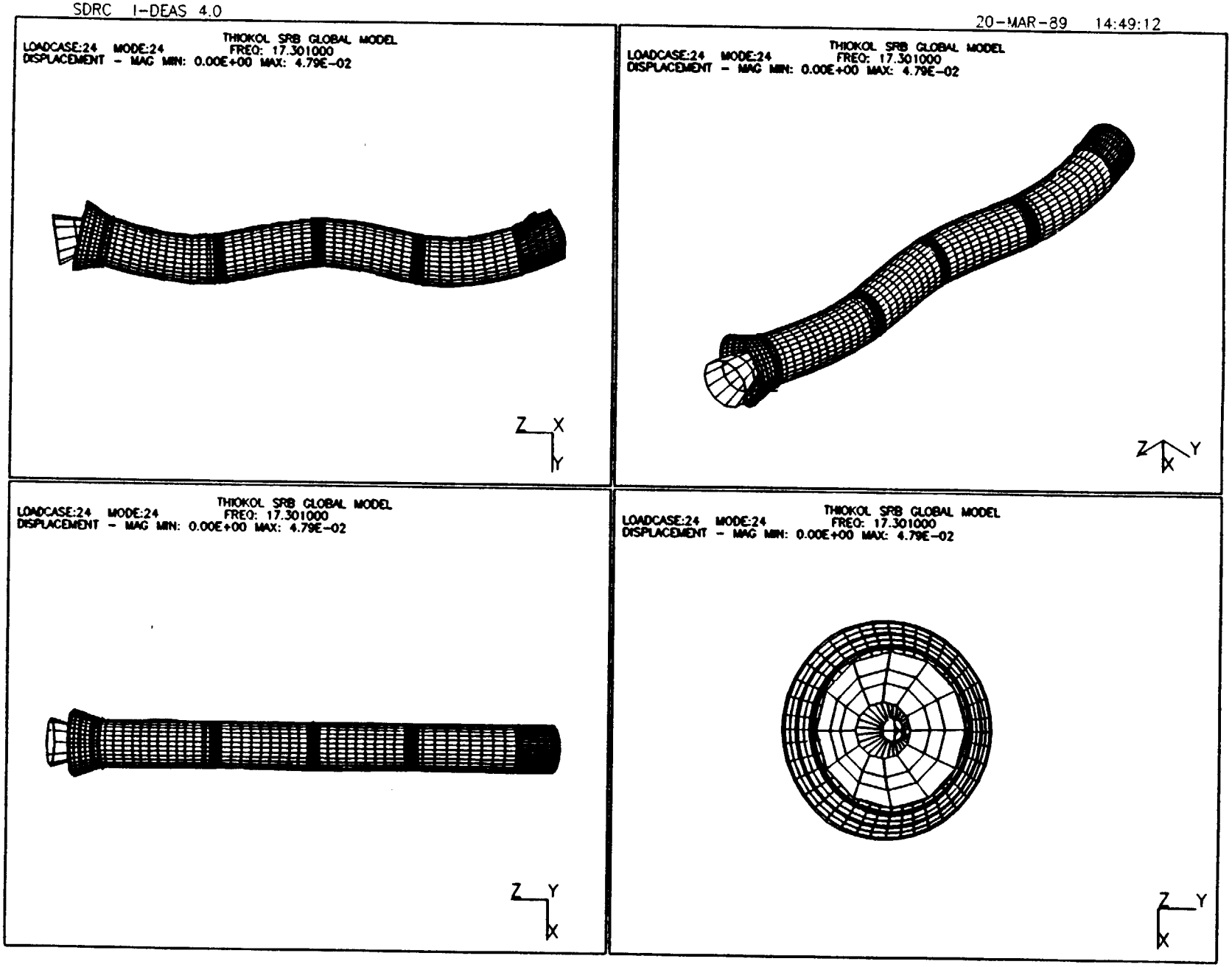

FLIGHT DISPLAY MODEL

SDRC I-DEAS 4.0 20-MAR-89 15:01:44

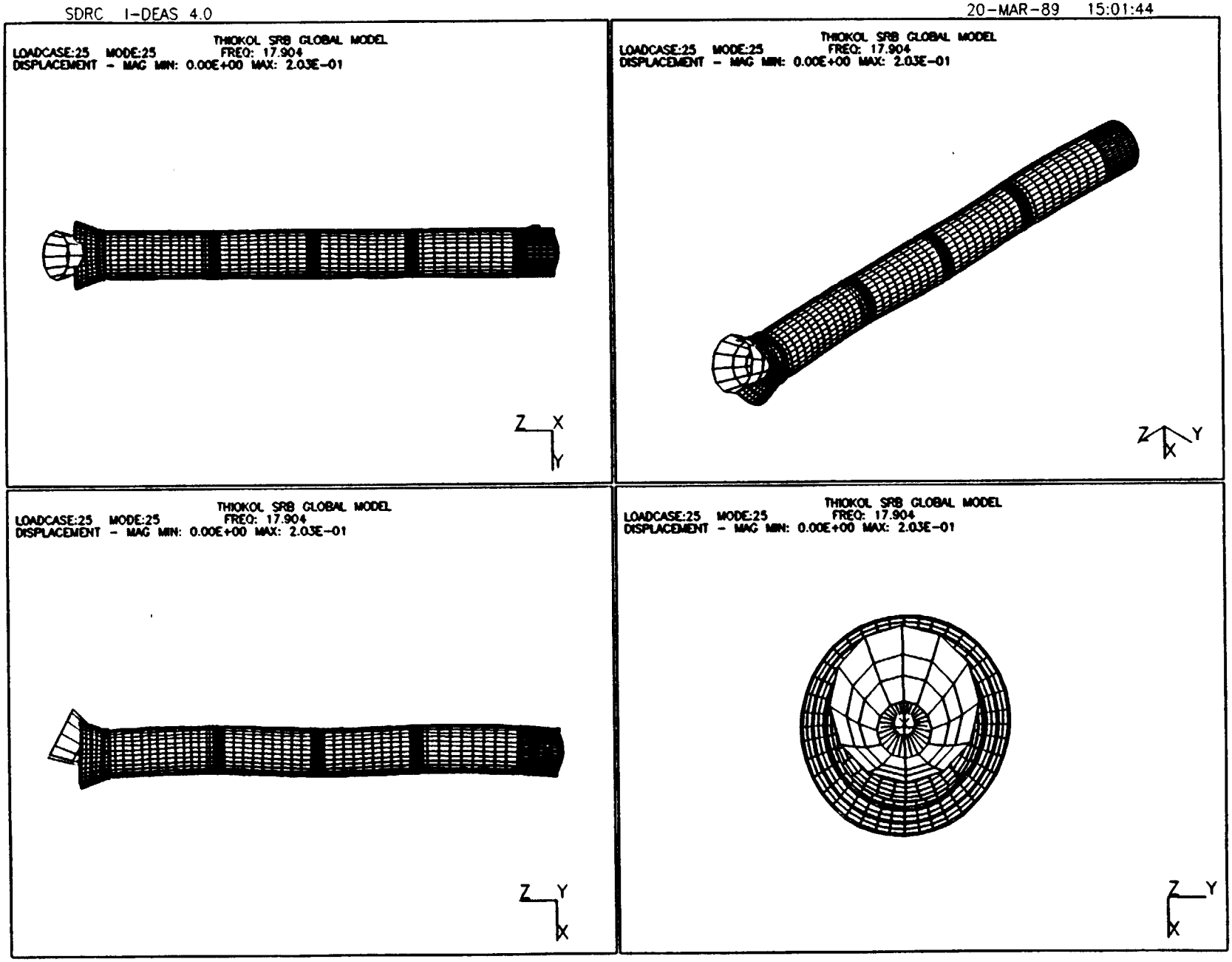

FLIGHT DISPLAY MODEL

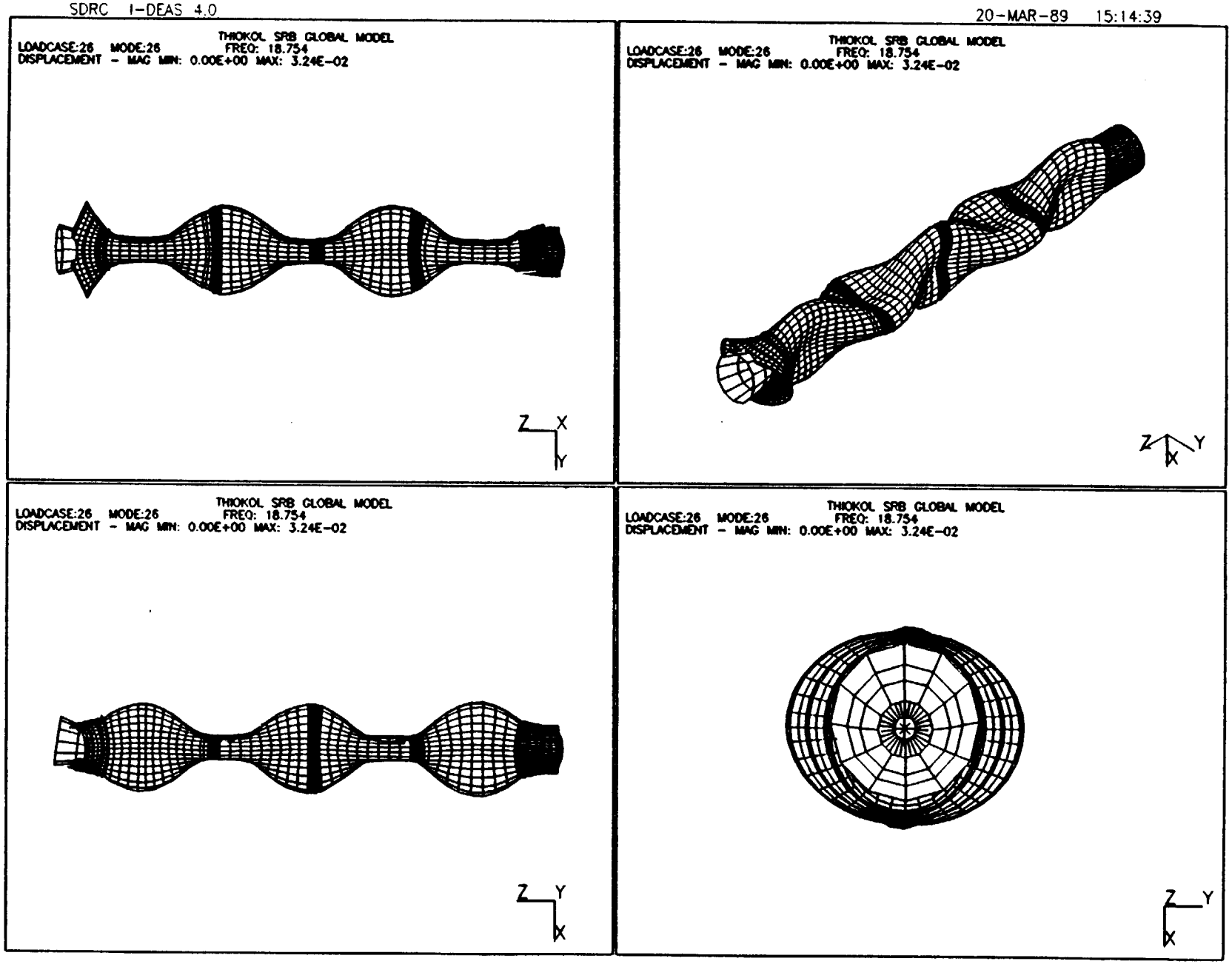

FLIGHT DISPLAY MODEL

SDRC I-DEAS 4.0 20-MAR-89 15:25:14

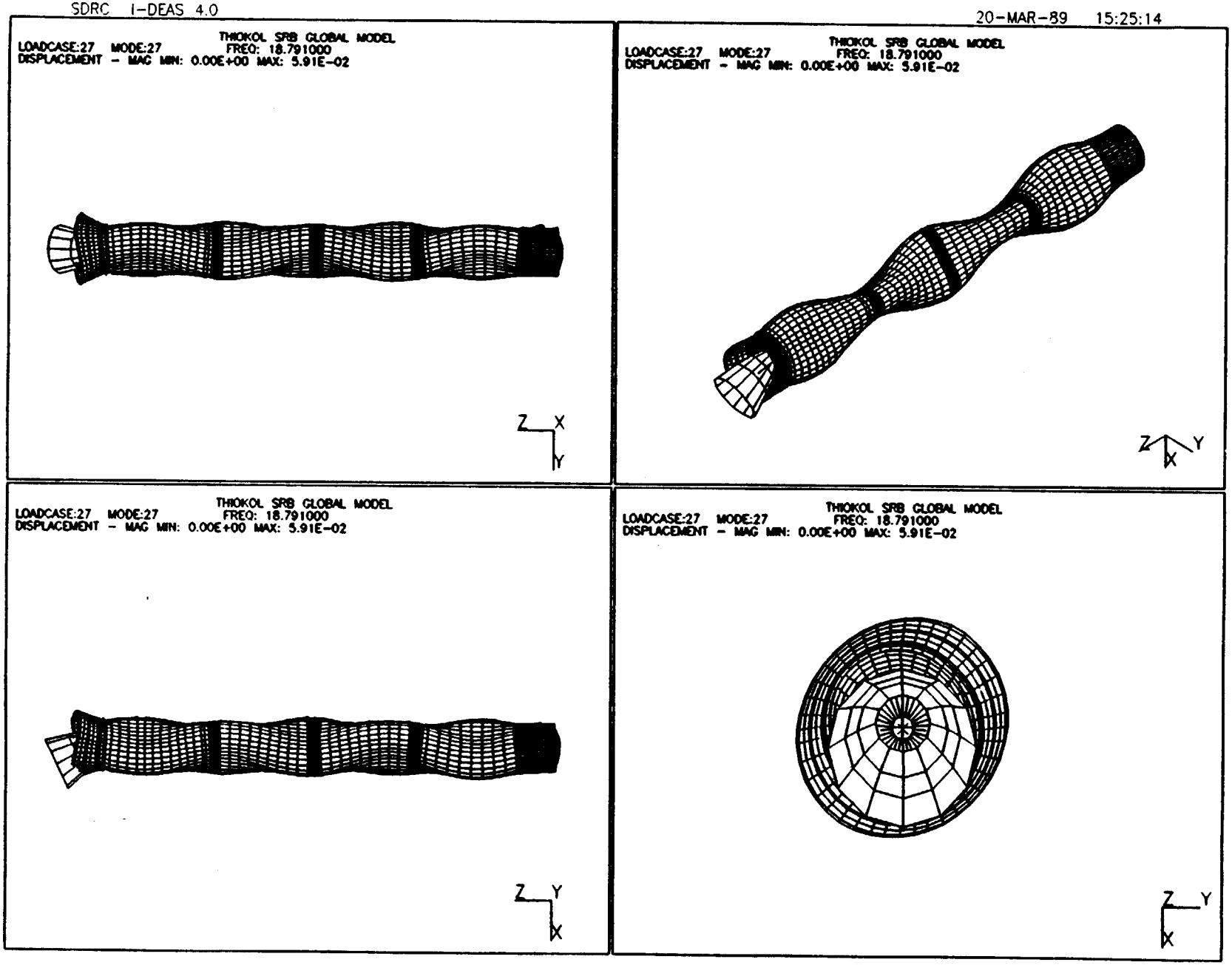

FLIGHT DISPLAY MODEL

SDRC I-DEAS 4.0 20-MAR-89 15:37:29

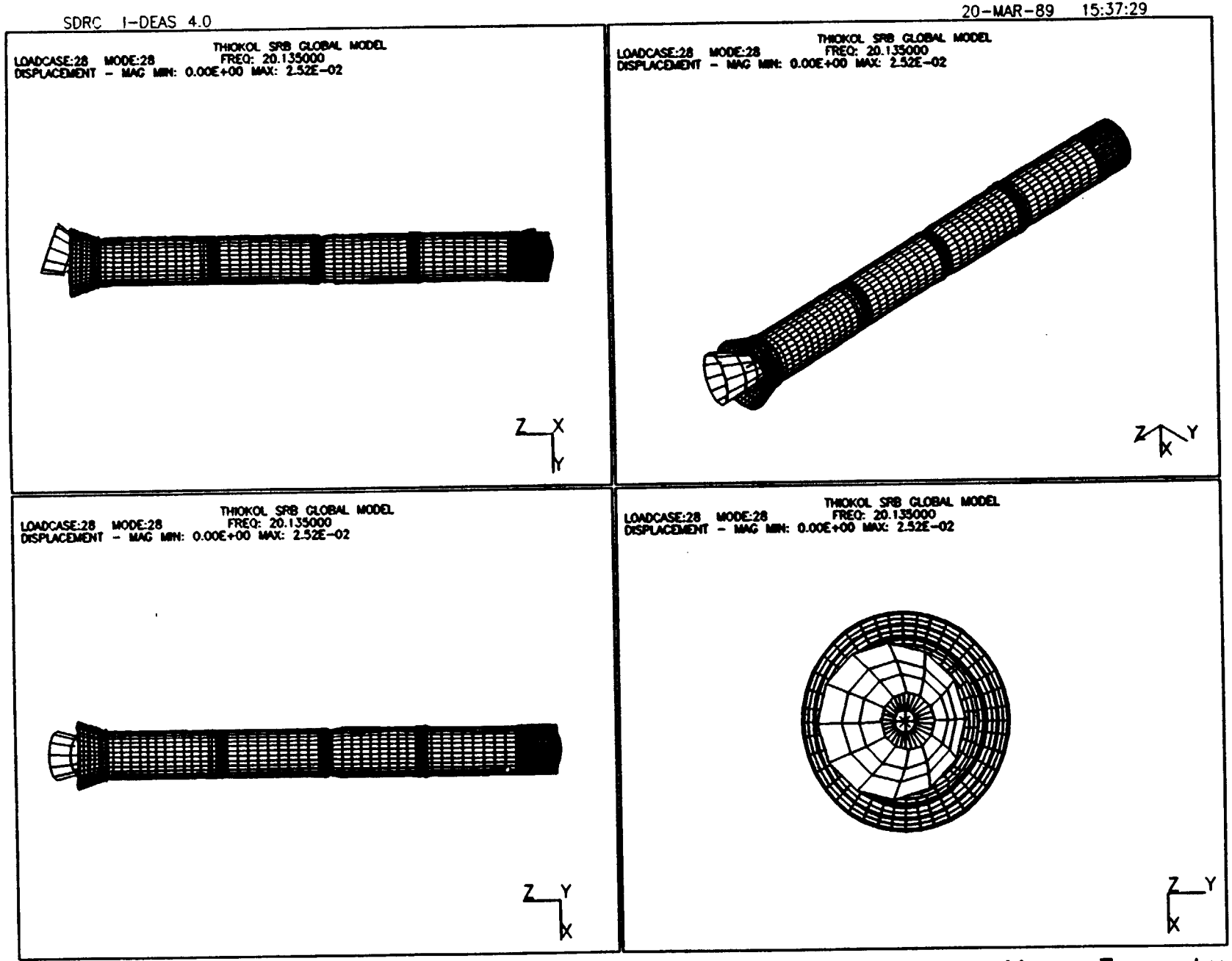

APPENDIX B

Reconstructed Liftoff Transient Loads

comparison of pressure profile

predicted by mti ballistics

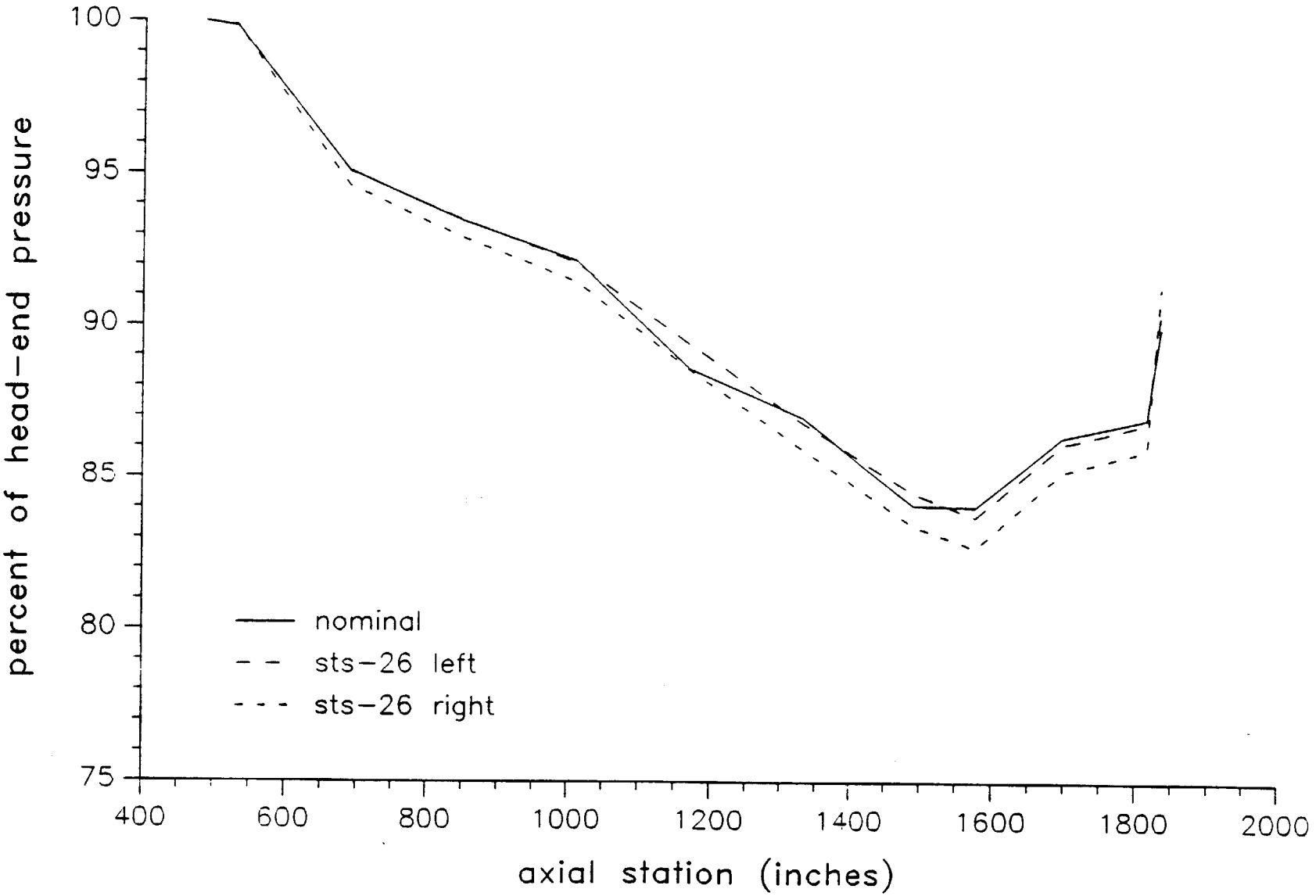

STS-26 RECONSTRUCTED HEAD-END PRESSURE

LEFT RSRM

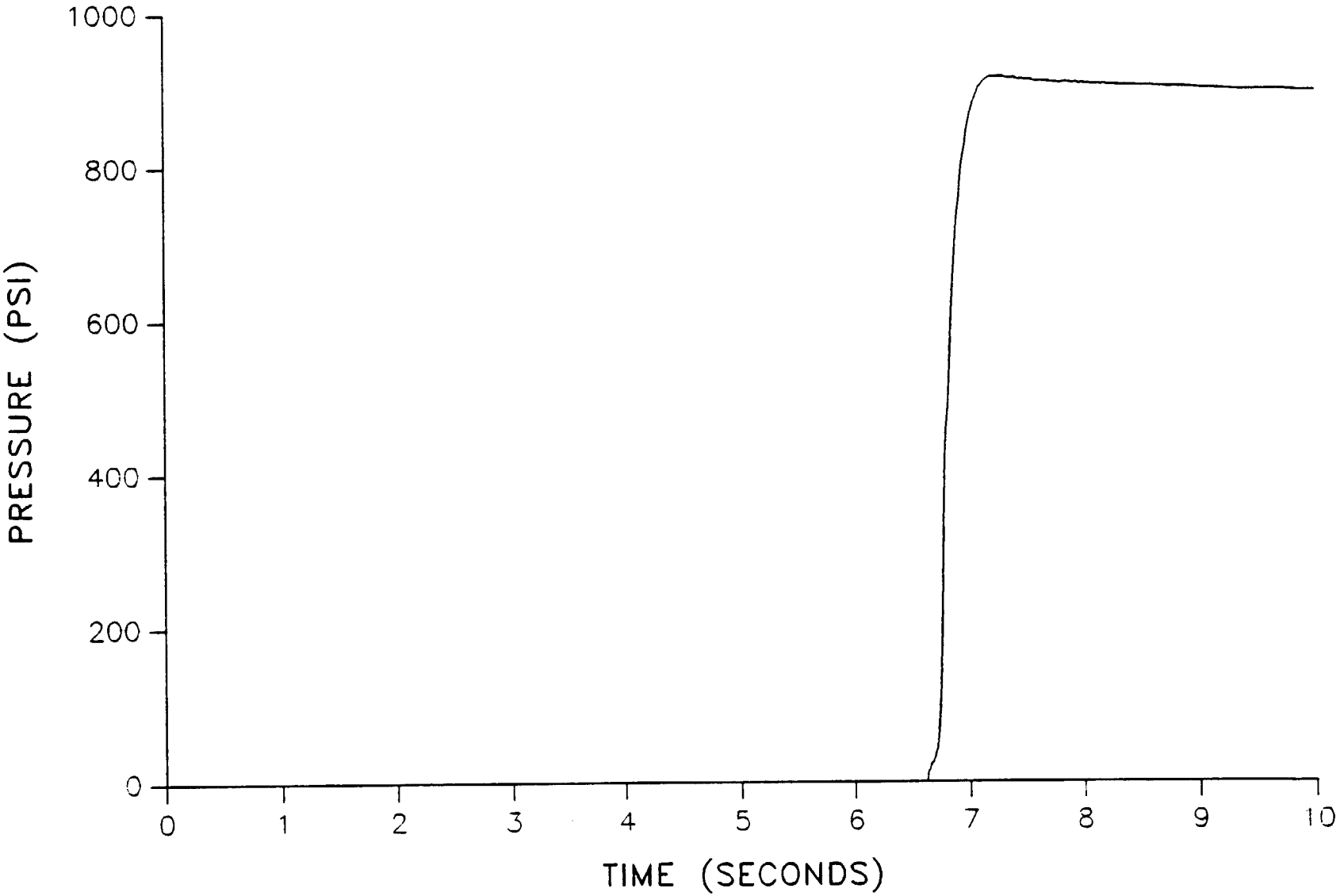

STS-26 RECONSTRUCTED FWD ATTACH LOADS

LEFT RSRM

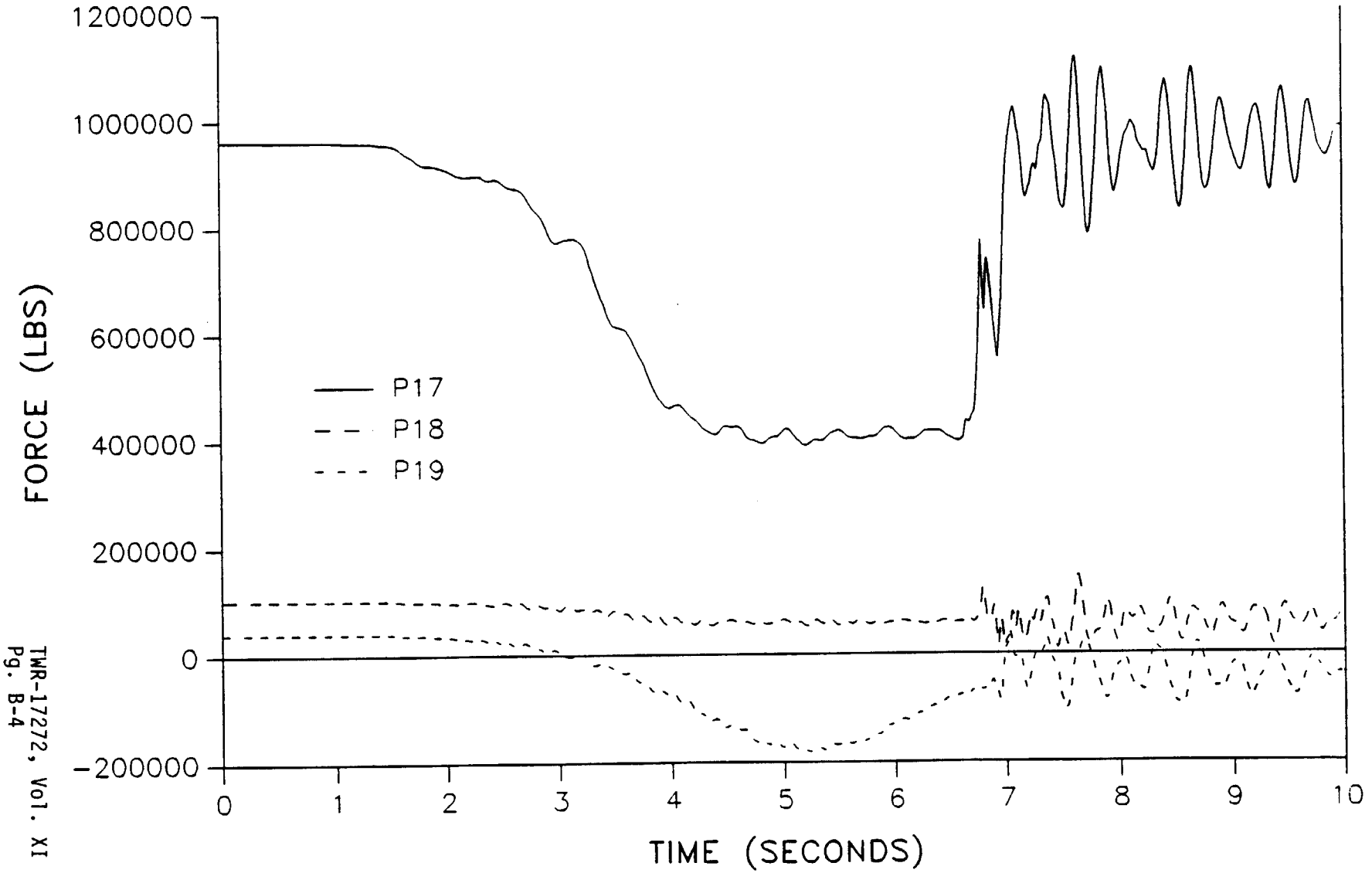

STS-26 RECONSTRUCTED ET ATTACH LOADS

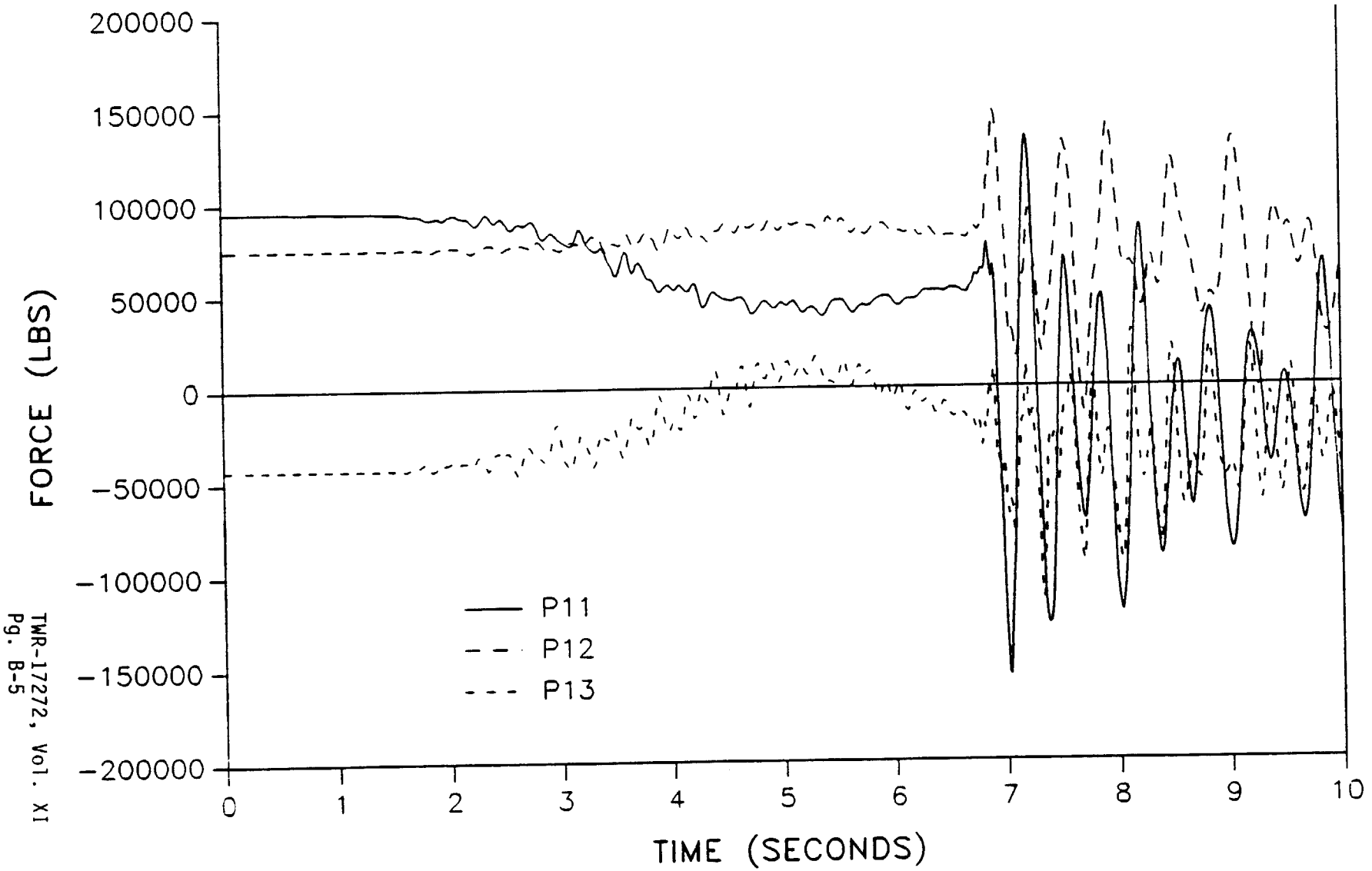

STS-26 RECONSTRUCTED TIE-DOWN BOLT LOADS

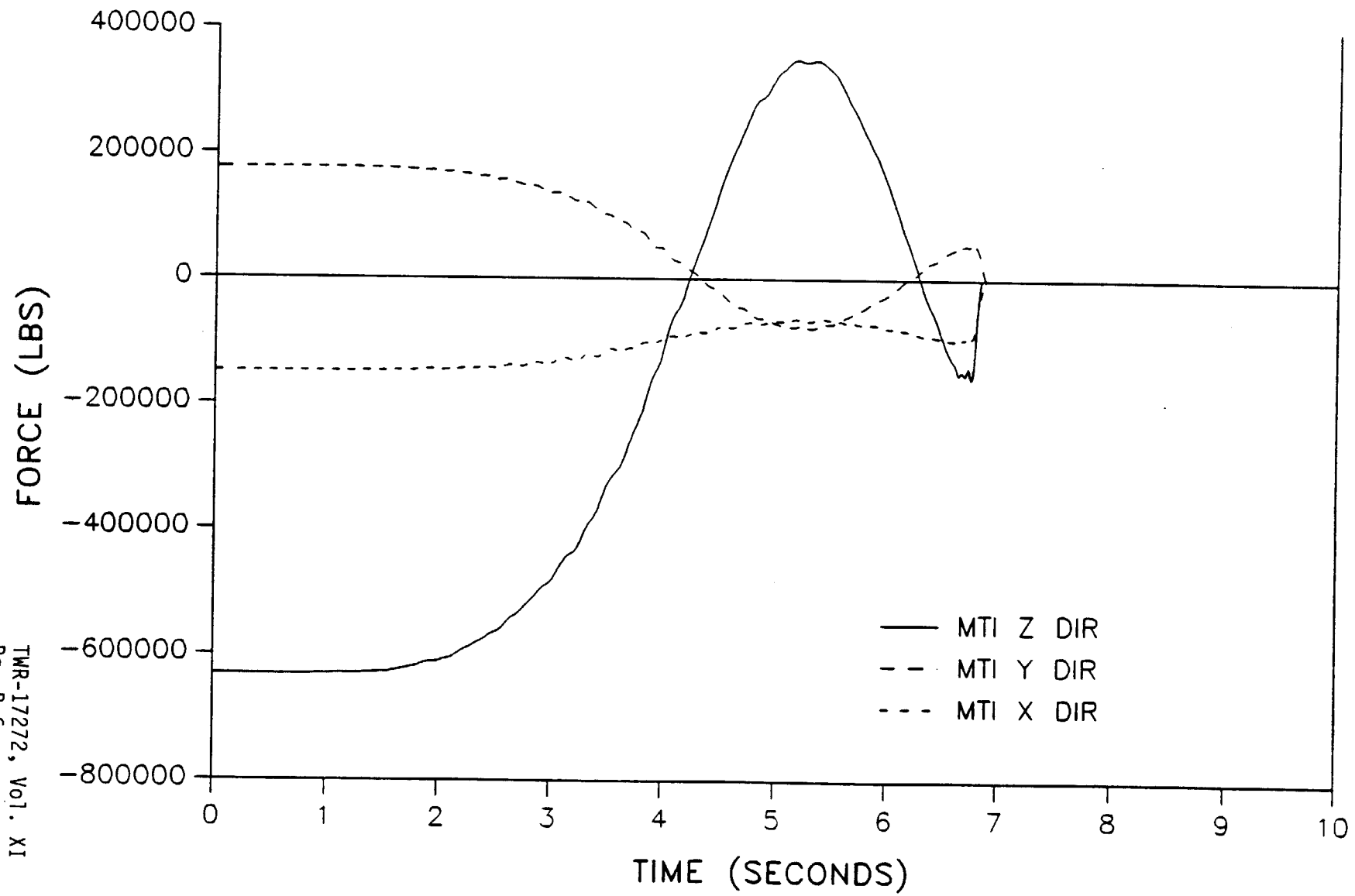

STS-26 RECONSTRUCTED TIE-DOWN BOLT LOADS

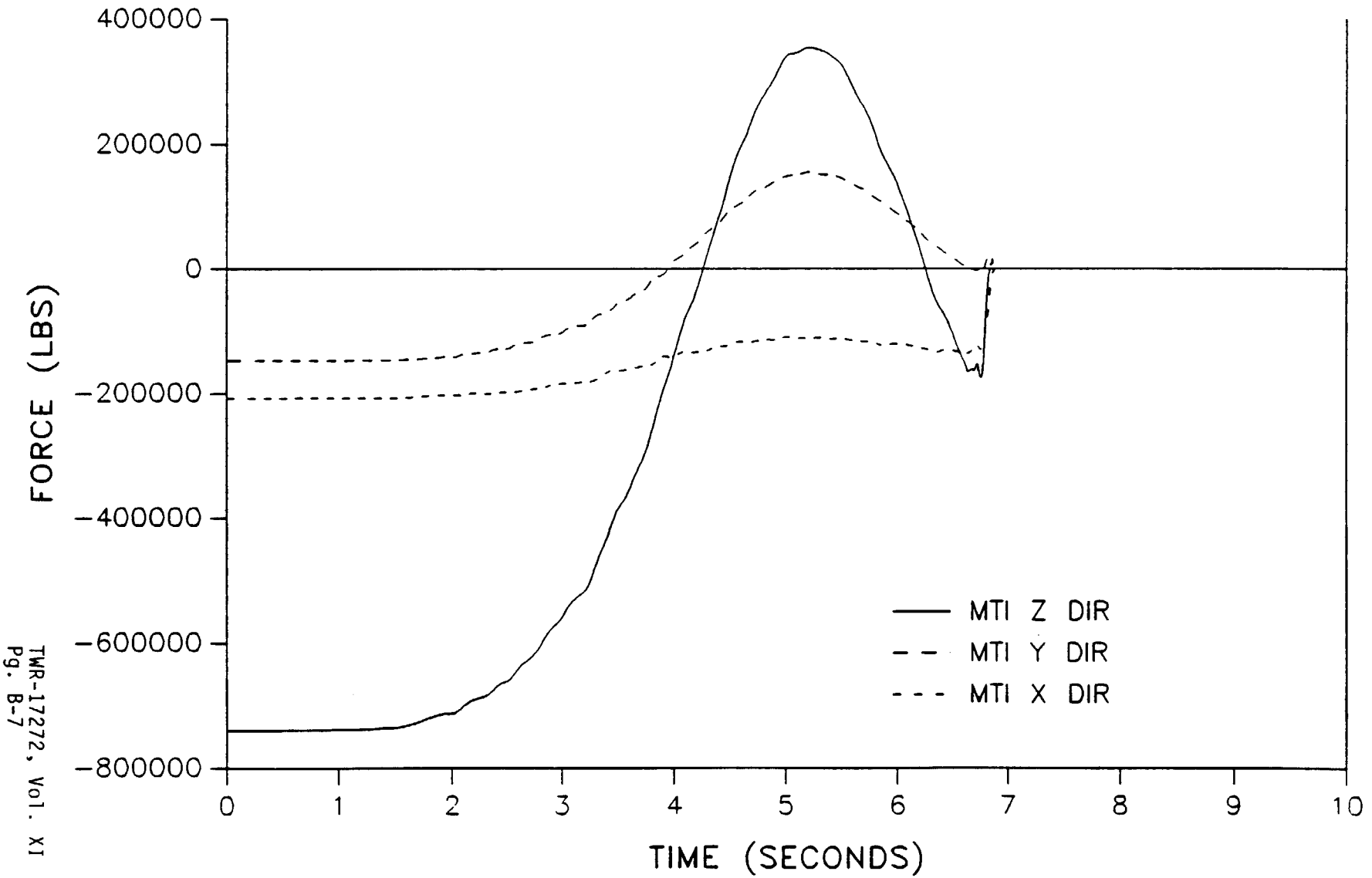

STS-26 RECONSTRUCTED TIE-DOWN BOLT LOADS

LEFT RSRM - BOLT #7

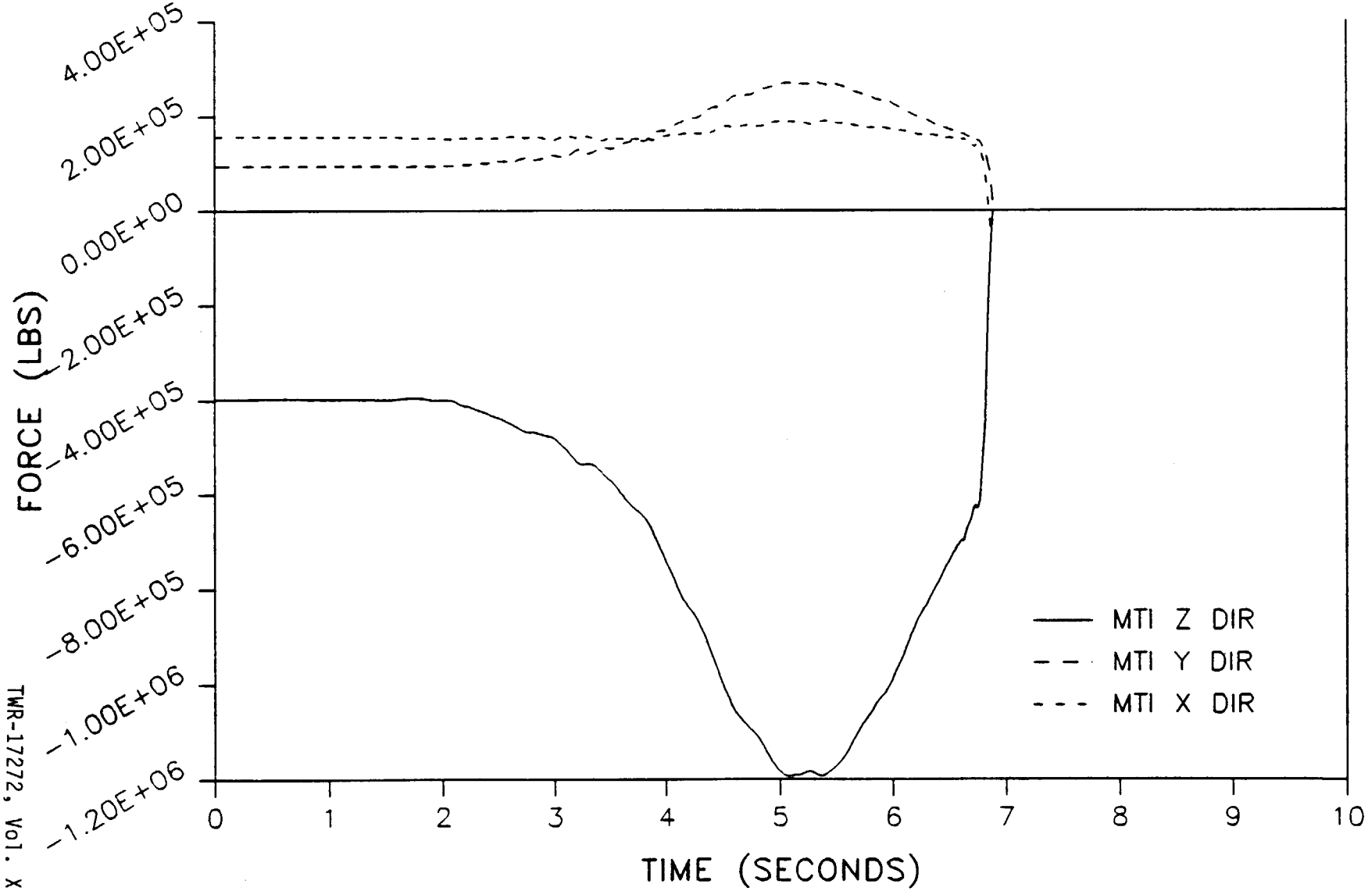

STS-26 RECONSTRUCTED TIE-DOWN BOLT LOADS

LEFT RSRM - BOLT #8

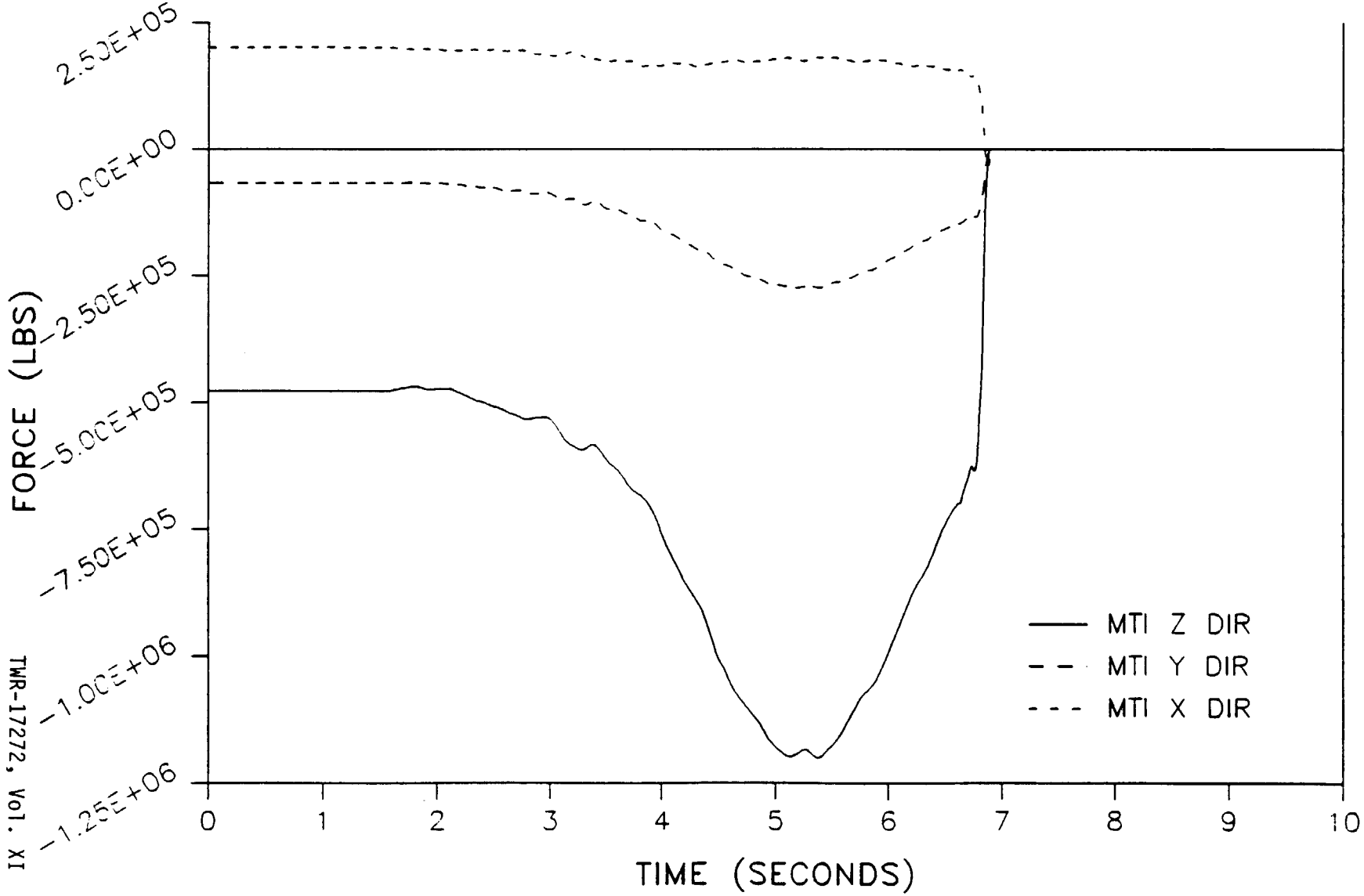

STS-26 RECONSTRUCTED CG OFFSET LOADS

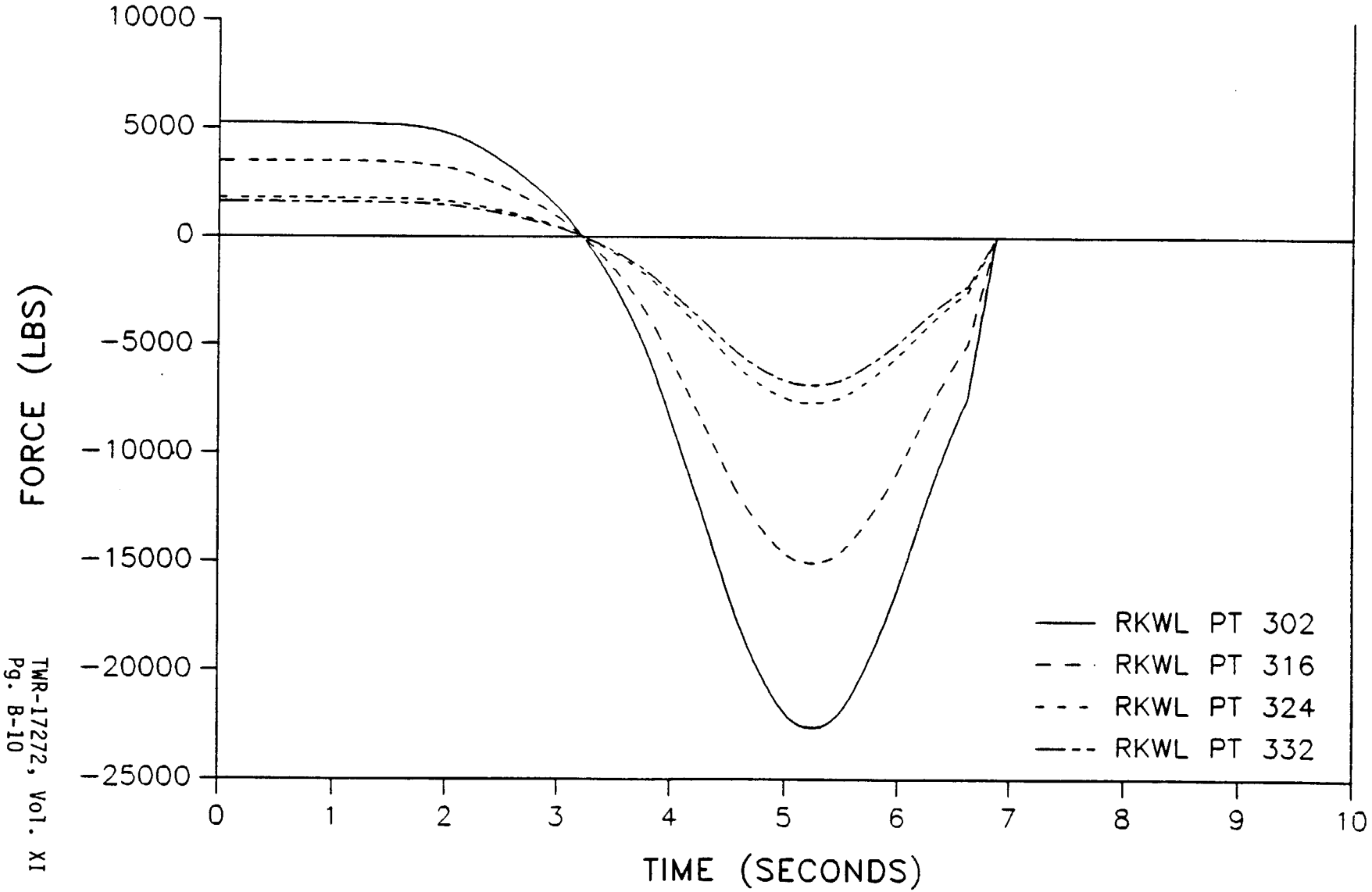

STS-26 RECONSTRUCTED NOZZLE LOADS

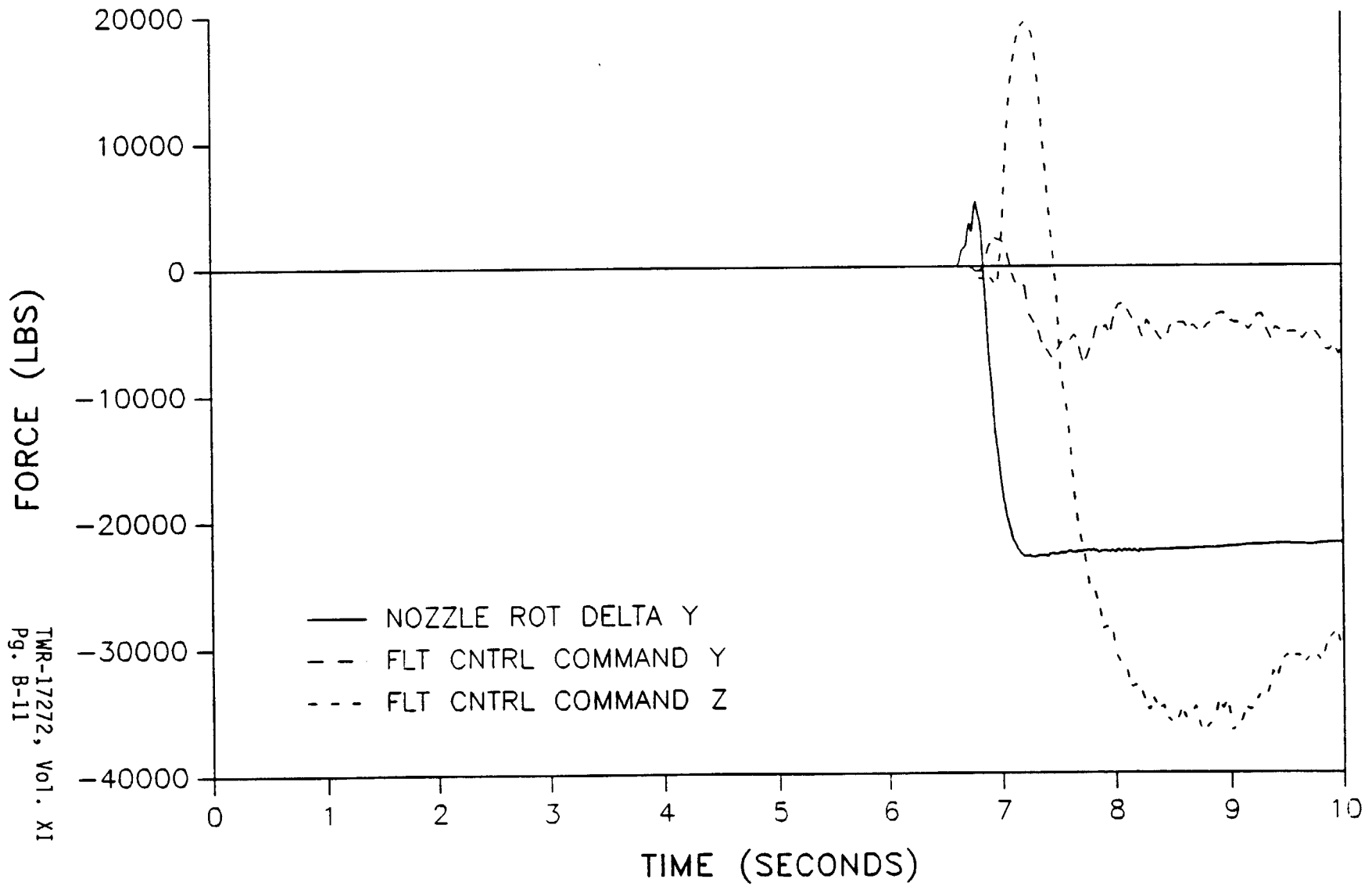

STS-26 RECONSTRUCTED HEAD-END PRESSURE

RIGHT RSRM

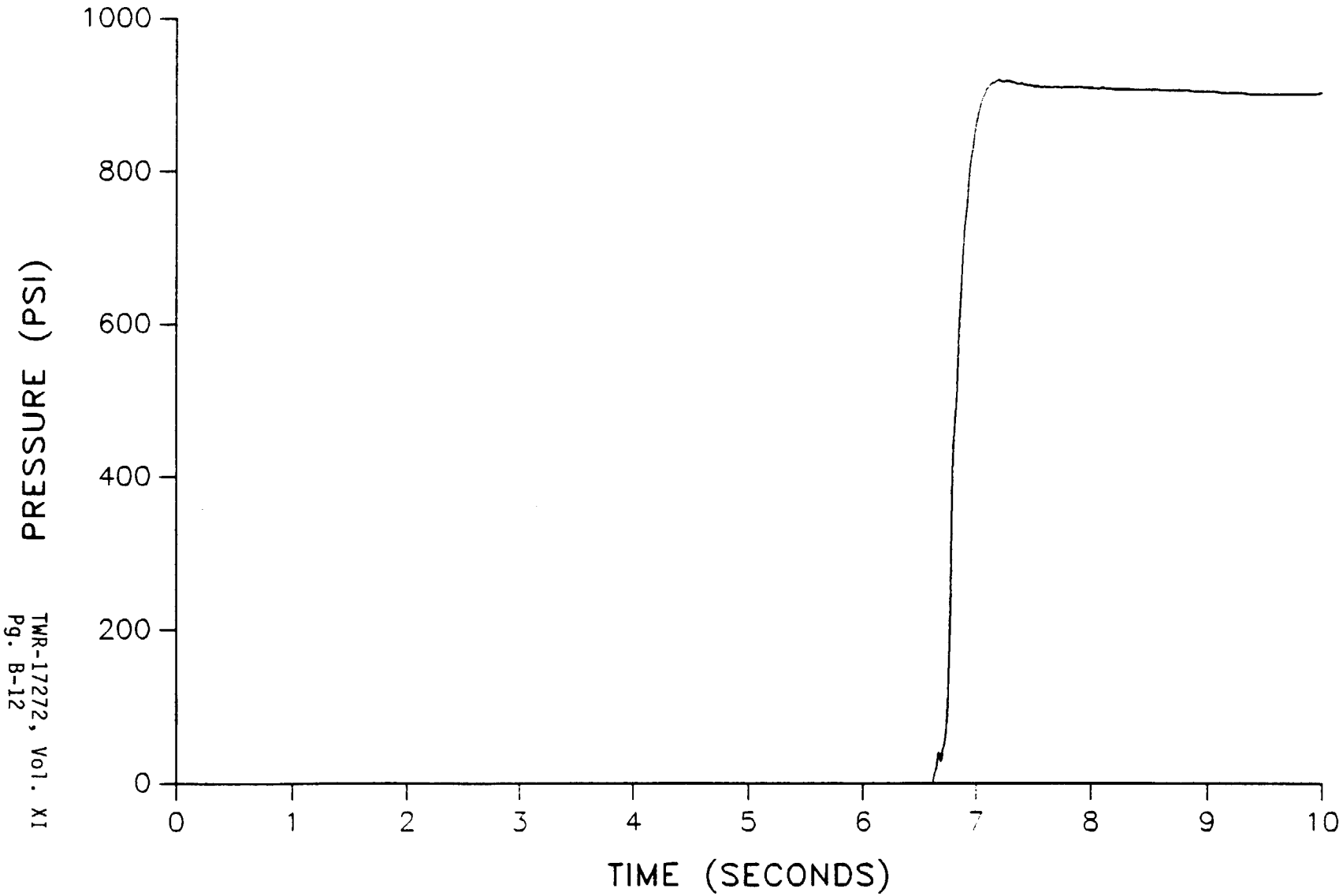

STS-26 RECONSTRUCTED FWD ATTACH LOADS

RIGHT RSRM

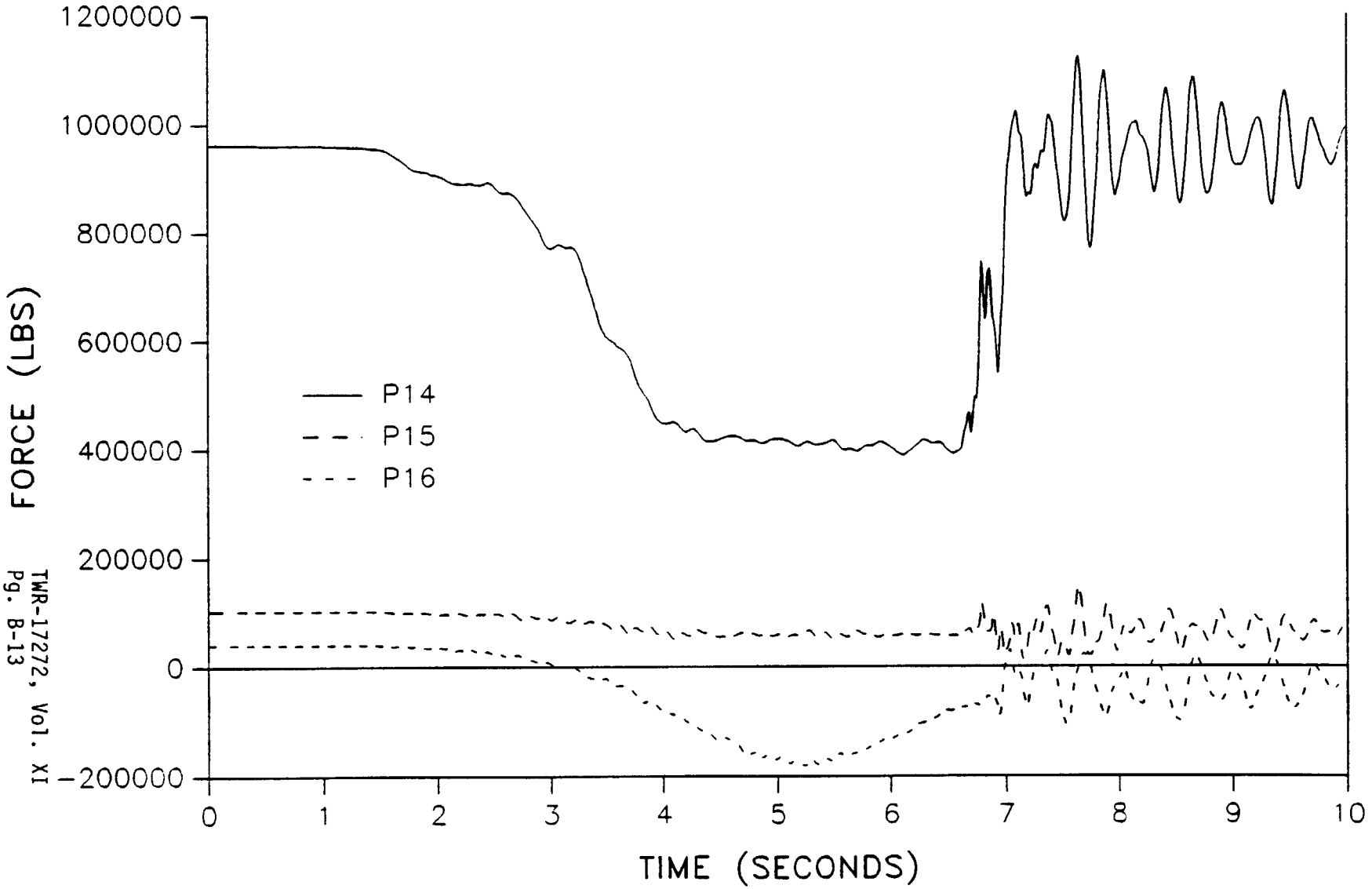

STS-26 RECONSTRUCTED ET ATTACH LOADS

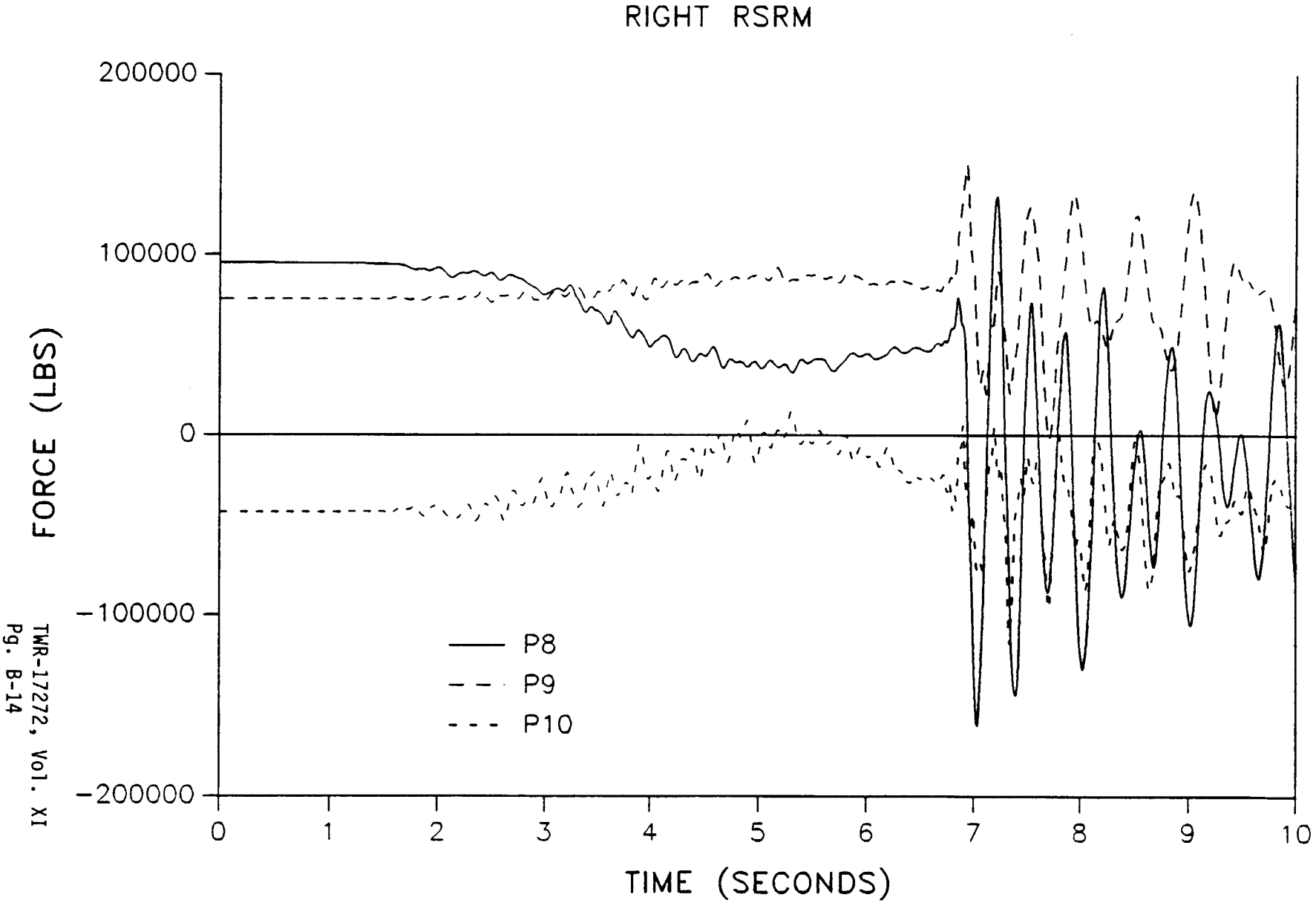

STS-26 RECONSTRUCTED TIE-DOWN BOLT LOADS

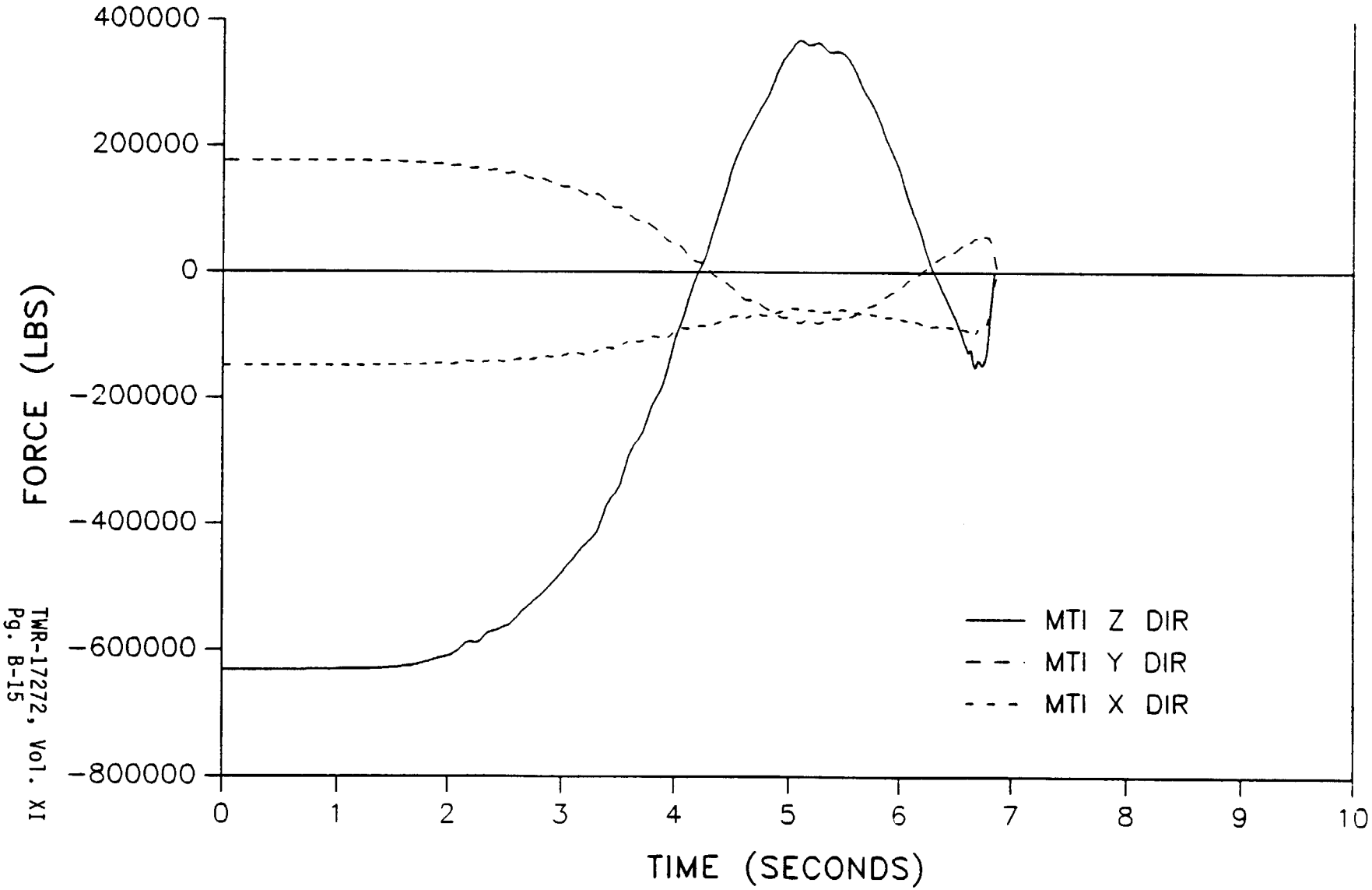

STS-26 RECONSTRUCTED TIE-DOWN BOLT LOADS

RIGHT RSRM - BOLT #2

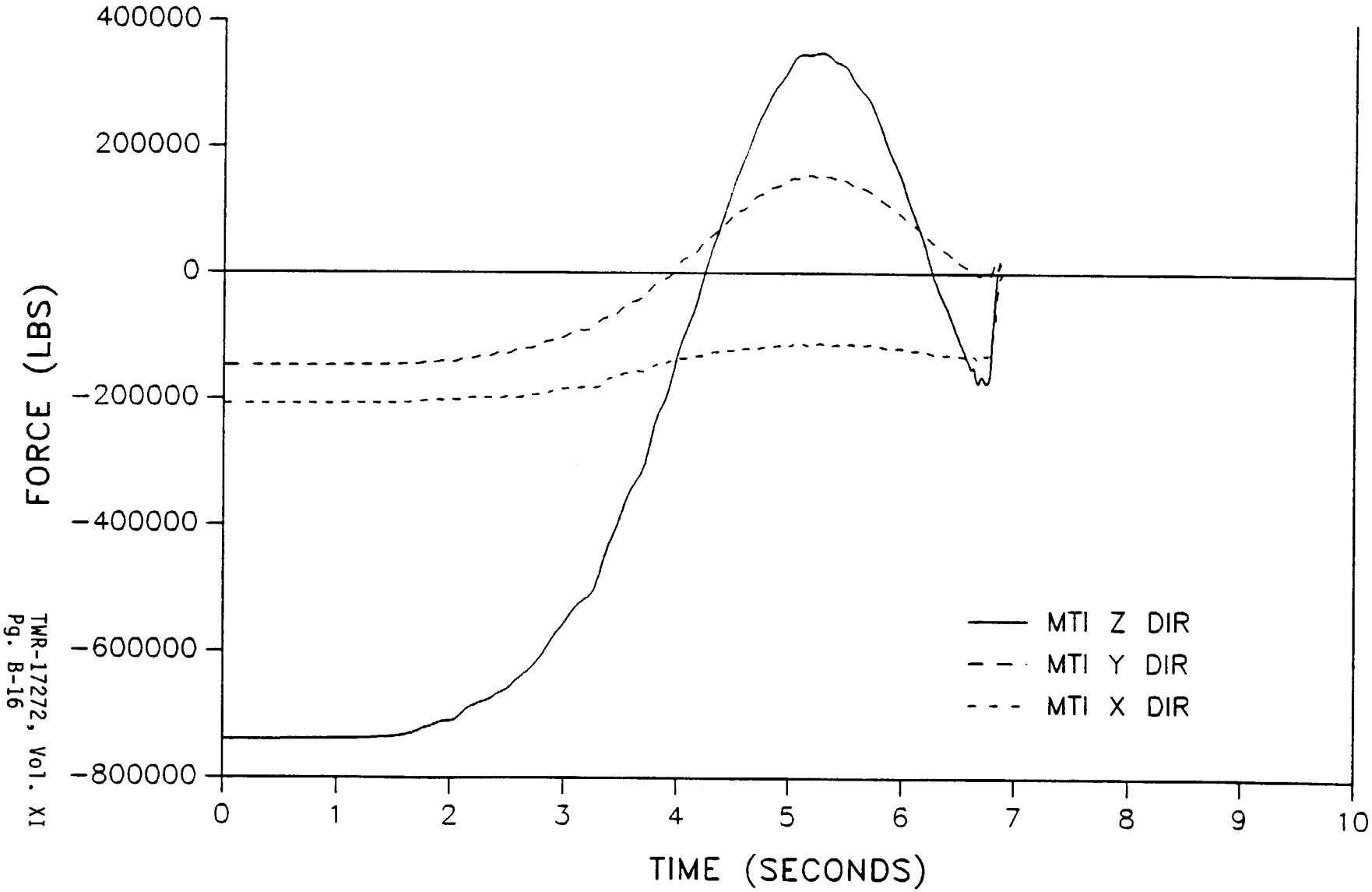

STS-26 RECONSTRUCTED TIE-DOWN BOLT LOADS

RIGHT RSRM - BOLT #3

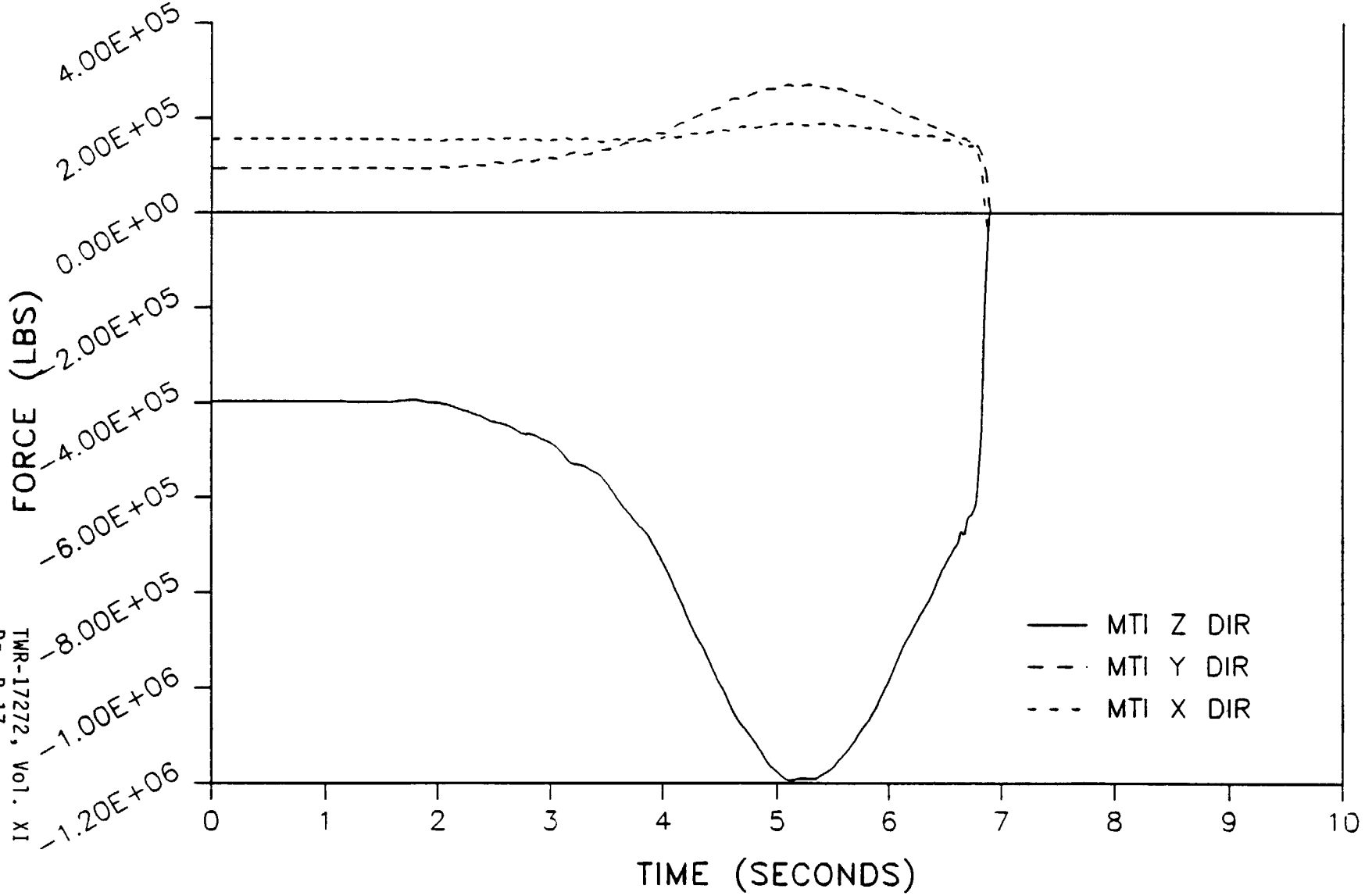

STS-26 RECONSTRUCTED TIE-DOWN BOLT LOADS

RIGHT RSRM - BOLT #4

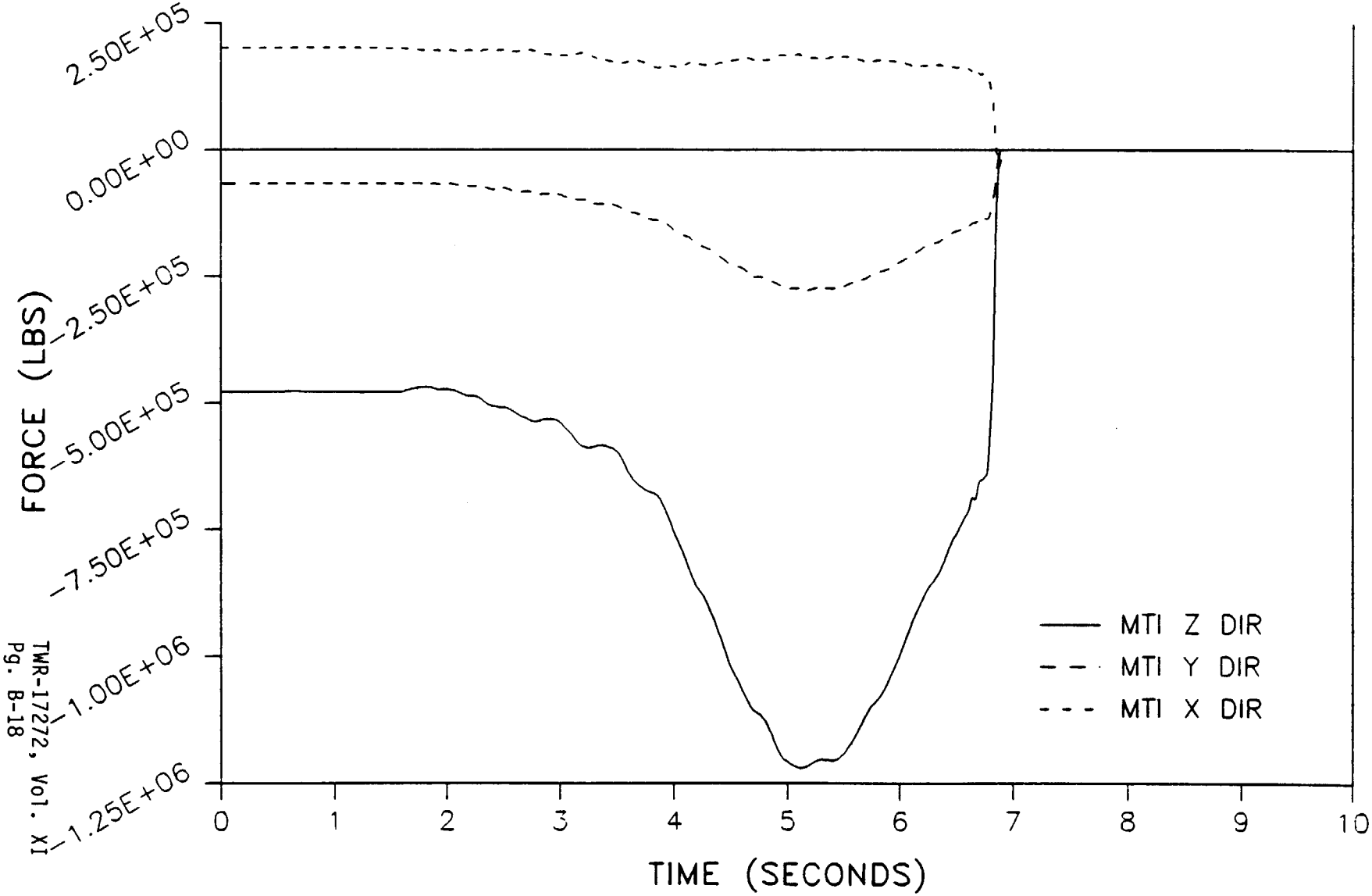

STS-26 RECONSTRUCTED CG OFFSET LOADS

RIGHT RSRM

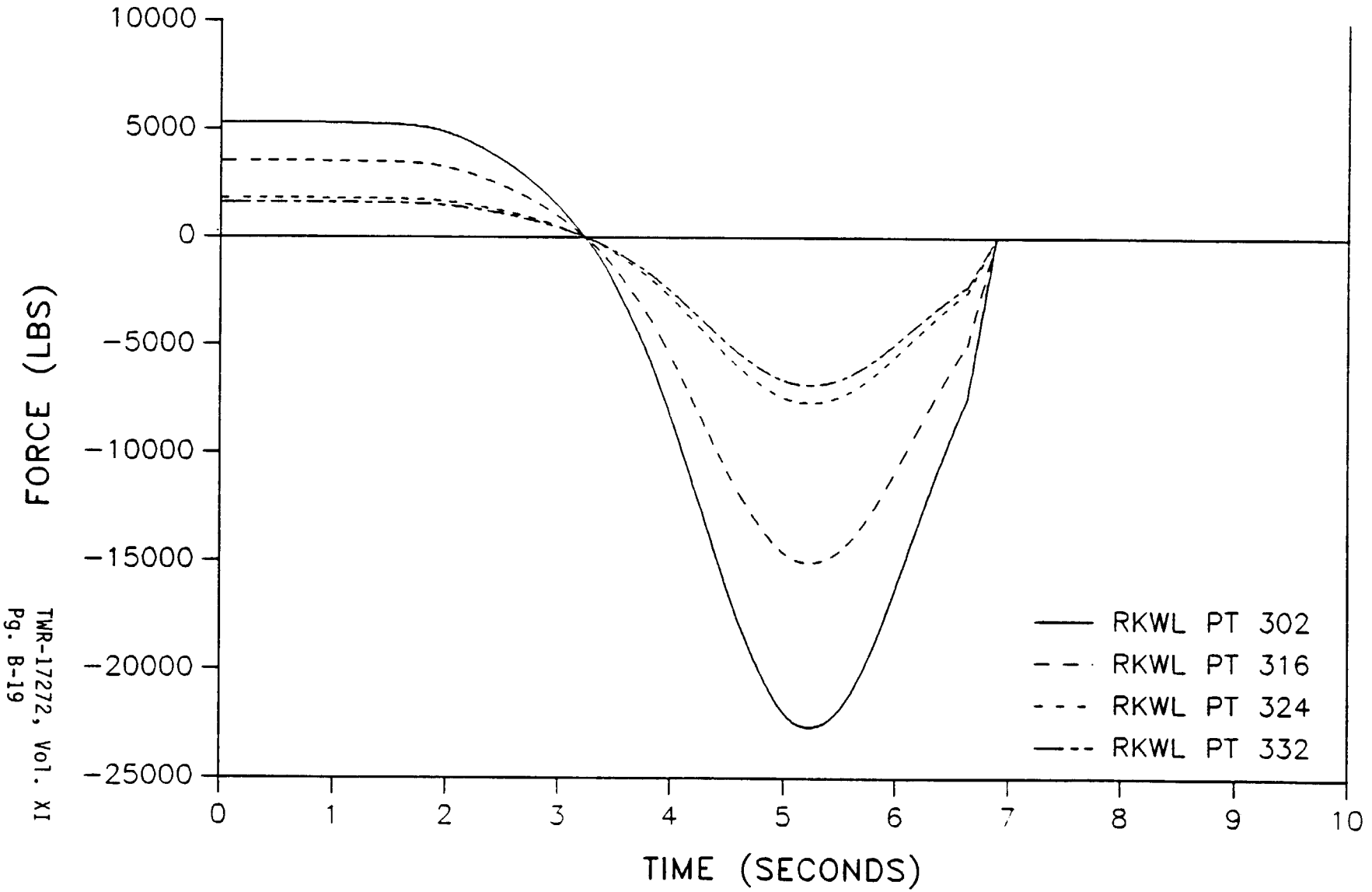

STS-26 RECONSTRUCTED NOZZLE LOADS

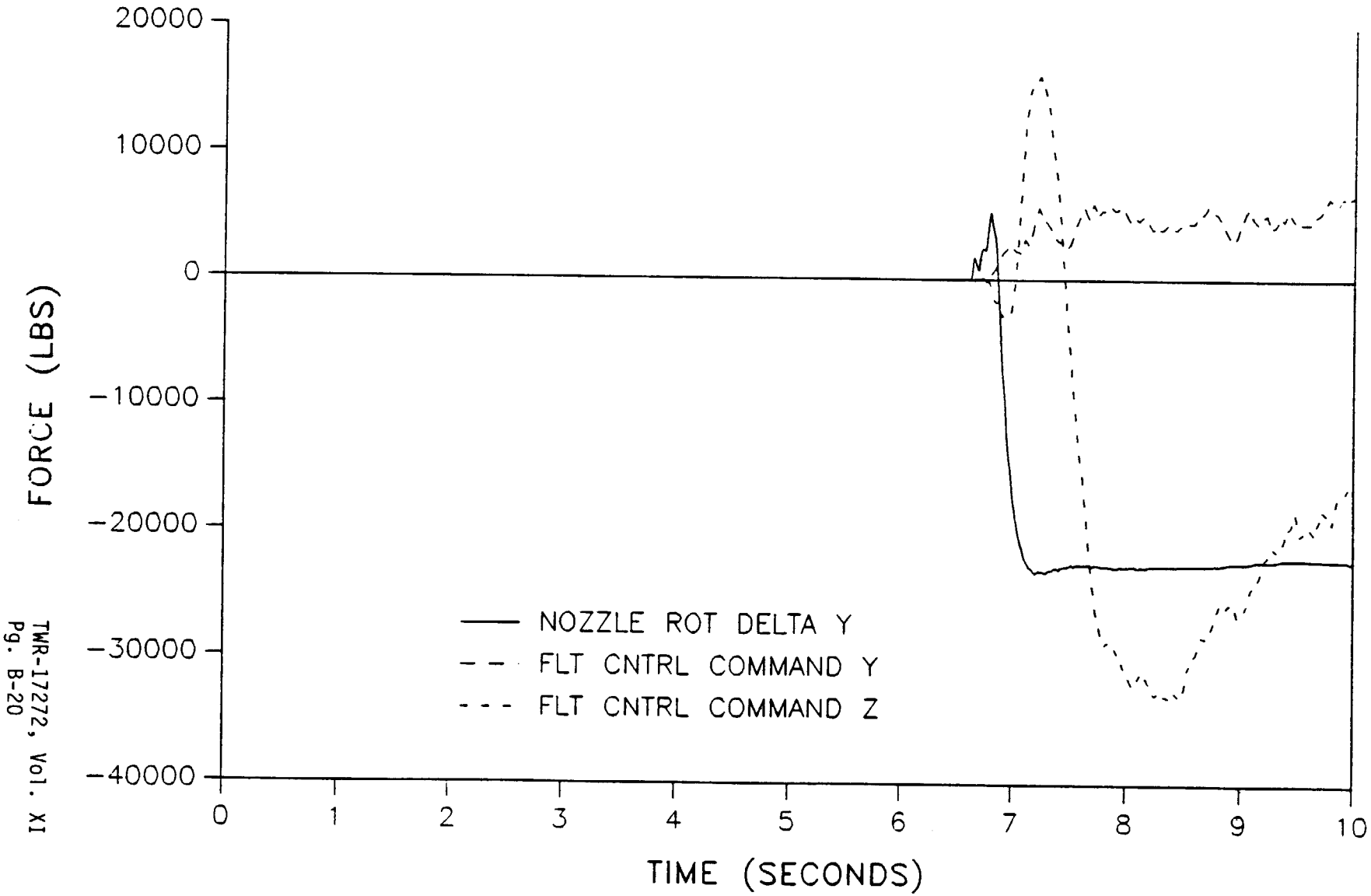

APPENDIX C

DFI Instrumentation List

DFI FLIGHT 1 INSTRUMENTATION

INST.NO	ANG. LOC.	STATION	MEAS. DIR	RANGE	REQ. ACC.	FM (hz)	DIG. (sps)	REMARKS	KSC INSTLD.	FLT. NO.	NOTES	OFI	PART NOS.
		LEFT	SRM										
B08D7160A	0.00	500.00	AXIAL	+/- 10 g's	+/- 10%	5-50		VIB. SRB		1-6	6		
B08D7161A	0.00	500.00	TANG.	+/- 10 g's	+/- 10%	5-50		VIB. SRB		1-6	6		
B08D7162A	0.00	500.00	RADIAL	+/- 10 g's	+/- 10%	5-50		VIB. SRB		1-6	6		
B08G7272A	N/A	771.50	HOOP	+6K,-2K	+/- 10%		80.00	STRAIN, GIRTH		1-6	2		1U75749-01
B08G7273A	N/A	847.00	HOOP	+6K,-2K	+/- 10%		160.00	STRAIN, GIRTH	X	1-6	2,3		1U75749-01
B08G7274A	N/A	848.75	HOOP	+6K,-2K	+/- 10%		160.00	STRAIN, GIRTH	X	1-6	2,3		1U75749-01
B08G7275A	N/A	850.20	HOOP	+6K,-2K	+/- 10%		160.00	STRAIN, GIRTH	X	1-6	2,3		1U75749-01
B08G7276A	N/A	852.80	HOOP	+6K,-2K	+/- 10%		160.00	STRAIN, GIRTH	X	1-6	2,3		1U75749-01
B08G7277A	N/A	855.50	HOOP	+6K,-2K	+/- 10%		160.00	STRAIN, GIRTH		1-6	2,3		1U75749-01
B08G7278A	N/A	857.50	HOOP	+6K,-2K	+/- 10%		160.00	STRAIN, GIRTH		1-6	2,3		1U75749-01
B08G7282A	N/A	1091.50	HOOP	+6K,-2K	+/- 10%		80.00	STRAIN, GIRTH		1-6	2		1U75749-01
B08G7283A	N/A	1167.00	HOOP	+6K,-2K	+/- 10%		160.00	STRAIN, GIRTH	X	1-6	2,3		1U75749-01
B08G7284A	N/A	1168.75	HOOP	+6K,-2K	+/- 10%		160.00	STRAIN, GIRTH	X	1-6	2,3		1U75749-01
B08G7285A	N/A	1170.20	HOOP	+6K,-2K	+/- 10%		160.00	STRAIN, GIRTH	X	1-6	2,3		1U75749-01
B08G7286A	N/A	1172.80	HOOP	+6K,-2K	+/- 10%		160.00	STRAIN, GIRTH	X	1-6	2,3		1U75749-01
B08G7287A	N/A	1175.25	HOOP	+6K,-2K	+/- 10%		160.00	STRAIN, GIRTH		1-6	2,3		1U75749-01
B08G7288A	N/A	1177.50	HOOP	+6K,-2K	+/- 10%		160.00	STRAIN, GIRTH		1-6	2,3		1U75749-01
B08G7292A	N/A	1411.80	HOOP	+6K,-2K	+/- 10%		80.00	STRAIN, GIRTH		1-6	2		1U75749-01
B08G7293A	N/A	1487.00	HOOP	+6K,-2K	+/- 10%		160.00	STRAIN, GIRTH	X	1-6	2,3		1U75749-01
B08G7294A	N/A	1488.75	HOOP	+6K,-2K	+/- 10%		160.00	STRAIN, GIRTH	X	1-6	2,3		1U75749-01
B08G7295A	N/A	1490.20	HOOP	+6K,-2K	+/- 10%		160.00	STRAIN, GIRTH	X	1-6	2,3		1U75749-01
B08G7296A	N/A	1492.80	HOOP	+6K,-2K	+/- 10%		160.00	STRAIN, GIRTH	X	1-6	2,3		1U75749-01
B08G7297A	N/A	1495.25	HOOP	+6K,-2K	+/- 10%		160.00	STRAIN, GIRTH		1-6	2,3		1U75749-01
B08G7298A	N/A	1497.50	HOOP	+6K,-2K	+/- 10%		160.00	STRAIN, GIRTH		1-6	2,3		1U75749-01
B08G7299A	N/A	1574.75	HOOP	+6K,-2K	+/- 10%		160.00	STRAIN, GIRTH		1-6	2,3		1U75749-01
B08G7300A	N/A	1576.40	HOOP	+6K,-2K	+/- 10%		160.00	STRAIN, GIRTH		1-6	2,3		1U75749-01
B08G7301A	N/A	1637.50	HOOP	+6K,-2K	+/- 10%		80.00	STRAIN, GIRTH		1-6	2		1U75749-01
B08G7302A	N/A	1694.75	HOOP	+6K,-2K	+/- 10%		160.00	STRAIN, GIRTH		1-6	2,3		1U75749-01
B08G7303A	N/A	1696.40	HOOP	+6K,-2K	+/- 10%		160.00	STRAIN, GIRTH		1-6	2,3		1U75749-01
B08G7305A	N/A	1834.75	HOOP	+6K,-2K	+/- 10%		160.00	STRAIN, GIRTH		1-6	2,3		1U75749-01
B08G7306A	N/A	1836.20	HOOP	+6K,-2K	+/- 10%		160.00	STRAIN, GIRTH		1-6	2,3		1U75749-01

DFI FLIGHT 1 INSTRUMENTATION

INST.NO	ANG. LOC.	STATION	MEAS. DIR	RANGE	REQ. ACC.	FM (hz)	DIG. (sps)	REMARKS	KSC INSTLD.	FLT. NO.	NOTES	OFI	PART NOS.
B08G7311A	N/A	1872.00	HOOP	+6K,-2K	+/- 10%		160.00	STRAIN, GIRTH		1-6	3,5		1U75749-01
B08G7312A	N/A	1873.50	HOOP	+6K,-2K	+/- 10%		80.00	STRAIN, GIRTH		1-6	3,5		1U75749-01
B08G7313A	N/A	1874.50	HOOP	+6K,-2K	+/- 10%		80.00	STRAIN, GIRTH		1-6	3,5		1U75749-01
B08G7314A	N/A	1876.00	HOOP	+6K,-2K	+/- 10%		160.00	STRAIN, GIRTH		1-6	3,5		1U75749-01
B08G7315A	N/A	1876.30	HOOP	+6K,-2K	+/- 10%		160.00	STRAIN, GIRTH		1-6	3,5		1U75749-01
B08G7316A	5.00	486.40	AXIAL	+6K,-2K	+/- 10%		160.00	STRAIN, BIAX		1-6	1		1U51212-02
B08G7317A	5.00	486.40	TANG.	+6K,-2K	+/- 10%		160.00	STRAIN, BIAX		1-6	1		1U51212-02
B08G7318A	0.00	556.50	AXIAL	+6K,-2K	+/- 10%		160.00	STRAIN, BIAX		1-6	1	X	1U51212-02
B08G7319A	0.00	556.50	TANG.	+6K,-2K	+/- 10%		160.00	STRAIN, BIAX		1-6	1	X	1U51212-02
B08G7320A	98.00	556.50	AXIAL	+6K,-2K	+/- 10%		80.00	STRAIN, BIAX		1-6	1	X	1U51212-02
B08G7321A	98.00	556.50	TANG.	+6K,-2K	+/- 10%		80.00	STRAIN, BIAX		1-6	1	X	1U51212-02
B08G7322A	180.00	556.50	AXIAL	+6K,-2K	+/- 10%		160.00	STRAIN, BIAX		1-6	1	X	1U51212-02
B08G7323A	180.00	556.50	TANG.	+6K,-2K	+/- 10%		160.00	STRAIN, BIAX		1-6	1	X	1U51212-02
B08G7324A	270.00	556.50	AXIAL	+6K,-2K	+/- 10%		80.00	STRAIN, BIAX		1-6	1	X	1U51212-02
B08G7325A	270.00	556.50	TANG.	+6K,-2K	+/- 10%		80.00	STRAIN, BIAX		1-6	1	X	1U51212-02
B08G7326A	0.00	876.50	AXIAL	+6K,-2K	+/- 10%		160.00	STRAIN, BIAX		1-6	1		1U51212-02
B08G7327A	0.00	876.50	TANG.	+6K,-2K	+/- 10%		160.00	STRAIN, BIAX		1-6	1		1U51212-02
B08G7328A	98.00	876.50	AXIAL	+6K,-2K	+/- 10%		80.00	STRAIN, BIAX		1-6	1		1U51212-02
B08G7329A	98.00	876.50	TANG.	+6K,-2K	+/- 10%		80.00	STRAIN, BIAX		1-6	1		1U51212-02
B08G7330A	180.00	876.50	AXIAL	+6K,-2K	+/- 10%		160.00	STRAIN, BIAX		1-6	1		1U51212-02
B08G7331A	180.00	876.50	TANG.	+6K,-2K	+/- 10%		160.00	STRAIN, BIAX		1-6	1		1U51212-02
B08G7332A	270.00	876.50	AXIAL	+6K,-2K	+/- 10%		80.00	STRAIN, BIAX		1-6	1		1U51212-02
B08G7333A	270.00	876.50	TANG.	+6K,-2K	+/- 10%		80.00	STRAIN, BIAX		1-6	1		1U51212-02
B08G7334A	0.00	1196.50	AXIAL	+6K,-2K	+/- 10%		160.00	STRAIN, BIAX		1-6	1		1U51212-02
B08G7335A	0.00	1196.50	TANG.	+6K,-2K	+/- 10%		160.00	STRAIN, BIAX		1-6	1		1U51212-02
B08G7336A	98.00	1196.50	AXIAL	+6K,-2K	+/- 10%		80.00	STRAIN, BIAX		1-6	1		1U51212-02
B08G7337A	98.00	1196.50	TANG.	+6K,-2K	+/- 10%		80.00	STRAIN, BIAX		1-6	1		1U51212-02
B08G7338A	180.00	1196.50	AXIAL	+6K,-2K	+/- 10%		160.00	STRAIN, BIAX		1-6	1		1U51212-02
B08G7339A	180.00	1196.50	TANG.	+6K,-2K	+/- 10%		160.00	STRAIN, BIAX		1-6	1		1U51212-02
B08G7340A	270.00	1196.50	AXIAL	+6K,-2K	+/- 10%		80.00	STRAIN, BIAX		1-6	1		1U51212-02
B08G7341A	270.00	1196.50	TANG.	+6K,-2K	+/- 10%		80.00	STRAIN, BIAX		1-6	1		1U51212-02
B08G7342A	0.00	1466.00	AXIAL	+6K,-2K	+/- 10%		160.00	STRAIN, BIAX		1-6	4		1U51212-02
B08G7343A	0.00	1466.00	TANG.	+6K,-2K	+/- 10%		160.00	STRAIN, BIAX		1-6	4		1U51212-02
B08G7344A	98.00	1466.00	AXIAL	+6K,-2K	+/- 10%		80.00	STRAIN, BIAX		1-6	4		1U51212-02

INST.NO	ANG. LOC.	STATION	MEAS. DIR	RANGE	REQ. ACC.	FM (hz)	DIG. (sps)	REMARKS	KSC INSTLD.	FLT. NO.	NOTES	OFI	PART NOS.
B08G7345A	98.00	1466.00	TANG.	+6K,-2K	+/- 10%		80.00	STRAIN, BIAX		1-6	4		1U51212-02
B08G7346A	180.00	1466.00	AXIAL	+6K,-2K	+/- 10%		160.00	STRAIN, BIAX		1-6	4		1U51212-02
B08G7347A	180.00	1466.00	TANG.	+6K,-2K	+/- 10%		160.00	STRAIN, BIAX		1-6	4		1U51212-02
B08G7348A	270.00	1466.00	AXIAL	+6K,-2K	+/- 10%		80.00	STRAIN, BIAX		1-6	4		1U51212-02
B08G7349A	270.00	1466.00	TANG.	+6K,-2K	+/- 10%		80.00	STRAIN, BIAX		1-6	4		1U51212-02
B08G7350A	180.00	1493.00	AXIAL	+6K,-2K	+/- 10%		160.00	STRAIN, BIAX	X	1-6	4		1U51212-02
B08G7351A	180.00	1493.00	TANG.	+6K,-2K	+/- 10%		160.00	STRAIN, BIAX	X	1-6	4		1U51212-02
B08G7352A	98.00	1493.00	AXIAL	+6K,-2K	+/- 10%		80.00	STRAIN, BIAX	X	1-6	4		1U51212-02
B08G7353A	98.00	1493.00	TANG.	+6K,-2K	+/- 10%		80.00	STRAIN, BIAX	X	1-6	4		1U51212-02
B08G7354A	0.00	1493.00	AXIAL	+6K,-2K	+/- 10%		160.00	STRAIN, BIAX	X	1-6	4		1U51212-02
B08G7355A	0.00	1493.00	TANG.	+6K,-2K	+/- 10%		160.00	STRAIN, BIAX	X	1-6	4		1U51212-02
B08G7356A	320.00	1493.00	AXIAL	+6K,-2K	+/- 10%		80.00	STRAIN, BIAX	X	1-6	4		1U51212-02
B08G7357A	320.00	1493.00	TANG.	+6K,-2K	+/- 10%		80.00	STRAIN, BIAX	X	1-6	4		1U51212-02
B08G7358A	300.00	1493.00	AXIAL	+6K,-2K	+/- 10%		160.00	STRAIN, BIAX	X	1-6	4		1U51212-02
B08G7359A	300.00	1493.00	TANG.	+6K,-2K	+/- 10%		160.00	STRAIN, BIAX	X	1-6	4		1U51212-02
B08G7360A	285.00	1493.00	AXIAL	+6K,-2K	+/- 10%		80.00	STRAIN, BIAX	X	1-6	4		1U51212-02
B08G7361A	285.00	1493.00	TANG.	+6K,-2K	+/- 10%		80.00	STRAIN, BIAX	X	1-6	4		1U51212-02
B08G7362A	270.00	1493.00	AXIAL	+6K,-2K	+/- 10%		160.00	STRAIN, BIAX	X	1-6	4		1U51212-02
B08G7363A	270.00	1493.00	TANG.	+6K,-2K	+/- 10%		160.00	STRAIN, BIAX	X	1-6	4		1U51212-02
B08G7364A	255.00	1493.00	AXIAL	+6K,-2K	+/- 10%		80.00	STRAIN, BIAX	X	1-6	4		1U51212-02
B08G7365A	255.00	1493.00	TANG.	+6K,-2K	+/- 10%		80.00	STRAIN, BIAX	X	1-6	4		1U51212-02
B08G7366A	220.00	1493.00	AXIAL	+6K,-2K	+/- 10%		160.00	STRAIN, BIAX	X	1-6	4		1U51212-02
B08G7367A	220.00	1493.00	TANG.	+6K,-2K	+/- 10%		160.00	STRAIN, BIAX	X	1-6	4		1U51212-02
B08G7386A	180.00	1501.00	AXIAL	+6K,-2K	+/- 10%		160.00	STRAIN, BIAX		1-6	4		1U51212-02
B08G7387A	180.00	1501.00	TANG.	+6K,-2K	+/- 10%		160.00	STRAIN, BIAX		1-6	4		1U51212-02
B08G7388A	98.00	1501.00	AXIAL	+6K,-2K	+/- 10%		80.00	STRAIN, BIAX		1-6	4		1U51212-02
B08G7389A	98.00	1501.00	TANG.	+6K,-2K	+/- 10%		80.00	STRAIN, BIAX		1-6	4		1U51212-02
B08G7390A	0.00	1501.00	AXIAL	+6K,-2K	+/- 10%		160.00	STRAIN, BIAX		1-6	4		1U51212-02
B08G7391A	0.00	1501.00	TANG.	+6K,-2K	+/- 10%		160.00	STRAIN, BIAX		1-6	4		1U51212-02
B08G7392A	320.00	1501.00	AXIAL	+6K,-2K	+/- 10%		80.00	STRAIN, BIAX		1-6	4	X	1U51212-02
B08G7393A	320.00	1501.00	TANG.	+6K,-2K	+/- 10%		80.00	STRAIN, BIAX		1-6	4	X	1U51212-02
B08G7394A	300.00	1501.00	AXIAL	+6K,-2K	+/- 10%		160.00	STRAIN, BIAX		1-6	4		1U51212-02
B08G7395A	300.00	1501.00	TANG.	+6K,-2K	+/- 10%		160.00	STRAIN, BIAX		1-6	4		1U51212-02
B08G7396A	285.00	1501.00	AXIAL	+6K,-2K	+/- 10%		80.00	STRAIN, BIAX		1-6	4	X	1U51212-02
B08G7397A	285.00	1501.00	TANG.	+6K,-2K	+/- 10%		80.00	STRAIN, BIAX		1-6	4	X	1U51212-02

DFI FLIGHT 1 INSTRUMENTATION

INST.NO	ANG. LOC.	STATION	MEAS. DIR	RANGE	REQ. ACC.	FM (hz)	DIG. (sps)	REMARKS	KSC INSTLD.	FLT. NO.	NOTES	OFI	PART NOS.
B08G7398A	270.00	1501.00	AXIAL	+6K,-2K	+/- 10%		160.00	STRAIN, BIAX		1-6	4		1U51212-02
B08G7399A	270.00	1501.00	TANG.	+6K,-2K	+/- 10%		160.00	STRAIN, BIAX		1-6	4		1U51212-02
B08G7400A	255.00	1501.00	AXIAL	+6K,-2K	+/- 10%		80.00	STRAIN, BIAX		1-6	4		1U51212-02
B08G7401A	255.00	1501.00	TANG.	+6K,-2K	+/- 10%		80.00	STRAIN, BIAX		1-6	4		1U51212-02
B08G7402A	220.00	1501.00	AXIAL	+6K,-2K	+/- 10%		160.00	STRAIN, BIAX		1-6	4	X	1U51212-02
B08G7403A	220.00	1501.00	TANG.	+6K,-2K	+/- 10%		160.00	STRAIN, BIAX		1-6	4	X	1U51212-02
B08G7404A	0.00	1797.00	AXIAL	+6K,-2K	+/- 10%		160.00	STRAIN, BIAX		1-6	10	X	1U51212-02
B08G7405A	0.00	1797.00	TANG.	+6K,-2K	+/- 10%		160.00	STRAIN, BIAX		1-6	10	X	1U51212-02
B08G7406A	98.00	1797.00	AXIAL	+6K,-2K	+/- 10%		80.00	STRAIN, BIAX		1-6	10	X	1U51212-02
B08G7407A	98.00	1797.00	TANG.	+6K,-2K	+/- 10%		80.00	STRAIN, BIAX		1-6	10	X	1U51212-02
B08G7408A	180.00	1797.00	AXIAL	+6K,-2K	+/- 10%		160.00	STRAIN, BIAX		1-6	10	X	1U51212-02
B08G7409A	180.00	1797.00	TANG.	+6K,-2K	+/- 10%		160.00	STRAIN, BIAX		1-6	10	X	1U51212-02
B08G7410A	270.00	1797.00	AXIAL	+6K,-2K	+/- 10%		80.00	STRAIN, BIAX		1-6	10	X	1U51212-02
B08G7411A	270.00	1797.00	TANG.	+6K,-2K	+/- 10%		80.00	STRAIN, BIAX		1-6	10	X	1U51212-02
B08G7412A	0.00	1875.00	AXIAL	+6K,-2K	+/- 10%		160.00	STRAIN, BIAX		1-6	5		1U51212-02
B08G7413A	0.00	1875.00	TANG.	+6K,-2K	+/-10%		160.00	STRAIN, BIAX		1-6	5		1U51212-02
B08G7414A	0.00	1871.00	AXIAL	+6K,-2K	+/- 10%		80.00	STRAIN, UNIAX		1-6	5		1U51212-02
B08G7415A	0.00	1868.00	TANG.	+6K,-2K	+/-10%		80.00	STRAIN, BIAX		1-6	5		1U51212-02
B08G7416A	0.00	1868.00	AXIAL	+6K,-2K	+/- 10%		160.00	STRAIN, BIAX		1-6	5		1U51212-02
B08G7417A	90.00	1975.00	AXIAL	+6K,-2K	+/- 10%		80.00	STRAIN, BIAX		1-6	5		1U51212-02
B08G7418A	90.00	1875.00	TANG.	+6K,-2K	+/-10%		160.00	STRAIN, BIAX		1-6	5		1U51212-02
B08G7419A	90.00	1871.00	AXIAL	+6K,-2K	+/- 10%		160.00	STRAIN, UNIAX		1-6	5		1U51212-02
B08G7420A	90.00	1868.00	TANG.	+6K,-2K	+/-10%		80.00	STRAIN, BIAX		1-6	5		1U51212-02
B08G7421A	90.00	1868.00	AXIAL	+6K,-2K	+/- 10%		80.00	STRAIN, BIAX		1-6	5		1U51212-02
B08G7422A	180.00	1875.00	AXIAL	+6K,-2K	+/- 10%		160.00	STRAIN, BIAX		1-6	5		1U51212-02
B08G7423A	180.00	1875.00	TANG.	+6K,-2K	+/-10%		160.00	STRAIN, BIAX		1-6	5		1U51212-02
B08G7424A	180.00	1871.00	AXIAL	+6K,-2K	+/- 10%		80.00	STRAIN, UNIAX		1-6	5		1U51212-02
B08G7425A	180.00	1868.00	TANG.	+6K,-2K	+/-10%		80.00	STRAIN, BIAX		1-6	5		1U51212-02
B08G7426A	180.00	1868.00	AXIAL	+6K,-2K	+/- 10%		160.00	STRAIN, BIAX		1-6	5		1U51212-02
B08G7427A	270.00	1875.00	AXIAL	+6K,-2K	+/- 10%		80.00	STRAIN, BIAX		1-6	5		1U51212-02
B08G7428A	270.00	1875.00	TANG.	+6K,-2K	+/-10%		160.00	STRAIN, BIAX		1-6	5		1U51212-02
B08G7429A	270.00	1871.00	AXIAL	+6K,-2K	+/- 10%		160.00	STRAIN, UNIAX		1-6	5		1U51212-02
B08G7430A	270.00	1868.00	TANG.	+6K,-2K	+/-10%		80.00	STRAIN, BIAX		1-6	5		1U51212-02
B08G7431A	270.00	1868.00	AXIAL	+6K,-2K	+/- 10%		80.00	STRAIN, BIAX		1-6	5		1U51212-02
B08G7440A	45.00	1922.00	AXIAL	+6K,-2K	+/- 10%		160.00	STRAIN, BIAX		1&5	5,14		1U51212-02

INST.NO	ANG. LOC.	STATION	MEAS. DIR	RANGE	REQ. ACC.	FM (hz)	DIG. (sps)	REMARKS	KSC INSTLD.	FLT. NO.	NOTES	OFI	PART NOS.
B08G7441A	45.00	1922.00	TANG.	+6K,-2K	+/- 10%		160.00	STRAIN, BIAX		1&5	5,14		1U51212-02
B07T7606A	191.00	486.40		0-400 deg	+/- 1%		10.00	TEMP. SRM		1-6	8		16A03055-1
B07T7607A	0.00	846.30		0-400 deg	+/- 1%		10.00	TEMP. SRM	X	1-6	8		16A03055-1
B07T7608A	120.00	846.30		0-400 deg	+/- 1%		10.00	TEMP. SRM	X	1-6	8		16A03055-1
B07T7609A	240.00	846.30		0-400 deg	+/- 1%		10.00	TEMP. SRM	X	1-6	8		16A03055-1
B07T7610A	0.00	1486.30		0-400 deg	+/- 1%		10.00	TEMP. SRM	X	1-6	8		16A03055-1
B07T7611A	120.00	1486.30		0-400 deg	+/- 1%		10.00	TEMP. SRM	X	1-6	8		16A03055-1
B07T7612A	240.00	1486.30		0-400 deg	+/- 1%		10.00	TEMP. SRM	X	1-6	8		16A03055-1
B07T7613A	0.00	1877.50		0-400 deg	+/- 1%		10.00	TEMP. SRM		1-6	8		16A03055-1
B07T7614A	90.00	1877.50		0-400 deg	+/- 1%		10.00	TEMP. SRM		1-6	5,12		16A03055-1
B07T7615A	180.00	1877.50		0-400 deg	+/- 1%		10.00	TEMP. SRM		1-6	5,12		16A03055-1
B07T7616A	270.00	1877.50		0-400 deg	+/- 1%		10.00	TEMP. SRM		1-6	5,12		16A03055-1
B07T7622A	180.00	1905.00		0-750 deg	+/- 1%		10.00	TEMP. SRM		1-6	5,12		16A03055-1
B07T7625A	240.00	1996.50		0-750 deg	+/- 1%		10.00	TEMP. SRM		1-6	5		16A03055-1
B47P1300A		487.00		0-1050 psia	+/- 2%		320.00	OPT		1-6	15	X	1U50188-07
B47P1301A		487.00		0-1050 psia	+/- 2%		320.00	OPT		1-6	15	X	1U50188-07
B47P1302A		487.00		0-1050 psia	+/- 2%		320.00	OPT		1-6	15	X	1U50188-07
B47P7310A	115.00	487.00		0-3000 psia	+/- 2%	DC-100		PRESSURE, IGNITER CHAMBE		1-6	7	X	1U50188-08
B08X7942E	270.00	1926.00					10.00	CONTINUITY, T	X	1-6	11		
		RIGHT	SRM										
B08D8151A	180.00	487.00	AXIAL					VIB				X	
B08D8152A	180.00	487.00	RADIAL					VIB				X	
B08D8153A	180.00	487.00	TANG.					VIB				X	
B08D8160A	180.00	500.00	AXIAL	+/- 10 g's	+/- 10%	5-50		VIB. SRB		1-6	6		
B08D8161A	180.00	500.00	TANG.	+/- 10 g's	+/- 10%	5-50		VIB. SRB		1-6	6		
B08D8163A	0.00	500.00	TANG.	+/- 10 g's	+/- 10%	5-50		VIB. SRB		1-6	6		
B08G8272A	N/A	771.50		+6K,-2K	+/- 10%		80.00	STRAIN, GIRTH		1-6	2		1U75749-01
B08G8273A	N/A	847.00		+6K,-2K	+/- 10%		160.00	STRAIN, GIRTH	X	1-6	2,3		1U75749-01
B08G8274A	N/A	848.75		+6K,-2K	+/- 10%		160.00	STRAIN, GIRTH	X	1-6	2,3		1U75749-01
B08G8275A	N/A	850.20		+6K,-2K	+/- 10%		160.00	STRAIN, GIRTH	X	1-6	2,3		1U75749-01

INST.NO	ANG. LOC.	STATION	MEAS. DIR	RANGE	REQ. ACC.	FM (hz)	DIG. (sps)	REMARKS	KSC INSTLD.	FLT. NO.	NOTES	OFI	PART NOS.
B08G8276A	N/A	852.80		+6K,-2K	+/- 10%		160.00	STRAIN, GIRTH	X	1-6	2,3		1U75749-01
B08G8277A	N/A	855.50		+6K,-2K	+/- 10%		160.00	STRAIN, GIRTH		1-6	2,3		1U75749-01
B08G8278A	N/A	857.50		+6K,-2K	+/- 10%		160.00	STRAIN, GIRTH		1-6	2,3		1U75749-01
B08G8282A	N/A	1091.50		+6K,-2K	+/- 10%		80.00	STRAIN, GIRTH		1-6	2		1U75749-01
B08G8283A	N/A	1167.00		+6K,-2K	+/- 10%		160.00	STRAIN, GIRTH	X	1-6	2,3		1U75749-01
B08G8284A	N/A	1168.75		+6K,-2K	+/- 10%		160.00	STRAIN, GIRTH	X	1-6	2,3		1U75749-01
B08G8285A	N/A	1170.20		+6K,-2K	+/- 10%		160.00	STRAIN, GIRTH	X	1-6	2,3		1U75749-01
B08G8286A	N/A	1172.50		+6K,-2K	+/- 10%		160.00	STRAIN, GIRTH	X	1-6	2,3		1U75749-01
B08G8287A	N/A	1175.25		+6K,-2K	+/- 10%		160.00	STRAIN, GIRTH		1-6	2,3		1U75749-01
B08G8288A	N/A	1177.50		+6K,-2K	+/- 10%		160.00	STRAIN, GIRTH		1-6	2,3		1U75749-01
B08G8292A	N/A	1411.80		+6K,-2K	+/- 10%		80.00	STRAIN, GIRTH		1-6	2		1U75749-01
B08G8293A	N/A	1487.00		+6K,-2K	+/- 10%		160.00	STRAIN, GIRTH	X	1-6	2,3		1U75749-01
B08G8294A	N/A	1488.75		+6K,-2K	+/- 10%		160.00	STRAIN, GIRTH	X	1-6	2,3		1U75749-01
B08G8295A	N/A	1490.20		+6K,-2K	+/- 10%		160.00	STRAIN, GIRTH	X	1-6	2,3		1U75749-01
B08G8296A	N/A	1492.80		+6K,-2K	+/- 10%		160.00	STRAIN, GIRTH	X	1-6	2,3		1U75749-01
B08G8297A	N/A	1495.25		+6K,-2K	+/- 10%		160.00	STRAIN, GIRTH		1-6	2,3		1U75749-01
B08G8298A	N/A	1497.50		+6K,-2K	+/- 10%		160.00	STRAIN, GIRTH		1-6	2,3		1U75749-01
B08G8299A	N/A	1574.75		+6K,-2K	+/- 10%		160.00	STRAIN, GIRTH		1-6	2,3		1U75749-01
B08G8300A	N/A	1576.40		+6K,-2K	+/- 10%		160.00	STRAIN, GIRTH		1-6	2,3		1U75749-01
B08G8301A	N/A	1637.50		+6K,-2K	+/- 10%		80.00	STRAIN, GIRTH		1-6	2		1U75749-01
B08G8302A	N/A	1694.75		+6K,-2K	+/-10%		160.00	STRAIN, GIRTH		1-6	2,3		1U75749-01
B08G8303A	N/A	1696.40		+6K,-2K	+/-10%		160.00	STRAIN, GIRTH		1-6	2,3		1U75749-01
B08G8305A	N/A	1834.75		+6K,-2K	+/-10%		160.00	STRAIN, GIRTH		1-6	2,3		1U75749-01
B08G8306A	N/A	1836.20		+6K,-2K	+/-10%		160.00	STRAIN, GIRTH		1-6	2,3		1U75749-01
B08G8311A	N/A	1872.00		+6K,-2K	+/- 10%		160.00	STRAIN, GIRTH		1-6	3,5		1U75749-01
B08G8312A	N/A	1873.50		+6K,-2K	+/- 10%		80.00	STRAIN, GIRTH		1-6	3,5		1U75749-01
B08G8313A	N/A	1874.50		+6K,-2K	+/- 10%		80.00	STRAIN, GIRTH		1-6	3,5		1U75749-01
B08G8314A	N/A	1876.00		+6K,-2K	+/- 10%		160.00	STRAIN, GIRTH		1-6	3,5		1U75749-01
B08G8315A	N/A	1876.30		+6K,-2K	+/- 10%		160.00	STRAIN, GIRTH		1-6	3,5		1U75749-01
B08G8316A	185.00	486.40	AXIAL	+6K,-2K	+/- 10%		160.00	STRAIN, BIAX		1-6	1		1U51212-02
B08G8317A	185.00	486.40	TANG.	+6K,-2K	+/- 10%		160.00	STRAIN, BIAX		1-6	1		1U51212-02
B08G8318A·	180.00	556.50	AXIAL	+6K,-2K	+/- 10%		160.00	STRAIN, BIAX		1-6	1	X	1U51212-02
B08G8319A·	180.00	556.50	TANG.	+6K,-2K	+/- 10%		160.00	STRAIN, BIAX		1-6	1	X	1U51212-02
B08G8320A·	82.00	556.50	AXIAL	+6K,-2K	+/- 10%		80.00	STRAIN, BIAX		1-6	1	X	1U51212-02

INST.NO	ANG. LOC.	STATION	MEAS. DIR	RANGE	REQ. ACC.	FM (hz)	DIG. (sps)	REMARKS	KSC INSTLD.	FLT. NO.	NOTES	OFI	PART NOS.
B08G8321A·	82.00	556.50	TANG.	+6K,-2K	+/- 10%		80.00	STRAIN, BIAX		1-6	1	X	1U51212-02
B08G8322A·	0.00	556.50	AXIAL	+6K,-2K	+/- 10%		160.00	STRAIN, BIAX		1-6	1	X	1U51212-02
B08G8323A·	0.00	556.50	TANG.	+6K,-2K	+/- 10%		160.00	STRAIN, BIAX		1-6	1	X	1U51212-02
B08G8324A·	270.00	556.50	AXIAL	+6K,-2K	+/- 10%		80.00	STRAIN, BIAX		1-6	1	X	1U51212-02
B08G8325A·	270.00	556.50	TANG.	+6K,-2K	+/- 10%		80.00	STRAIN, BIAX		1-6	1	X	1U51212-02
B08G8326A·	180.00	876.50	AXIAL	+6K,-2K	+/- 10%		160.00	STRAIN, BIAX		1-6	1		1U51212-02
B08G8327A·	180.00	876.50	TANG.	+6K,-2K	+/- 10%		160.00	STRAIN, BIAX		1-6	1		1U51212-02
B08G8328A·	82.00	876.50	AXIAL	+6K,-2K	+/- 10%		80.00	STRAIN, BIAX		1-6	1		1U51212-02
B08G8329A·	82.00	876.50	TANG.	+6K,-2K	+/- 10%		80.00	STRAIN, BIAX		1-6	1		1U51212-02
B08G8330A·	0.00	876.50	AXIAL	+6K,-2K	+/- 10%		160.00	STRAIN, BIAX		1-6	1		1U51212-02
B08G8331A·	0.00	876.50	TANG.	+6K,-2K	+/- 10%		160.00	STRAIN, BIAX		1-6	1		1U51212-02
B08G8332A·	270.00	876.50	AXIAL	+6K,-2K	+/- 10%		80.00	STRAIN, BIAX		1-6	1		1U51212-02
B08G8333A·	270.00	876.50	TANG.	+6K,-2K	+/- 10%		80.00	STRAIN, BIAX		1-6	1		1U51212-02
B08G8334A·	180.00	1196.50	AXIAL	+6K,-2K	+/- 10%		160.00	STRAIN, BIAX		1-6	1		1U51212-02
B08G8335A·	180.00	1196.50	TANG.	+6K,-2K	+/- 10%		160.00	STRAIN, BIAX		1-6	1		1U51212-02
B08G8336A·	82.00	1196.50	AXIAL	+6K,-2K	+/- 10%		80.00	STRAIN, BIAX		1-6	1		1U51212-02
B08G8337A·	82.00	1196.50	TANG.	+6K,-2K	+/- 10%		80.00	STRAIN, BIAX		1-6	1		1U51212-02
B08G8338A·	0.00	1196.50	AXIAL	+6K,-2K	+/- 10%		160.00	STRAIN, BIAX		1-6	1		1U51212-02
B08G8339A·	0.00	1196.50	TANG.	+6K,-2K	+/- 10%		160.00	STRAIN, BIAX		1-6	1		1U51212-02
B08G8340A·	270.00	1196.50	AXIAL	+6K,-2K	+/- 10%		80.00	STRAIN, BIAX		1-6	1		1U51212-02
B08G8341A·	270.00	1196.50	TANG.	+6K,-2K	+/- 10%		80.00	STRAIN, BIAX		1-6	1		1U51212-02
B08G8342A·	180.00	1466.00	AXIAL	+6K,-2K	+/- 10%		160.00	STRAIN, BIAX		1-6	4		1U51212-02
B08G8343A·	180.00	1466.00	TANG.	+6K,-2K	+/- 10%		160.00	STRAIN, BIAX		1-6	4		1U51212-02
B08G8344A·	82.00	1466.00	AXIAL	+6K,-2K	+/- 10%		80.00	STRAIN, BIAX		1-6	4		1U51212-02
B08G8345A·	82.00	1466.00	TANG.	+6K,-2K	+/- 10%		80.00	STRAIN, BIAX		1-6	4		1U51212-02
B08G8346A·	0.00	1466.00	AXIAL	+6K,-2K	+/- 10%		160.00	STRAIN, BIAX		1-6	4		1U51212-02
B08G8347A·	0.00	1466.00	TANG.	+6K,-2K	+/- 10%		160.00	STRAIN, BIAX		1-6	4		1U51212-02
B08G8348A·	270.00	1466.00	AXIAL	+6K,-2K	+/- 10%		80.00	STRAIN, BIAX		1-6	4		1U51212-02
B08G8349A·	270.00	1466.00	TANG.	+6K,-2K	+/- 10%		80.00	STRAIN, BIAX		1-6	4		1U51212-02
B08G8350A·	0.00	1493.00	AXIAL	+6K,-2K	+/- 10%		160.00	STRAIN, BIAX	X	1-6	4		1U51212-02
B08G8351A·	0.00	1493.00	TANG.	+6K,-2K	+/- 10%		160.00	STRAIN, BIAX	X	1-6	4		1U51212-02
B08G8352A·	82.00	1493.00	AXIAL	+6K,-2K	+/- 10%		80.00	STRAIN, BIAX	X	1-6	4		1U51212-02
B08G8353A·	82.00	1493.00	TANG.	+6K,-2K	+/- 10%		80.00	STRAIN, BIAX	X	1-6	4		1U51212-02
B08G8354A·	180.00	1493.00	AXIAL	+6K,-2K	+/- 10%		160.00	STRAIN, BIAX	X	1-6	4		1U51212-02
B08G8355A·	180.00	1493.00	TANG.	+6K,-2K	+/- 10%		160.00	STRAIN, BIAX	X	1-6	4		1U51212-02

INST NO	ANG. LOC.	STATION	MEAS. DIR	RANGE	REQ. ACC.	FM (hz)	DIG. (sps)	REMARKS	KSC INSTLD.	FLT. NO.	NOTES	OFI	PART NOS.
B08G8356A	220.00	1493.00	AXIAL	+6K,-2K	+/- 10%		80.00	STRAIN, BIAX	X	1-6	4		1U51212-02
B08G8357A	220.00	1493.00	TANG.	+6K,-2K	+/- 10%		80.00	STRAIN, BIAX	X	1-6	4		1U51212-02
B08G8358A	240.00	1493.00	AXIAL	+6K,-2K	+/- 10%		160.00	STRAIN, BIAX	X	1-6	4		1U51212-02
B08G8359A	240.00	1493.00	TANG.	+6K,-2K	+/- 10%		160.00	STRAIN, BIAX	X	1-6	4		1U51212-02
B08G8360A	255.00	1493.00	AXIAL	+6K,-2K	+/- 10%		80.00	STRAIN, BIAX	X	1-6	4		1U51212-02
B08G8361A	255.00	1493.00	TANG.	+6K,-2K	+/- 10%		80.00	STRAIN, BIAX	X	1-6	4		1U51212-02
B08G8362A	270.00	1493.00	AXIAL	+6K,-2K	+/- 10%		160.00	STRAIN, BIAX	X	1-6	4		1U51212-02
B08G8363A	270.00	1493.00	TANG.	+6K,-2K	+/- 10%		160.00	STRAIN, BIAX	X	1-6	4		1U51212-02
B08G8364A	285.00	1493.00	AXIAL	+6K,-2K	+/- 10%		80.00	STRAIN, BIAX	X	1-6	4		1U51212-02
B08G8365A	285.00	1493.00	TANG.	+6K,-2K	+/- 10%		80.00	STRAIN, BIAX	X	1-6	4		1U51212-02
B08G8366A	320.00	1493.00	AXIAL	+6K,-2K	+/- 10%		160.00	STRAIN, BIAX	X	1-6	4		1U51212-02
B08G8367A	320.00	1493.00	TANG.	+6K,-2K	+/- 10%		160.00	STRAIN, BIAX	X	1-6	4		1U51212-02
B08G8386A	0.00	1501.00	AXIAL	+6K,-2K	+/- 10%		160.00	STRAIN, BIAX		1-6	4		1U51212-02
B08G8387A	0.00	1501.00	TANG.	+6K,-2K	+/- 10%		160.00	STRAIN, BIAX		1-6	4		1U51212-02
B08G8388A	82.00	1501.00	AXIAL	+6K,-2K	+/- 10%		80.00	STRAIN, BIAX		1-6	4		1U51212-02
B08G8389A	82.00	1501.00	TANG.	+6K,-2K	+/- 10%		80.00	STRAIN, BIAX		1-6	4		1U51212-02
B08G8390A	180.00	1501.00	AXIAL	+6K,-2K	+/- 10%		160.00	STRAIN, BIAX		1-6	4		1U51212-02
B08G8391A	180.00	1501.00	TANG.	+6K,-2K	+/- 10%		160.00	STRAIN, BIAX		1-6	4		1U51212-02
B08G8392A	220.00	1501.00	AXIAL	+6K,-2K	+/- 10%		80.00	STRAIN, BIAX		1-6	4	X	1U51212-02
B08G8393A	220.00	1501.00	TANG.	+6K,-2K	+/- 10%		80.00	STRAIN, BIAX		1-6	4	X	1U51212-02
B08G8394A	240.00	1501.00	AXIAL	+6K,-2K	+/- 10%		160.00	STRAIN, BIAX		1-6	4		1U51212-02
B08G8395A	240.00	1501.00	TANG.	+6K,-2K	+/- 10%		160.00	STRAIN, BIAX		1-6	4		1U51212-02
B08G8396A	255.00	1501.00	AXIAL	+6K,-2K	+/- 10%		80.00	STRAIN, BIAX		1-6	4	X	1U51212-02
B08G8397A	255.00	1501.00	TANG.	+6K,-2K	+/- 10%		80.00	STRAIN, BIAX		1-6	4	X	1U51212-02
B08G8398A	270.00	1501.00	AXIAL	+6K,-2K	+/- 10%		160.00	STRAIN, BIAX		1-6	4		1U51212-02
B08G8399A	270.00	1501.00	TANG.	+6K,-2K	+/- 10%		160.00	STRAIN, BIAX		1-6	4		1U51212-02
B08G8400A	285.00	1501.00	AXIAL	+6K,-2K	+/- 10%		80.00	STRAIN, BIAX		1-6	4		1U51212-02
B08G8401A	285.00	1501.00	TANG.	+6K,-2K	+/- 10%		80.00	STRAIN, BIAX		1-6	4		1U51212-02
B08G8402A	320.00	1501.00	AXIAL	+6K,-2K	+/- 10%		160.00	STRAIN, BIAX		1-6	4	X	1U51212-02
B08G8403A	320.00	1501.00	TANG.	+6K,-2K	+/- 10%		160.00	STRAIN, BIAX		1-6	4	X	1U51212-02
B08G8404A	180.00	1797.00	AXIAL	+6K,-2K	+/- 10%		160.00	STRAIN, BIAX		1-6	10	X	1U51212-02
B08G8405A	180.00	1797.00	TANG.	+6K,-2K	+/- 10%		160.00	STRAIN, BIAX		1-6	10	X	1U51212-02
B08G8406A	82.00	1797.00	AXIAL	+6K,-2K	+/- 10%		80.00	STRAIN, BIAX		1-6	10	X	1U51212-02
B08G8407A	82.00	1797.00	TANG.	+6K,-2K	+/- 10%		80.00	STRAIN, BIAX		1-6	10	X	1U51212-02
B08G8408A	0.00	1797.00	AXIAL	+6K,-2K	+/- 10%		160.00	STRAIN, BIAX		1-6	10	X	1U51212-02

INST.NO	ANG. LOC.	STATION	MEAS. DIR	RANGE	REQ. ACC.	FM (hz)	DIG. (sps)	REMARKS	KSC INSTLD.	FLT. NO.	NOTES	OFI	PART NOS.
B08G8409A	0.00	1797.00	TANG.	+6K,-2K	+/- 10%		160.00	STRAIN, BIAX		1-6	10	X	1U51212-02
B08G8410A	270.00	1797.00	AXIAL	+6K,-2K	+/- 10%		80.00	STRAIN, BIAX		1-6	10	X	1U51212-02
B08G8411A	270.00	1797.00	TANG.	+6K,-2K	+/- 10%		80.00	STRAIN, BIAX		1-6	10	X	1U51212-02
B08G8412A	180.00	1875.00	AXIAL	+6K,-2K	+/- 10%		160.00	STRAIN, BIAX		1-6	5		1U51212-02
B08G8413A	180.00	1875.00	TANG.	+6K,-2K	+/-10%		160.00	STRAIN, BIAX		1-6	5		1U51212-02
B08G8414A	180.00	1871.00	AXIAL	+6K,-2K	+/- 10%		80.00	STRAIN, UNIAX		1-6	5		1U51212-02
B08G8415A	180.00	1868.00	TANG.	+6K,-2K	+/-10%		80.00	STRAIN, BIAX		1-6	5		1U51212-02
B08G8416A	180.00	1868.00	AXIAL	+6K,-2K	+/- 10%		160.00	STRAIN, BIAX		1-6	5		1U51212-02
B08G8417A	90.00	1875.00	AXIAL	+6K,-2K	+/- 10%		80.00	STRAIN, BIAX		1-6	5		1U51212-02
B08G8418A	90.00	1875.00	TANG.	+6K,-2K	+/-10%		160.00	STRIAN, BIAX		1-6	5		1U51212-02
B08G8419A	90.00	1871.00	AXIAL	+6K,-2K	+/- 10%		160.00	STRAIN, UNIAX		1-6	5		1U51212-02
B08G8420A	90.00	1868.00	TANG.	+6K,-2K	+/-10%		80.00	STRAIN, BIAX		1-6	5		1U51212-02
B08G8421A	90.00	1868.00	AXIAL	+6K,-2K	+/- 10%		80.00	STRAIN, BIAX		1-6	5		1U51212-02
B08G8422A	0.00	1875.00	AXIAL	+6K,-2K	+/- 10%		160.00	STRAIN, BIAX		1-6	5		1U51212-02
B08G8423A	0.00	1875.00	TANG.	+6K,-2K	+/-10%		160.00	STRAIN, BIAX		1-6	5		1U51212-02
B08G8424A	0.00	1871.00	AXIAL	+6K,-2K	+/- 10%		80.00	STRAIN, UNIAX		1-6	5		1U51212-02
B08G8425A	0.00	1868.00	TANG.	+6K,-2K	+/-10%		80.00	STRAIN, BIAX		1-6	5		1U51212-02
B08G8426A	0.00	1868.00	AXIAL	+6K,-2K	+/- 10%		160.00	STRAIN, BIAX		1-6	5		1U51212-02
B08G8427A	270.00	1875.00	AXIAL	+6K,-2K	+/- 10%		80.00	STRAIN, BIAX		1-6	5		1U51212-02
B08G8428A	270.00	1875.00	TANG.	+6K,-2K	+/-10%		160.00	STRAIN, BIAX		1-6	5		1U51212-02
B08G8429A	270.00	1871.00	AXIAL	+6K,-2K	+/- 10%		160.00	STRAIN, UNIAX		1-6	5		1U51212-02
B08G8430A	270.00	1868.00	TANG.	+6K,-2K	+/-10%		80.00	STRAIN, BIAX		1-6	5		1U51212-02
B08G8431A	270.00	1868.00	AXIAL	+6K,-2K	+/- 10%		80.00	STRAIN, BIAX		1-6	5		1U51212-02
B08G8440A	45.00	1922.00	AXIAL	+6K,-2K	+/- 10%		160.00	STRAIN, BIAX		1&5	5,14		1U51212-02
B08G8441A	45.00	1922.00	TANG.	+6K,-2K	+/- 10%		160.00	STRAIN, BIAX		1&5	5,14		1U51212-02
B07T8606A	191.00	486.40		0-400 deg	+/- 1%		10.00	TEMP. SRM		1-6	8		16A03055-1
B07T8607A	180.00	846.30		0-400 deg	+/- 1%		10.00	TEMP. SRM	X	1-6	8		16A03055-1
B07T8608A	60.00	846.30		0-400 deg	+/- 1%		10.00	TEMP. SRM	X	1-6	8		16A03055-1
B07T8609A	300.00	846.30		0-400 deg	+/- 1%		10.00	TEMP. SRM	X	1-6	8		16A03055-1
B07T8610A	180.00	1486.30		0-400 deg	+/- 1%		10.00	TEMP. SRM	X	1-6	8		16A03055-1
B07T8611A	60.00	1486.30		0-400 deg	+/- 1%		10.00	TEMP. SRM	X	1-6	8		16A03055-1
B07T8612A	300.00	1486.30		0-400 deg	+/- 1%		10.00	TEMP. SRM	X	1-6	8		16A03055-1
B07T8613A	180.00	1877.50		0-400 deg	+/- 1%		10.00	TEMP. SRM		1-6	8		16A03055-1
B07T8614A	90.00	1877.50		0-400 deg	+/- 1%		10.00	TEMP. SRM		1-6	5,12		16A03055-1

DFI FLIGHT 1 INSTRUMENTATION

INST.NO	ANG. LOC.	STATION	MEAS. DIR	RANGE	REQ. ACC.	FM (hz)	DIG. (sps)	REMARKS	KSC INSTLD.	FLT. NO.	NOTES	OFI	PART NOS.
B07T8615A	0.00	1877.50		0-400 deg	+/- 1%		10.00	TEMP. SRM		1-6	5,12		16A03055-1
B07T8616A	270.00	1877.50		0-400 deg	+/- 1%		10.00	TEMP. SRM		1-6	5,12		16A03055-1
B07T8622A	0.00	1905.00		0-750 deg	+/- 1%		10.00	TEMP. SRM		1-6	5		16A03055-1
B07T8625A	300.00	1996.50		0-750 deg	+/- 1%		10.00	TEMP. SRM		1-6	5		
B47P2300A		487.00		0-1050 psia	+/-2%		320.00	OPT		1-6	15		1U50188-07
B47P2301A		487.00		0-1050 psia	+/-2%		320.00	OPT		1-6	15		1U50188-07
B47P2302A		487.00		0-1050 psia	+/-2%		320.00	OPT		1-6	15		1U50188-07
B47P8310A	115.00	487.00		0-3000 psia	+/- 2%	DC-100		PRESSURE, IGNITER CHAMBE		1-6	7		1U50188-08
B08X8942E	270.00	1926.00					10.00	CONTINUITY, T	X	1-6	11		

APPENDIX D

Radial Growth Plots

PREDICTED VS MEASURED RADIAL GROWTH

360L001 GIRTH GAGE B08G7273A – STATION 847.00

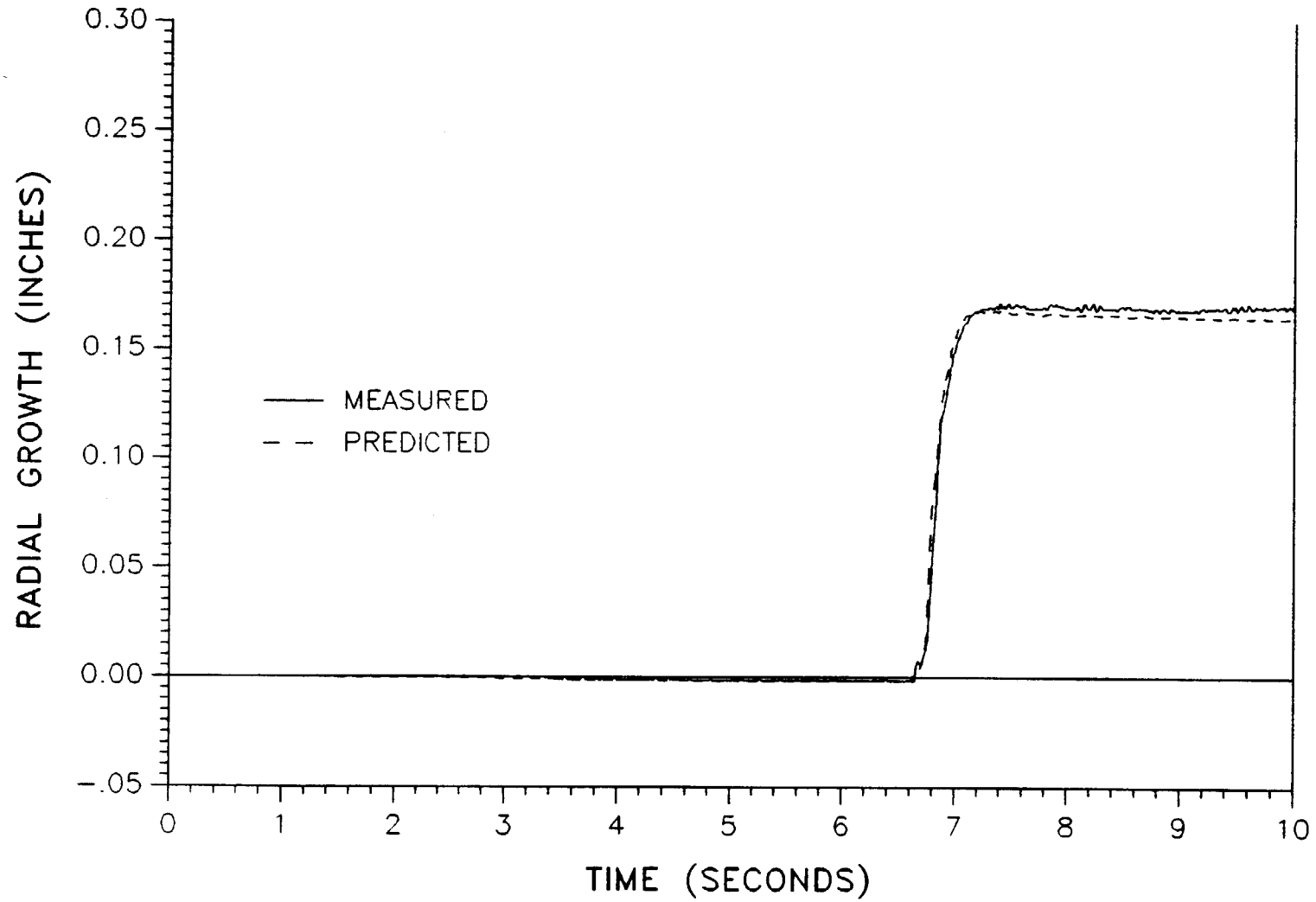

PREDICTED VS MEASURED RADIAL GROWTH

360L001 GIRTH GAGE B08G7274A - STATION 848.75

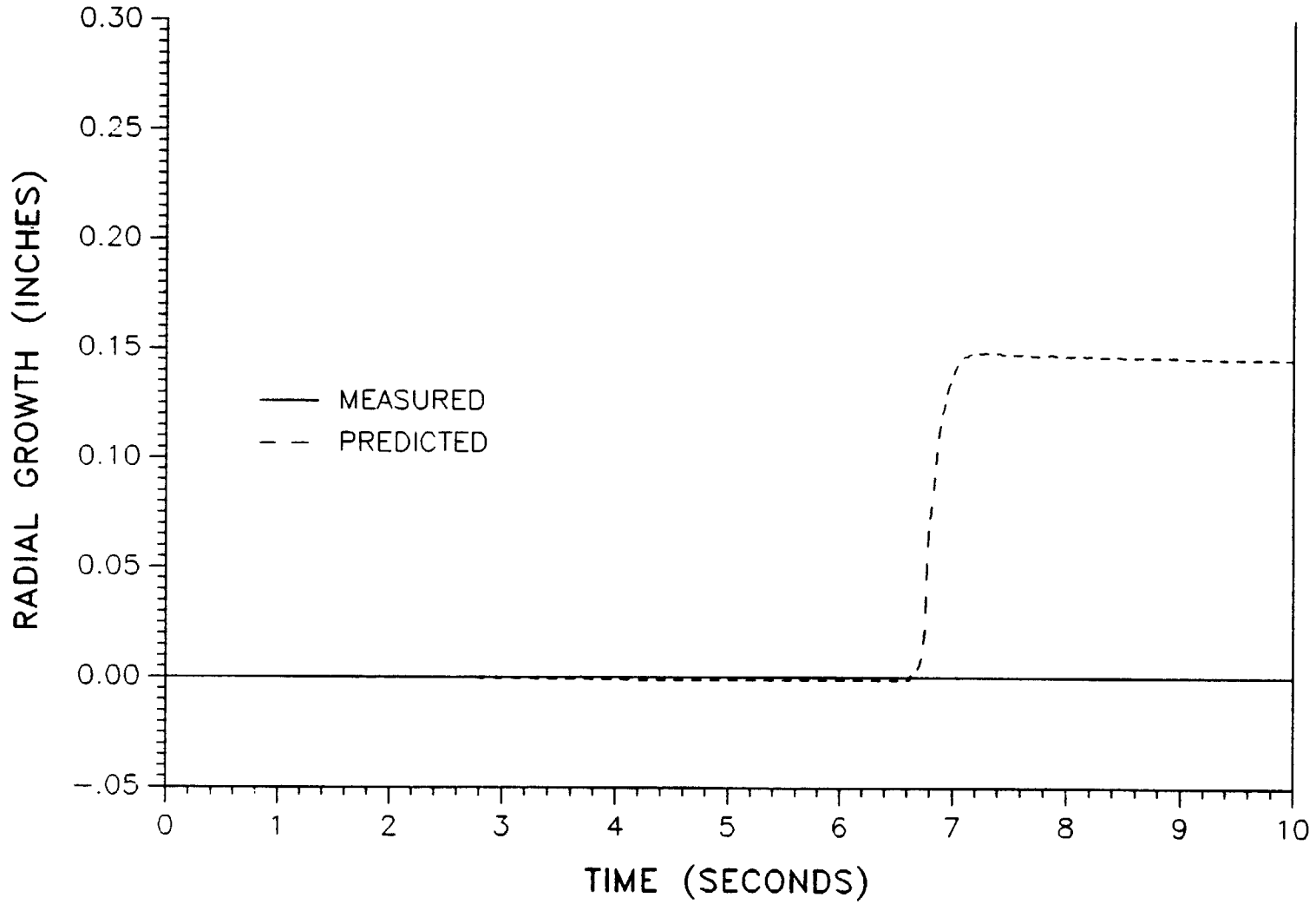

PREDICTED VS MEASURED RADIAL GROWTH

360L001 GIRTH GAGE B08G7275A – STATION 850.20

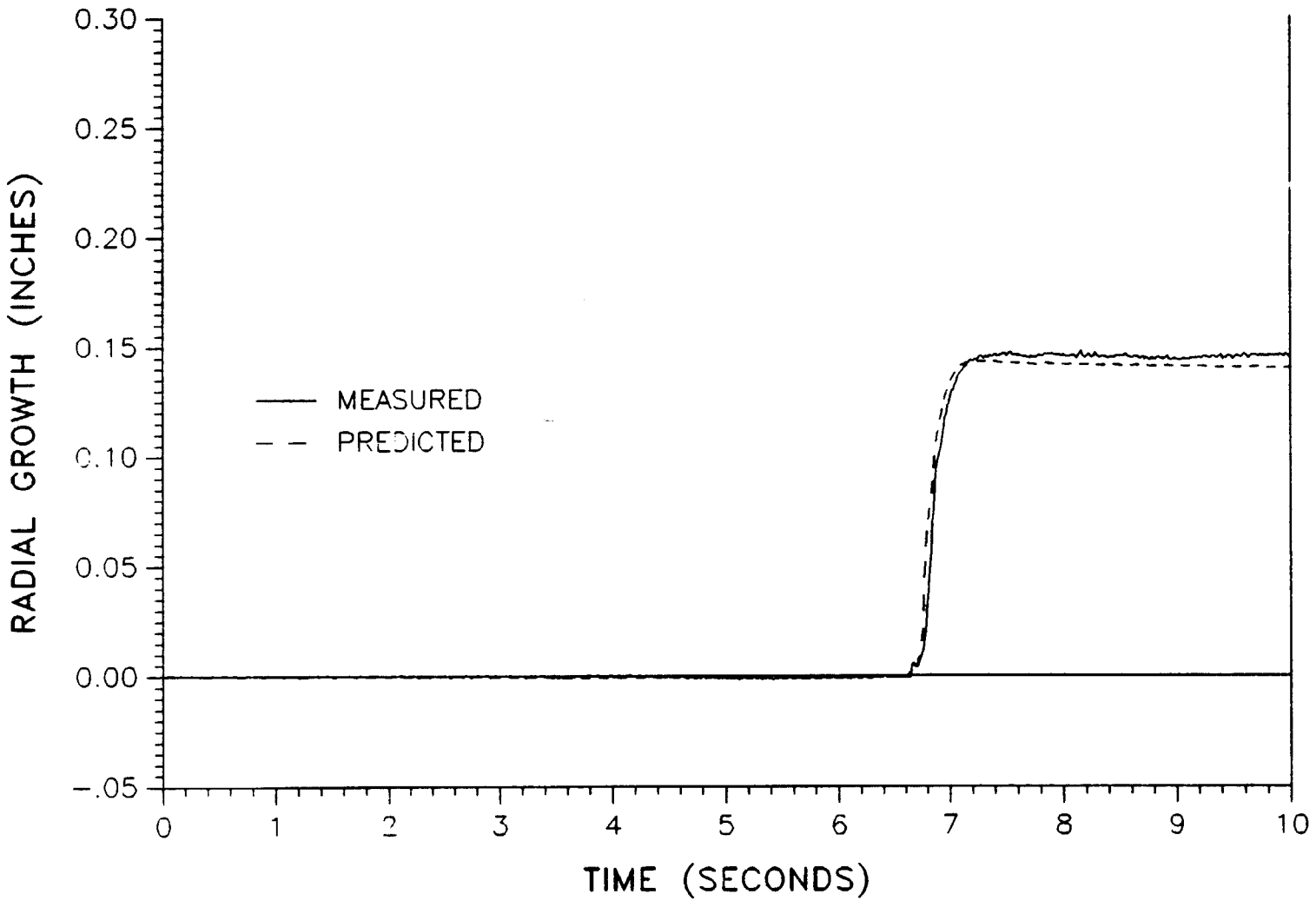

PREDICTED VS MEASURED RADIAL GROWTH

360L001 GIRTH GAGE B08G7276A – STATION 852.80

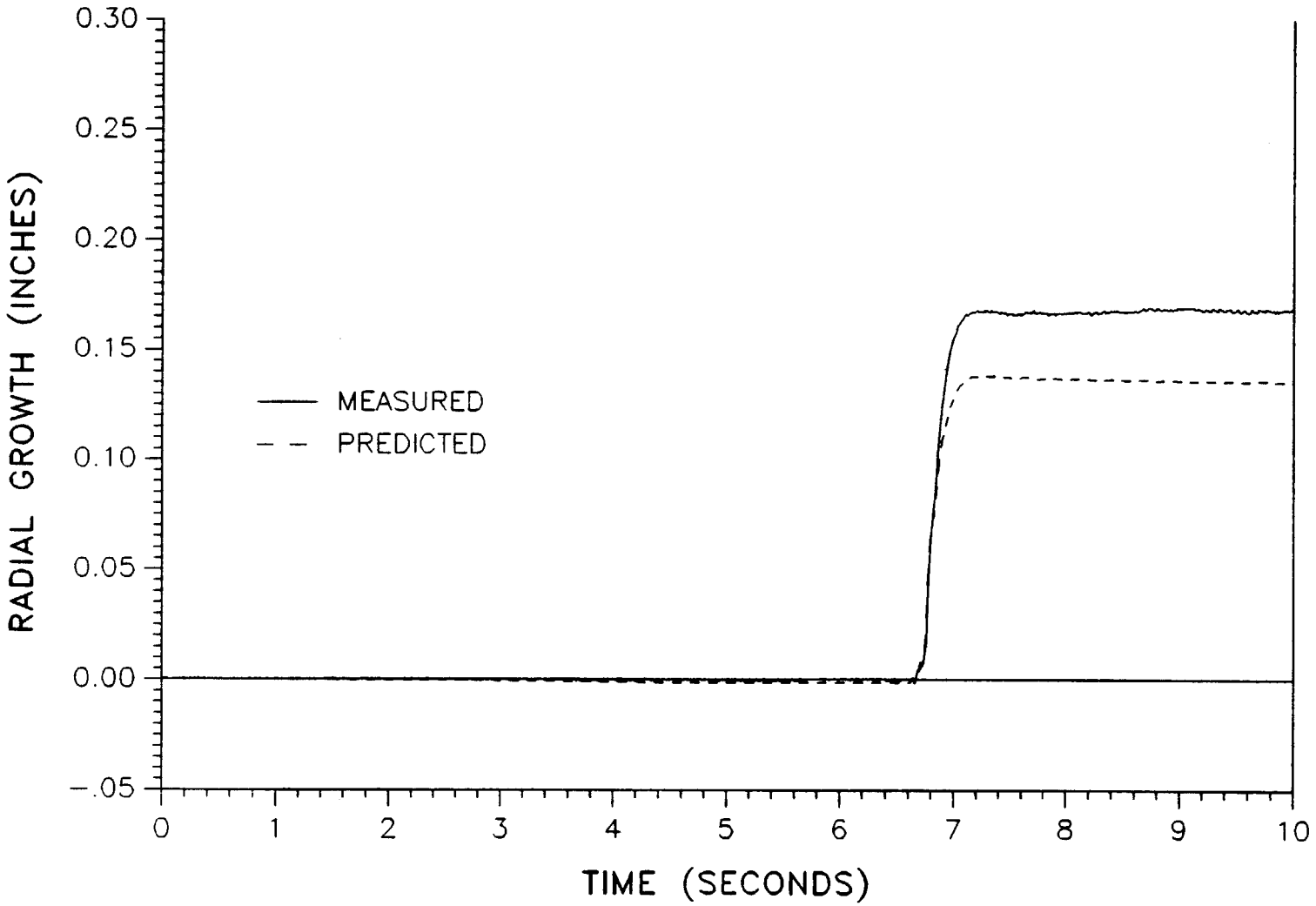

PREDICTED VS MEASURED RADIAL GROWTH

360L001 GIRTH GAGE B08G7277A - STATION 855.50

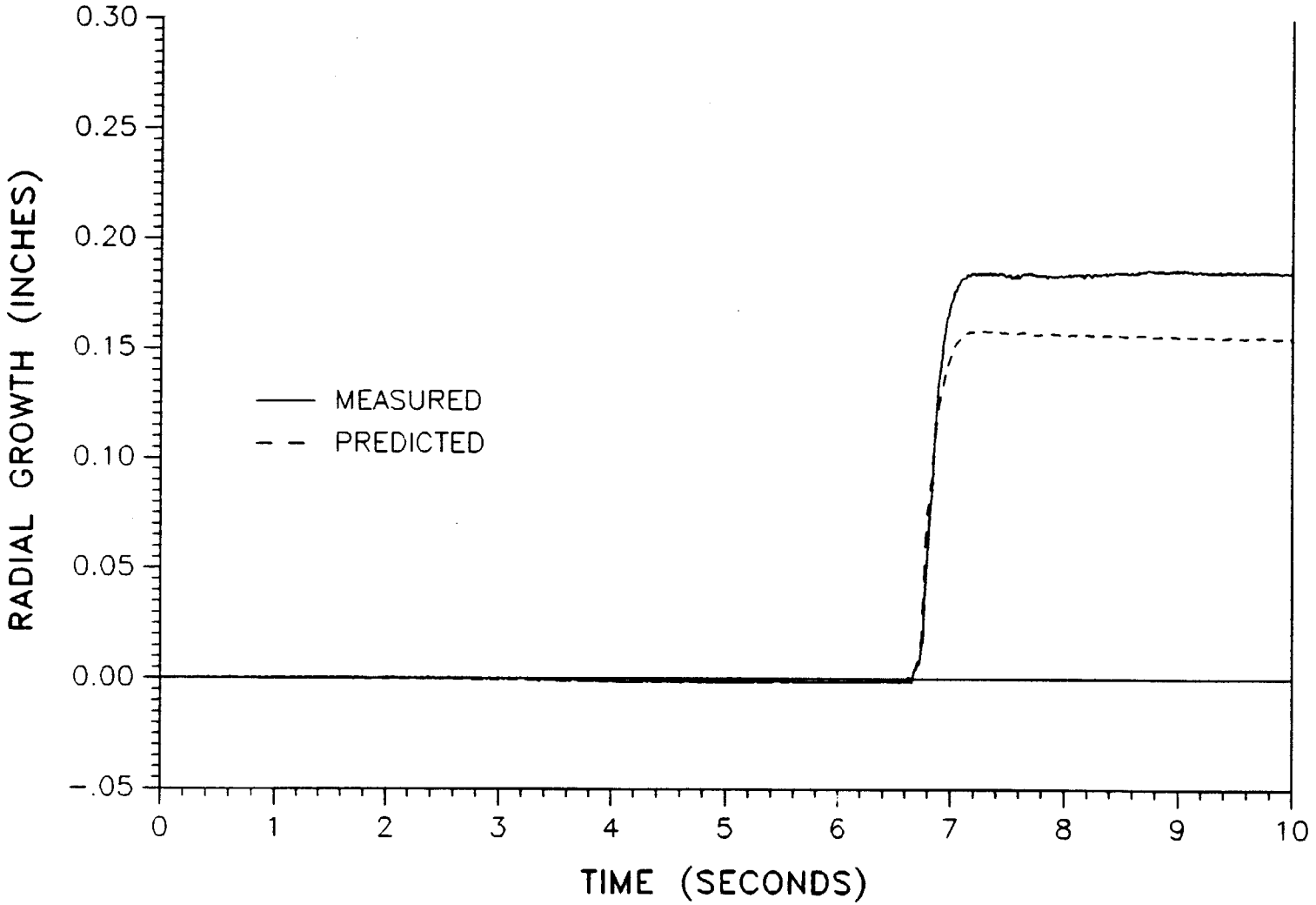

PREDICTED VS MEASURED RADIAL GROWTH

360L001 GIRTH GAGE B08G7278A – STATION 857.50

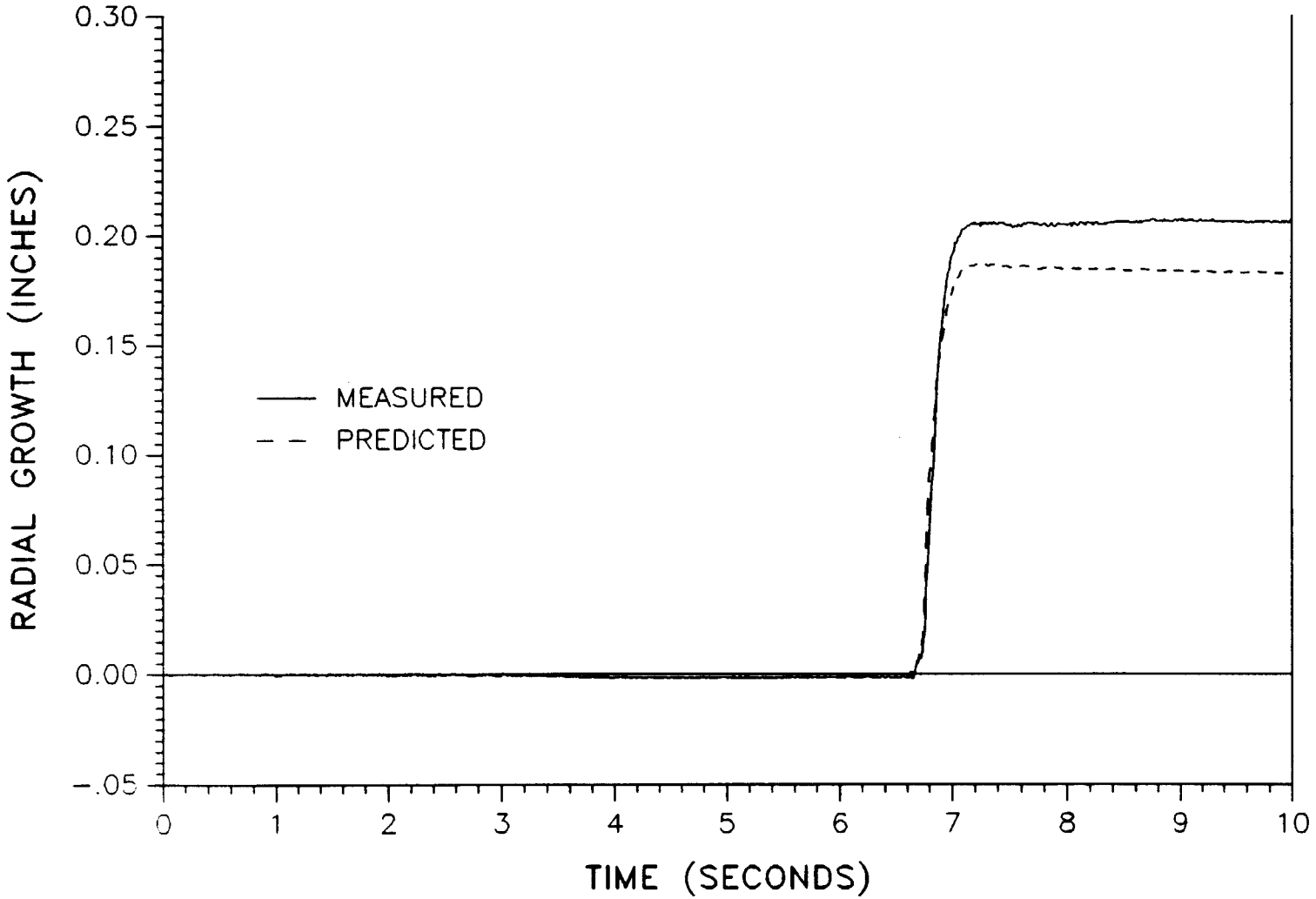

PREDICTED VS MEASURED RADIAL GROWTH

360L001 GIRTH GAGE B08G7282A – STATION 1091.50

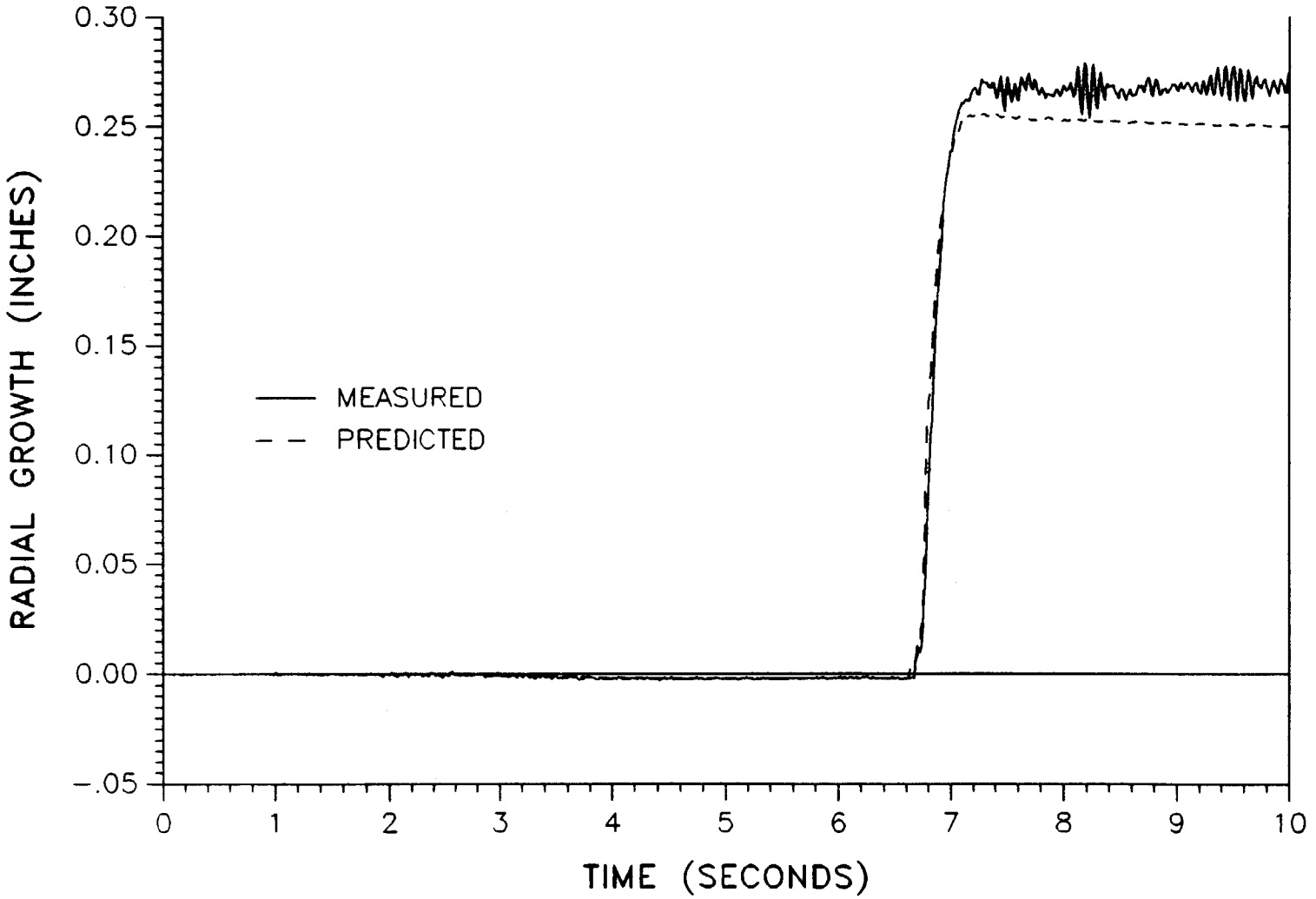

PREDICTED VS MEASURED RADIAL GROWTH

360L001 GIRTH GAGE B08G7283A – STATION 1167.00

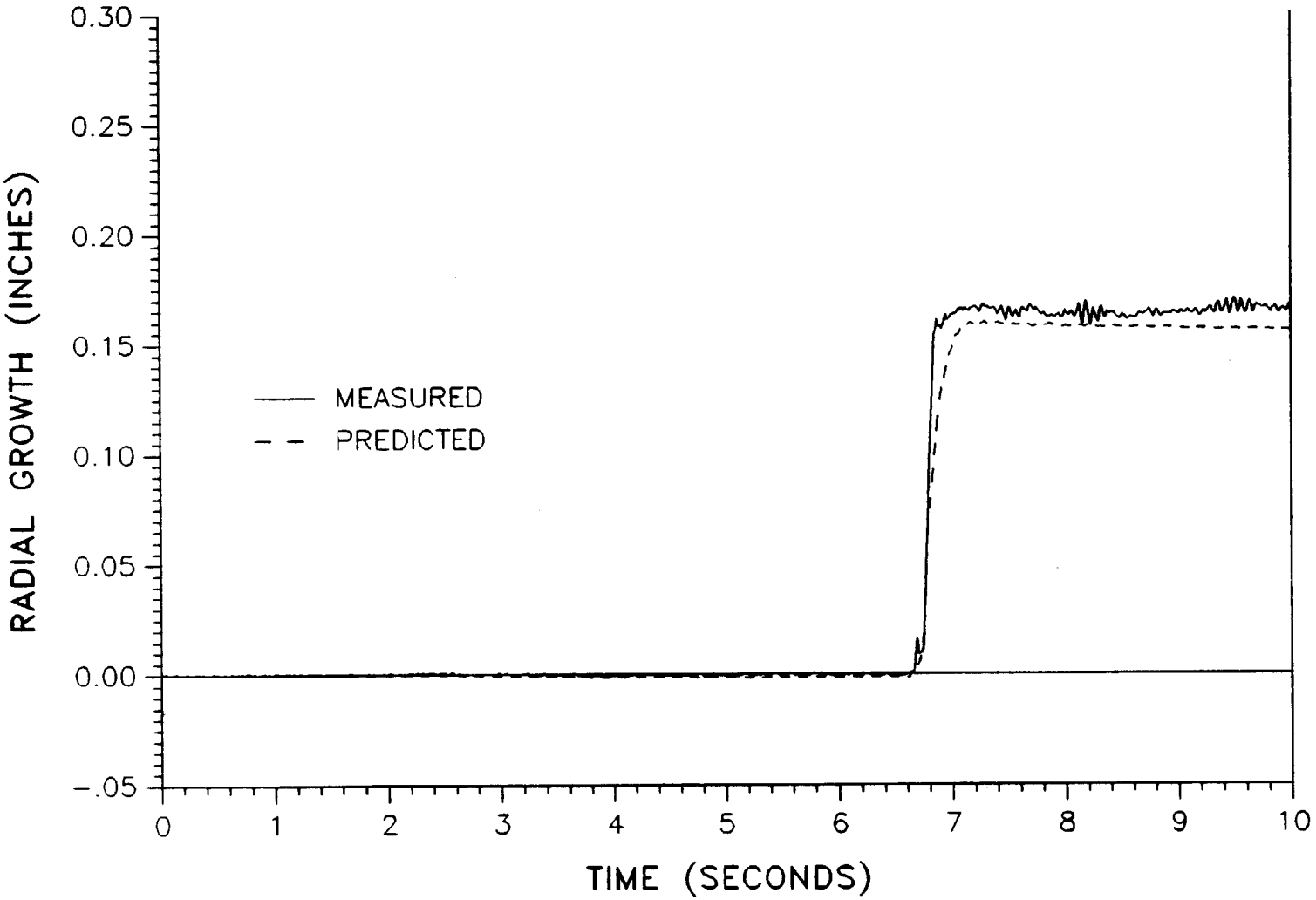

PREDICTED VS MEASURED RADIAL GROWTH

360L001 GIRTH GAGE B08G7284A – STATION 1168.75

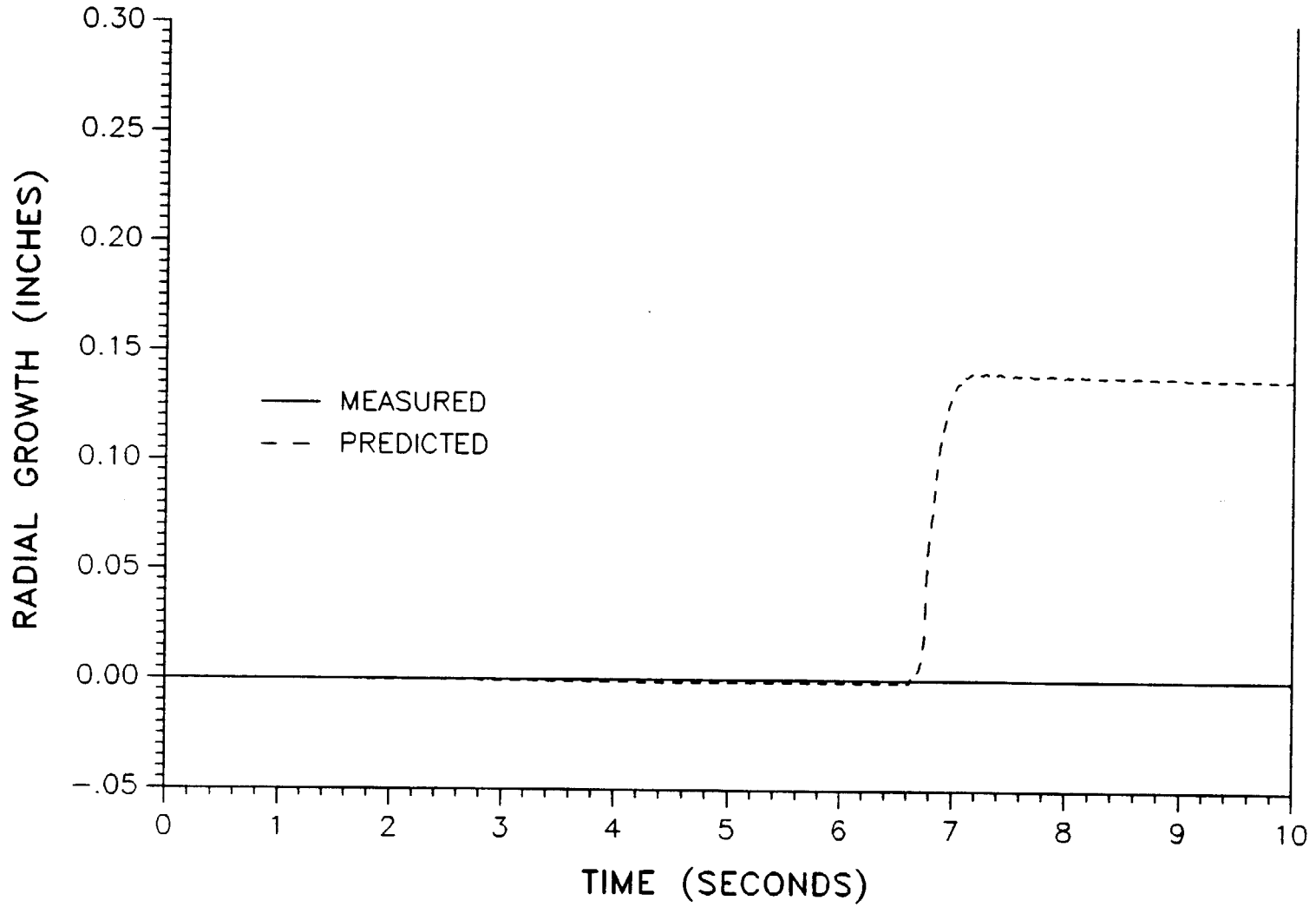

PREDICTED VS MEASURED RADIAL GROWTH

360L001 GIRTH GAGE B08G7285A – STATION 1170.20

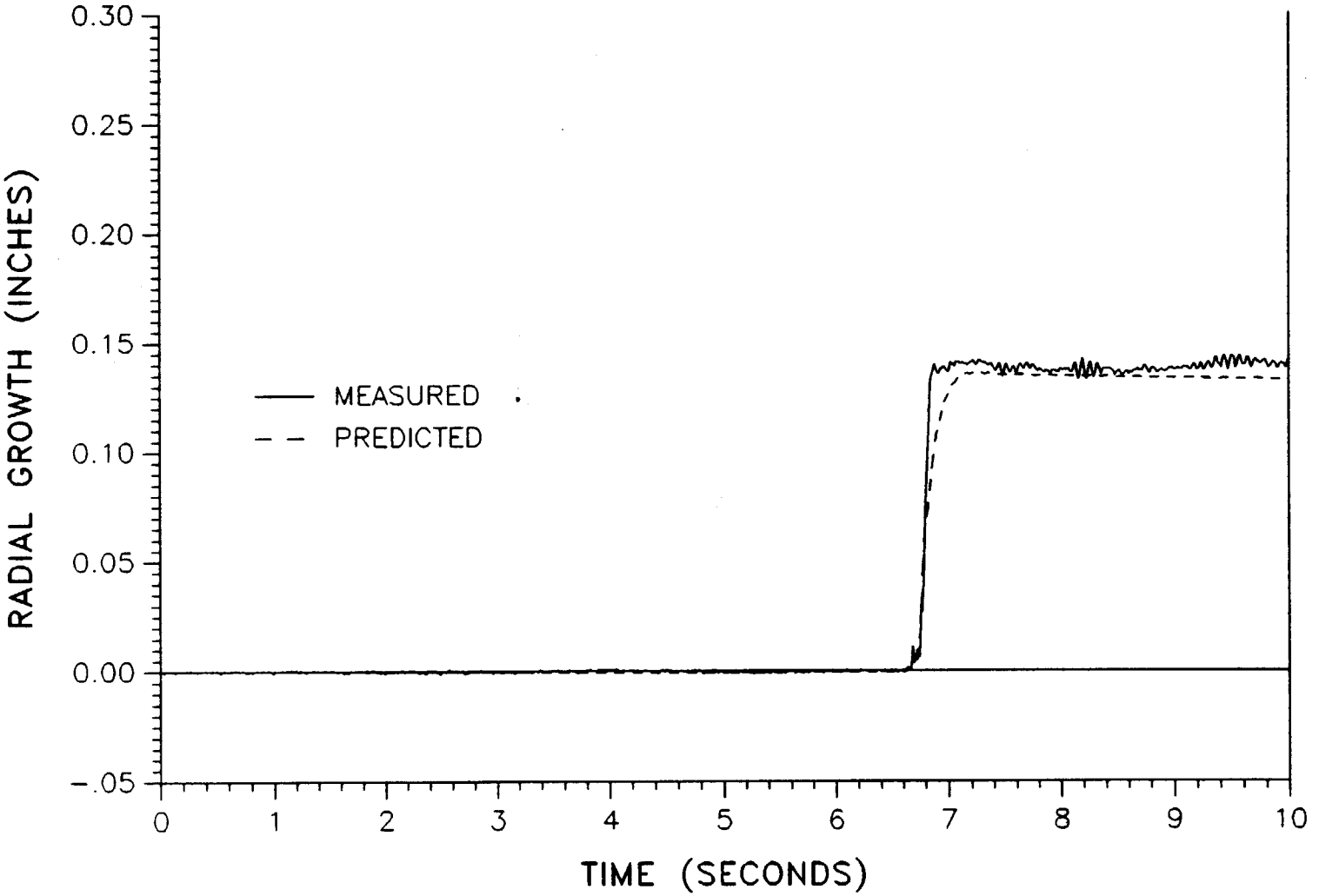

PREDICTED VS MEASURED RADIAL GROWTH

360L001 GIRTH GAGE B08G7286A - STATION 1172.80

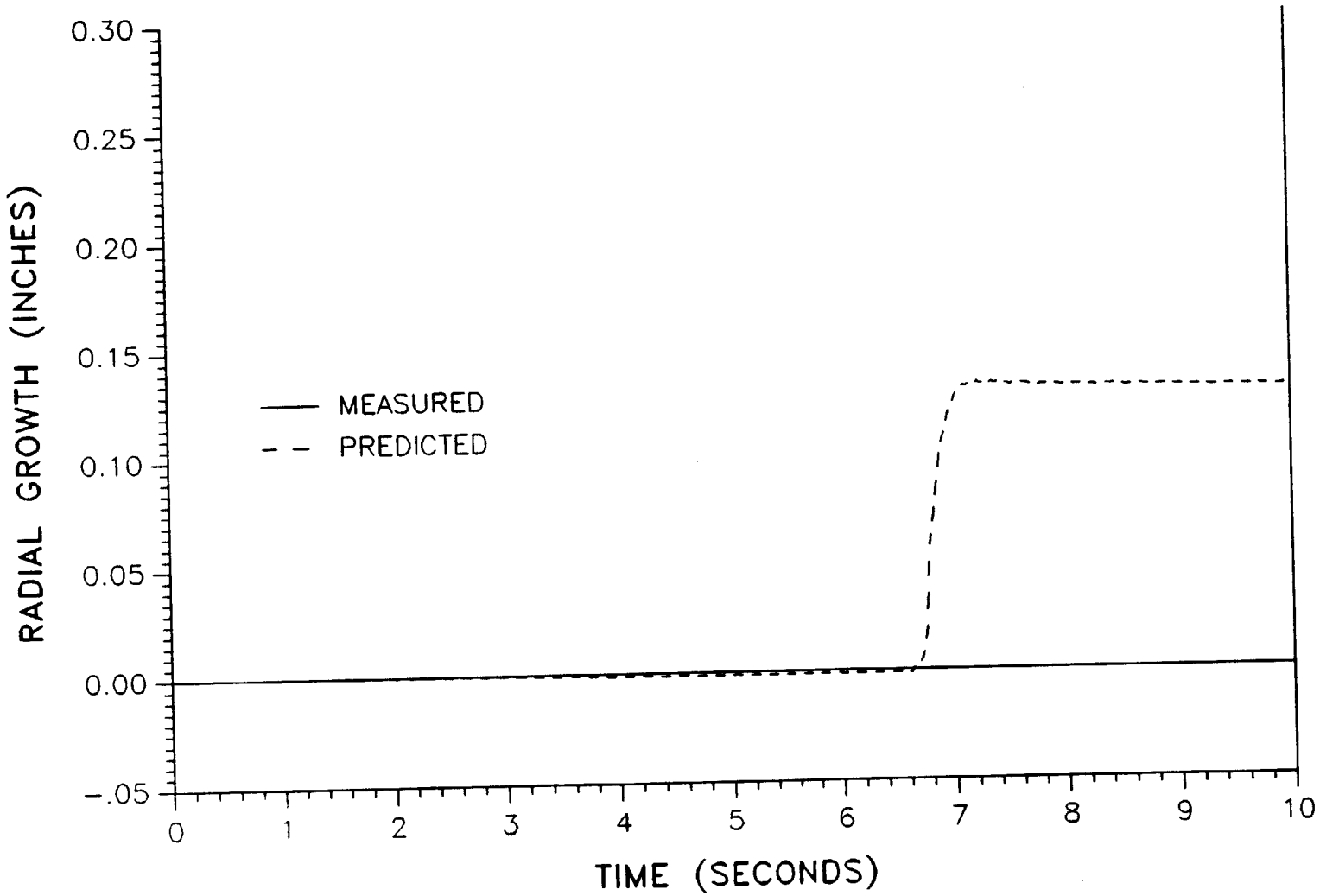

PREDICTED VS MEASURED RADIAL GROWTH

360L001 GIRTH GAGE B08G7287A – STATION 1175.25

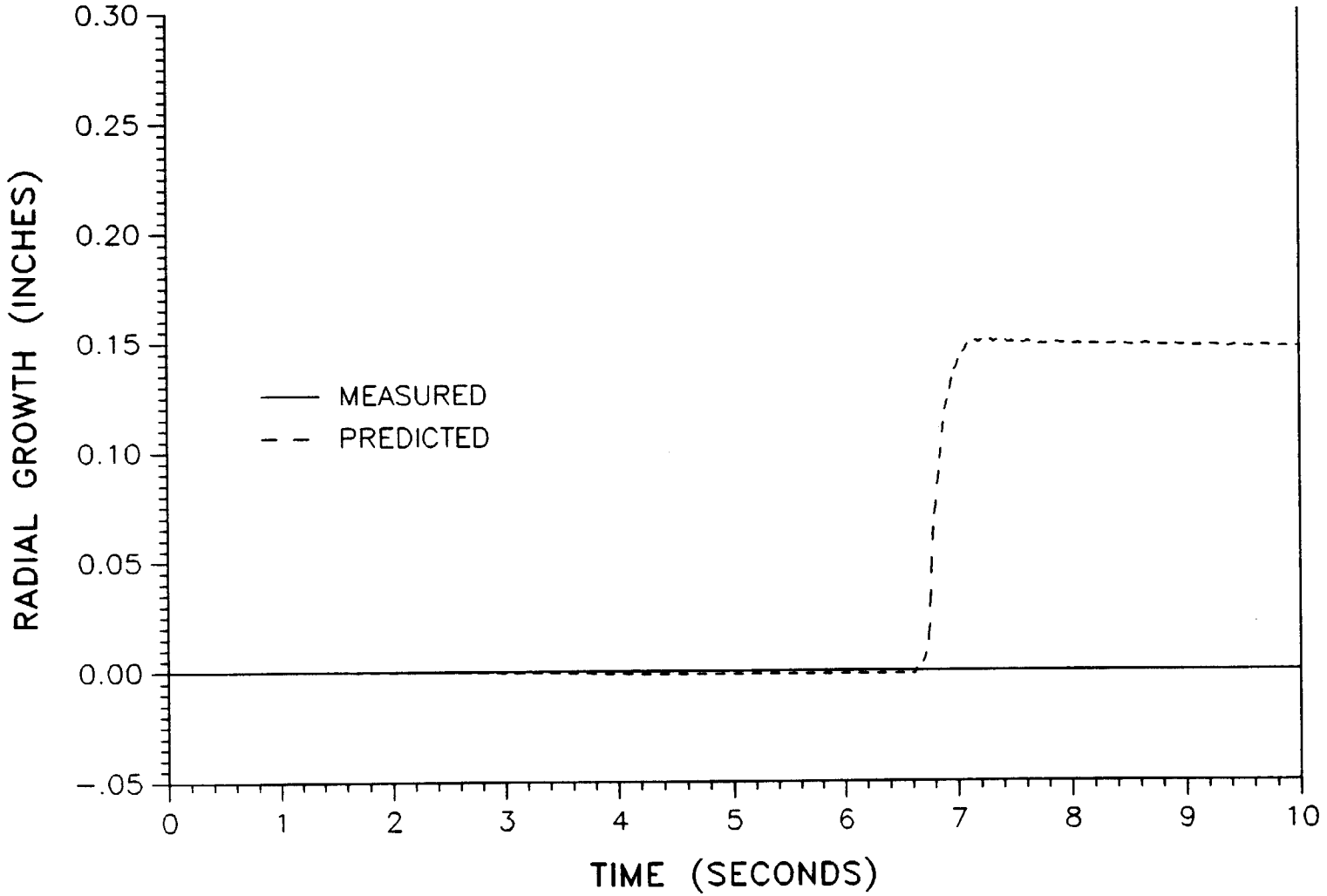

PREDICTED VS MEASURED RADIAL GROWTH

360L001 GIRTH GAGE B08G7288A - STATION 1177.50

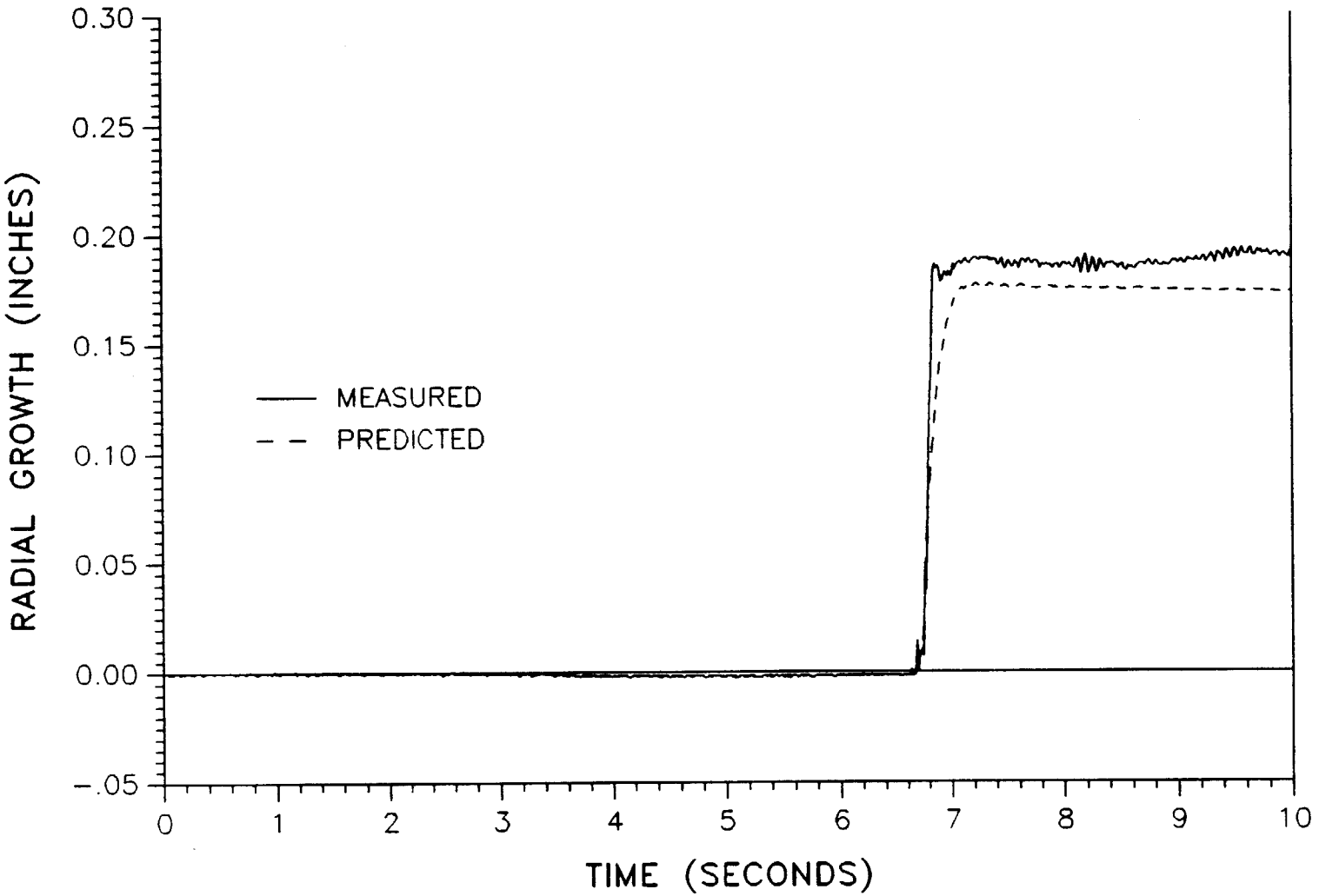

PREDICTED VS MEASURED RADIAL GROWTH

360L001 GIRTH GAGE B08G7292A – STATION 1411.80

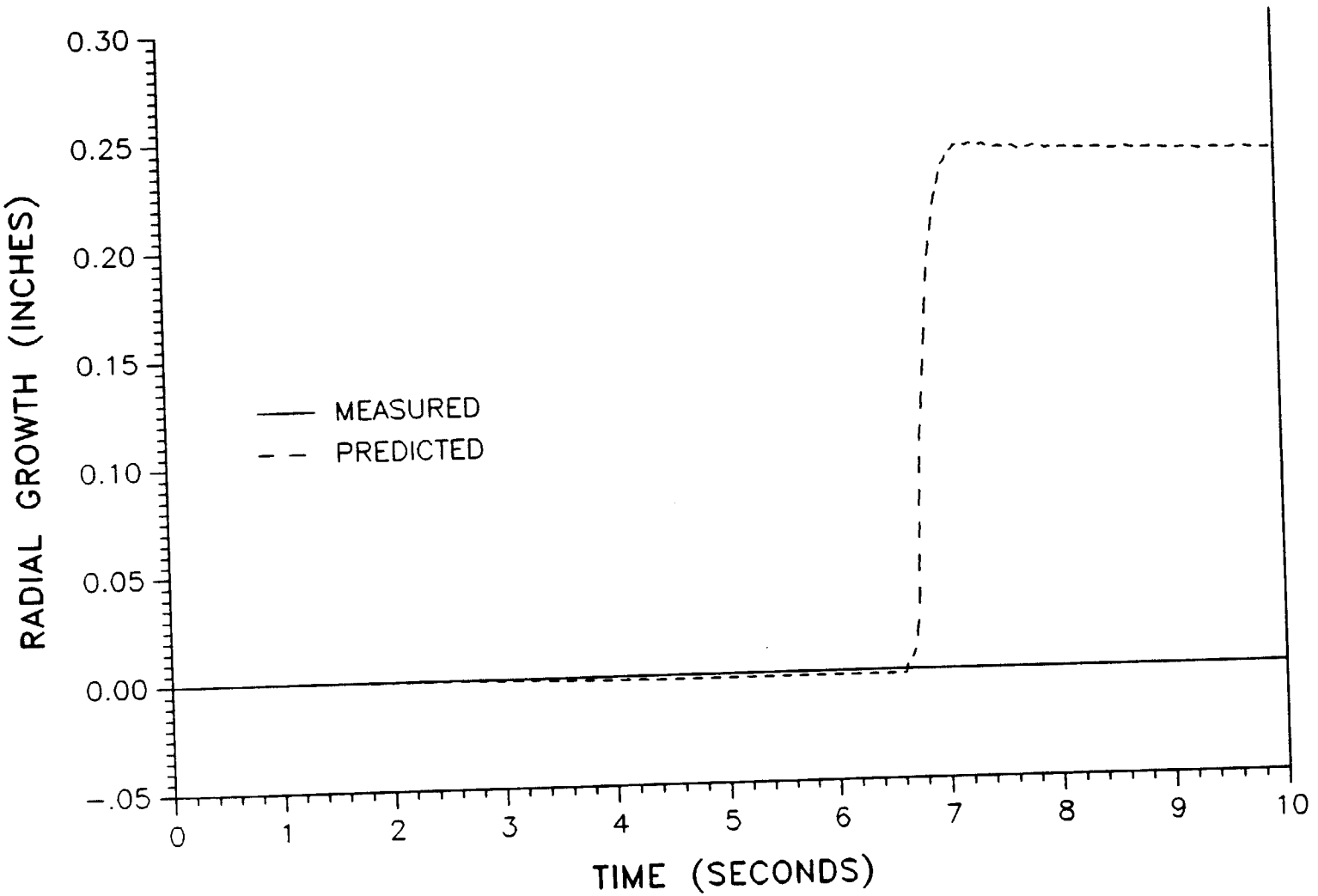

PREDICTED VS MEASURED RADIAL GROWTH

360L001 GIRTH GAGE B08G7293A – STATION 1487.00

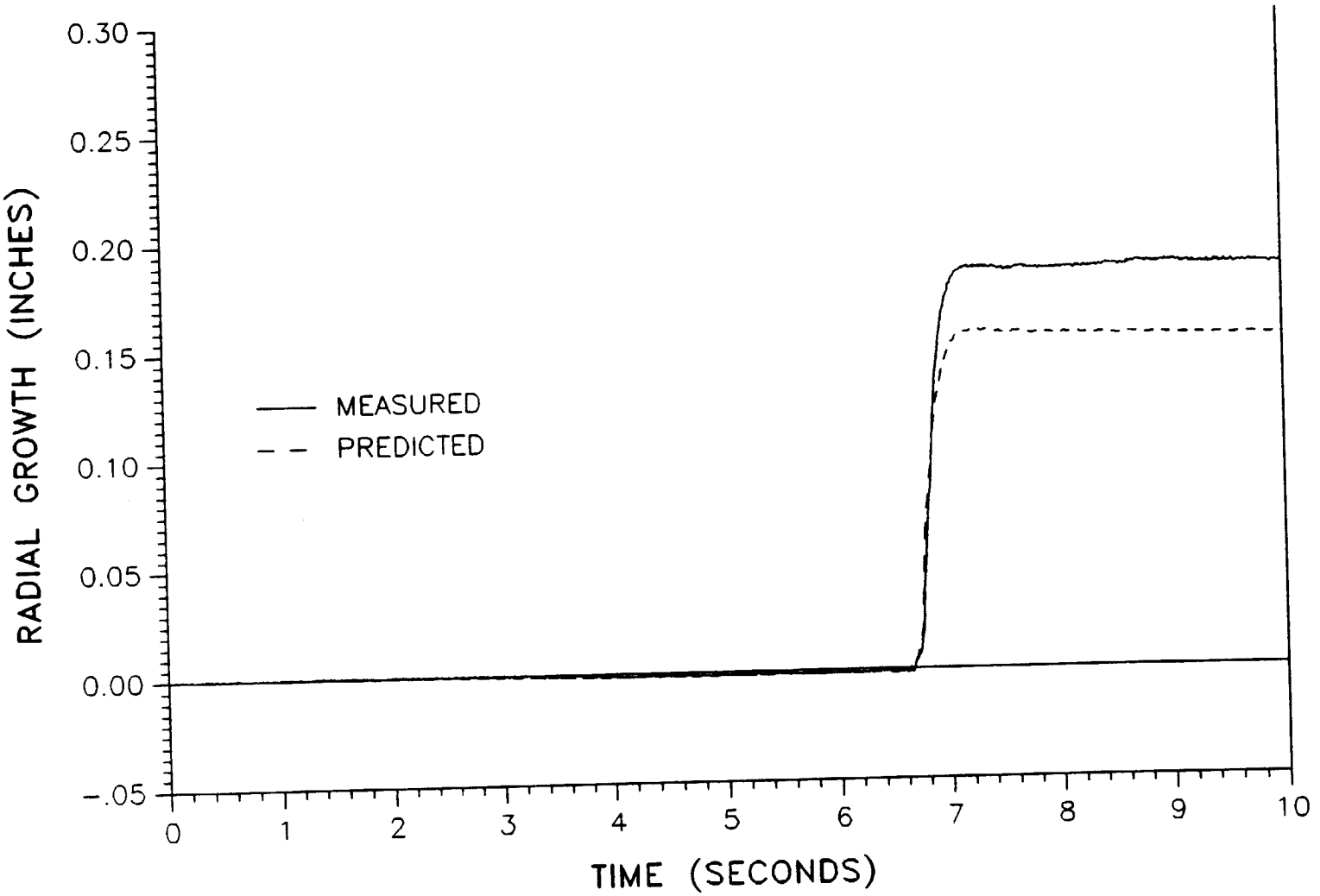

PREDICTED VS MEASURED RADIAL GROWTH

360L001 GIRTH GAGE B08G7294A – STATION 1488.75

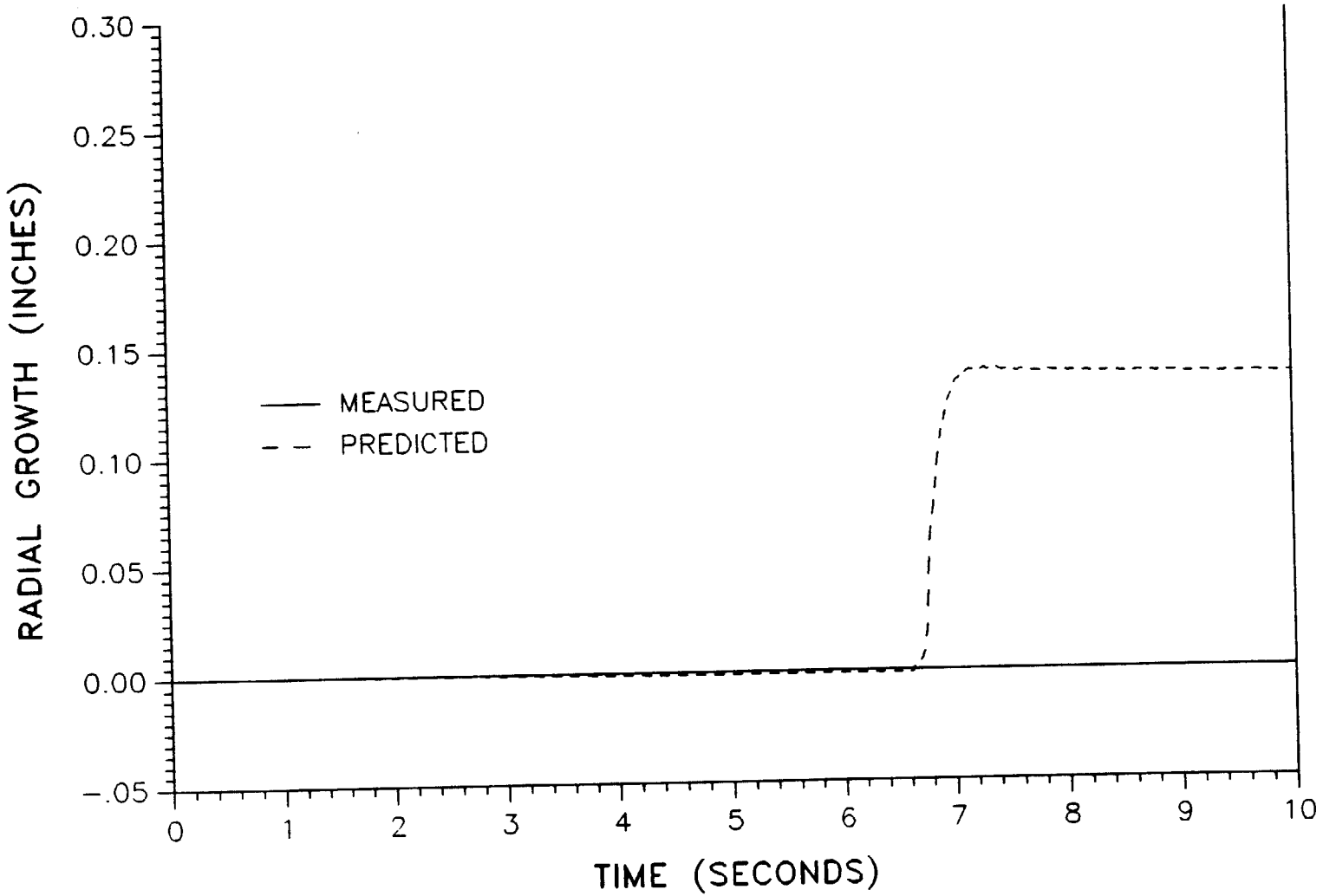

PREDICTED VS MEASURED RADIAL GROWTH

360L001 GIRTH GAGE B08G7295A – STATION 1490.20

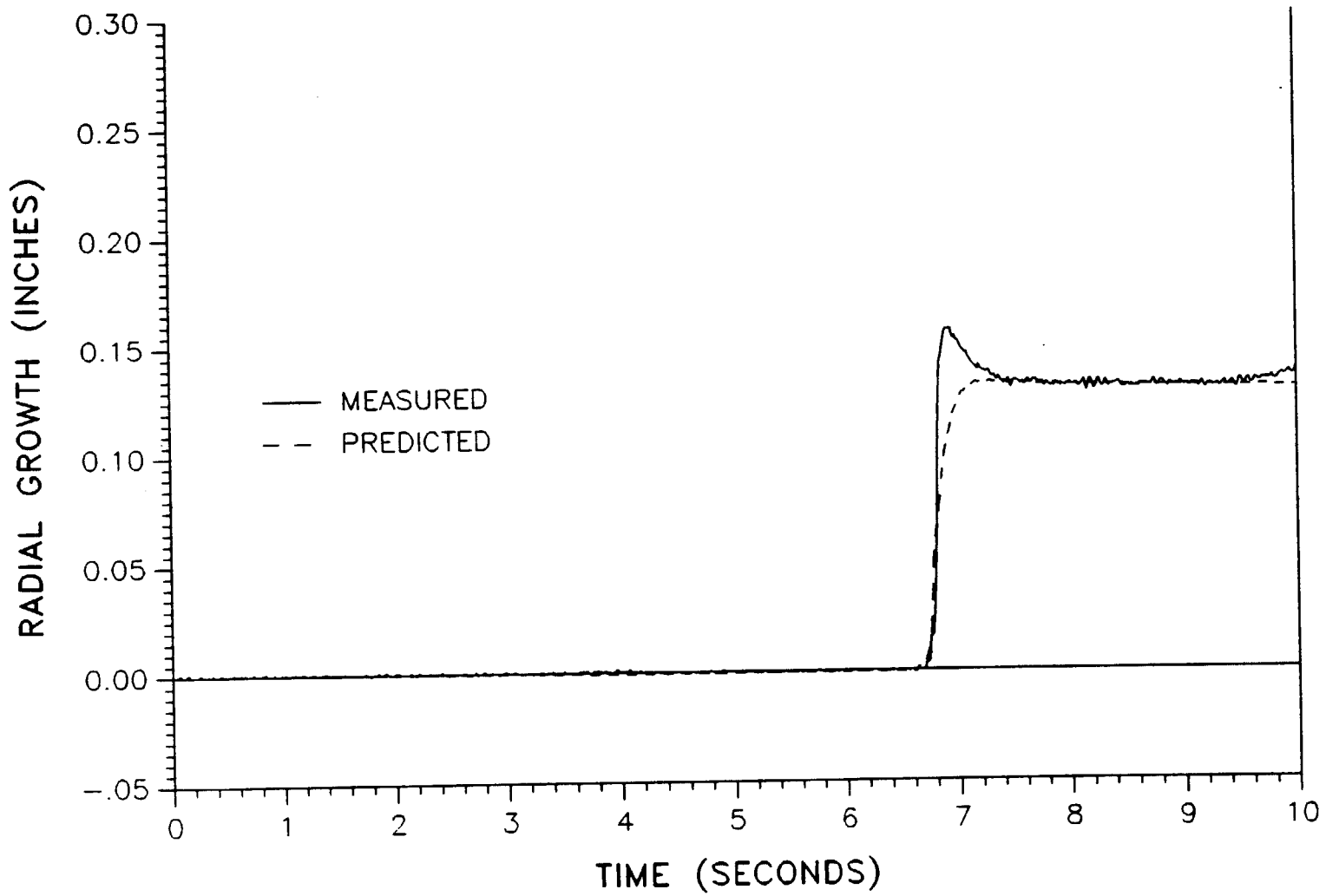

PREDICTED VS MEASURED RADIAL GROWTH

360L001 GIRTH GAGE B08G7296A - STATION 1492.80

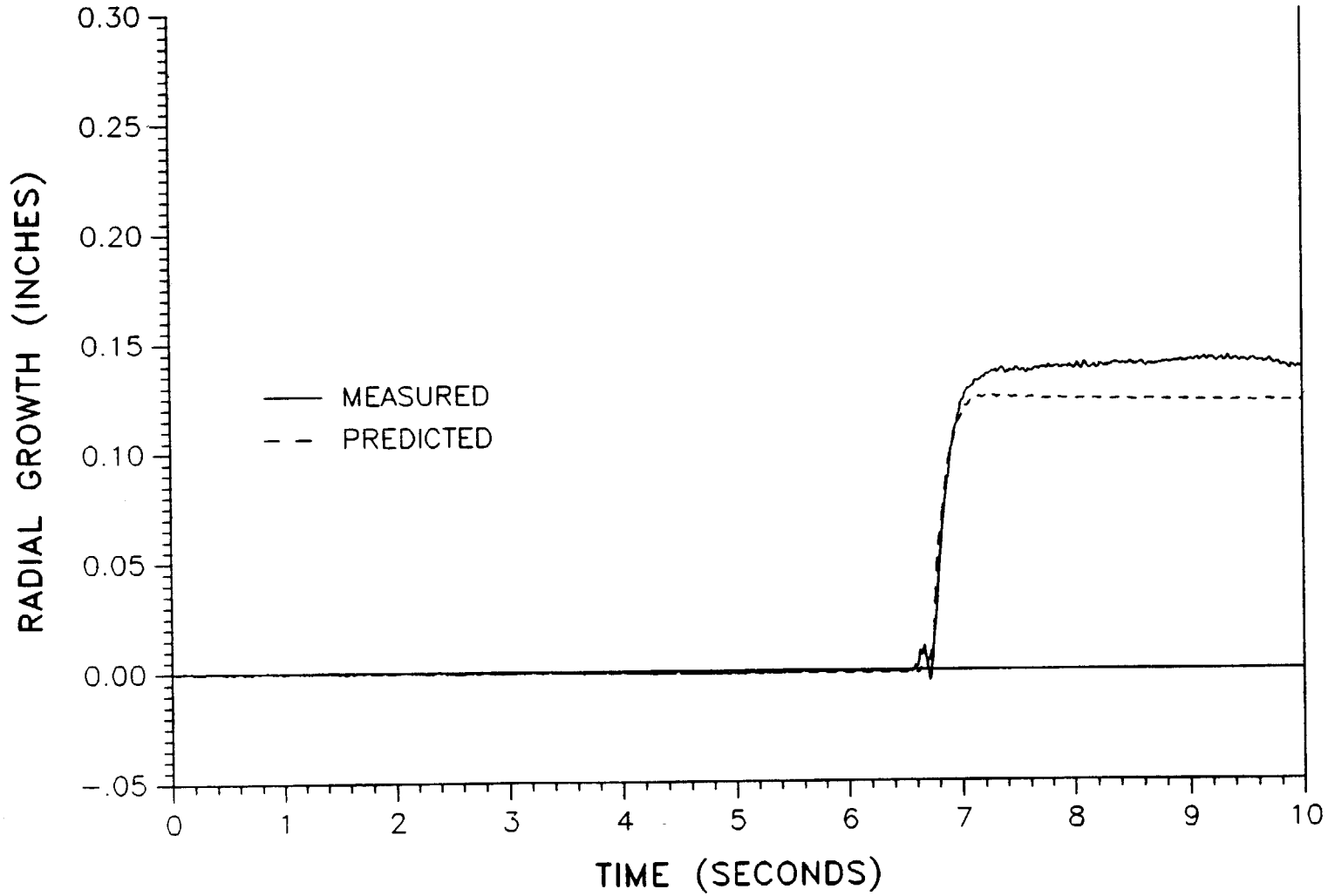

PREDICTED VS MEASURED RADIAL GROWTH

360L001 GIRTH GAGE B08G7297A – STATION 1495.25

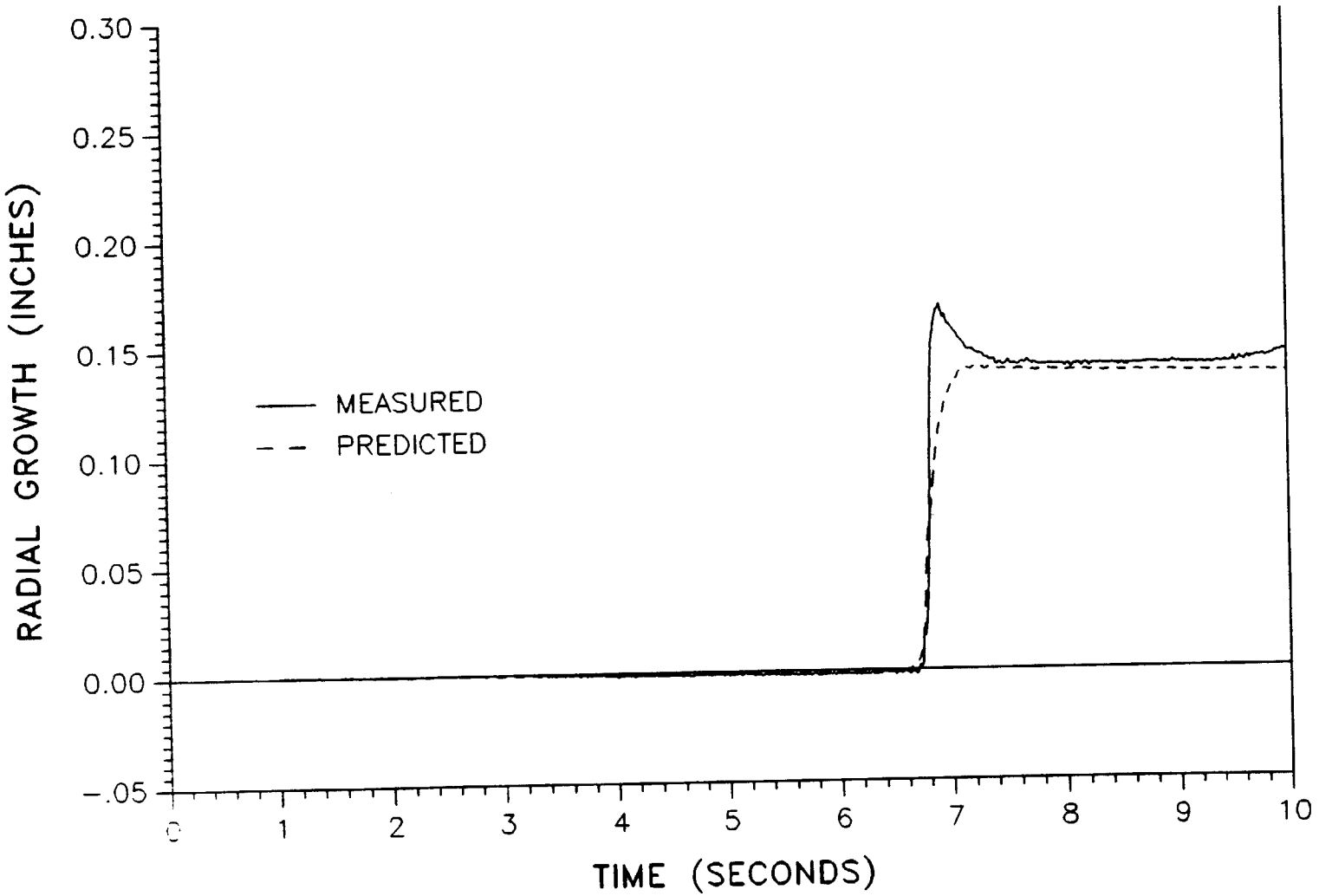

PREDICTED VS MEASURED RADIAL GROWTH

360L001 GIRTH GAGE B08G7298A – STATION 1497.50

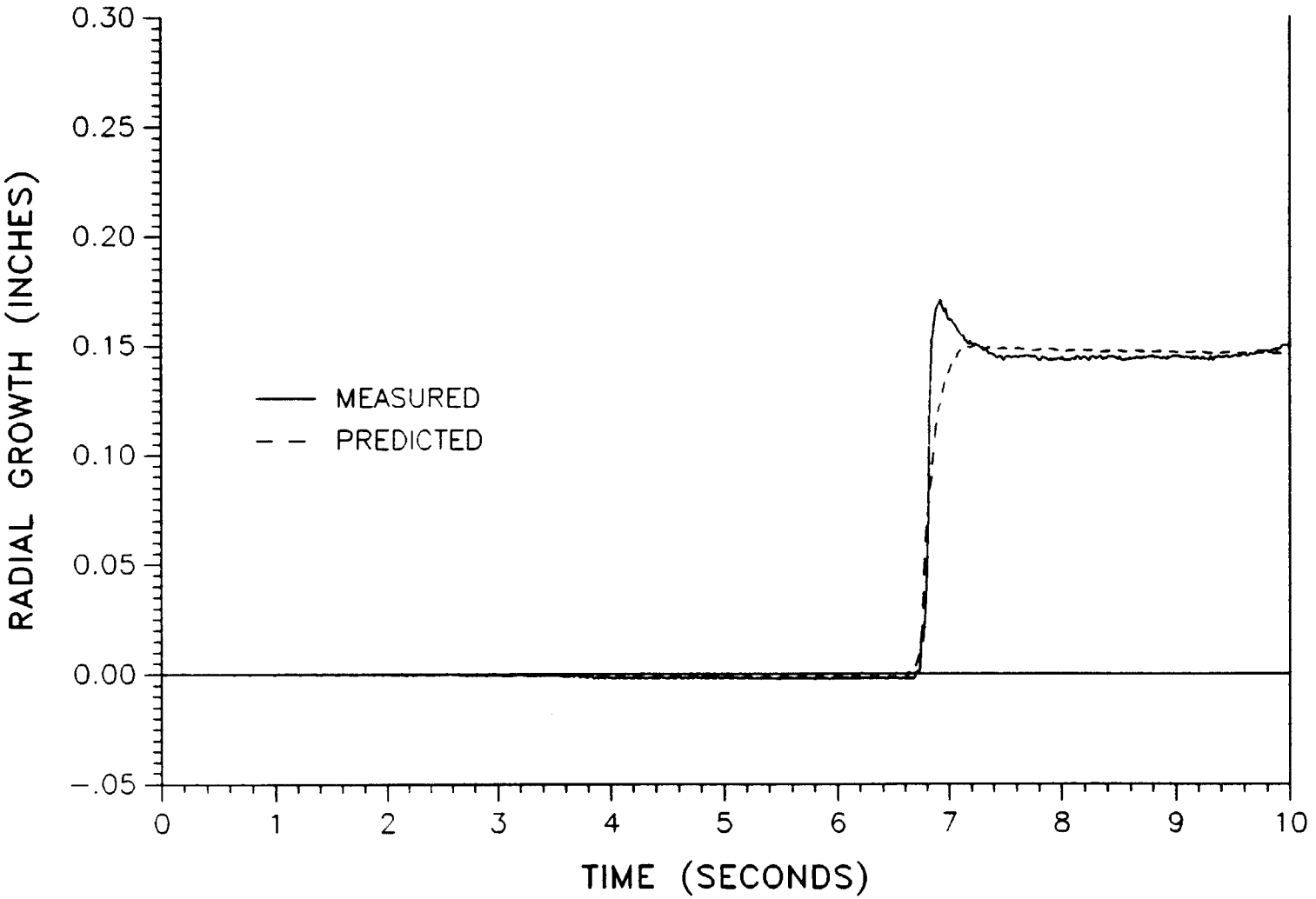

PREDICTED VS MEASURED RADIAL GROWTH

360L001 GIRTH GAGE B08G7299A – STATION 1574.75

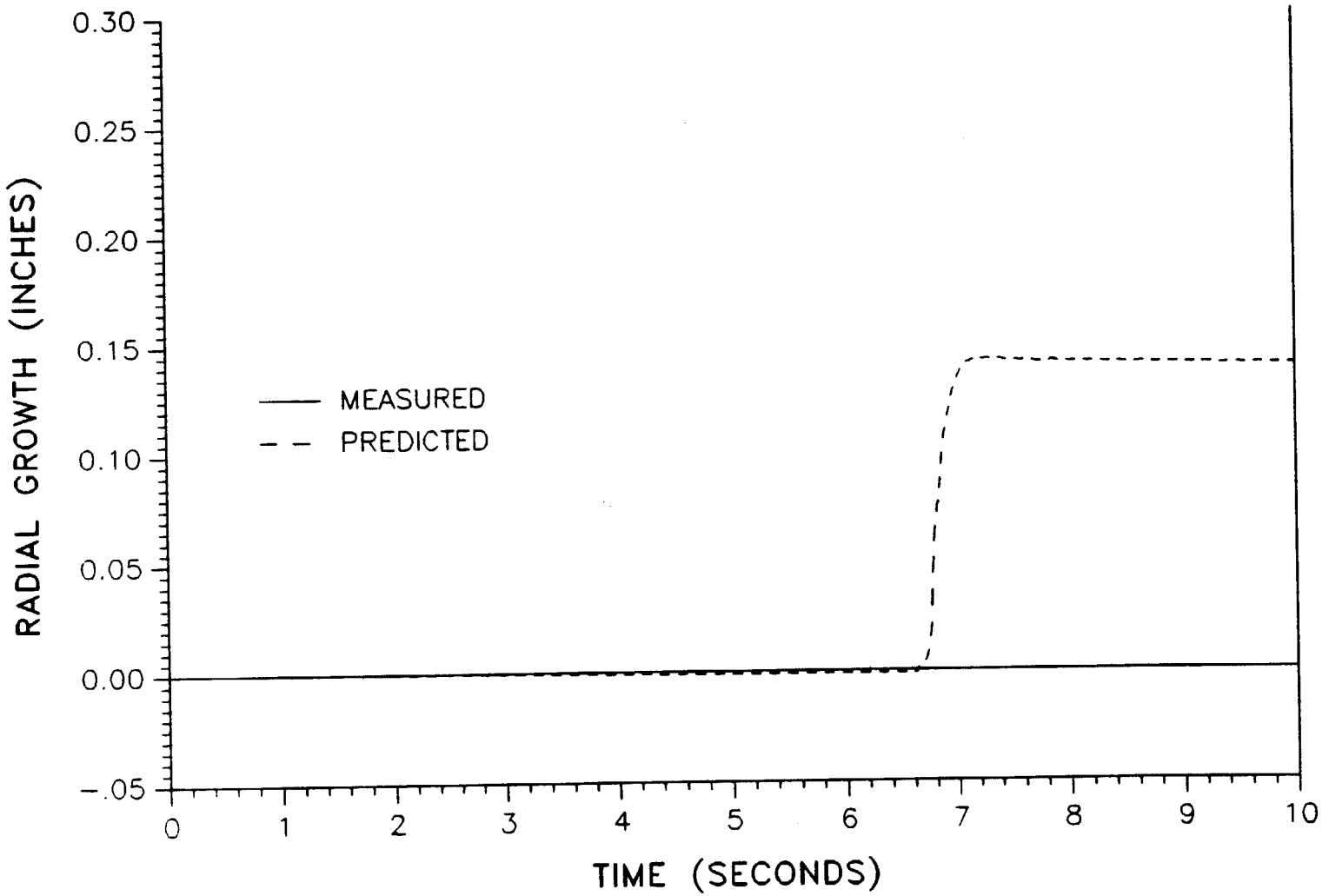

PREDICTED VS MEASURED RADIAL GROWTH

360L001 GIRTH GAGE B08G7300A – STATION 1576.40

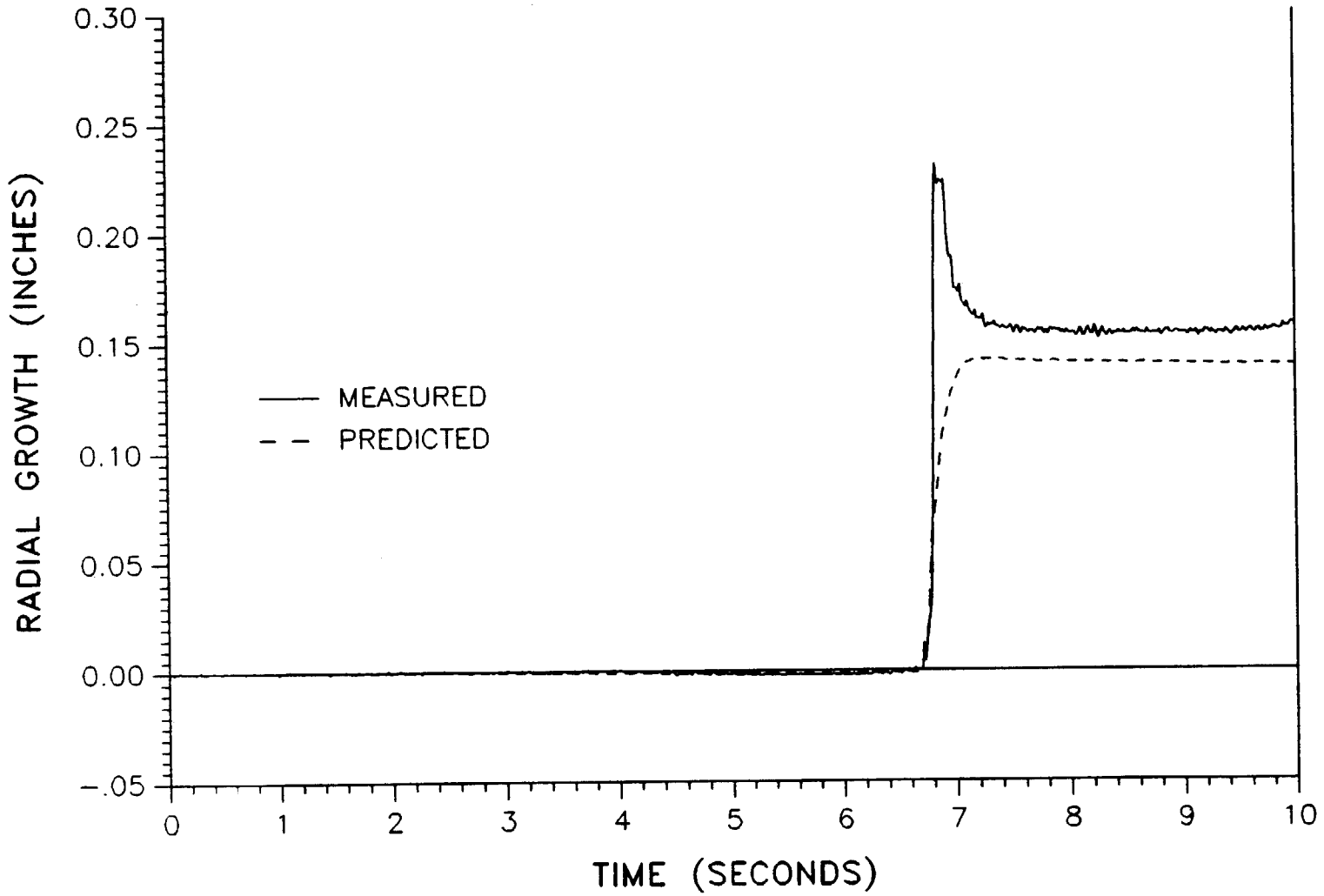

PREDICTED VS MEASURED RADIAL GROWTH

360L001 GIRTH GAGE B08G7301A – STATION 1637.50

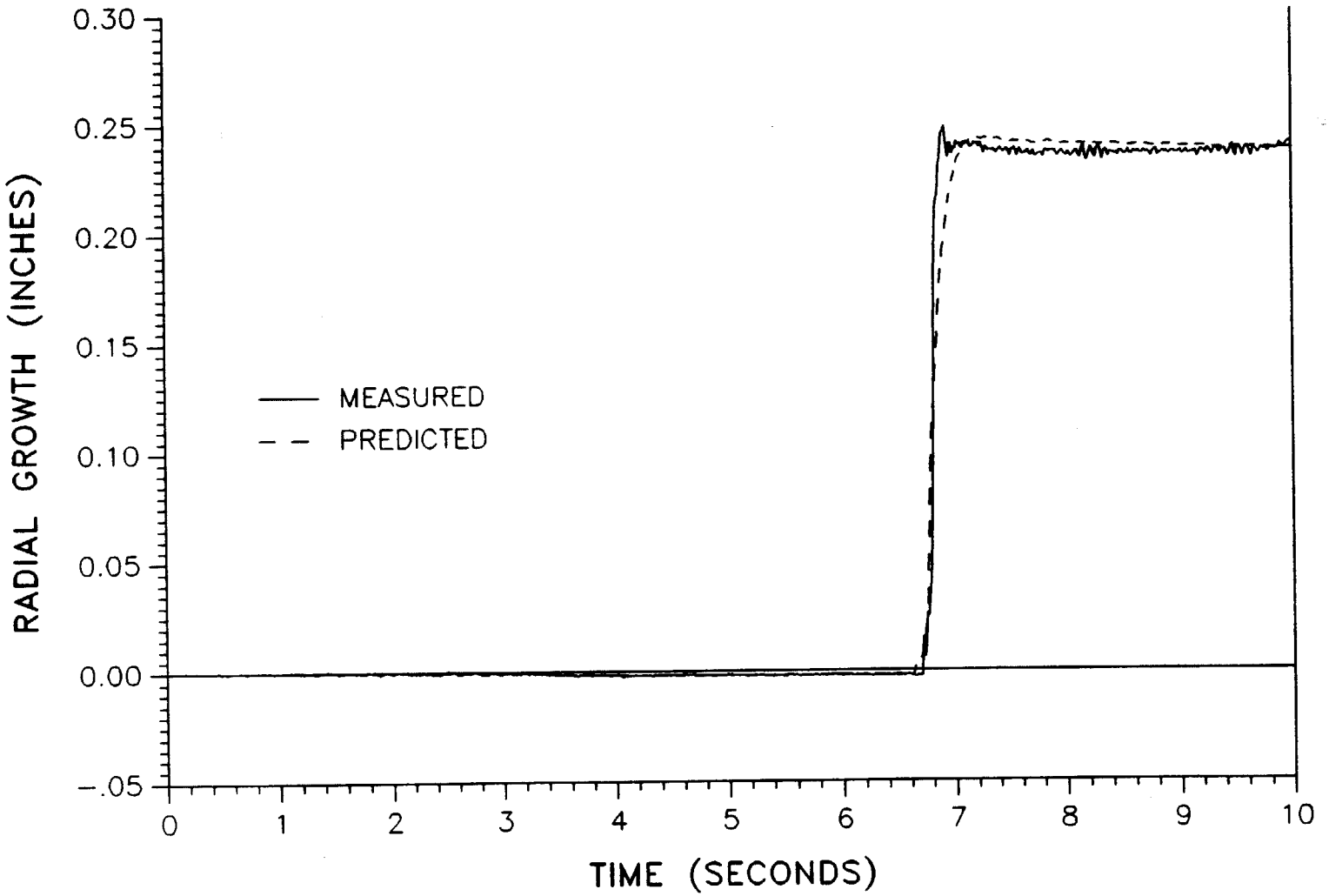

PREDICTED VS MEASURED RADIAL GROWTH

360L001 GIRTH GAGE B08G7302A – STATION 1694.75

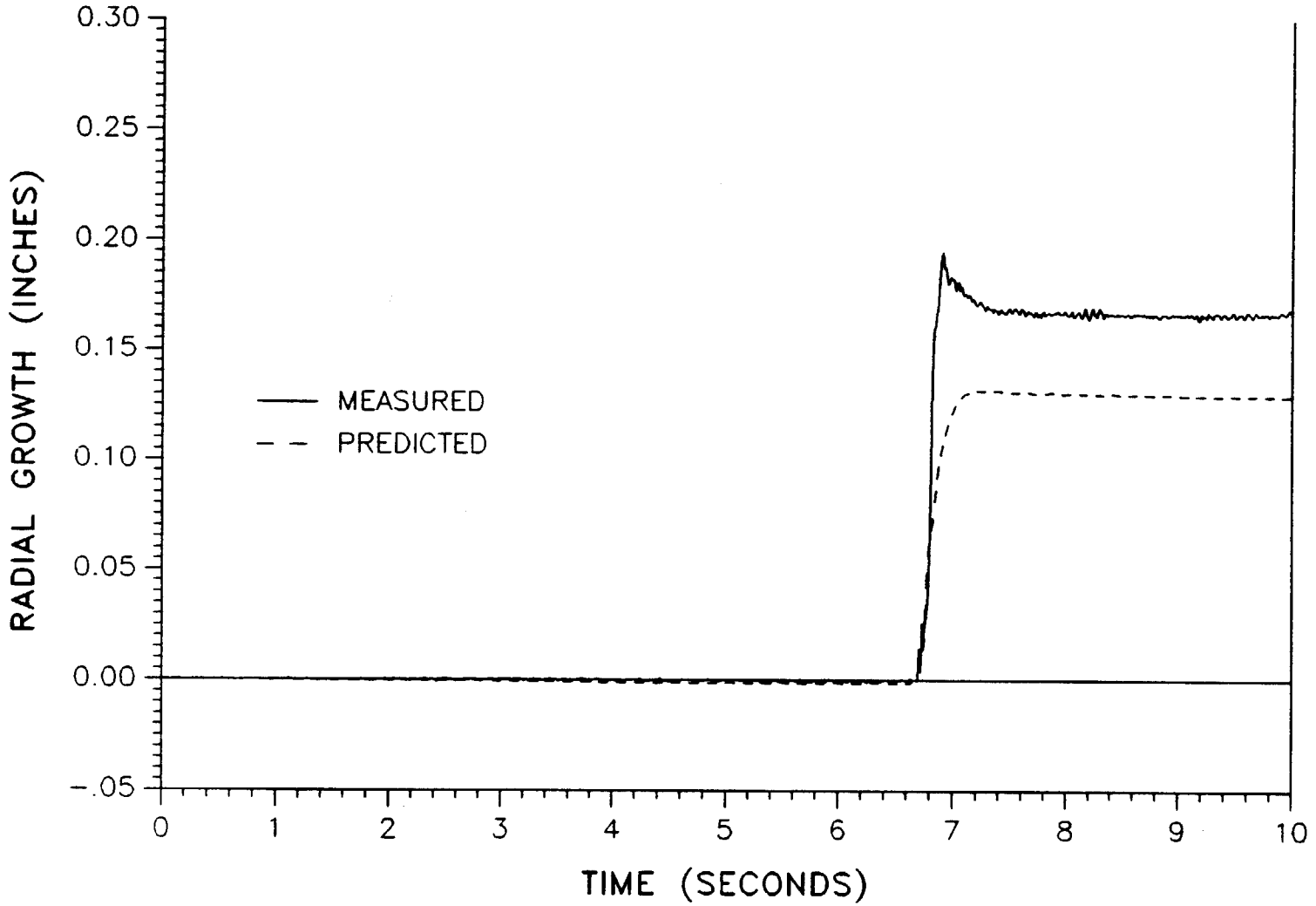

PREDICTED VS MEASURED RADIAL GROWTH

360L001 GIRTH GAGE B08G7303A – STATION 1696.40

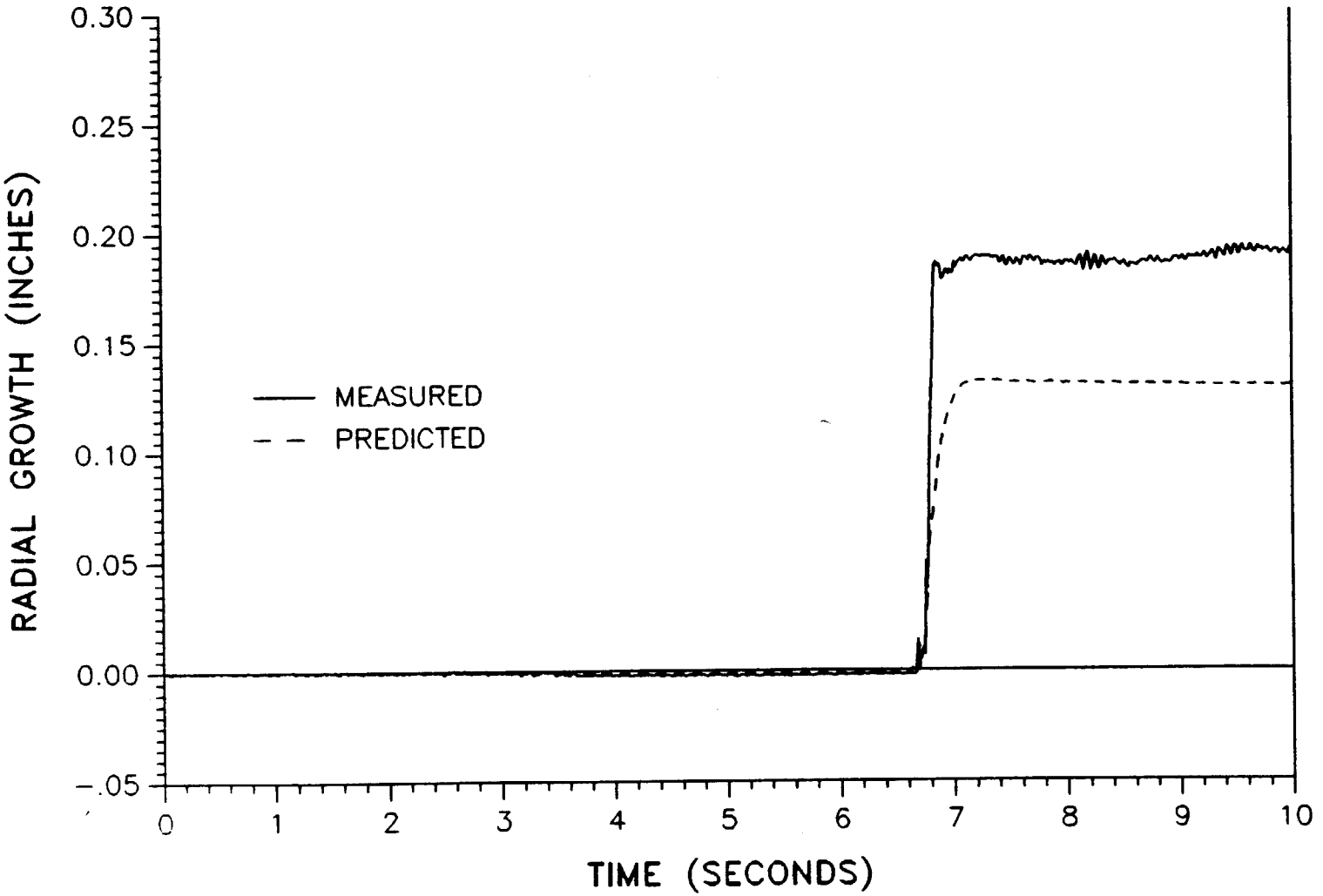

PREDICTED VS MEASURED RADIAL GROWTH

360L001 GIRTH GAGE B08G7272A - STATION 771.50

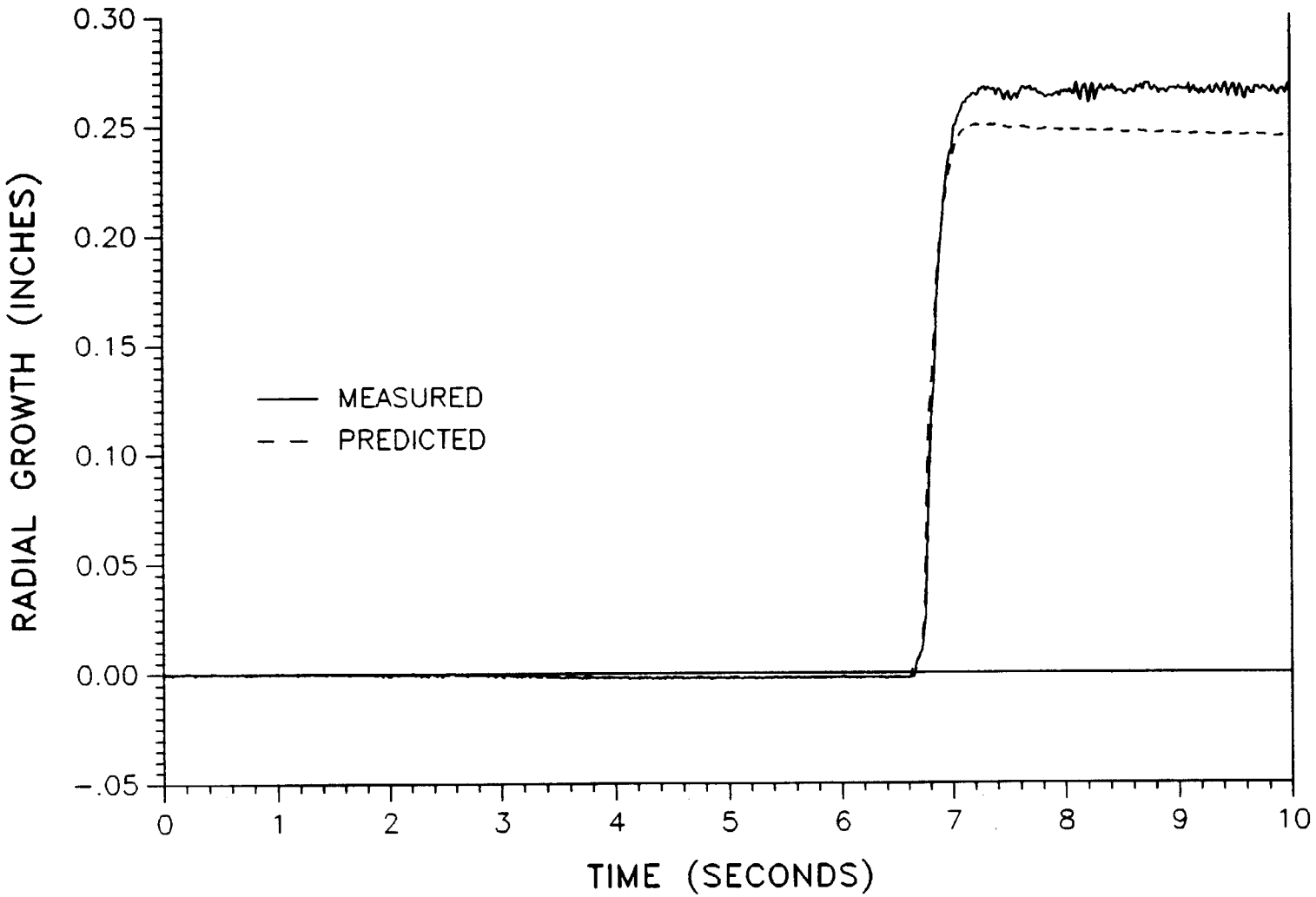

PREDICTED VS MEASURED RADIAL GROWTH

360L001 GIRTH GAGE B08G8272A - STATION 771.50

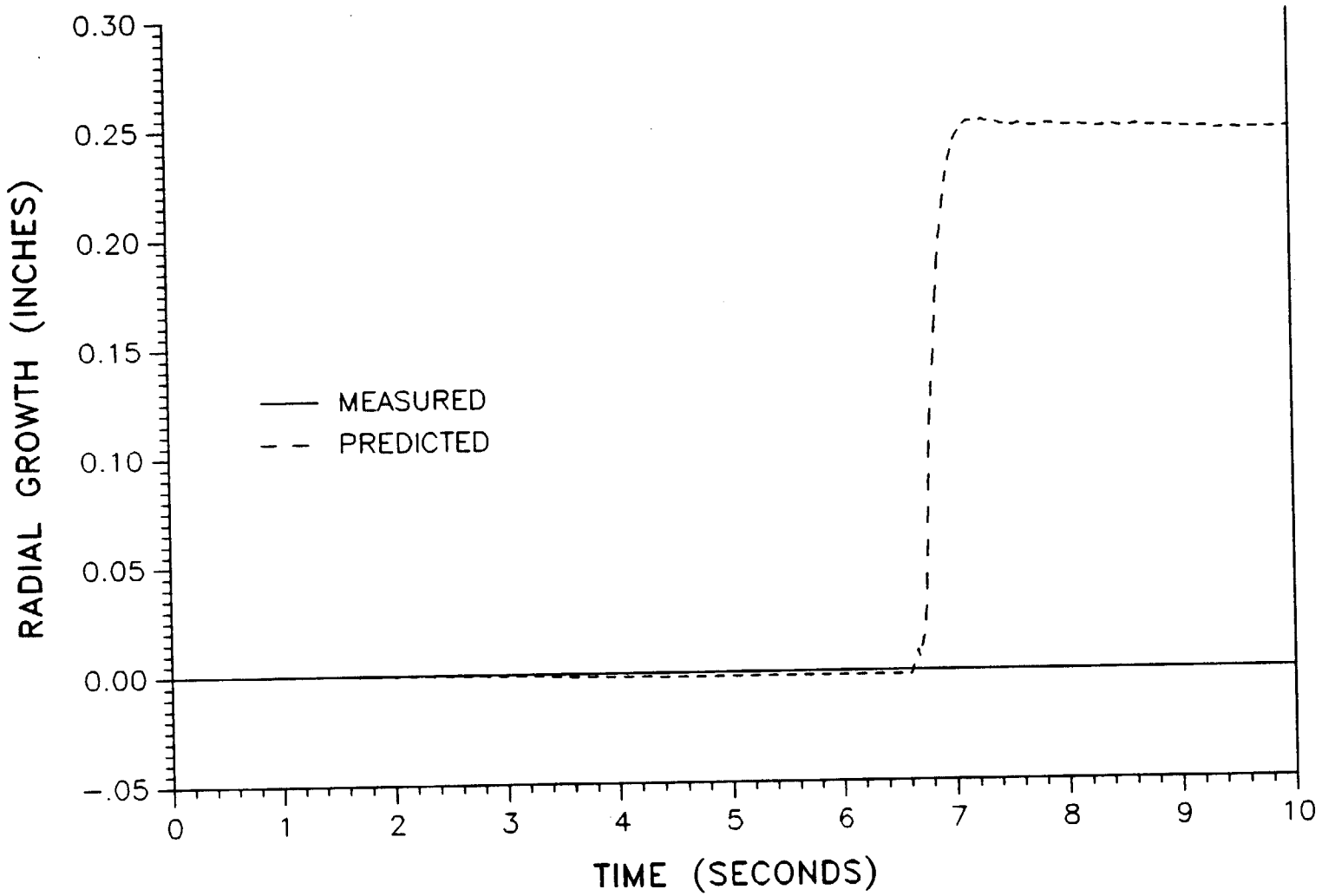

PREDICTED VS MEASURED RADIAL GROWTH

360L001 GIRTH GAGE B08G8273A - STATION 847.00

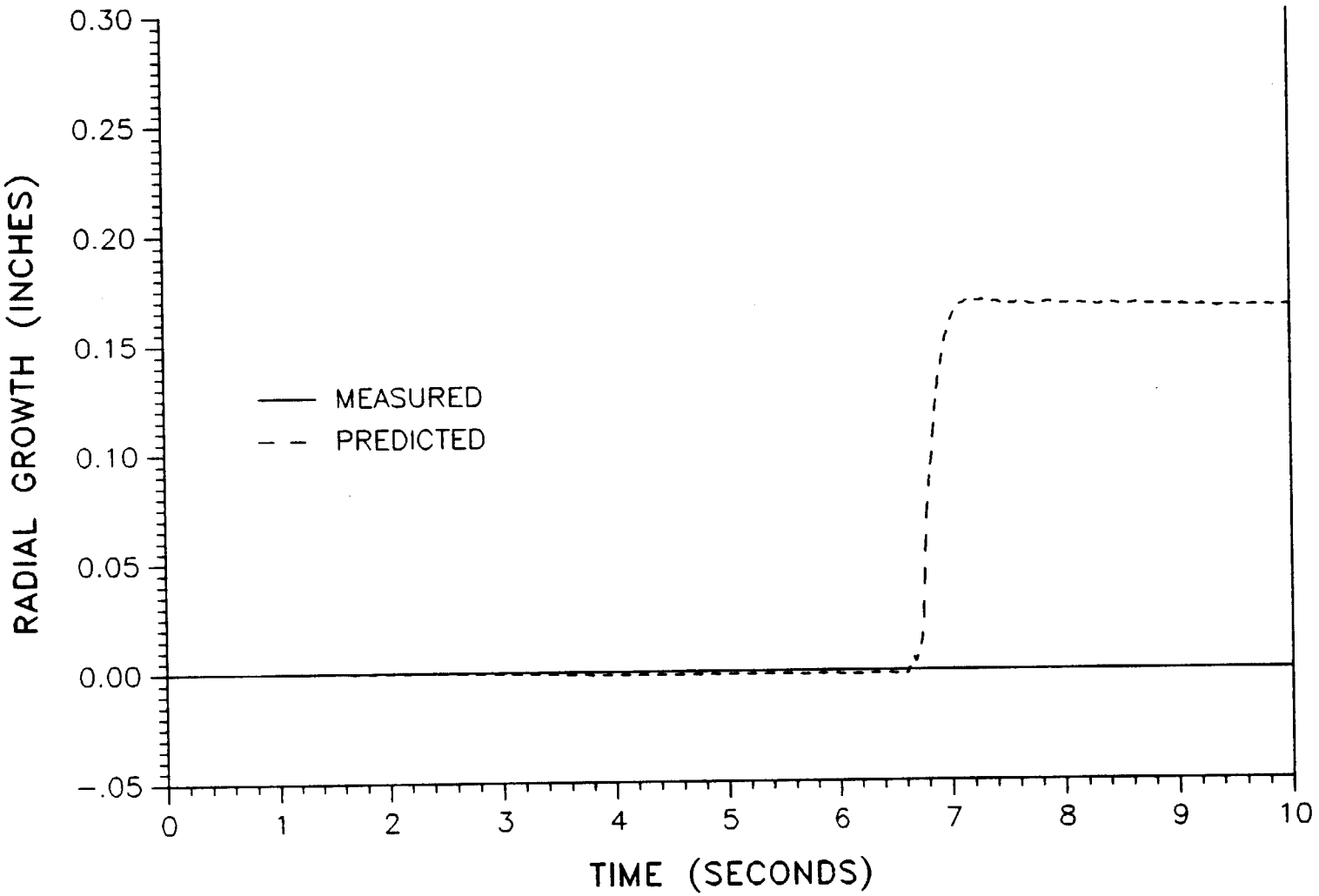

PREDICTED VS MEASURED RADIAL GROWTH

360L001 GIRTH GAGE B08G8274A - STATION 849.05

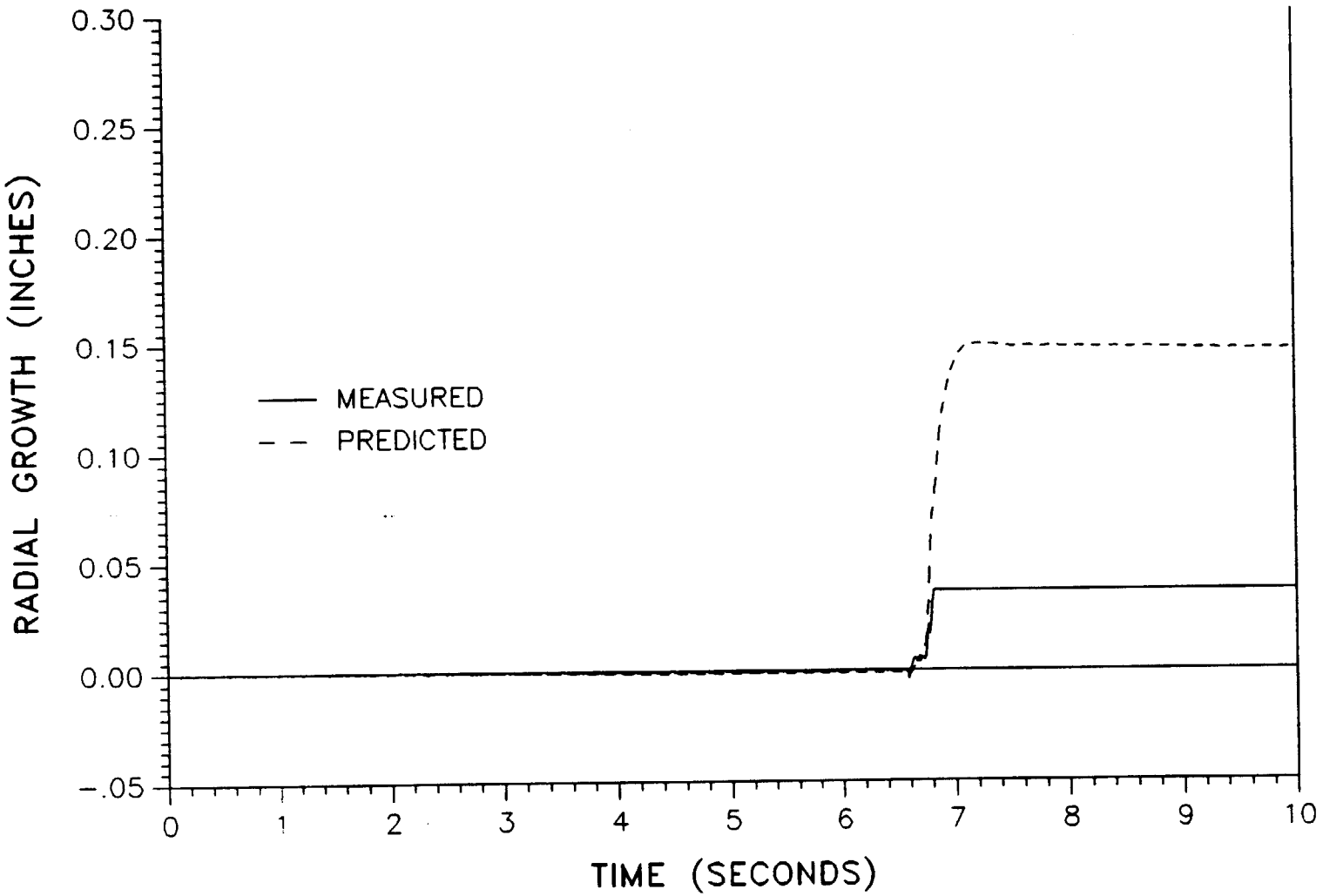

PREDICTED VS MEASURED RADIAL GROWTH

360L001 GIRTH GAGE B08G8275A – STATION 850.20

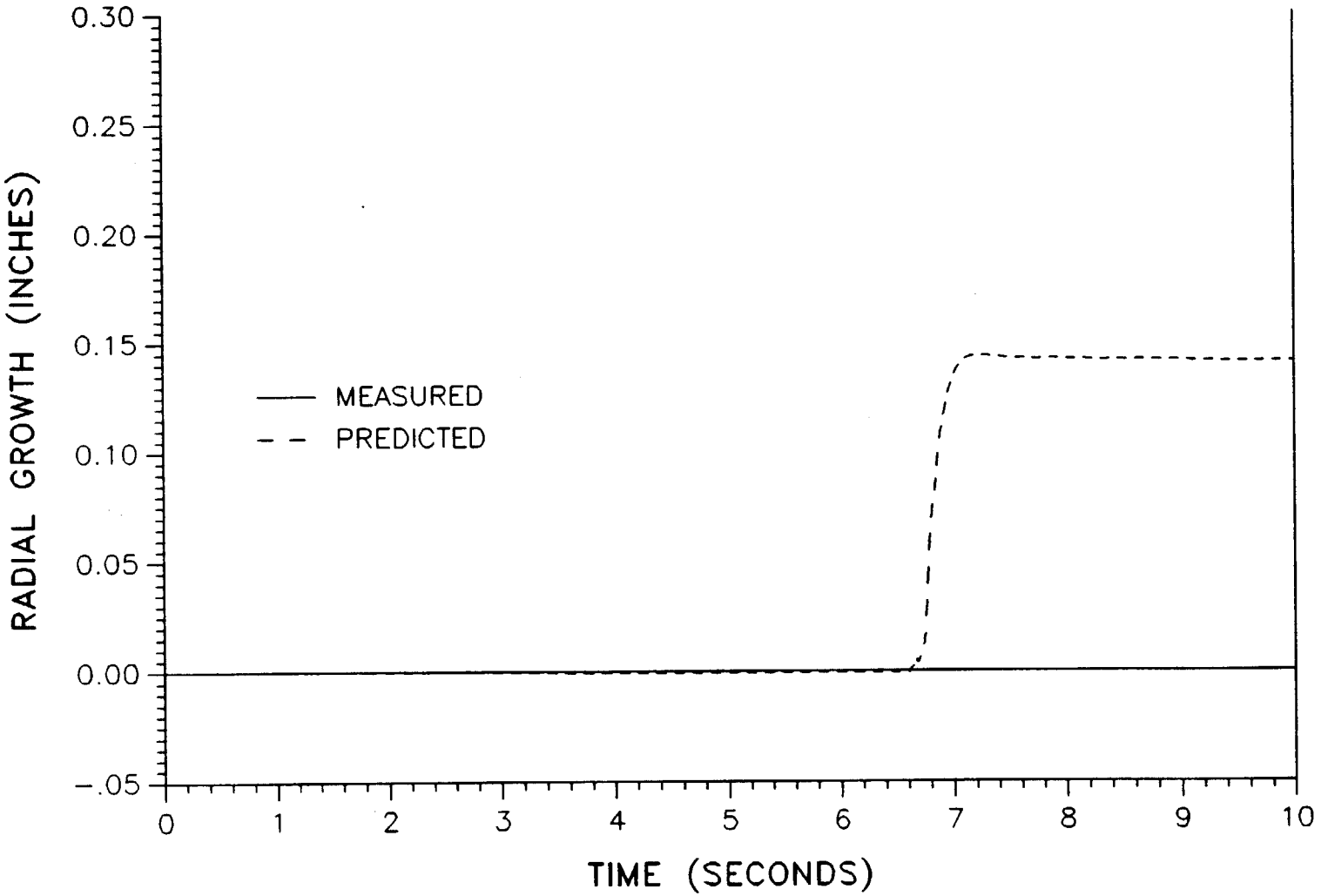

PREDICTED VS MEASURED RADIAL GROWTH

360L001 GIRTH GAGE B08G8276A – STATION 852.80

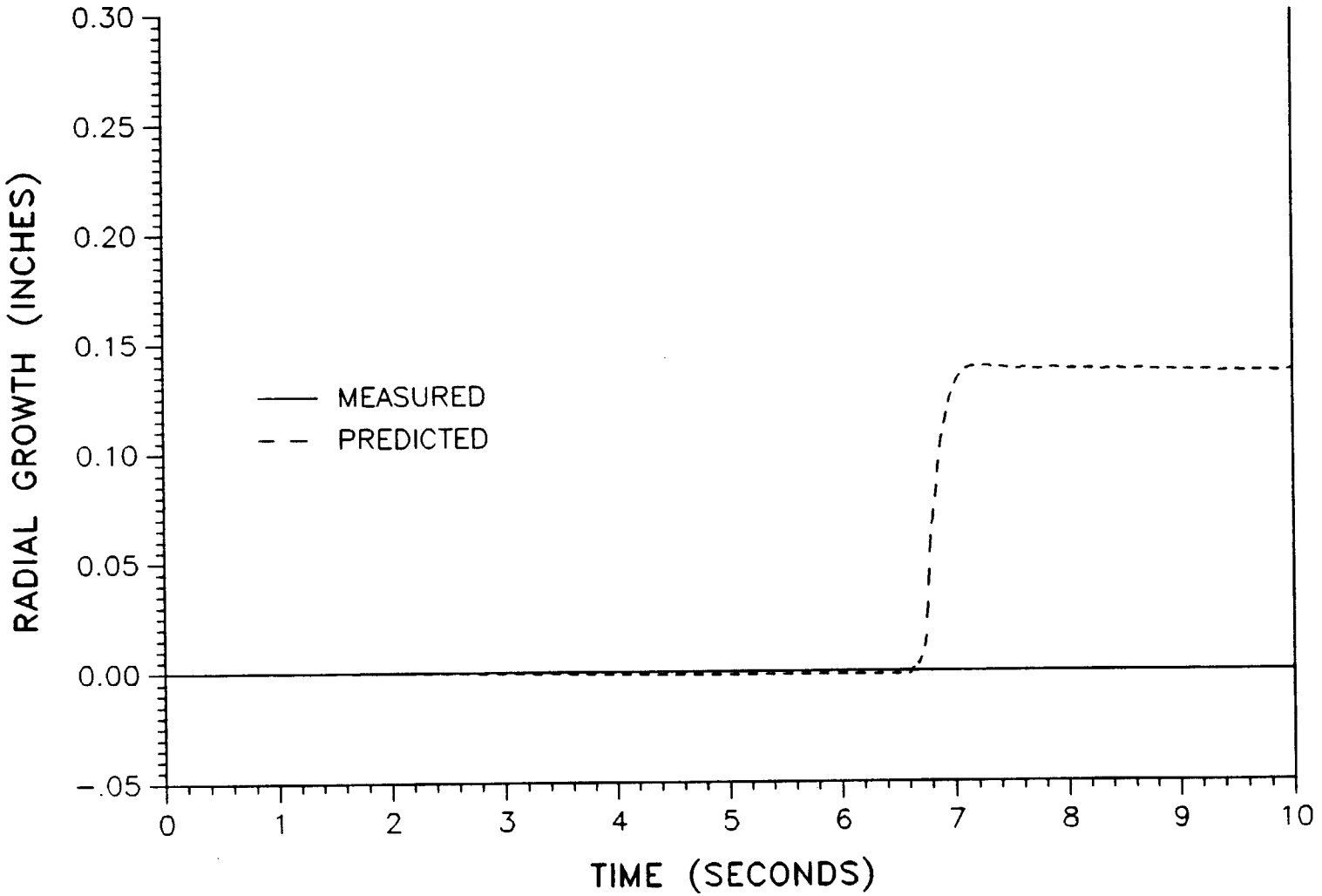

PREDICTED VS MEASURED RADIAL GROWTH

360L001 GIRTH GAGE B08G8277A – STATION 854.83

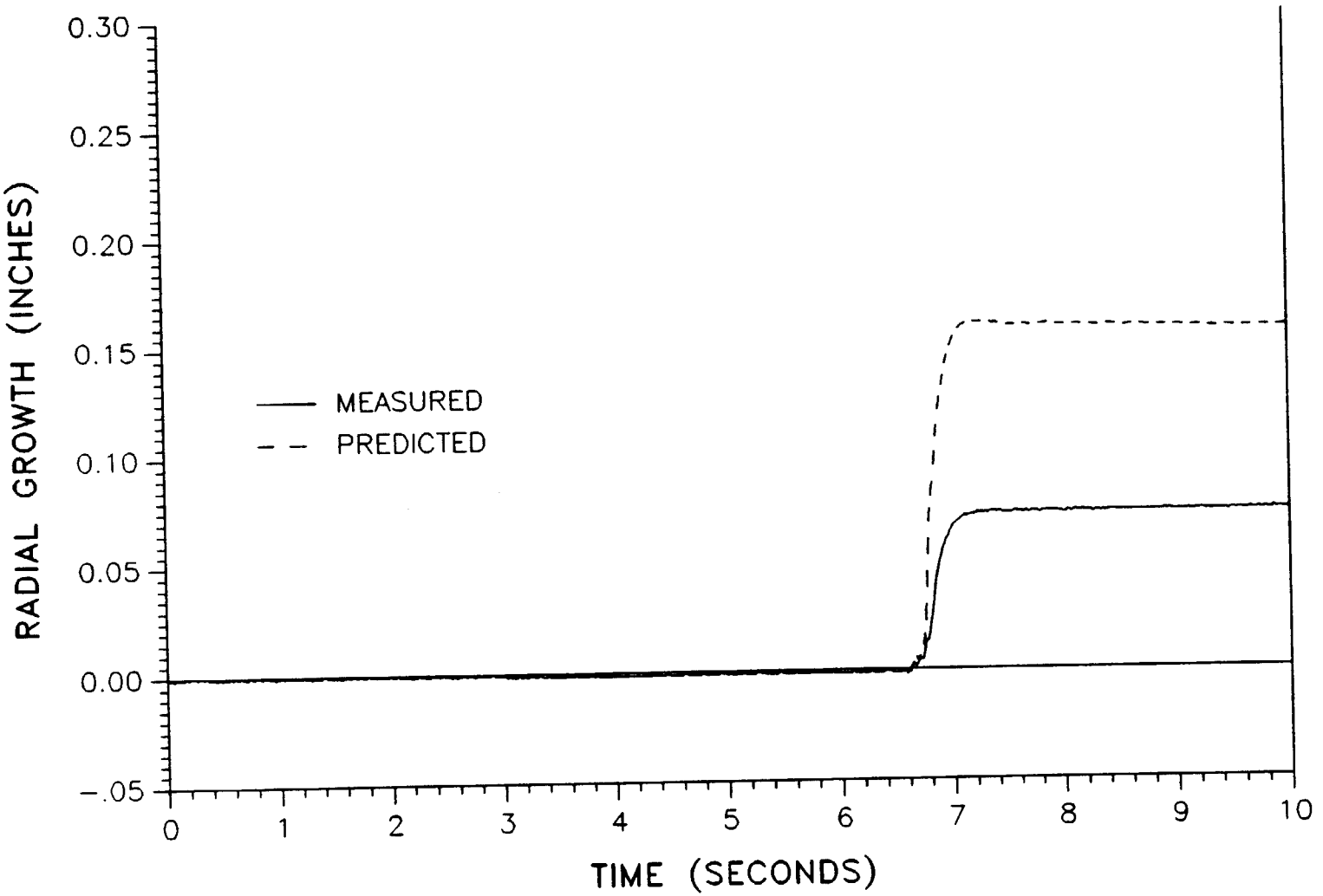

PREDICTED VS MEASURED RADIAL GROWTH

360L001 GIRTH GAGE B08G8278A - STATION 857.47

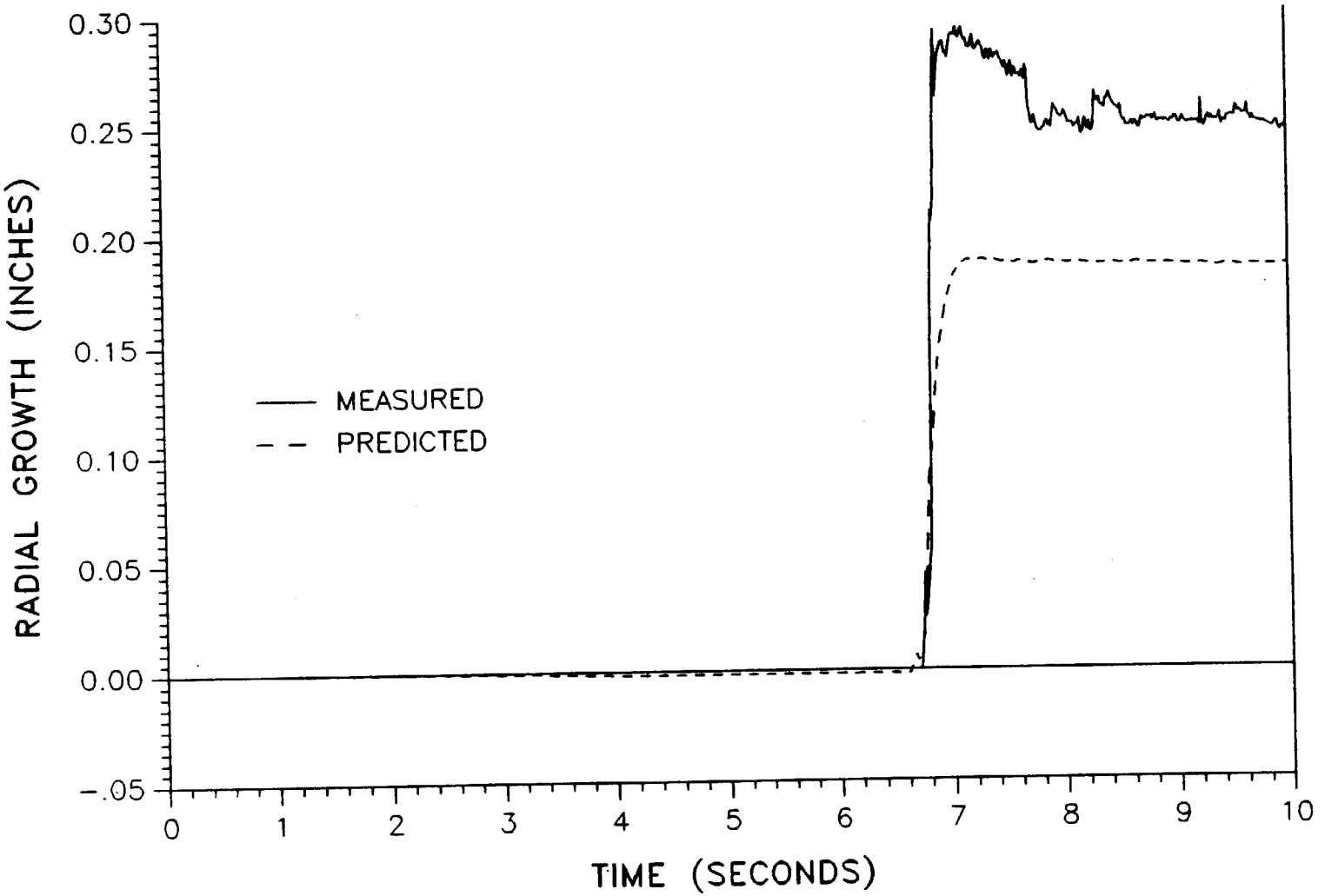

PREDICTED VS MEASURED RADIAL GROWTH

360L001 GIRTH GAGE B08G8282A – STATION 1091.50

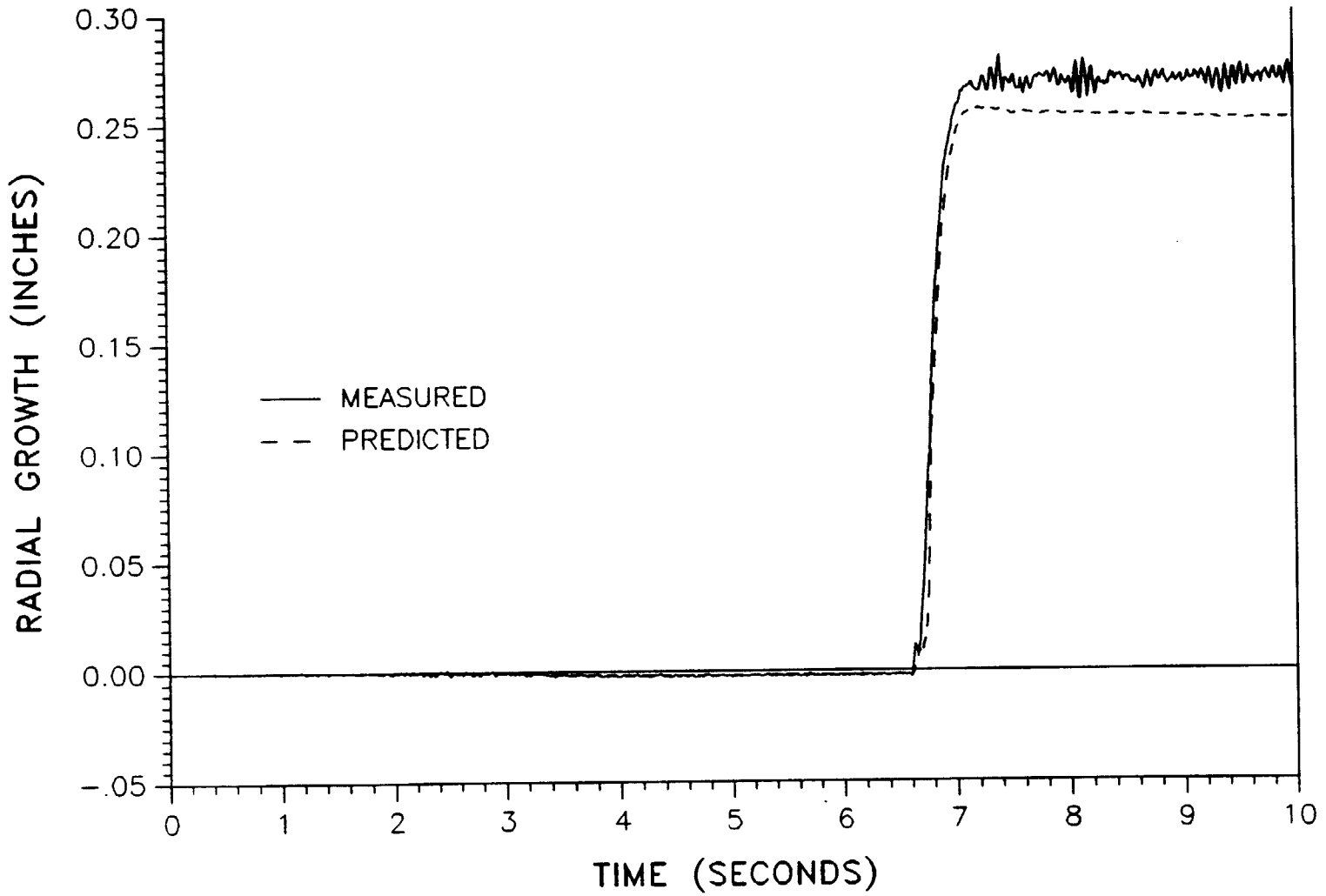

PREDICTED VS MEASURED RADIAL GROWTH

360L001 GIRTH GAGE B08G8283A – STATION 1167.43

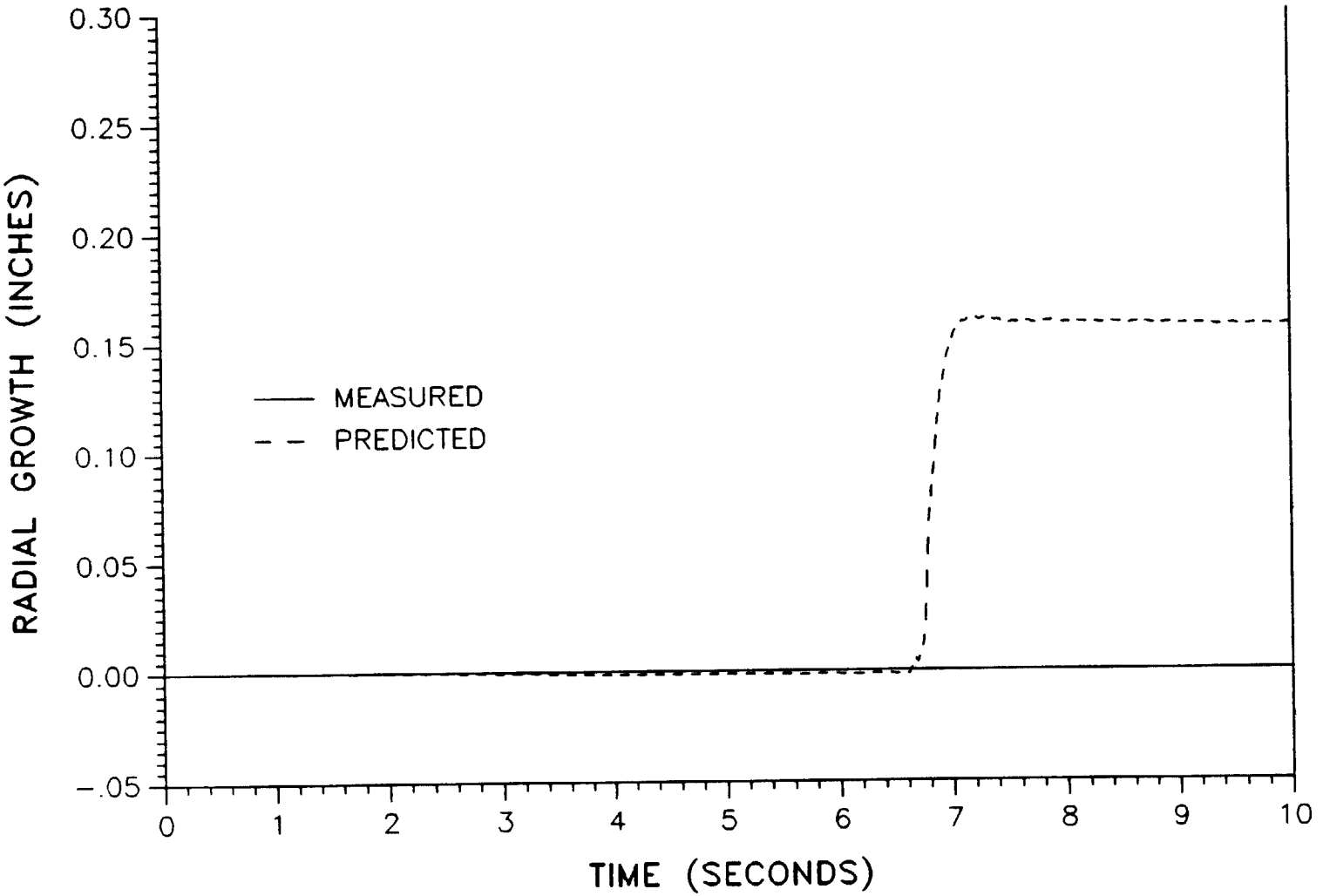

PREDICTED VS MEASURED RADIAL GROWTH

360L001 GIRTH GAGE B08G8284A – STATION 1168.75

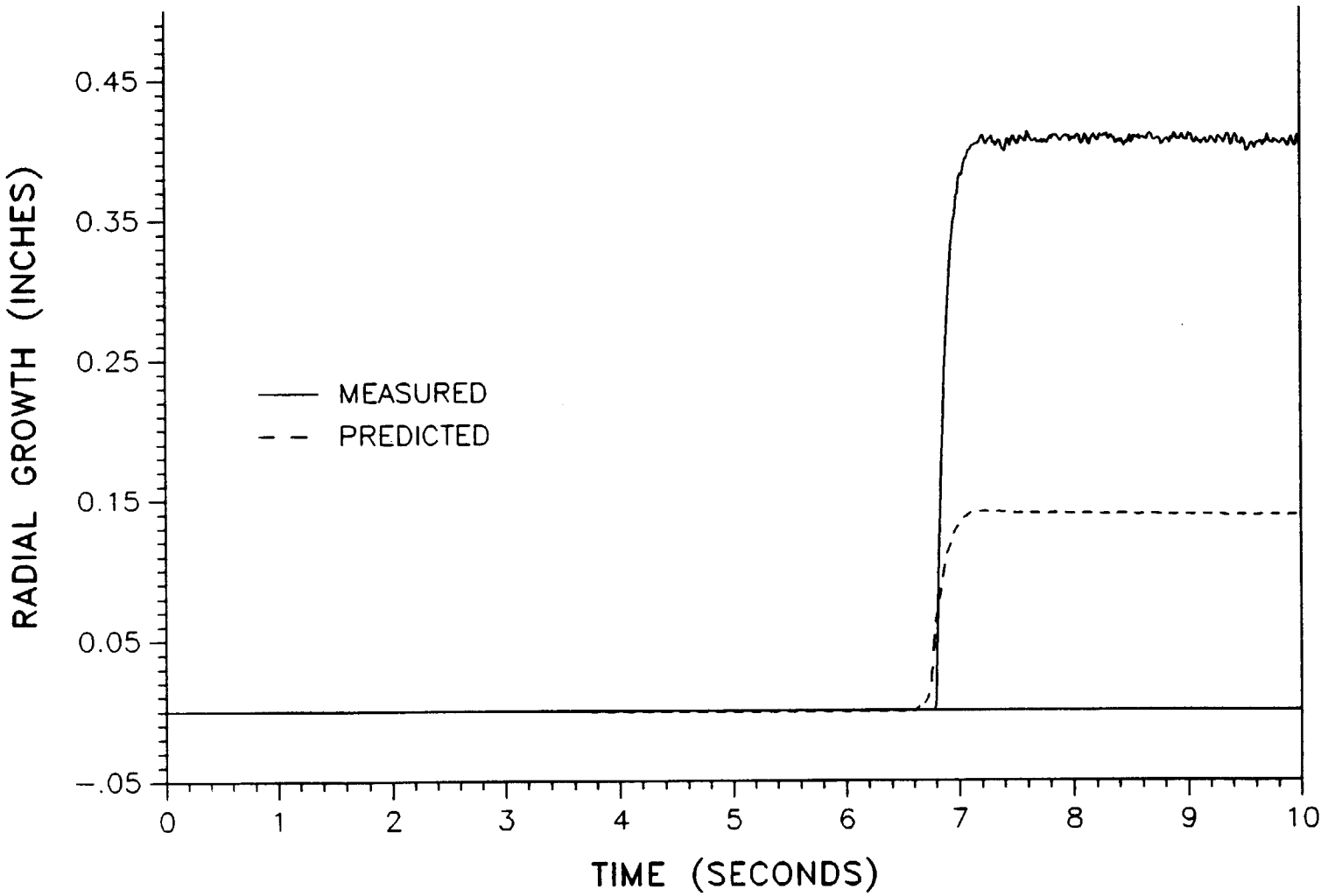

PREDICTED VS MEASURED RADIAL GROWTH

360L001 GIRTH GAGE B08G8285A – STATION 1170.38

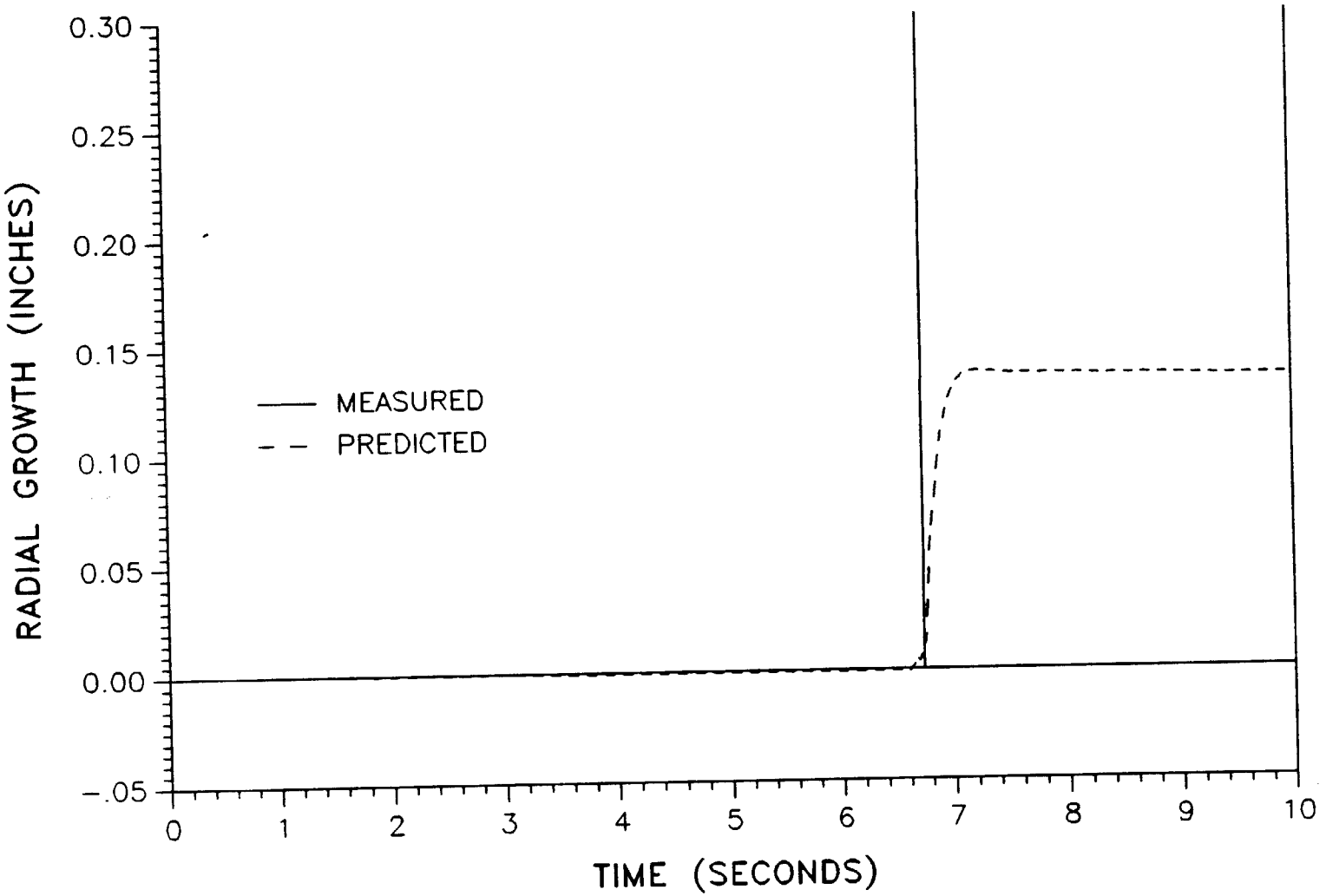

PREDICTED VS MEASURED RADIAL GROWTH

360L001 GIRTH GAGE B08G8286A – STATION 1172.73

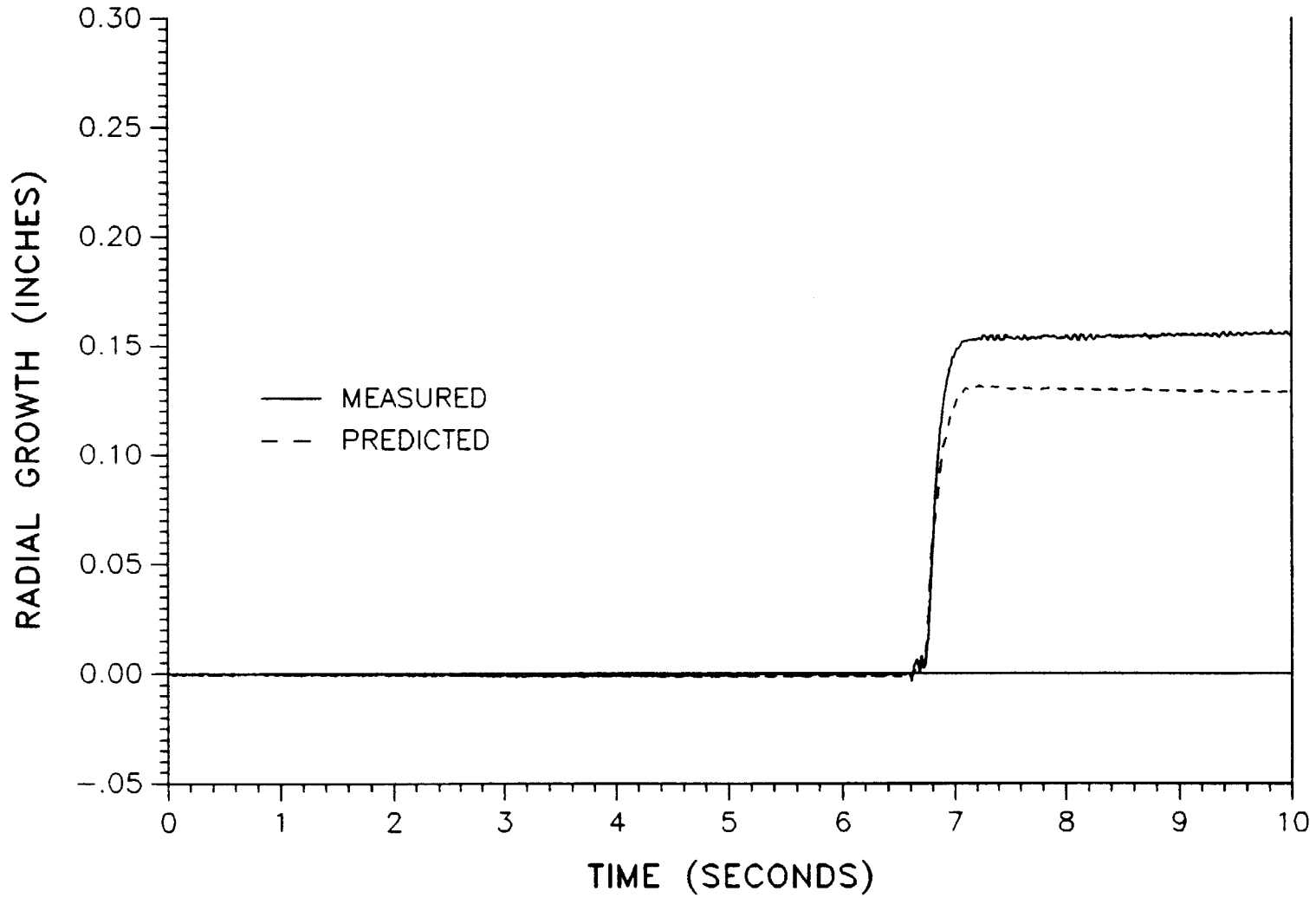

PREDICTED VS MEASURED RADIAL GROWTH

360L001 GIRTH GAGE B08G8287A – STATION 1175.25

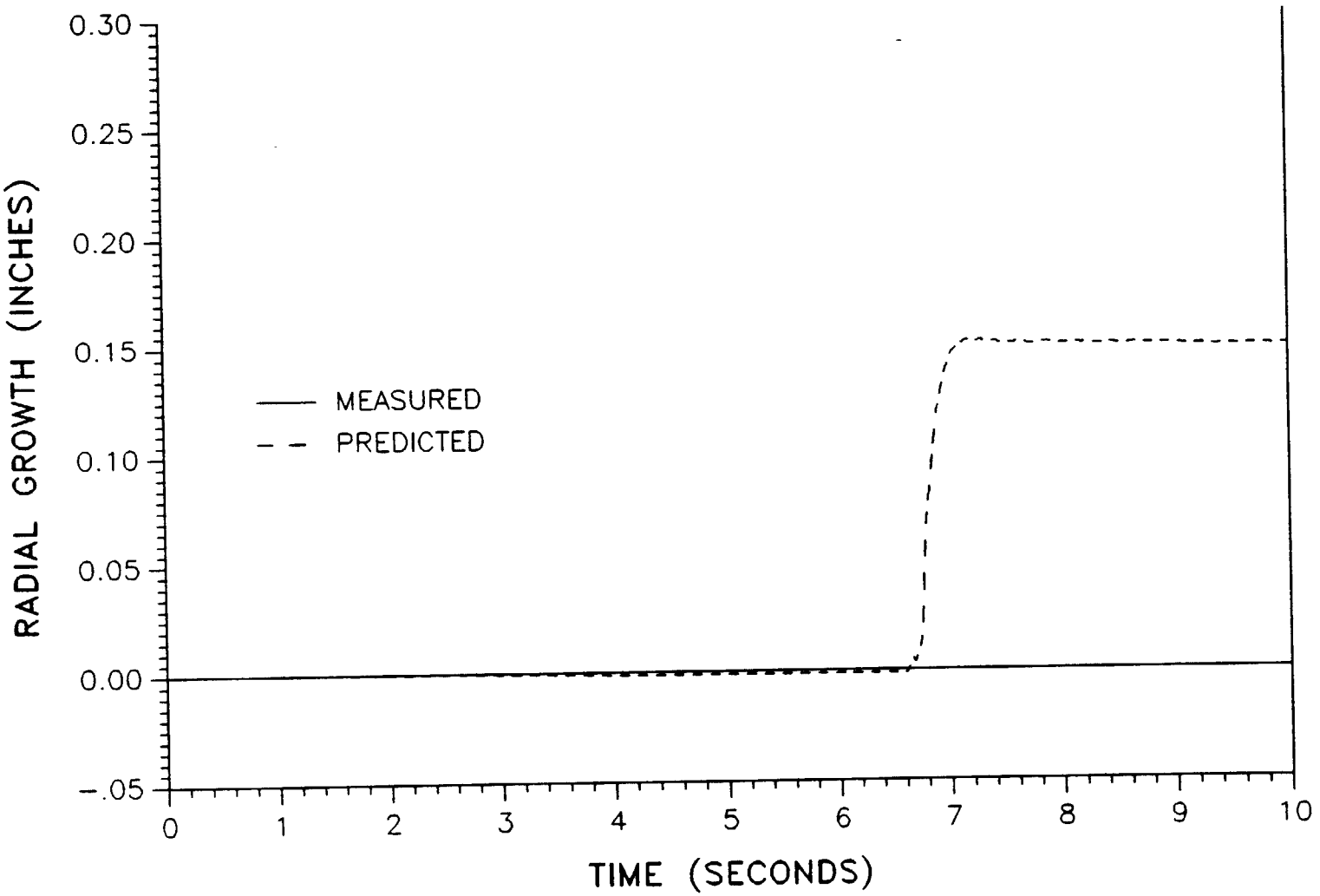

PREDICTED VS MEASURED RADIAL GROWTH

360L001 GIRTH GAGE B08G8288A – STATION 1177.47

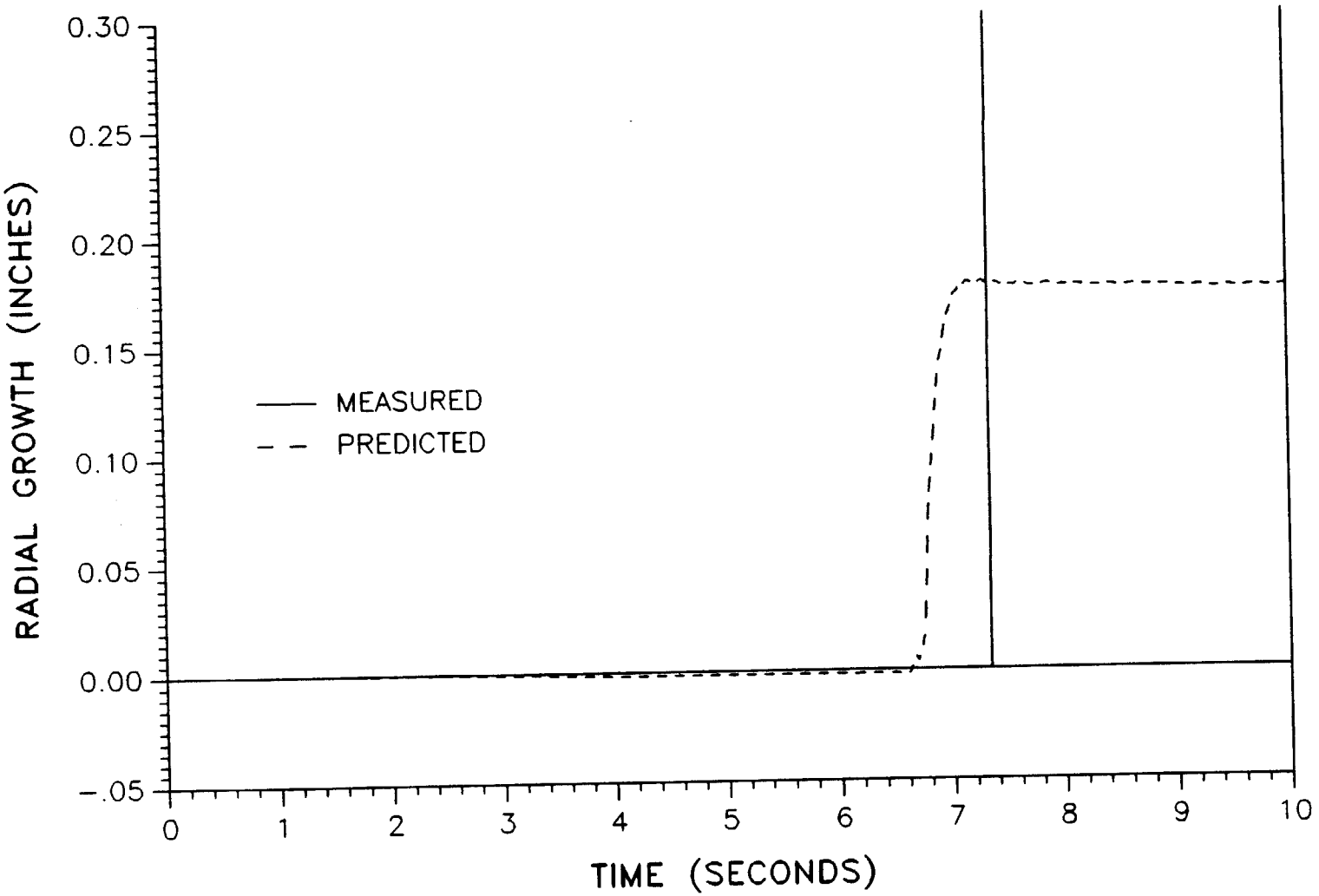

PREDICTED VS MEASURED RADIAL GROWTH

360L001 GIRTH GAGE B08G8292A – STATION 1411.80

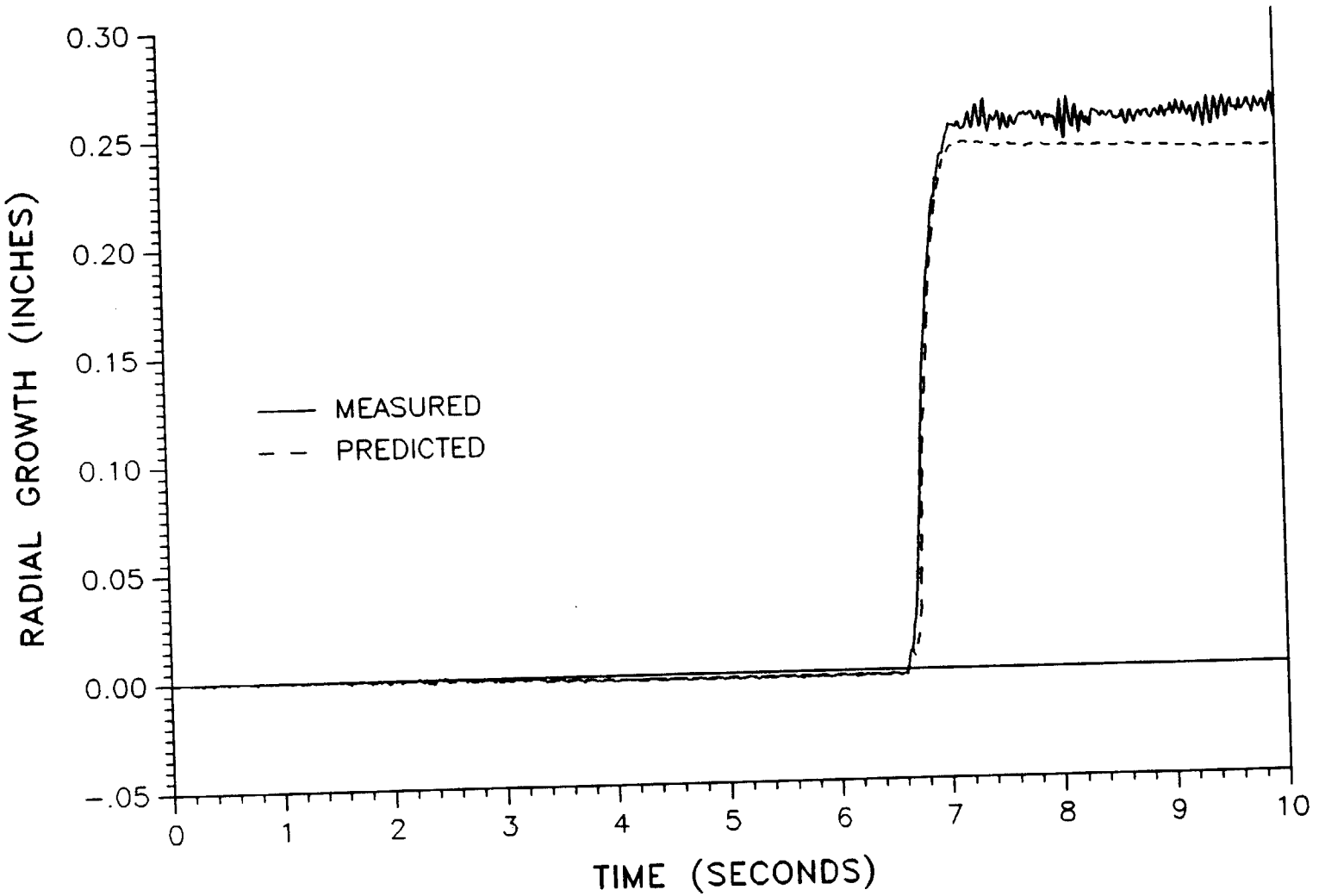

PREDICTED VS MEASURED RADIAL GROWTH

360L001 GIRTH GAGE B08G8293A - STATION 1487.43

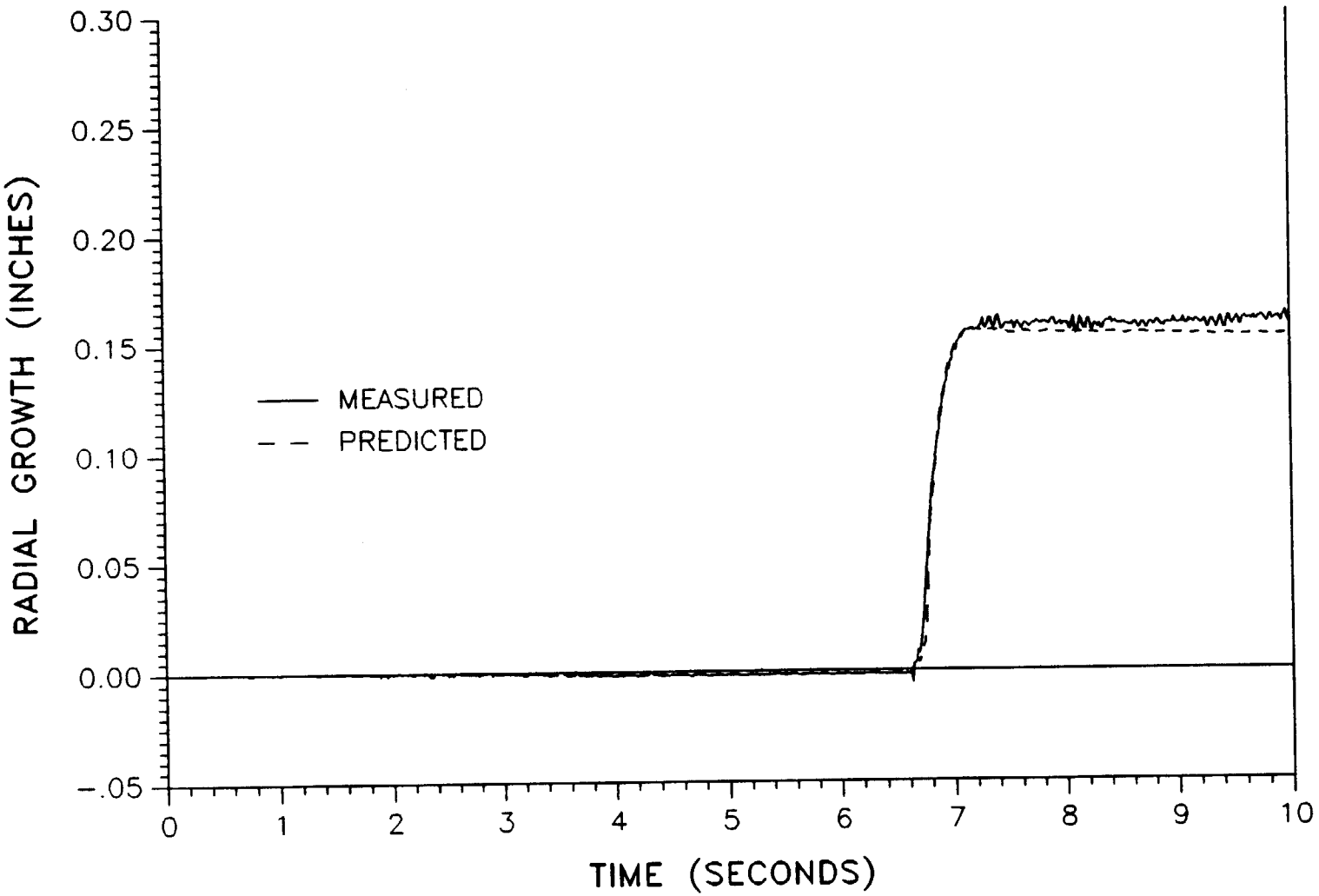

PREDICTED VS MEASURED RADIAL GROWTH

360L001 GIRTH GAGE B08G8294A – STATION 1489.05

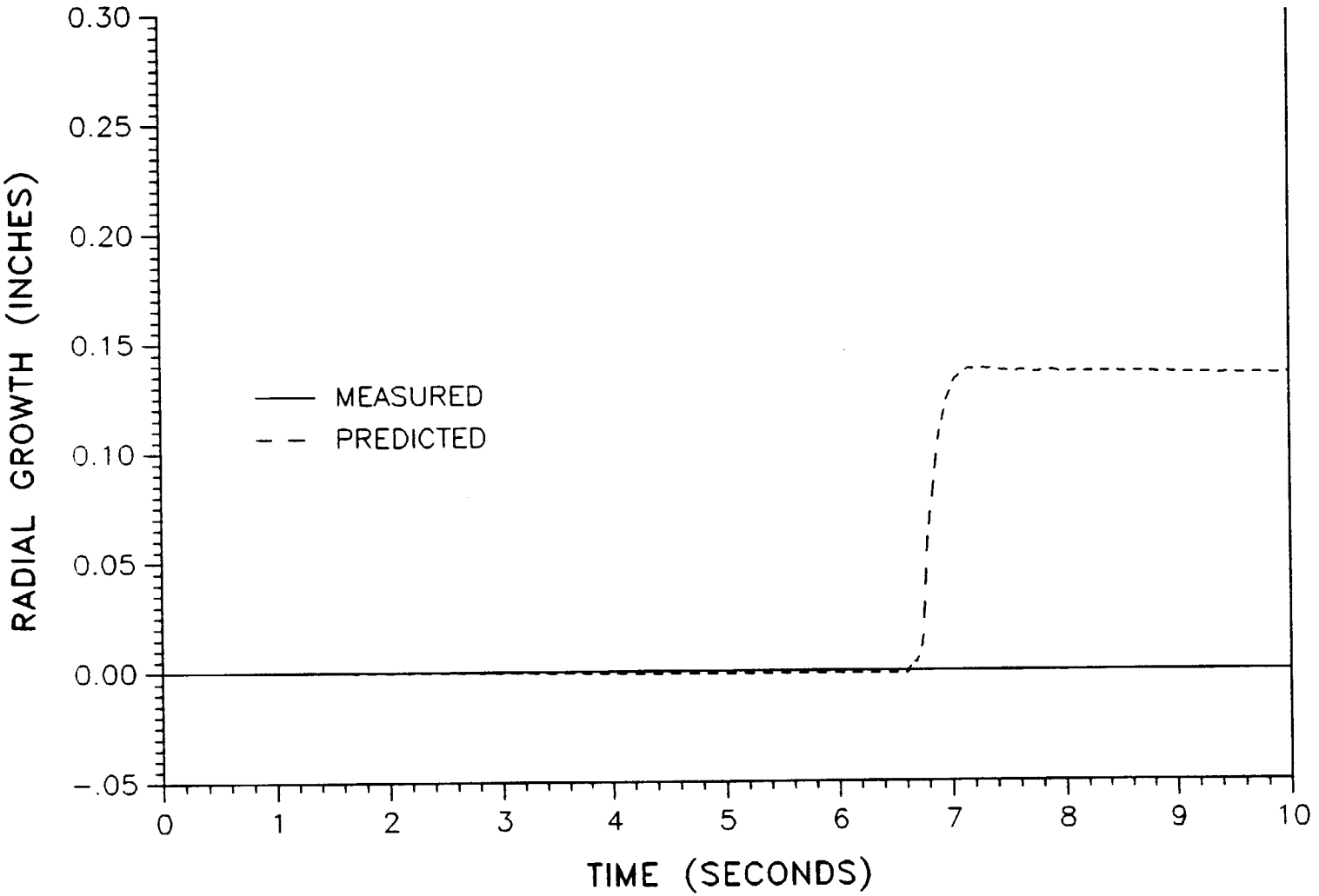

PREDICTED VS MEASURED RADIAL GROWTH

360L001 GIRTH GAGE B08G8295A – STATION 1490.20

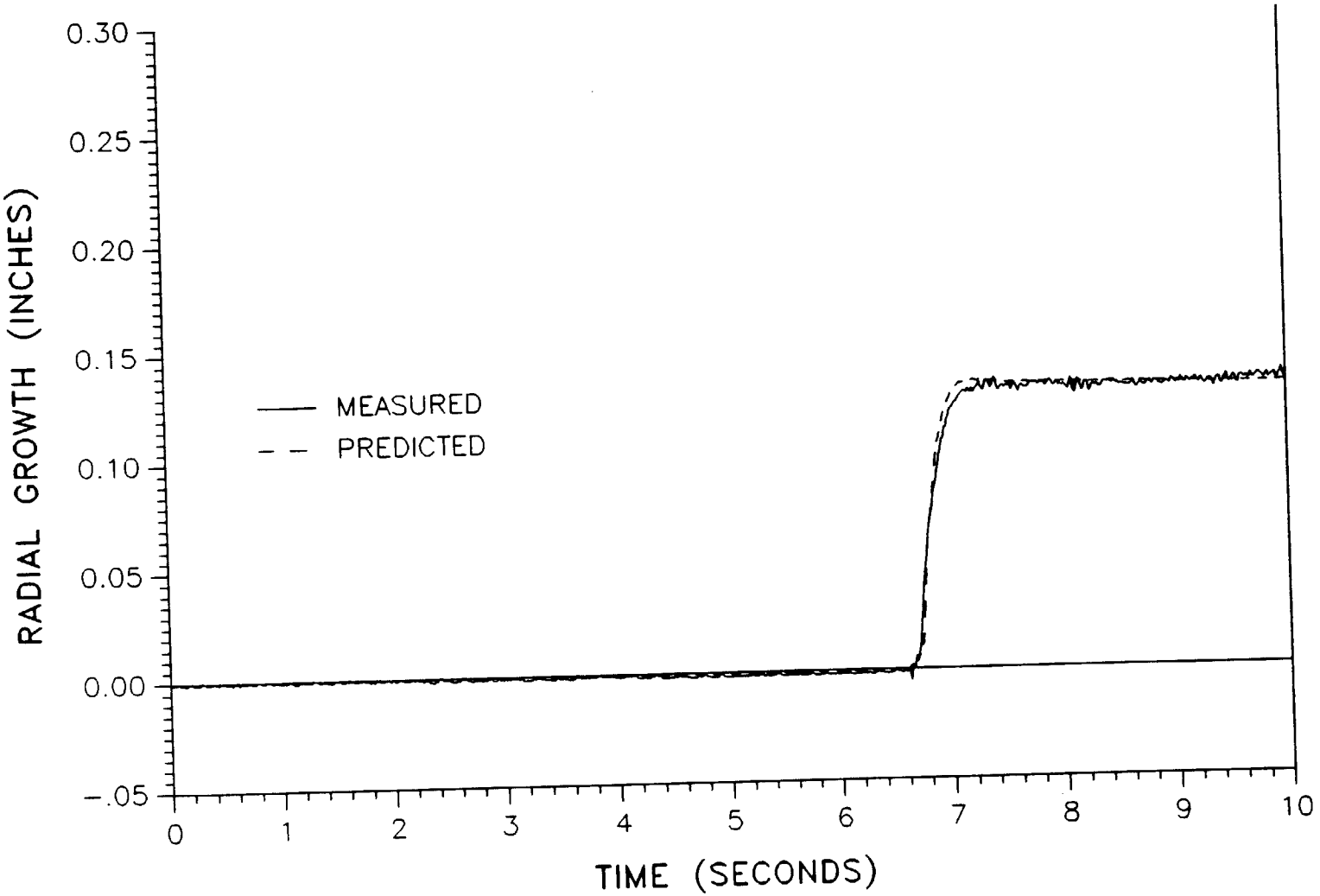

PREDICTED VS MEASURED RADIAL GROWTH

360L001 GIRTH GAGE B08G8296A – STATION 1492.73

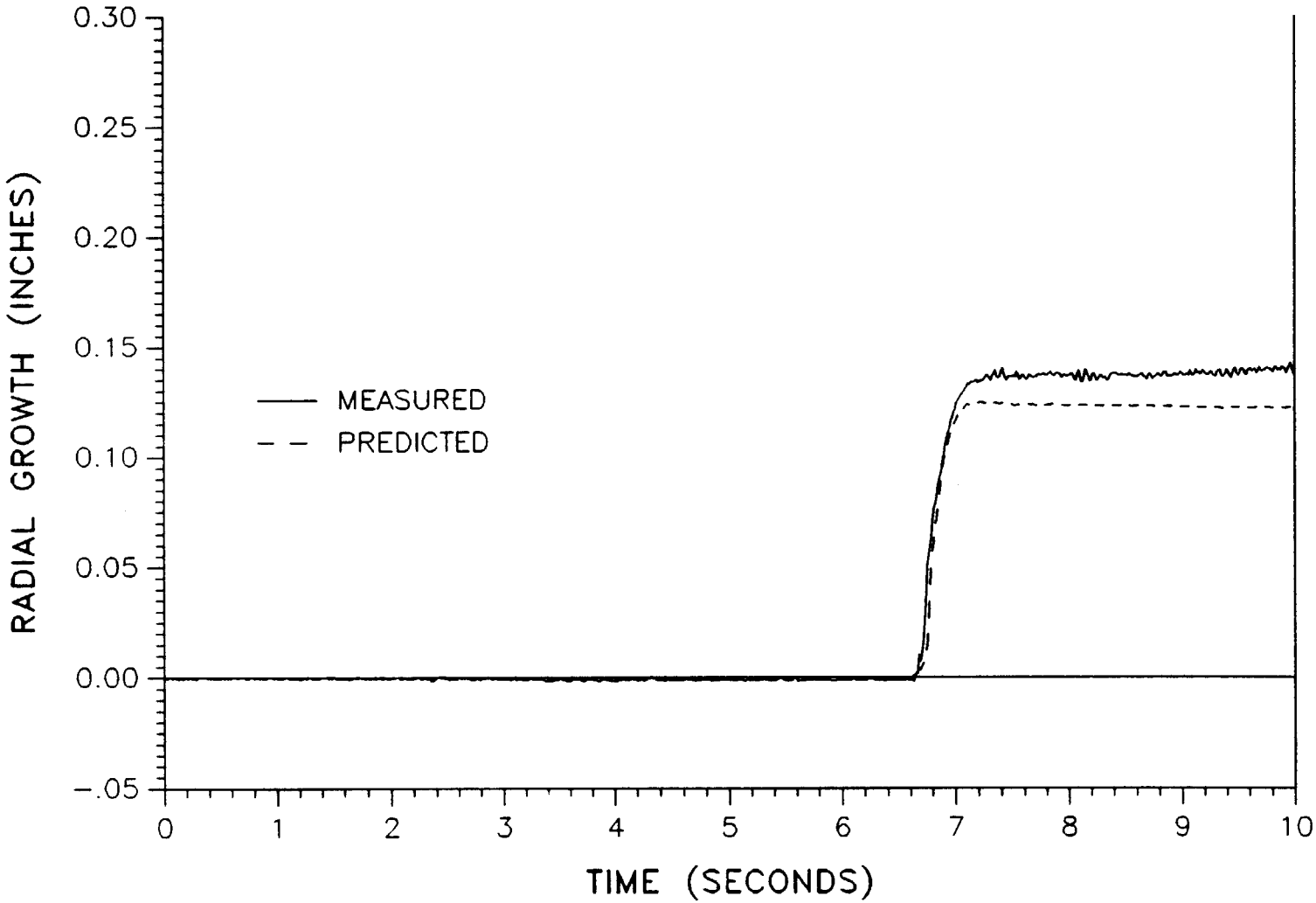

PREDICTED VS MEASURED RADIAL GROWTH

360L001 GIRTH GAGE B08G8297A – STATION 1494.83

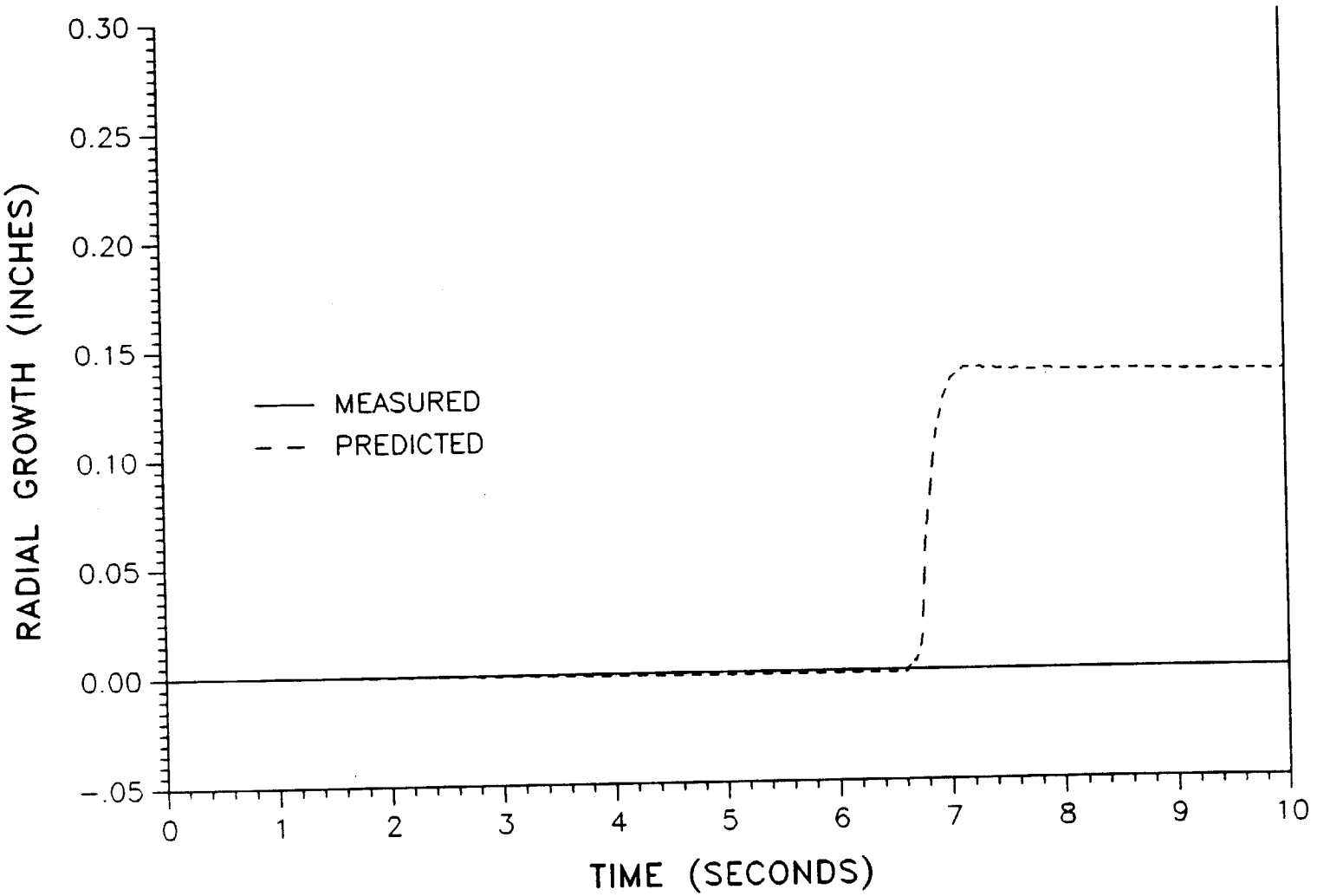

PREDICTED VS MEASURED RADIAL GROWTH

360L001 GIRTH GAGE B08G8298A – STATION 1497.50

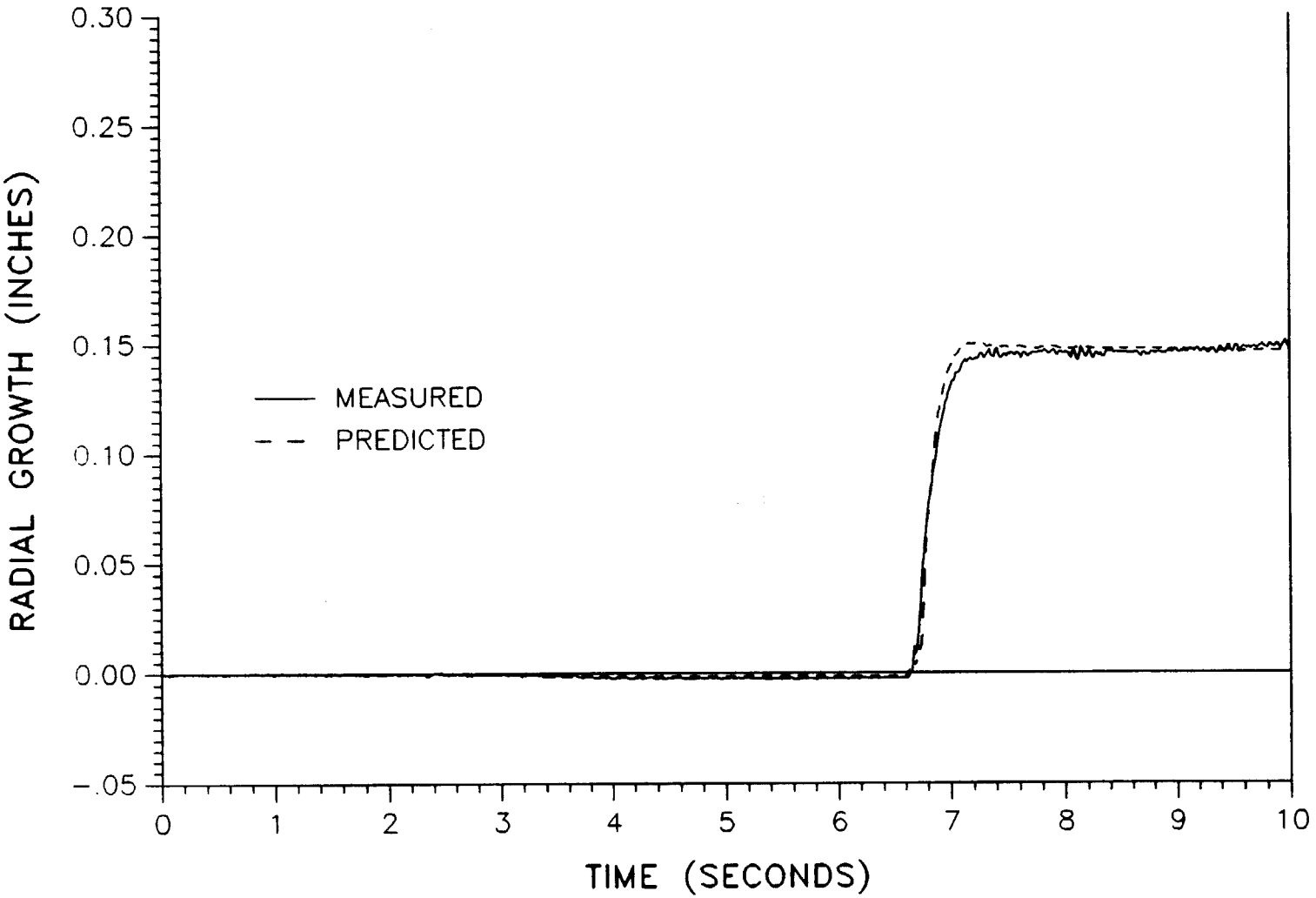

PREDICTED VS MEASURED RADIAL GROWTH

360L001 GIRTH GAGE B08G8299A – STATION 1574.75

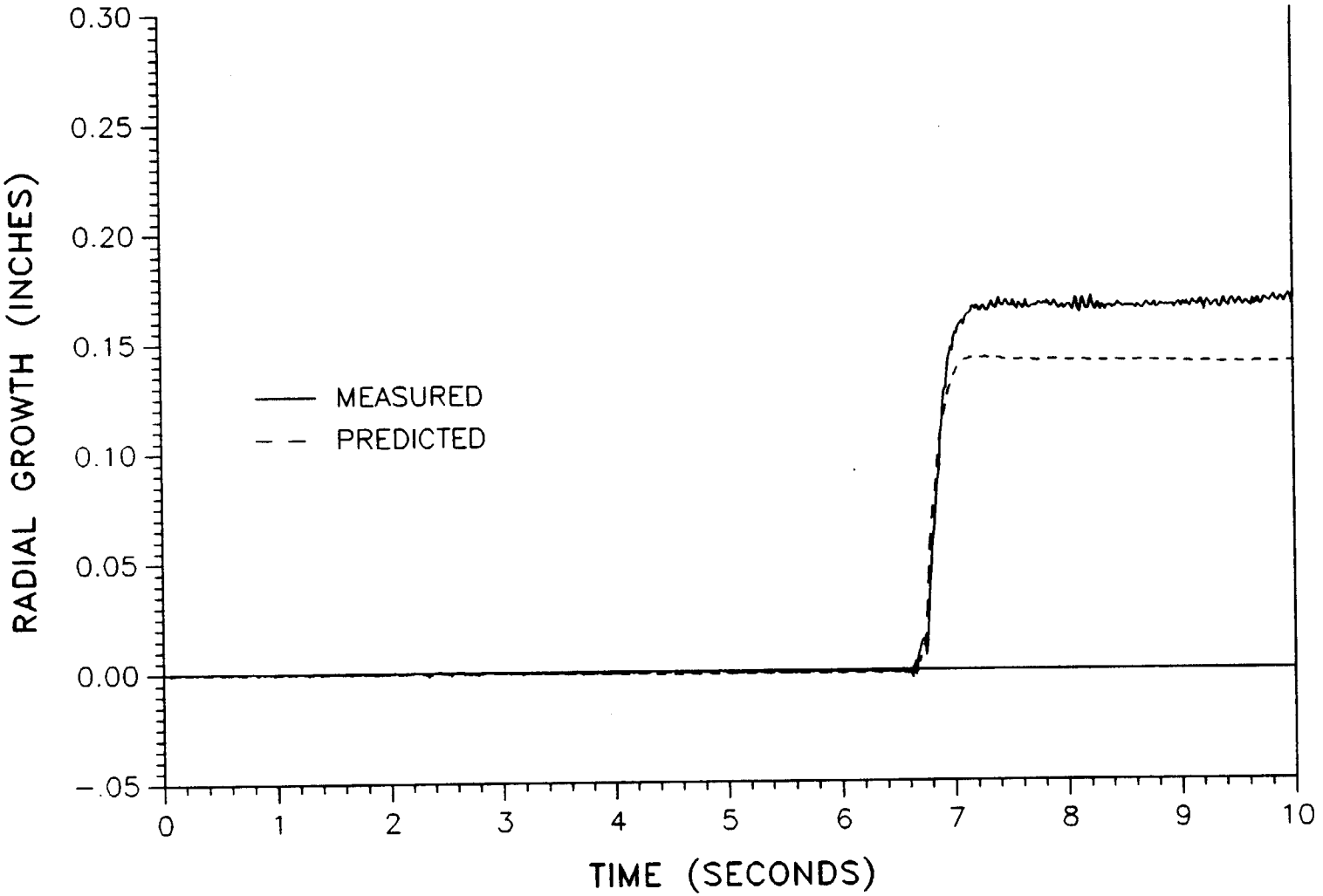

PREDICTED VS MEASURED RADIAL GROWTH

360L001 GIRTH GAGE B08G8300A – STATION 1576.40

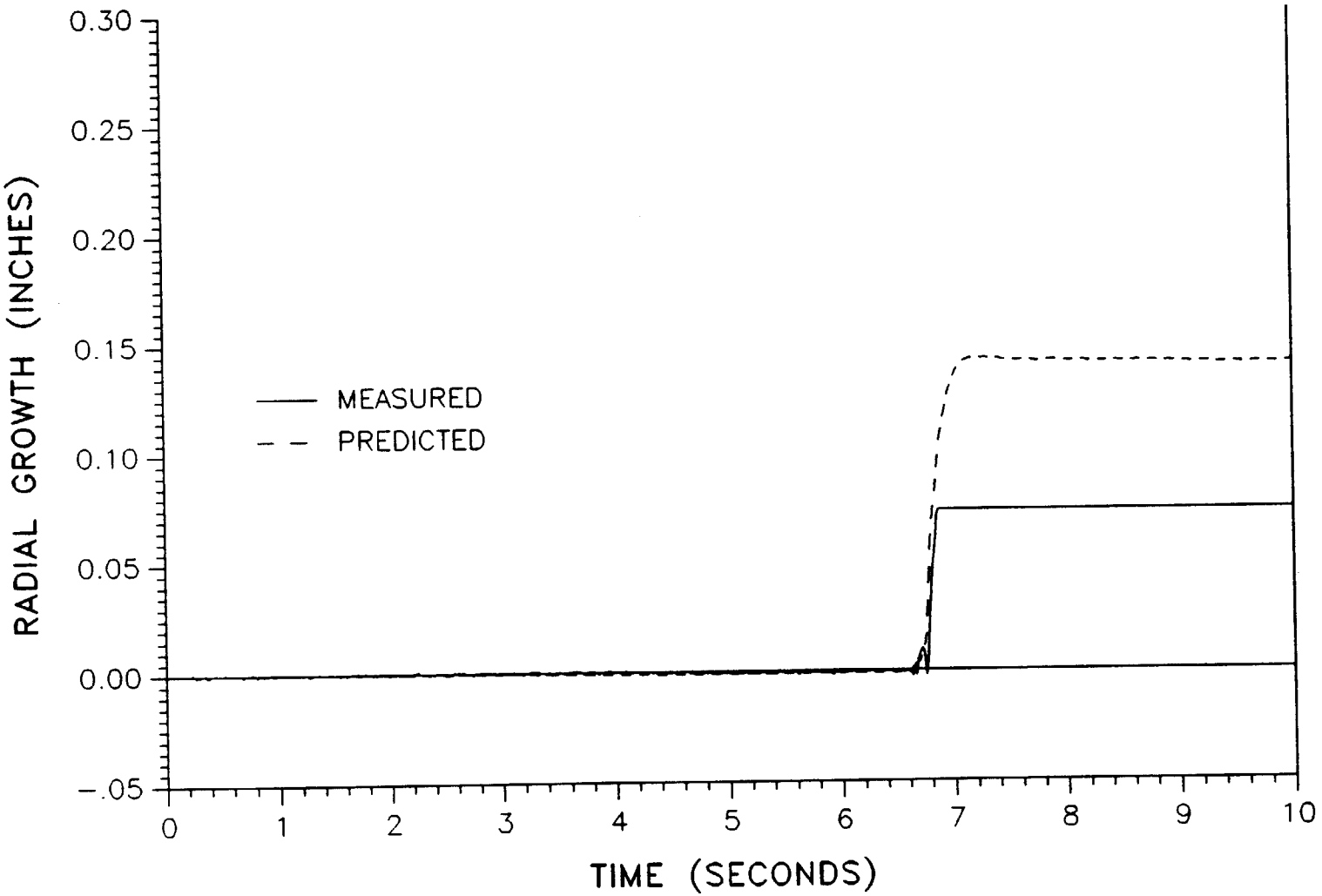

PREDICTED VS MEASURED RADIAL GROWTH

360L001 GIRTH GAGE B08G8301A – STATION 1637.50

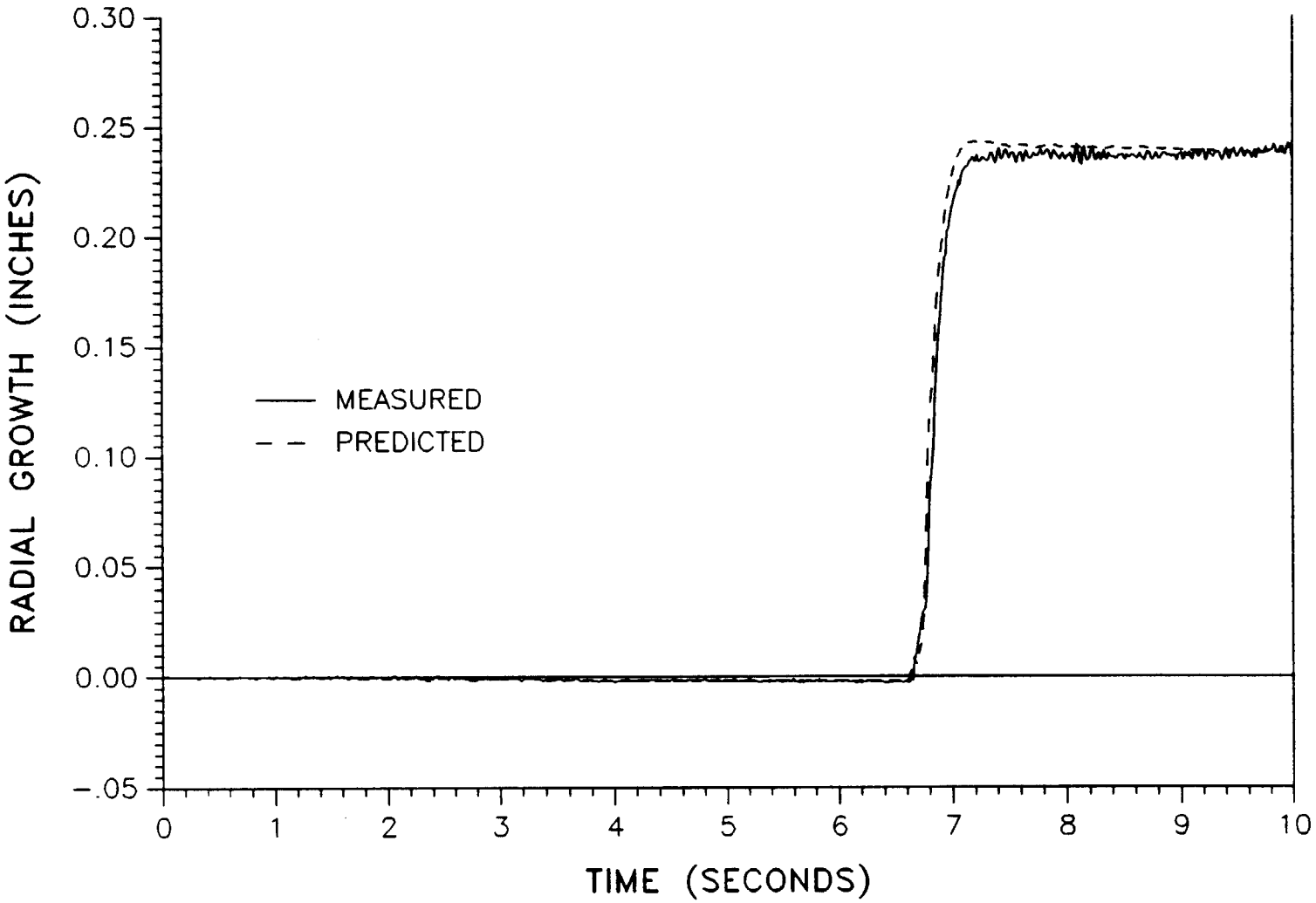

PREDICTED VS MEASURED RADIAL GROWTH

360L001 GIRTH GAGE B08G8302A – STATION 1694.75

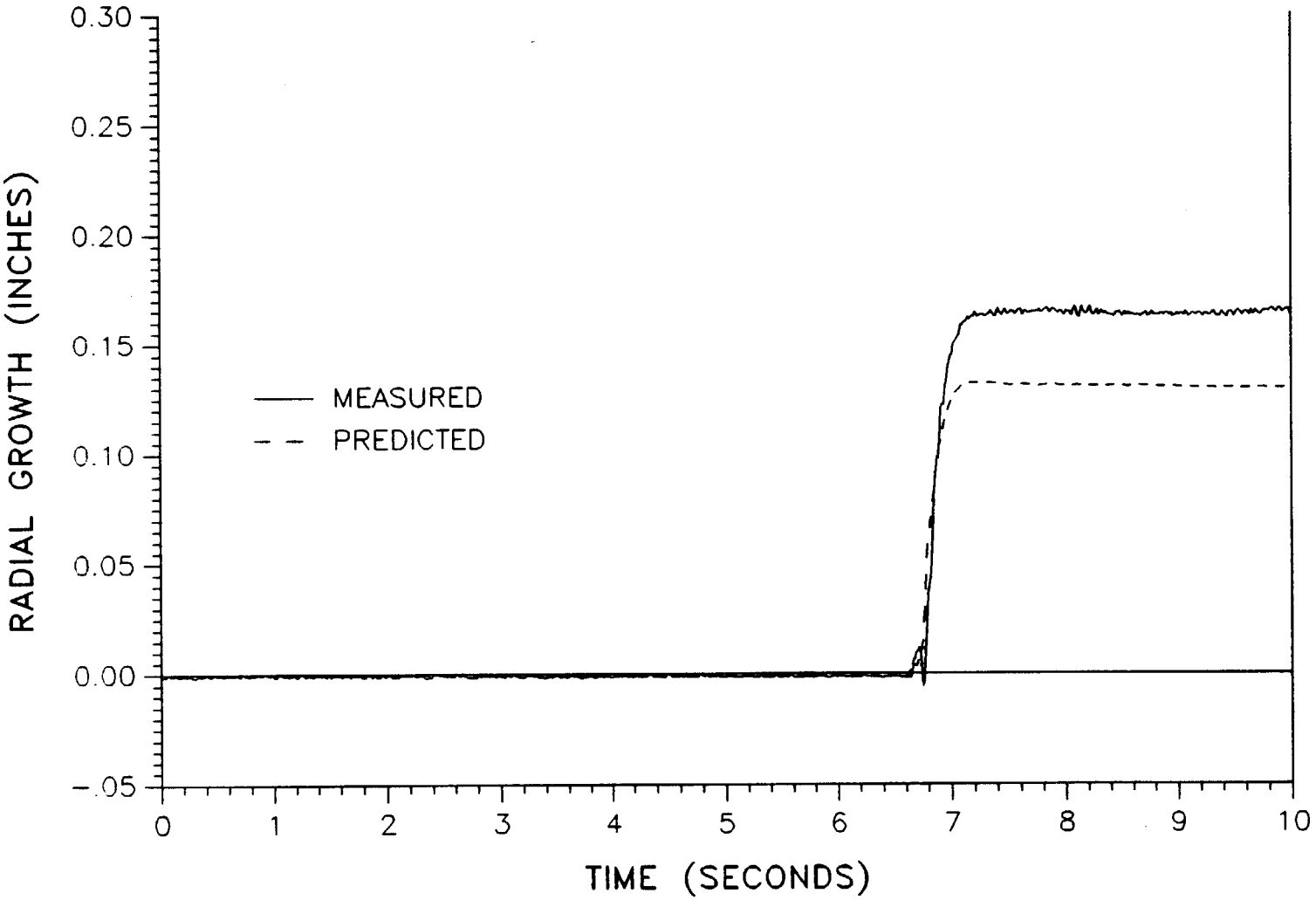

PREDICTED VS MEASURED RADIAL GROWTH

360L001 GIRTH GAGE B08G8303A - STATION 1696.40

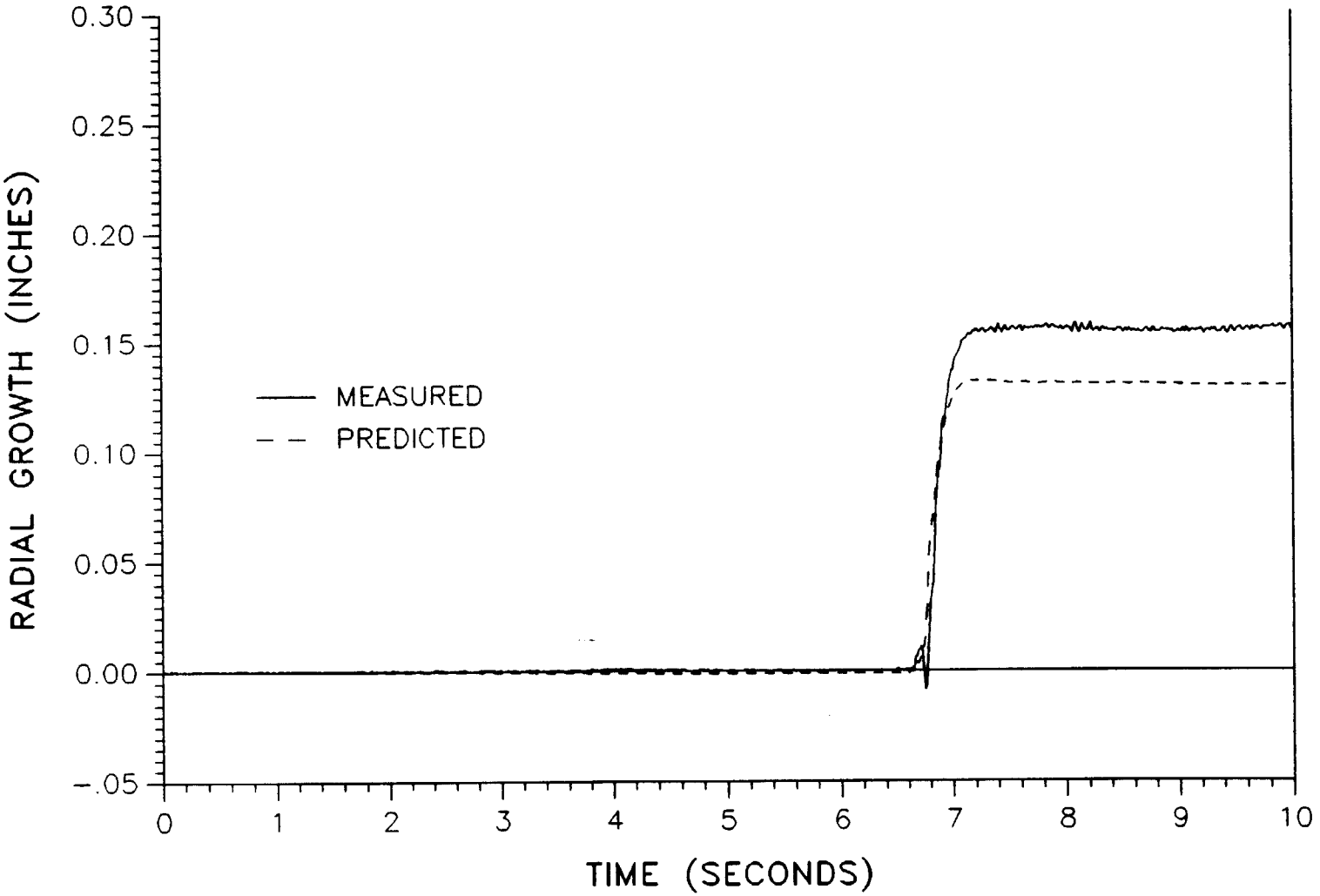

APPENDIX E

Hoop Strain Plots

PREDICTED VS MEASURED HOOP STRAIN

360L001 STRAIN GAGE B08G7319A – STATION 556.5 AT 0 DEGREES

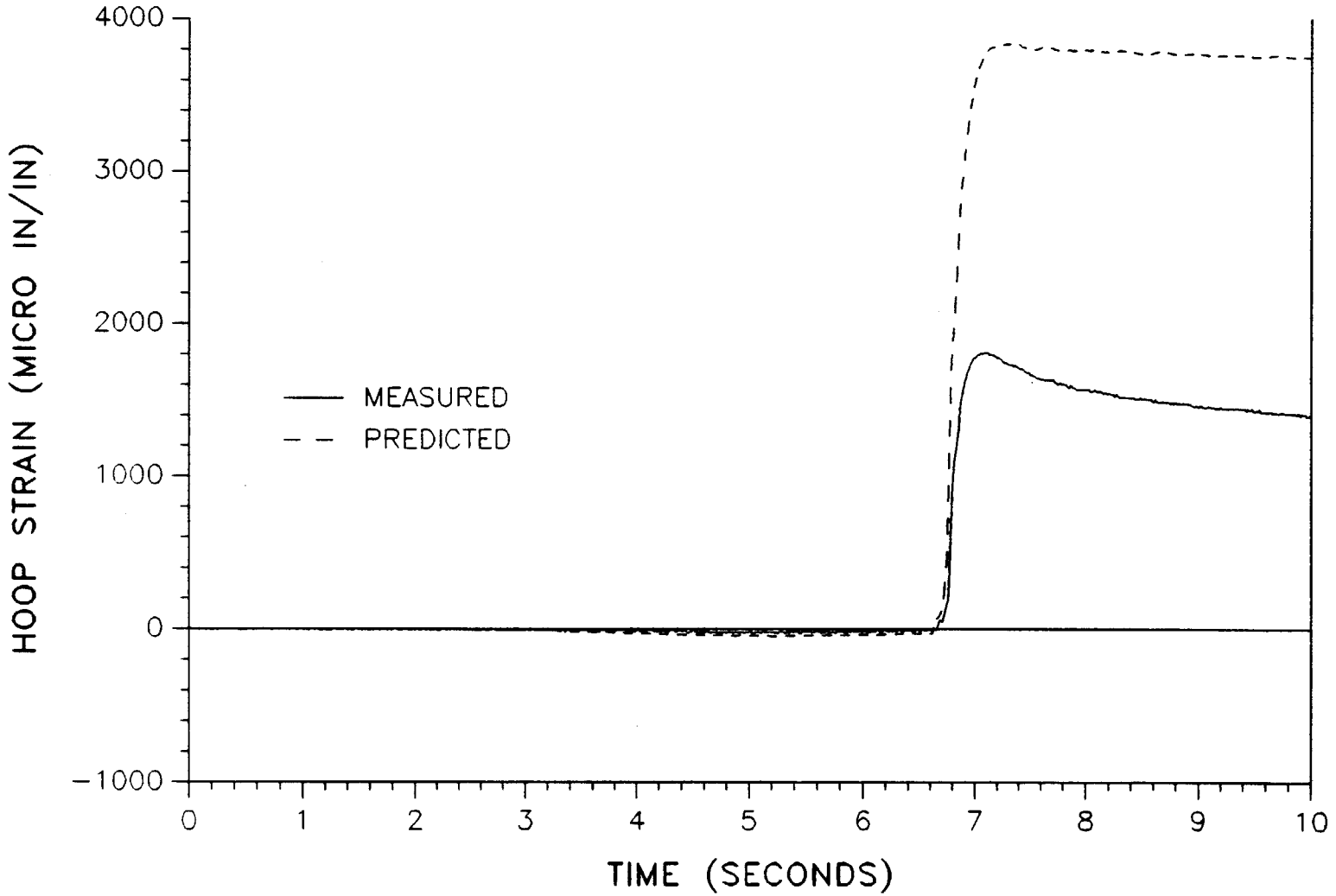

PREDICTED VS MEASURED HOOP STRAIN

360L001 STRAIN GAGE B08G7321A – STATION 556.5 AT 98 DEGREES

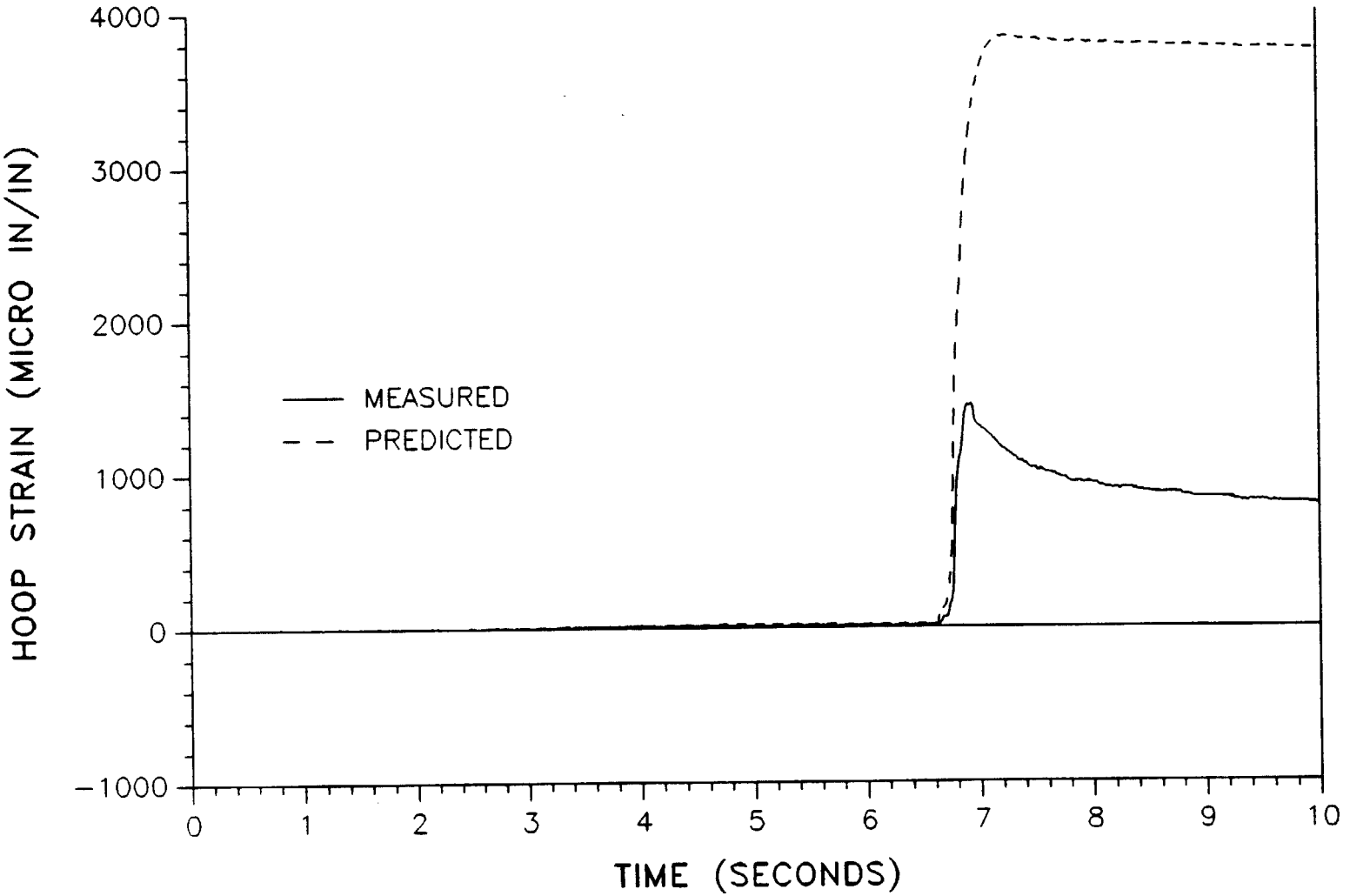

PREDICTED VS MEASURED HOOP STRAIN

360L001 STRAIN GAGE B08G7323A – STATION 556.5 AT 180 DEGREES

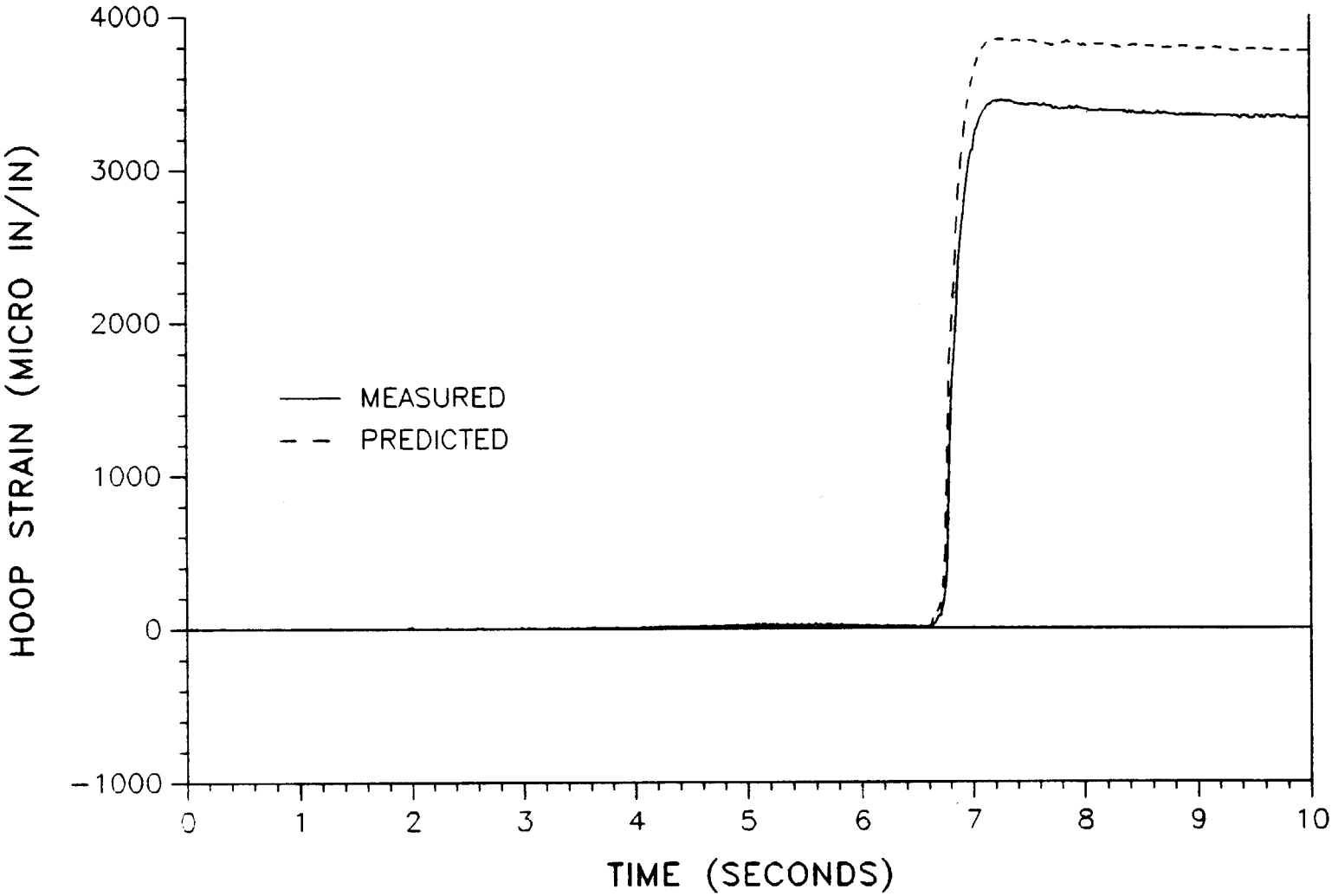

PREDICTED VS MEASURED HOOP STRAIN

360L001 STRAIN GAGE B08G7325A – STATION 556.5 AT 270 DEGREES

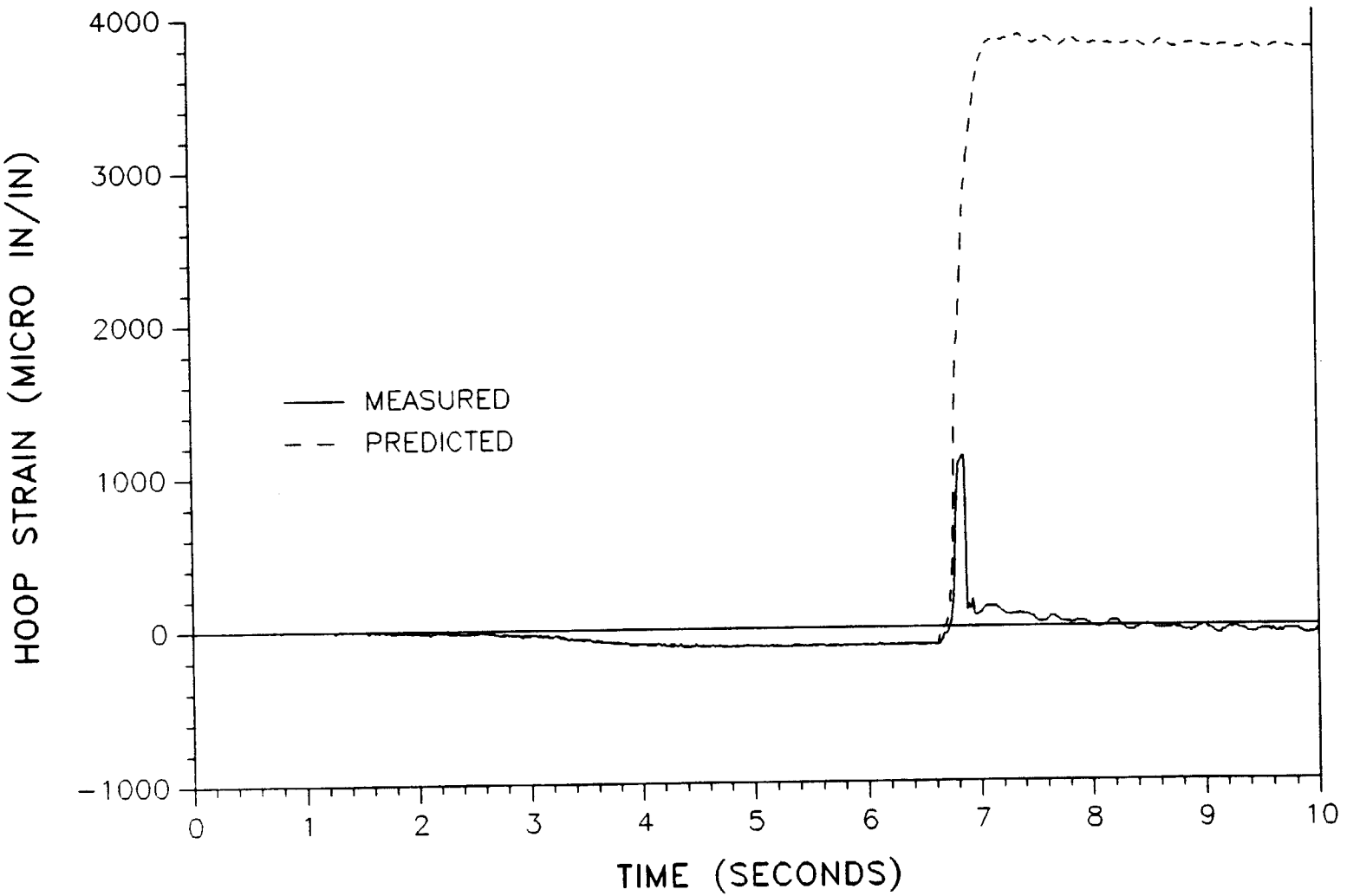

PREDICTED VS MEASURED HOOP STRAIN

360L001 STRAIN GAGE B08G7327A – STATION 876.5 AT 0 DEGREES

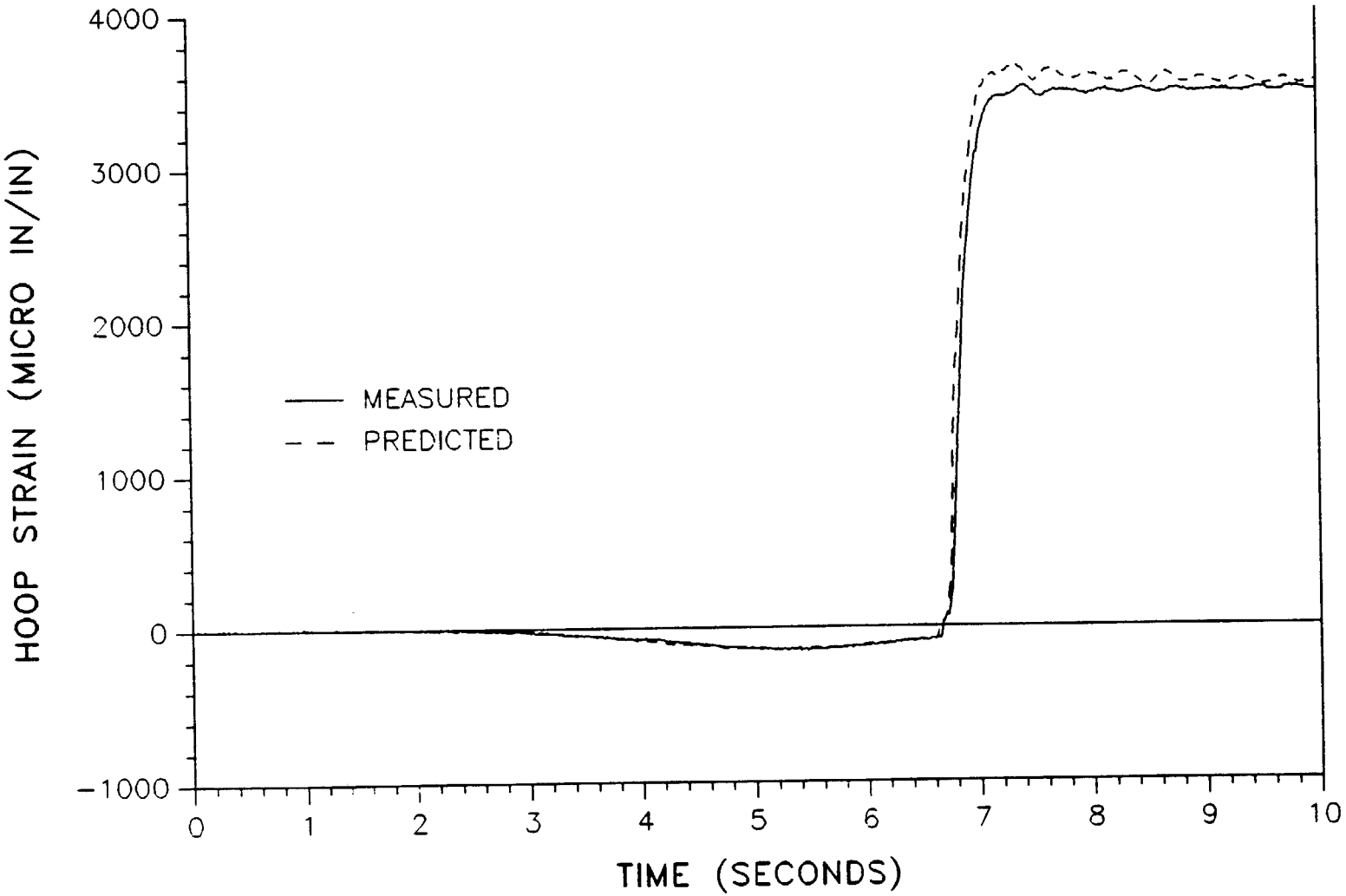

PREDICTED VS MEASURED HOOP STRAIN

360L001 STRAIN GAGE B08G7329A – STATION 876.5 AT 98 DEGREES

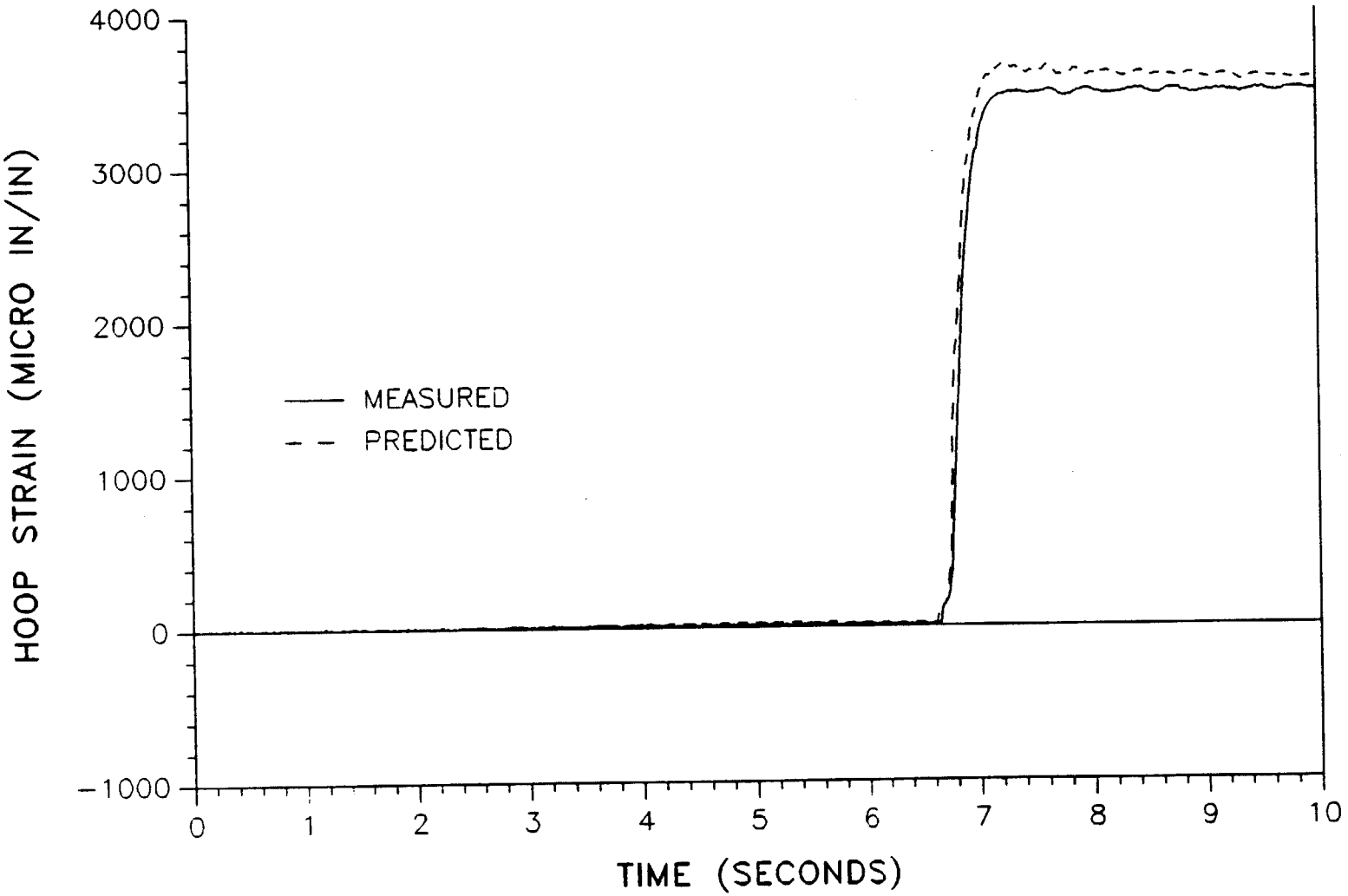

PREDICTED VS MEASURED HOOP STRAIN

360L001 STRAIN GAGE B08G7331A – STATION 876.5 AT 180 DEGREES

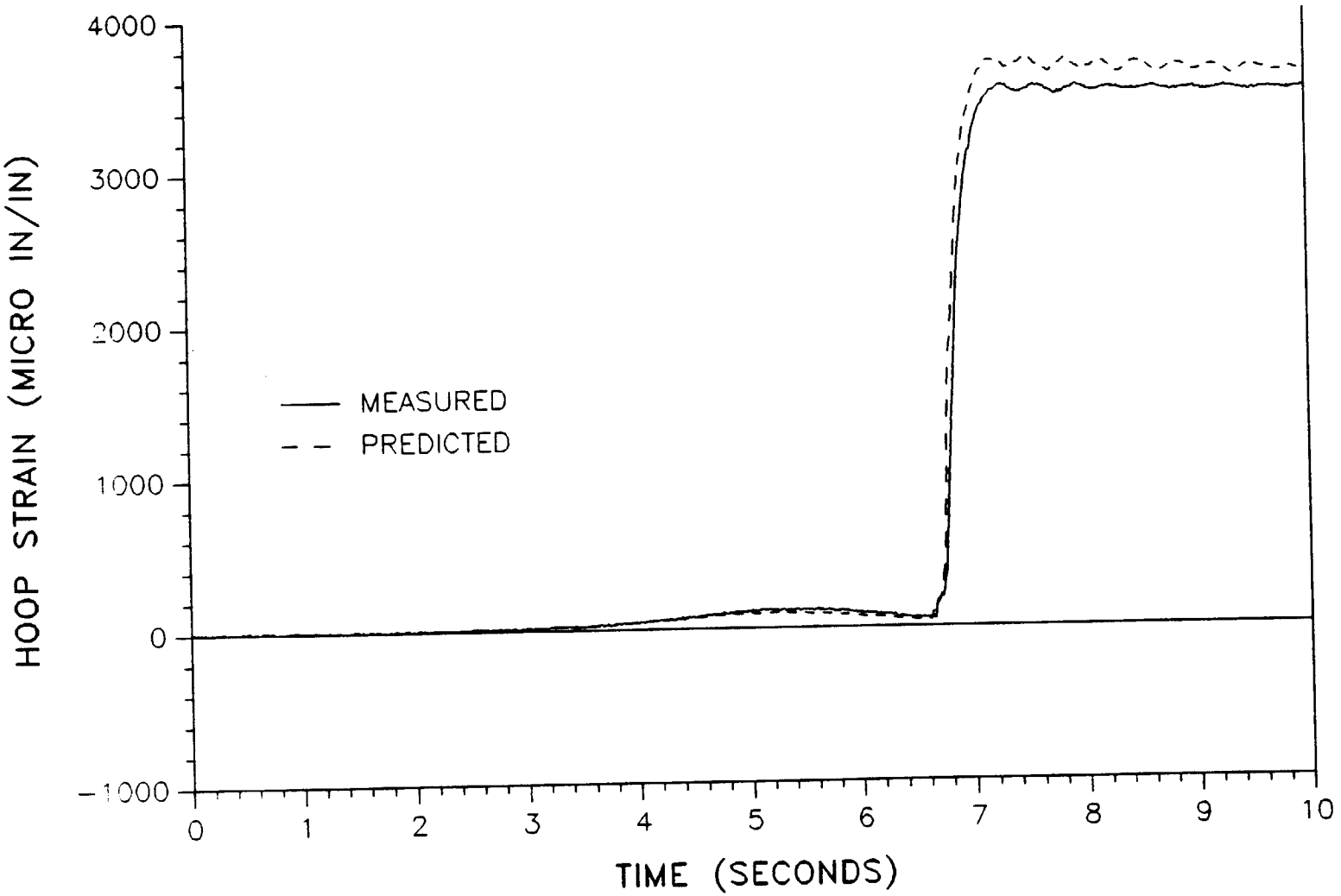

PREDICTED VS MEASURED HOOP STRAIN

360L001 STRAIN GAGE B08G7333A – STATION 876.5 AT 270 DEGREES

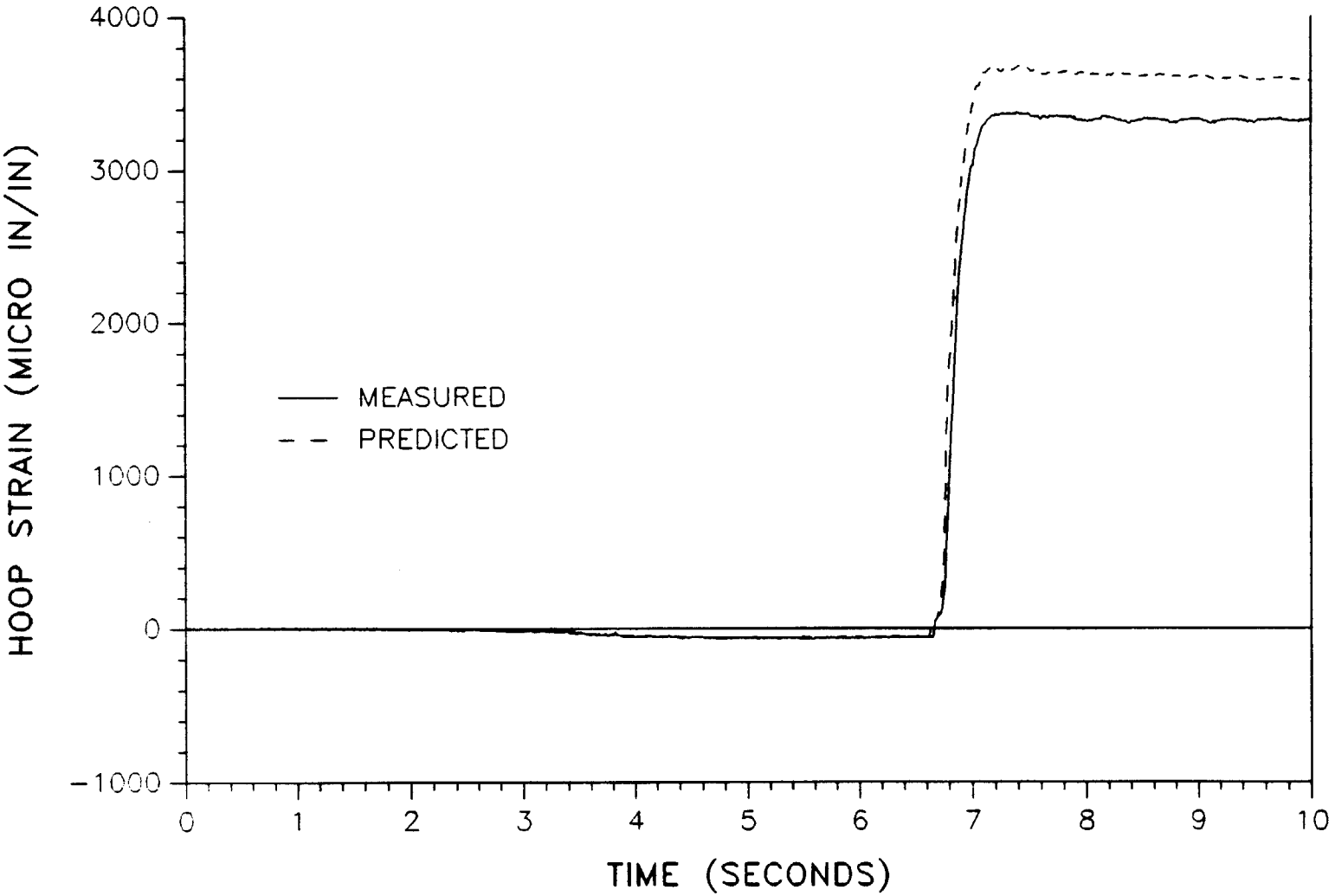

PREDICTED VS MEASURED HOOP STRAIN

360L001 STRAIN GAGE B08G7335A – STATION 1196.5 AT 0 DEGREES

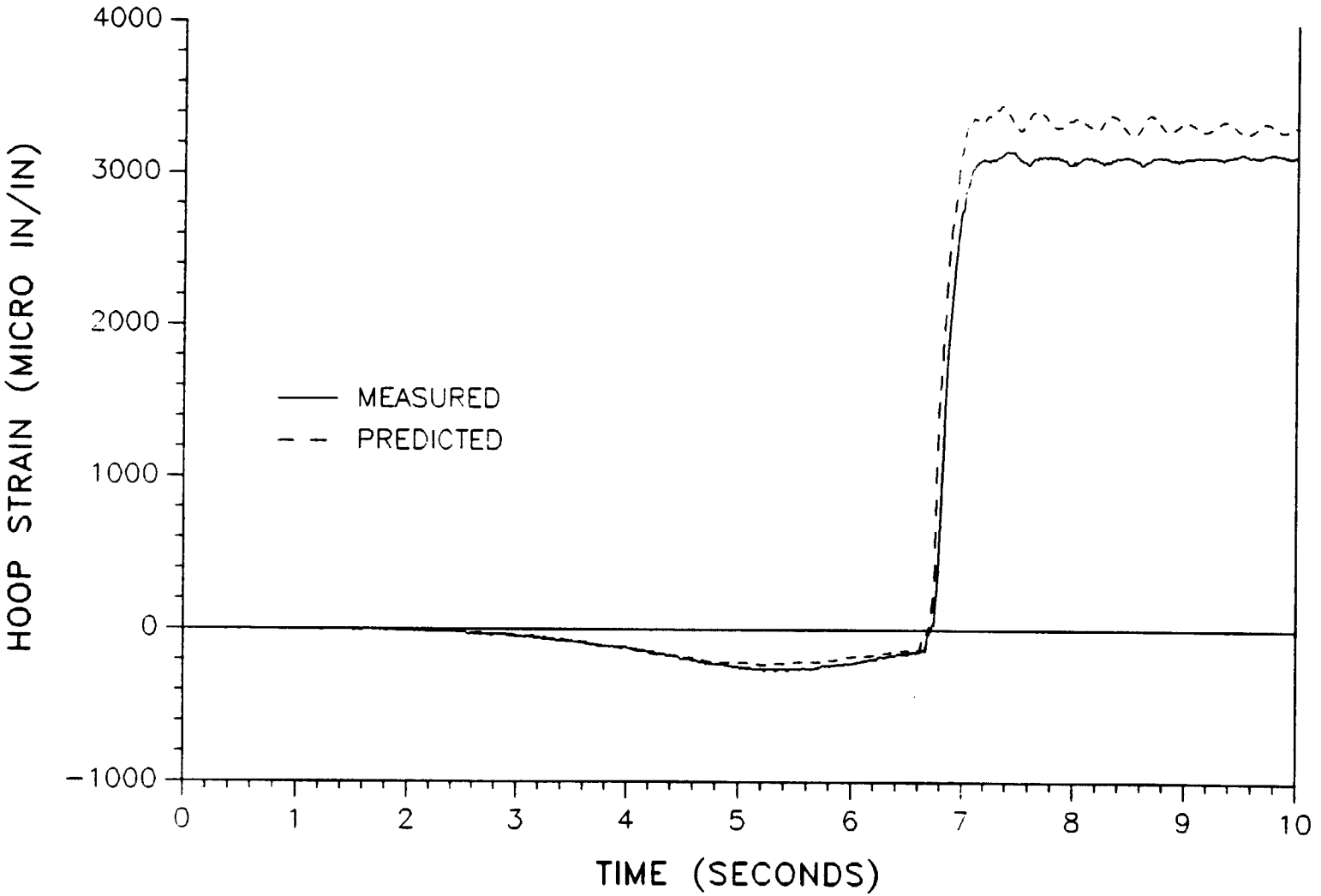

PREDICTED VS MEASURED HOOP STRAIN

360L001 STRAIN GAGE B08G7337A – STATION 1196.5 AT 98 DEGREES

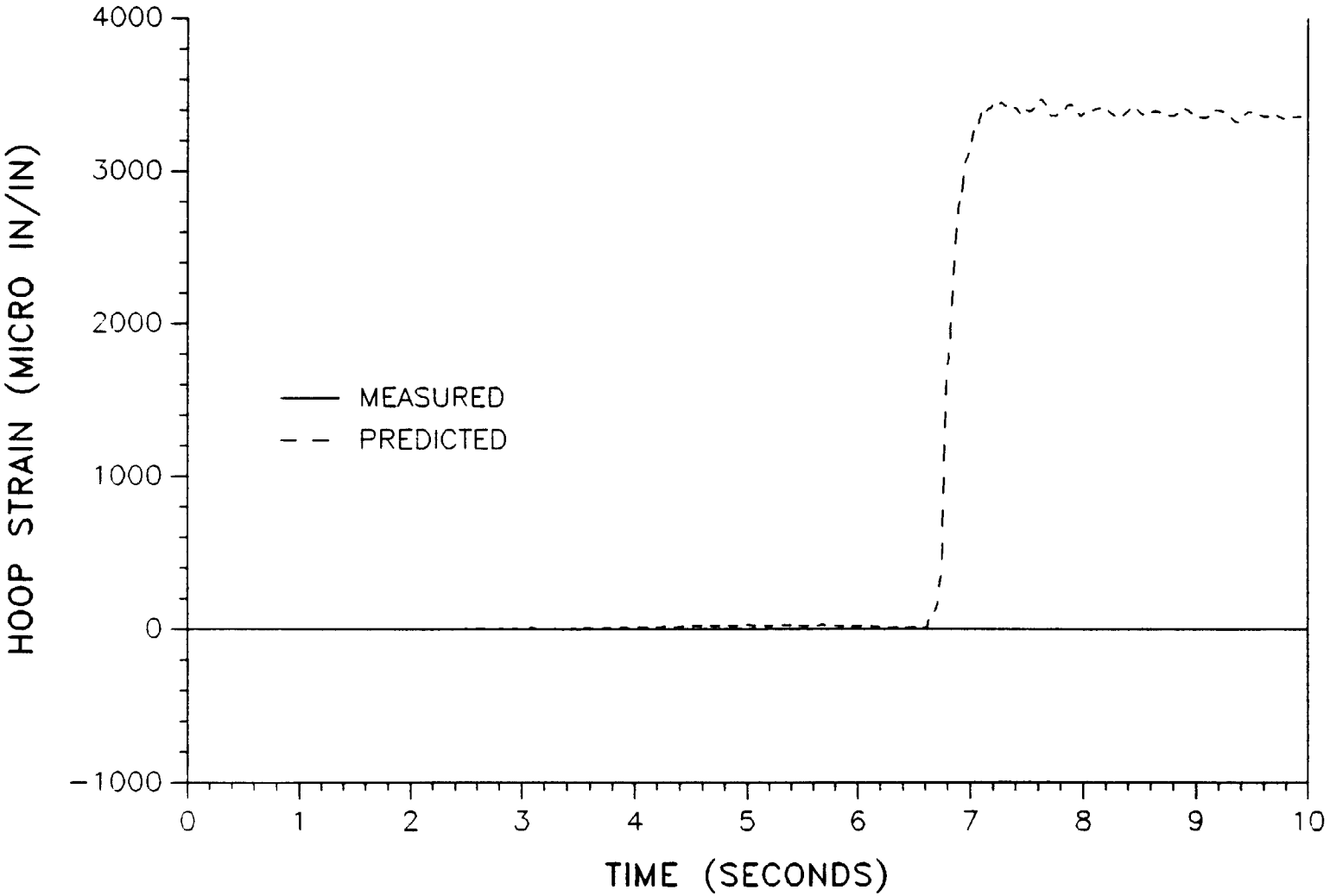

PREDICTED VS MEASURED HOOP STRAIN

360L001 STRAIN GAGE B08G7339A – STATION 1196.5 AT 180 DEGREES

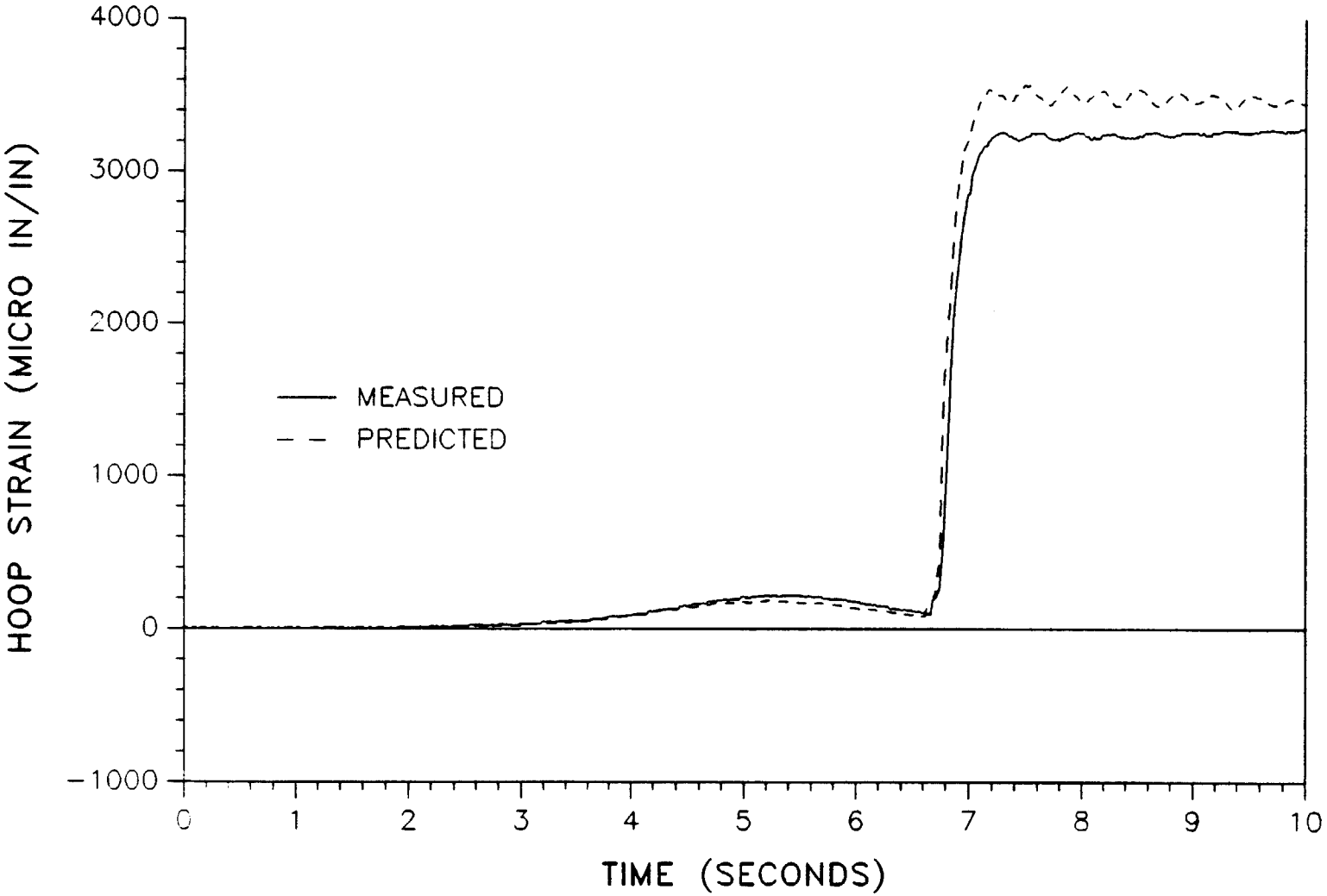

PREDICTED VS MEASURED HOOP STRAIN

360L001 STRAIN GAGE B08G7341A – STATION 1196.5 AT 270 DEGREES

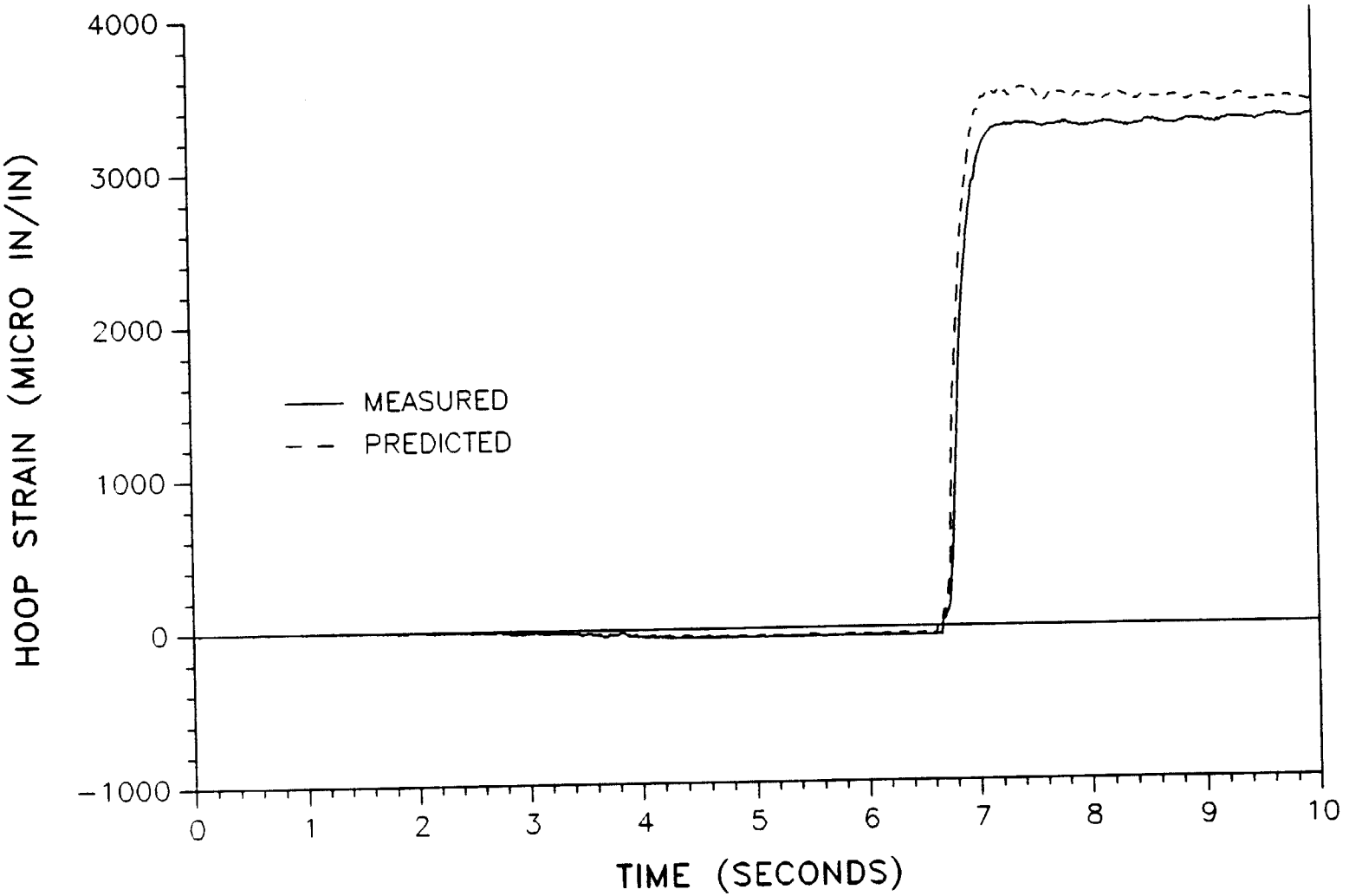

PREDICTED VS MEASURED HOOP STRAIN

360L001 STRAIN GAGE B08G7343A – STATION 1466.0 AT 0 DEGREES

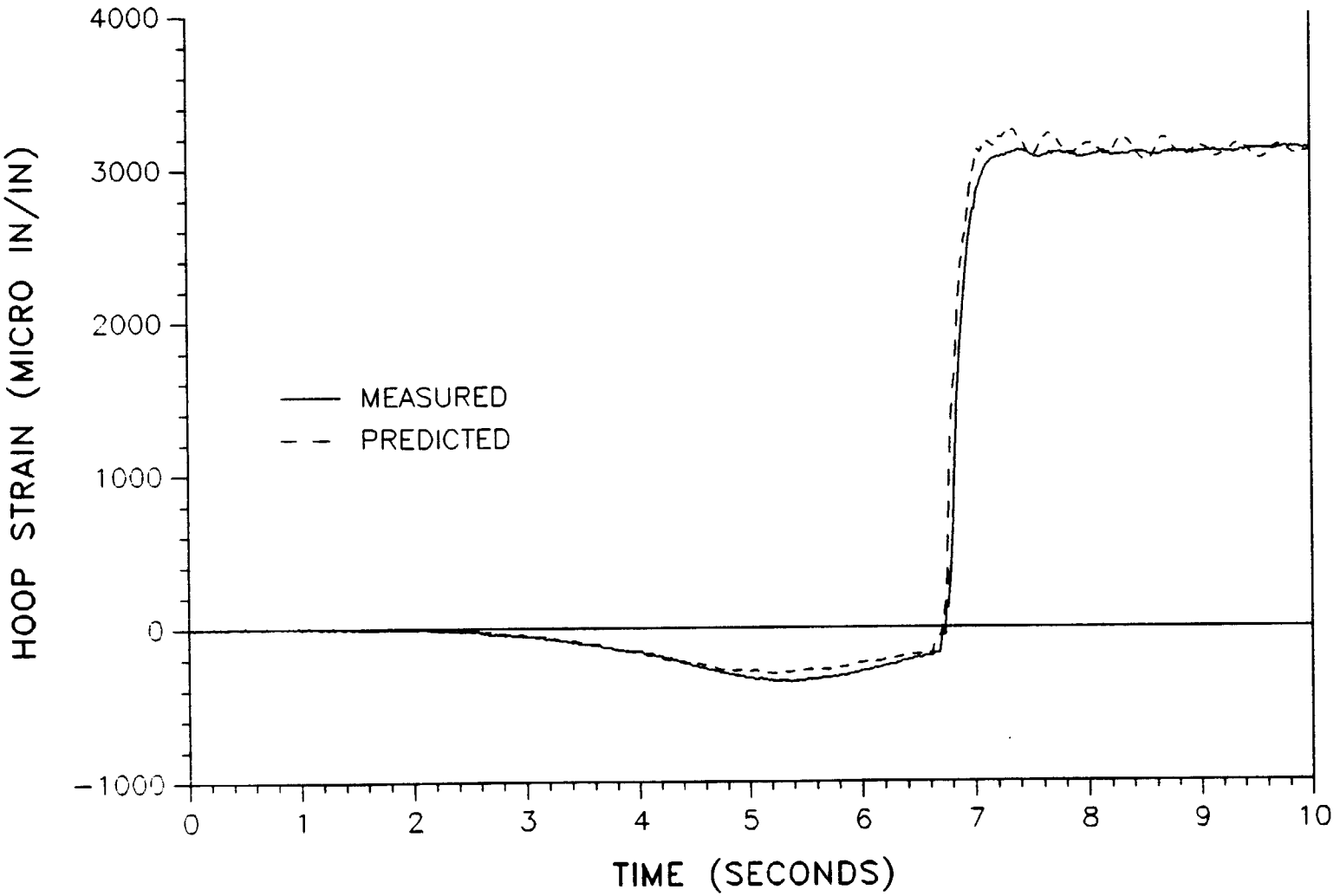

PREDICTED VS MEASURED HOOP STRAIN

360L001 STRAIN GAGE B08G7345A – STATION 1466.0 AT 98 DEGREES

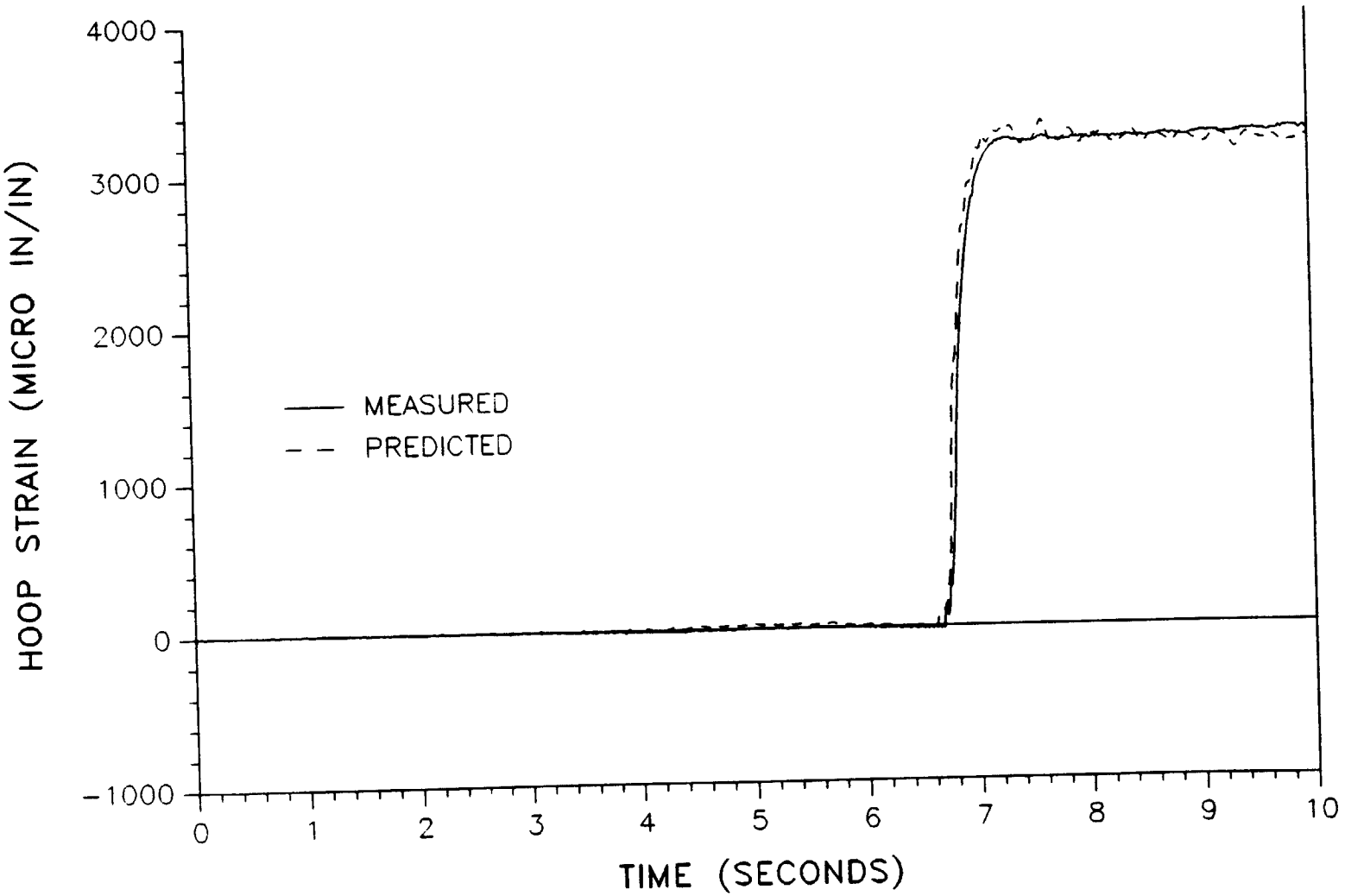

PREDICTED VS MEASURED HOOP STRAIN

360L001 STRAIN GAGE B08G7347A – STATION 1466.0 AT 180 DEGREES

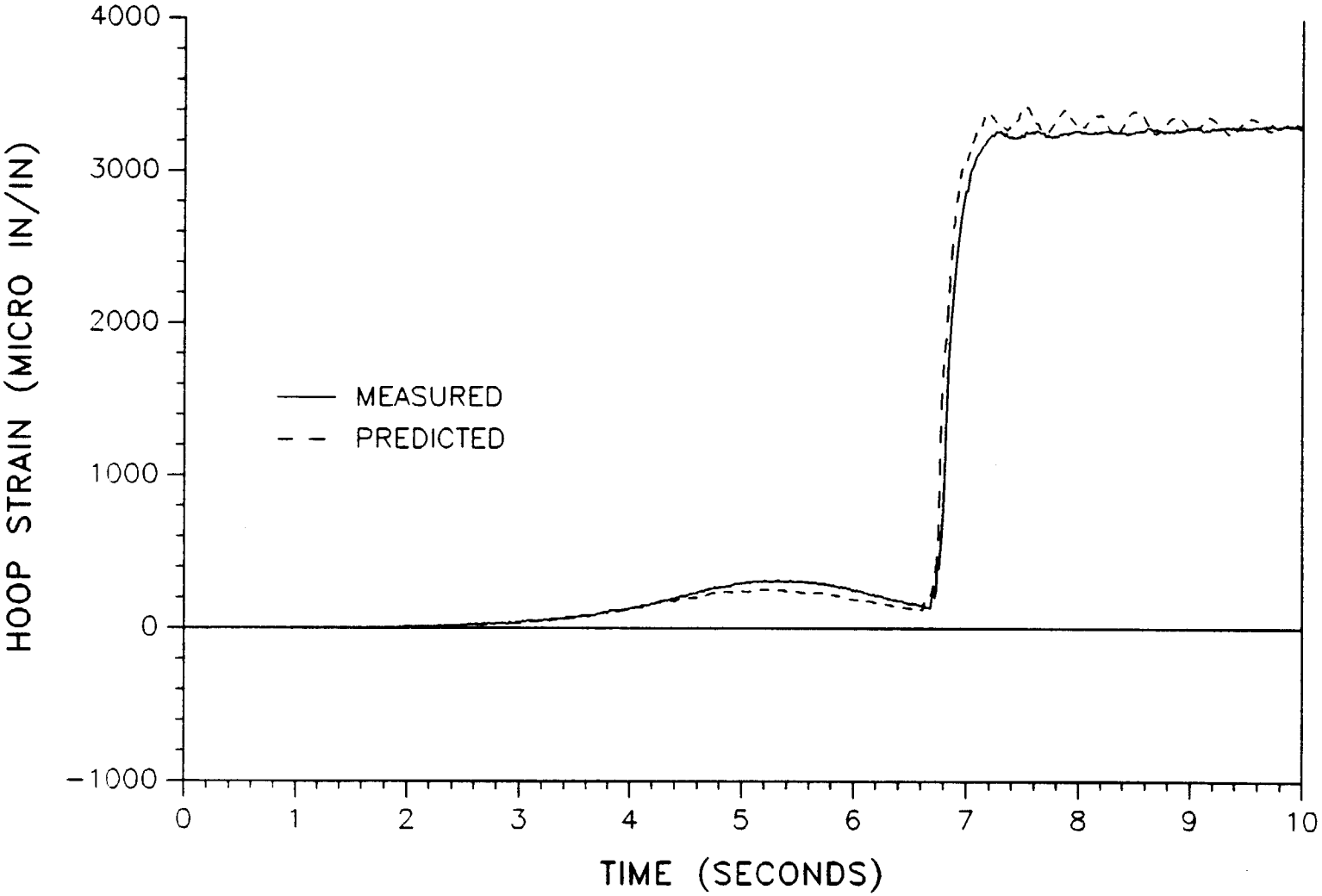

PREDICTED VS MEASURED HOOP STRAIN

360L001 STRAIN GAGE B08G7349A – STATION 1466.0 AT 270 DEGREES

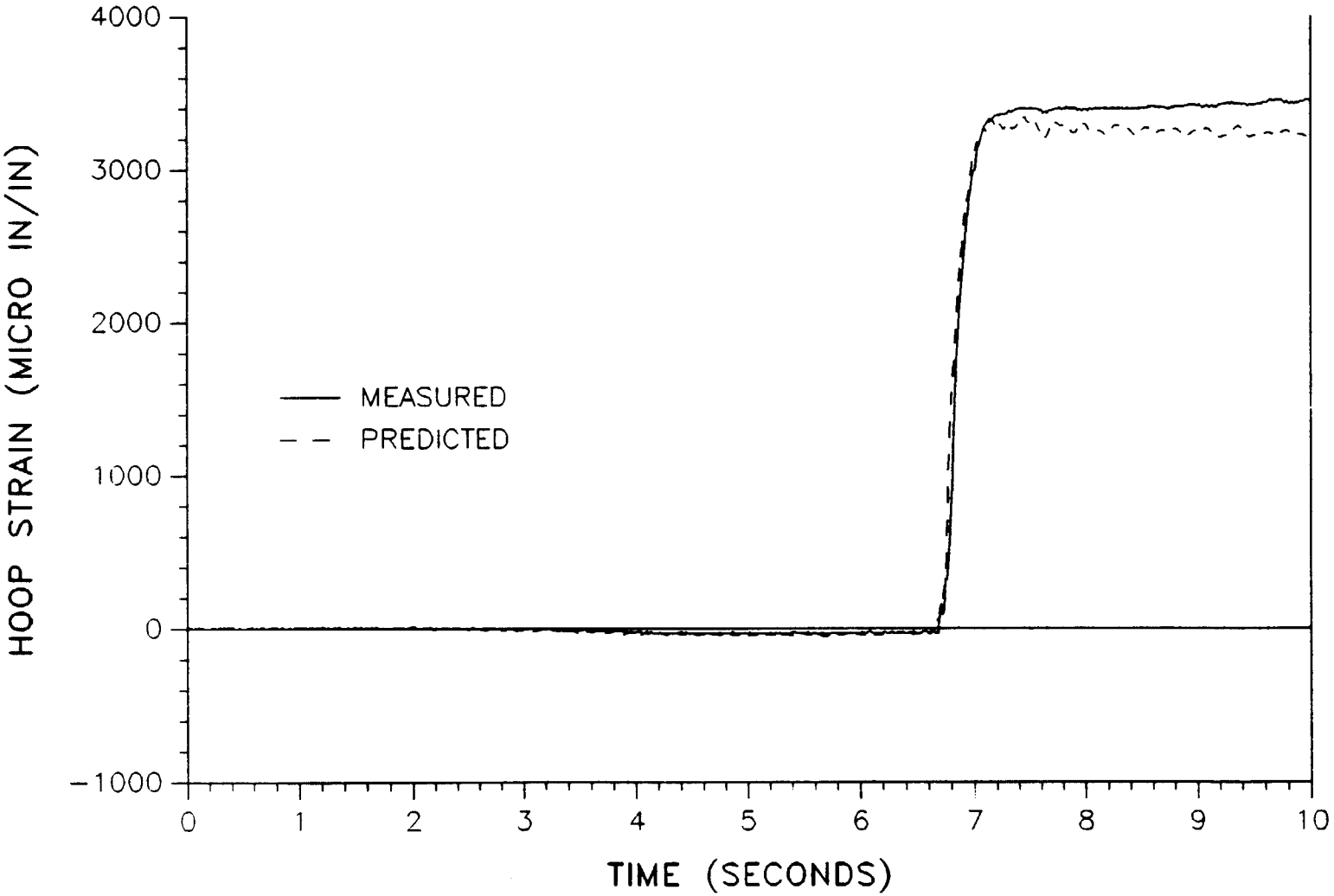

PREDICTED VS MEASURED HOOP STRAIN

360L001 STRAIN GAGE B08G7355A – STATION 1493.0 AT 0 DEGREES

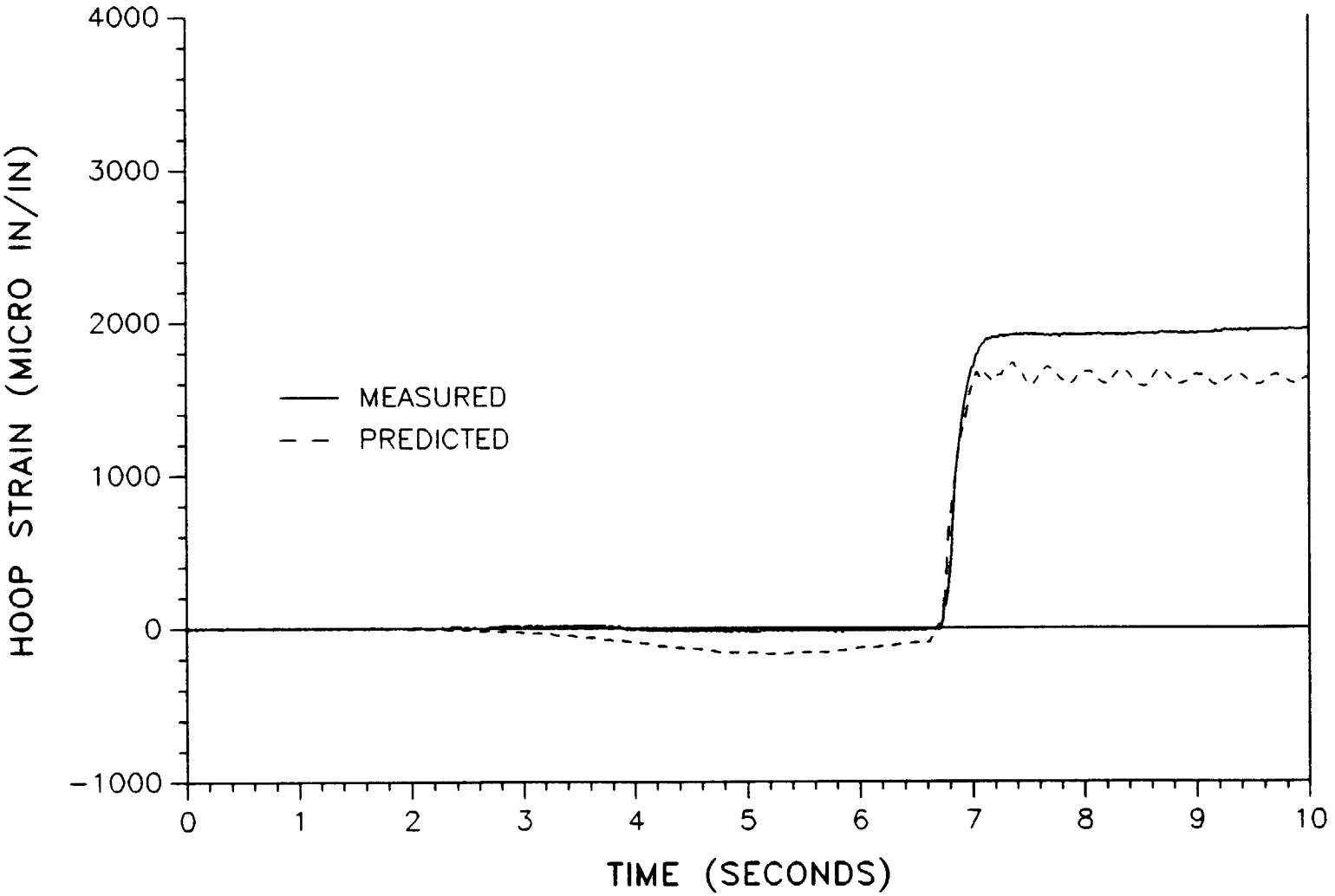

PREDICTED VS MEASURED HOOP STRAIN

360L001 STRAIN GAGE B08G7353A – STATION 1493.0 AT 98 DEGREES

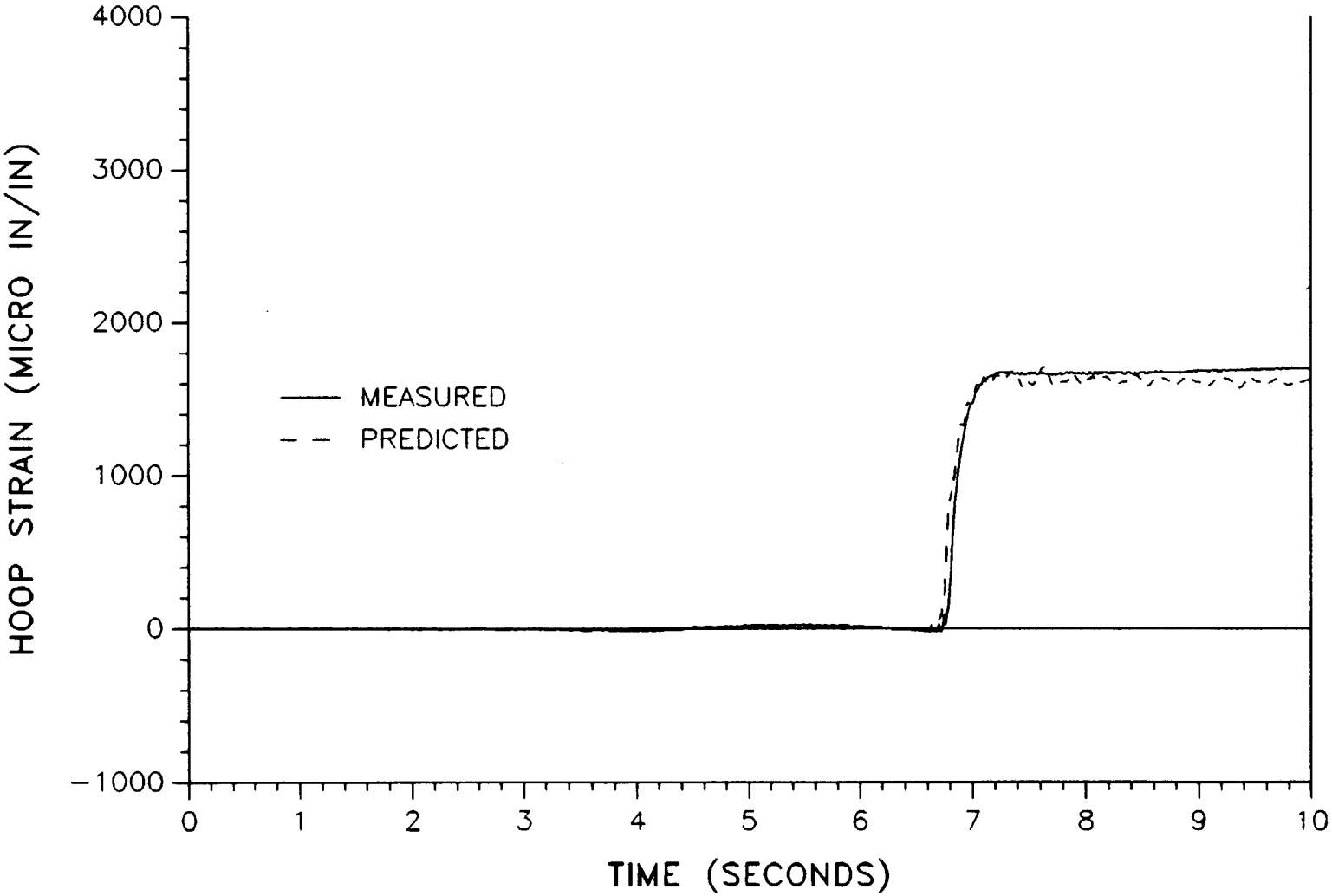

PREDICTED VS MEASURED HOOP STRAIN

360L001 STRAIN GAGE B08G7351A – STATION 1493.0 AT 180 DEGREES

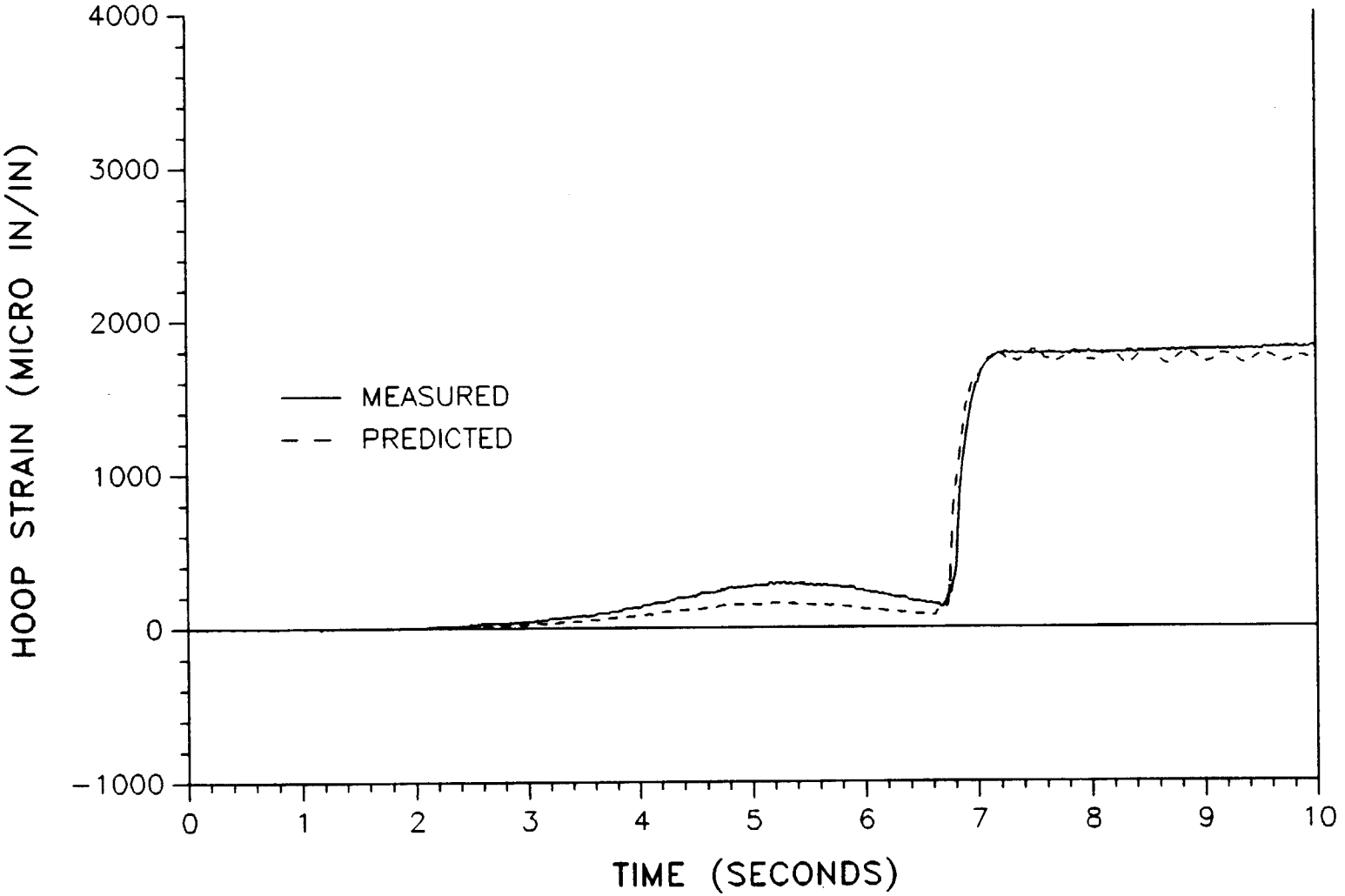

PREDICTED VS MEASURED HOOP STRAIN

360L001 STRAIN GAGE B08G7367A – STATION 1493.0 AT 220 DEGREES

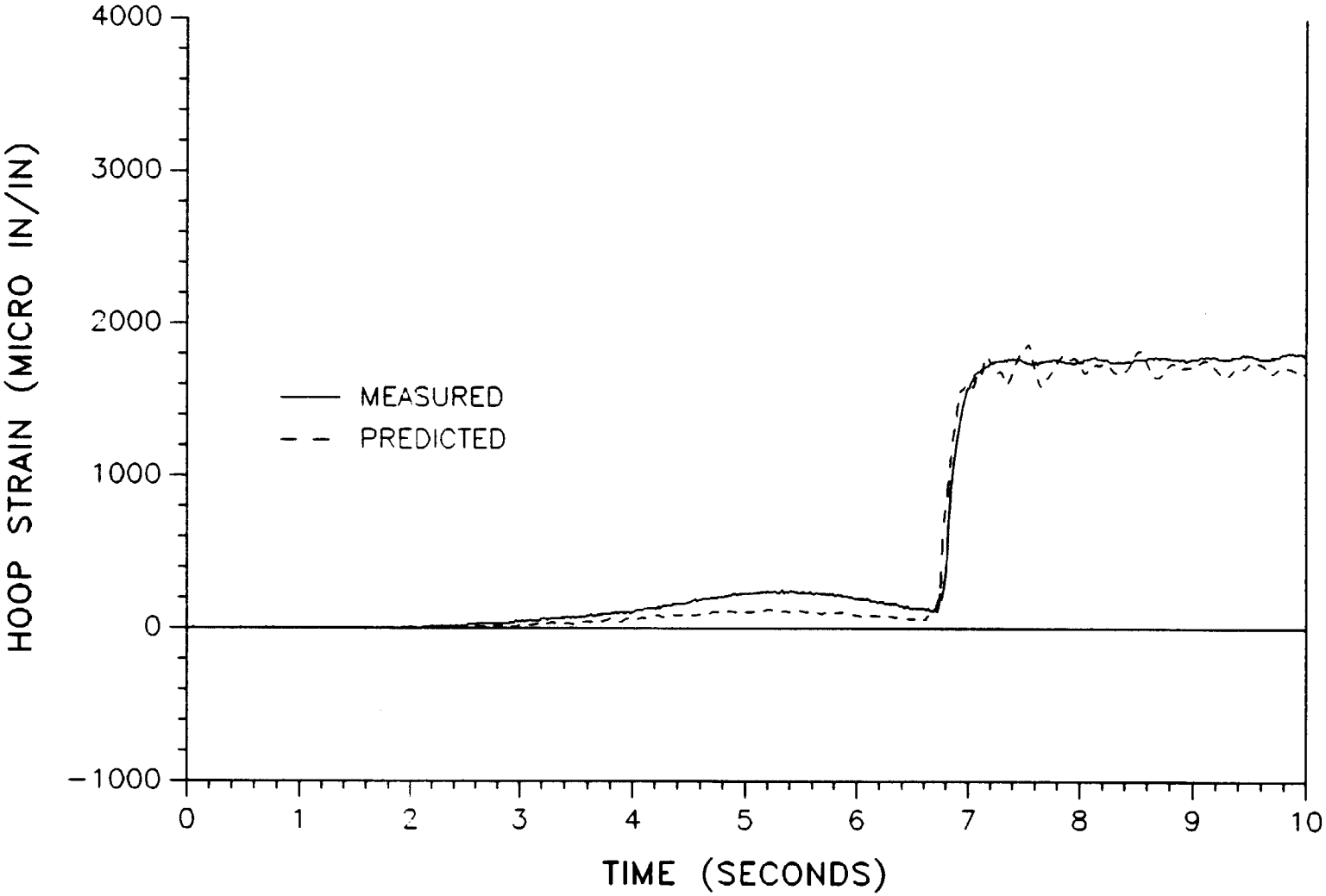

PREDICTED VS MEASURED HOOP STRAIN

360L001 STRAIN GAGE B08G7365A – STATION 1493.0 AT 255 DEGREES

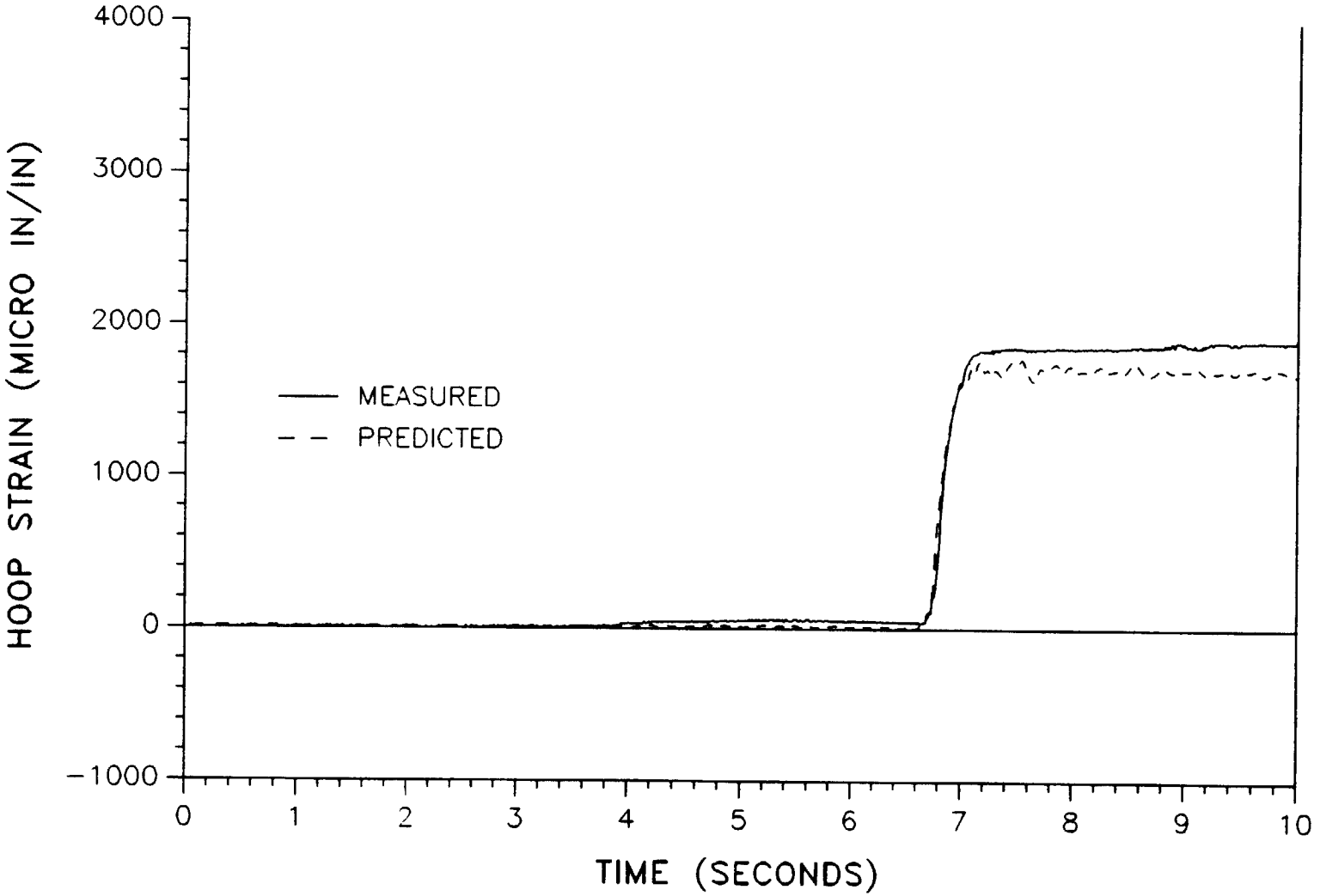

PREDICTED VS MEASURED HOOP STRAIN

360L001 STRAIN GAGE B08G7363A – STATION 1493.0 AT 270 DEGREES

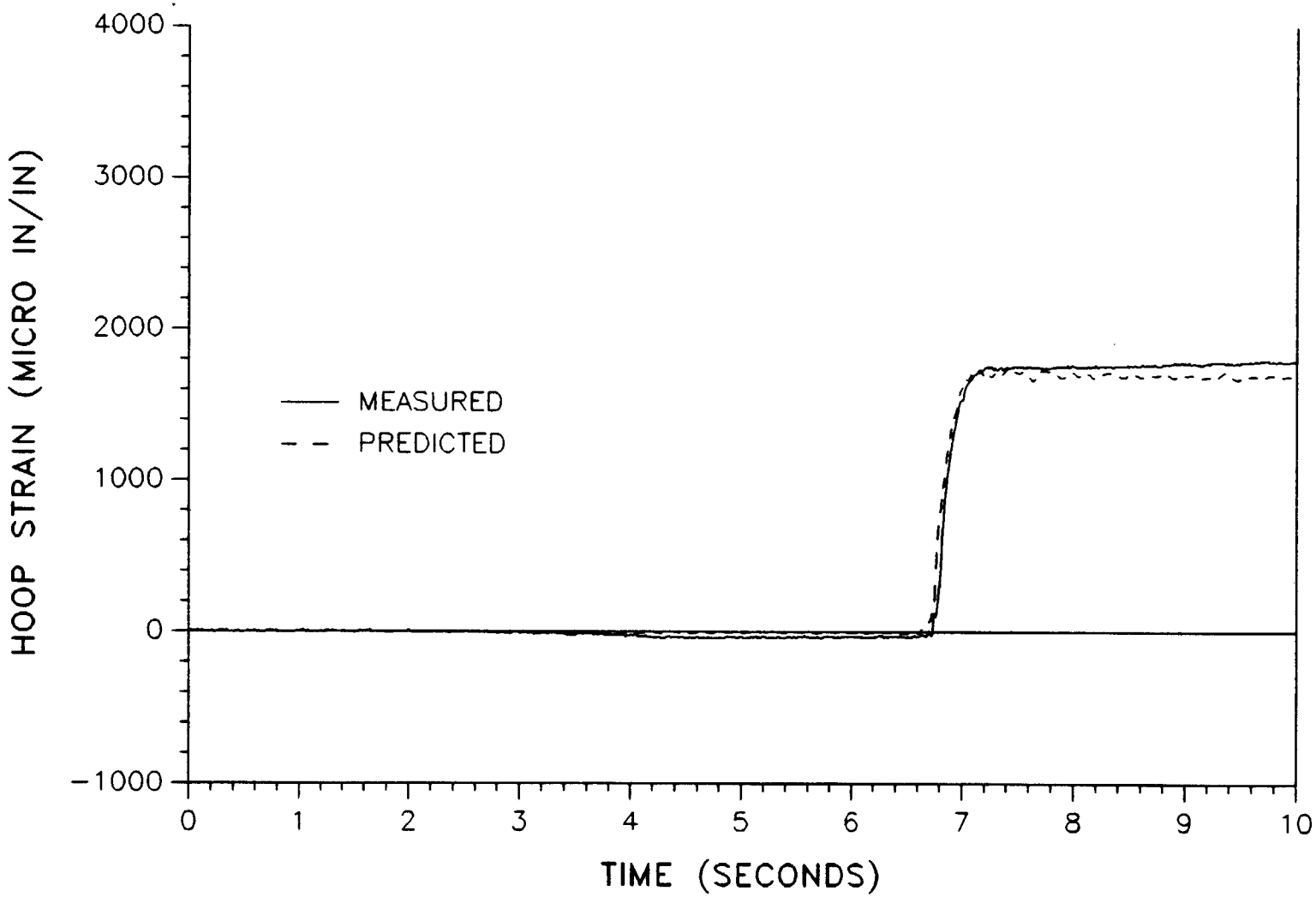

PREDICTED VS MEASURED HOOP STRAIN

360L001 STRAIN GAGE B08G7361A – STATION 1493.0 AT 285 DEGREES

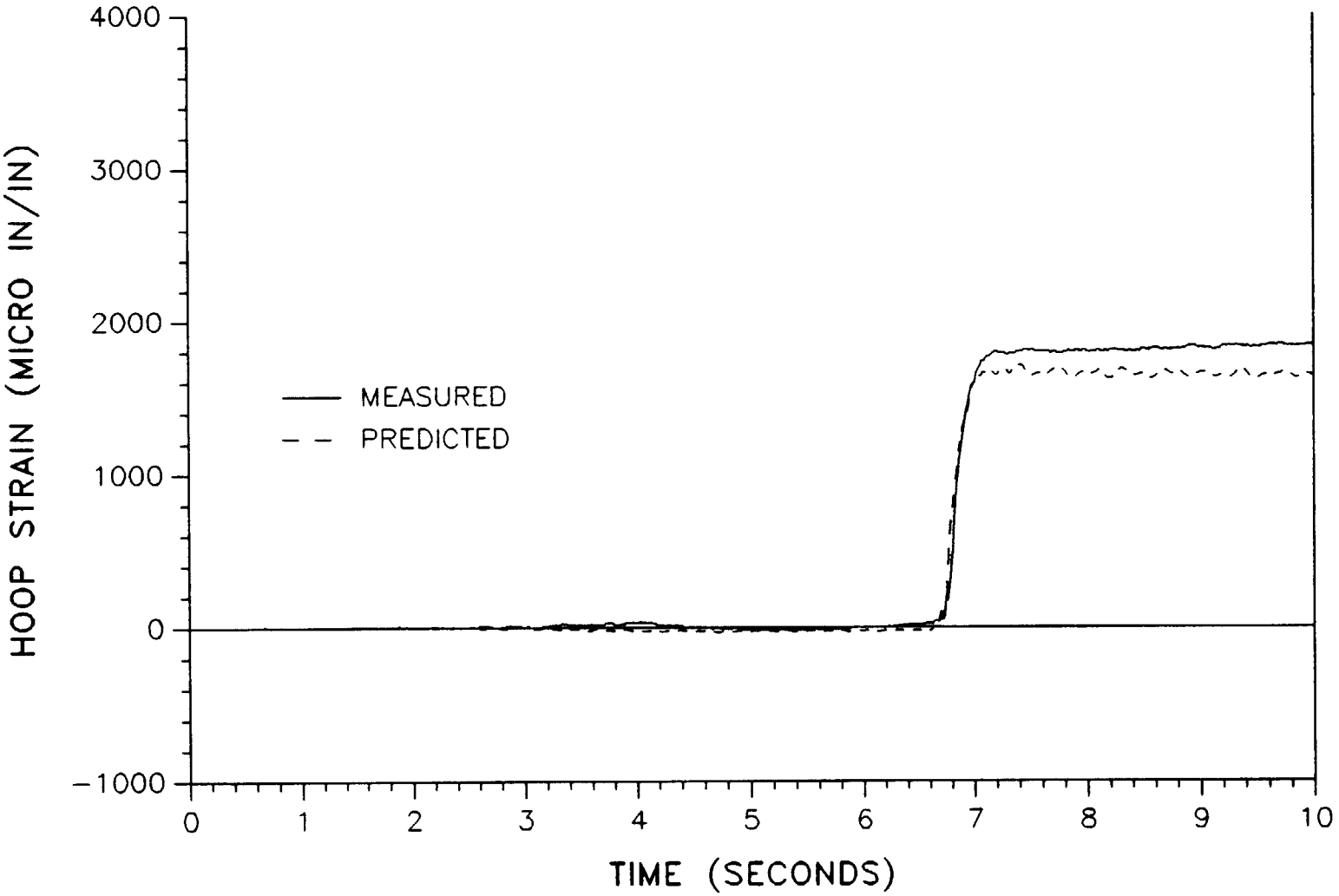

PREDICTED VS MEASURED HOOP STRAIN

360L001 STRAIN GAGE B08G7359A – STATION 1493.0 AT 300 DEGREES

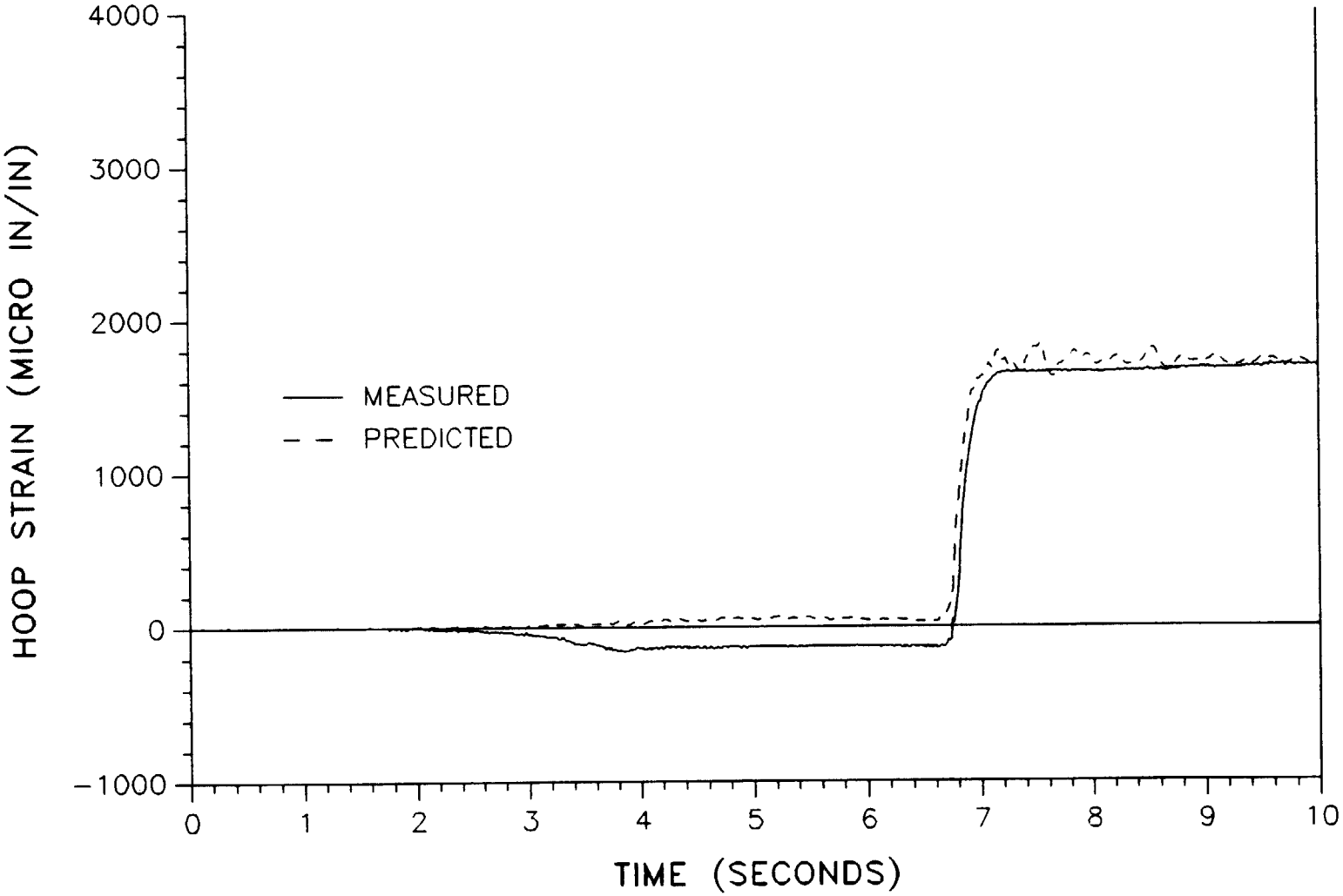

PREDICTED VS MEASURED HOOP STRAIN

360L001 STRAIN GAGE B08G7357A – STATION 1493.0 AT 320 DEGREES

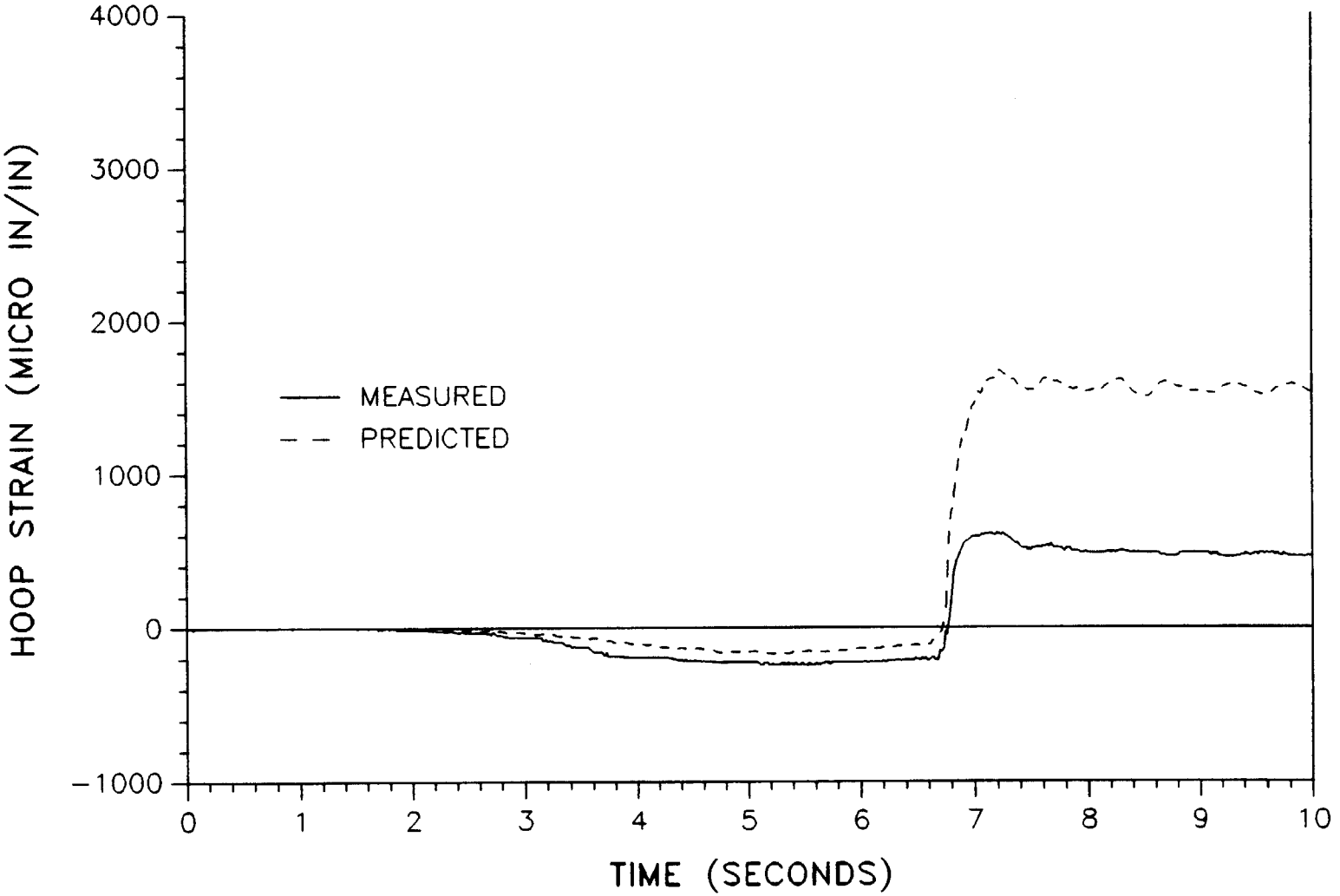

PREDICTED VS MEASURED HOOP STRAIN

360L001 STRAIN GAGE B08G7391A – STATION 1501.0 AT 0 DEGREES

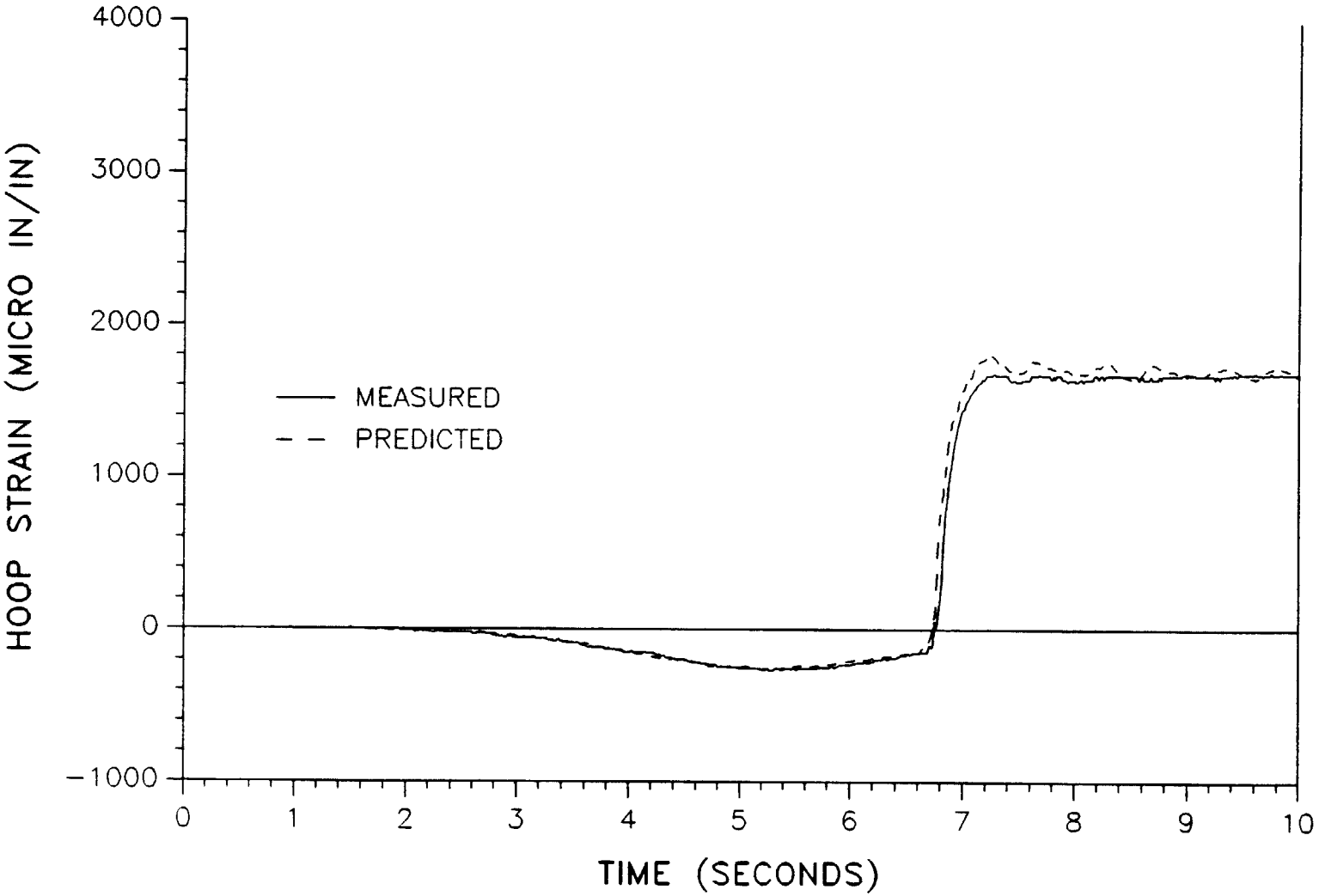

PREDICTED VS MEASURED HOOP STRAIN

360L001 STRAIN GAGE B08G7389A – STATION 1501.0 AT 98 DEGREES

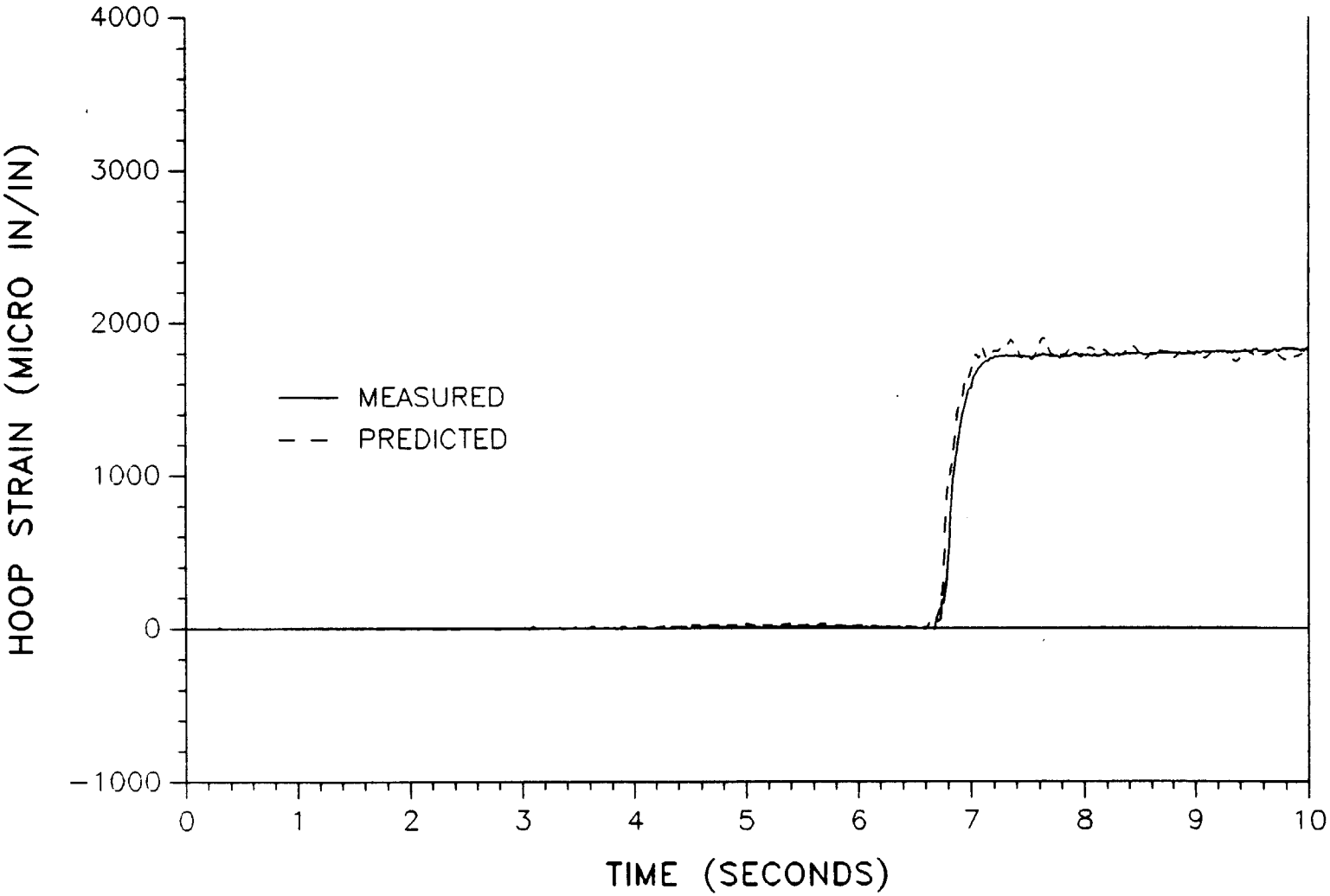

PREDICTED VS MEASURED HOOP STRAIN

360L001 STRAIN GAGE B08G7387A – STATION 1501.0 AT 180 DEGREES

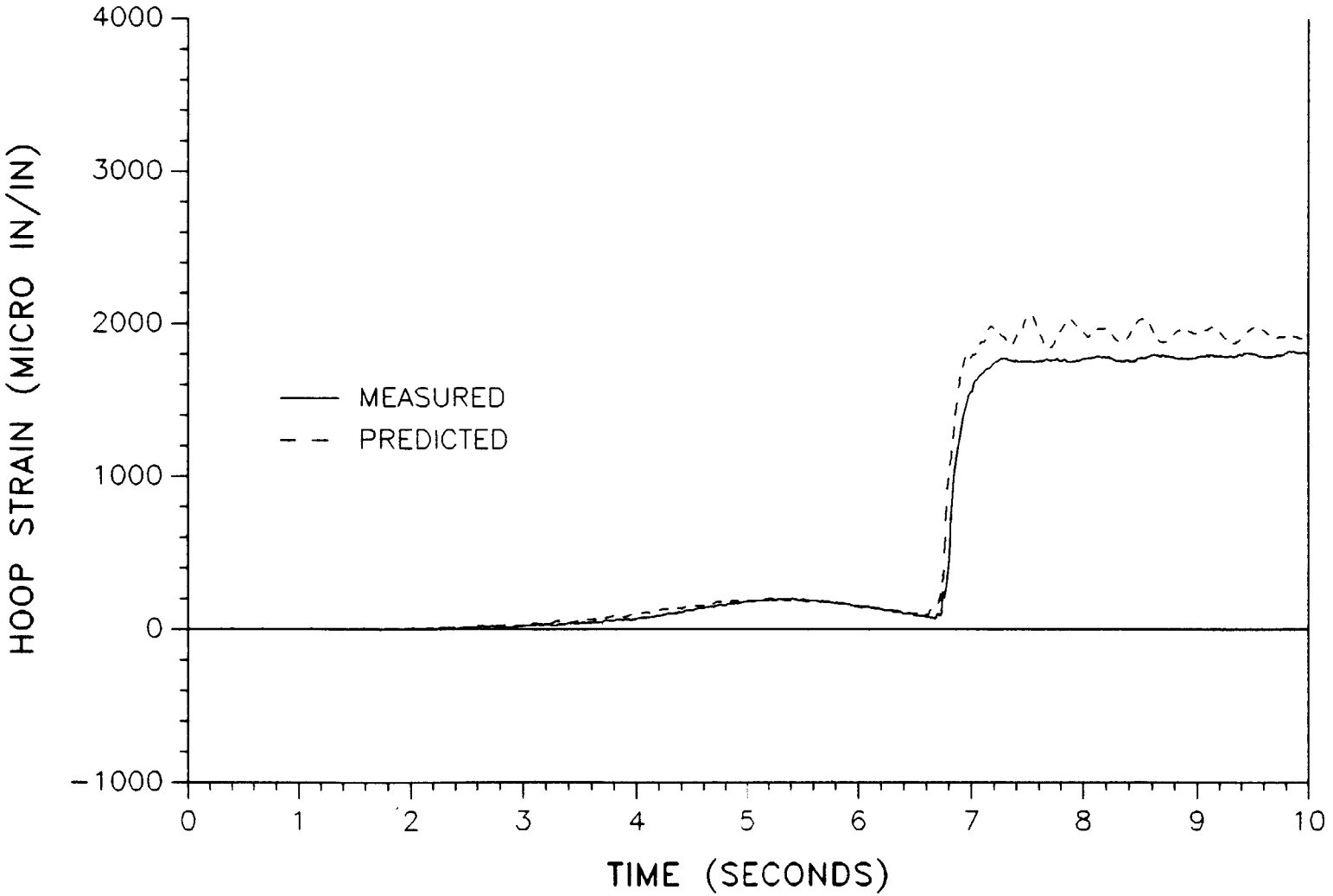

PREDICTED VS MEASURED HOOP STRAIN

360L001 STRAIN GAGE B08G7403A – STATION 1501.0 AT 220 DEGREES

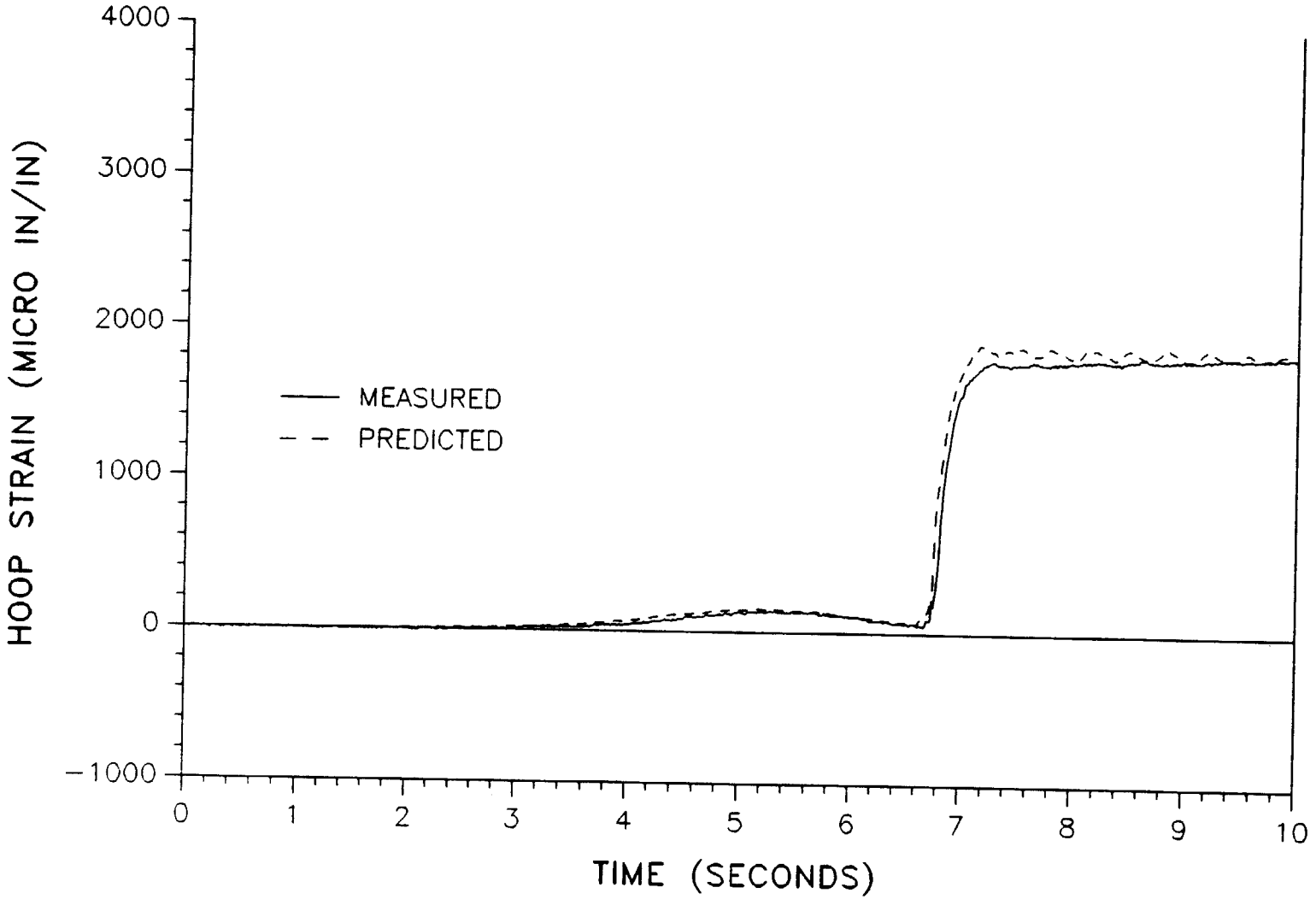

PREDICTED VS MEASURED HOOP STRAIN

360L001 STRAIN GAGE B08G7401A – STATION 1501.0 AT 255 DEGREES

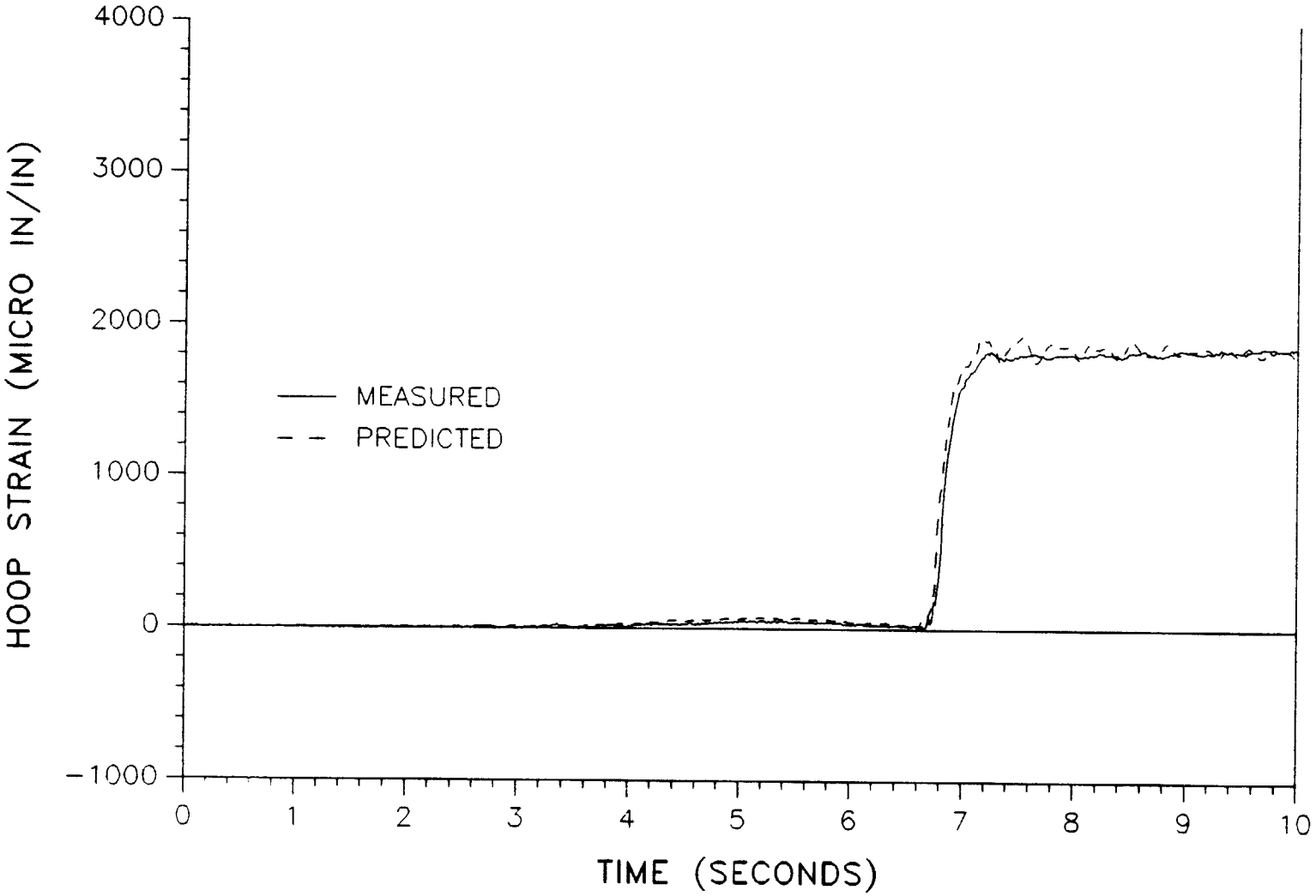

PREDICTED VS MEASURED HOOP STRAIN

360L001 STRAIN GAGE B08G7399A – STATION 1501.0 AT 270 DEGREES

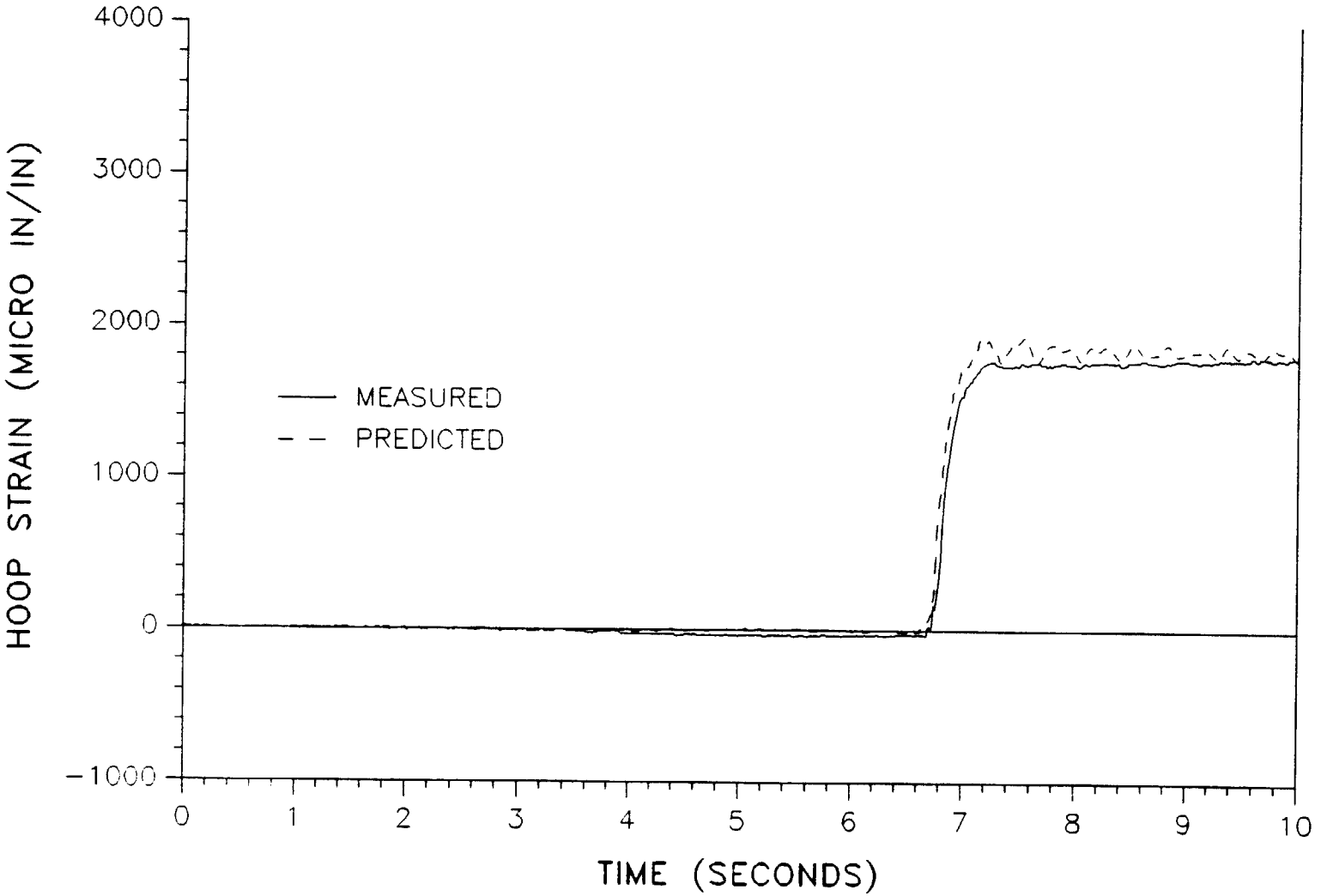

PREDICTED VS MEASURED HOOP STRAIN

360L001 STRAIN GAGE B08G7397A – STATION 1501.0 AT 285 DEGREES

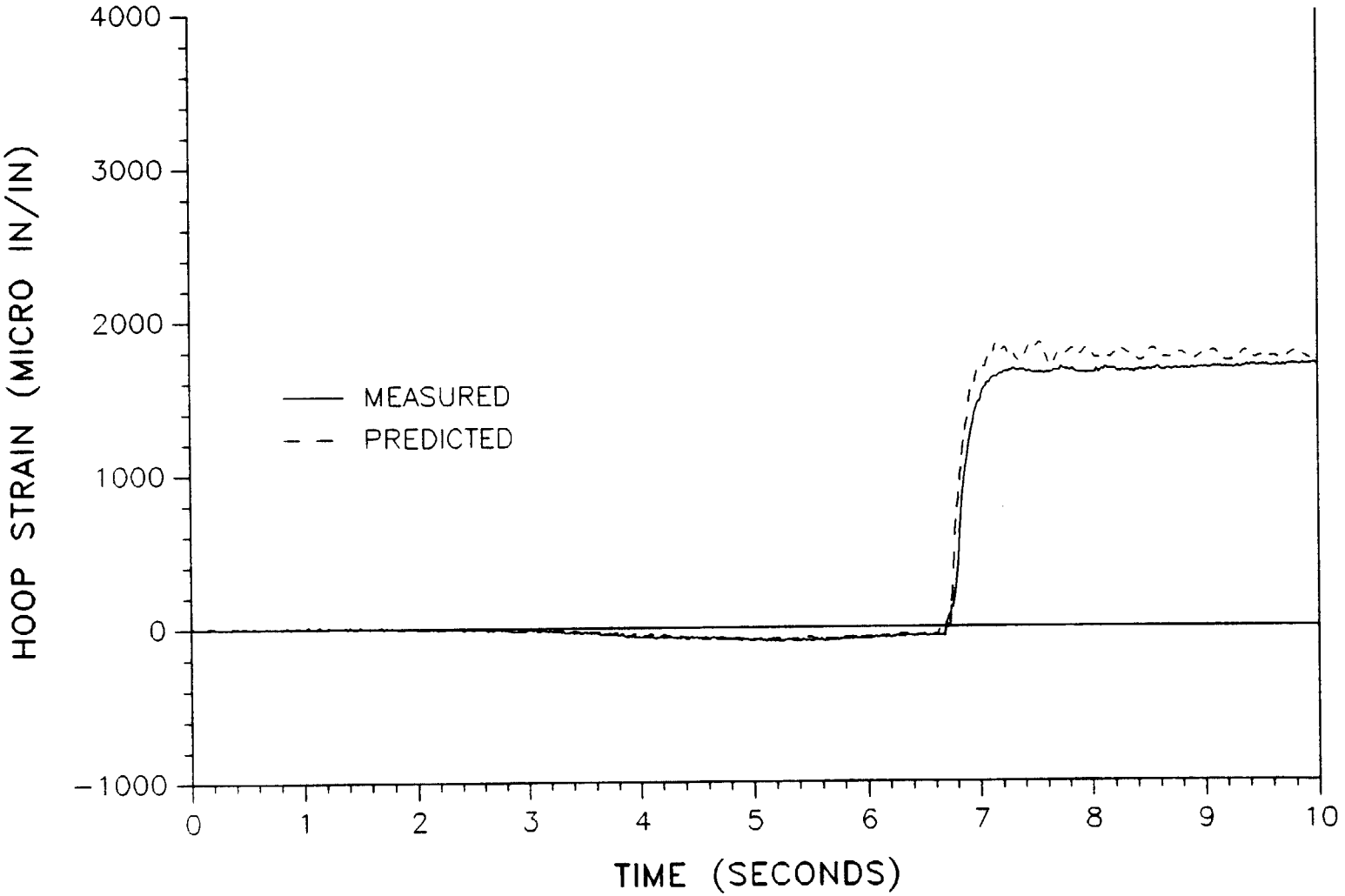

PREDICTED VS MEASURED HOOP STRAIN

360L001 STRAIN GAGE B08G7395A – STATION 1501.0 AT 300 DEGREES

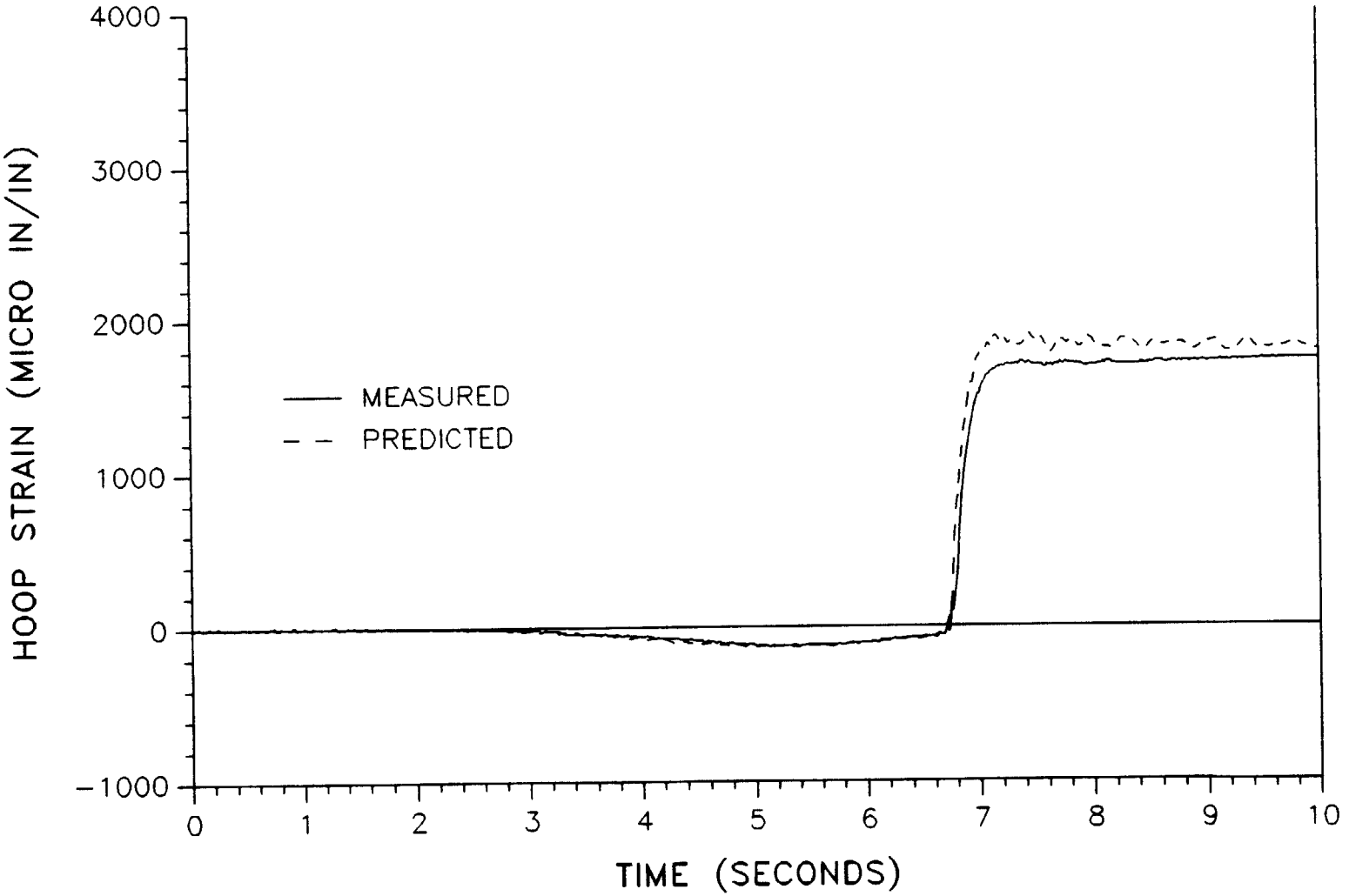

PREDICTED VS MEASURED HOOP STRAIN

360L001 STRAIN GAGE B08G7393A – STATION 1501.0 AT 320 DEGREES

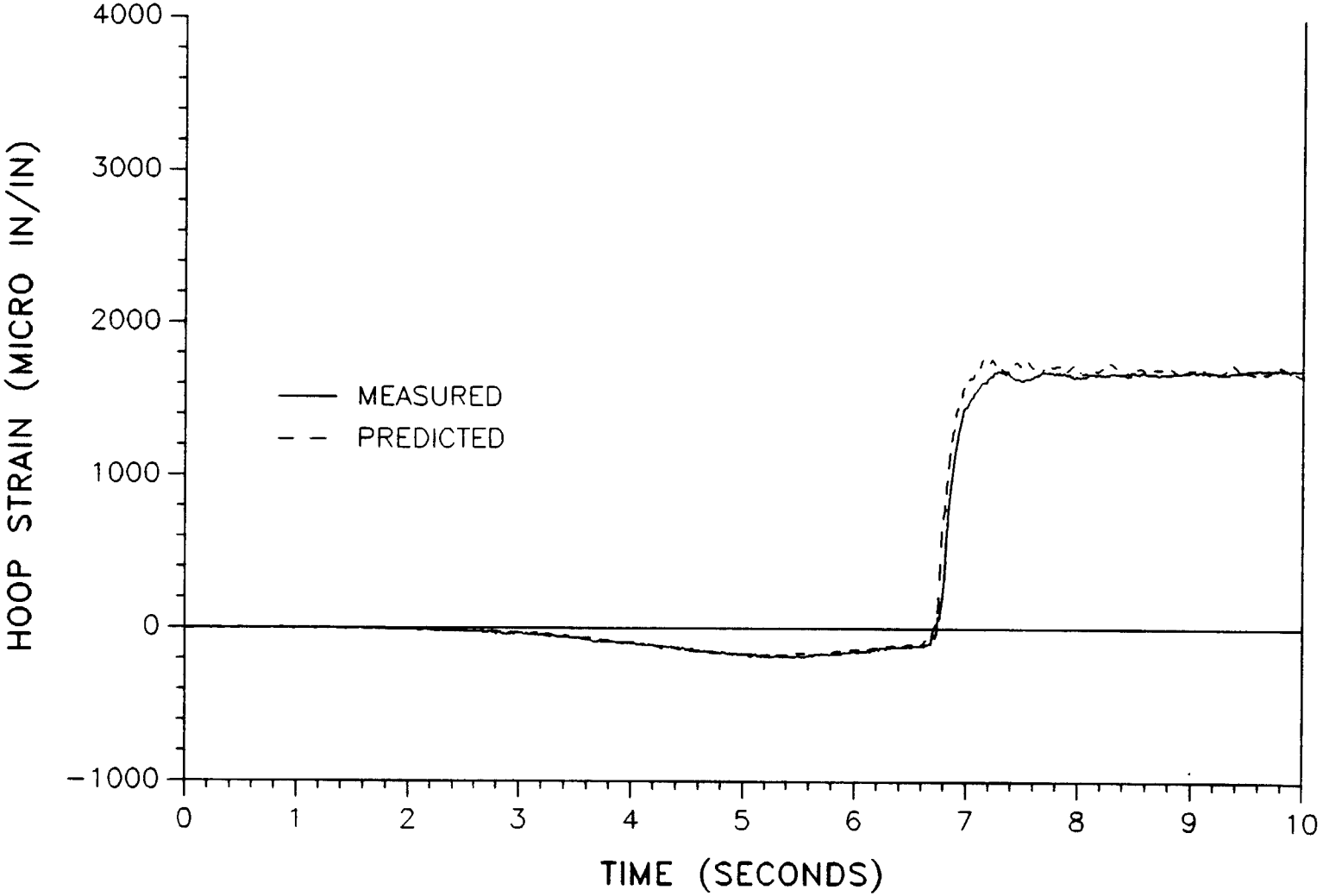

PREDICTED VS MEASURED HOOP STRAIN

360L001 STRAIN GAGE B08G7405A – STATION 1797.0 AT 0 DEGREES

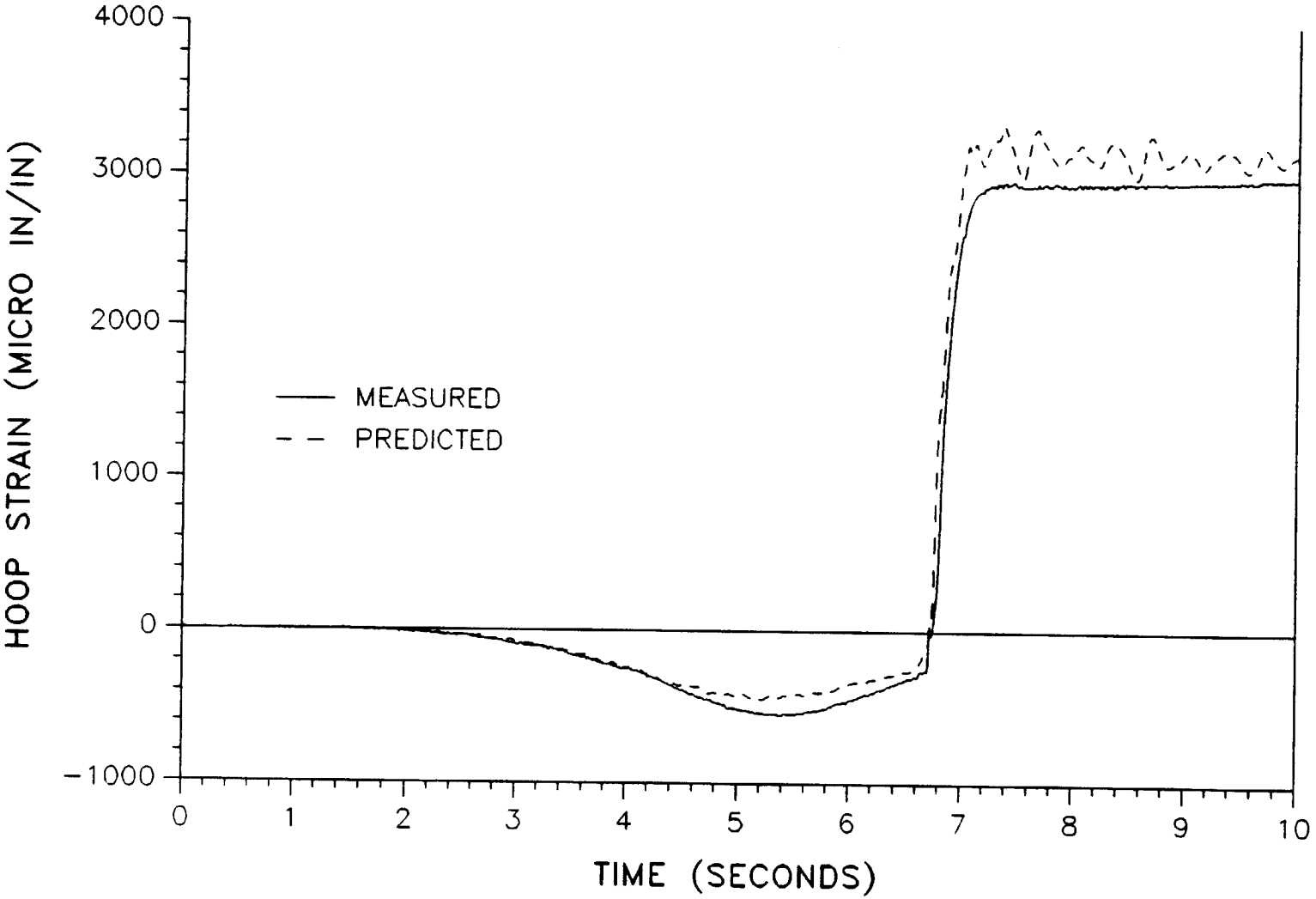

PREDICTED VS MEASURED HOOP STRAIN

360L001 STRAIN GAGE B08G7407A – STATION 1797.0 AT 98 DEGREES

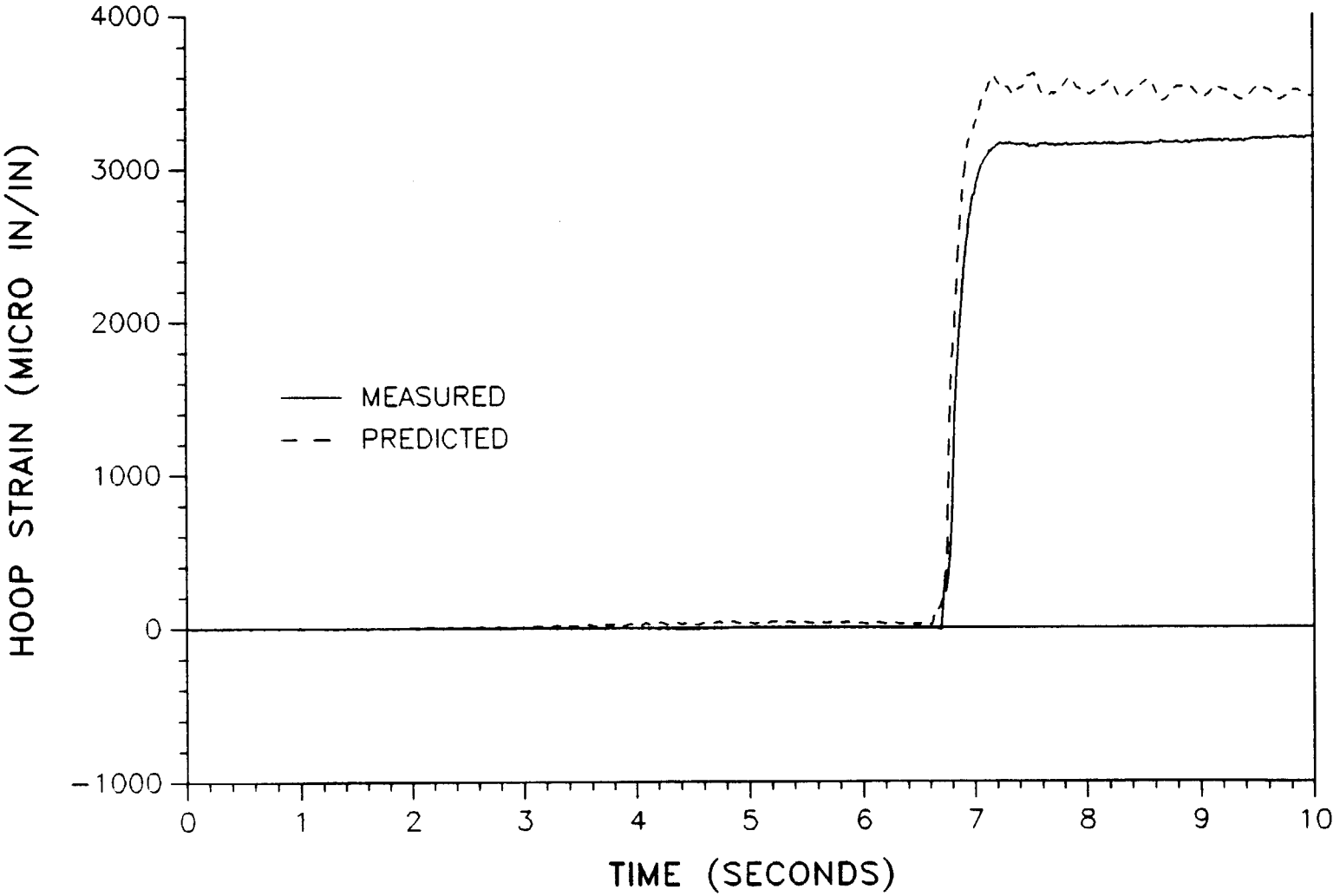

PREDICTED VS MEASURED HOOP STRAIN

360L001 STRAIN GAGE B08G7409A – STATION 1797.0 AT 180 DEGREES

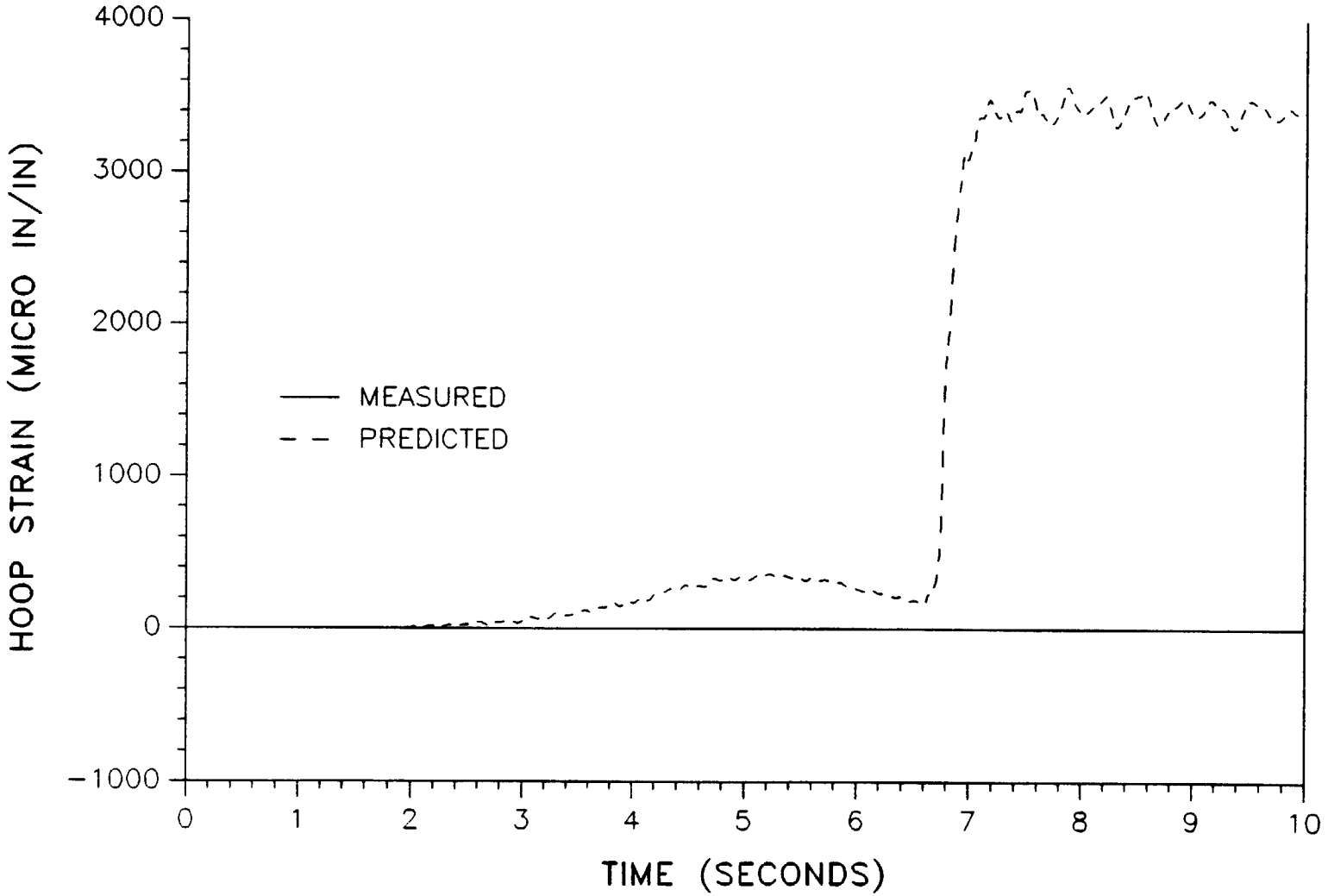

PREDICTED VS MEASURED HOOP STRAIN

360L001 STRAIN GAGE B08G7411A – STATION 1797.0 AT 270 DEGREES

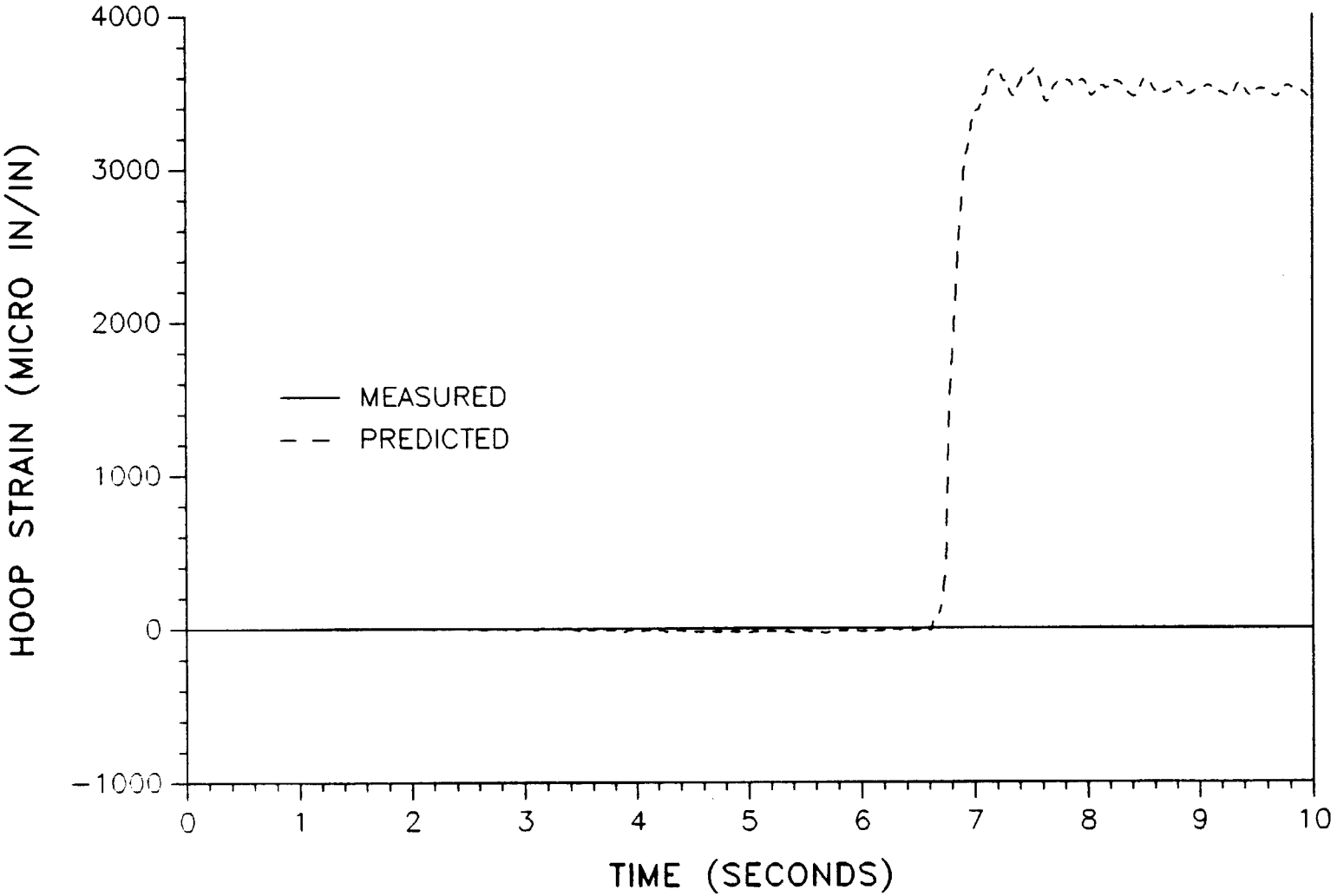

PREDICTED VS MEASURED HOOP STRAIN

360L001 STRAIN GAGE B08G8323A – STATION 556.5 AT 0 DEGREES

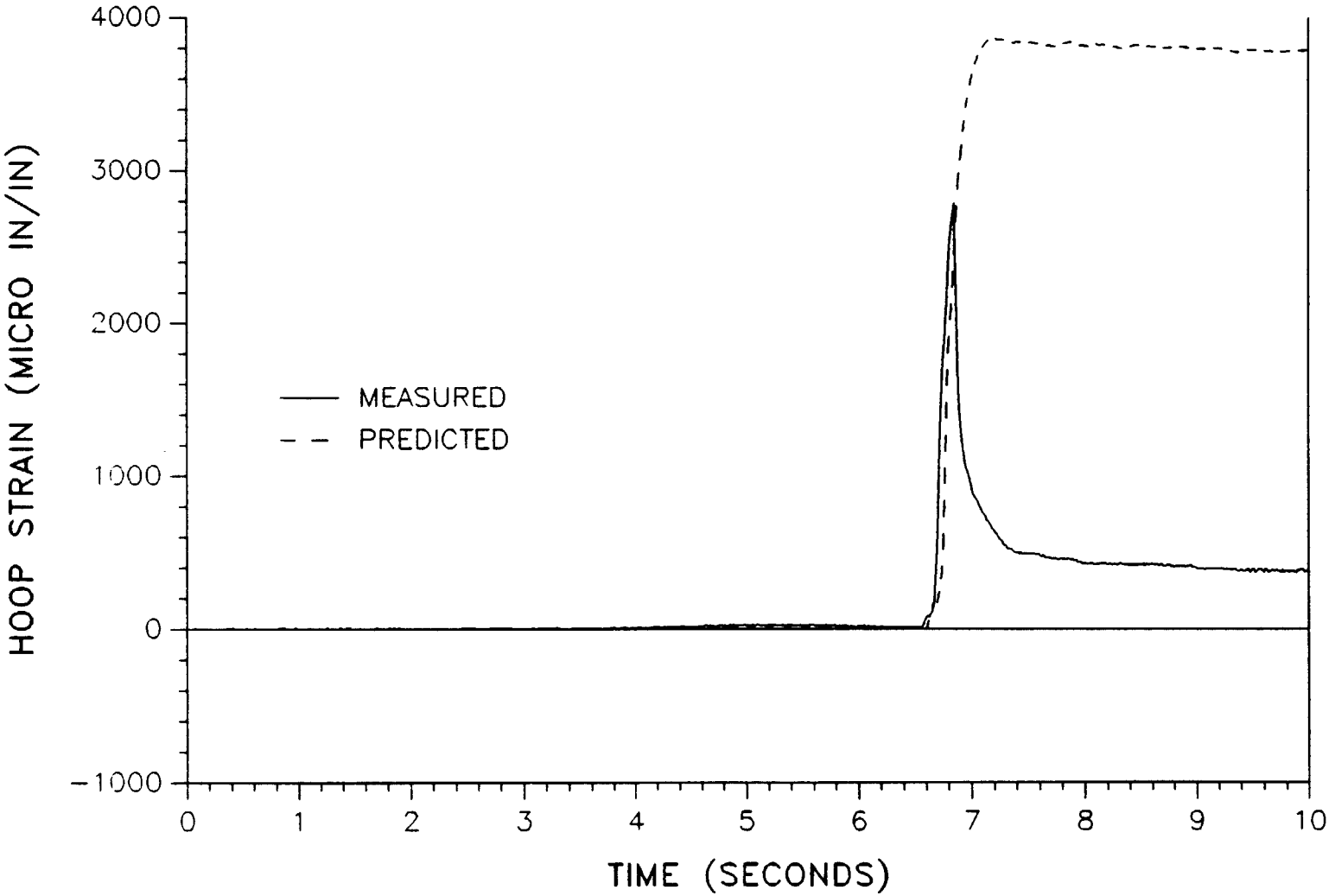

PREDICTED VS MEASURED HOOP STRAIN

360L001 STRAIN GAGE B08G8321A – STATION 556.5 AT 82 DEGREES

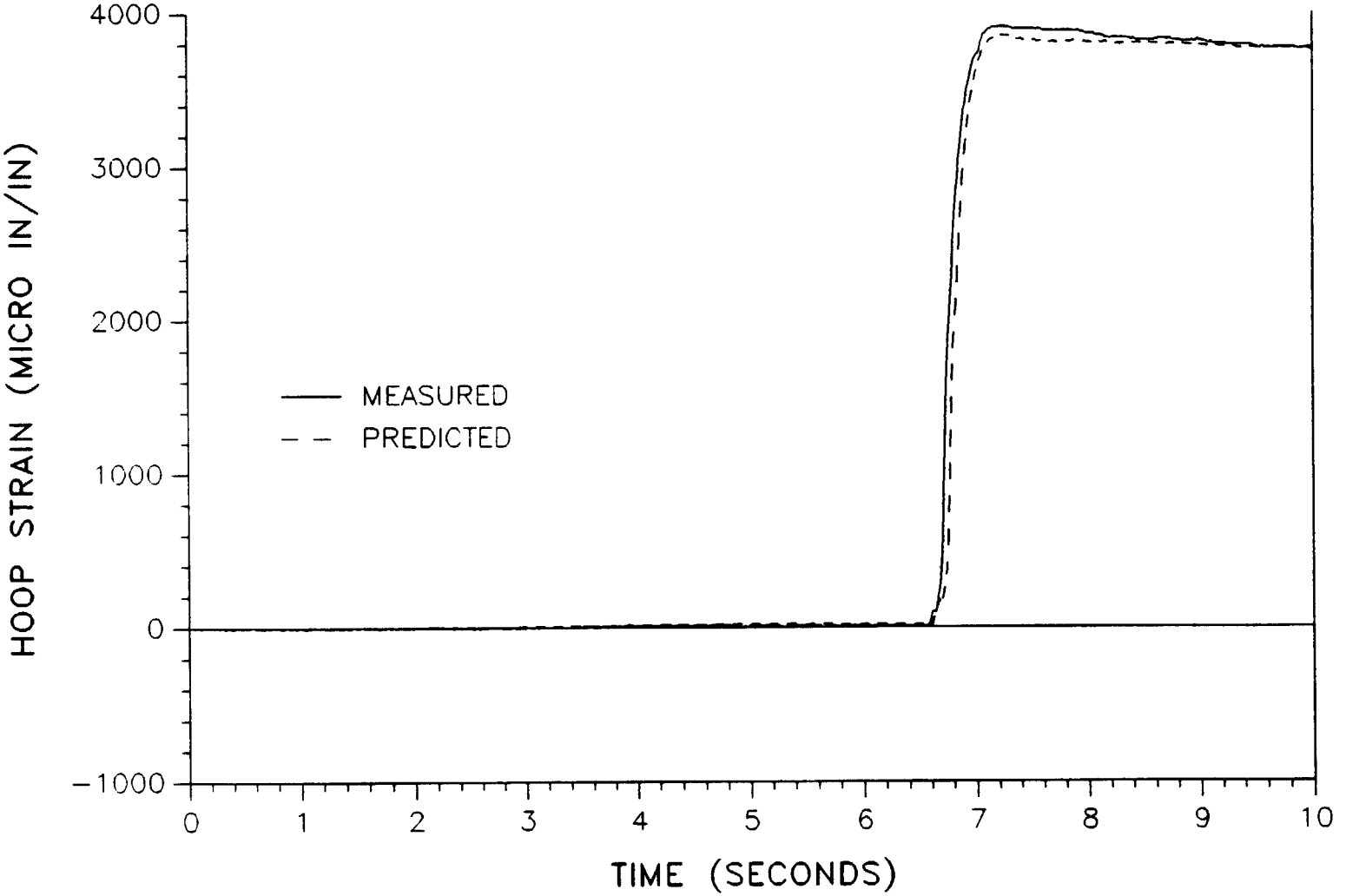

PREDICTED VS MEASURED HOOP STRAIN

360L001 STRAIN GAGE B08G8319A – STATION 556.5 AT 180 DEGREES

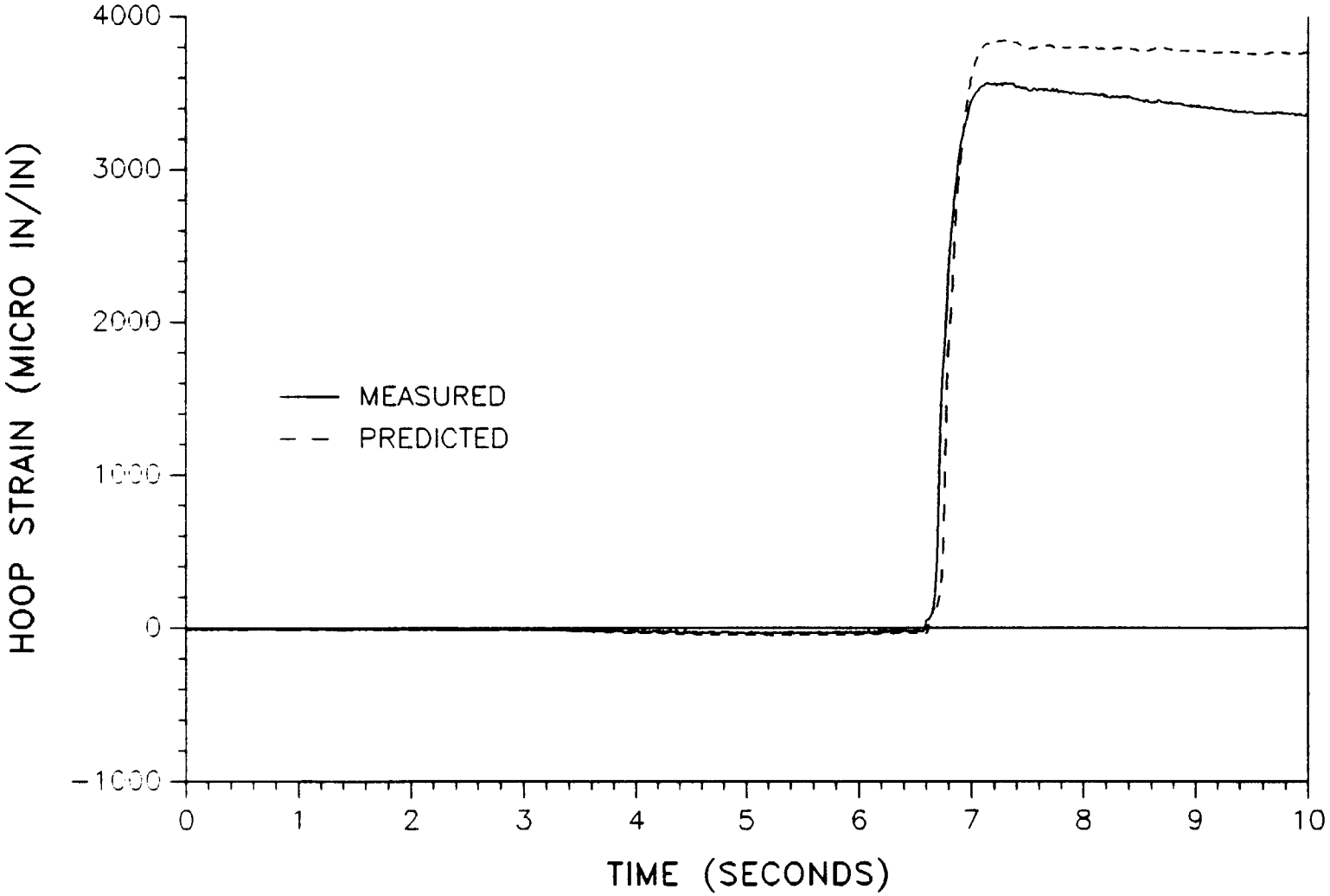

PREDICTED VS MEASURED HOOP STRAIN

360L001 STRAIN GAGE B08G7325A – STATION 556.5 AT 270 DEGREES

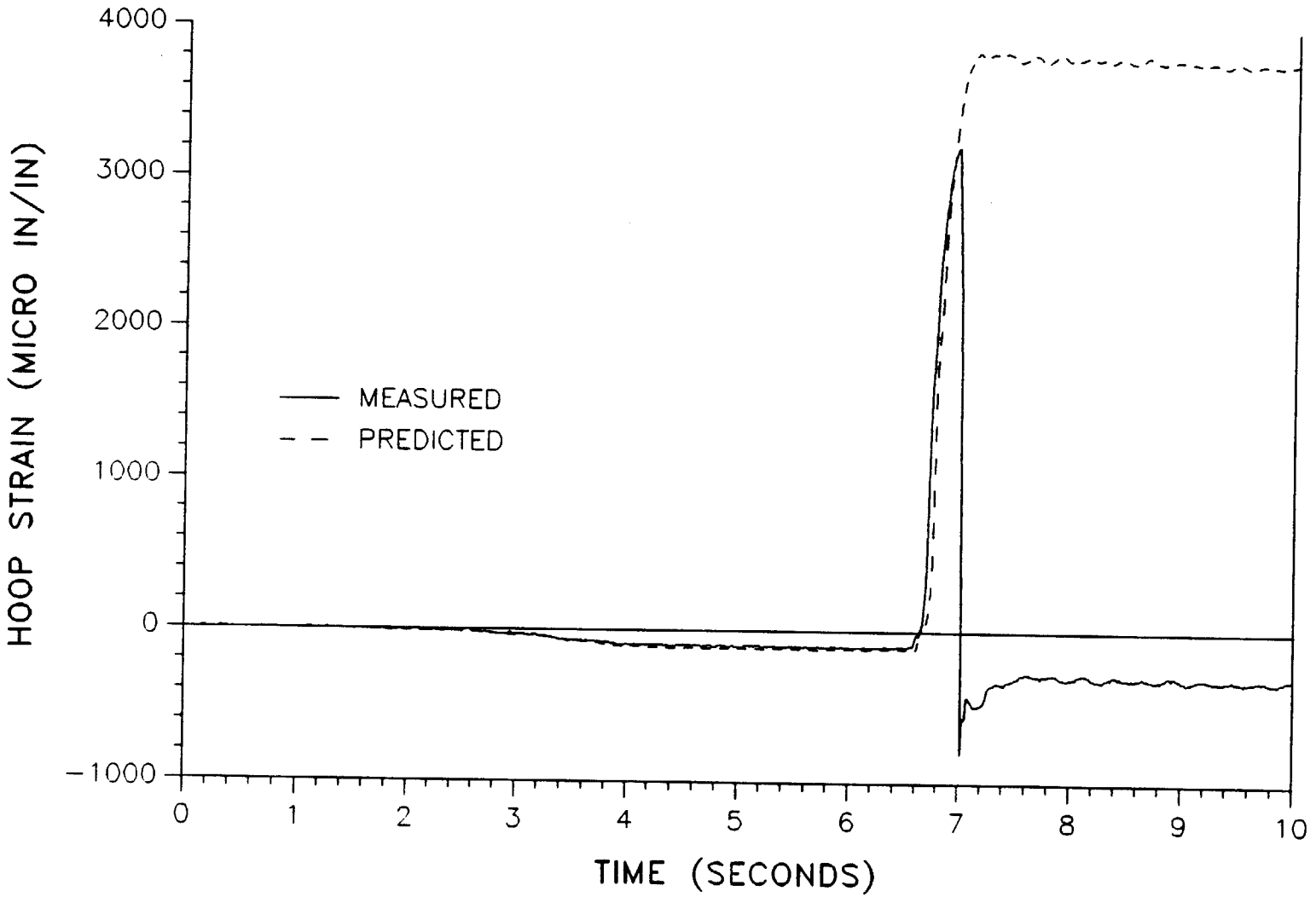

PREDICTED VS MEASURED HOOP STRAIN

360L001 STRAIN GAGE B08G8331A – STATION 876.5 AT 0 DEGREES

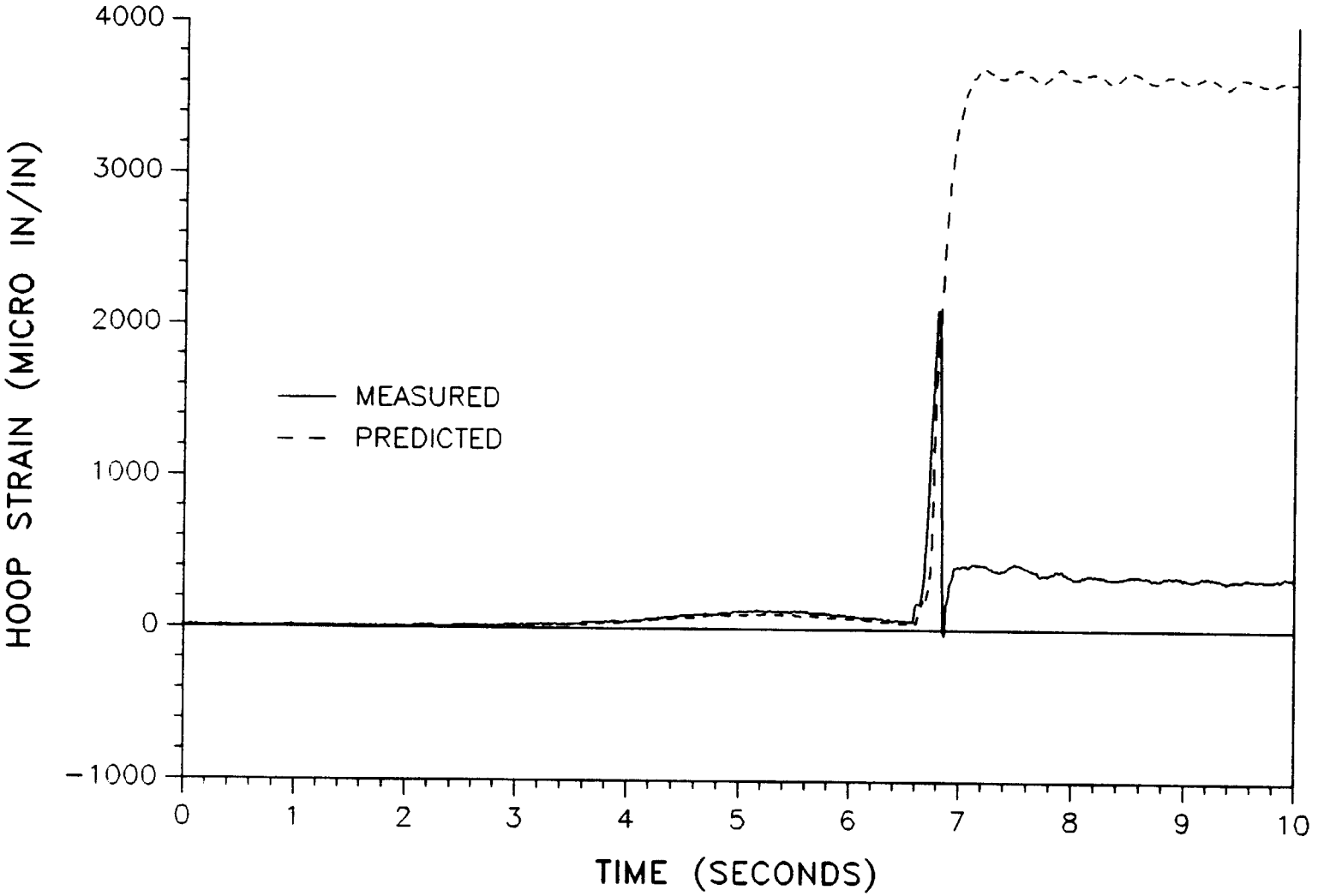

PREDICTED VS MEASURED HOOP STRAIN

360L001 STRAIN GAGE B08G8329A – STATION 876.5 AT 82 DEGREES

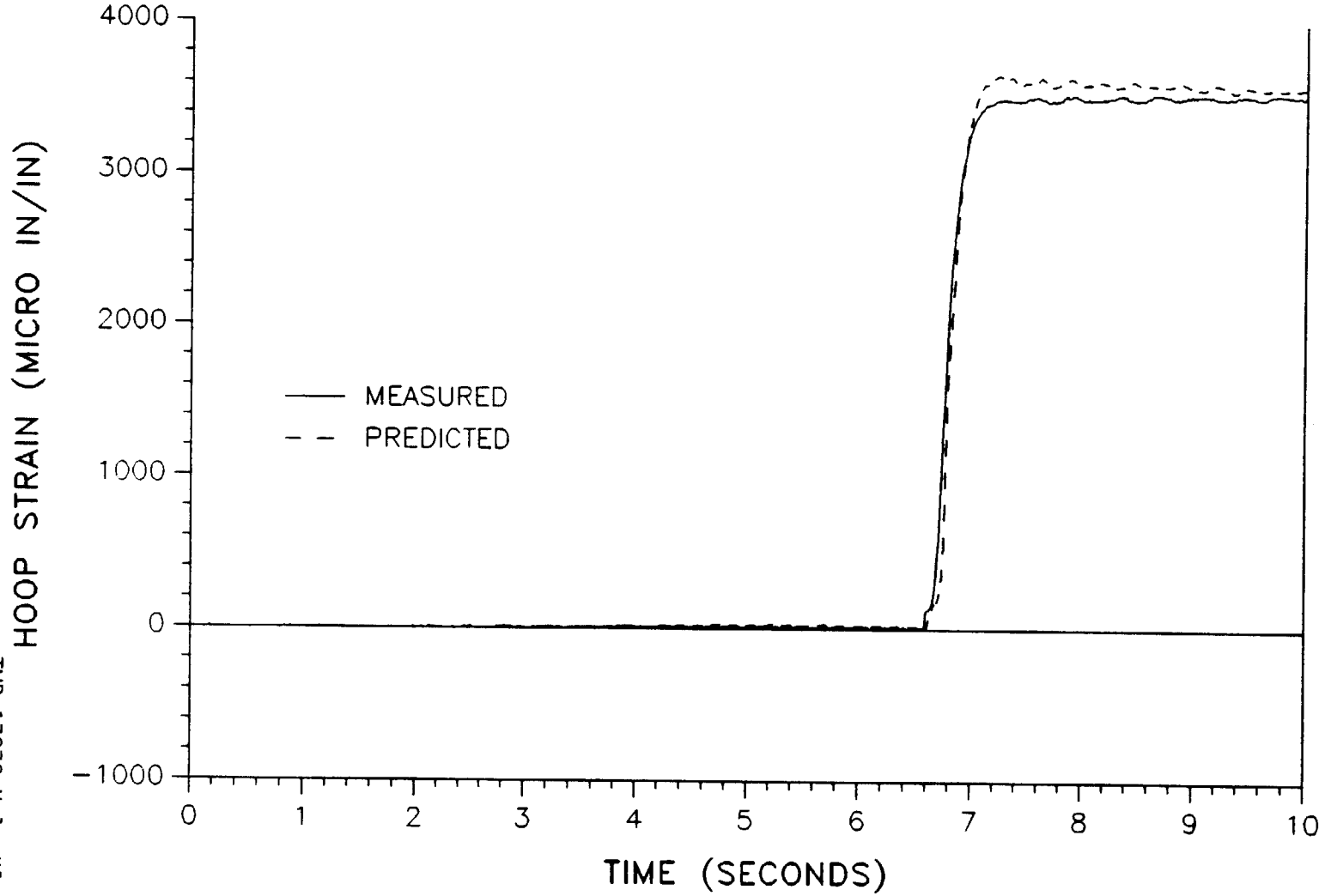

PREDICTED VS MEASURED HOOP STRAIN

360L001 STRAIN GAGE B08G8327A – STATION 876.5 AT 180 DEGREES

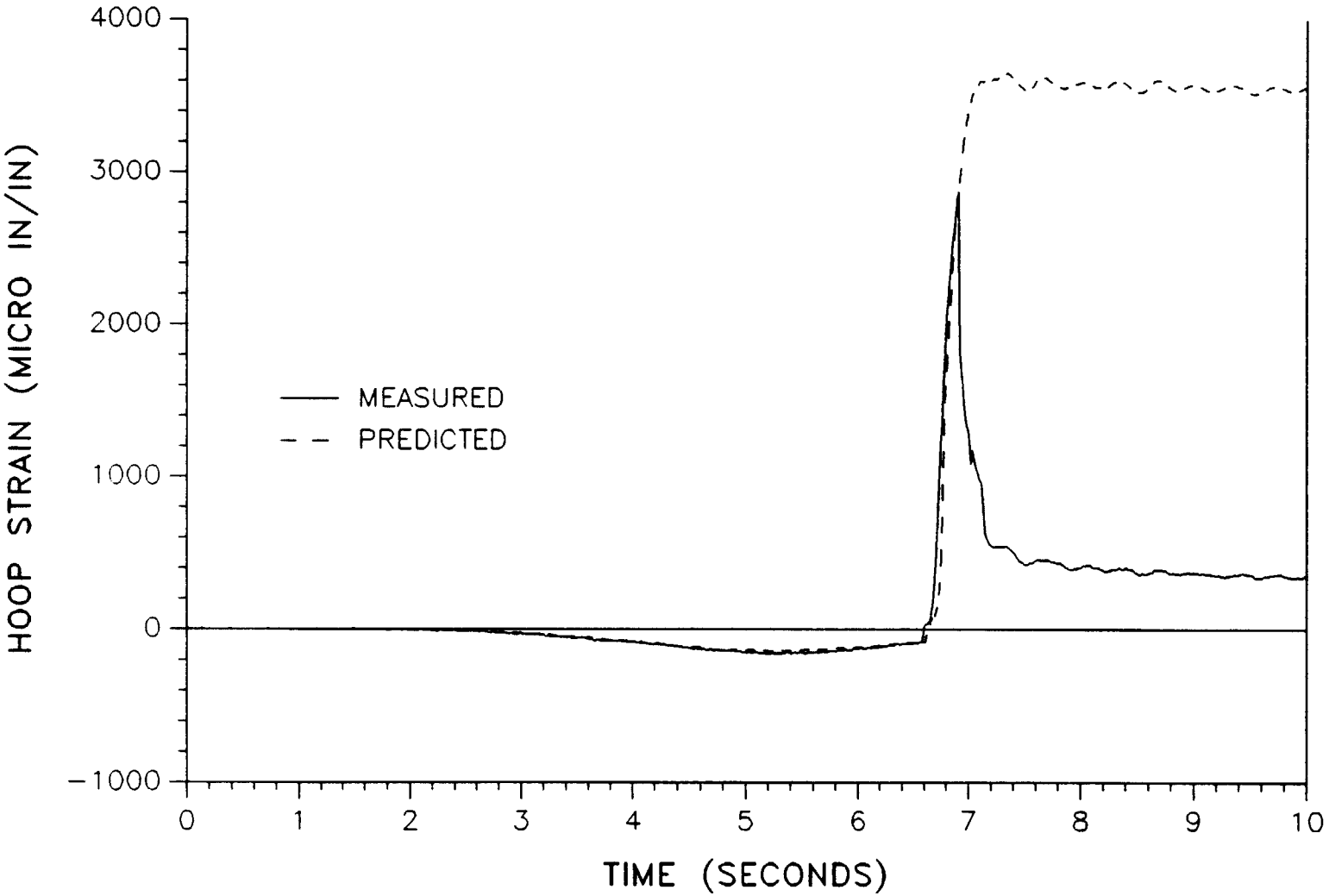

PREDICTED VS MEASURED HOOP STRAIN

360L001 STRAIN GAGE B08G8333A – STATION 876.5 AT 270 DEGREES

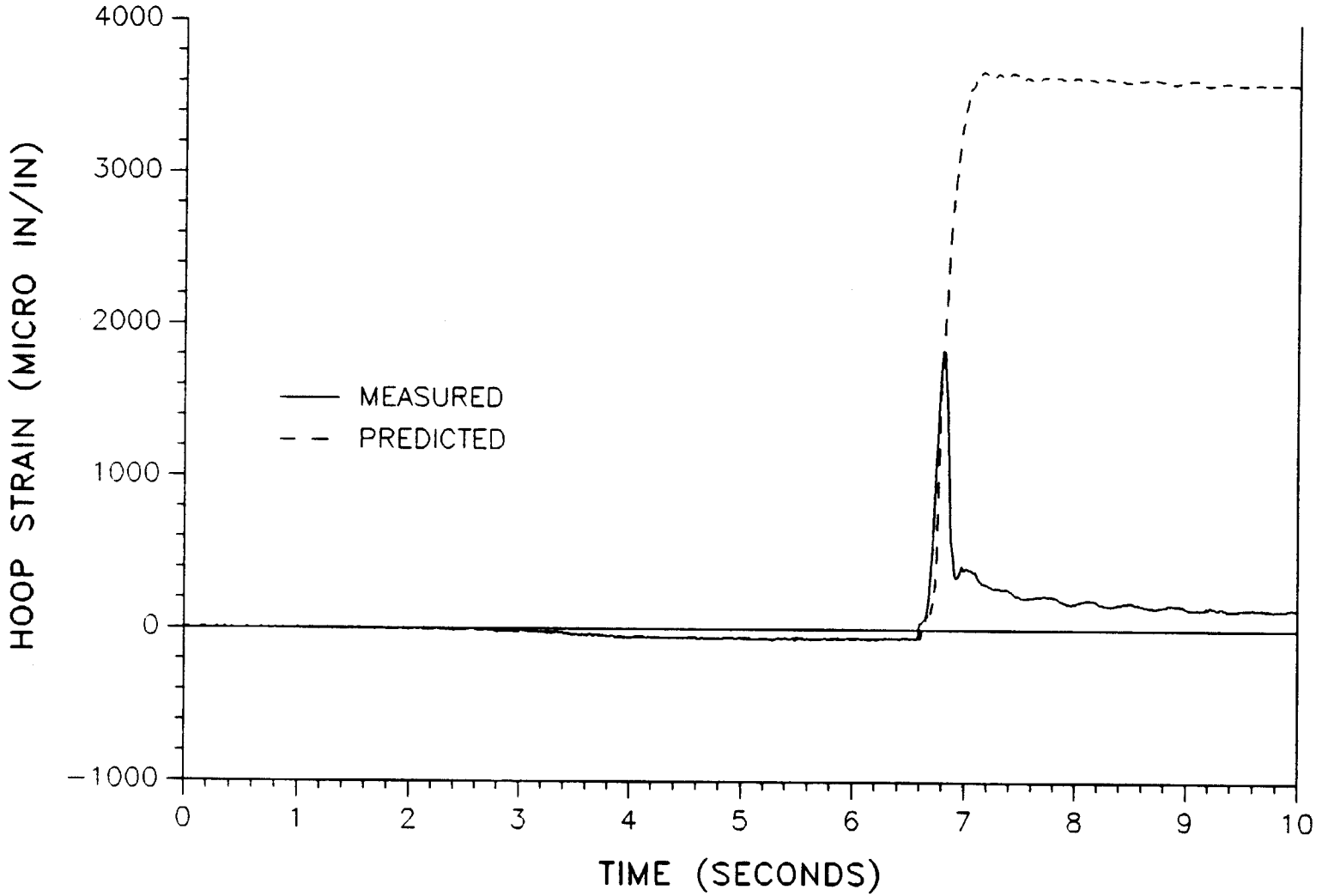

PREDICTED VS MEASURED HOOP STRAIN

360L001 STRAIN GAGE B08G8339A – STATION 1196.5 AT 0 DEGREES

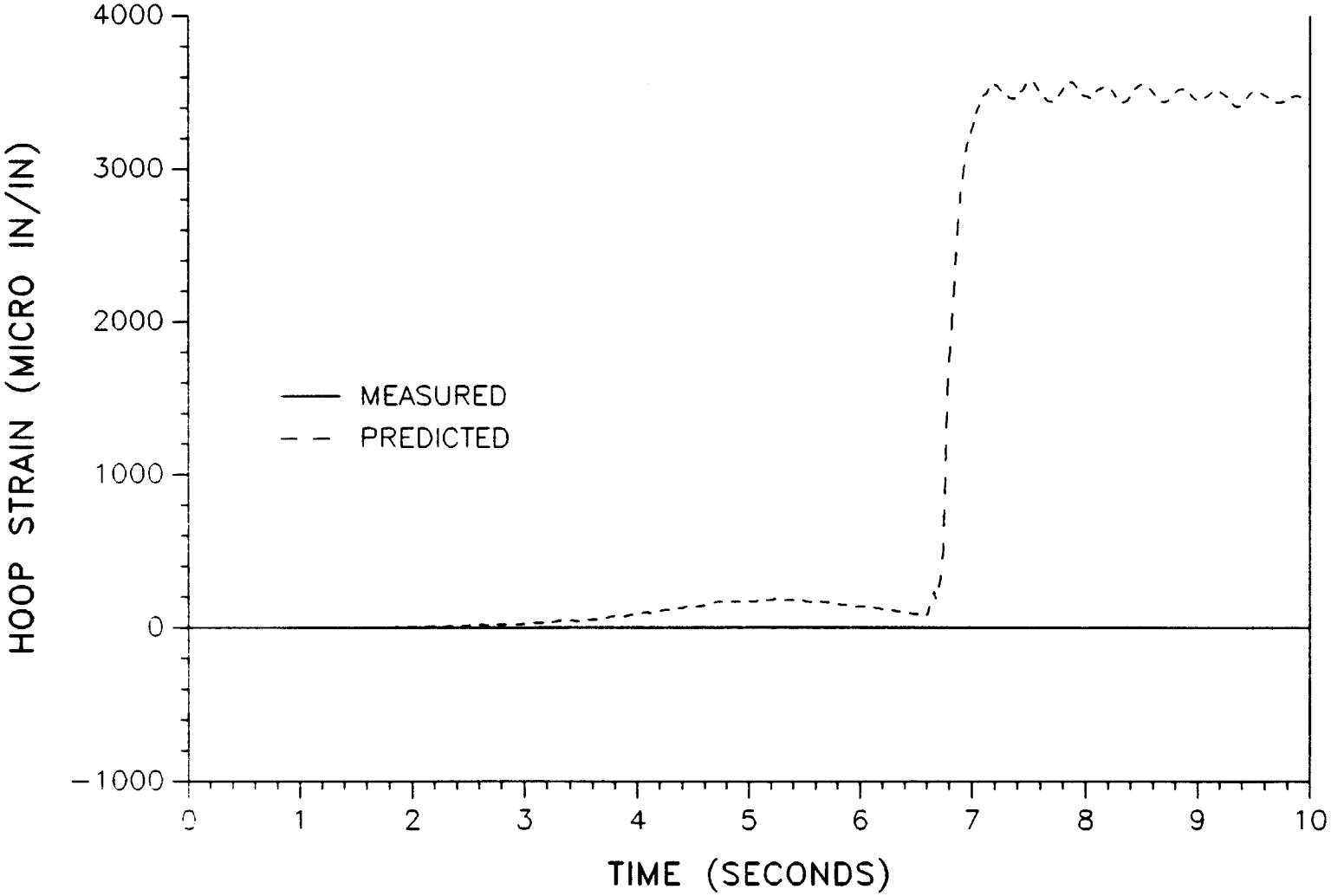

PREDICTED VS MEASURED HOOP STRAIN

360L001 STRAIN GAGE B08G8337A – STATION 1196.5 AT 82 DEGREES

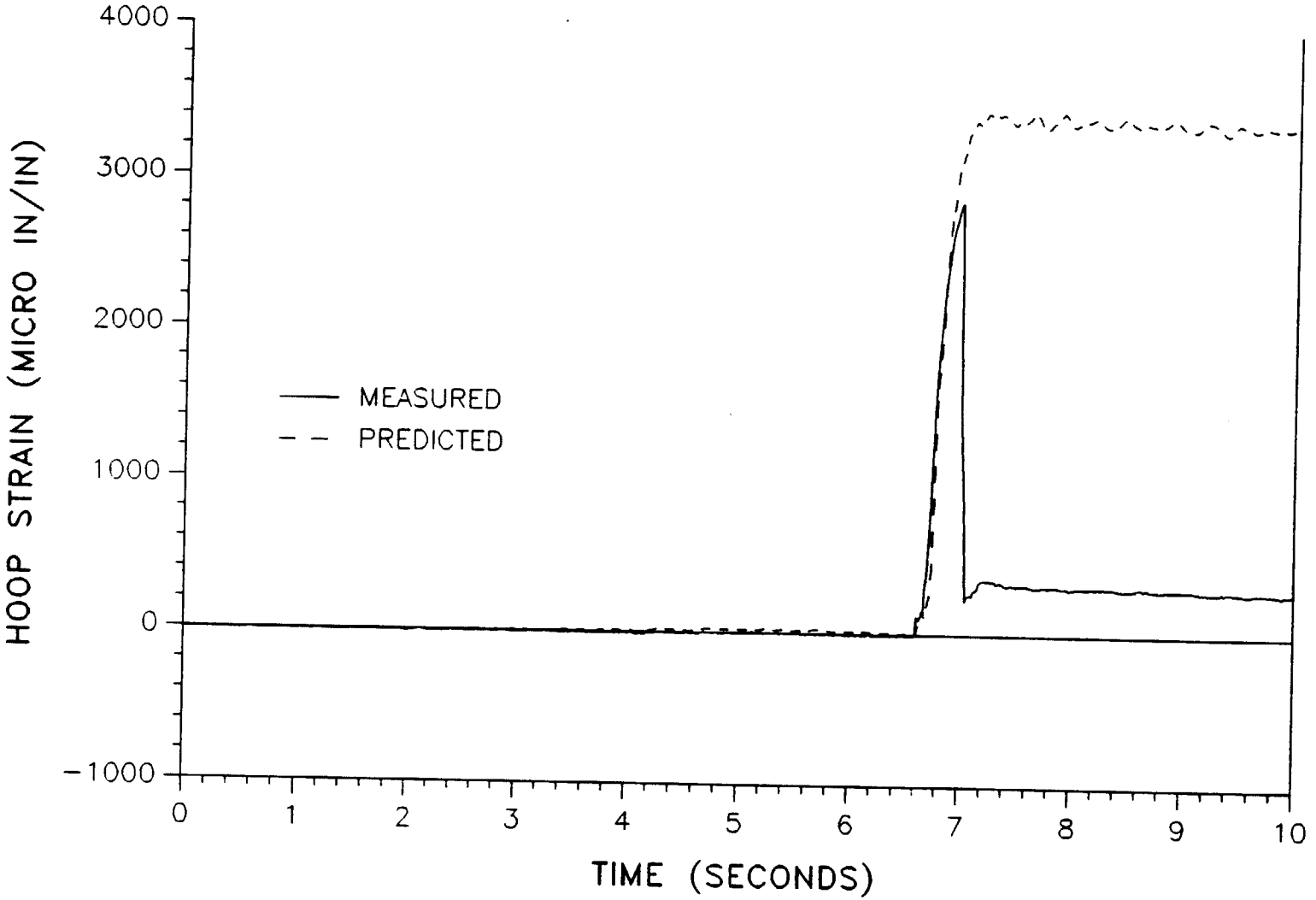

PREDICTED VS MEASURED HOOP STRAIN

360L001 STRAIN GAGE B08G8335A – STATION 1196.5 AT 180 DEGREES

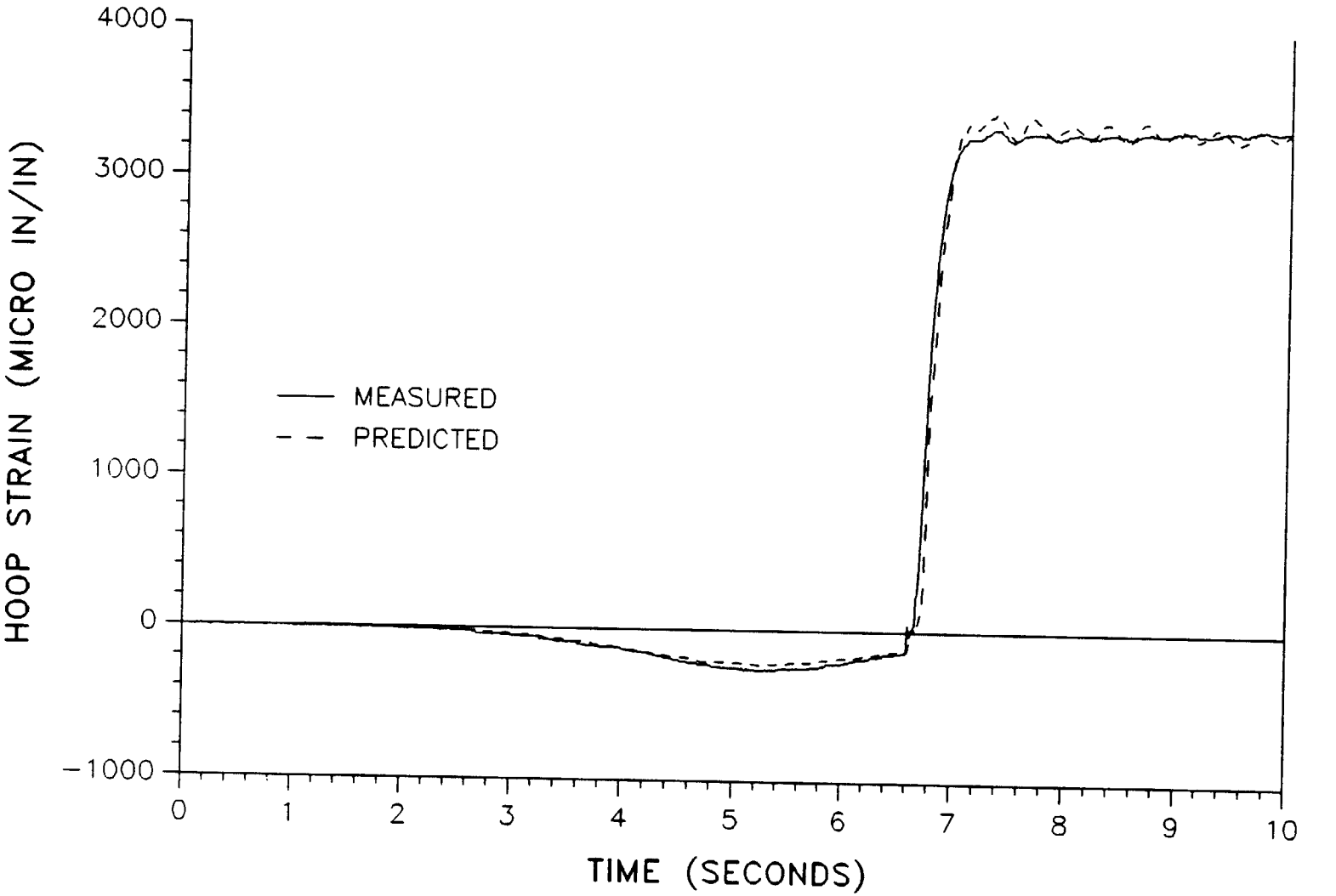

PREDICTED VS MEASURED HOOP STRAIN

360L001 STRAIN GAGE B08G8341A – STATION 1196.5 AT 270 DEGREES

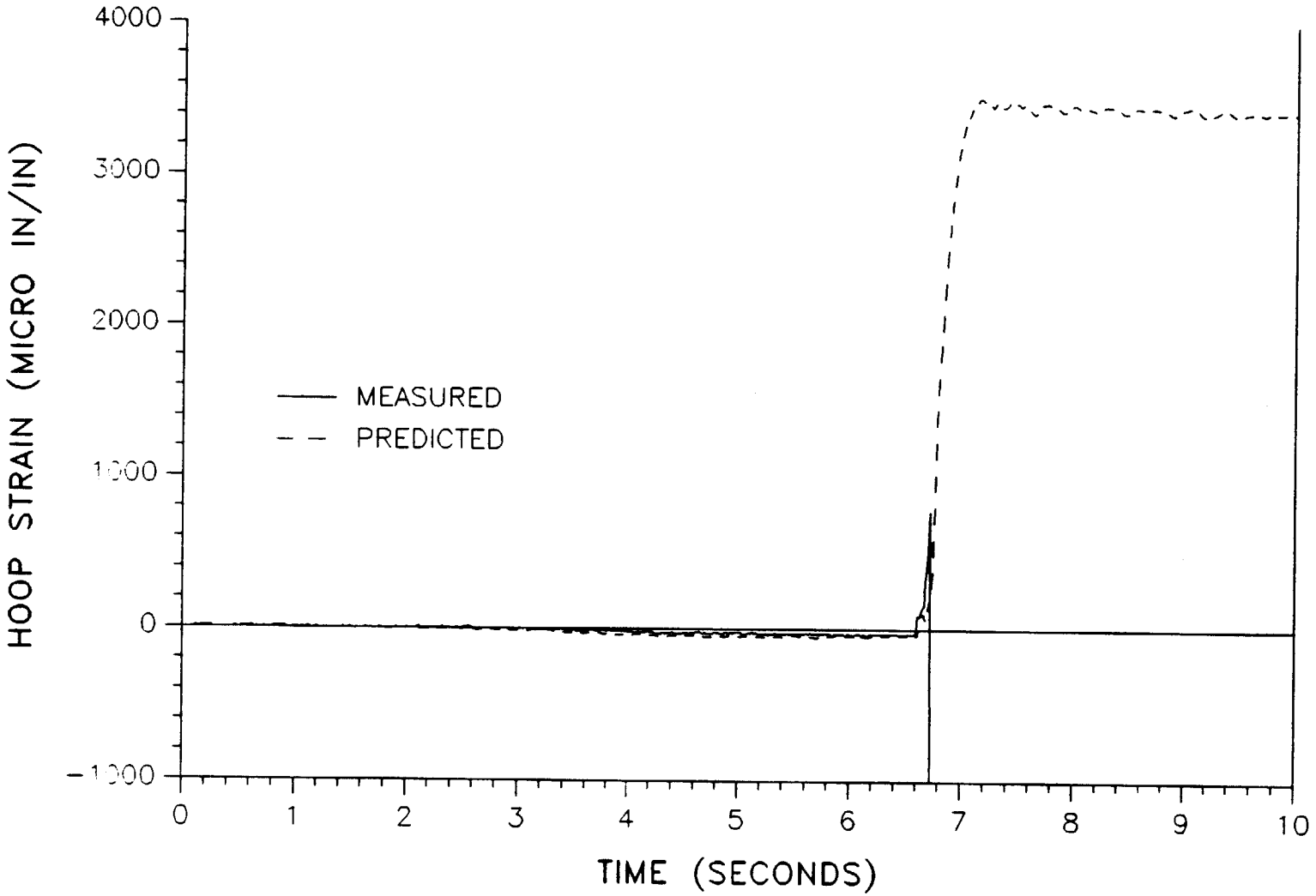

PREDICTED VS MEASURED HOOP STRAIN

360L001 STRAIN GAGE B08G8347A – STATION 1466.0 AT 0 DEGREES

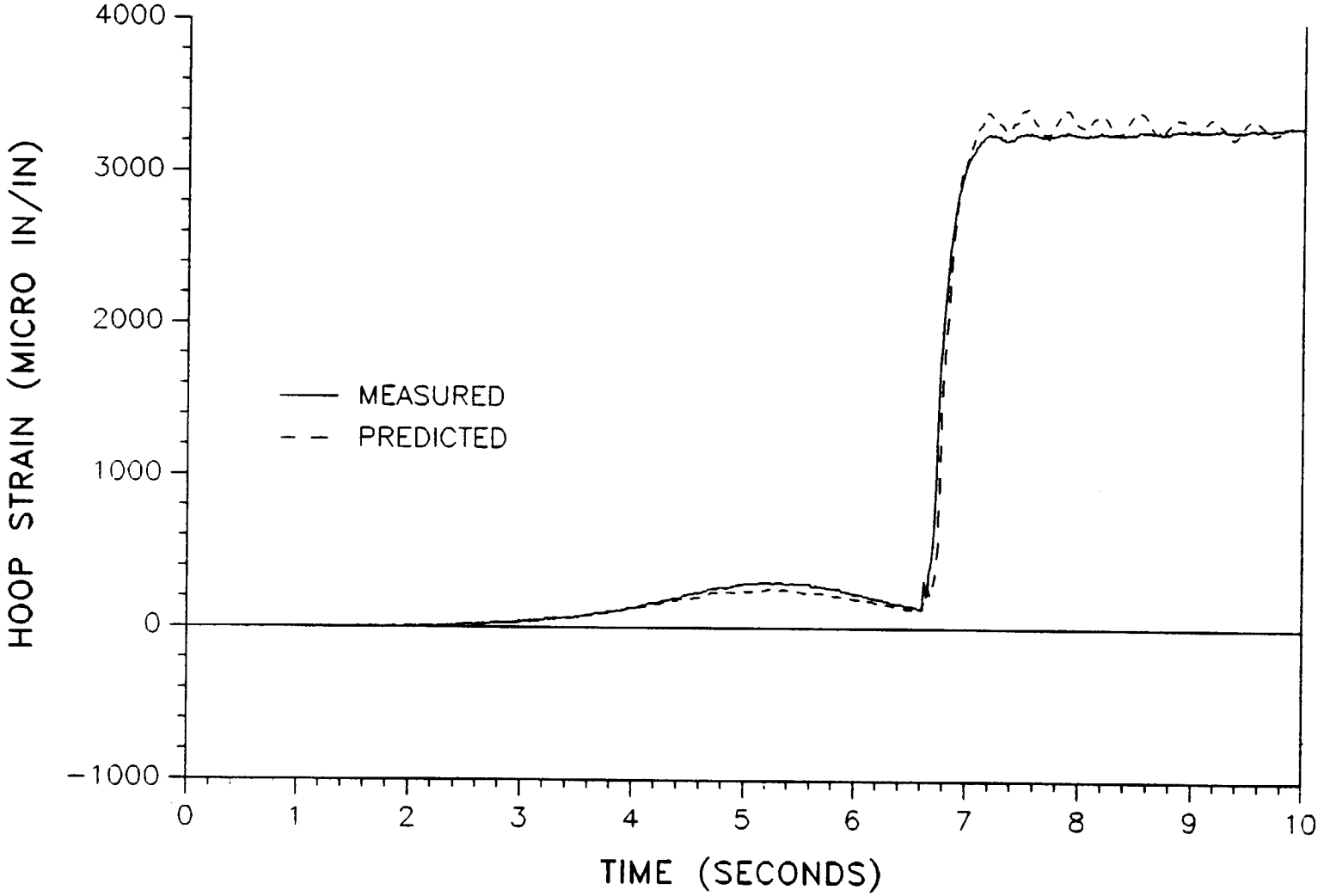

PREDICTED VS MEASURED HOOP STRAIN

360L001 STRAIN GAGE B08G8345A – STATION 1466.0 AT 82 DEGREES

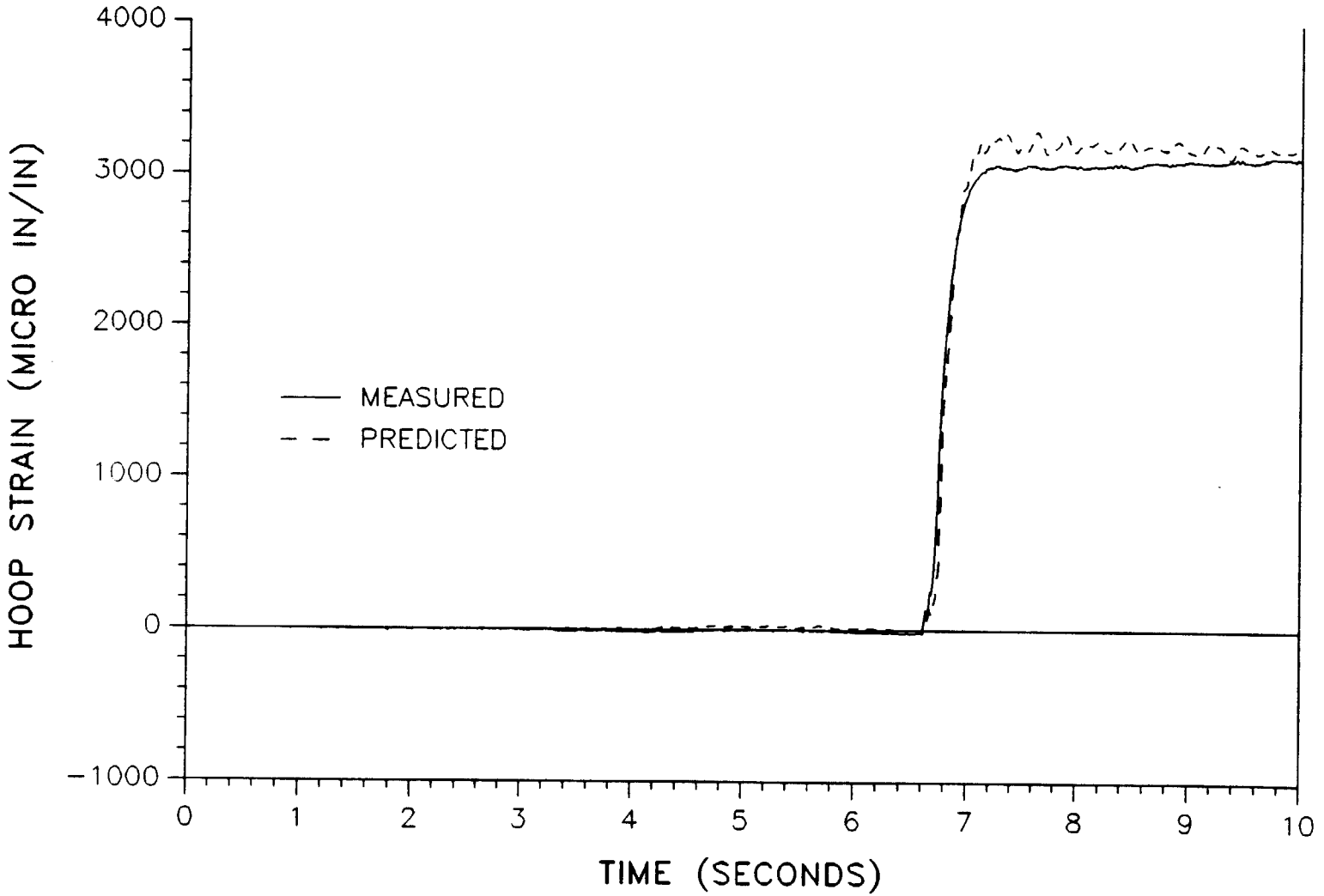

PREDICTED VS MEASURED HOOP STRAIN

360L001 STRAIN GAGE B08G8343A – STATION 1466.0 AT 180 DEGREES

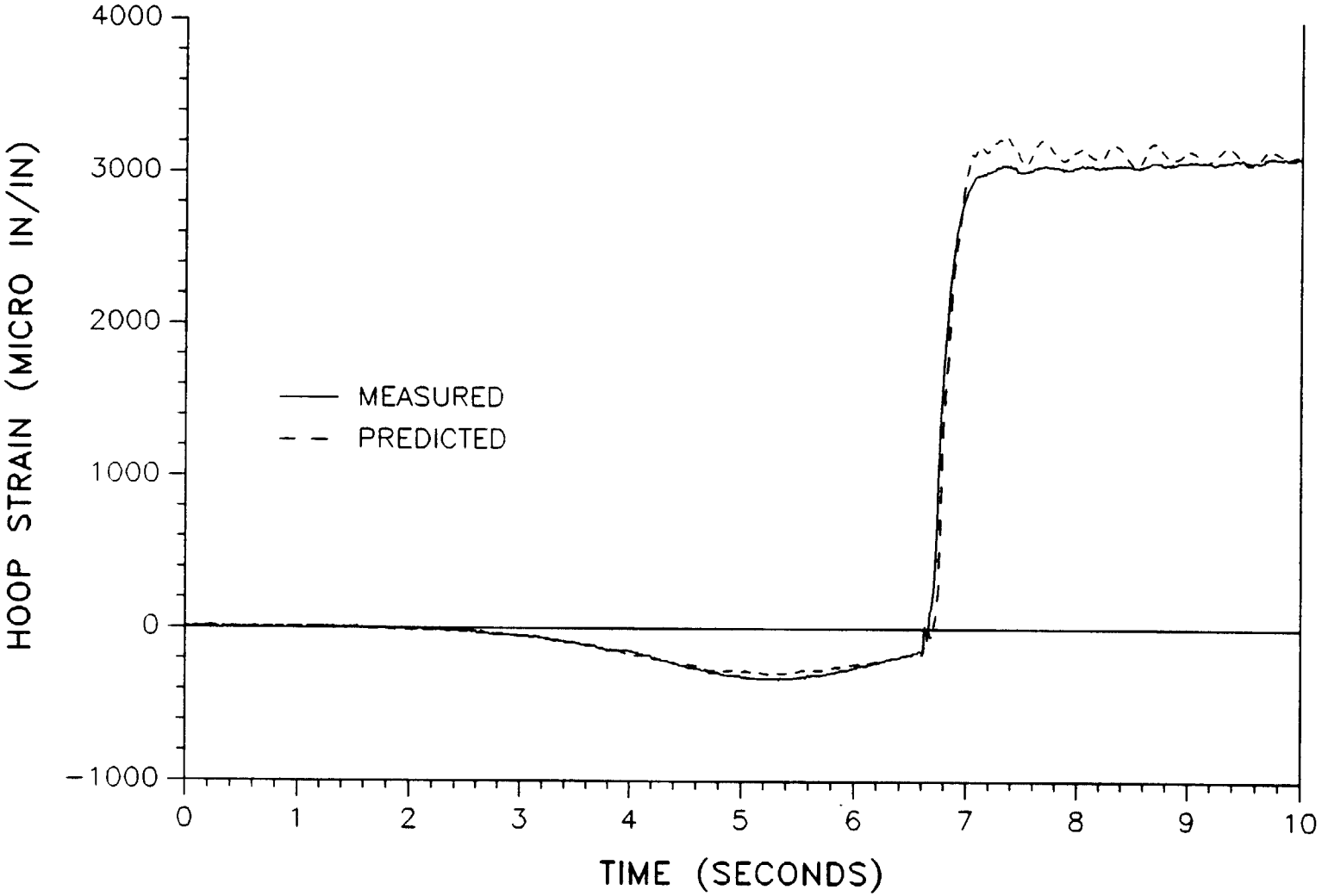

PREDICTED VS MEASURED HOOP STRAIN

360L001 STRAIN GAGE B08G8349A – STATION 1466.0 AT 270 DEGREES

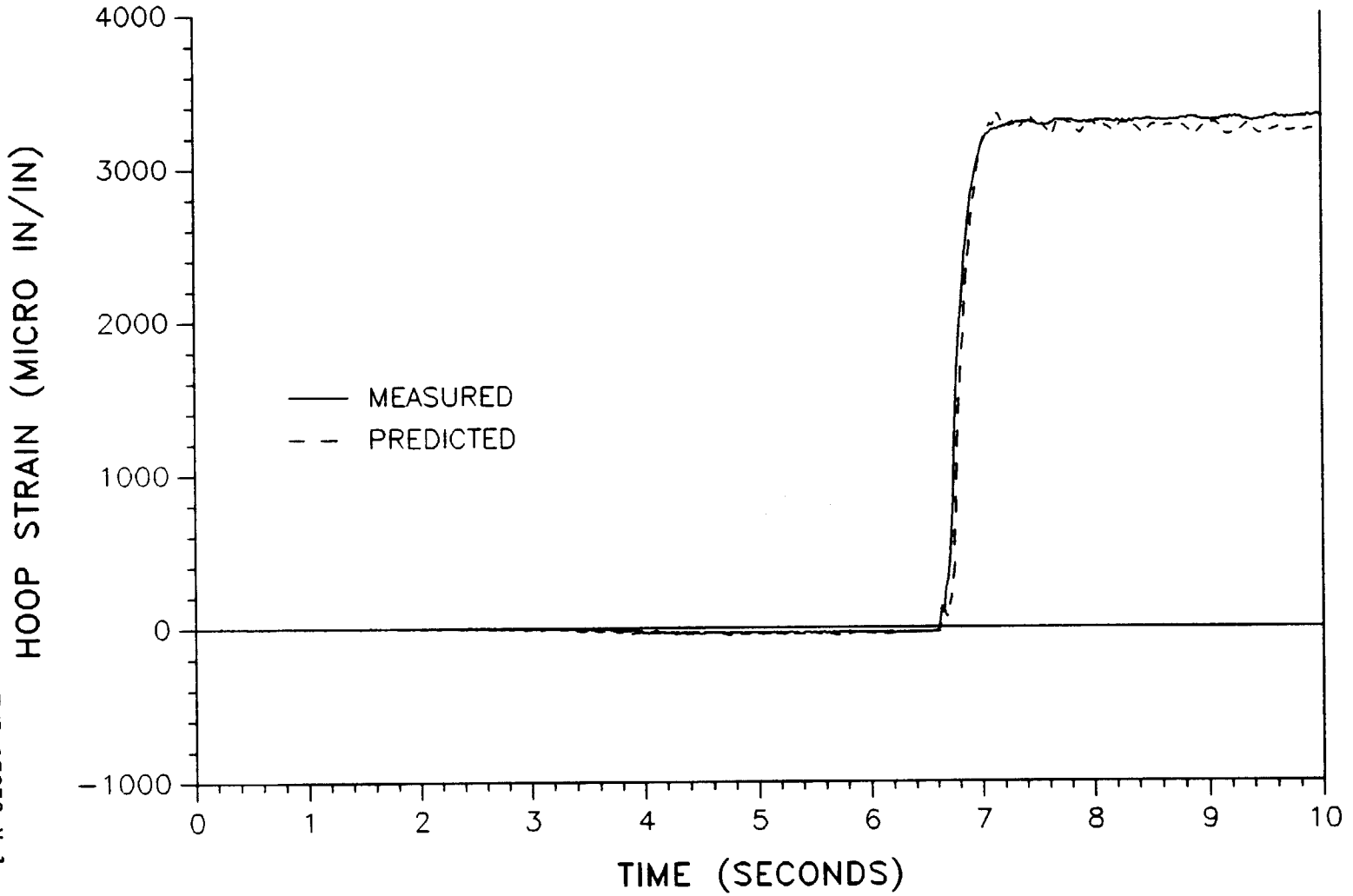

PREDICTED VS MEASURED HOOP STRAIN

360L001 STRAIN GAGE B08G8351A – STATION 1493.0 AT 0 DEGREES

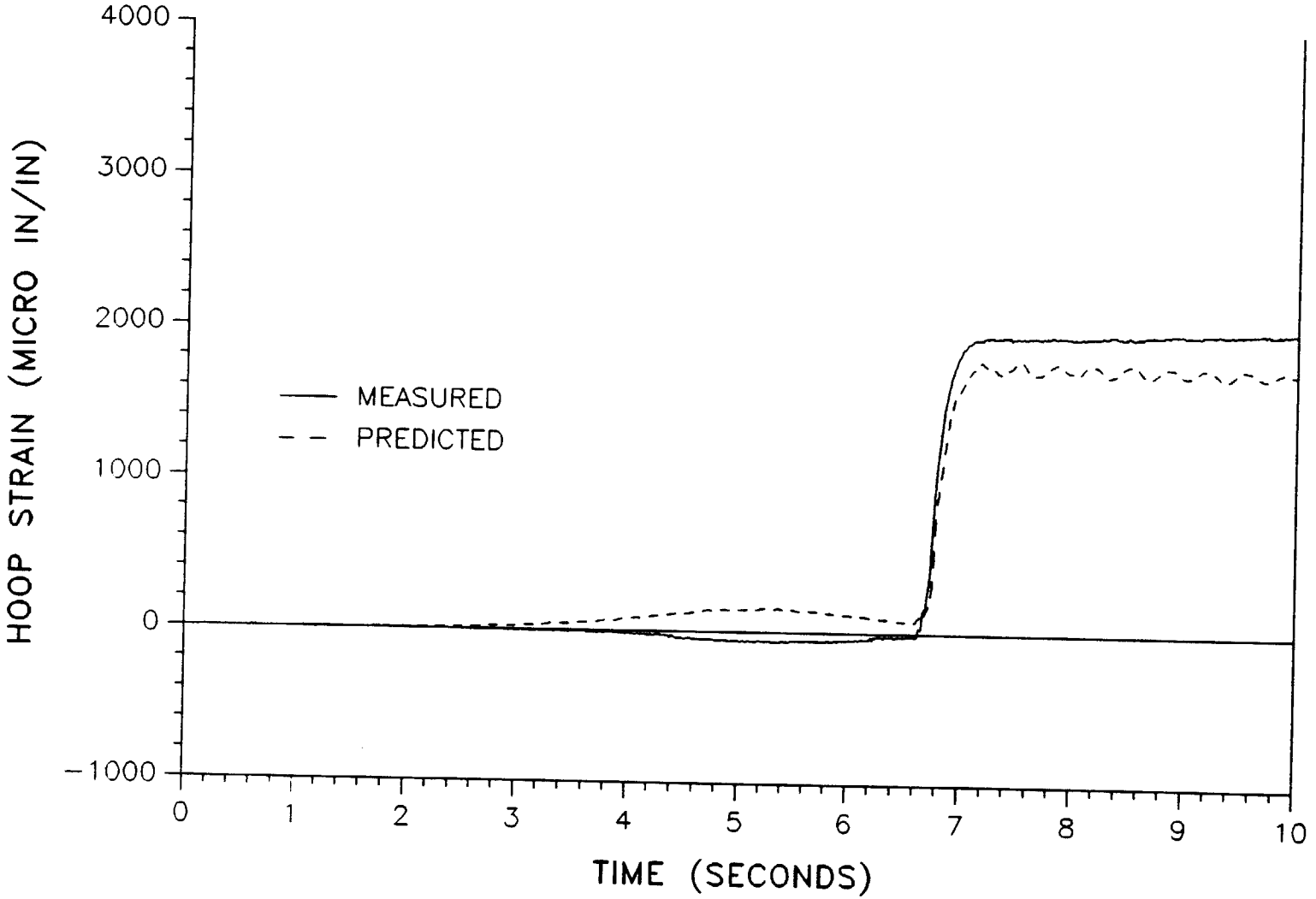

PREDICTED VS MEASURED HOOP STRAIN

360L001 STRAIN GAGE B08G8353A – STATION 1493.0 AT 82 DEGREES

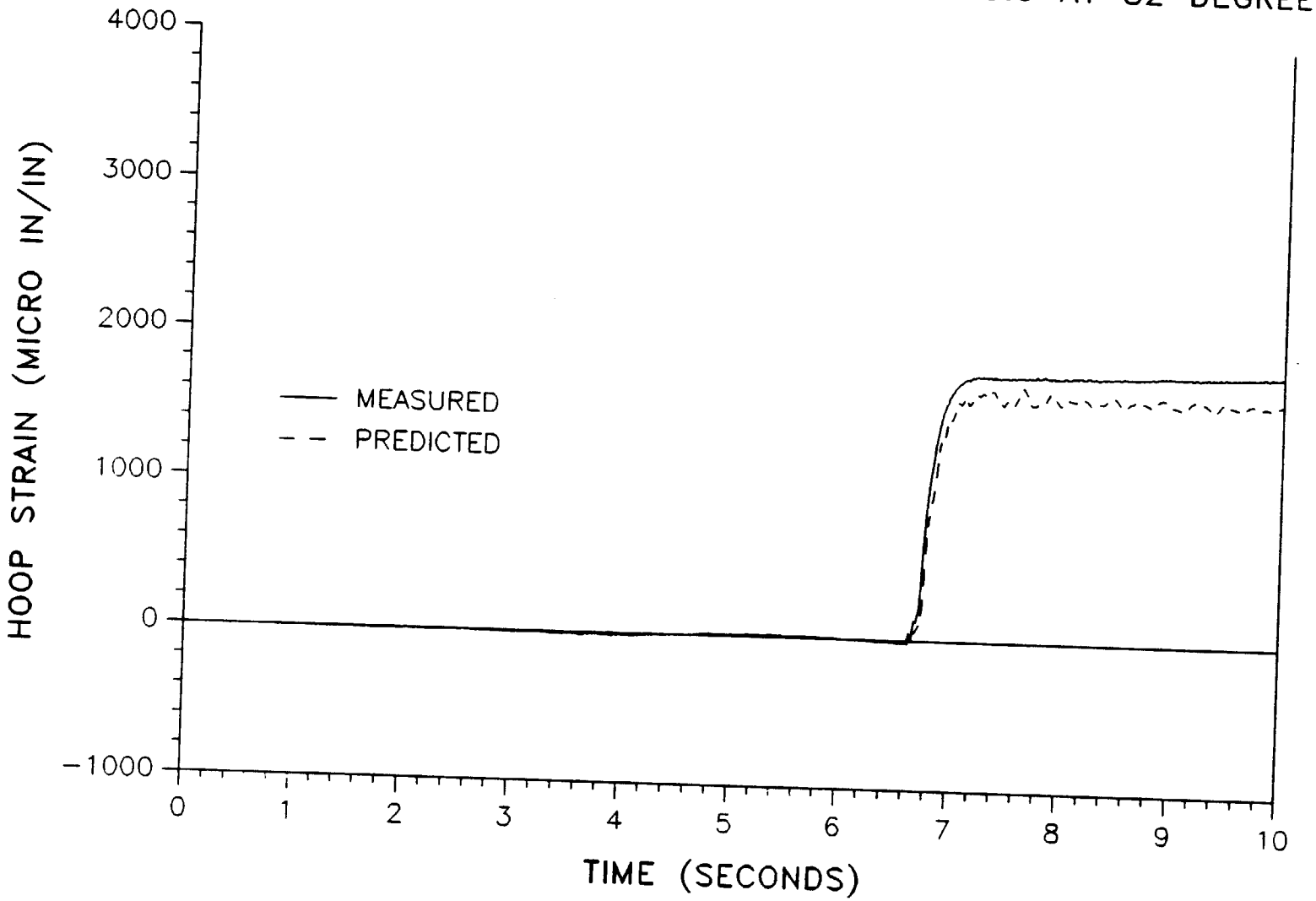

PREDICTED VS MEASURED HOOP STRAIN

360L001 STRAIN GAGE B08G8355A – STATION 1493.0 AT 180 DEGREES

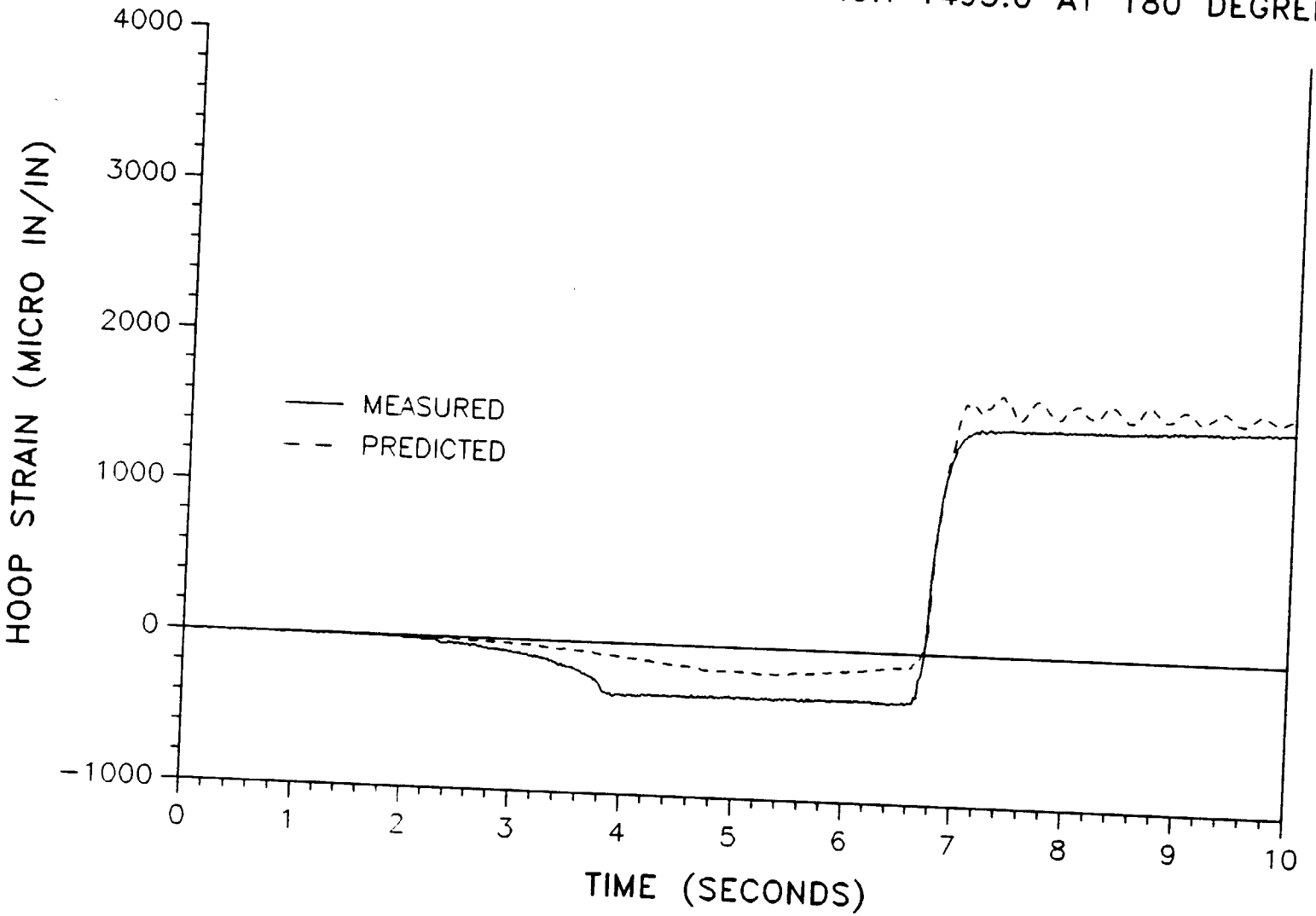

PREDICTED VS MEASURED HOOP STRAIN

360L001 STRAIN GAGE B08G8357A – STATION 1493.0 AT 220 DEGREES

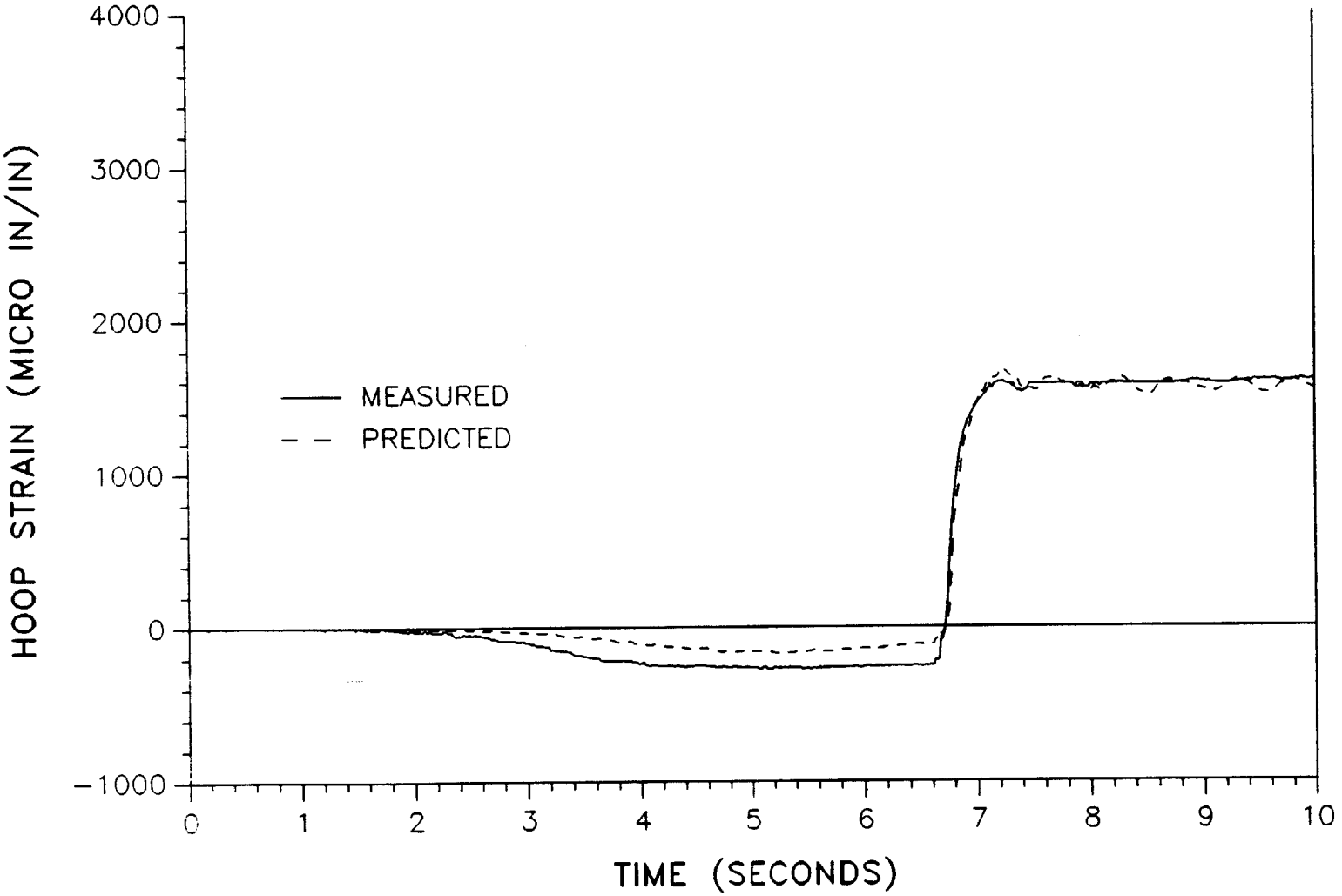

PREDICTED VS MEASURED HOOP STRAIN

360L001 STRAIN GAGE B08G8359A – STATION 1493.0 AT 240 DEGREES

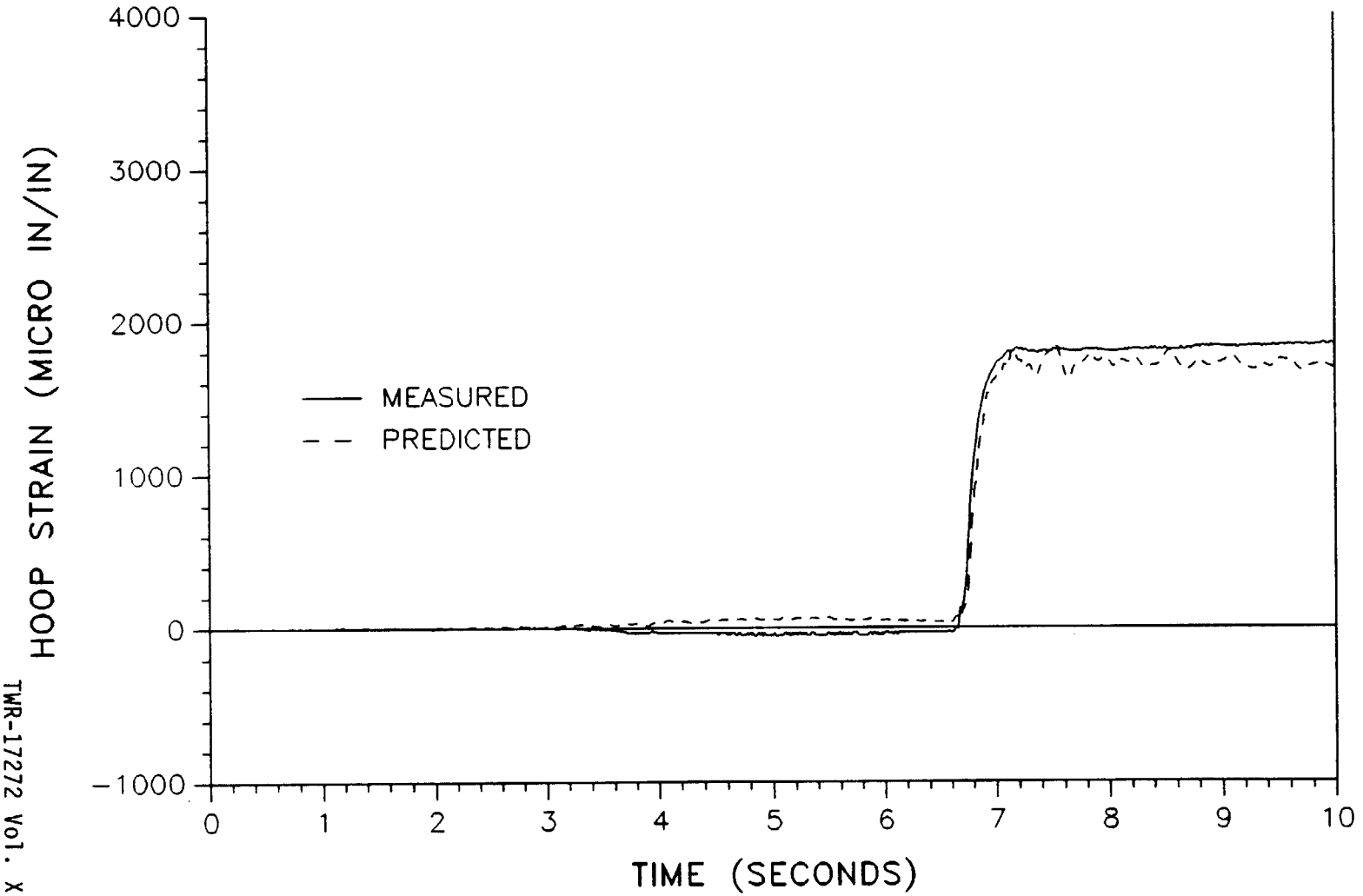

PREDICTED VS MEASURED HOOP STRAIN

360L001 STRAIN GAGE B08G8361A – STATION 1493.0 AT 255 DEGREES

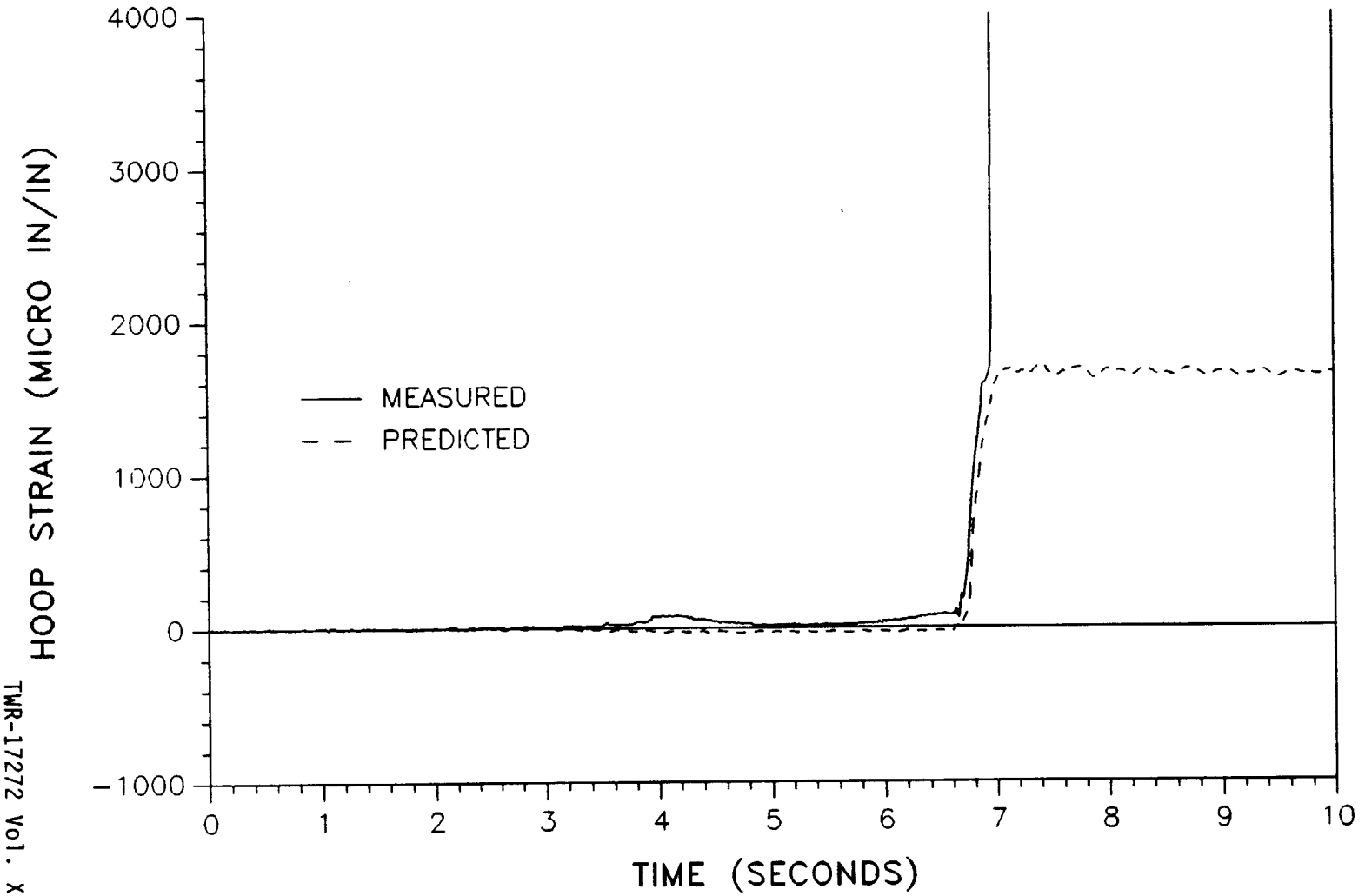

PREDICTED VS MEASURED HOOP STRAIN

360L001 STRAIN GAGE B08G8363A – STATION 1493.0 AT 270 DEGREES

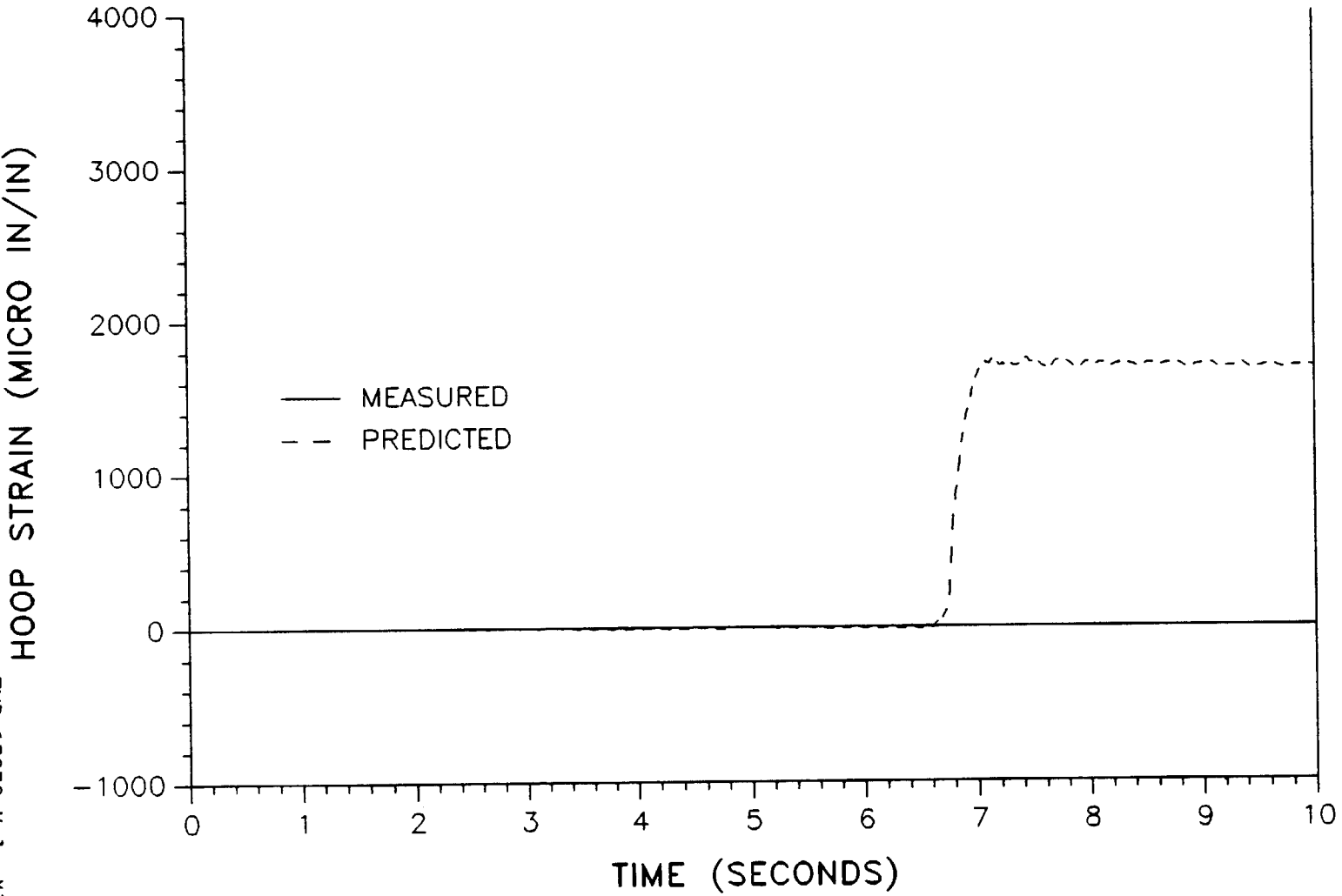

PREDICTED VS MEASURED HOOP STRAIN

360L001 STRAIN GAGE B08G8365A – STATION 1493.0 AT 285 DEGREES

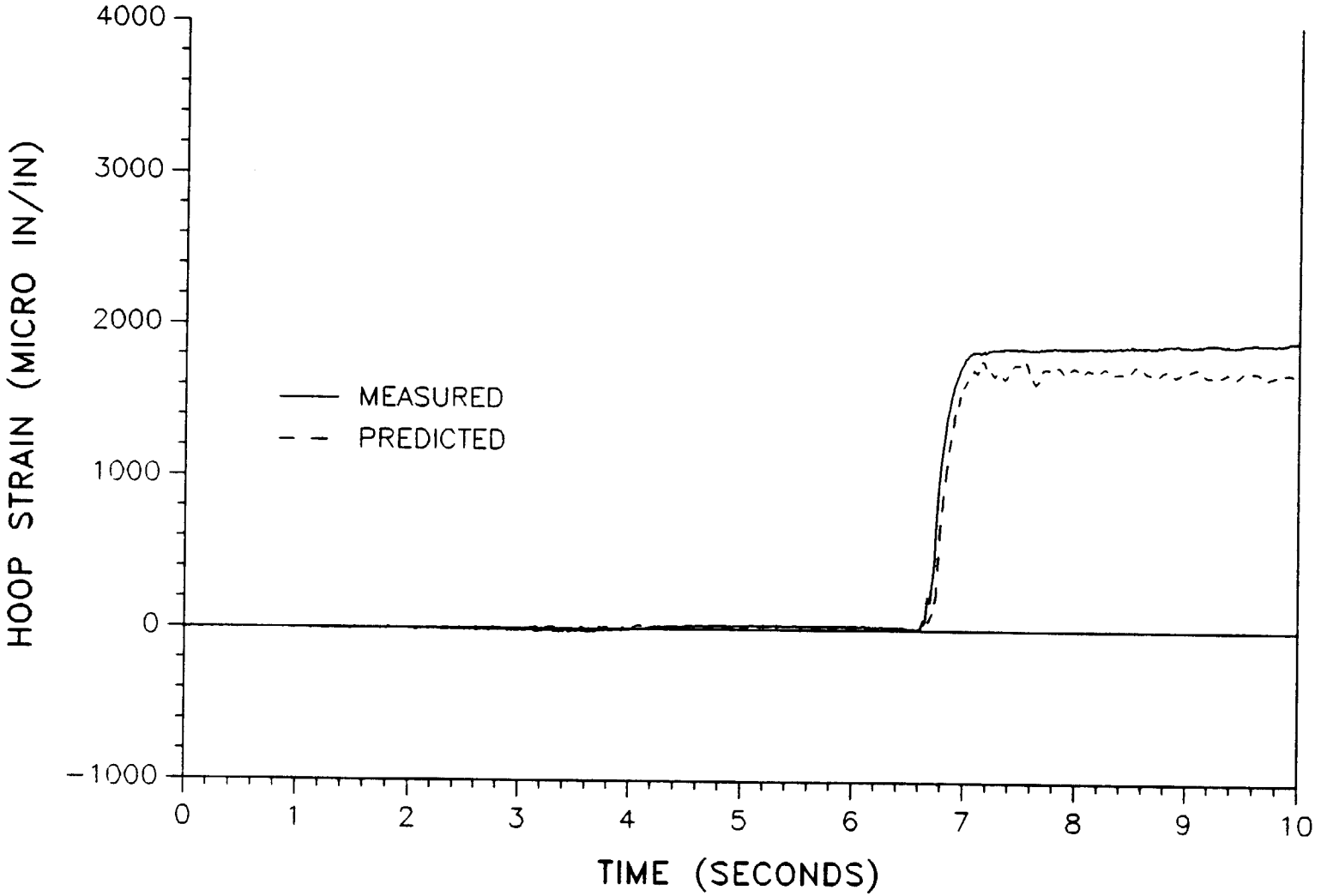

PREDICTED VS MEASURED HOOP STRAIN

360L001 STRAIN GAGE B08G8367A – STATION 1493.0 AT 320 DEGREES

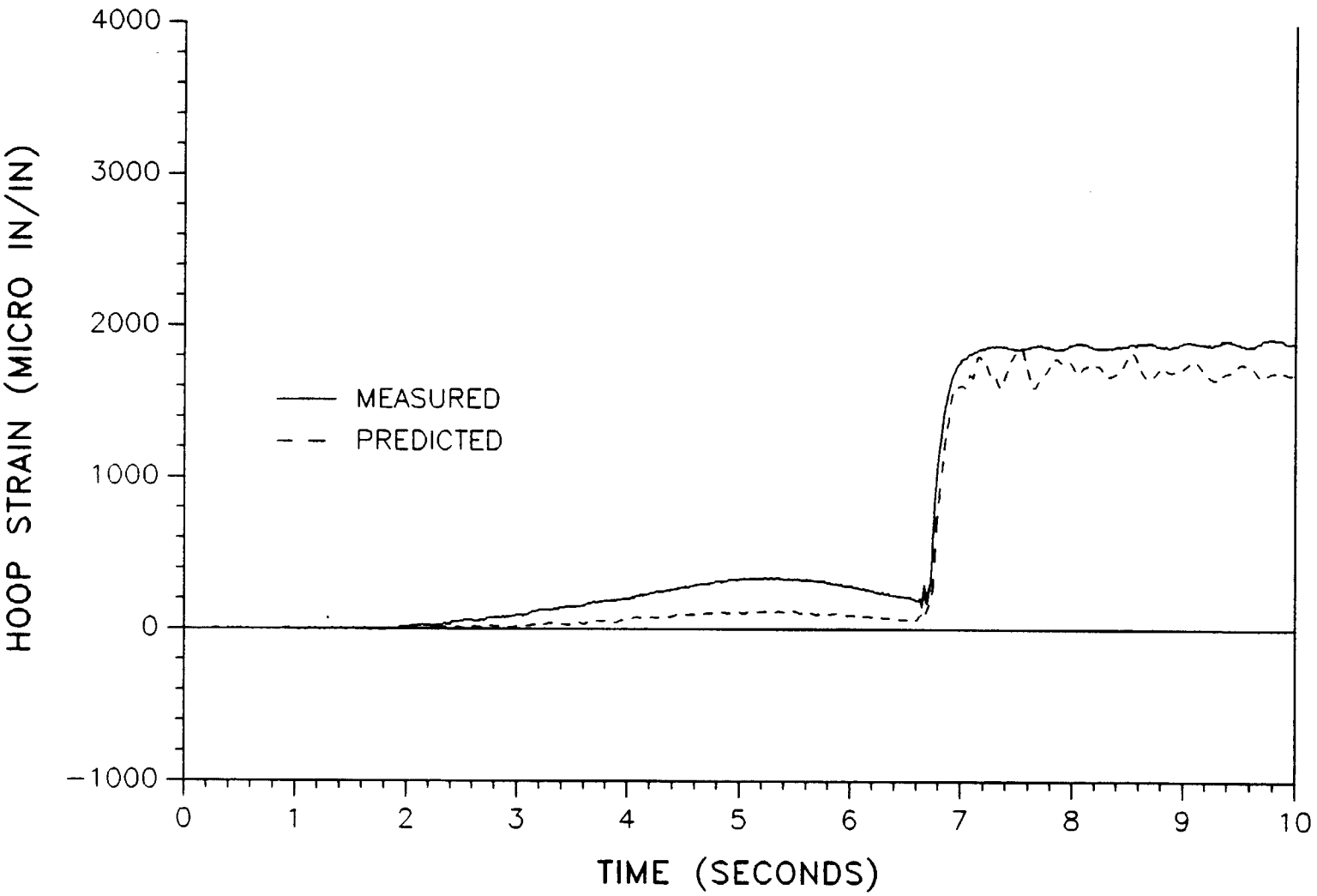

PREDICTED VS MEASURED HOOP STRAIN

360L001 STRAIN GAGE B08G8387A – STATION 1501.0 AT 0 DEGREES

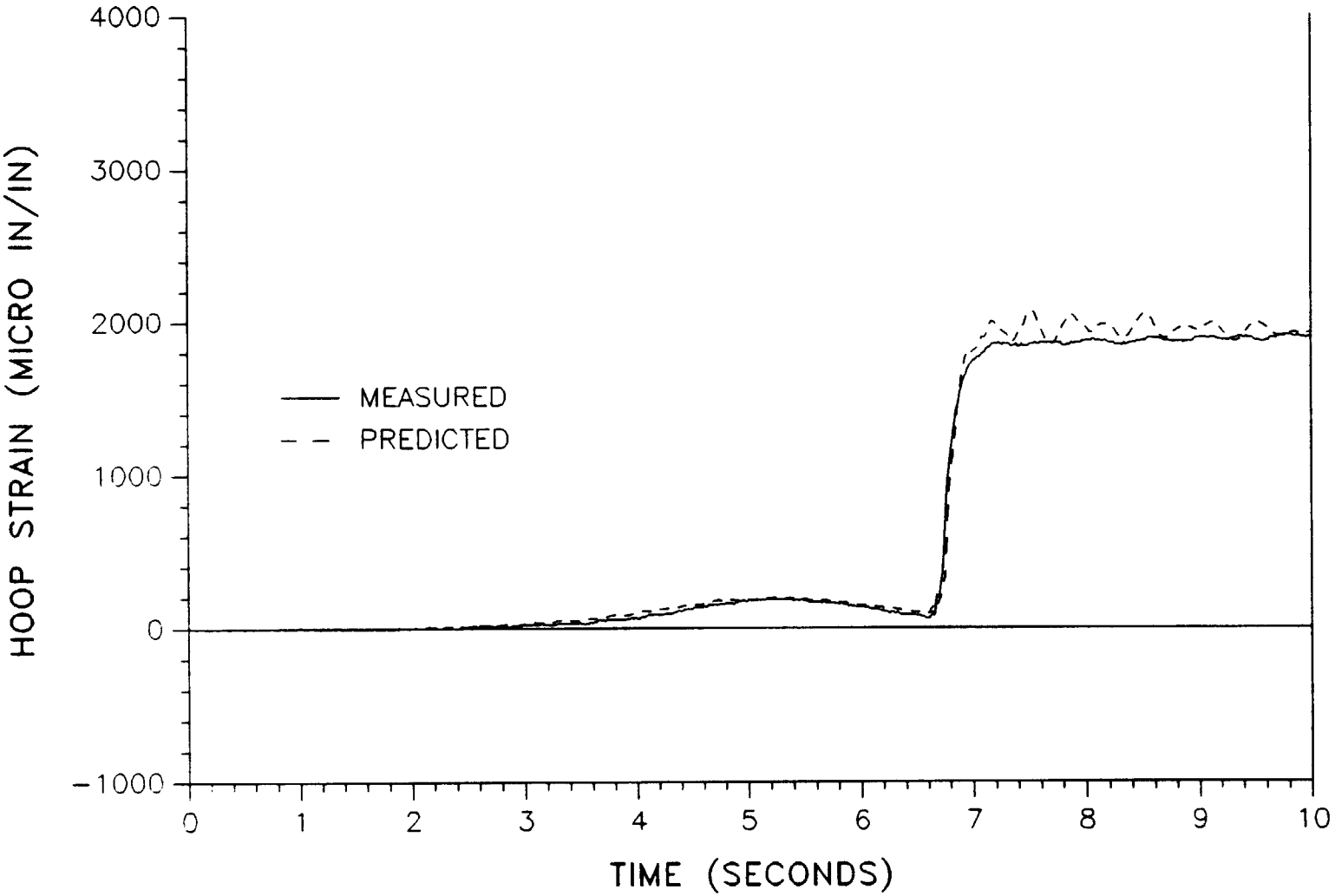

PREDICTED VS MEASURED HOOP STRAIN

360L001 STRAIN GAGE B08G8389A – STATION 1501.0 AT 82 DEGREES

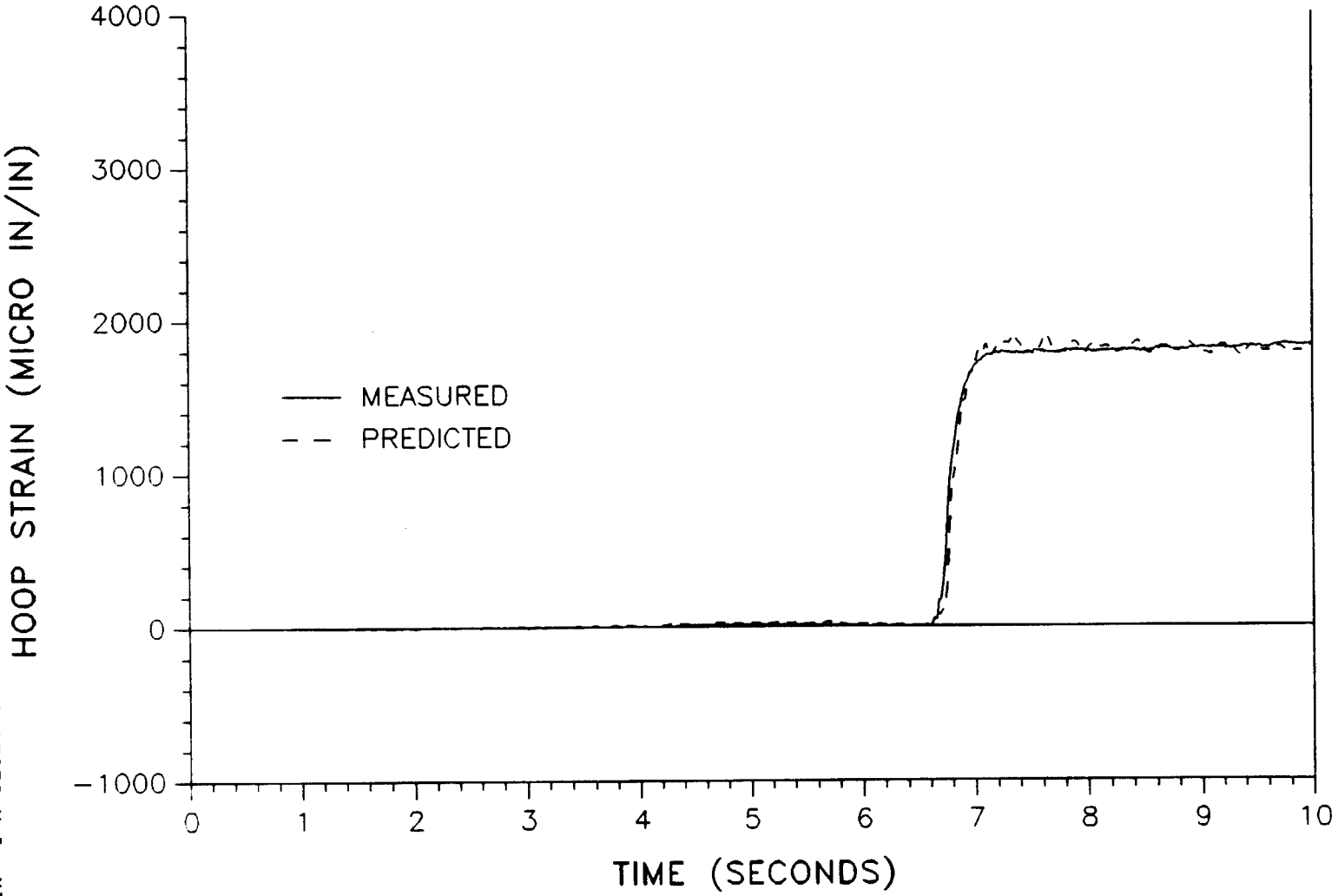

PREDICTED VS MEASURED HOOP STRAIN

360L001 STRAIN GAGE B08G8391A – STATION 1501.0 AT 180 DEGREES

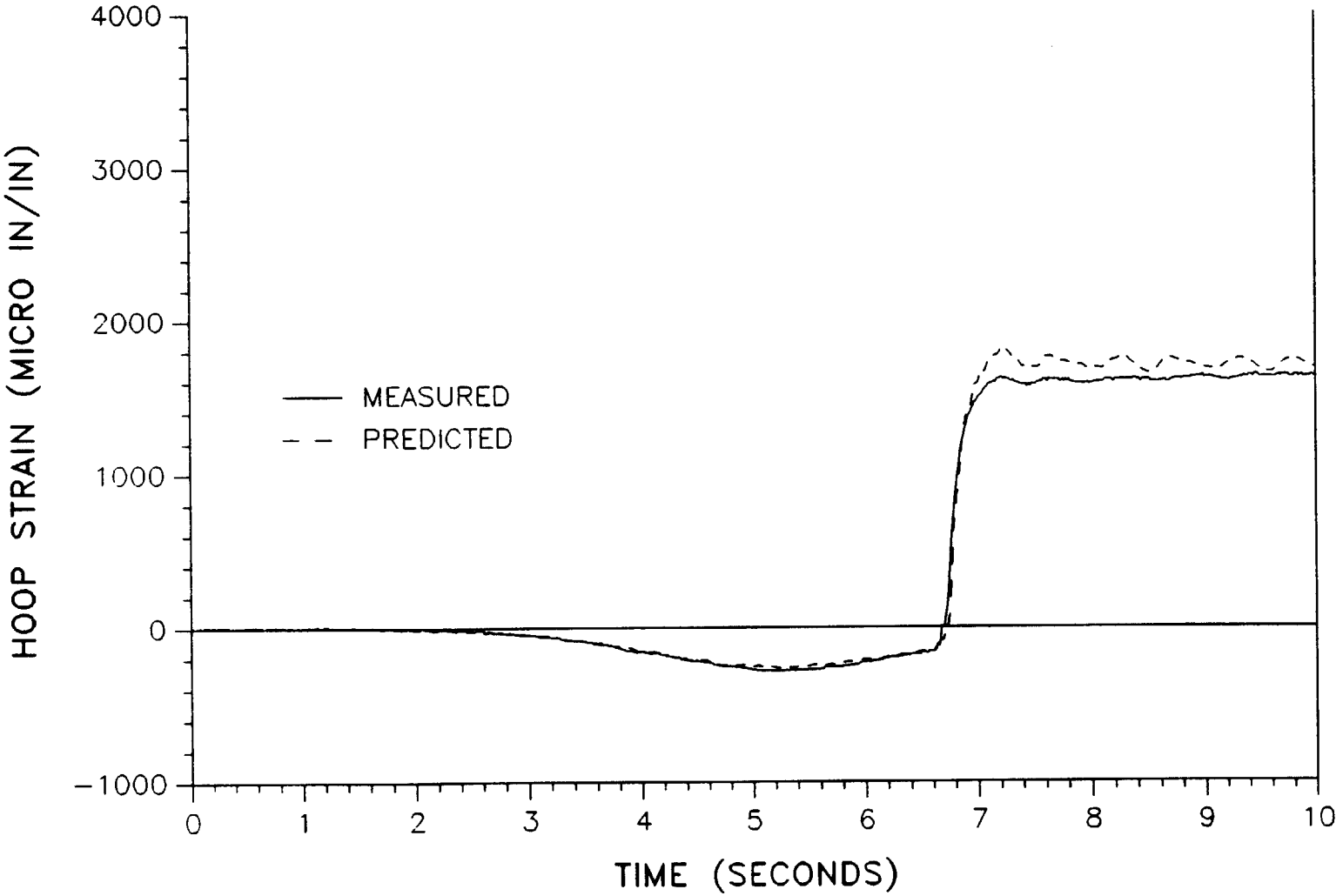

PREDICTED VS MEASURED HOOP STRAIN

360L001 STRAIN GAGE B08G8393A – STATION 1501.0 AT 220 DEGREES

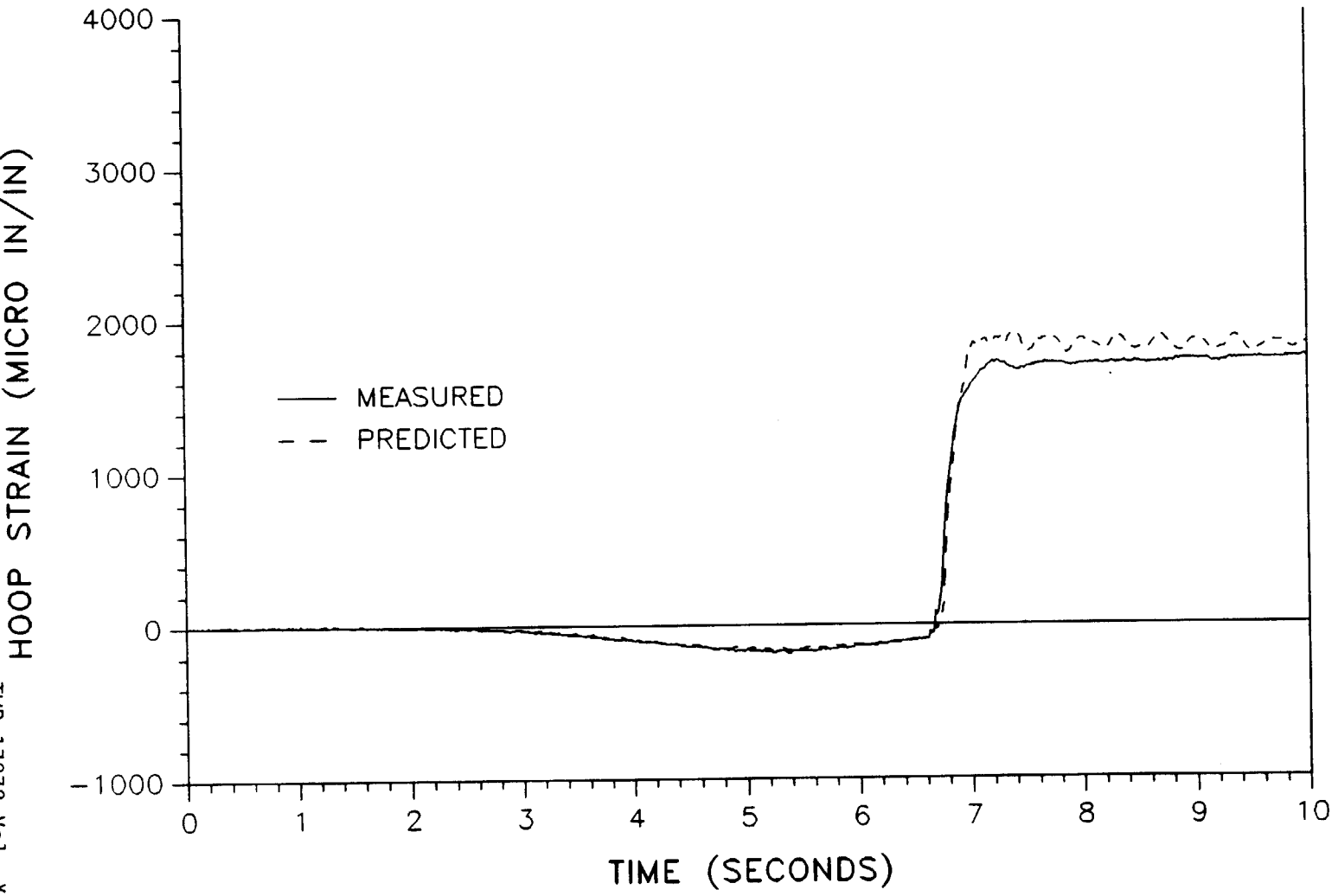

PREDICTED VS MEASURED HOOP STRAIN

360L001 STRAIN GAGE B08G8395A – STATION 1501.0 AT 240 DEGREES

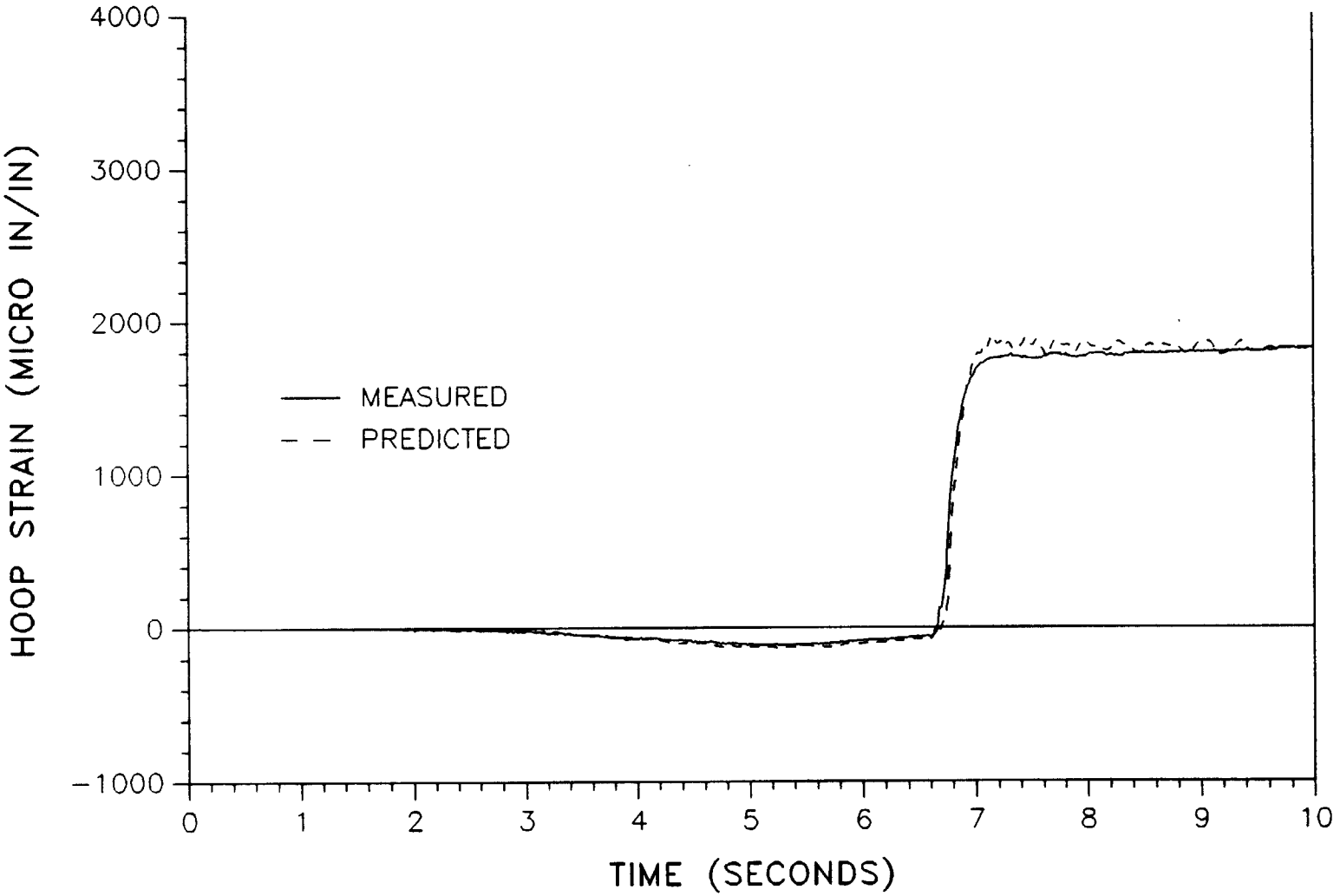

PREDICTED VS MEASURED HOOP STRAIN

360L001 STRAIN GAGE B08G8397A – STATION 1501.0 AT 255 DEGREES

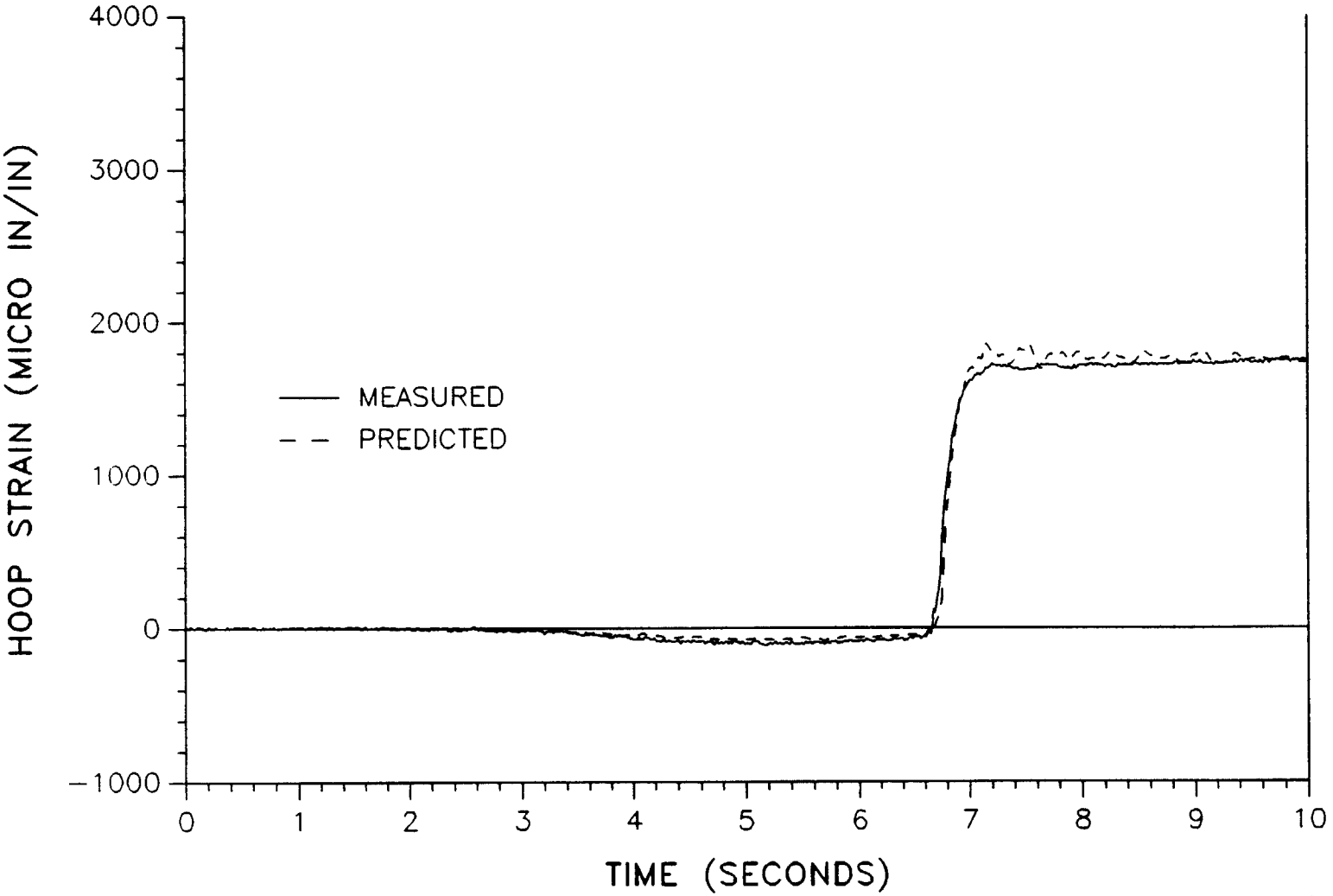

PREDICTED VS MEASURED HOOP STRAIN

360L001 STRAIN GAGE B08G8399A – STATION 1501.0 AT 270 DEGREES

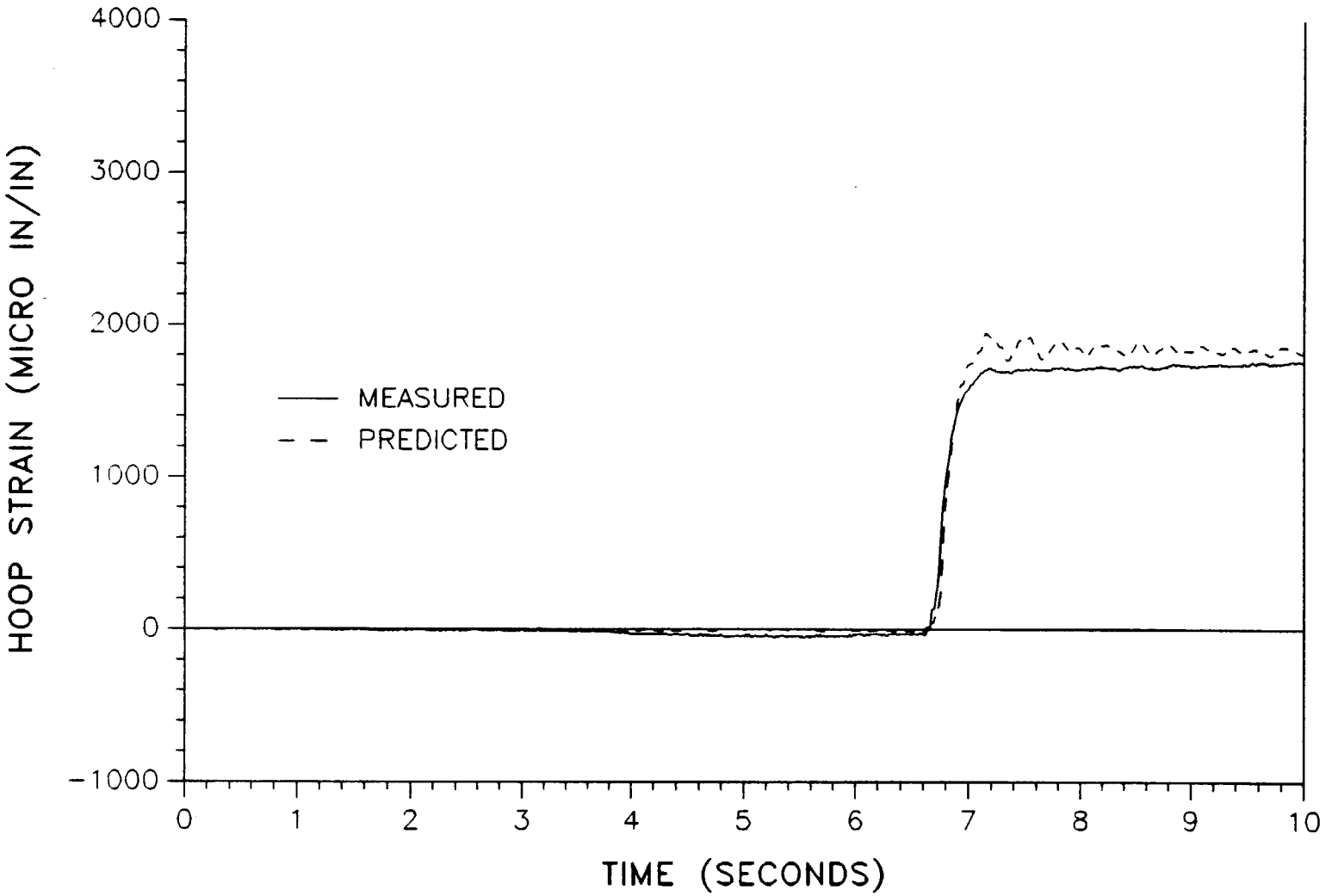

PREDICTED VS MEASURED HOOP STRAIN

360L001 STRAIN GAGE B08G8401A – STATION 1501.0 AT 285 DEGREES

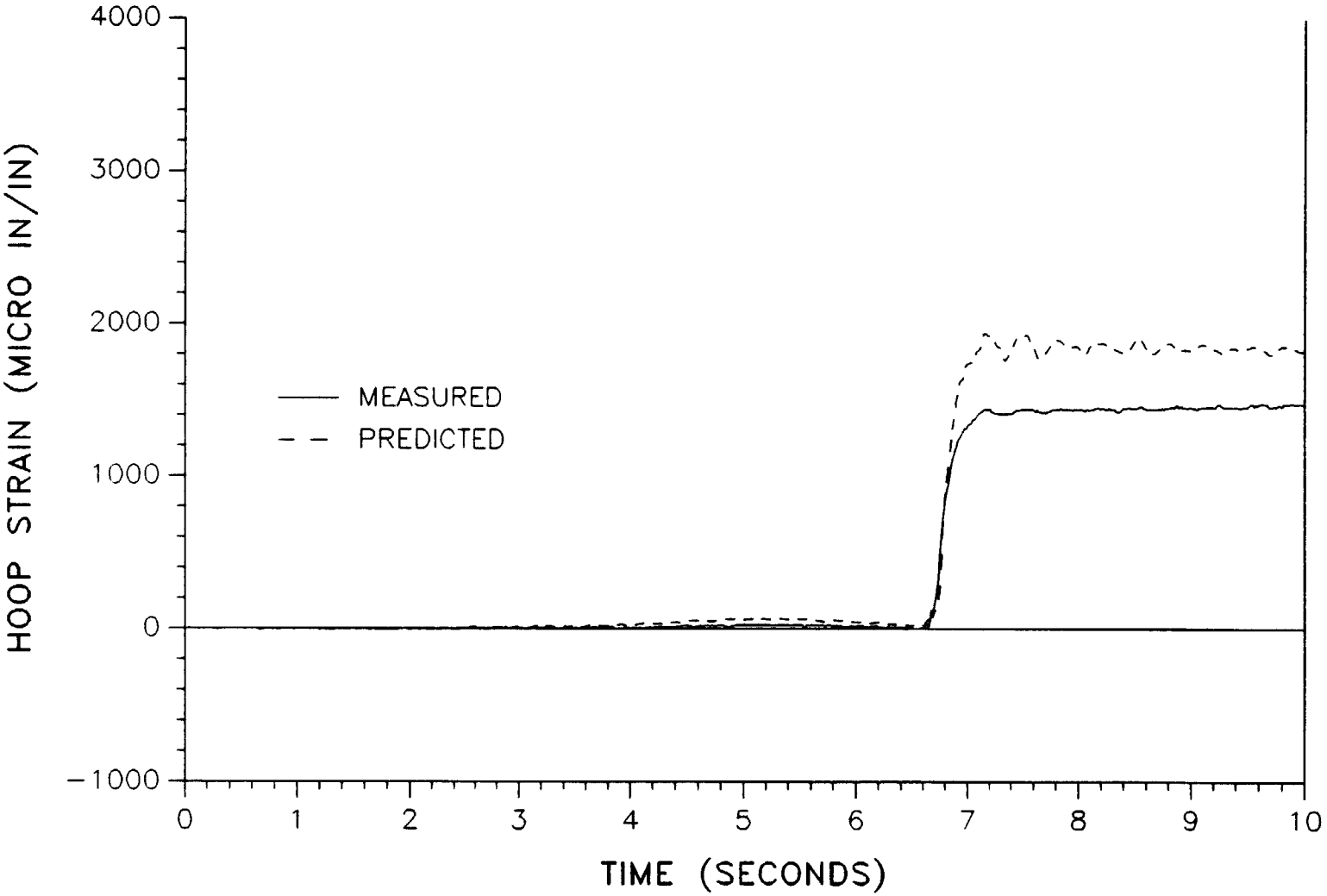

PREDICTED VS MEASURED HOOP STRAIN

360L001 STRAIN GAGE B08G8403A – STATION 1501.0 AT 320 DEGREES

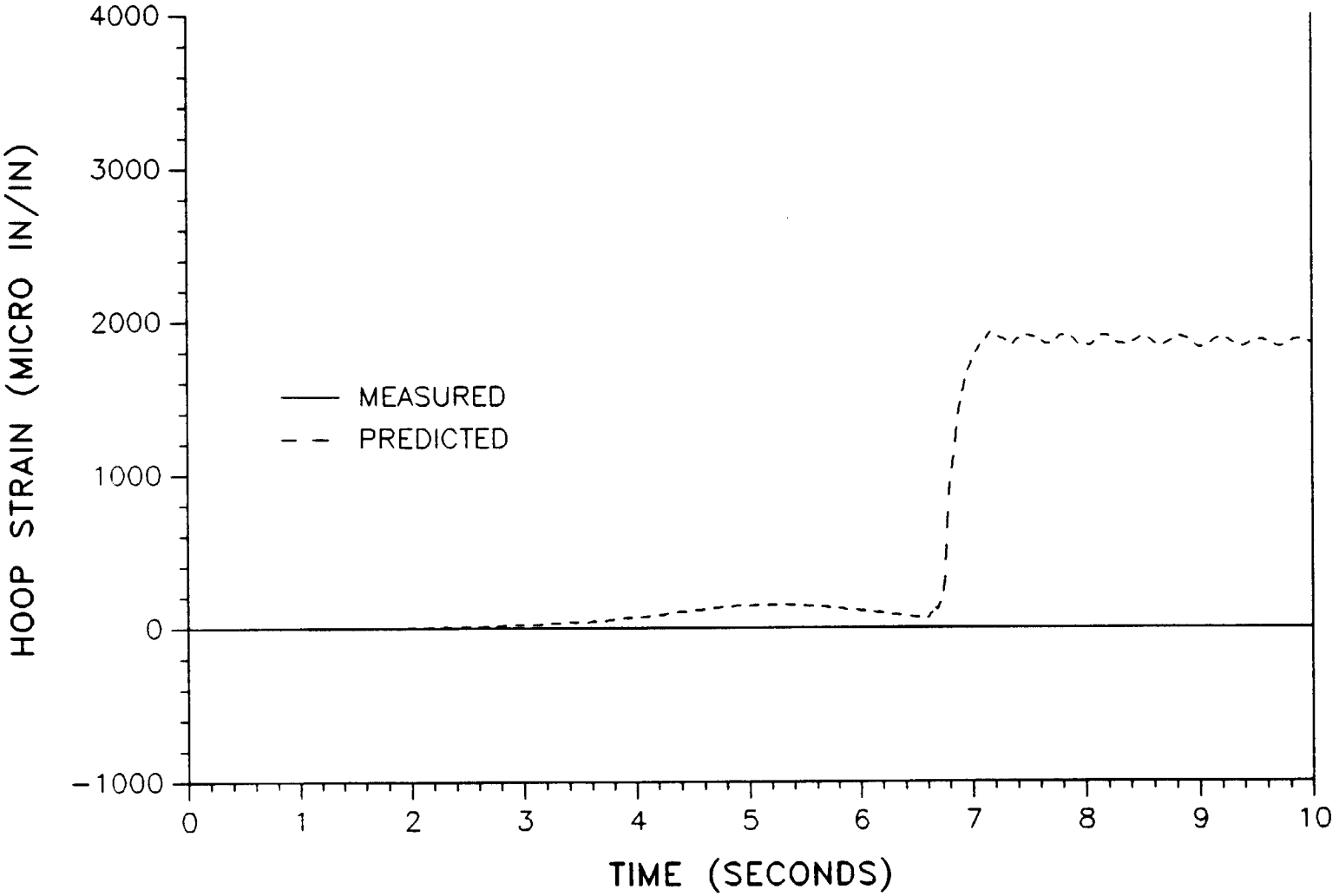

PREDICTED VS MEASURED HOOP STRAIN

360L001 STRAIN GAGE B08G8409A – STATION 1797.0 AT 0 DEGREES

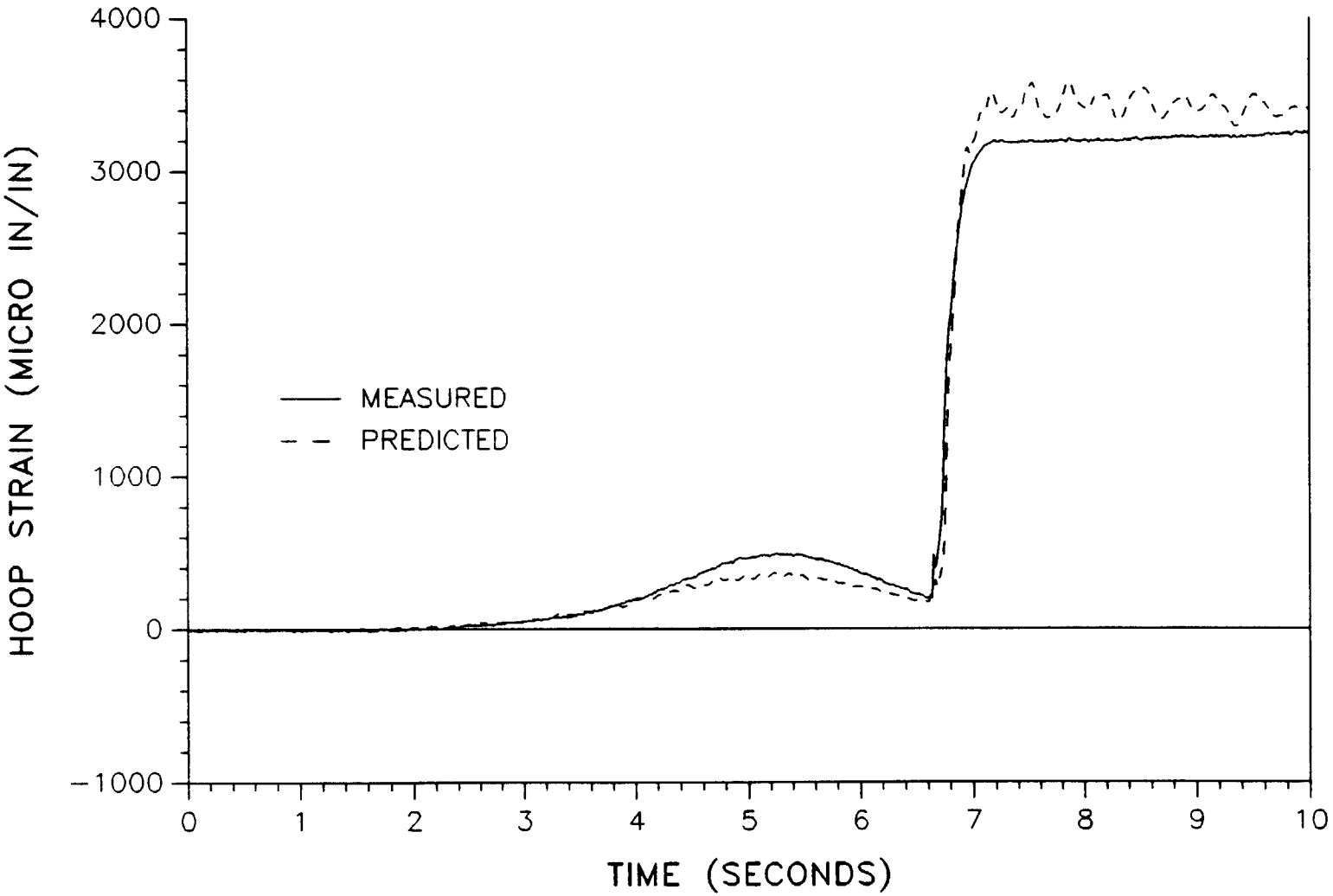

PREDICTED VS MEASURED HOOP STRAIN

360L001 STRAIN GAGE B08G8407A – STATION 1797.0 AT 82 DEGREES

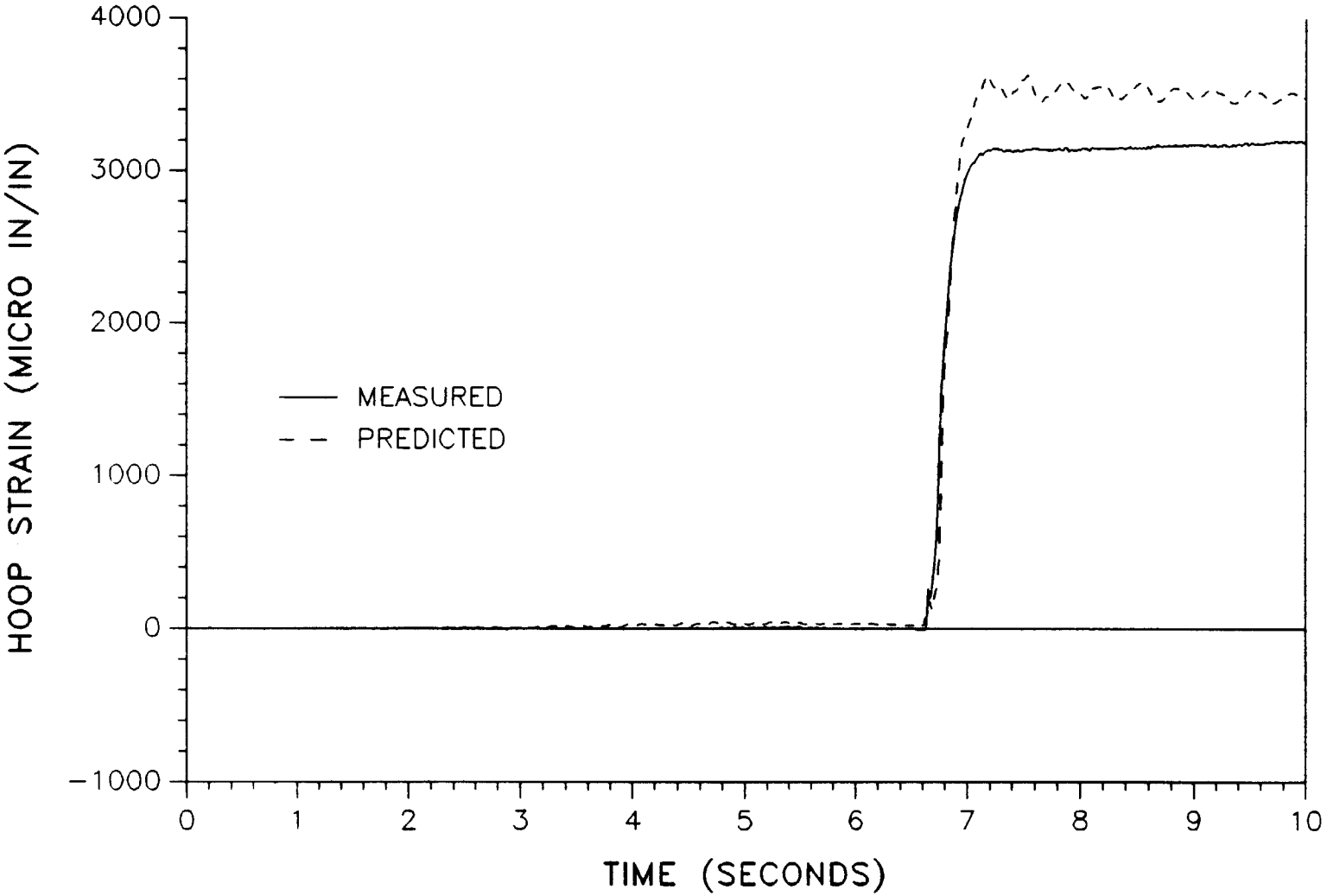

PREDICTED VS MEASURED HOOP STRAIN

360L001 STRAIN GAGE B08G8405A – STATION 1797.0 AT 180 DEGREES

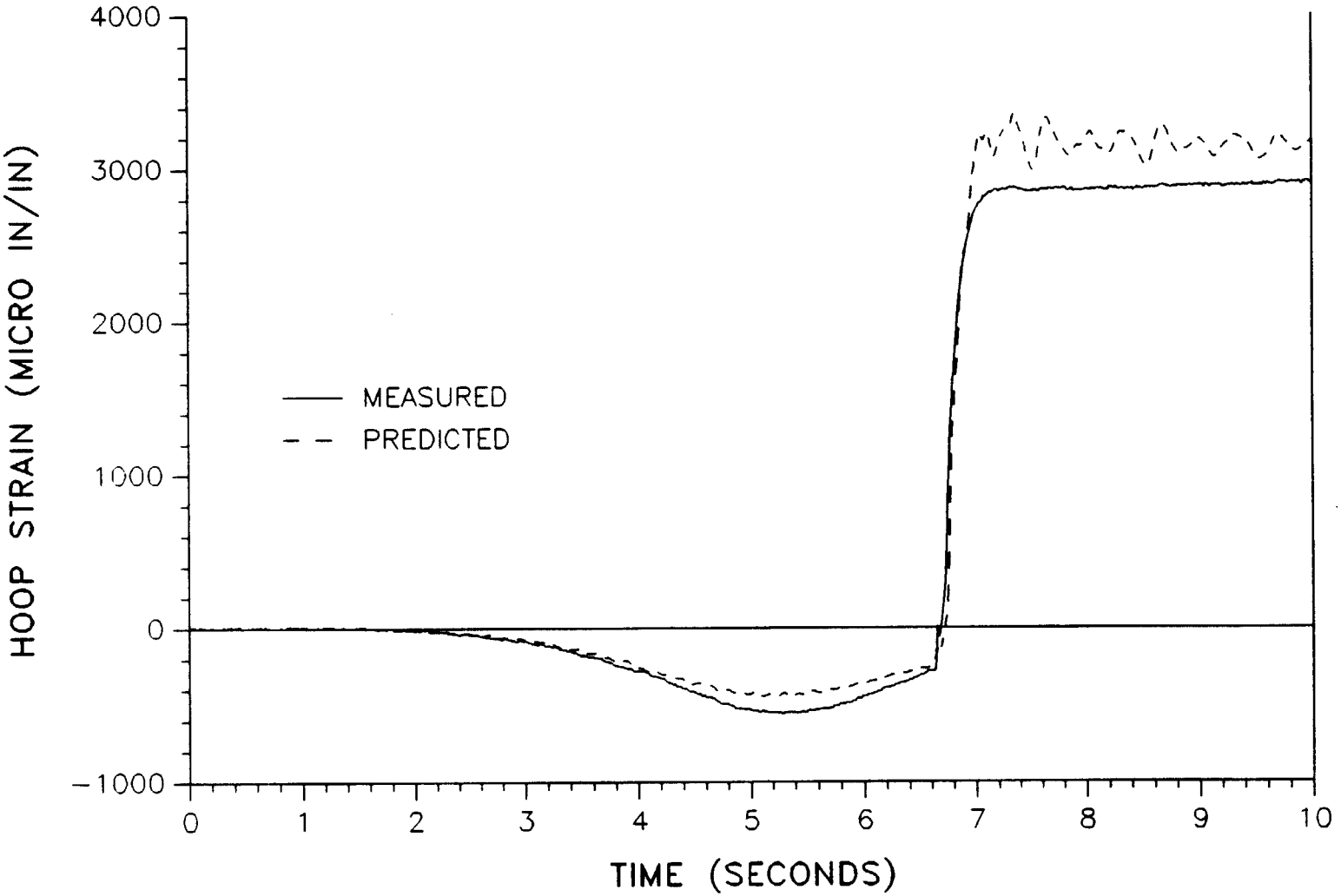

PREDICTED VS MEASURED HOOP STRAIN

360L001 STRAIN GAGE B08G8411A – STATION 1797.0 AT 270 DEGREES

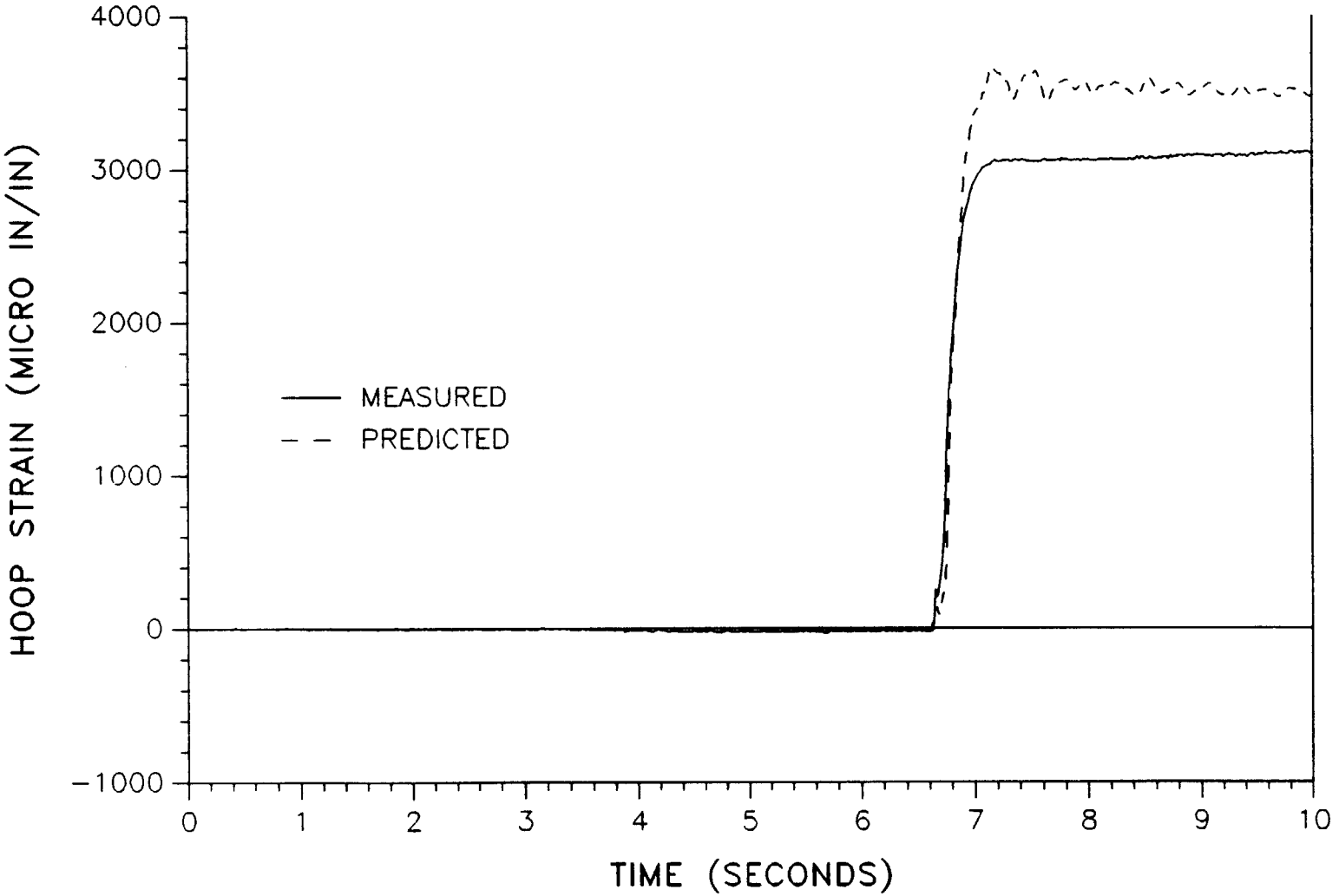

APPENDIX F

Axial Strain Plots

PREDICTED VS MEASURED AXIAL STRAIN

360L001 STRAIN GAGE B08G7318A – STATION 556.5 AT 0 DEGREES

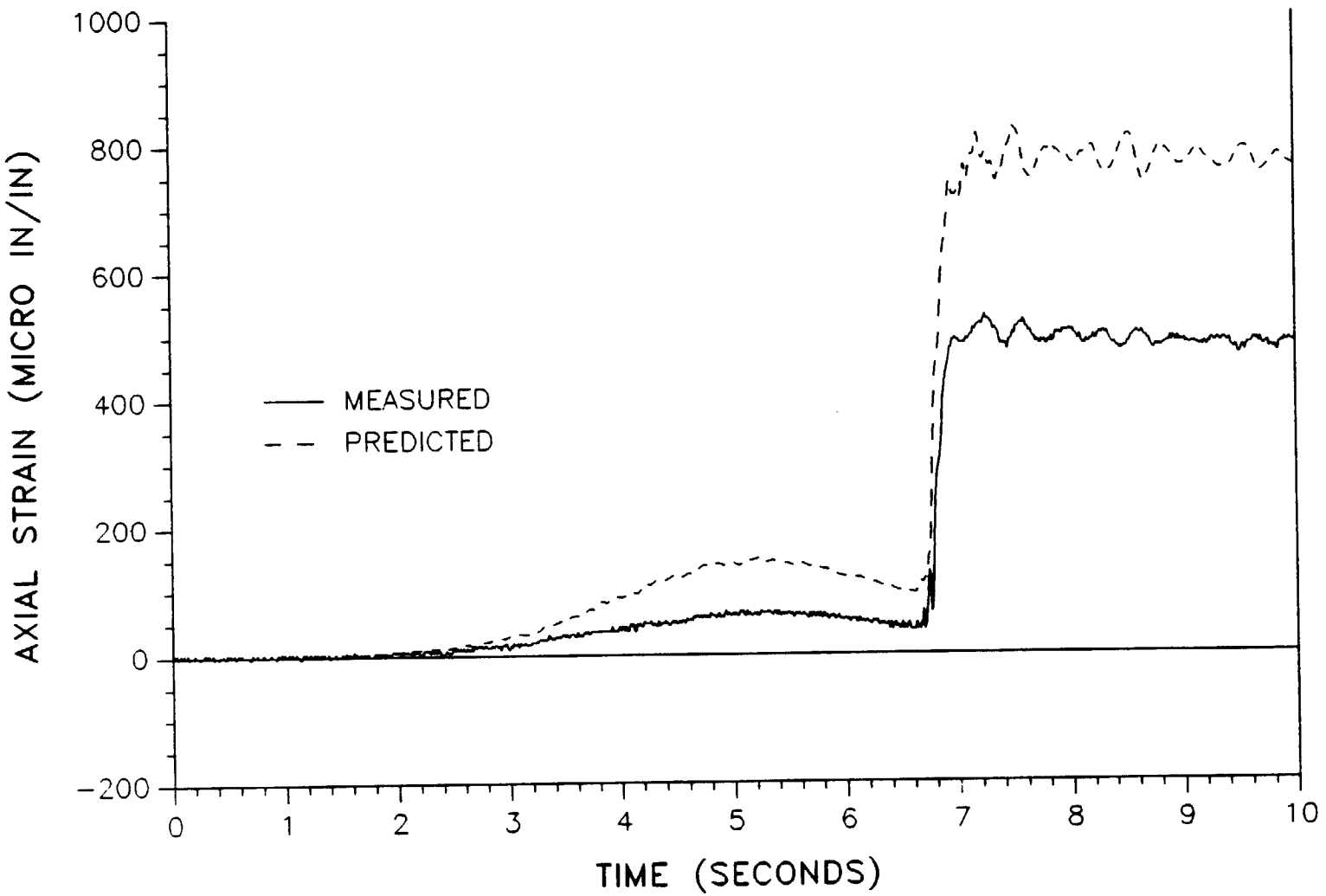

PREDICTED VS MEASURED AXIAL STRAIN

360L001 STRAIN GAGE B08G7320A – STATION 556.5 AT 98 DEGREES

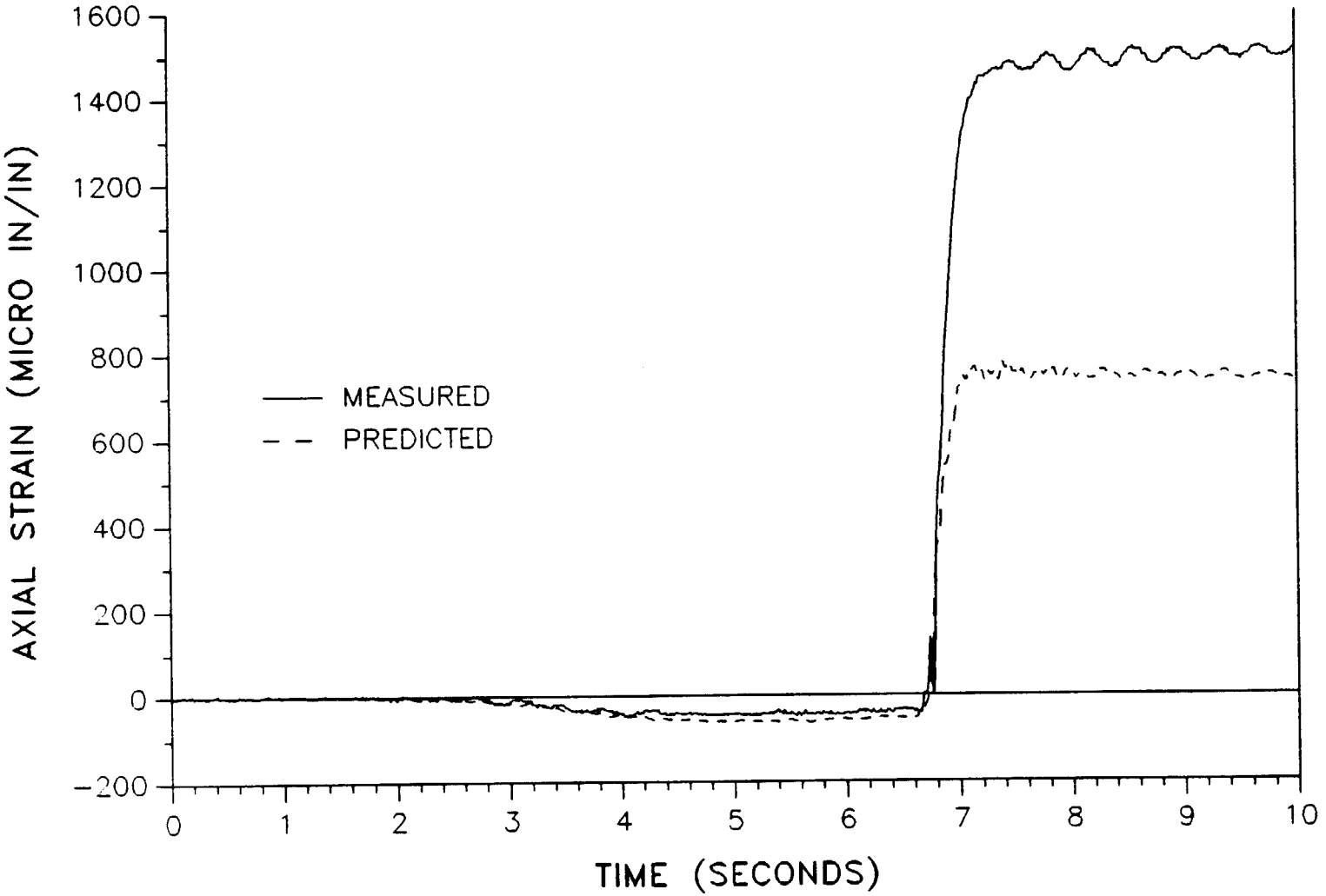

PREDICTED VS MEASURED AXIAL STRAIN

360L001 STRAIN GAGE B08G7322A – STATION 556.5 AT 180 DEGREES

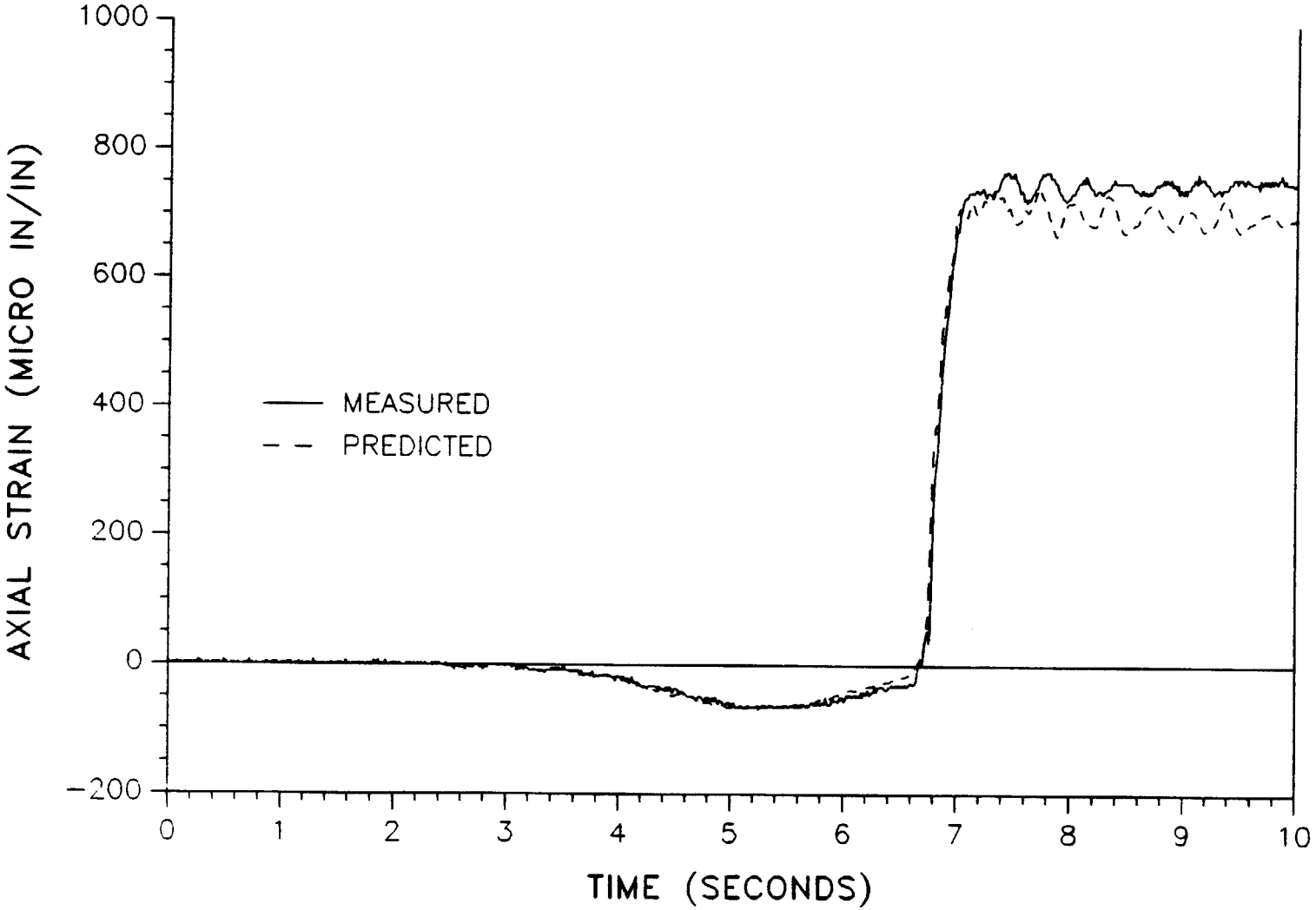

PREDICTED VS MEASURED AXIAL STRAIN

360L001 STRAIN GAGE B08G7324A – STATION 556.5 AT 270 DEGREES

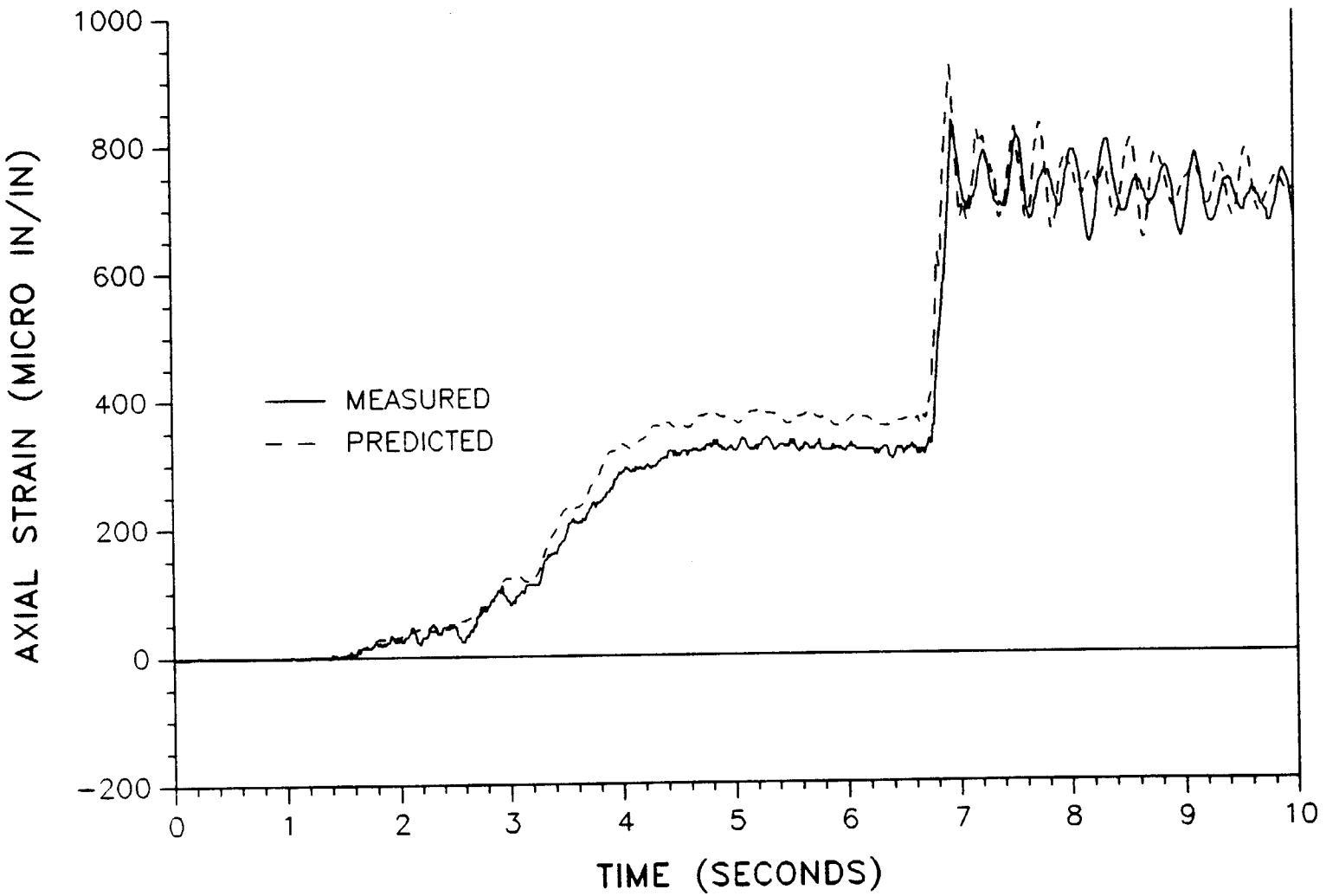

PREDICTED VS MEASURED AXIAL STRAIN

360L001 STRAIN GAGE B08G7326A – STATION 876.5 AT 0 DEGREES

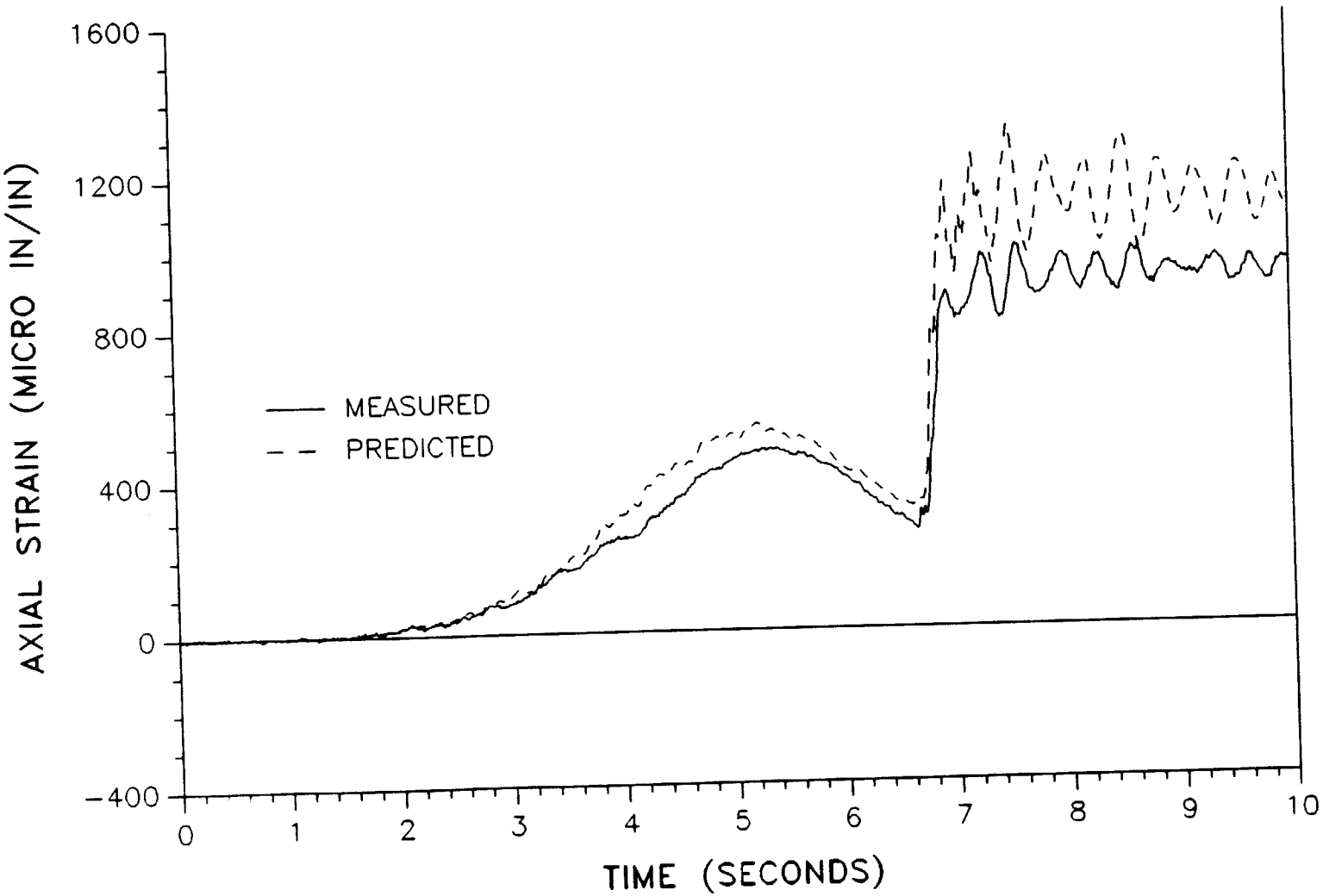

PREDICTED VS MEASURED AXIAL STRAIN

360L001 STRAIN GAGE B08G7328A – STATION 876.5 AT 98 DEGREES

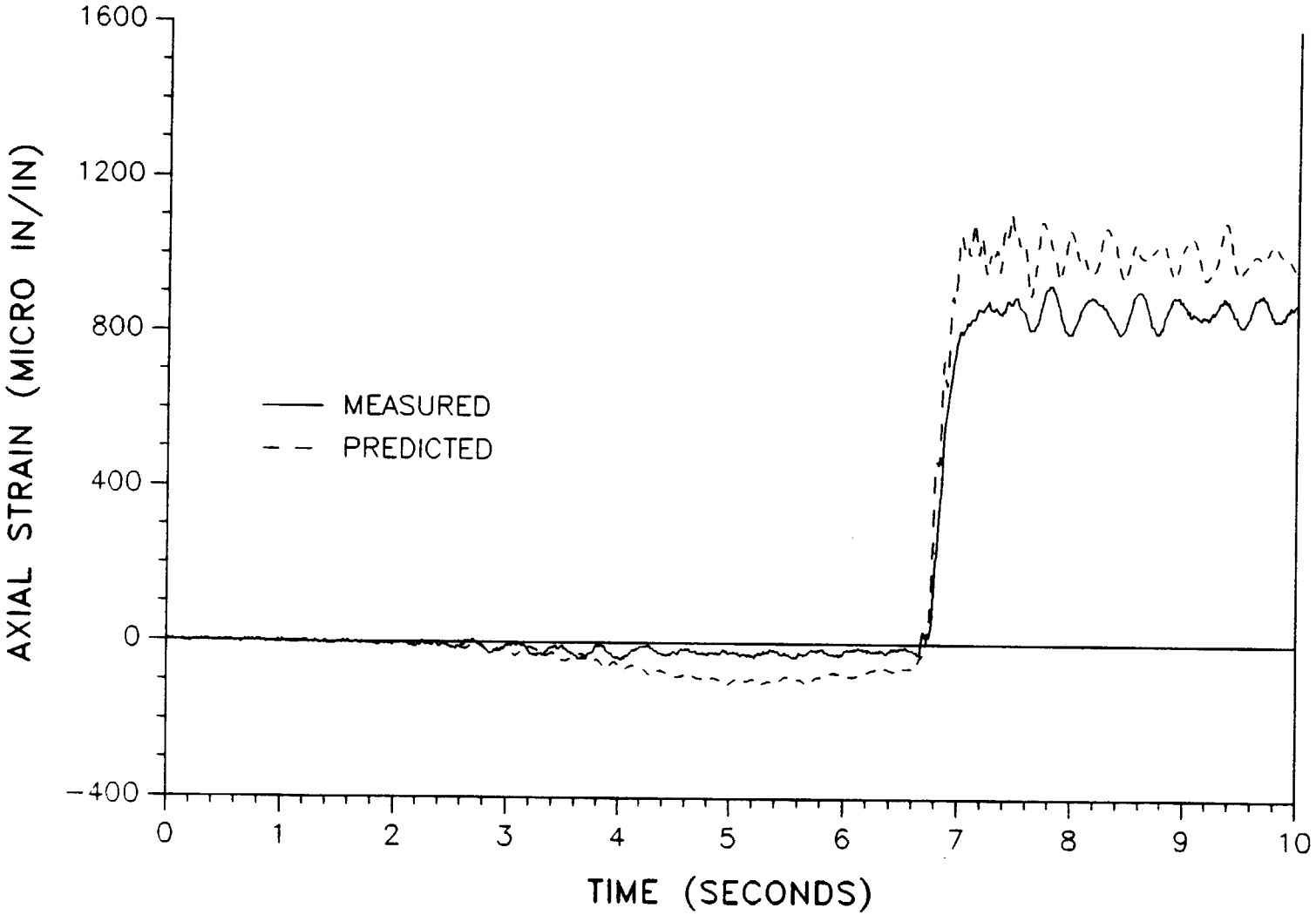

PREDICTED VS MEASURED AXIAL STRAIN

360L001 STRAIN GAGE B08G7330A – STATION 876.5 AT 180 DEGREES

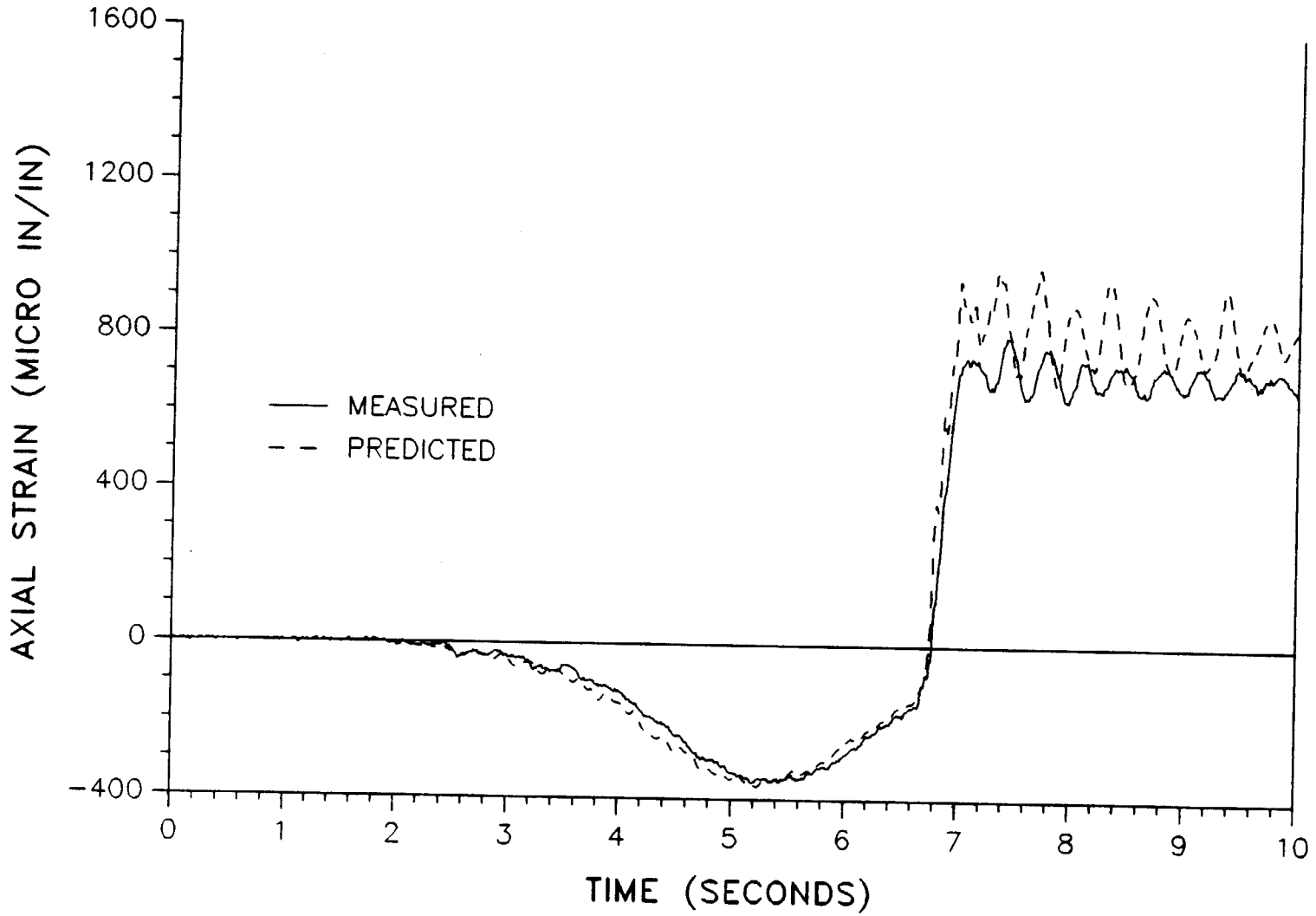

PREDICTED VS MEASURED AXIAL STRAIN

360L001 STRAIN GAGE B08G7332A – STATION 876.5 AT 270 DEGREES

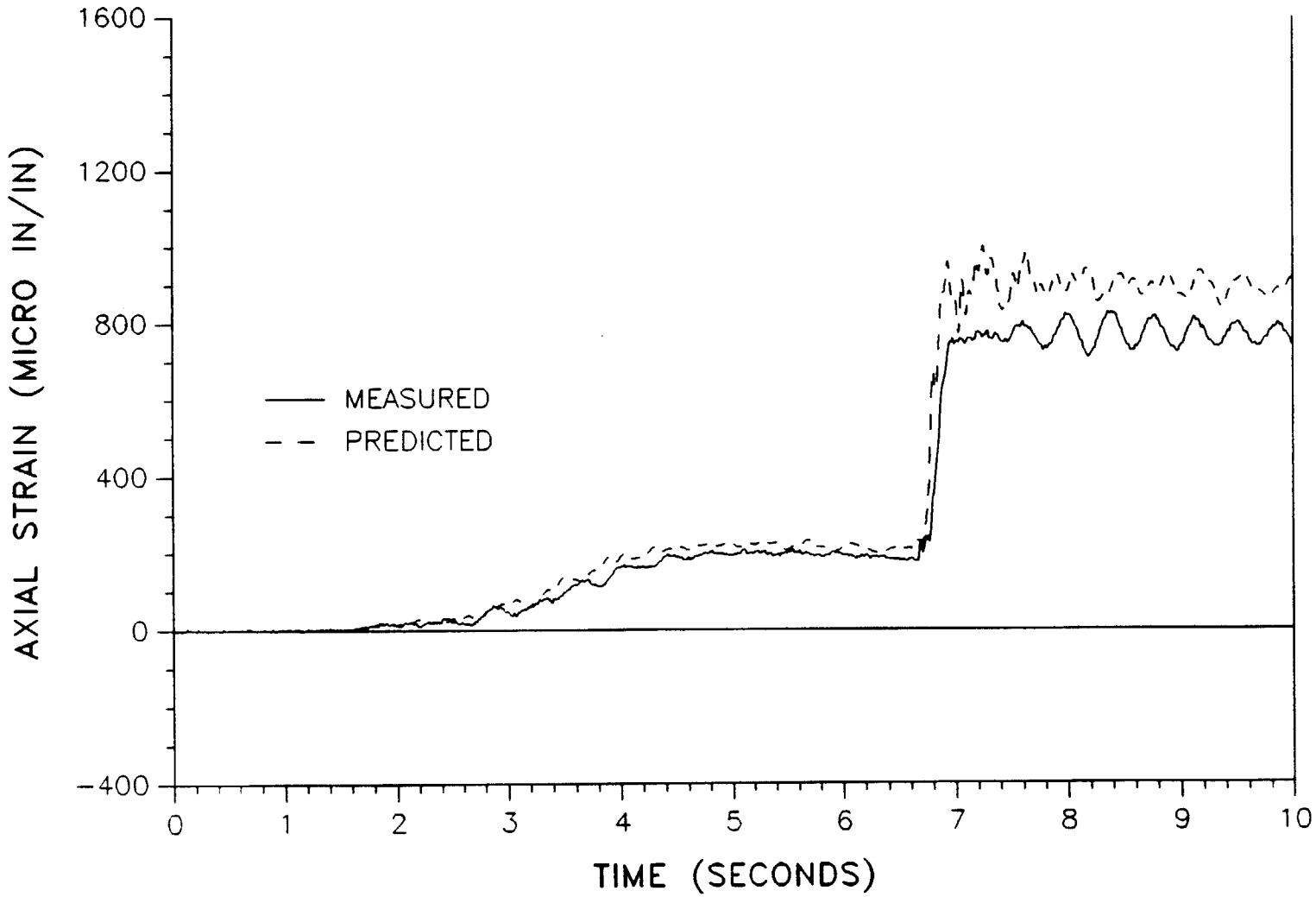

PREDICTED VS MEASURED AXIAL STRAIN

360L001 STRAIN GAGE B08G7334A – STATION 1196.5 AT 0 DEGREES

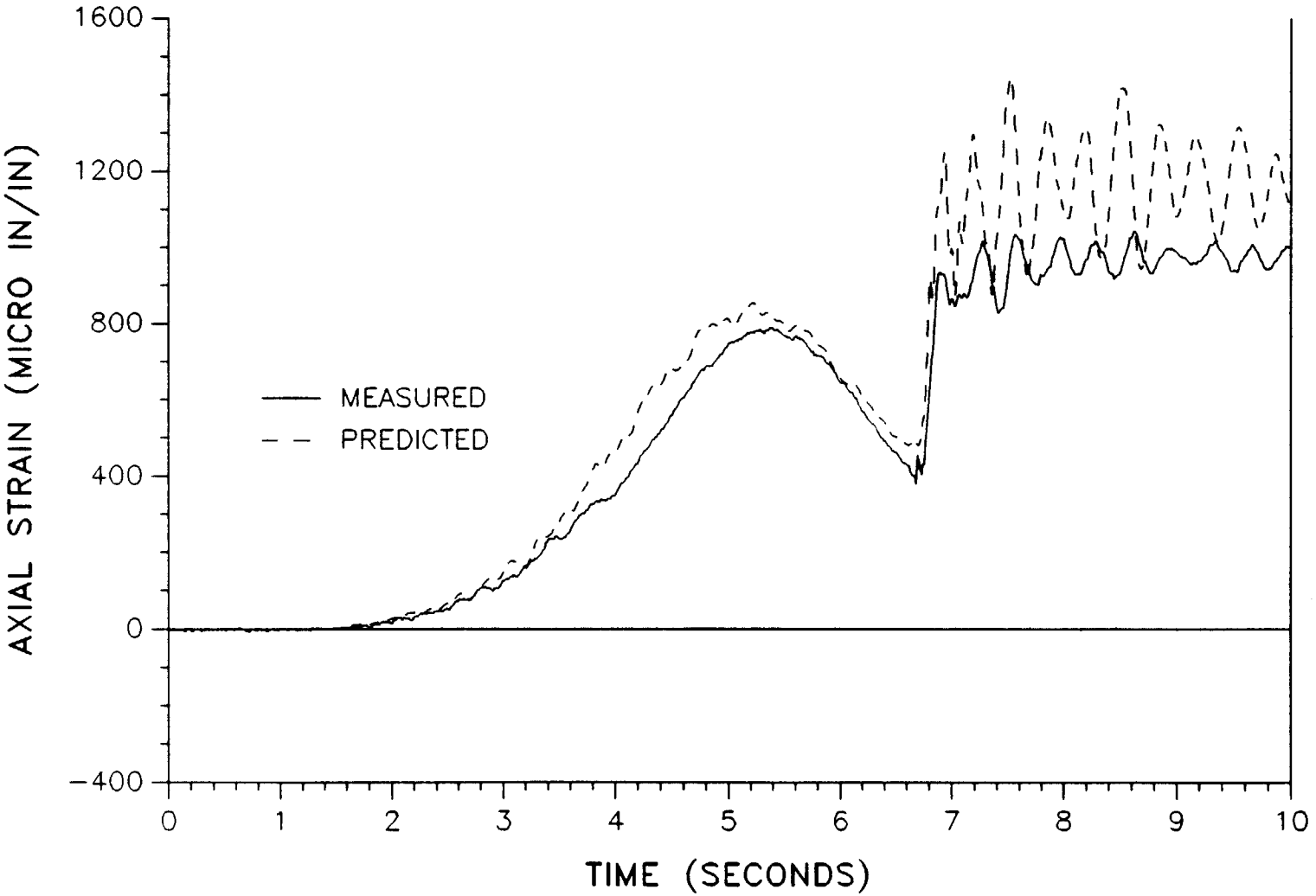

PREDICTED VS MEASURED AXIAL STRAIN

360L001 STRAIN GAGE B08G7336A – STATION 1196.5 AT 98 DEGREES

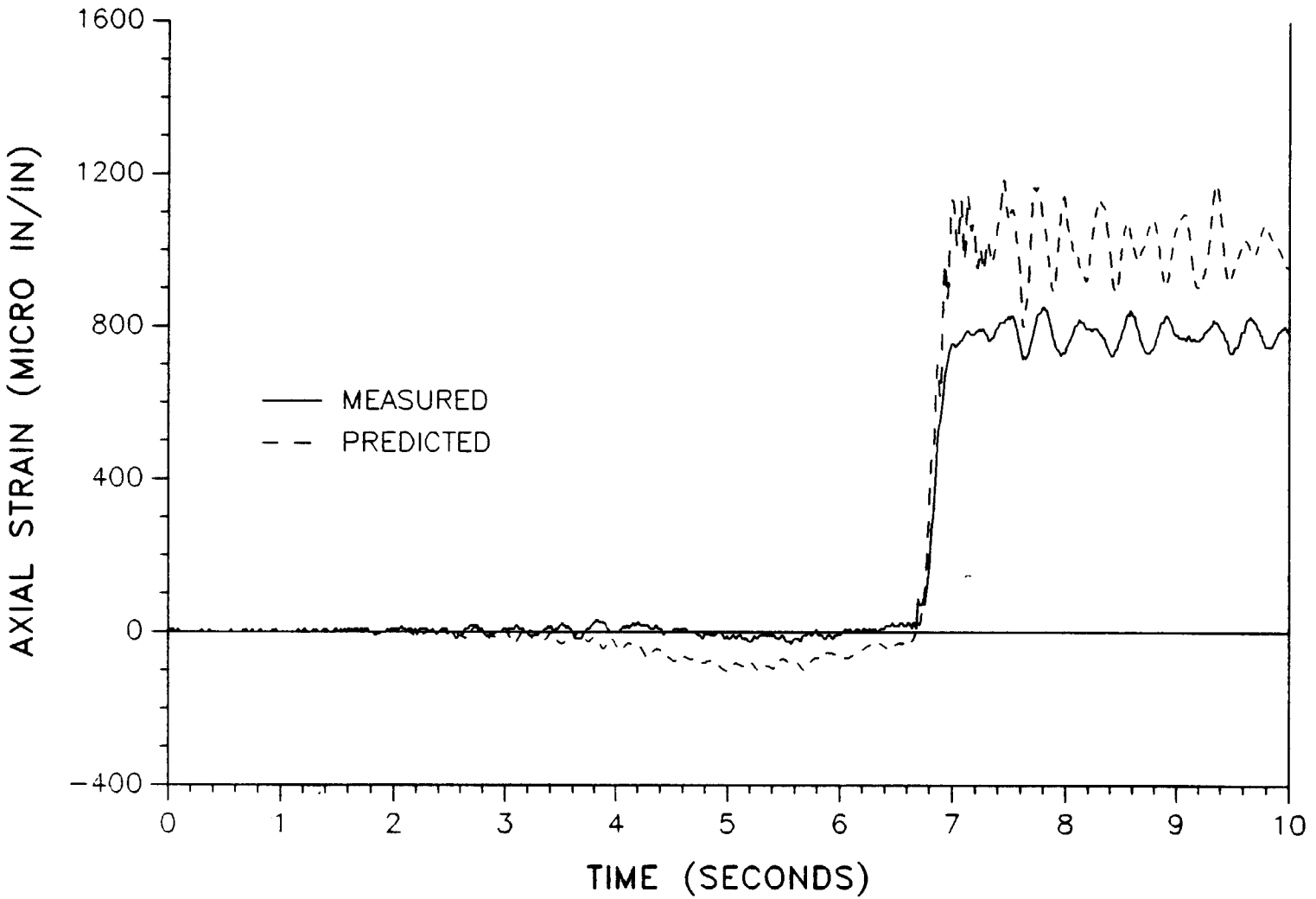

PREDICTED VS MEASURED AXIAL STRAIN

360L001 STRAIN GAGE B08G7338A – STATION 1196.5 AT 180 DEGREES

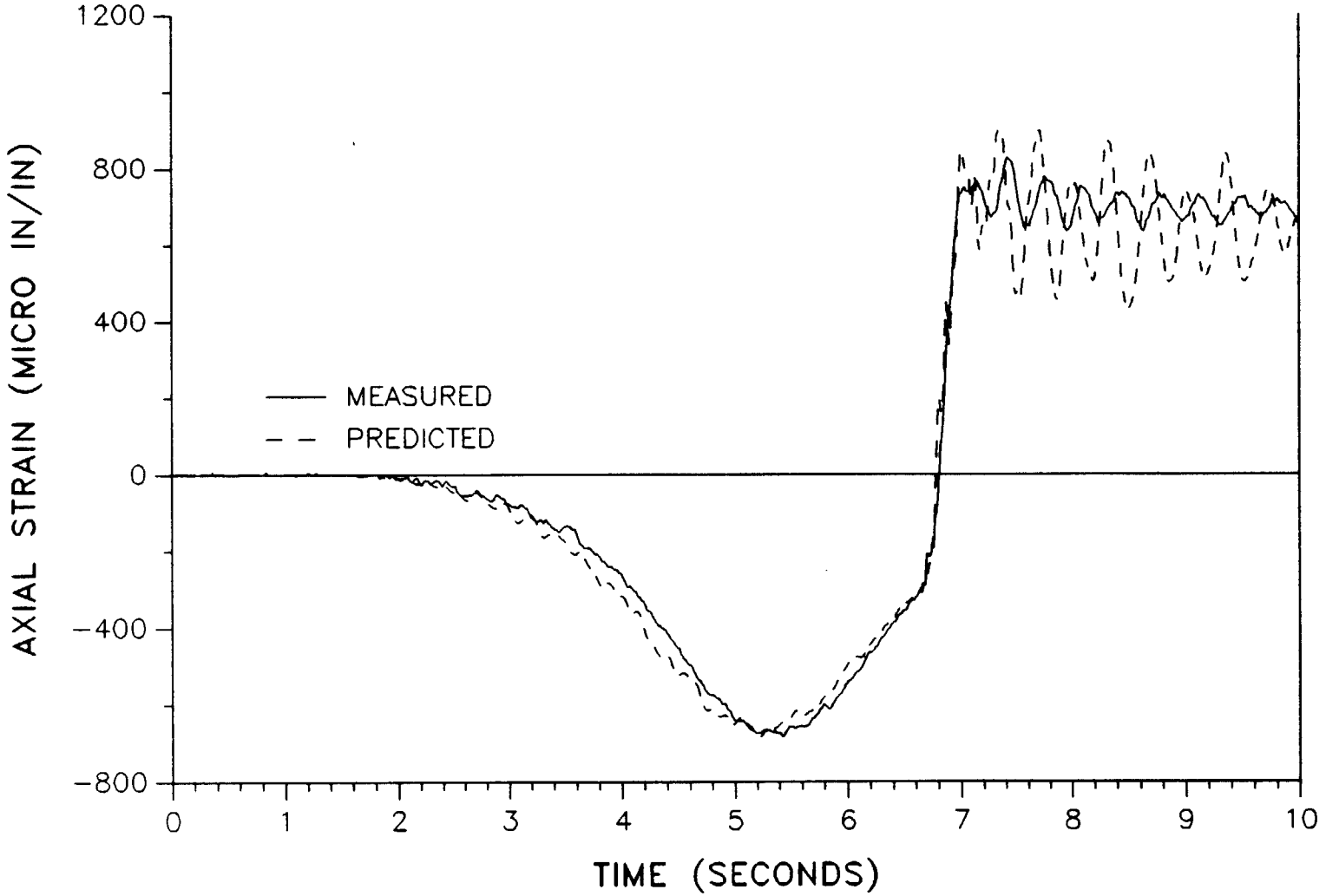

PREDICTED VS MEASURED AXIAL STRAIN

360L001 STRAIN GAGE B08G7340A – STATION 1196.5 AT 270 DEGREES

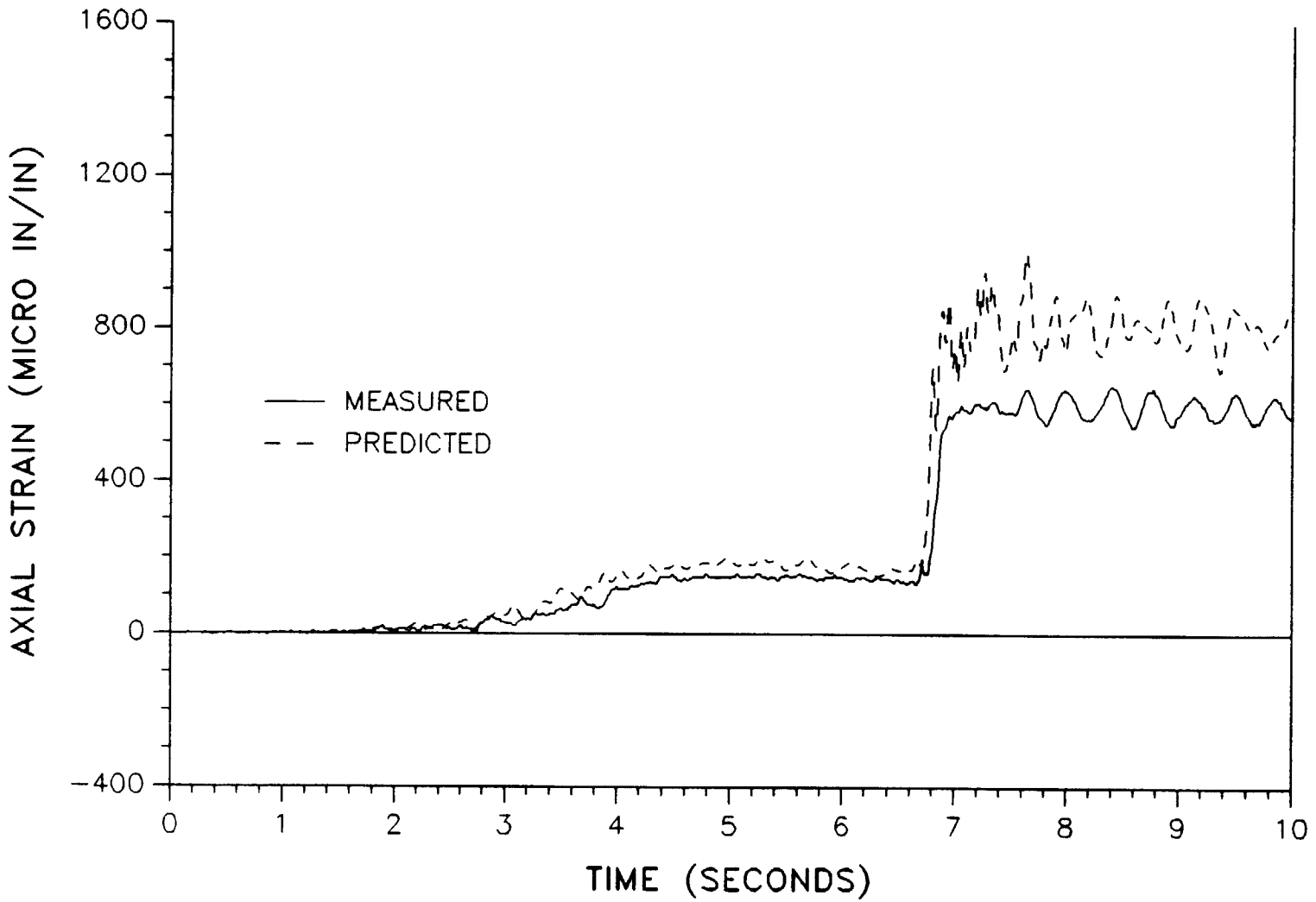

PREDICTED VS MEASURED AXIAL STRAIN

360L001 STRAIN GAGE B08G7342A – STATION 1466.0 AT 0 DEGREES

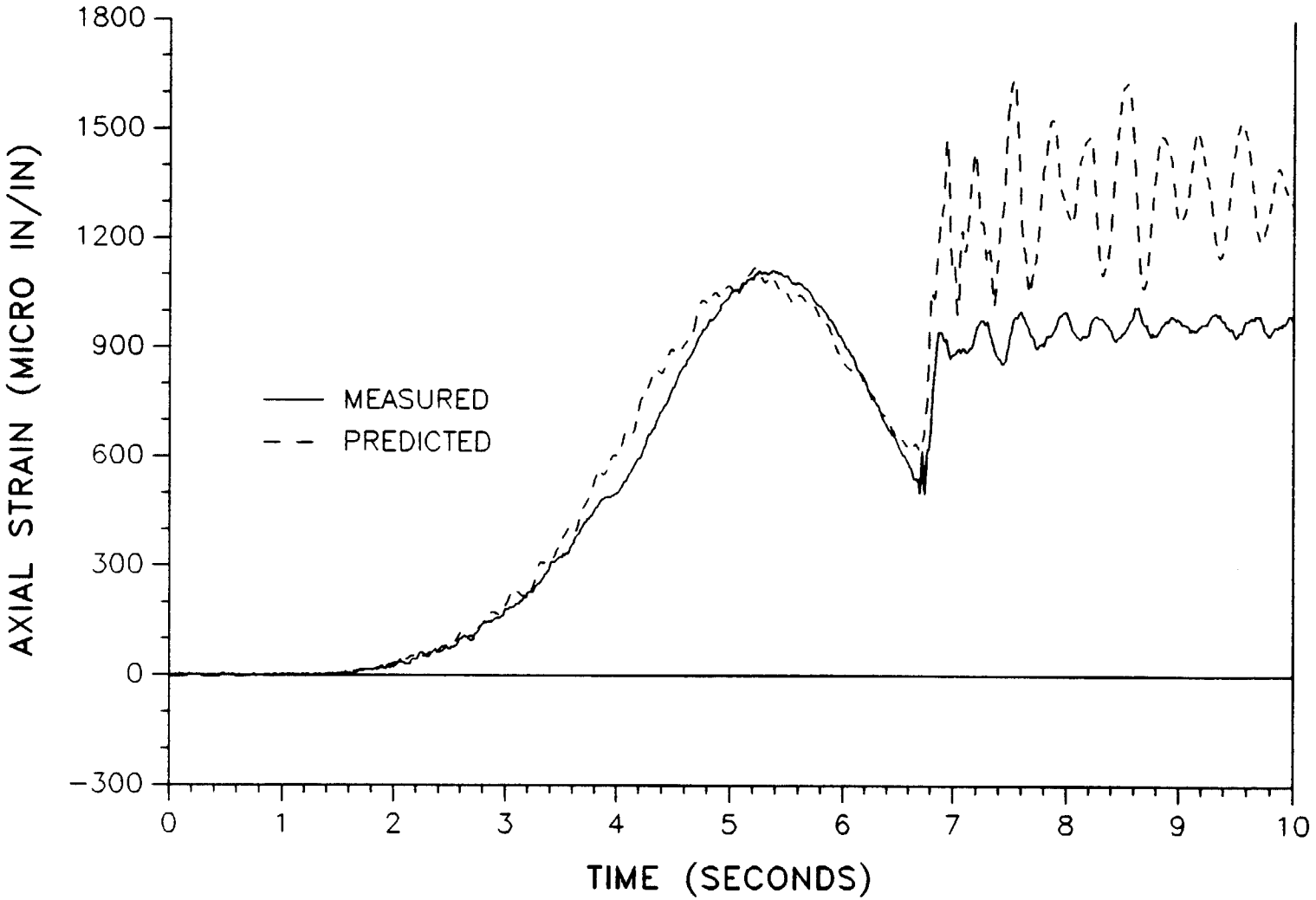

PREDICTED VS MEASURED AXIAL STRAIN

360L001 STRAIN GAGE B08G7344A – STATION 1466.0 AT 98 DEGREES

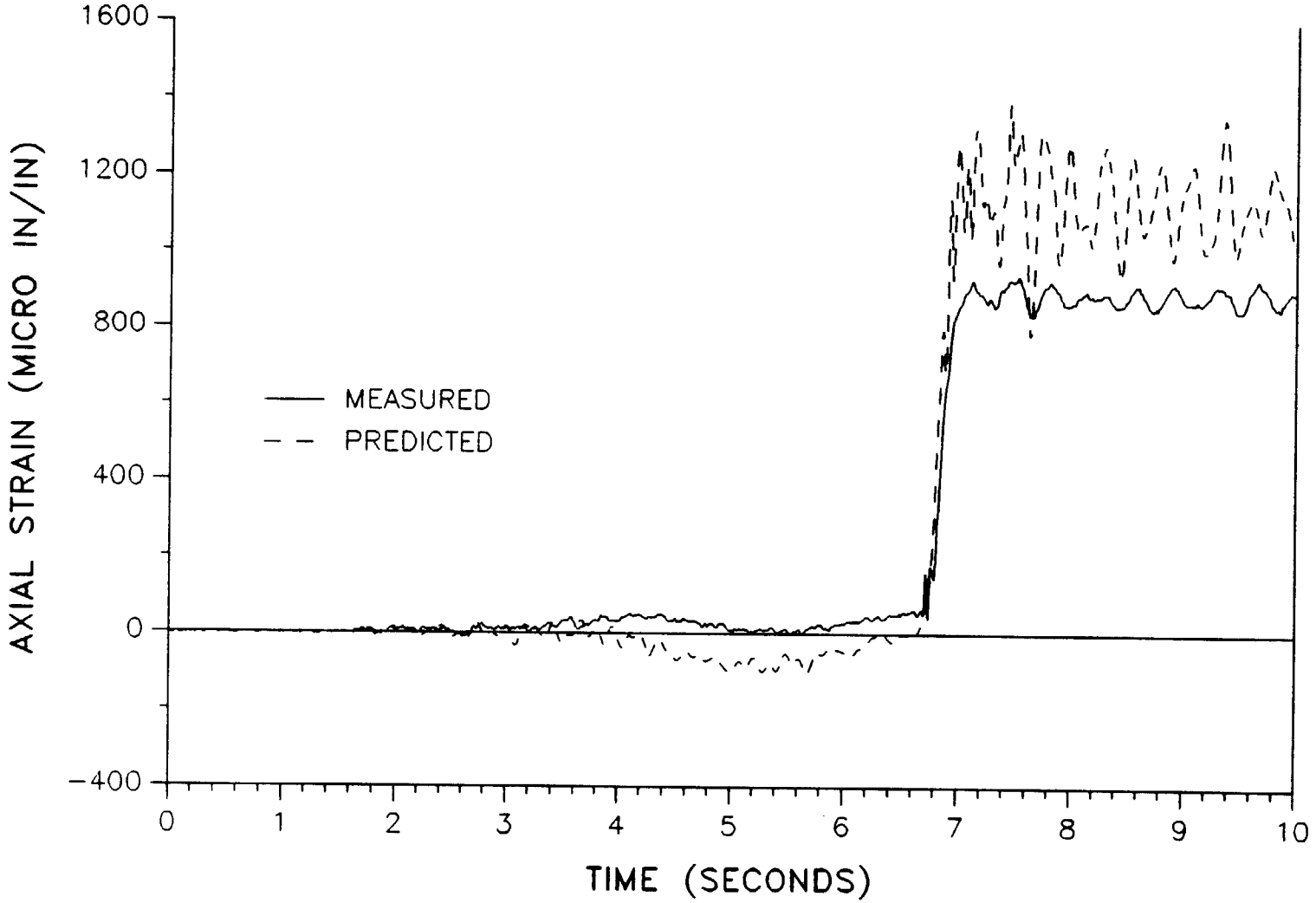

PREDICTED VS MEASURED AXIAL STRAIN

360L001 STRAIN GAGE B08G7346A – STATION 1466.0 AT 180 DEGREES

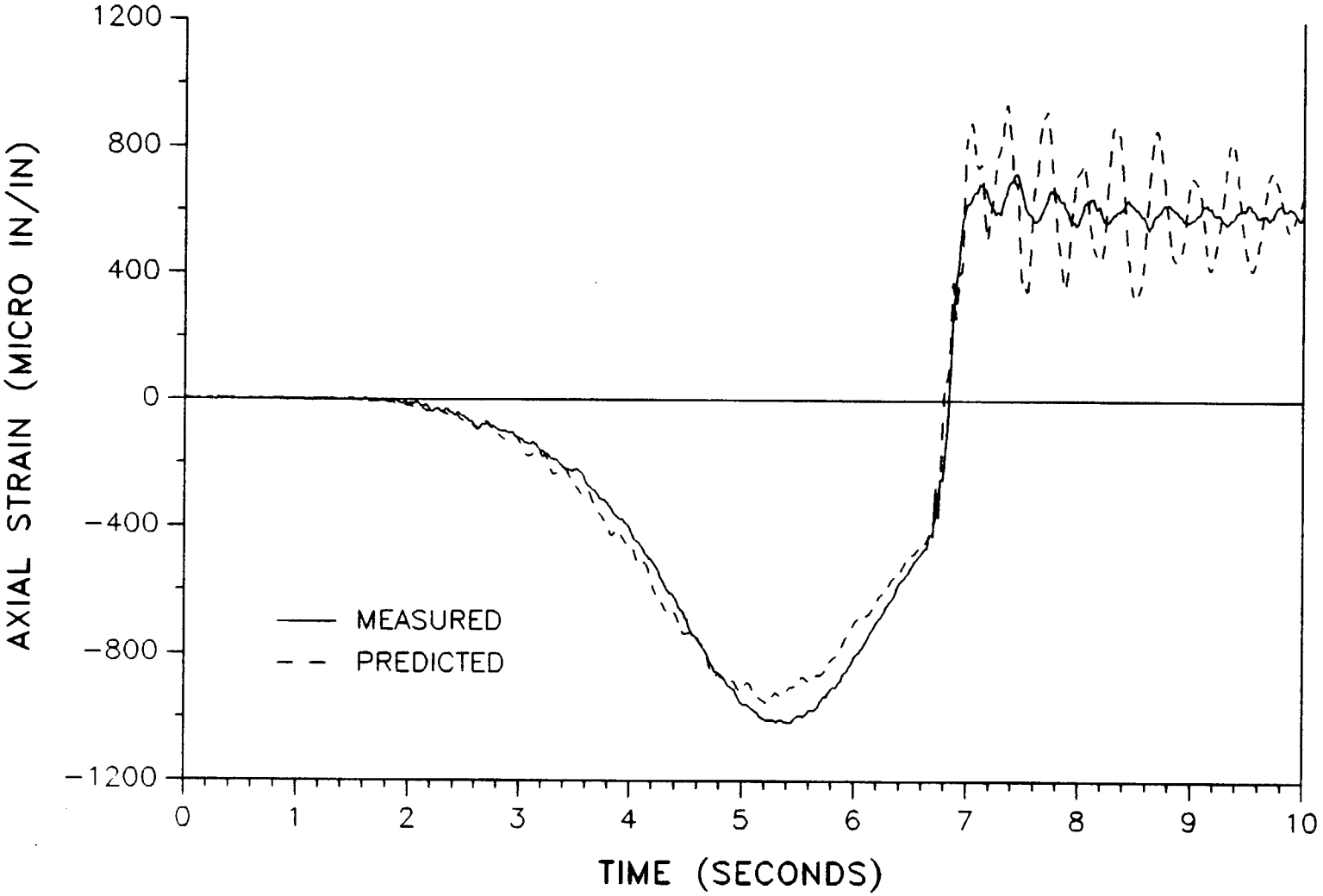

PREDICTED VS MEASURED AXIAL STRAIN

360L001 STRAIN GAGE B08G7348A – STATION 1466.0 AT 270 DEGREES

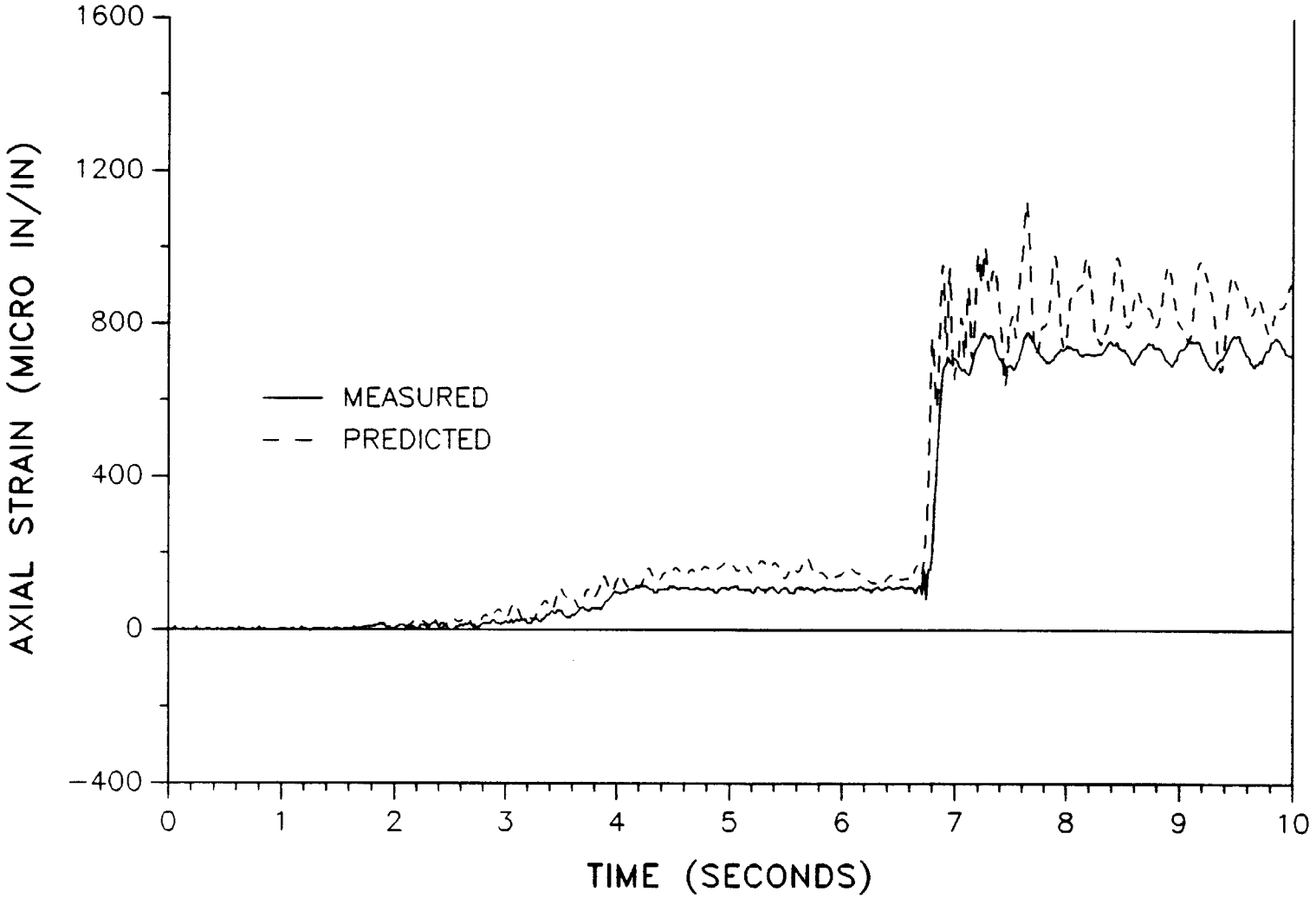

PREDICTED VS MEASURED AXIAL STRAIN

360L001 STRAIN GAGE B08G7354A – STATION 1493.0 AT 0 DEGREES

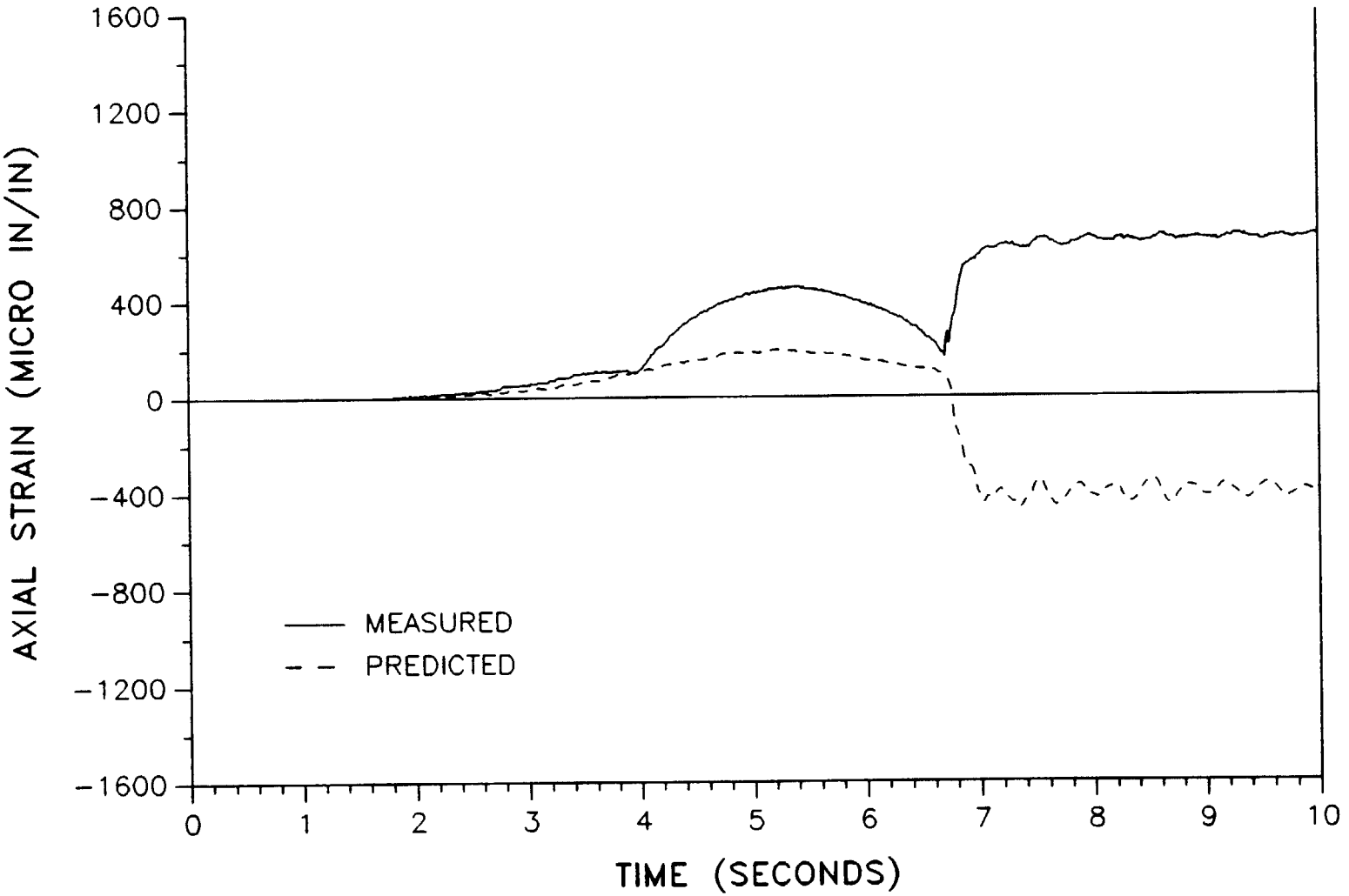

PREDICTED VS MEASURED AXIAL STRAIN

360L001 STRAIN GAGE B08G7352A – STATION 1493.0 AT 98 DEGREES

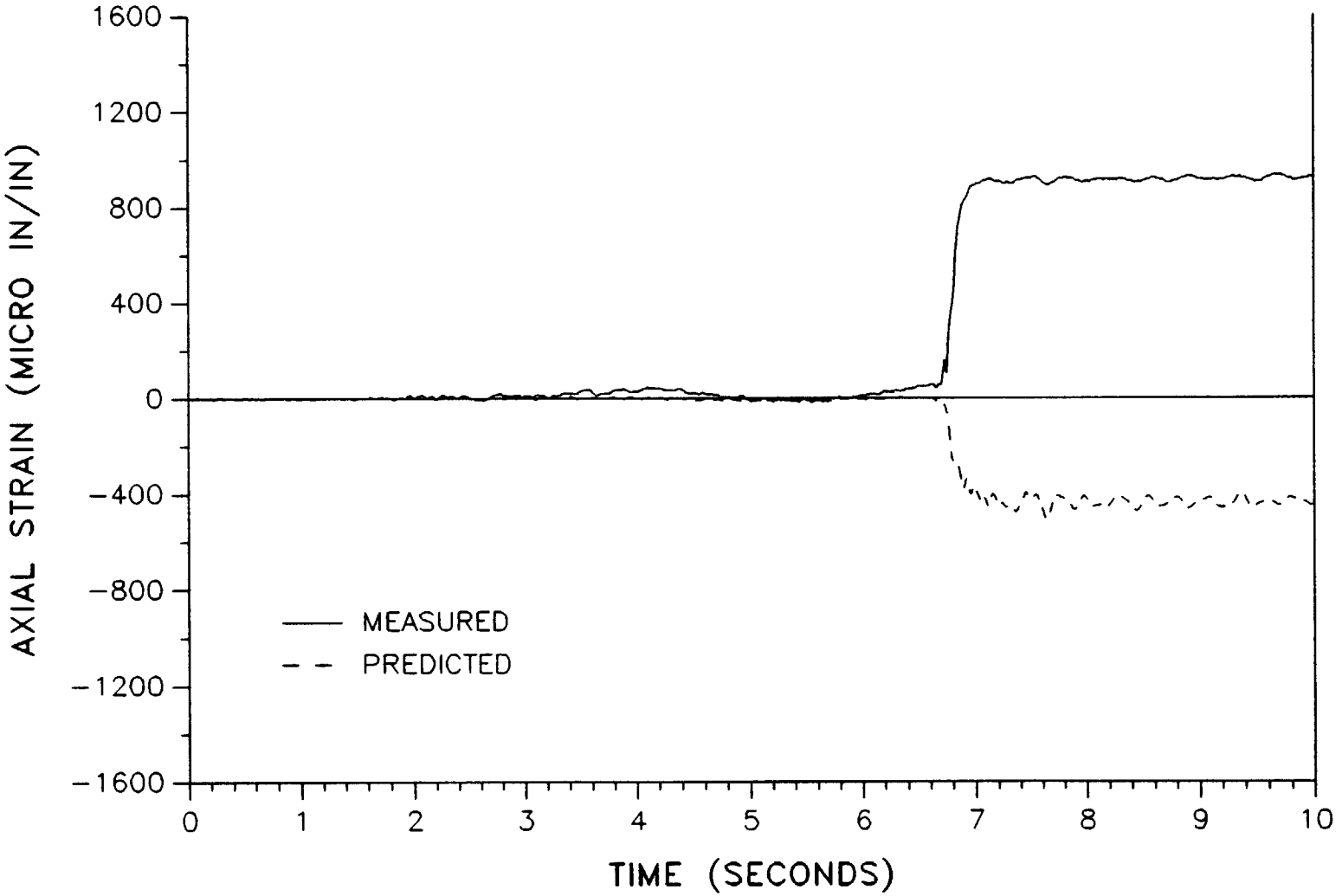

PREDICTED VS MEASURED AXIAL STRAIN

360L001 STRAIN GAGE B08G7350A – STATION 1493.0 AT 180 DEGREES

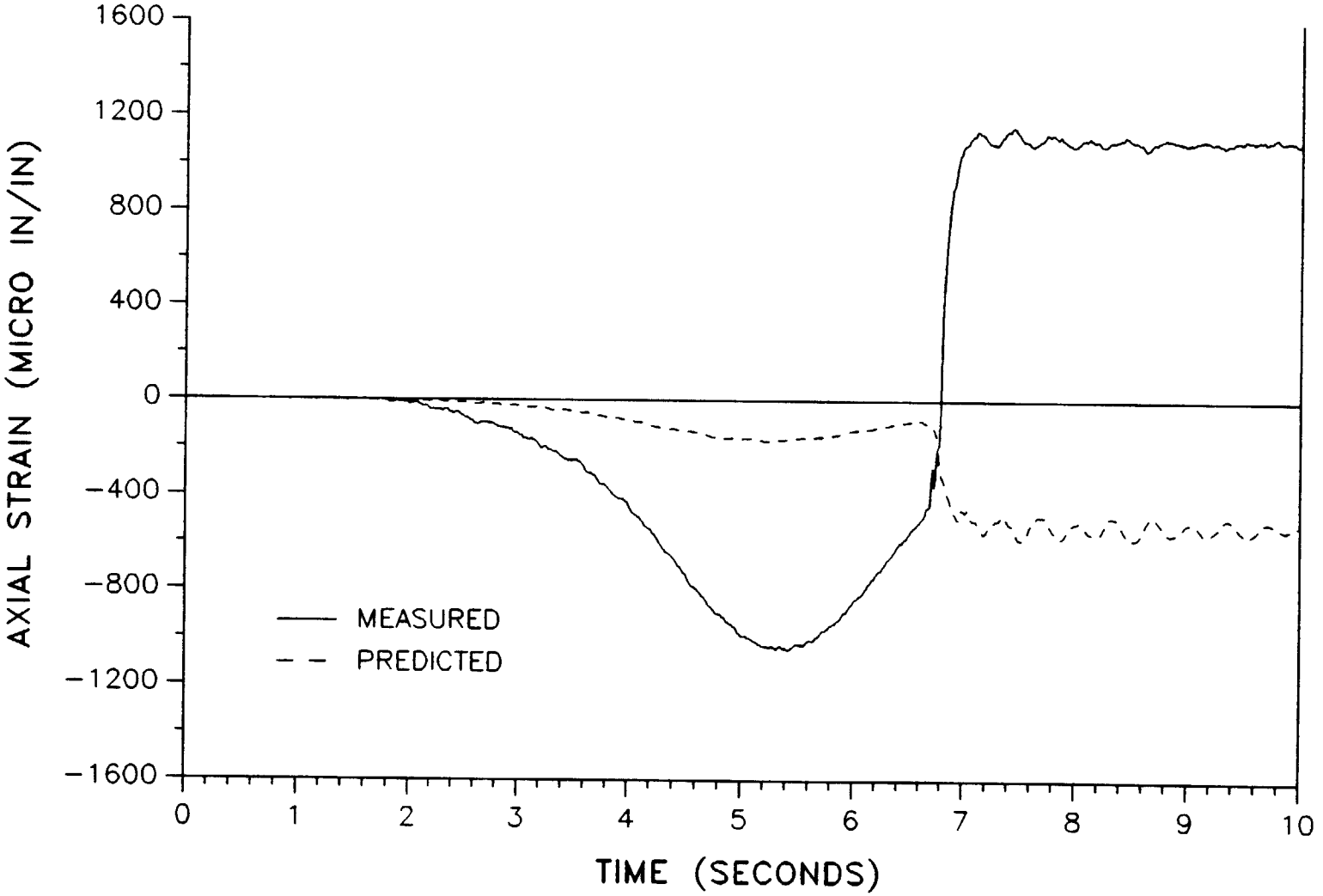

PREDICTED VS MEASURED AXIAL STRAIN

360L001 STRAIN GAGE B08G7366A – STATION 1493.0 AT 220 DEGREES

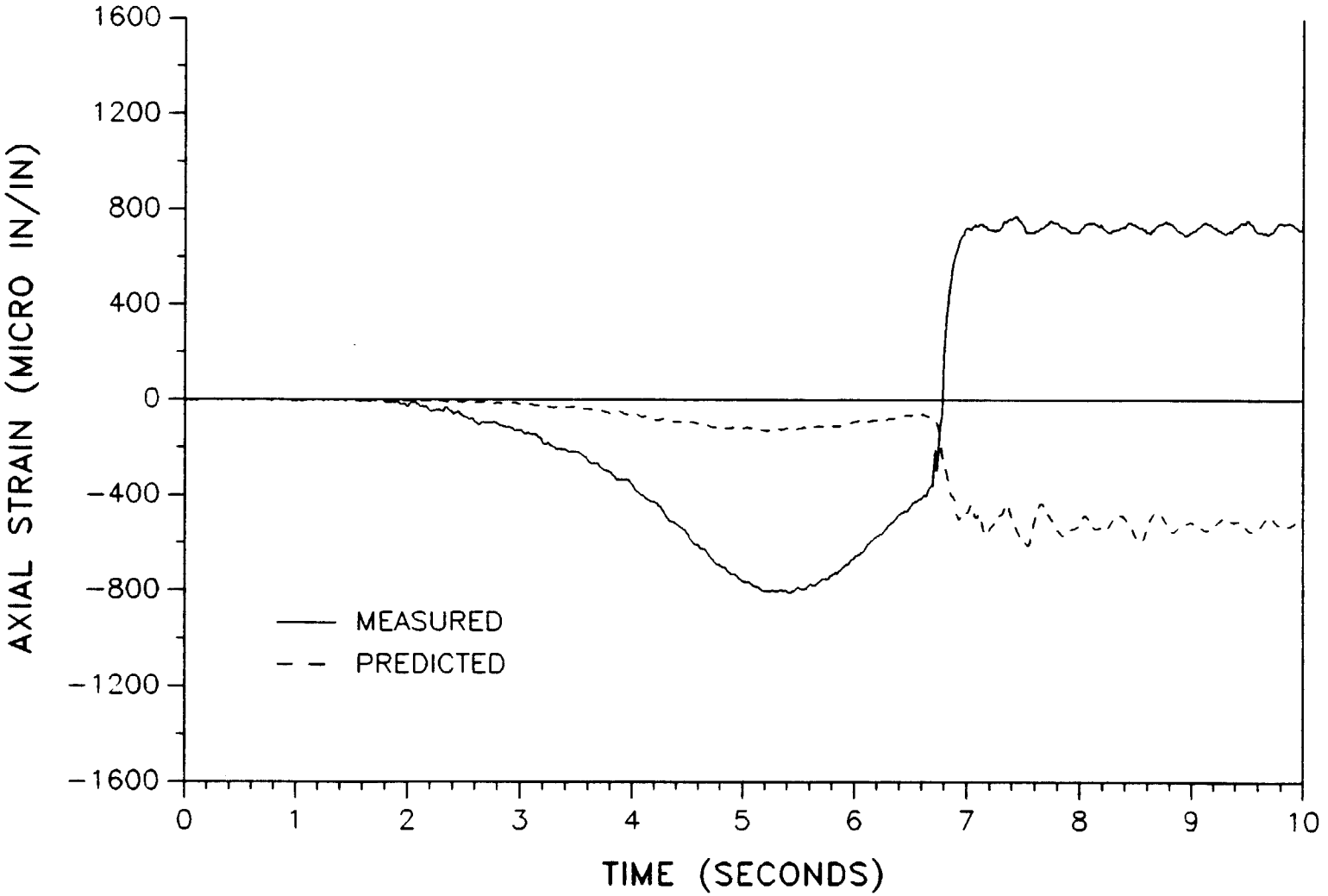

PREDICTED VS MEASURED AXIAL STRAIN

360L001 STRAIN GAGE B08G7364A – STATION 1493.0 AT 255 DEGREES

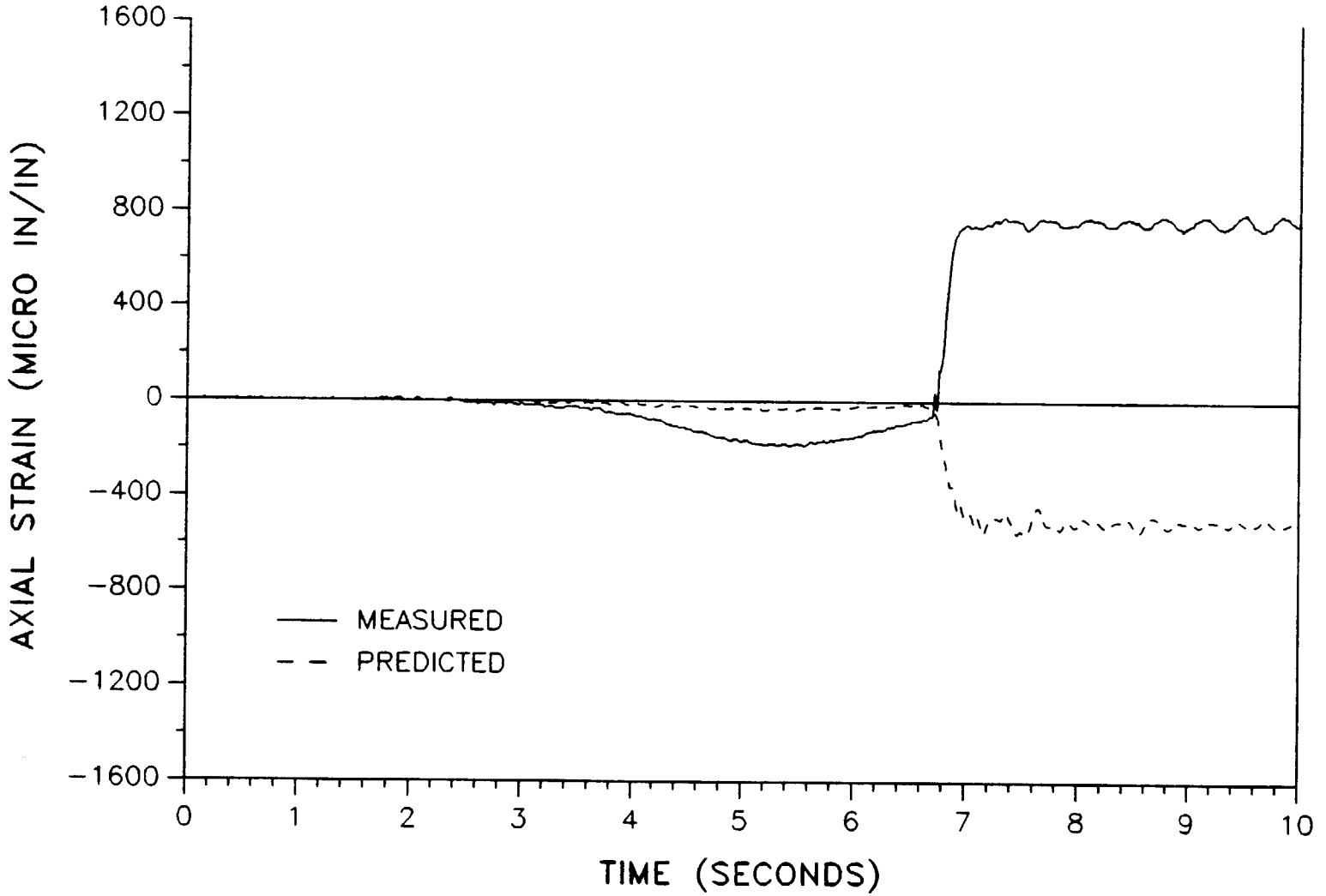

PREDICTED VS MEASURED AXIAL STRAIN

360L001 STRAIN GAGE B08G7360A – STATION 1493.0 AT 270 DEGREES

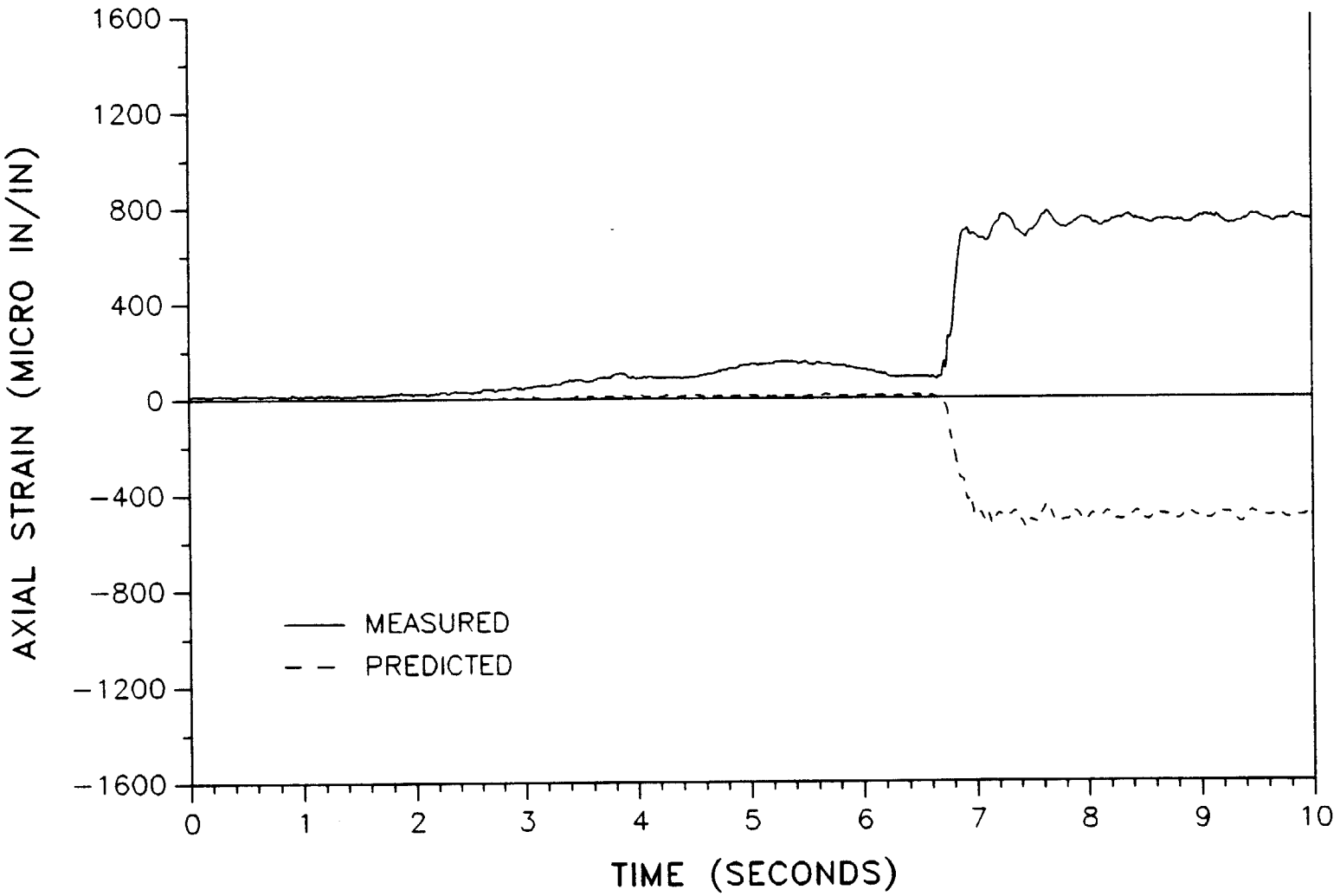

PREDICTED VS MEASURED AXIAL STRAIN

360L001 STRAIN GAGE B08G7362A – STATION 1493.0 AT 285 DEGREES

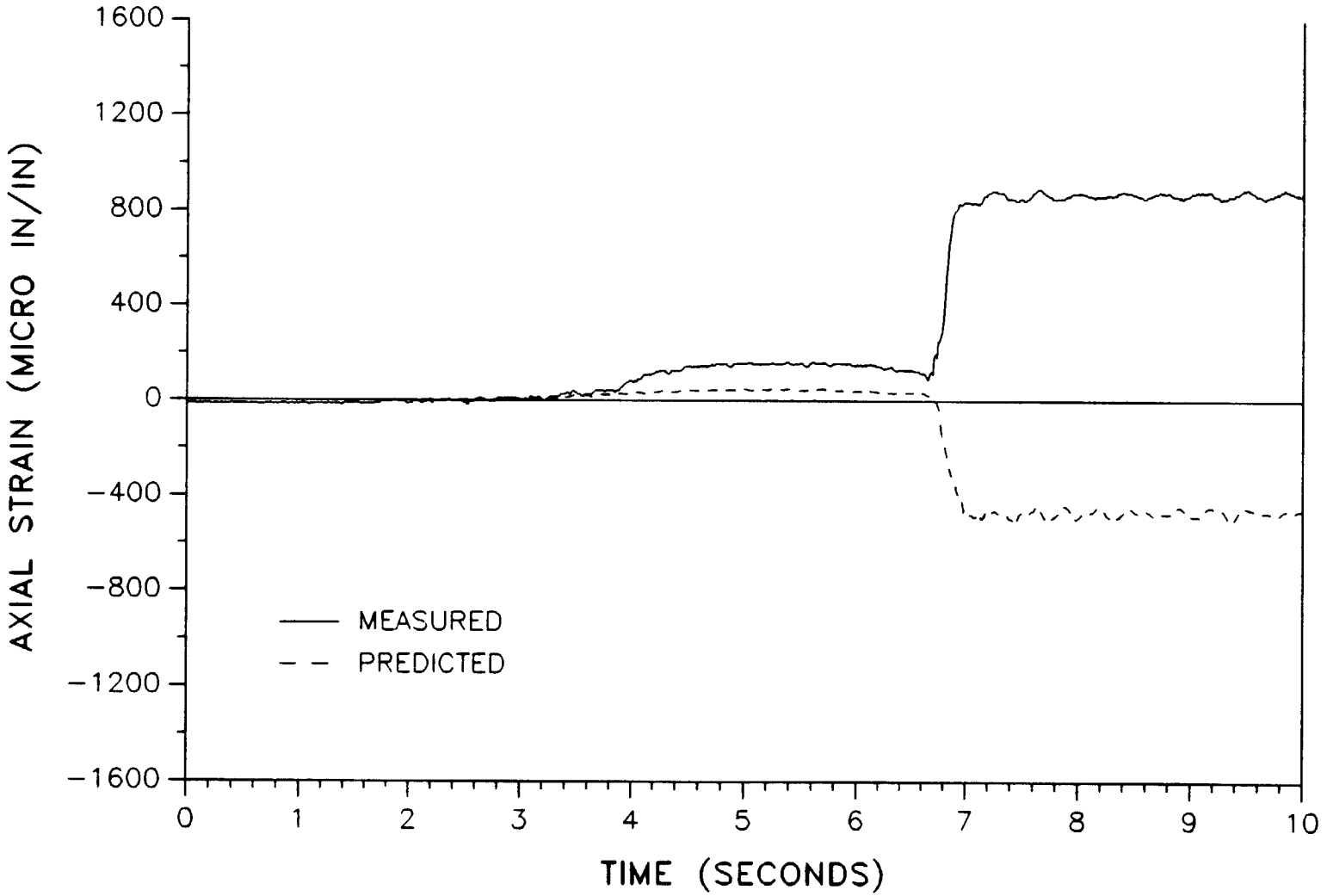

PREDICTED VS MEASURED AXIAL STRAIN

360L001 STRAIN GAGE B08G7358A – STATION 1493.0 AT 300 DEGREES

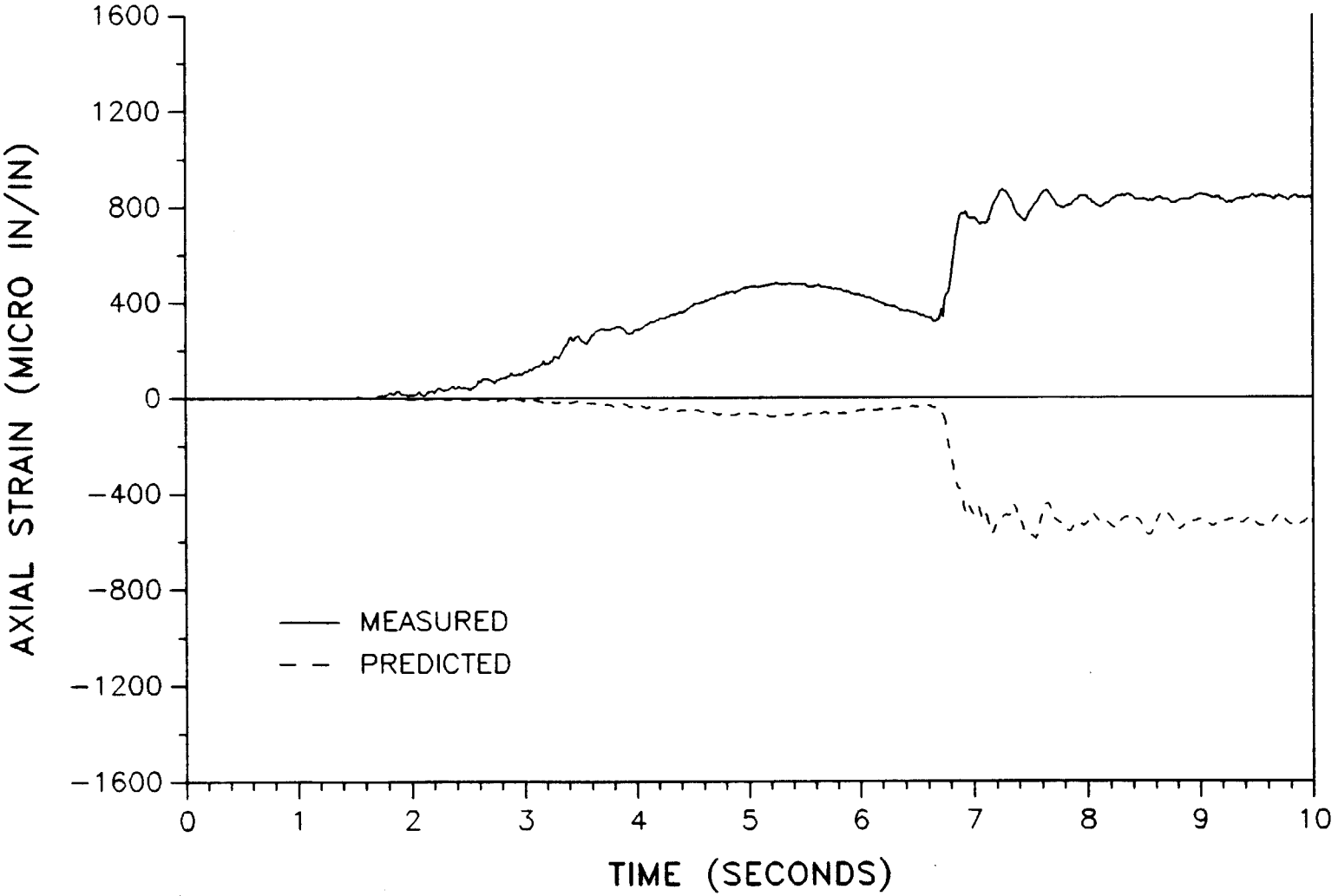

PREDICTED VS MEASURED AXIAL STRAIN

360L001 STRAIN GAGE B08G7356A – STATION 1493.0 AT 320 DEGREES

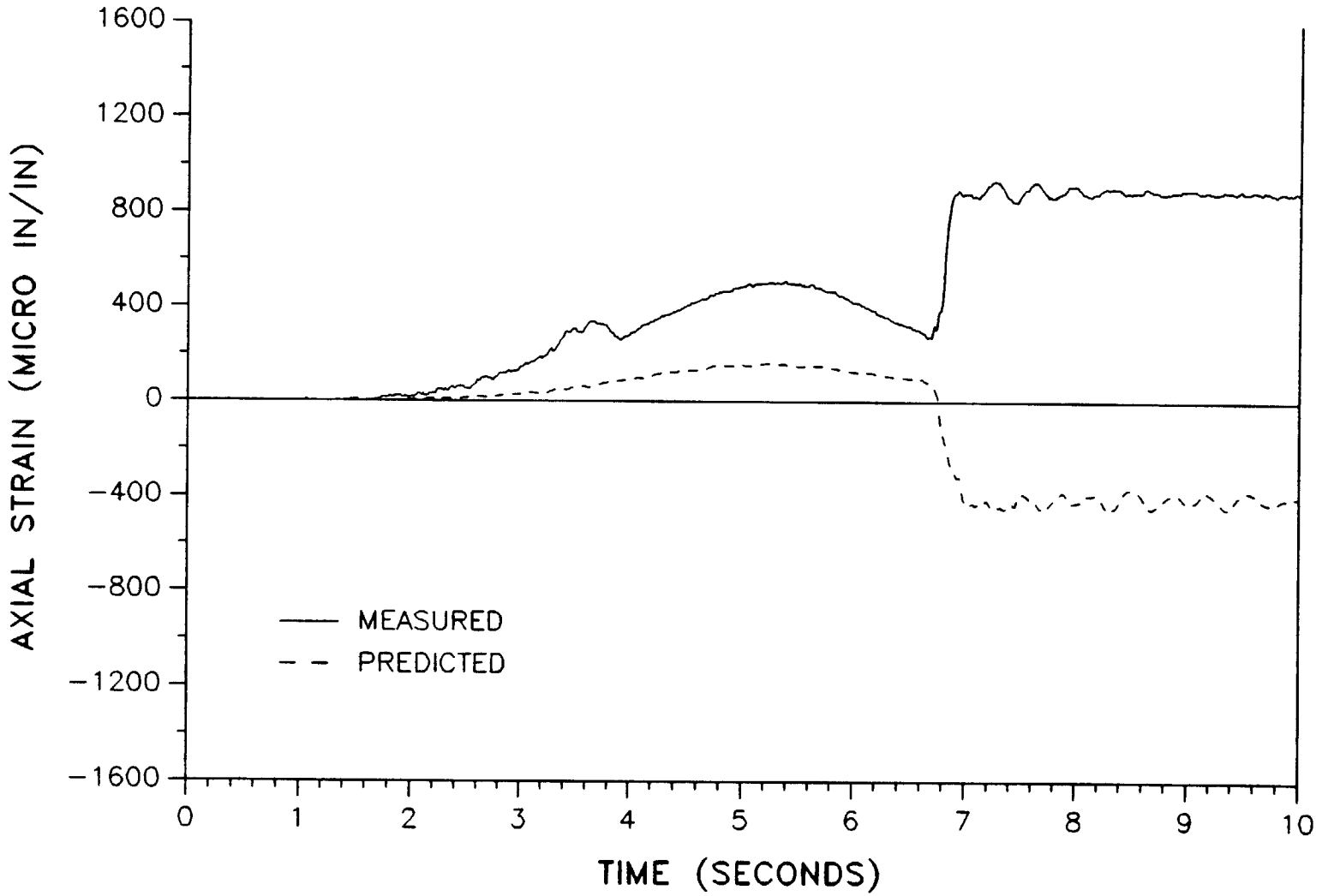

PREDICTED VS MEASURED AXIAL STRAIN

360L001 STRAIN GAGE B08G7390A – STATION 1501.0 AT 0 DEGREES

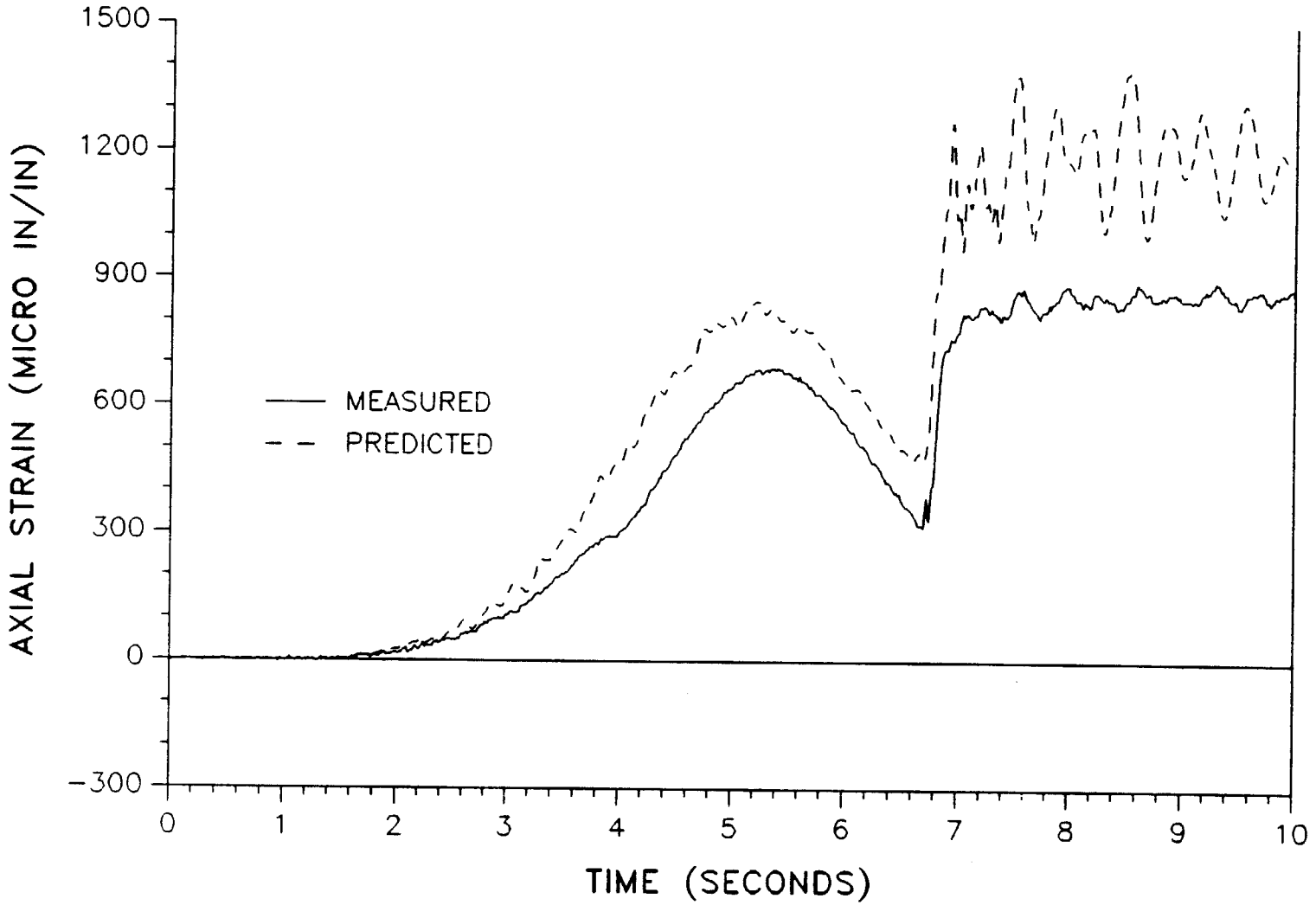

PREDICTED VS MEASURED AXIAL STRAIN

360L001 STRAIN GAGE B08G7388A – STATION 1501.0 AT 98 DEGREES

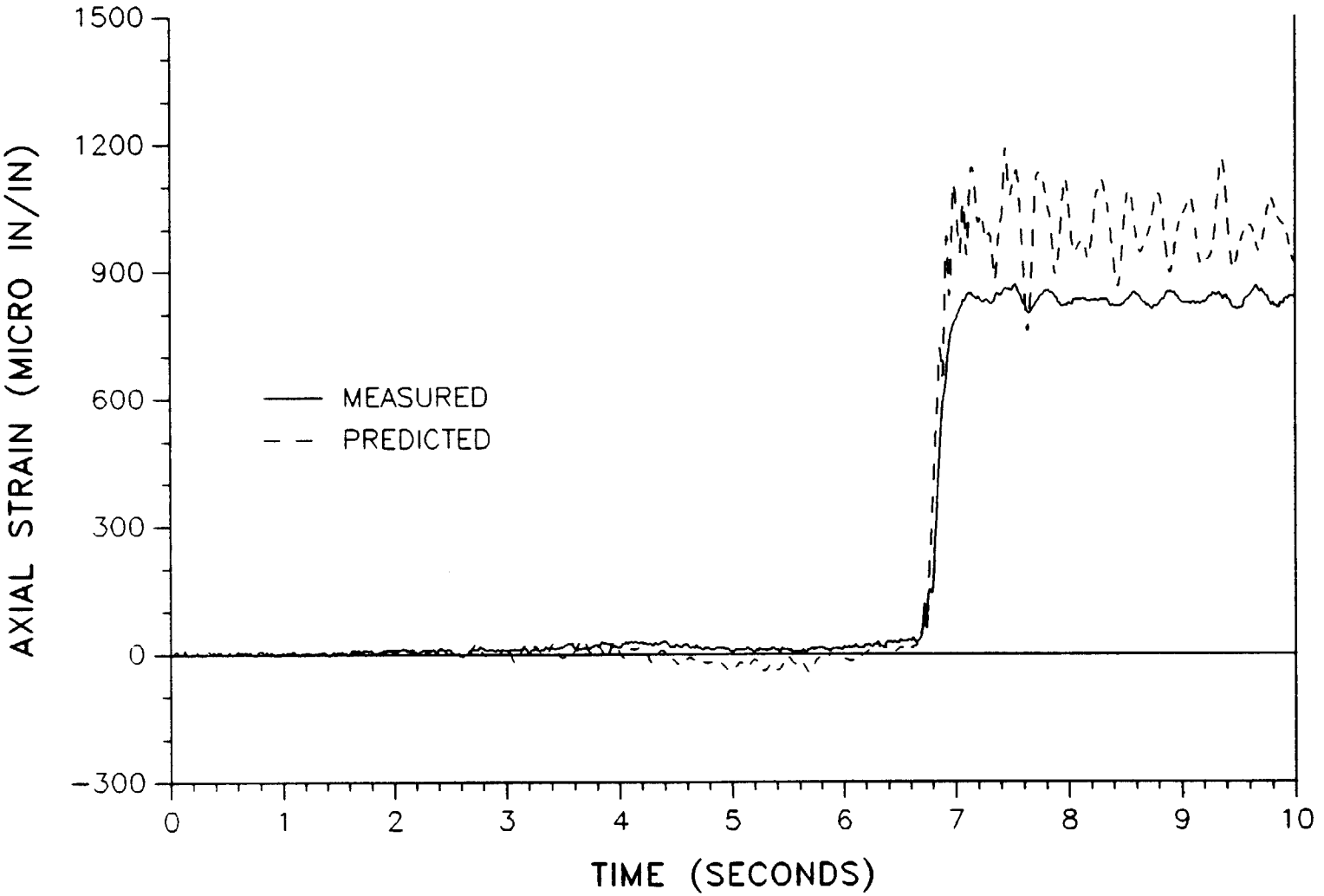

PREDICTED VS MEASURED AXIAL STRAIN

360L001 STRAIN GAGE B08G7386A – STATION 1501.0 AT 180 DEGREES

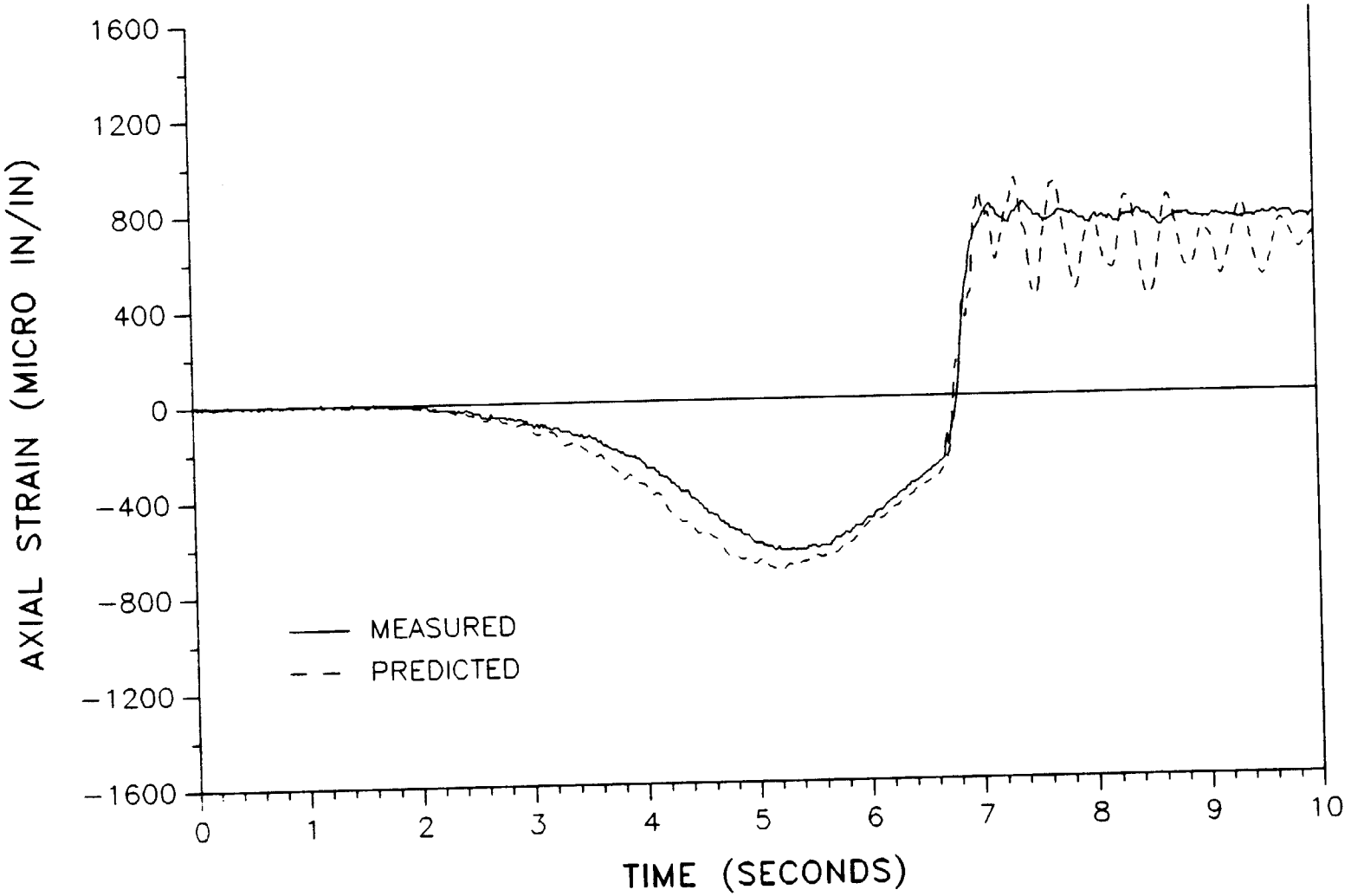

PREDICTED VS MEASURED AXIAL STRAIN

360L001 STRAIN GAGE B08G7402A – STATION 1501.0 AT 220 DEGREES

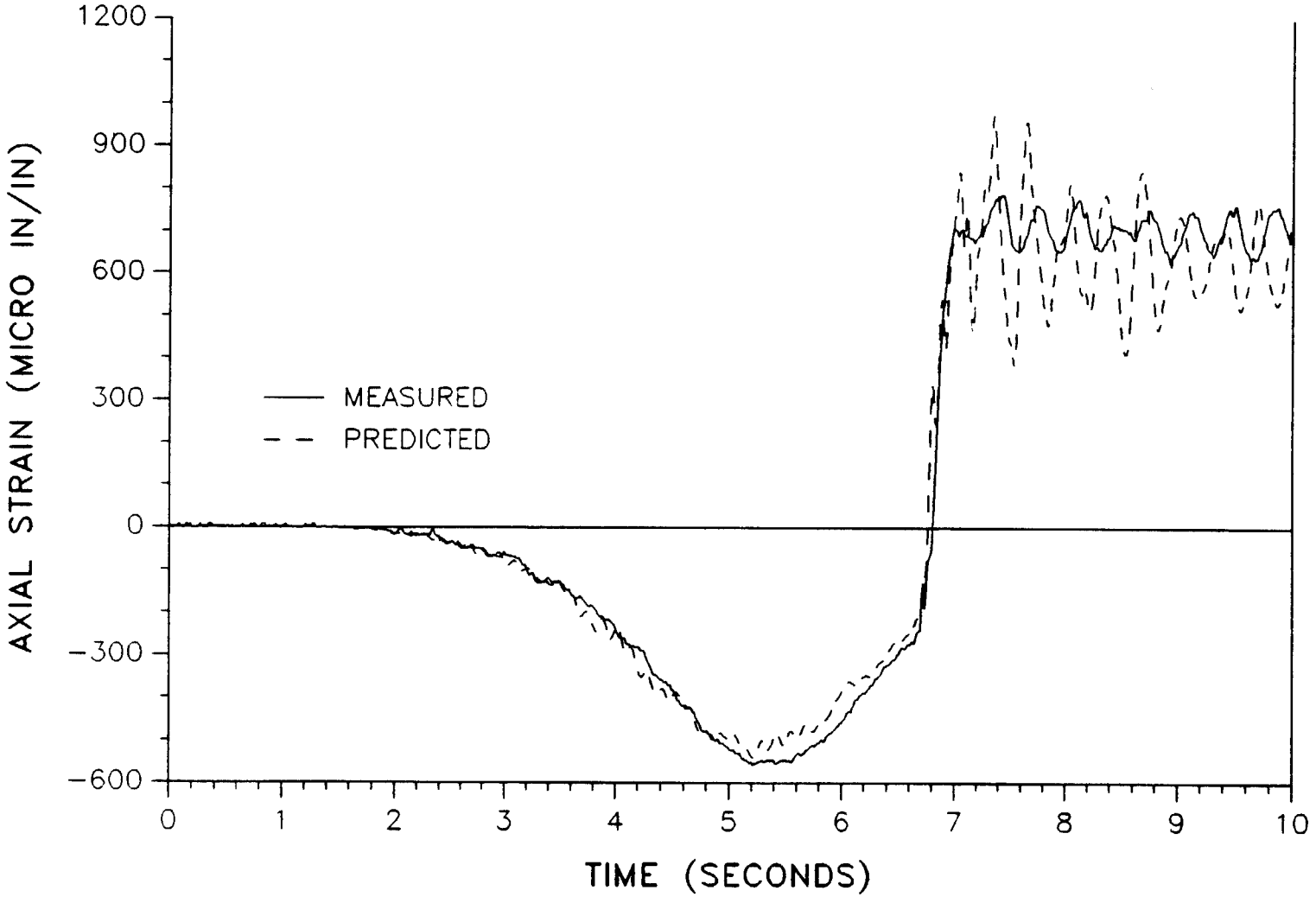

PREDICTED VS MEASURED AXIAL STRAIN

360L001 STRAIN GAGE B08G7400A – STATION 1501.0 AT 255 DEGREES

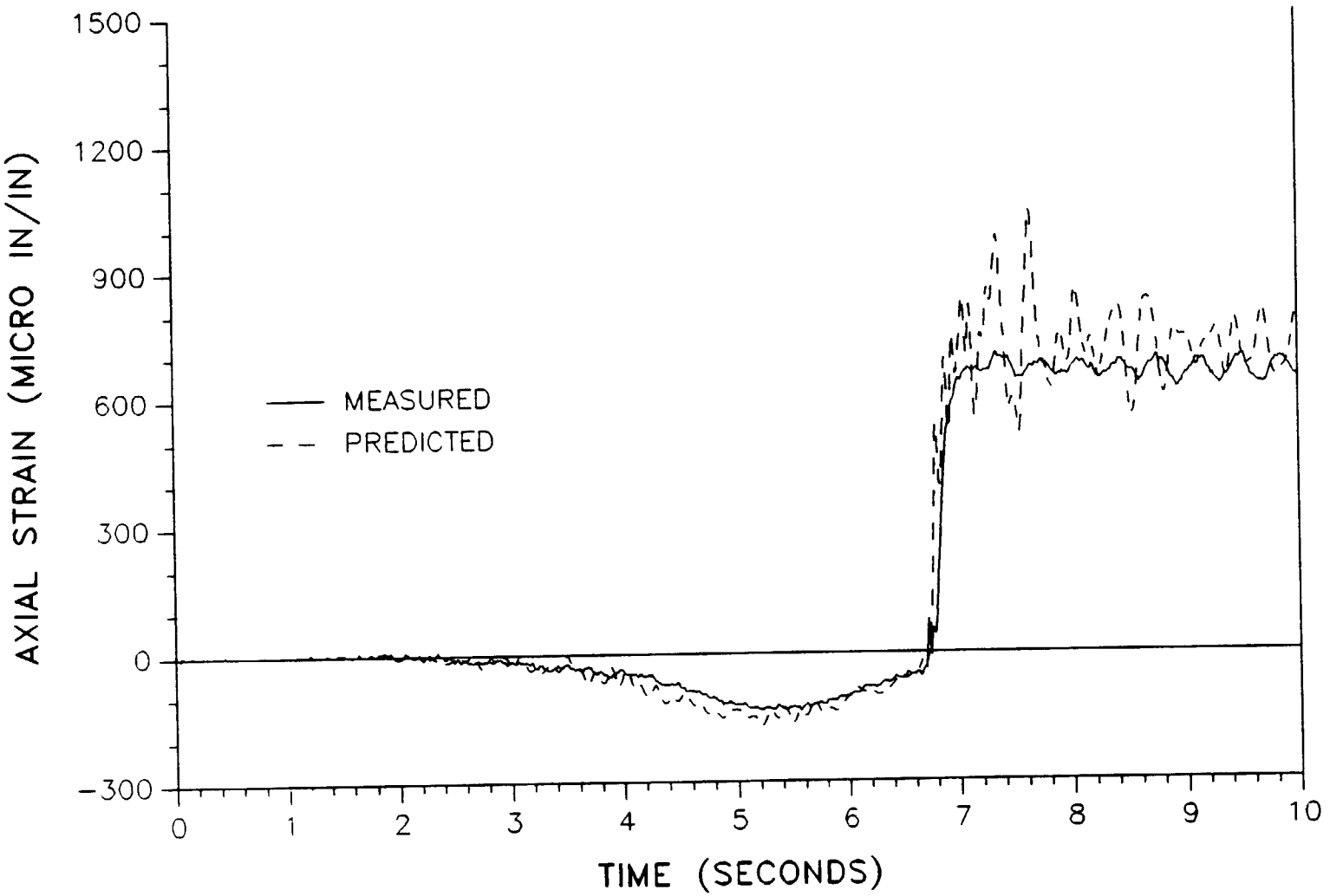

PREDICTED VS MEASURED AXIAL STRAIN

360L001 STRAIN GAGE B08G7398A – STATION 1501.0 AT 270 DEGREES

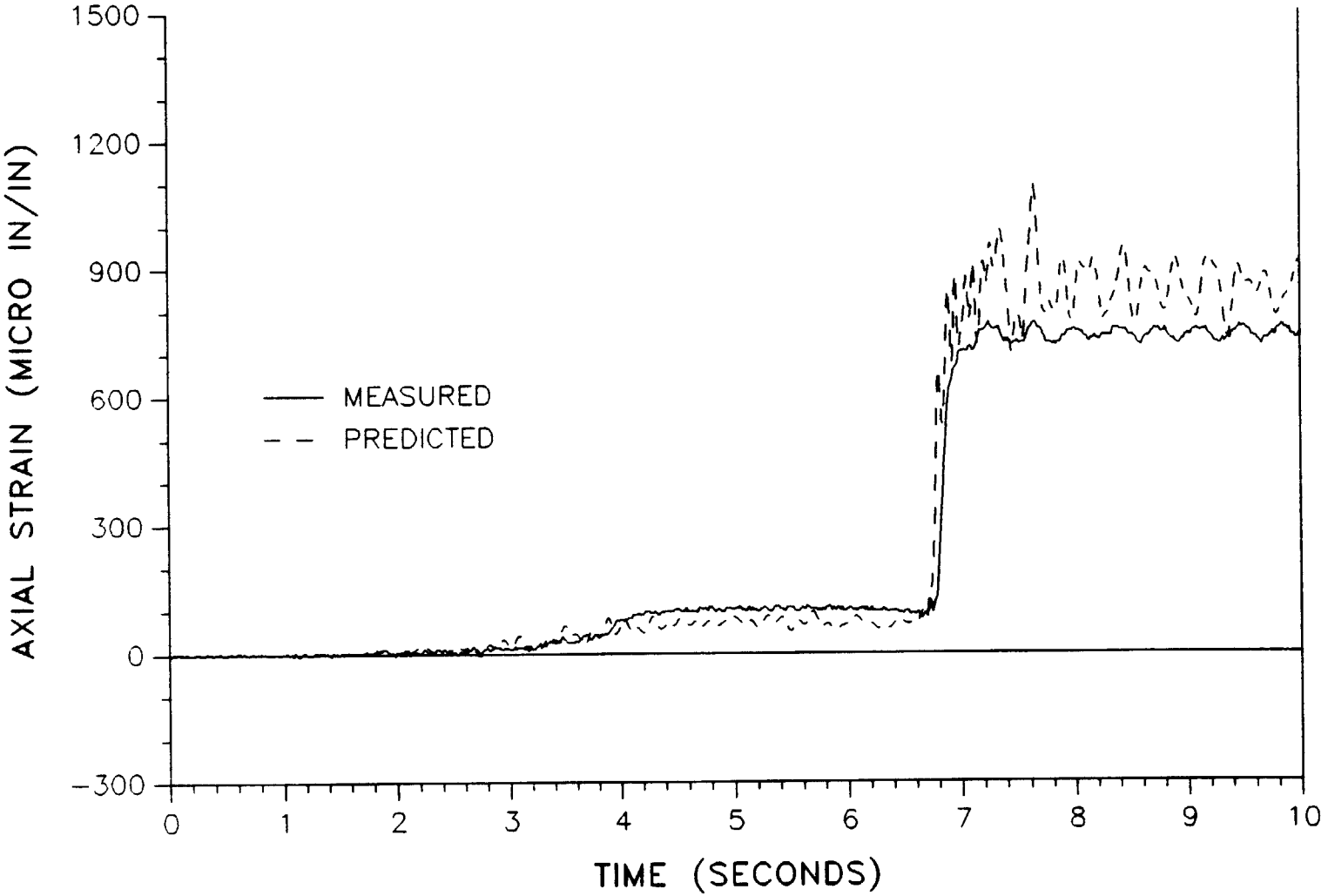

PREDICTED VS MEASURED AXIAL STRAIN

360L001 STRAIN GAGE B08G7396A – STATION 1501.0 AT 285 DEGREES

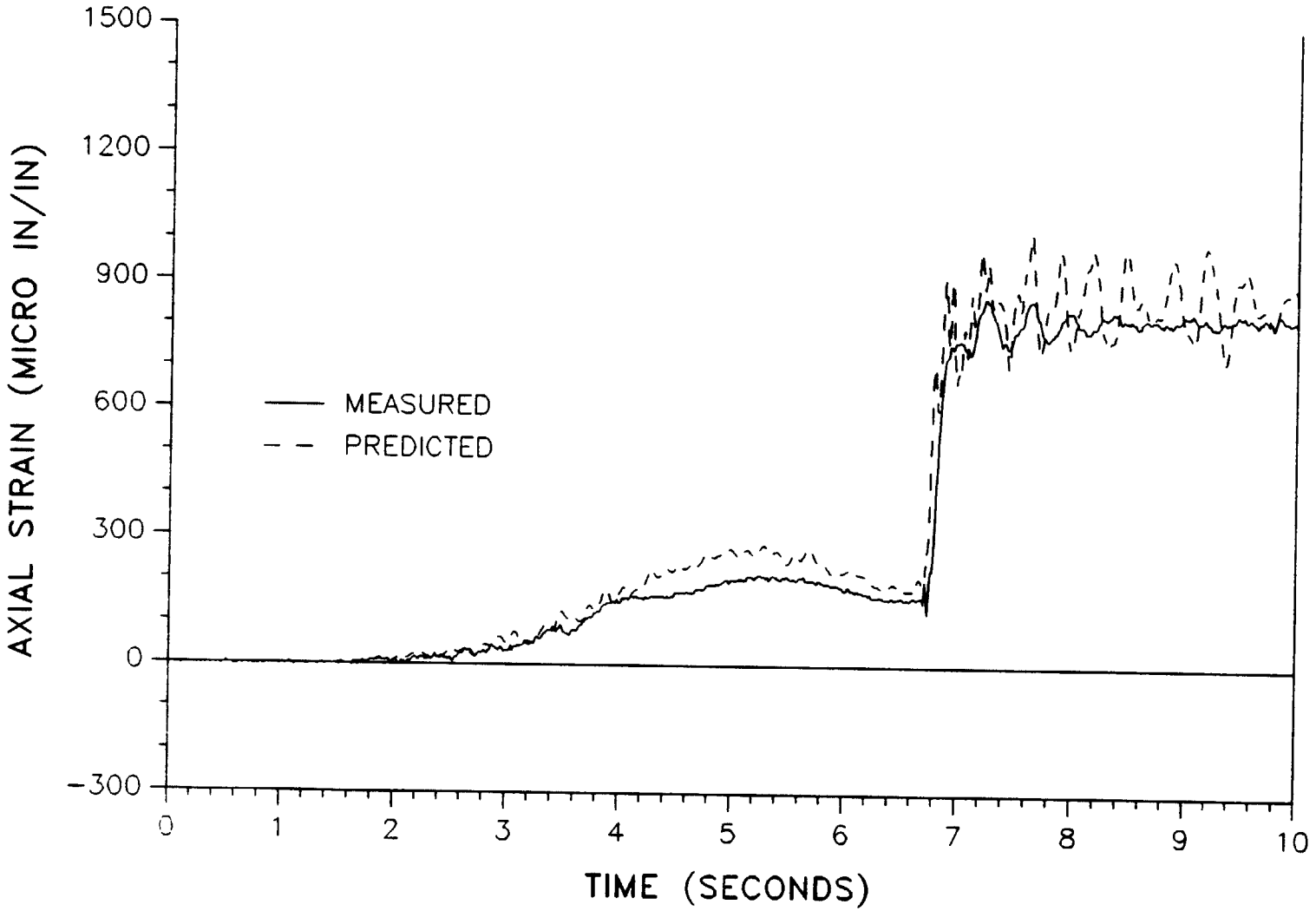

PREDICTED VS MEASURED AXIAL STRAIN

360L001 STRAIN GAGE B08G7394A – STATION 1501.0 AT 300 DEGREES

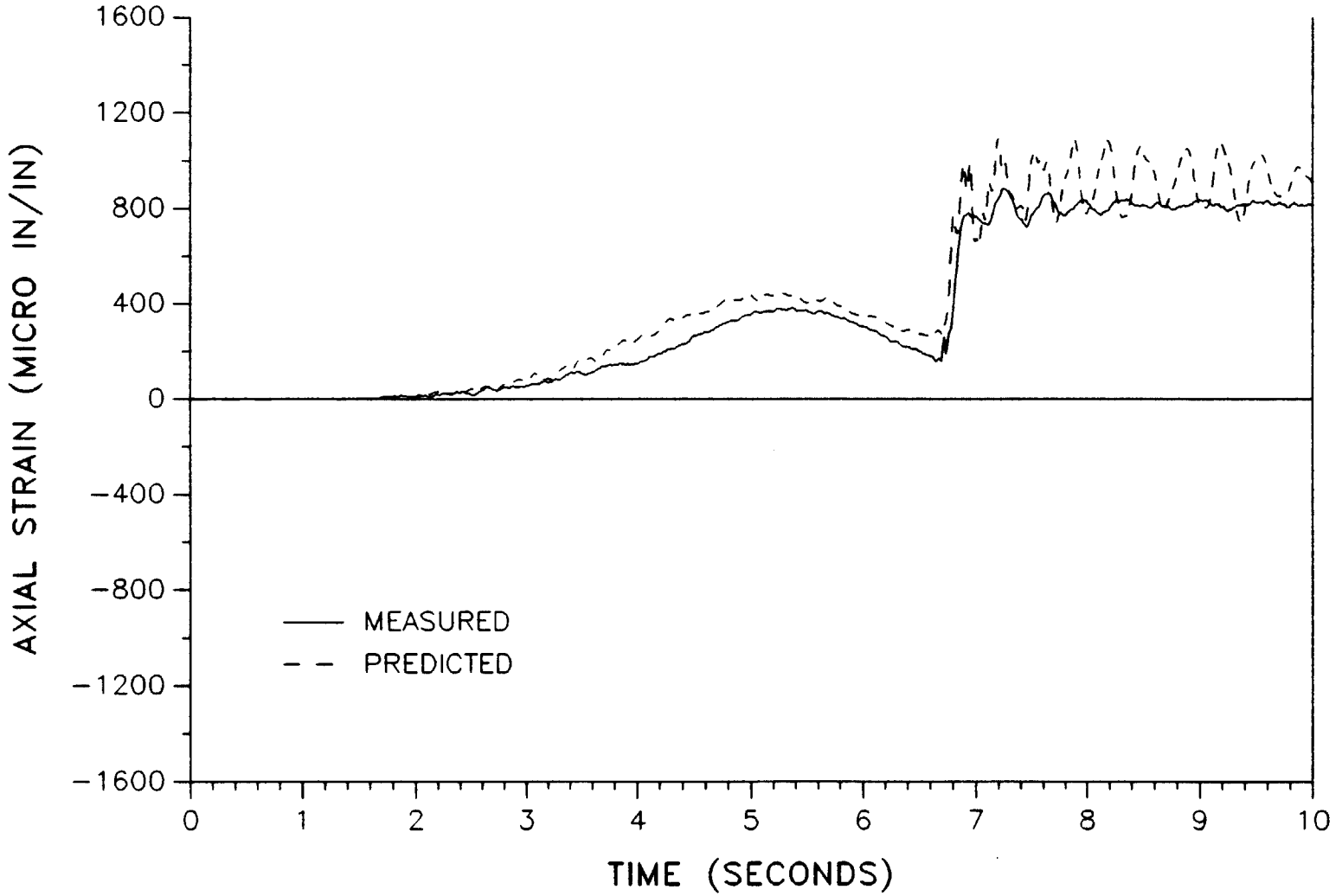

PREDICTED VS MEASURED AXIAL STRAIN

360L001 STRAIN GAGE B08G7392A – STATION 1501.0 AT 320 DEGREES

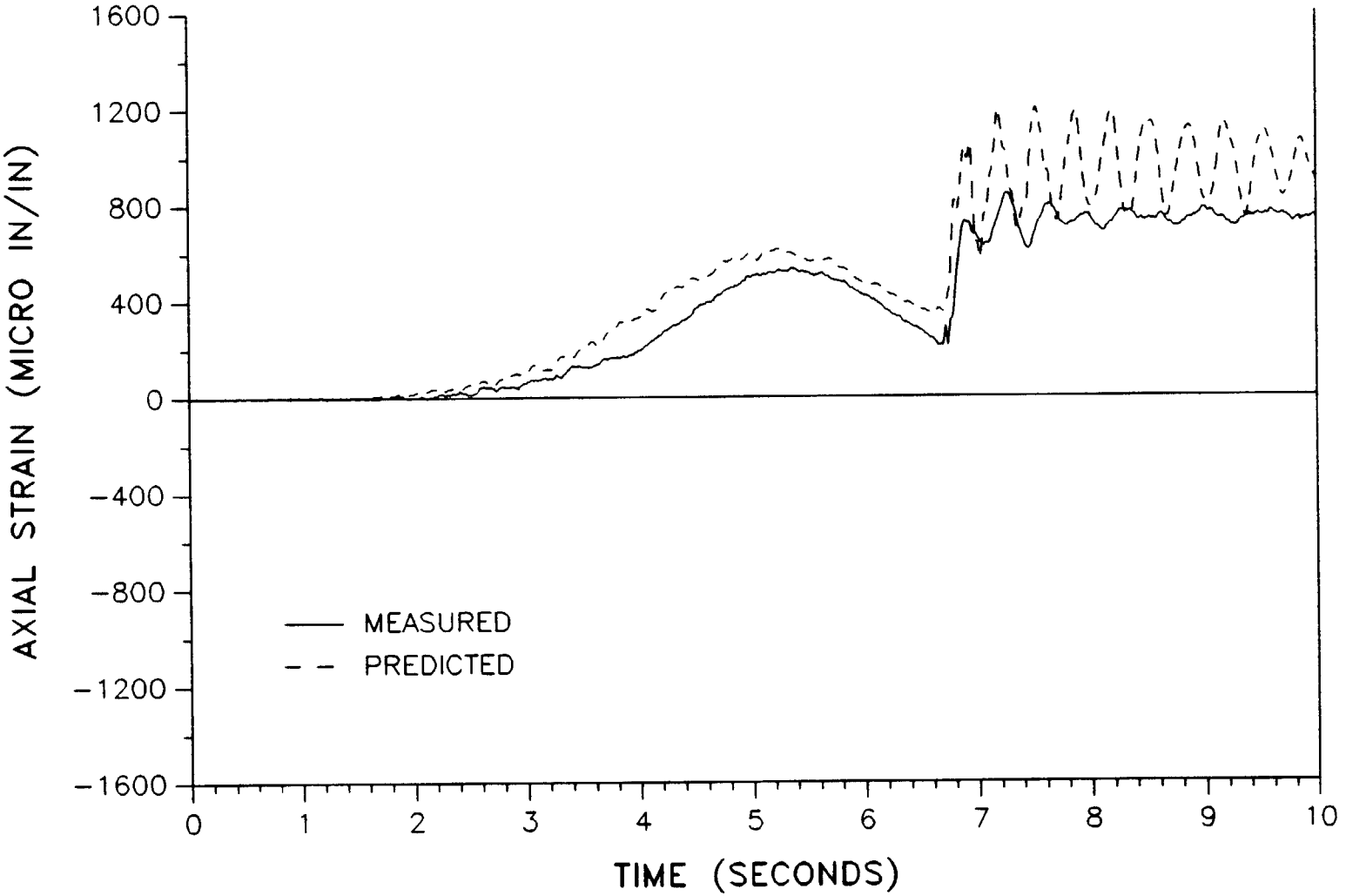

PREDICTED VS MEASURED AXIAL STRAIN

360L001 STRAIN GAGE B08G7404A – STATION 1797.0 AT 0 DEGREES

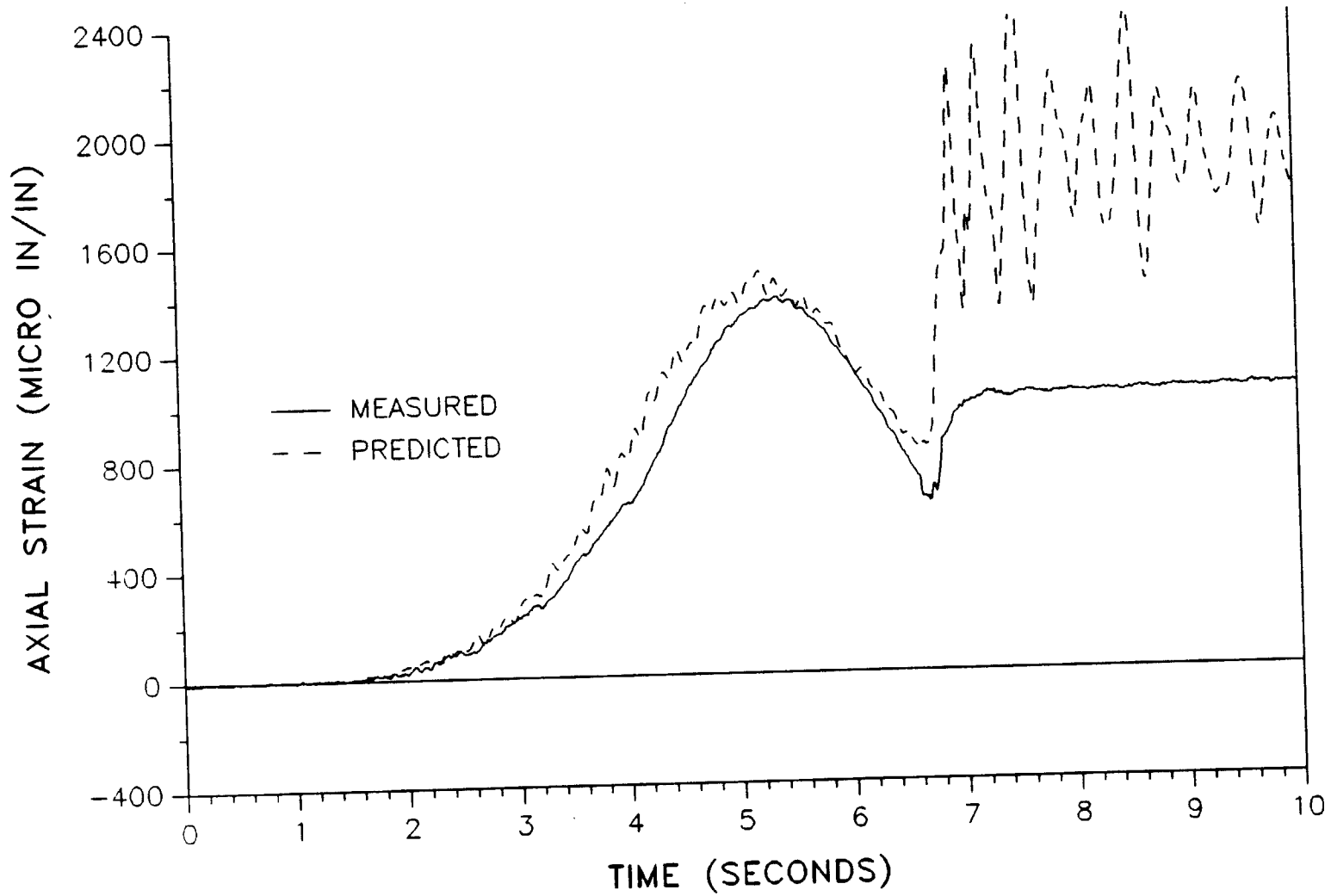

PREDICTED VS MEASURED AXIAL STRAIN

360L001 STRAIN GAGE B08G7406A – STATION 1797.0 AT 98 DEGREES

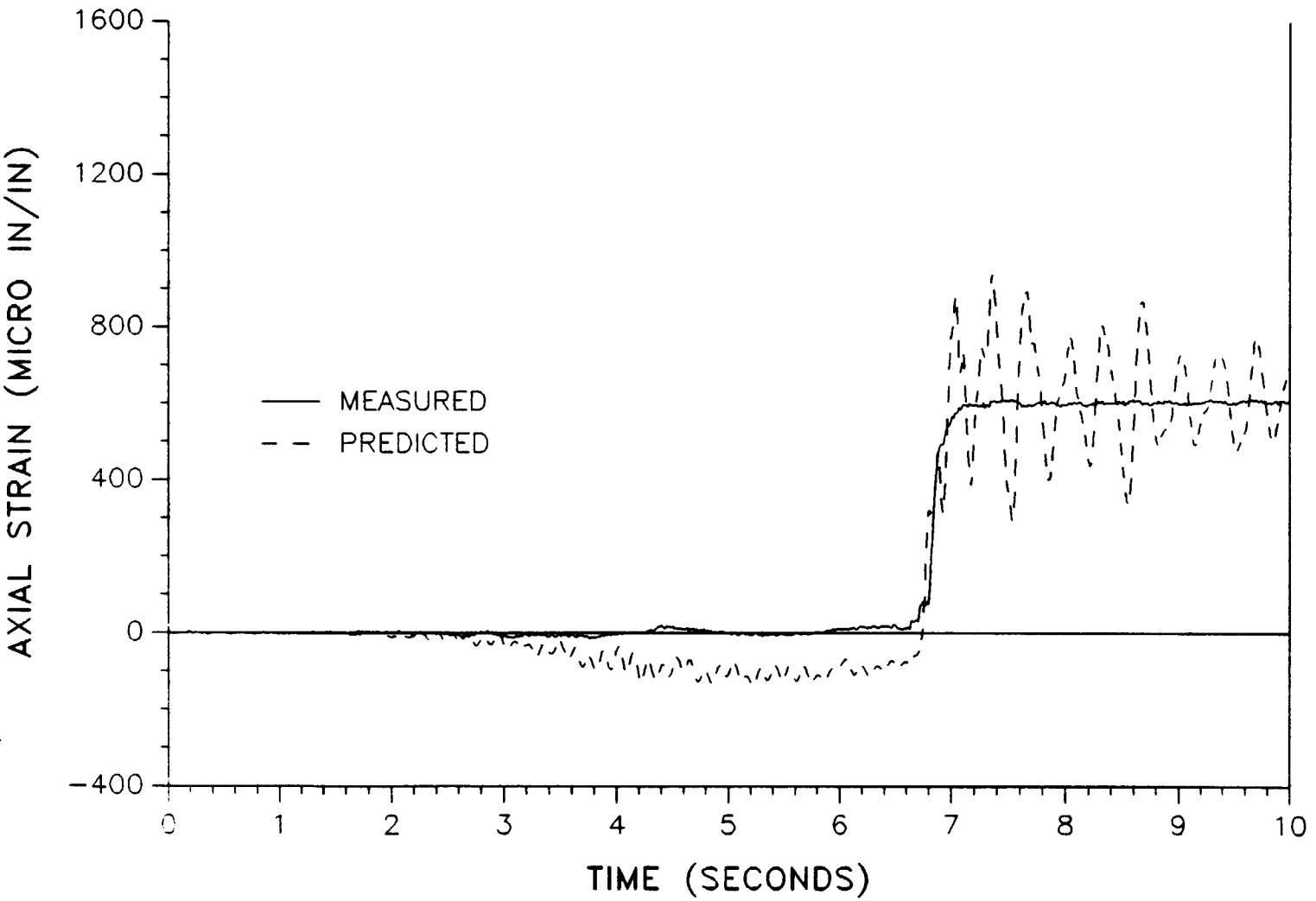

PREDICTED VS MEASURED AXIAL STRAIN

360L001 STRAIN GAGE B08G7408A – STATION 1797.0 AT 180 DEGREES

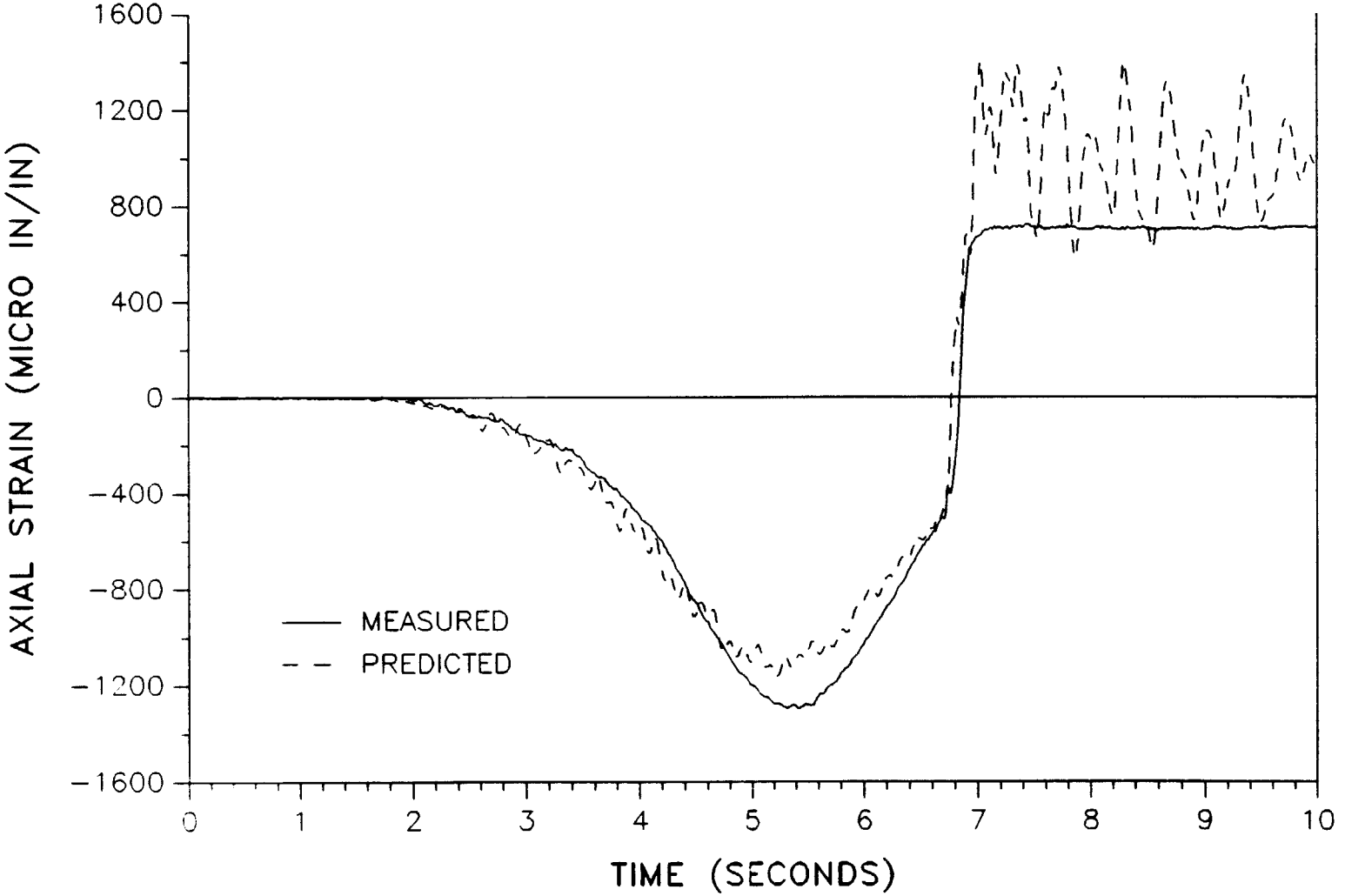

PREDICTED VS MEASURED AXIAL STRAIN

360L001 STRAIN GAGE B08G7410A – STATION 1797.0 AT 270 DEGREES

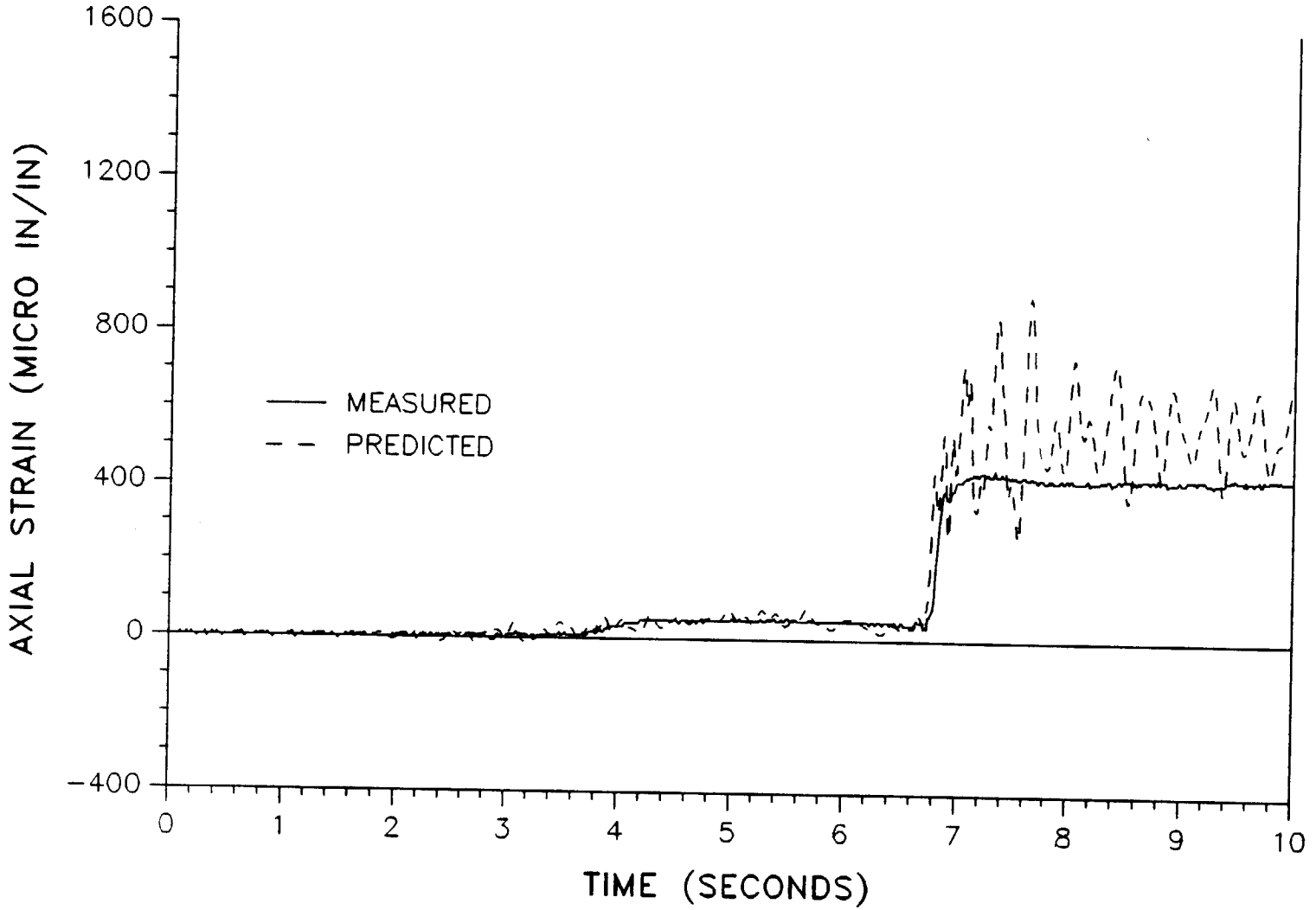

PREDICTED VS MEASURED AXIAL STRAIN

360L001 STRAIN GAGE B08G8322A – STATION 556.5 AT 0 DEGREES

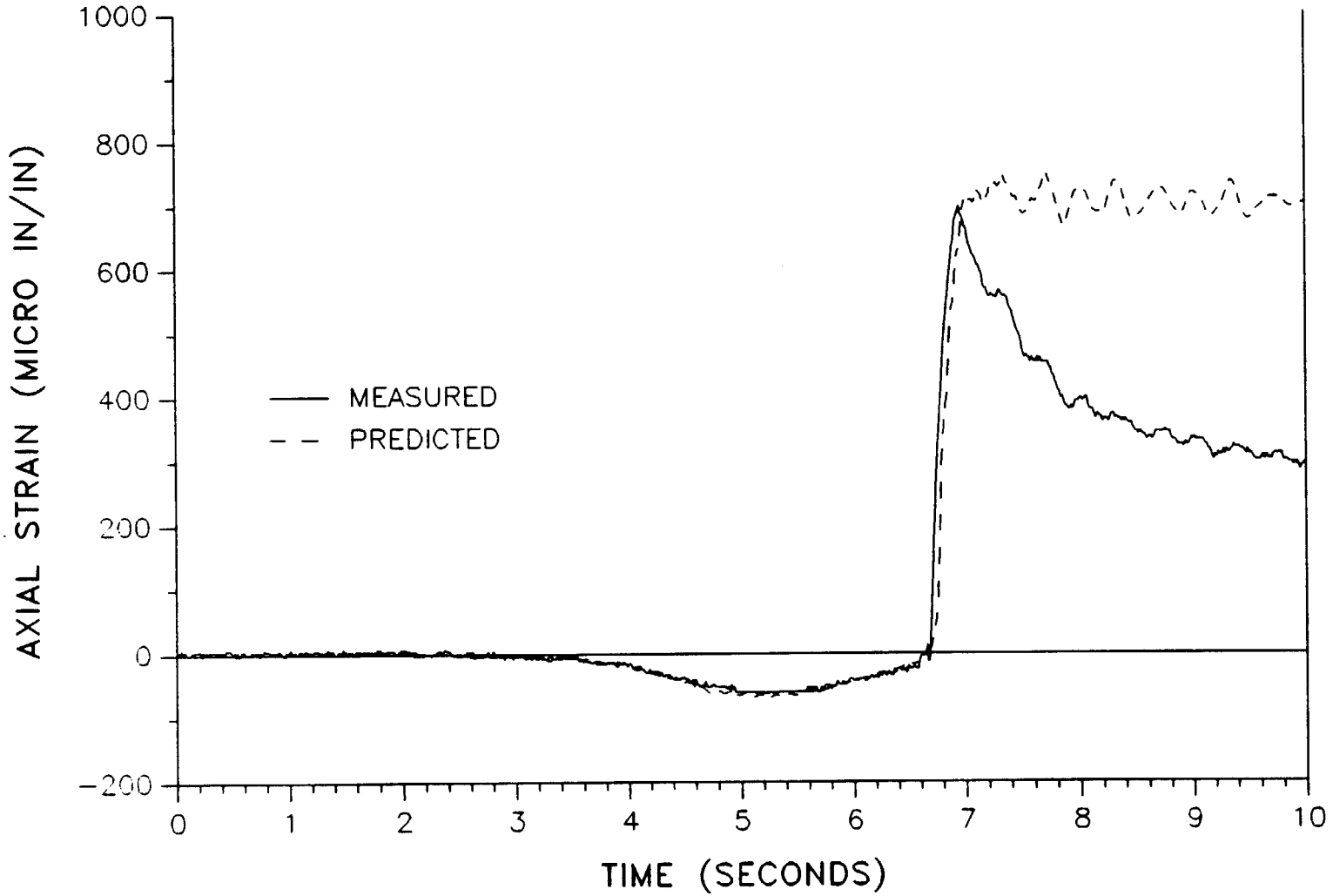

PREDICTED VS MEASURED AXIAL STRAIN

360L001 STRAIN GAGE B08G8320A – STATION 556.5 AT 82 DEGREES

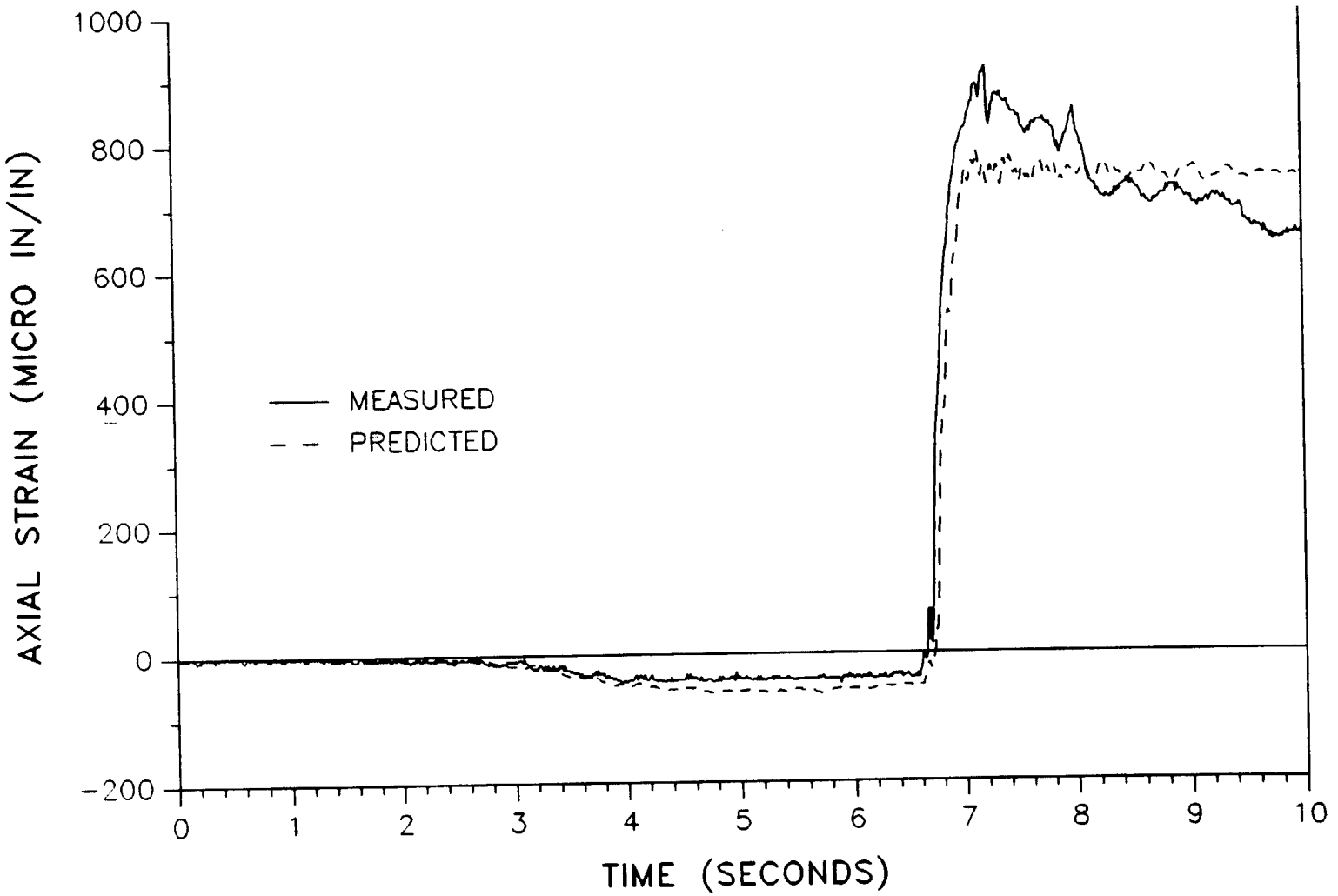

PREDICTED VS MEASURED AXIAL STRAIN

360L001 STRAIN GAGE B08G8318A – STATION 556.5 AT 180 DEGREES

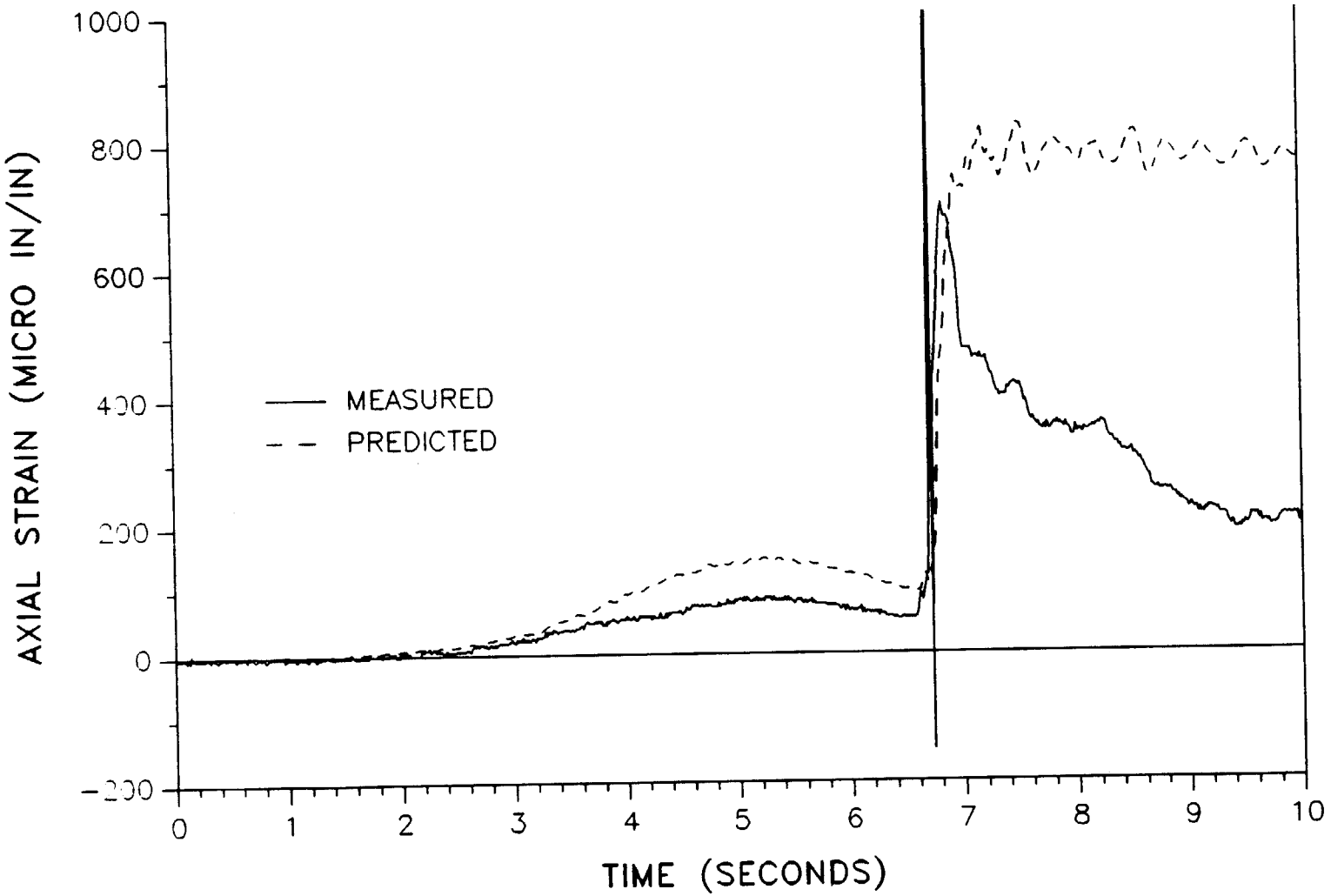

PREDICTED VS MEASURED AXIAL STRAIN

360L001 STRAIN GAGE B08G8324A – STATION 556.5 AT 270 DEGREES

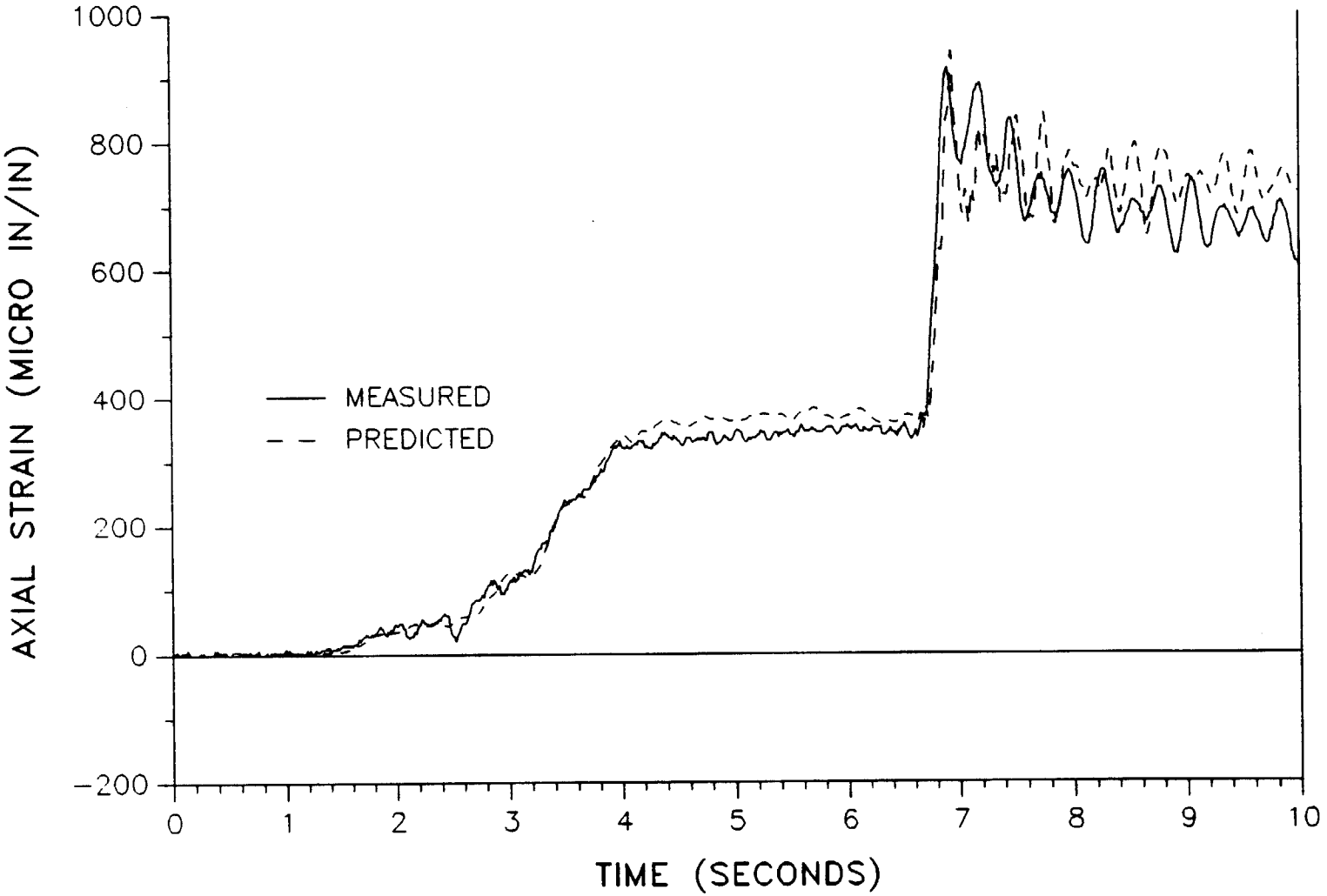

PREDICTED VS MEASURED AXIAL STRAIN

360L001 STRAIN GAGE B08G8330A – STATION 876.5 AT 0 DEGREES

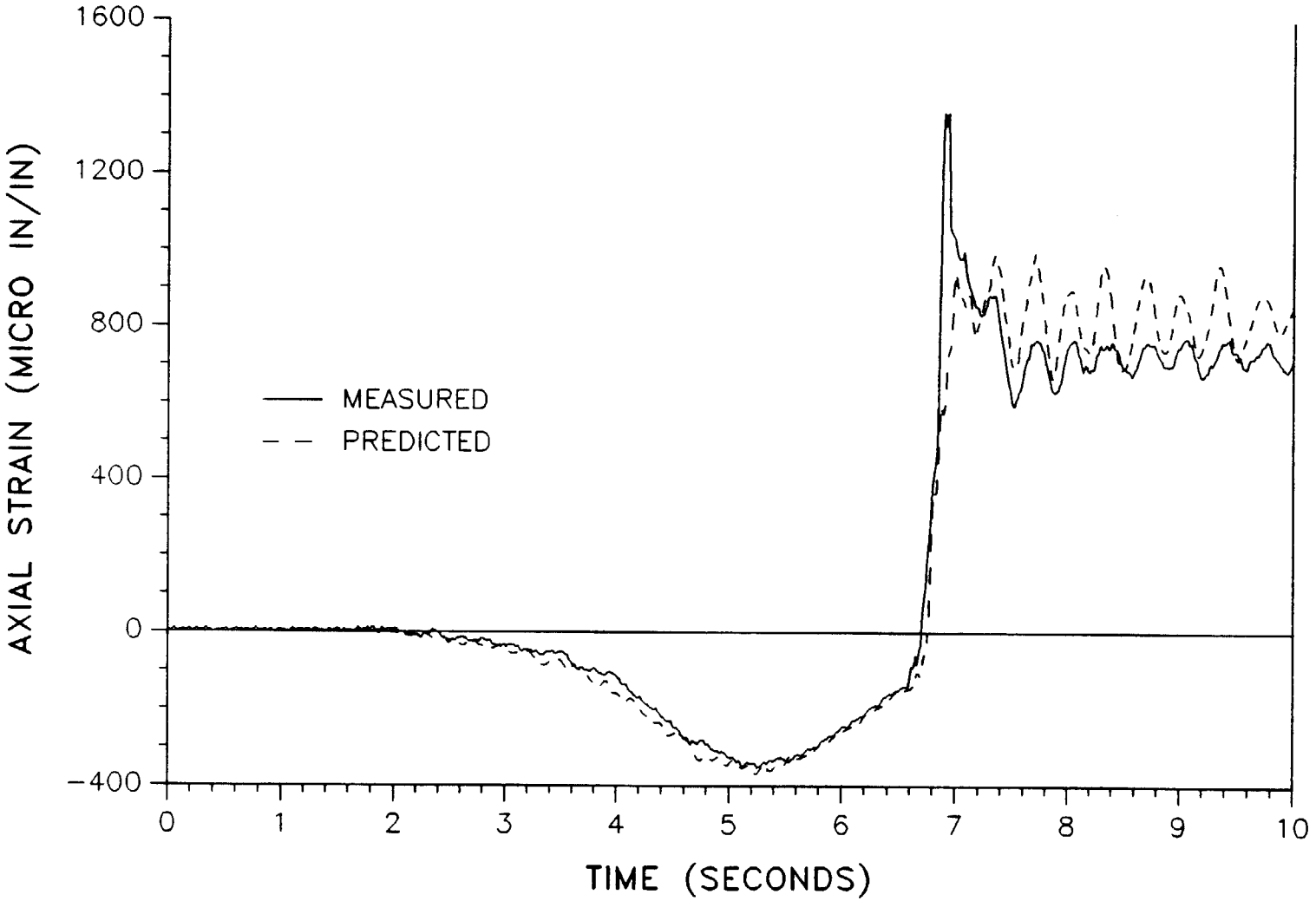

PREDICTED VS MEASURED AXIAL STRAIN

360L001 STRAIN GAGE B08G8328A – STATION 876.5 AT 82 DEGREES

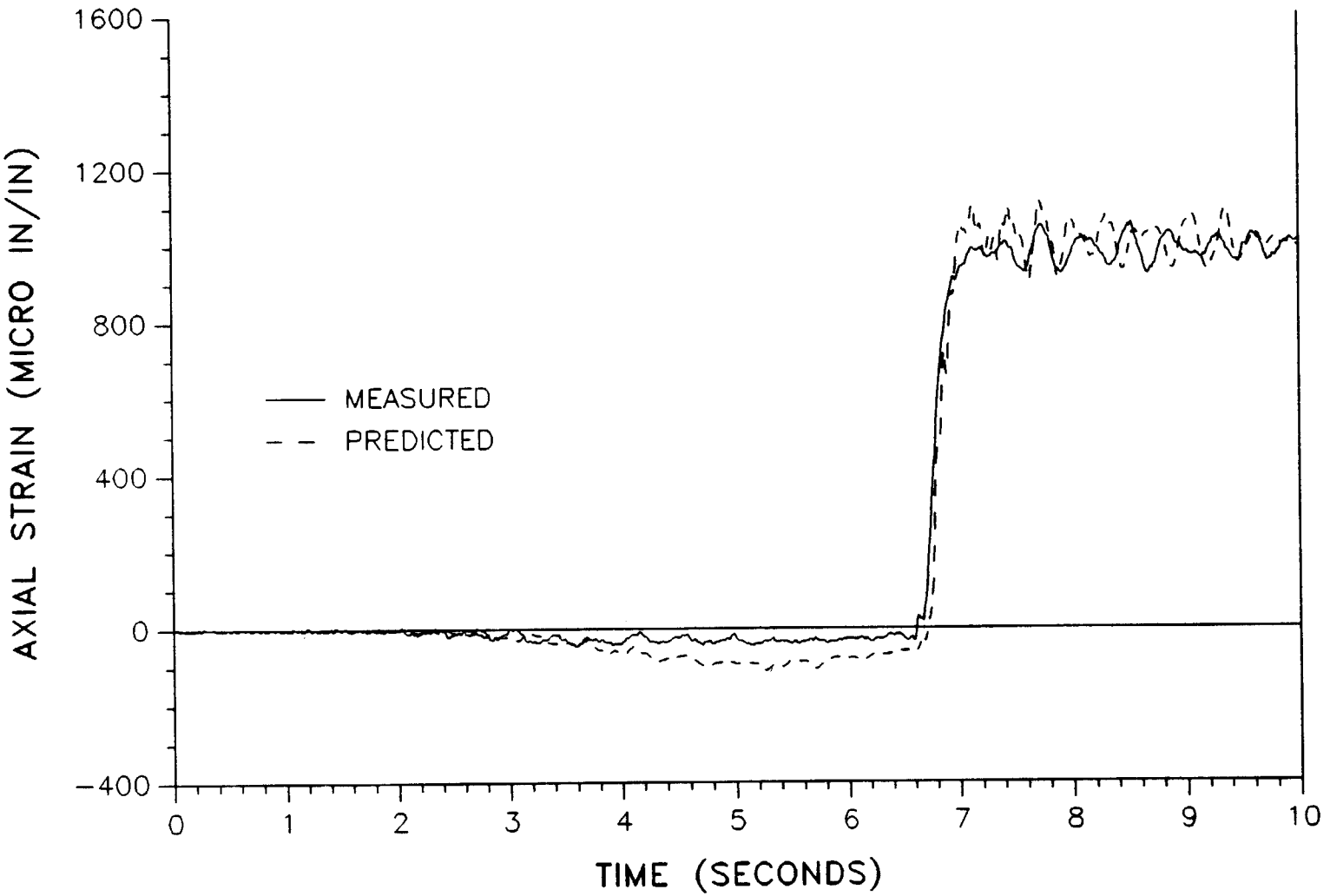

PREDICTED VS MEASURED AXIAL STRAIN

360L001 STRAIN GAGE B08G8326A – STATION 876.5 AT 180 DEGREES

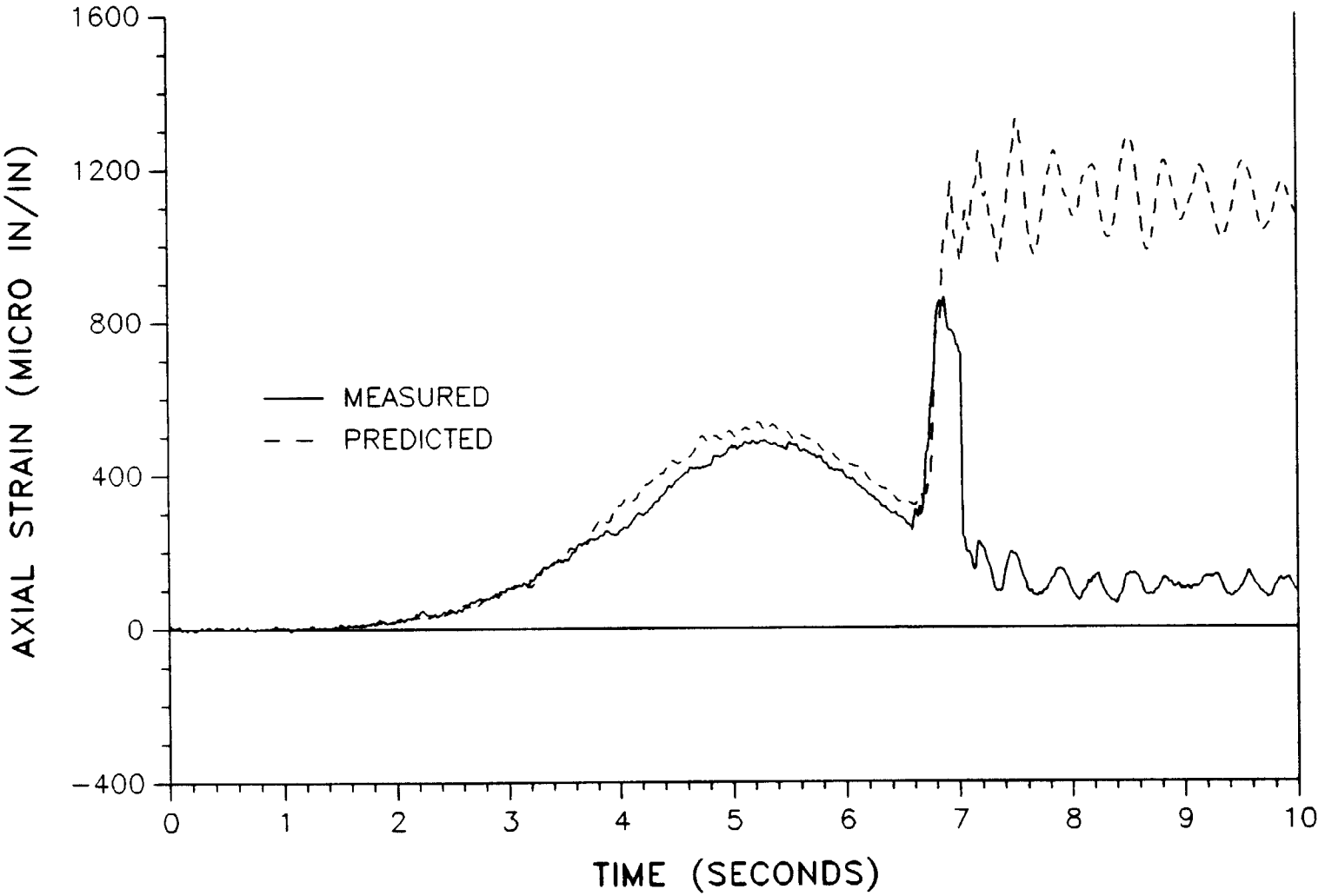

PREDICTED VS MEASURED AXIAL STRAIN

360L001 STRAIN GAGE B08G8332A – STATION 876.5 AT 270 DEGREES

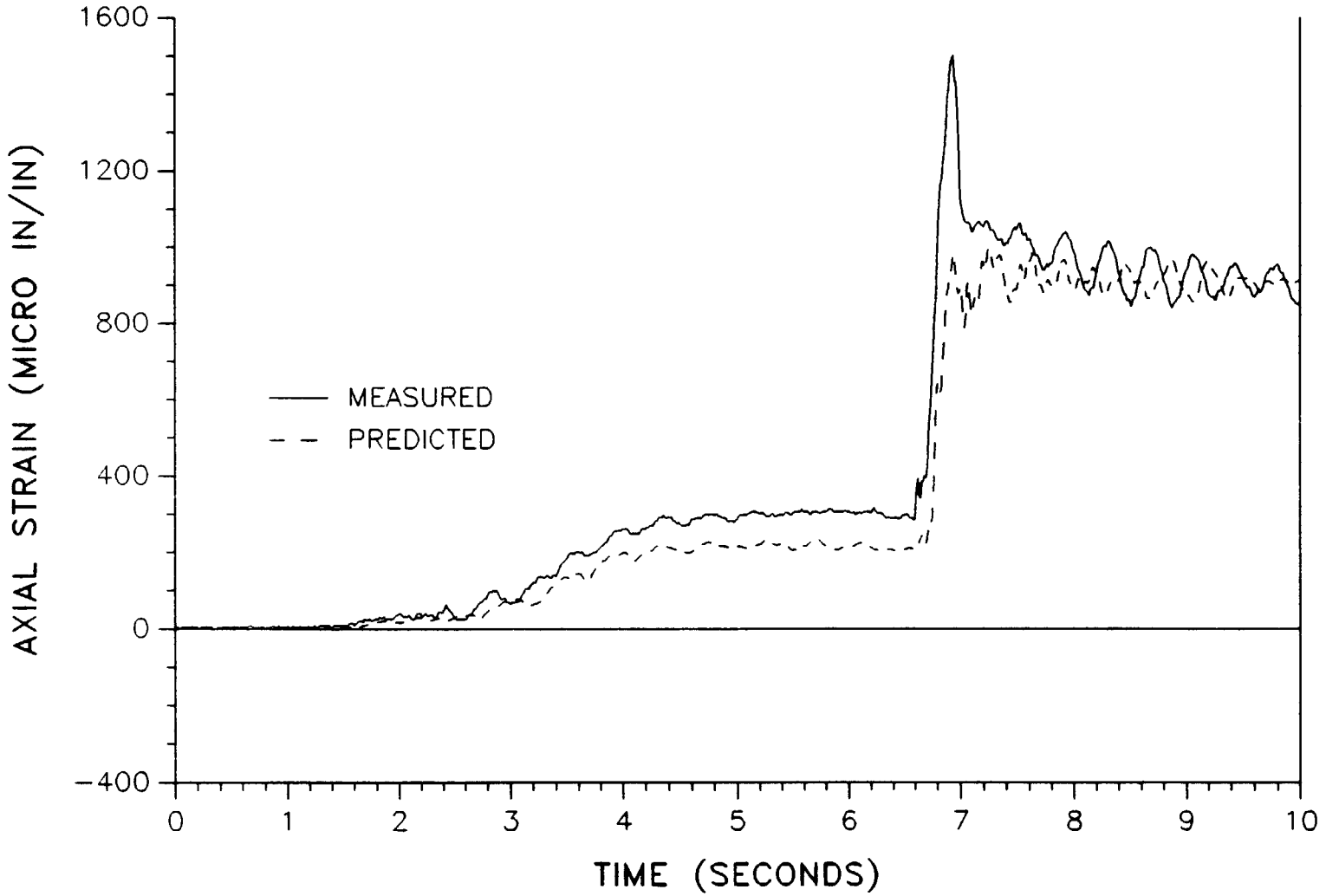

PREDICTED VS MEASURED AXIAL STRAIN

360L001 STRAIN GAGE B08G8338A – STATION 1196.5 AT 0 DEGREES

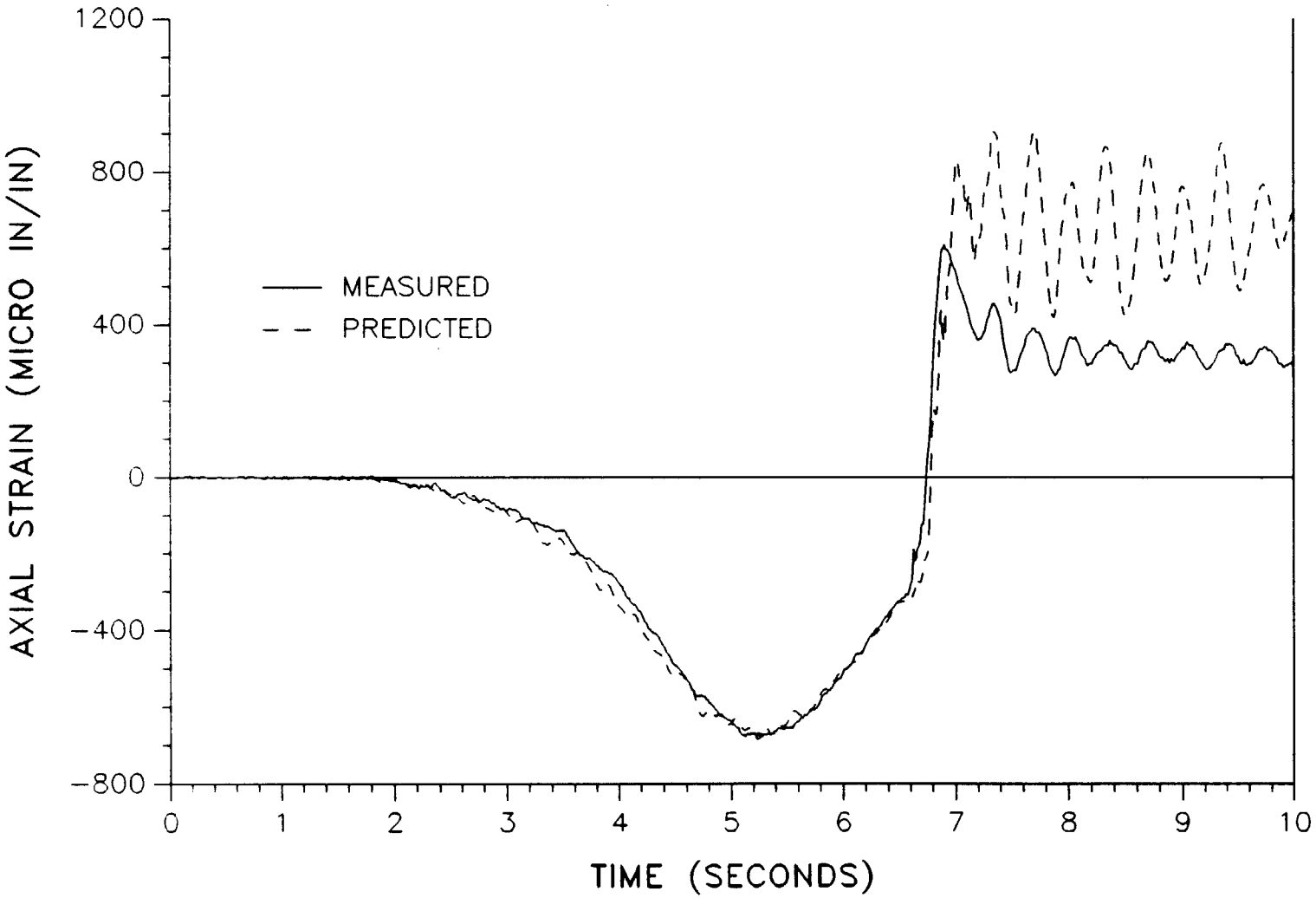

PREDICTED VS MEASURED AXIAL STRAIN

360L001 STRAIN GAGE B08G8336A – STATION 1196.5 AT 82 DEGREES

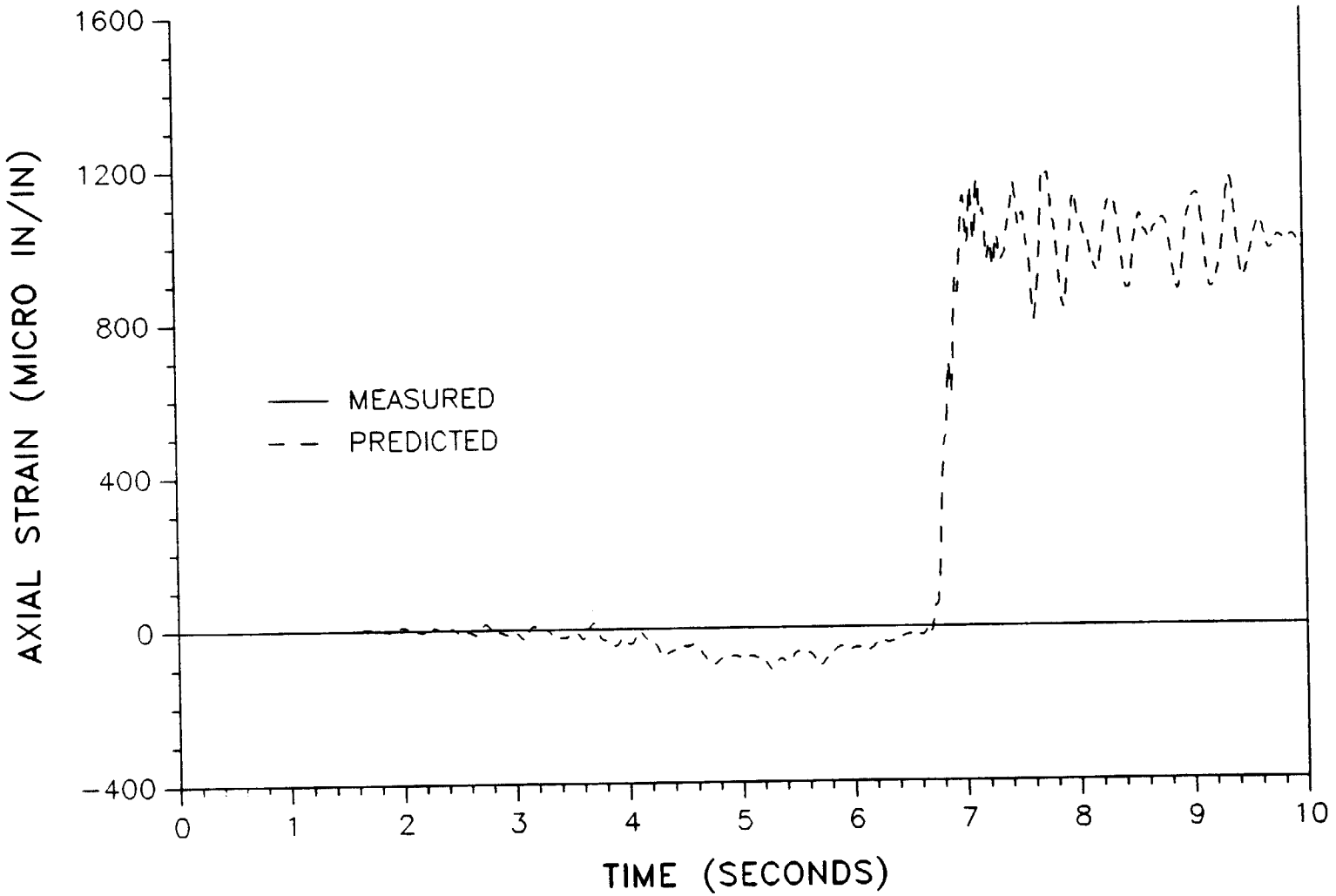

PREDICTED VS MEASURED AXIAL STRAIN

360L001 STRAIN GAGE B08G8334A – STATION 1196.5 AT 180 DEGREES

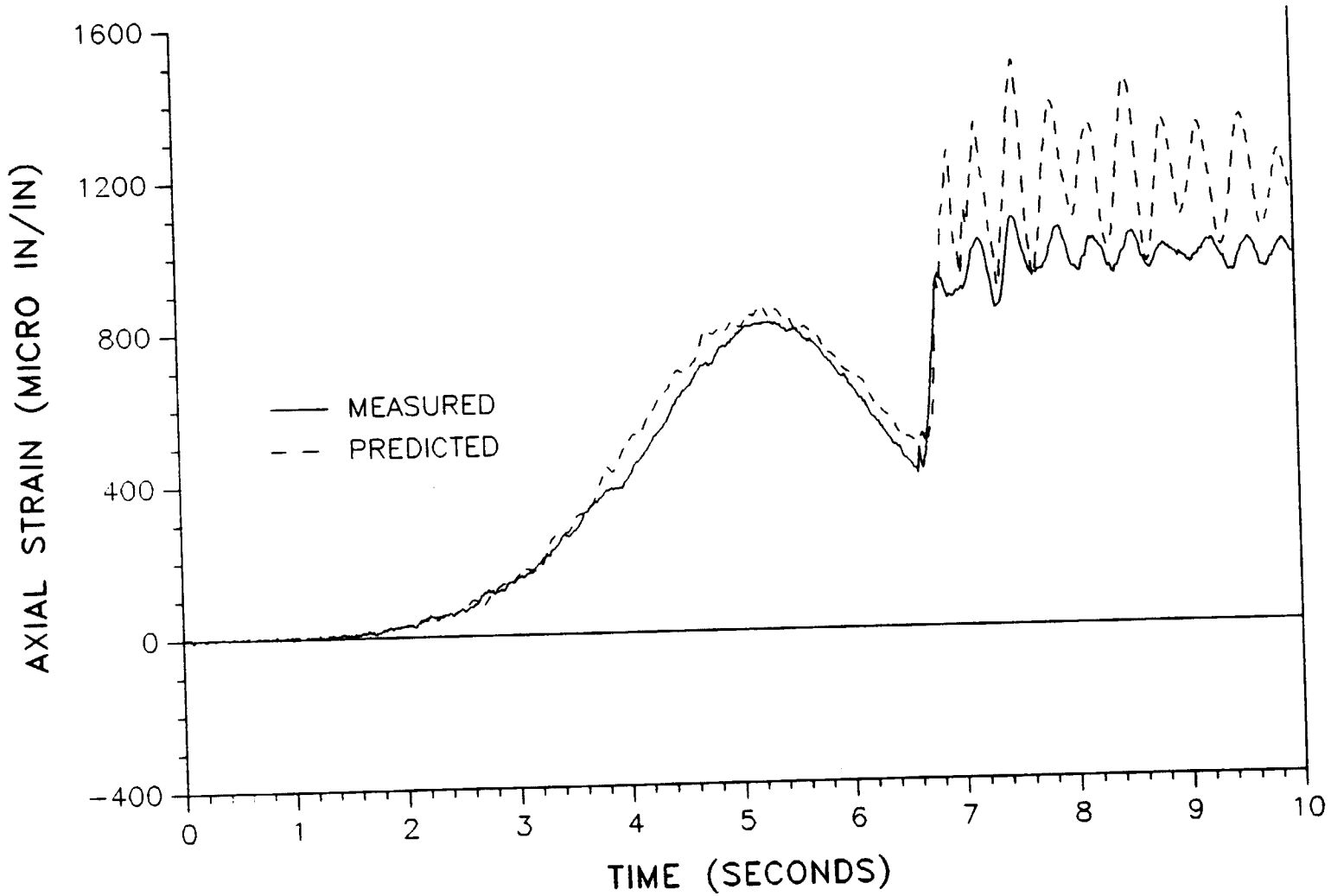

PREDICTED VS MEASURED AXIAL STRAIN

360L001 STRAIN GAGE B08G8340A – STATION 1196.5 AT 270 DEGREES

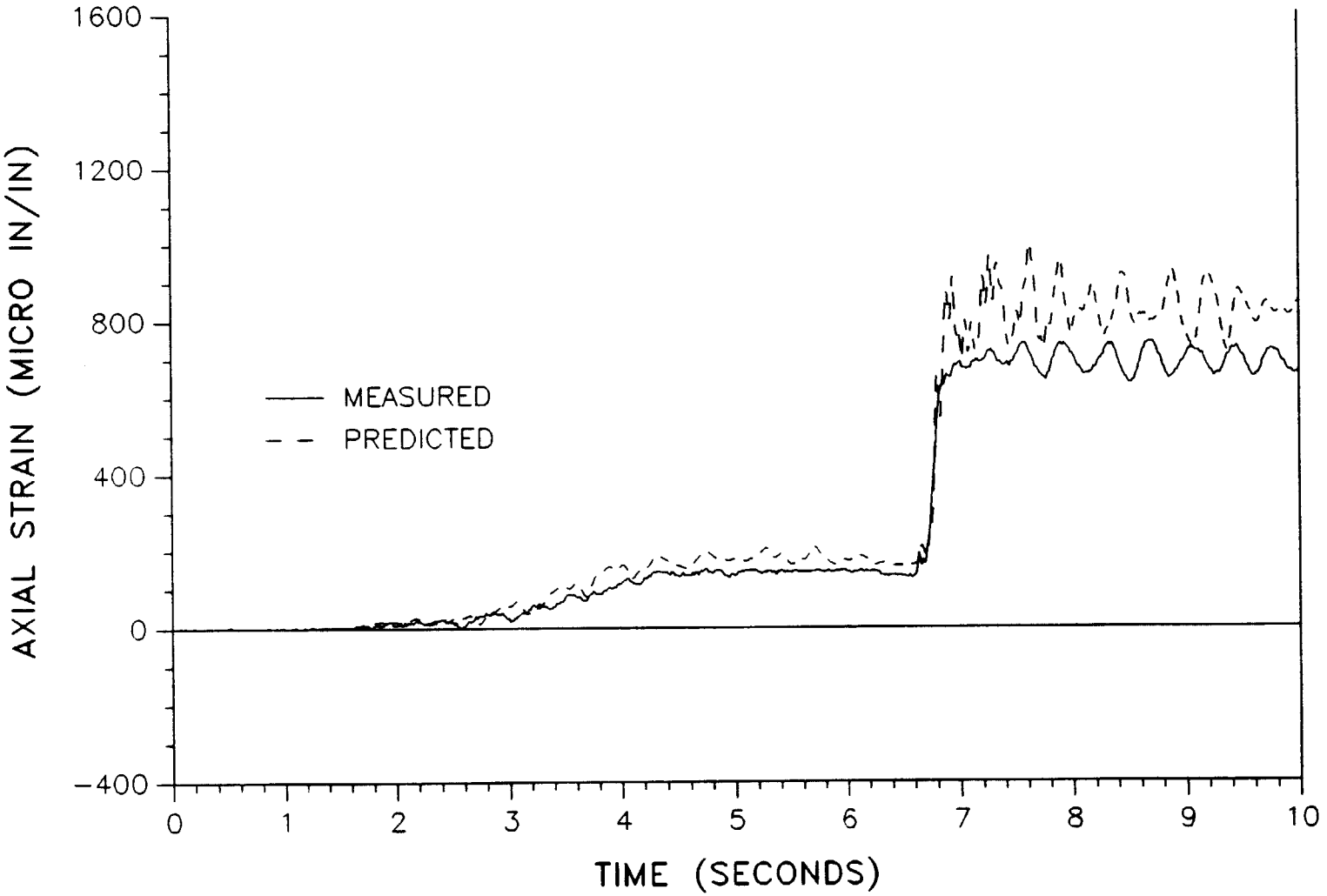

PREDICTED VS MEASURED AXIAL STRAIN

360L001 STRAIN GAGE B08G8346A – STATION 1466.0 AT 0 DEGREES

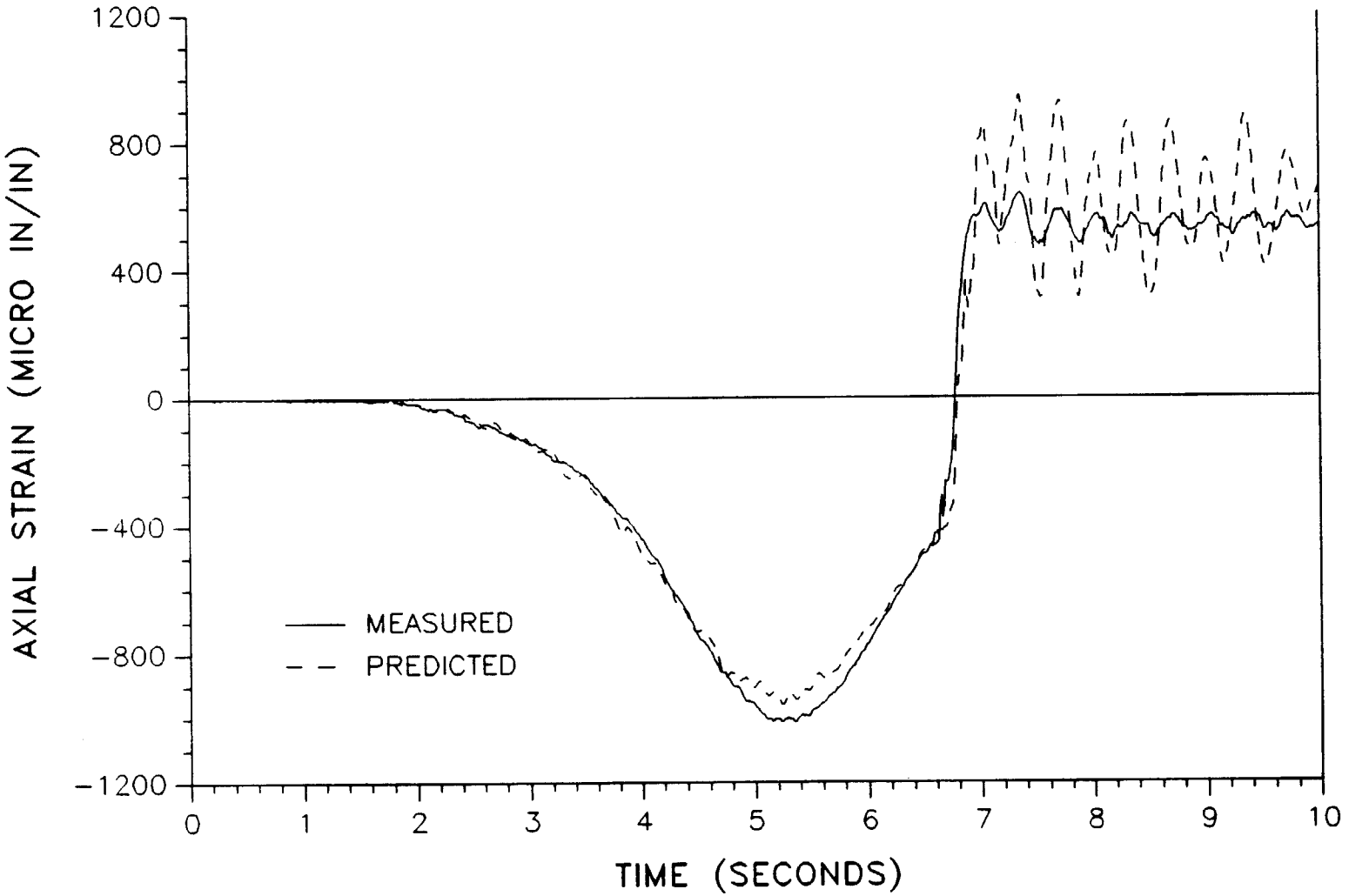

PREDICTED VS MEASURED AXIAL STRAIN

360L001 STRAIN GAGE B08G8344A – STATION 1466.0 AT 82 DEGREES

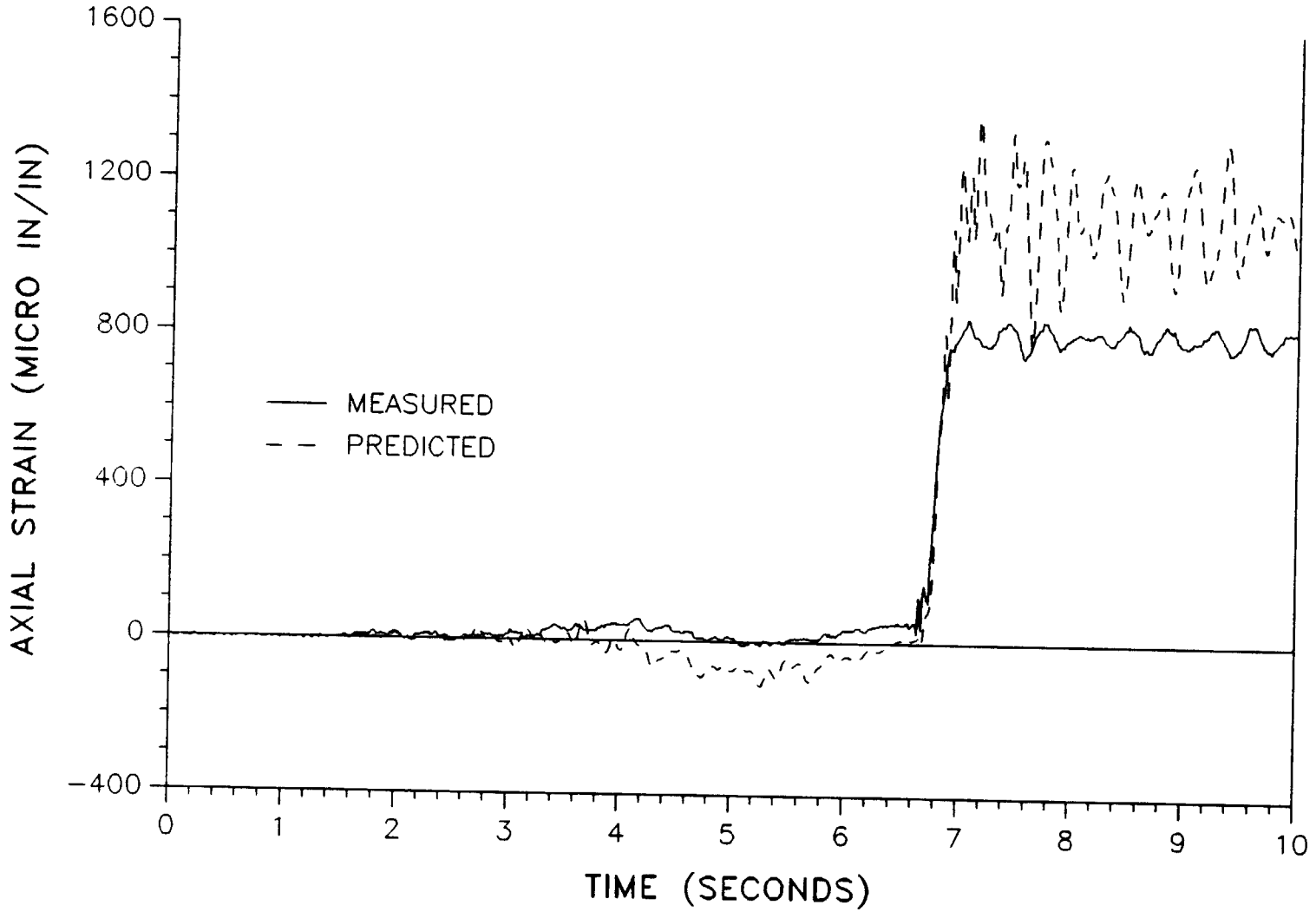

PREDICTED VS MEASURED AXIAL STRAIN

360L001 STRAIN GAGE B08G8342A – STATION 1466.0 AT 180 DEGREES

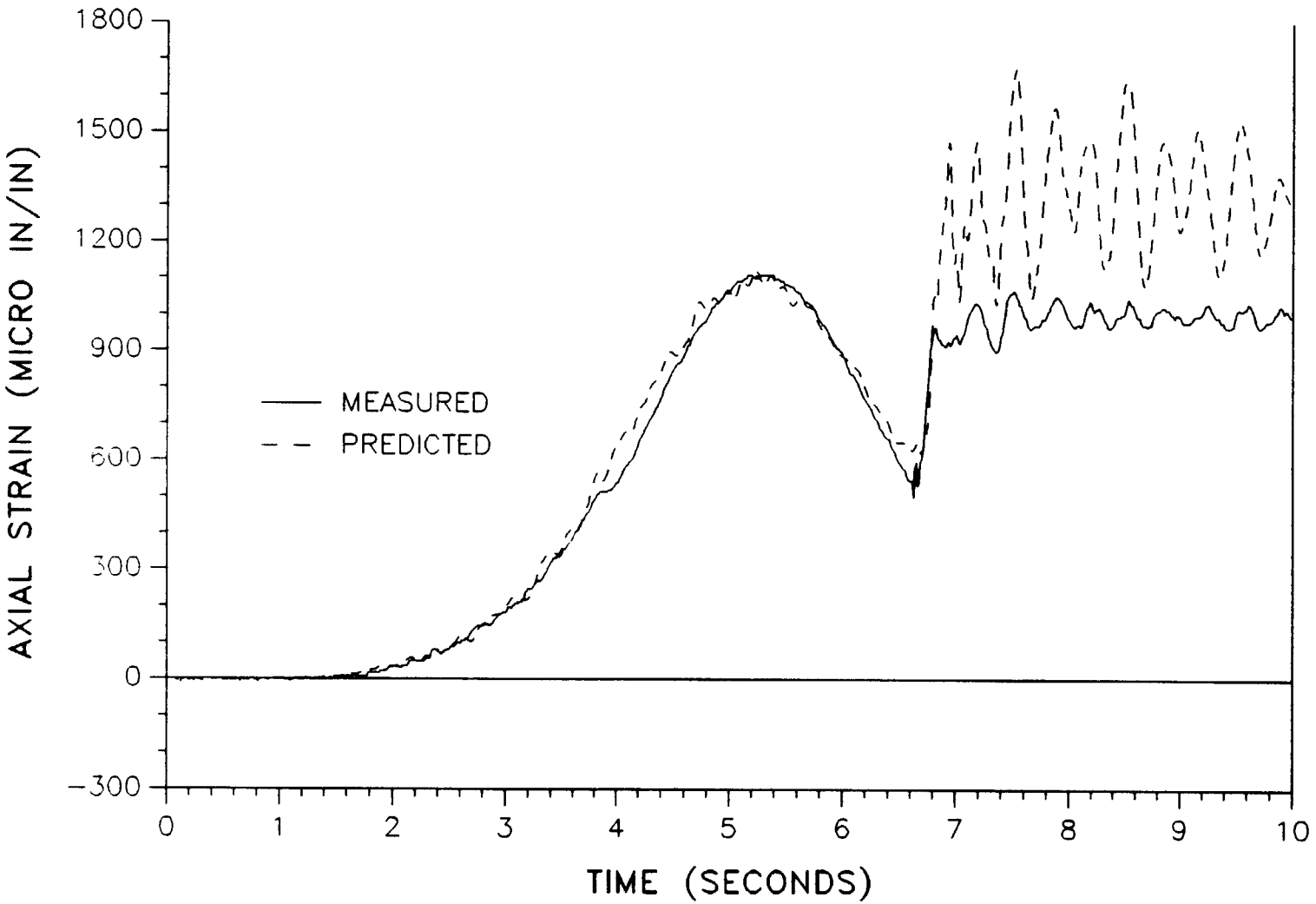

PREDICTED VS MEASURED AXIAL STRAIN

360L001 STRAIN GAGE B08G8348A – STATION 1466.0 AT 270 DEGREES

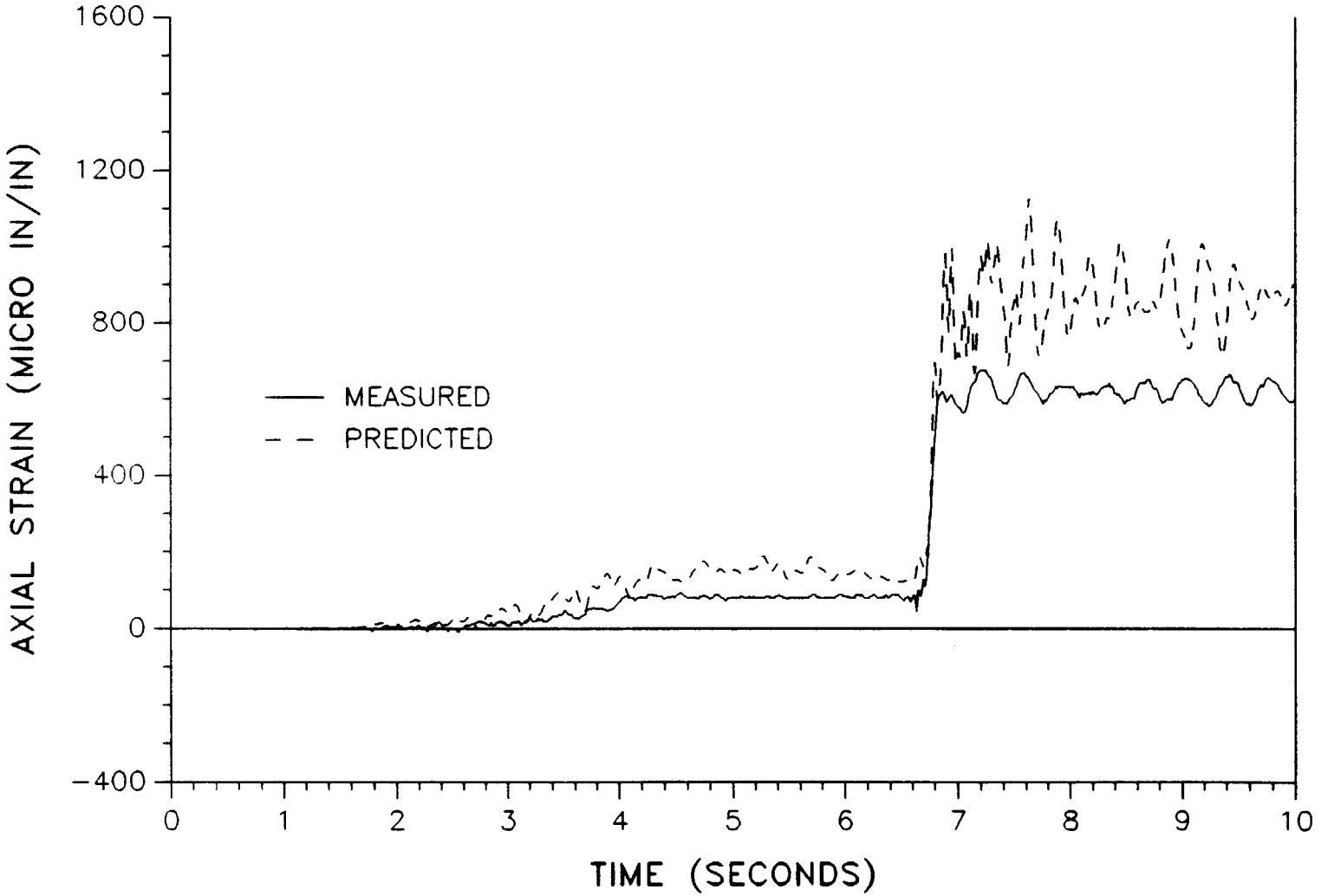

PREDICTED VS MEASURED AXIAL STRAIN

360L001 STRAIN GAGE B08G8350A – STATION 1493.0 AT 0 DEGREES

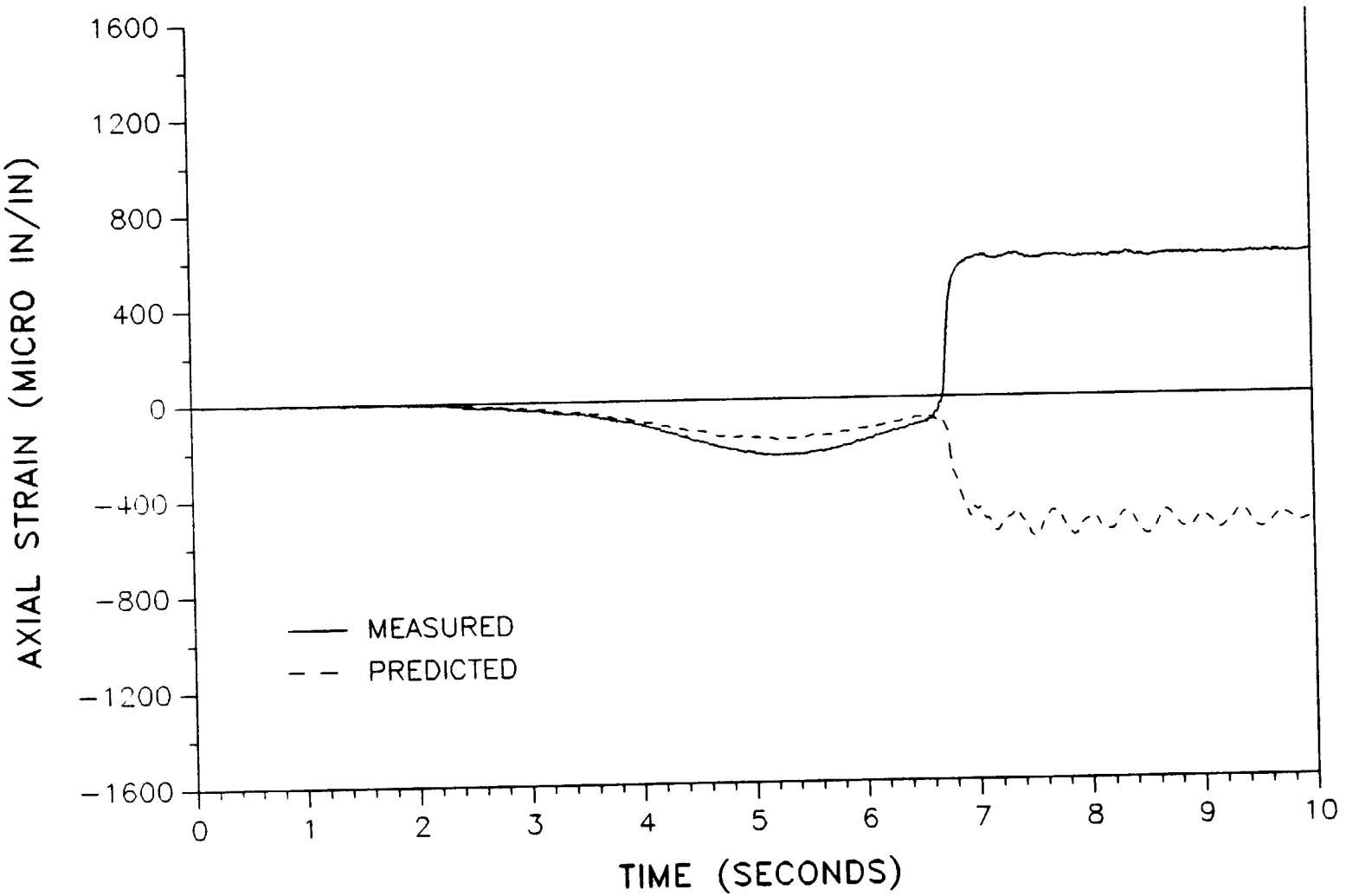

PREDICTED VS MEASURED AXIAL STRAIN

360L001 STRAIN GAGE B08G8352A – STATION 1493.0 AT 82 DEGREES

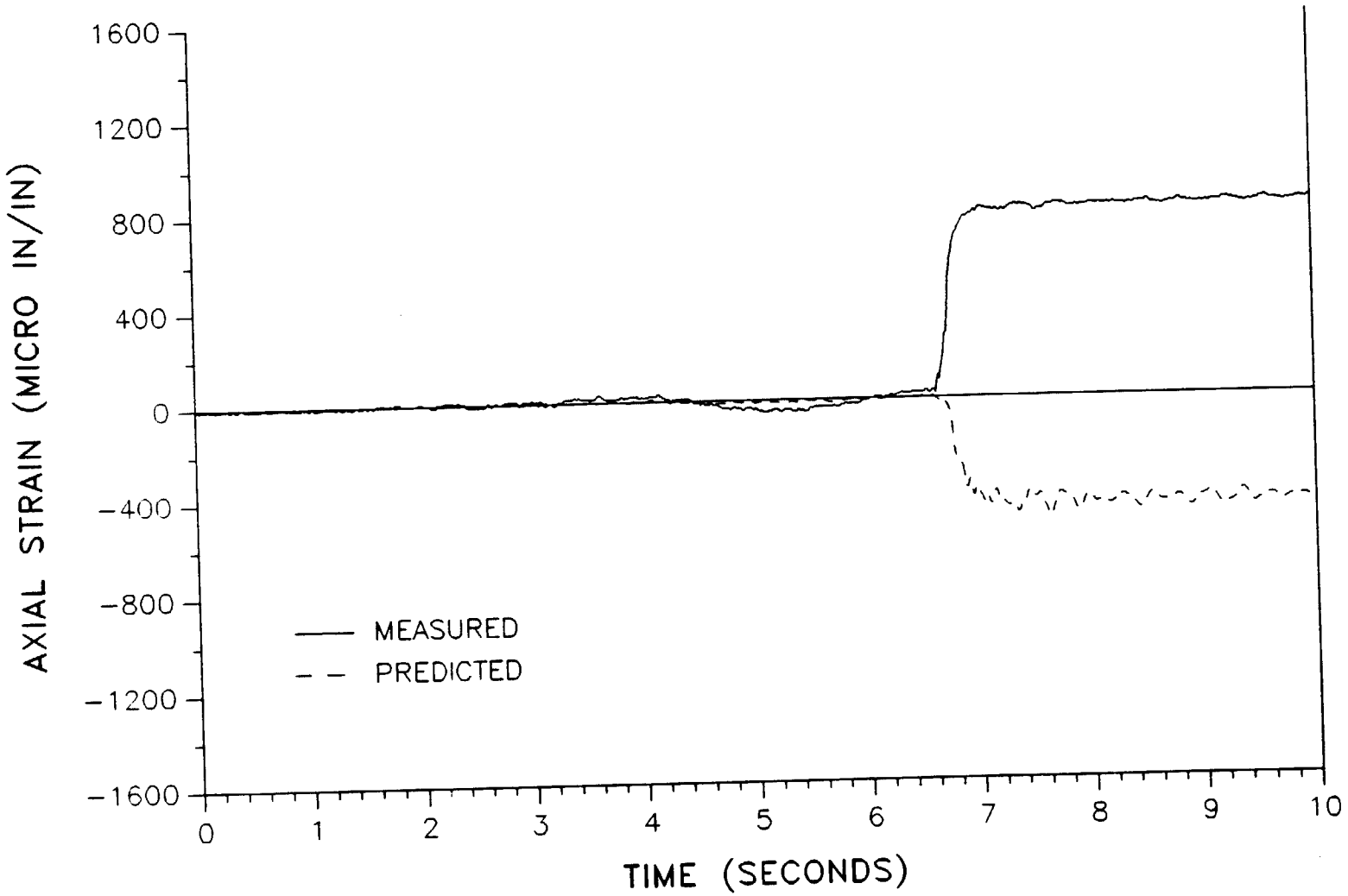

PREDICTED VS MEASURED AXIAL STRAIN

360L001 STRAIN GAGE B08G8354A – STATION 1493.0 AT 180 DEGREES

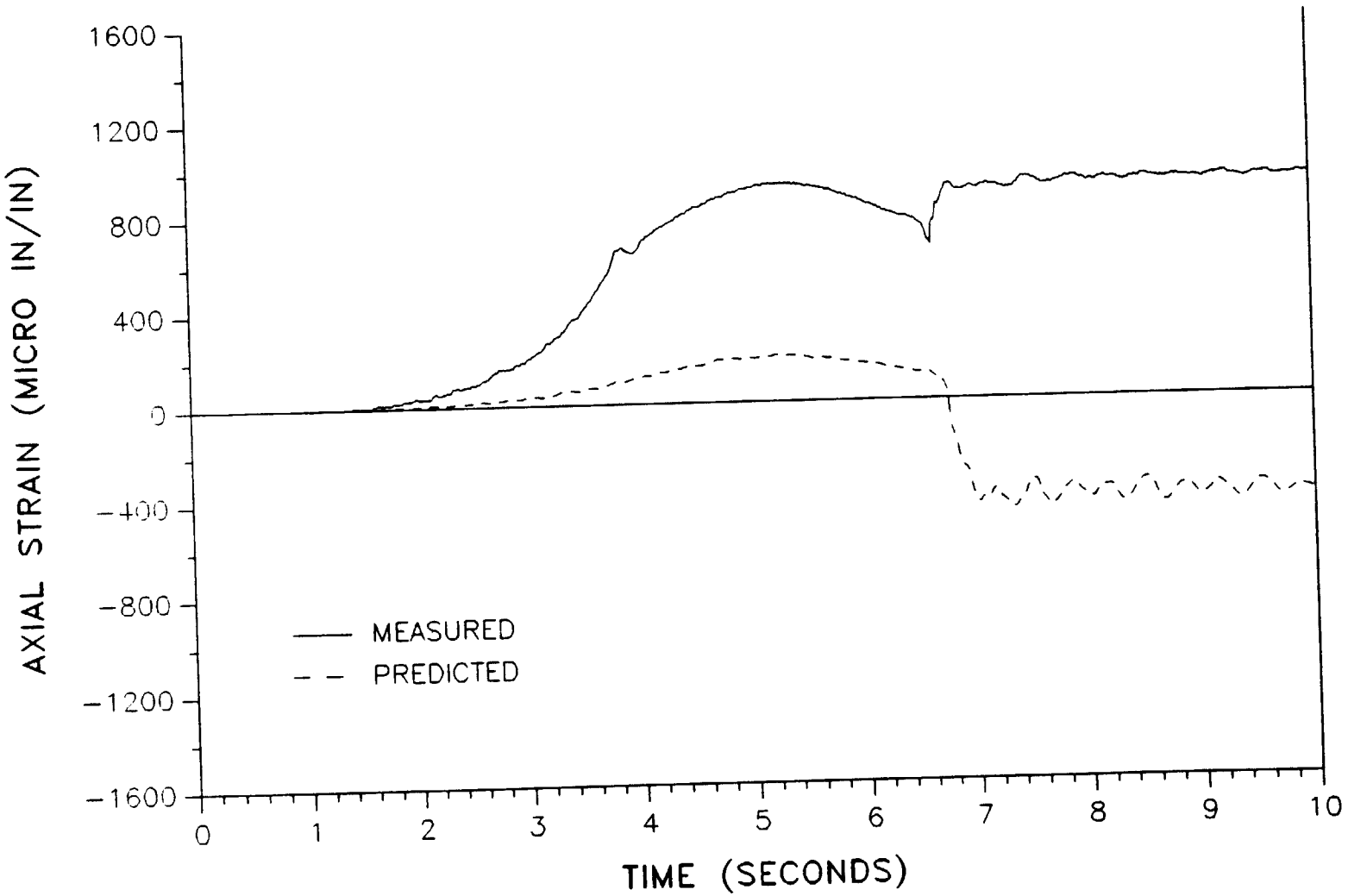

PREDICTED VS MEASURED AXIAL STRAIN

360L001 STRAIN GAGE B08G8356A – STATION 1493.0 AT 220 DEGREES

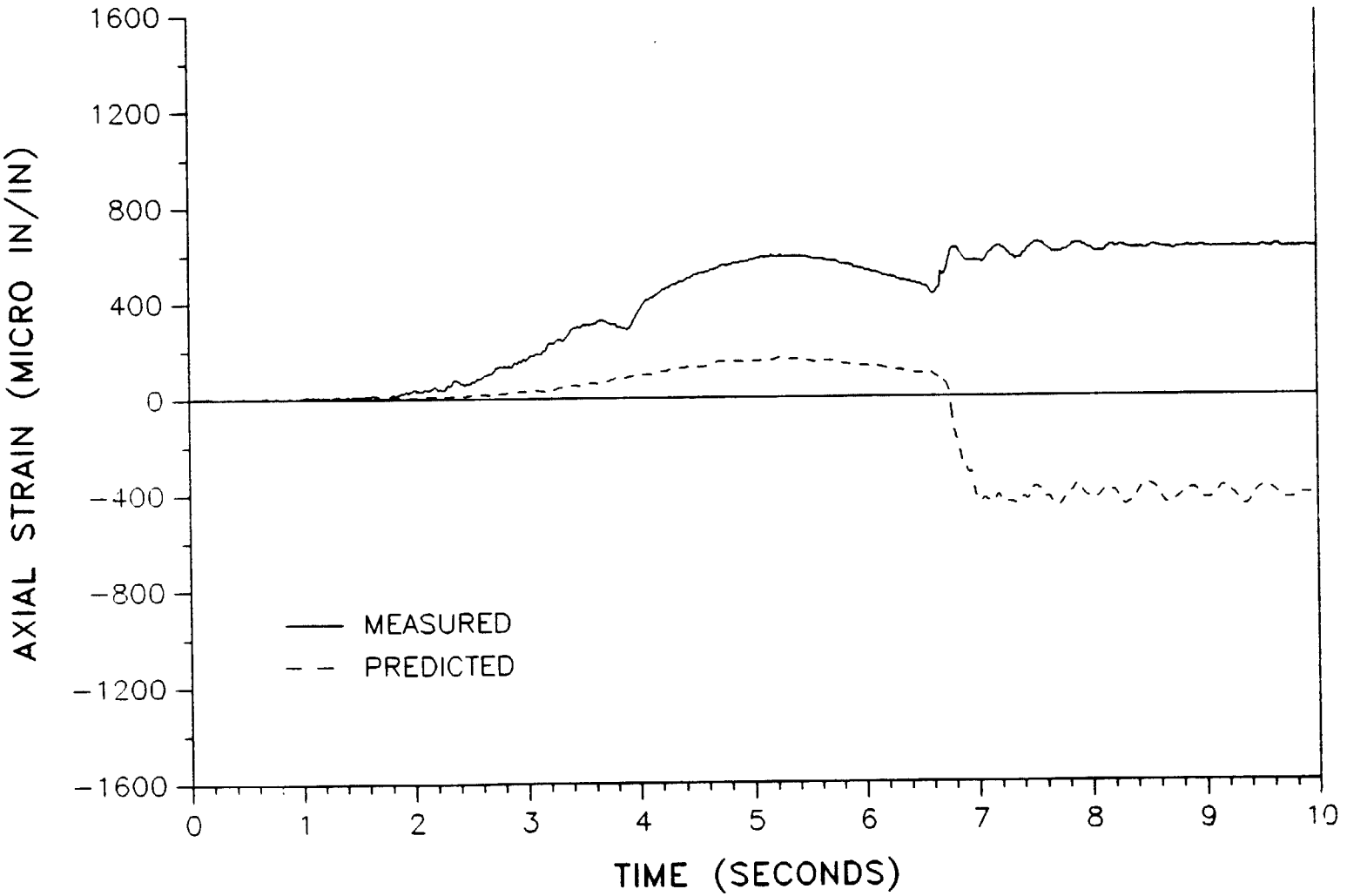

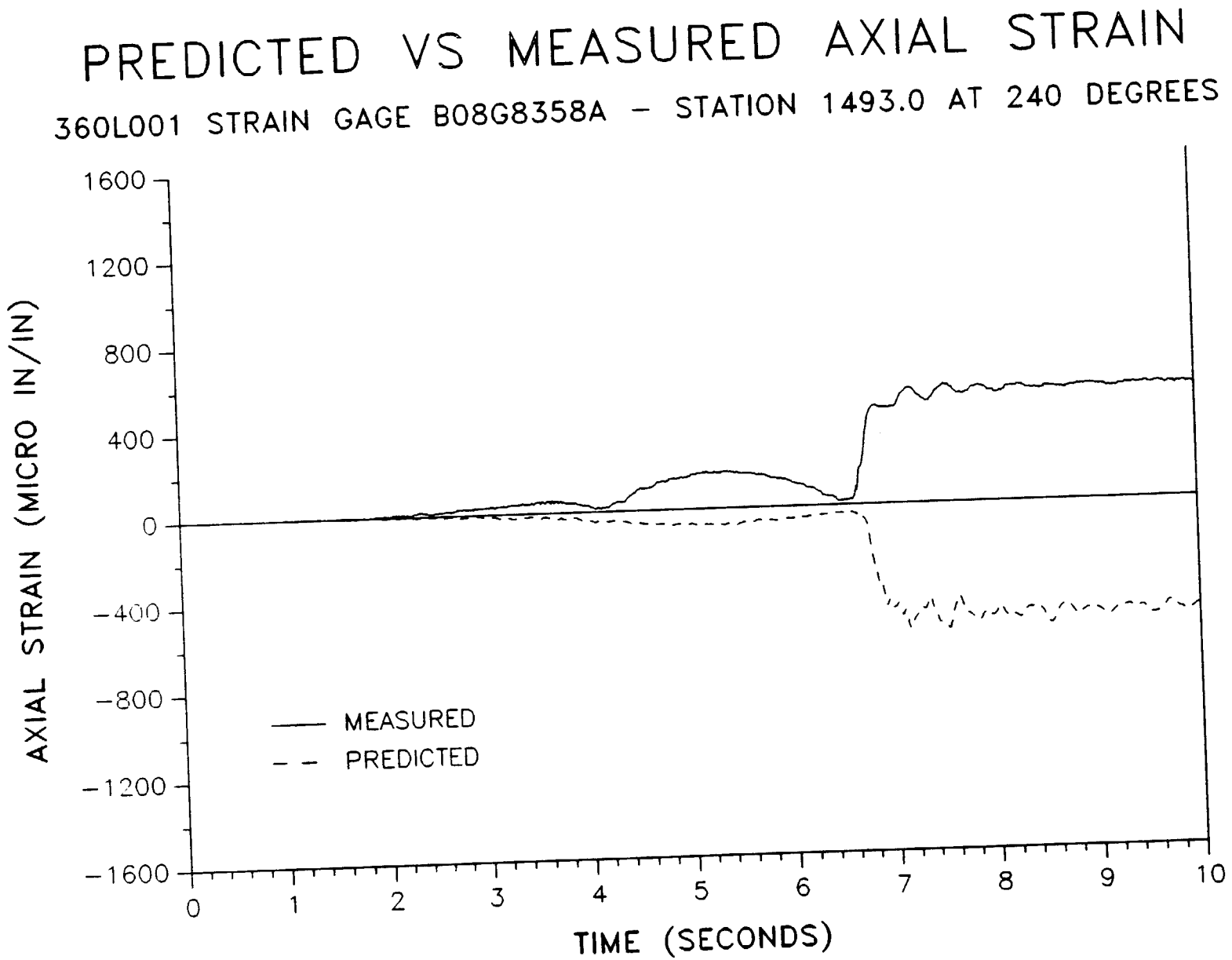
PREDICTED VS MEASURED AXIAL STRAIN
360L001 STRAIN GAGE B08G8358A – STATION 1493.0 AT 240 DEGREES
AXIAL STRAIN (MICRO IN/IN)
1600
1200
800
400
0
-400
-800
-1200
-1600
0
1
2
3
4
5
6
7
8
9
10
TIME (SECONDS)
MEASURED
PREDICTED

PREDICTED VS MEASURED AXIAL STRAIN

360L001 STRAIN GAGE B08G8360A – STATION 1493.0 AT 255 DEGREES

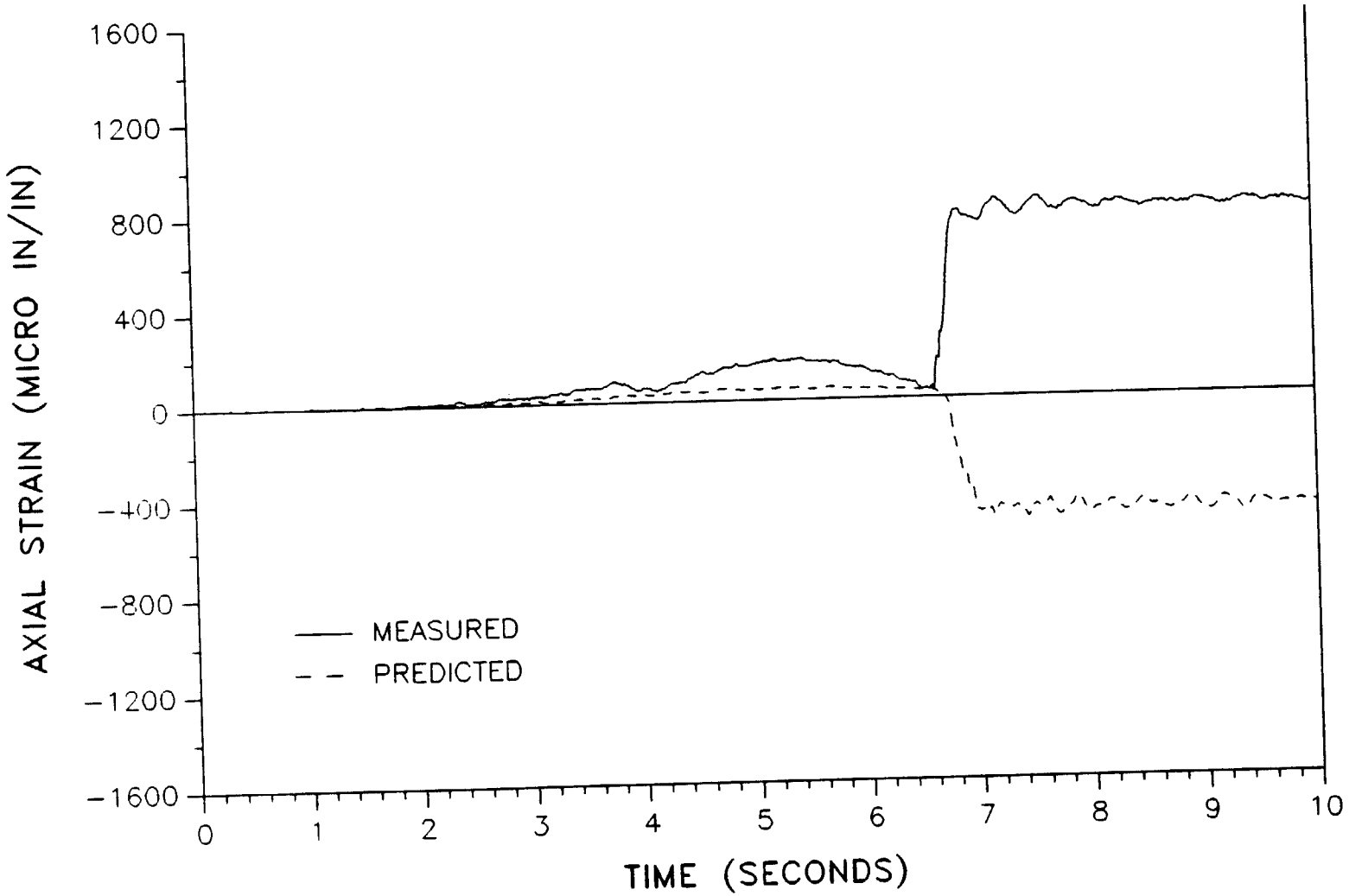

PREDICTED VS MEASURED AXIAL STRAIN

360L001 STRAIN GAGE B08G8362A – STATION 1493.0 AT 270 DEGREES

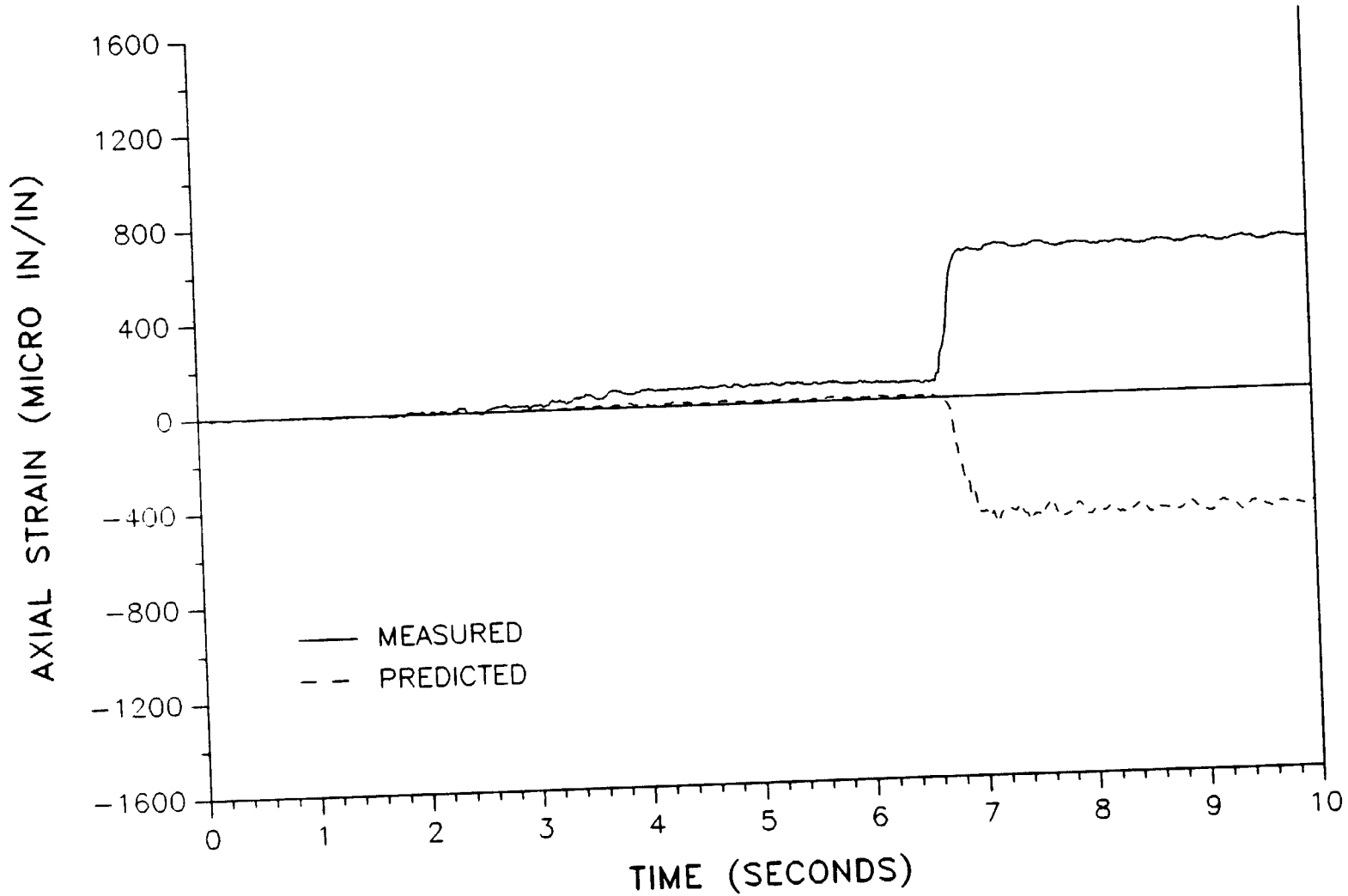

PREDICTED VS MEASURED AXIAL STRAIN

360L001 STRAIN GAGE B08G8364A – STATION 1493.0 AT 285 DEGREES

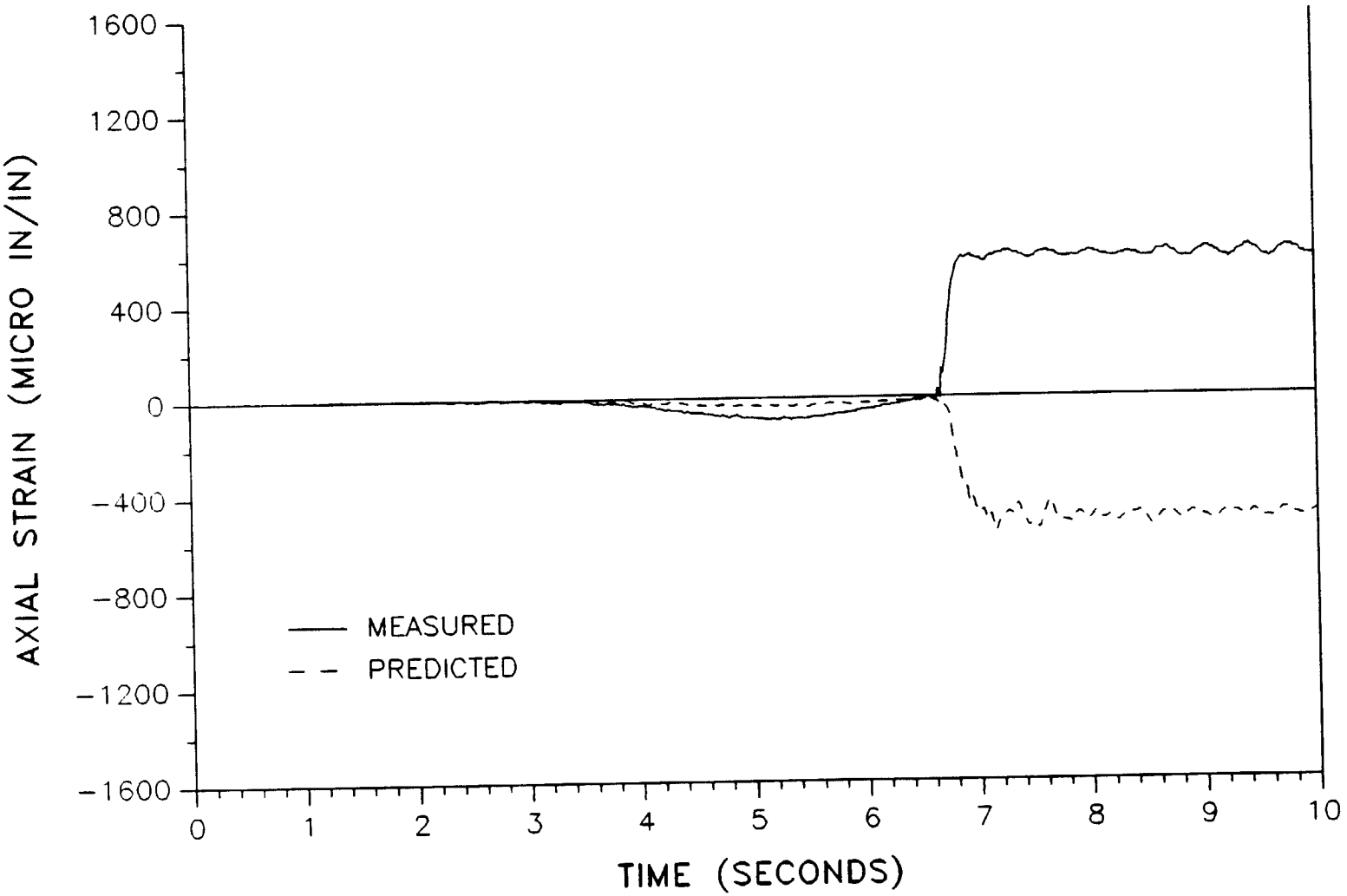

PREDICTED VS MEASURED AXIAL STRAIN

360L001 STRAIN GAGE B08G8366A – STATION 1493.0 AT 320 DEGREES

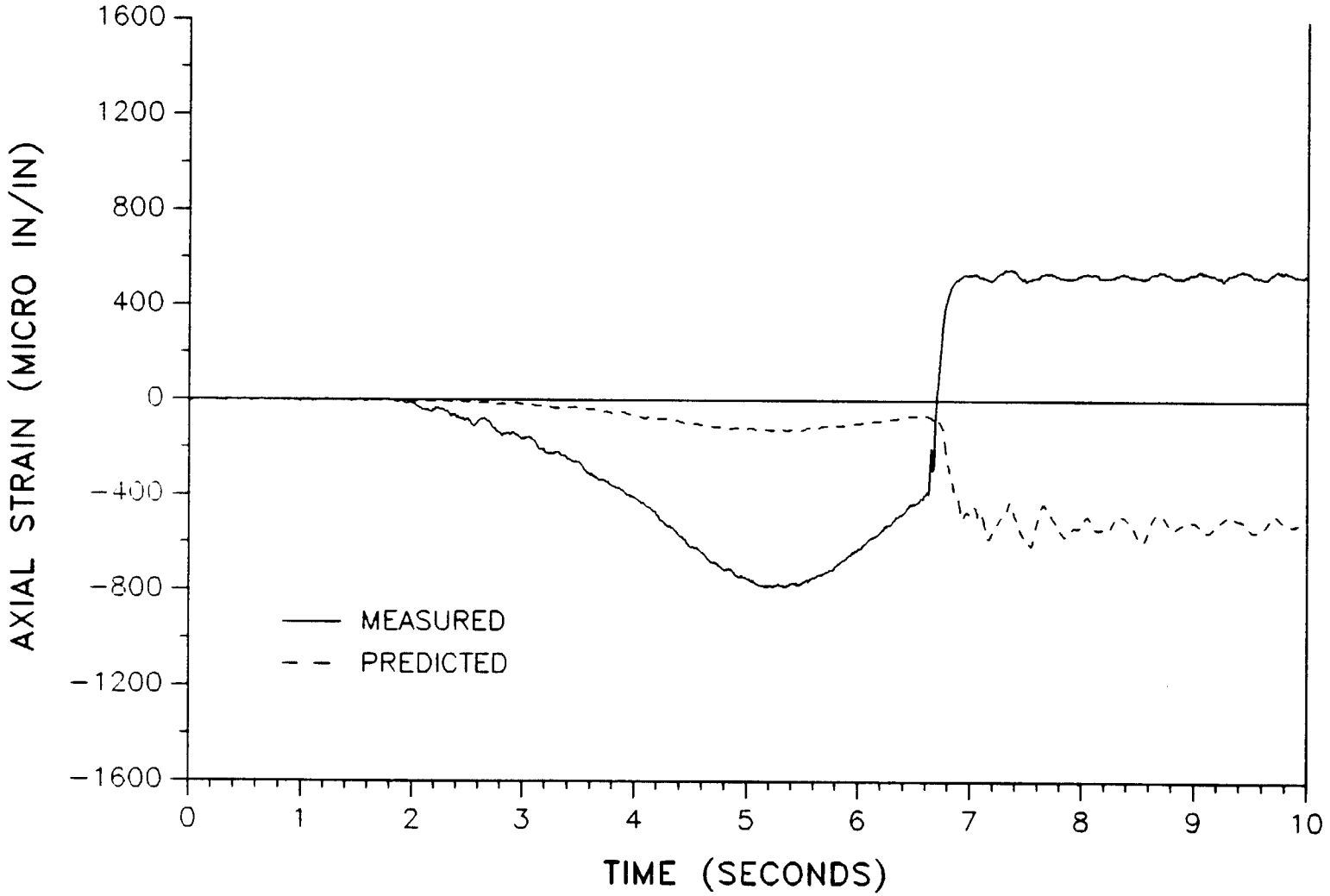

PREDICTED VS MEASURED AXIAL STRAIN

360L001 STRAIN GAGE B08G8386A – STATION 1501.0 AT 0 DEGREES

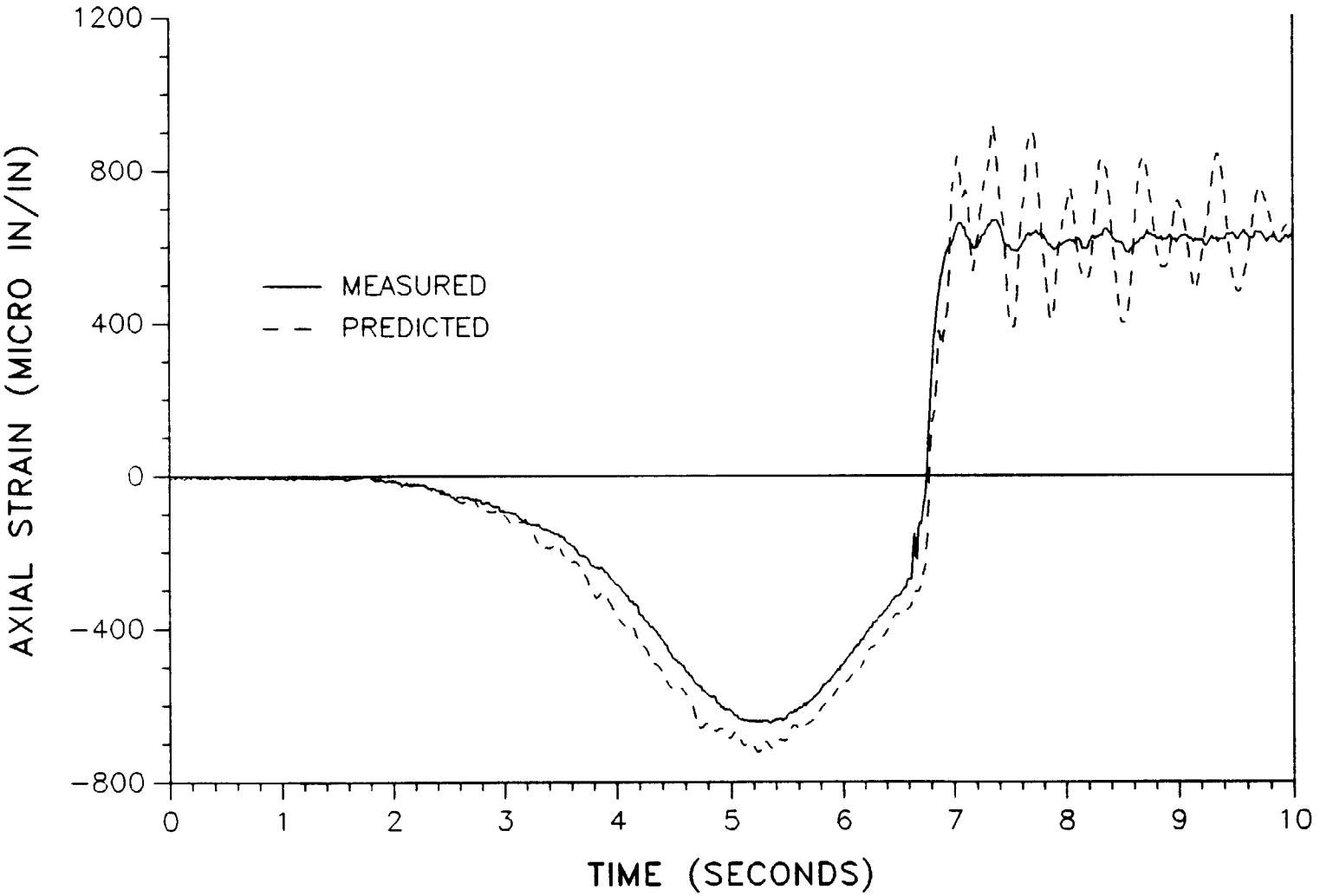

PREDICTED VS MEASURED AXIAL STRAIN

360L001 STRAIN GAGE B08G8388A – STATION 1501.0 AT 82 DEGREES

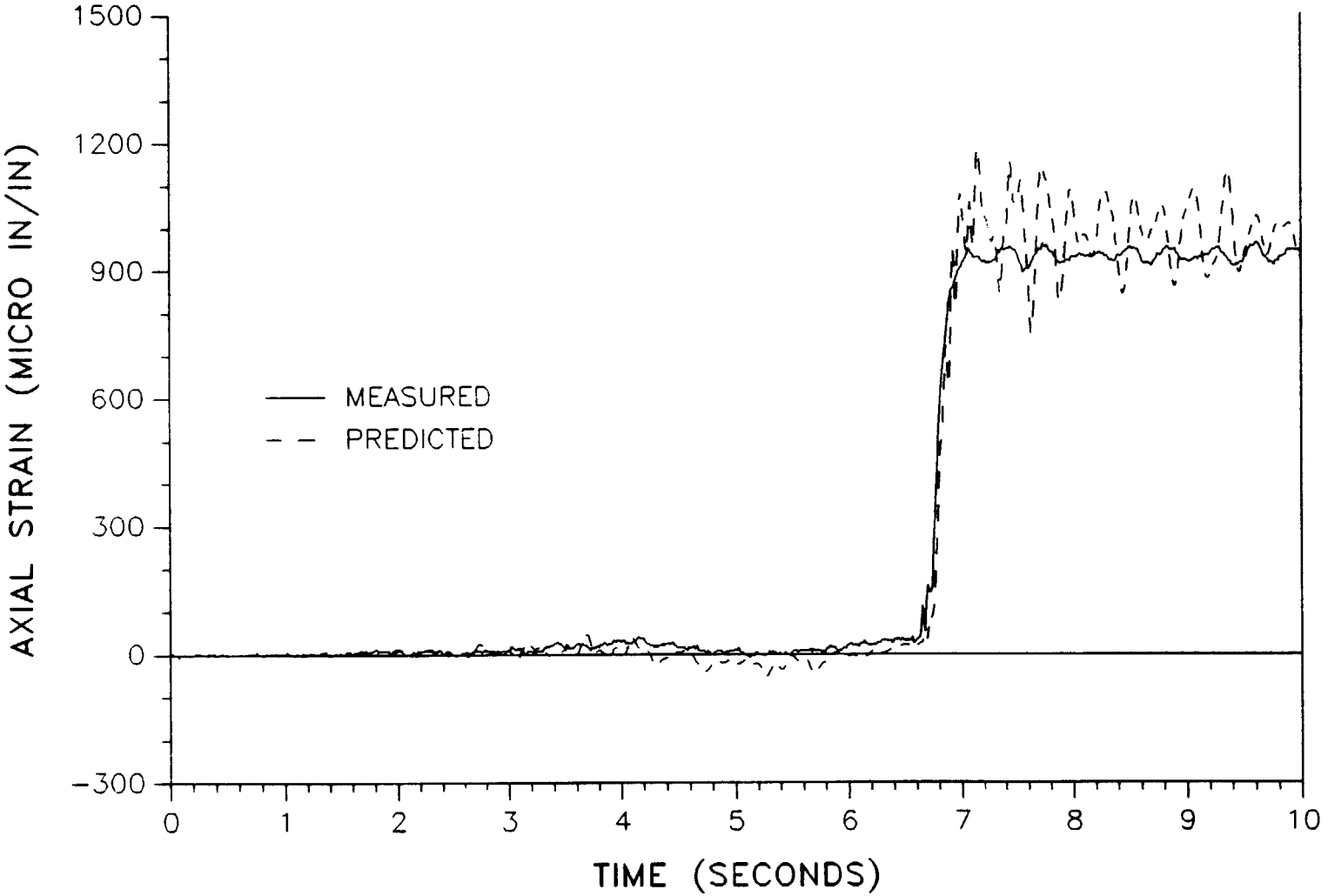

PREDICTED VS MEASURED AXIAL STRAIN

360L001 STRAIN GAGE B08G8390A – STATION 1501.0 AT 180 DEGREES

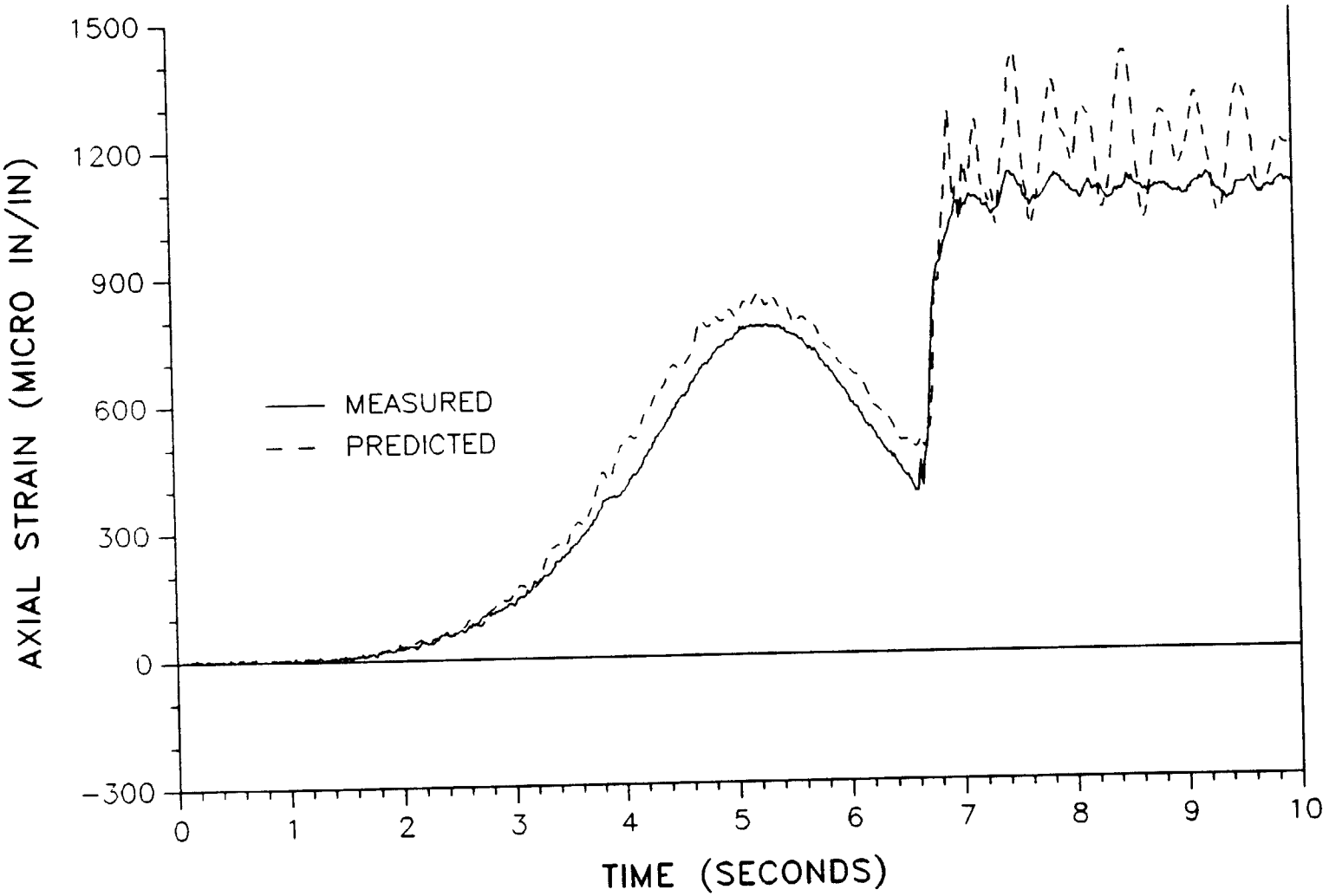

PREDICTED VS MEASURED AXIAL STRAIN

360L001 STRAIN GAGE B08G8392A – STATION 1501.0 AT 220 DEGREES

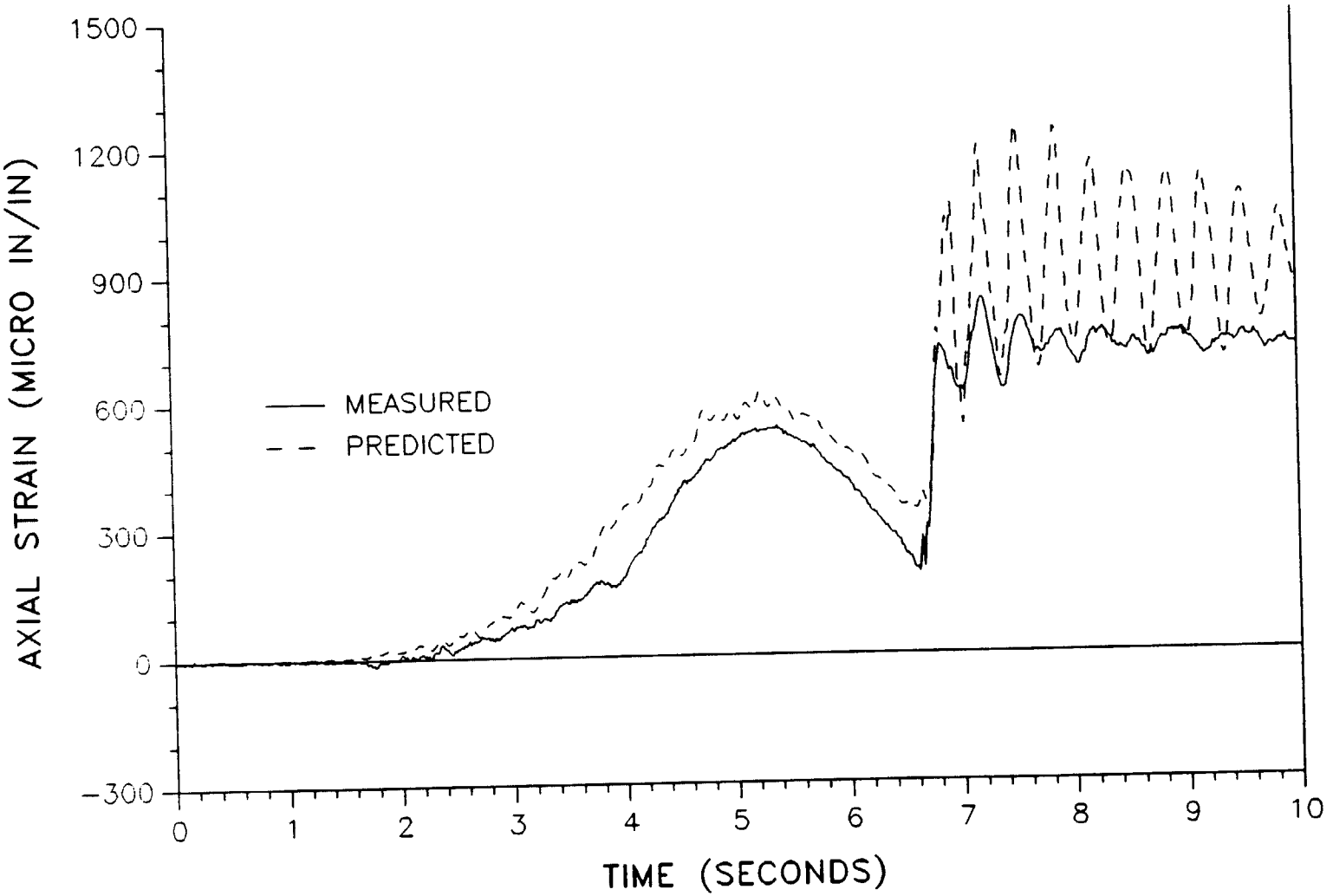

PREDICTED VS MEASURED AXIAL STRAIN

360L001 STRAIN GAGE B08G8394A – STATION 1501.0 AT 240 DEGREES

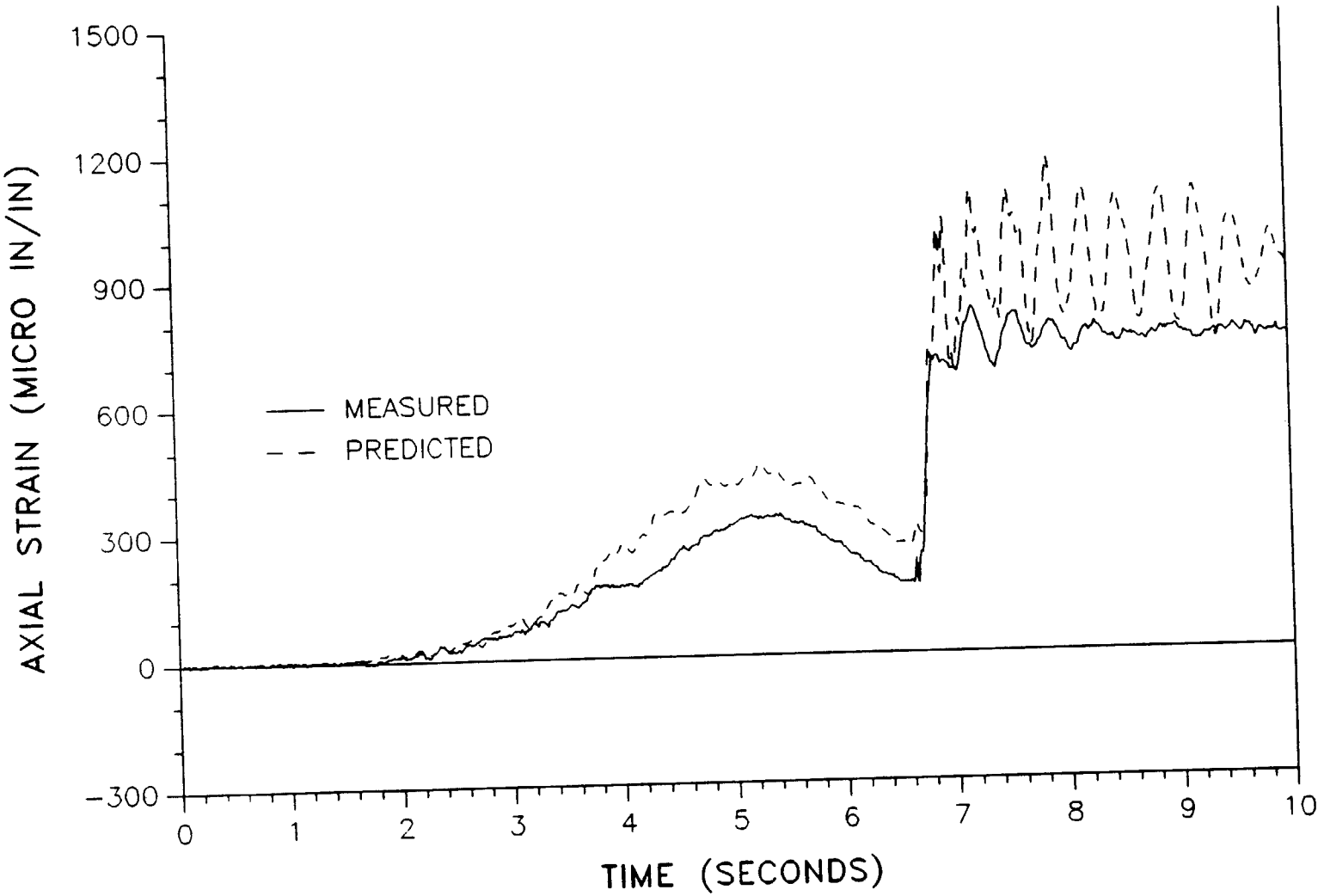

PREDICTED VS MEASURED AXIAL STRAIN

360L001 STRAIN GAGE B08G8396A – STATION 1501.0 AT 255 DEGREES

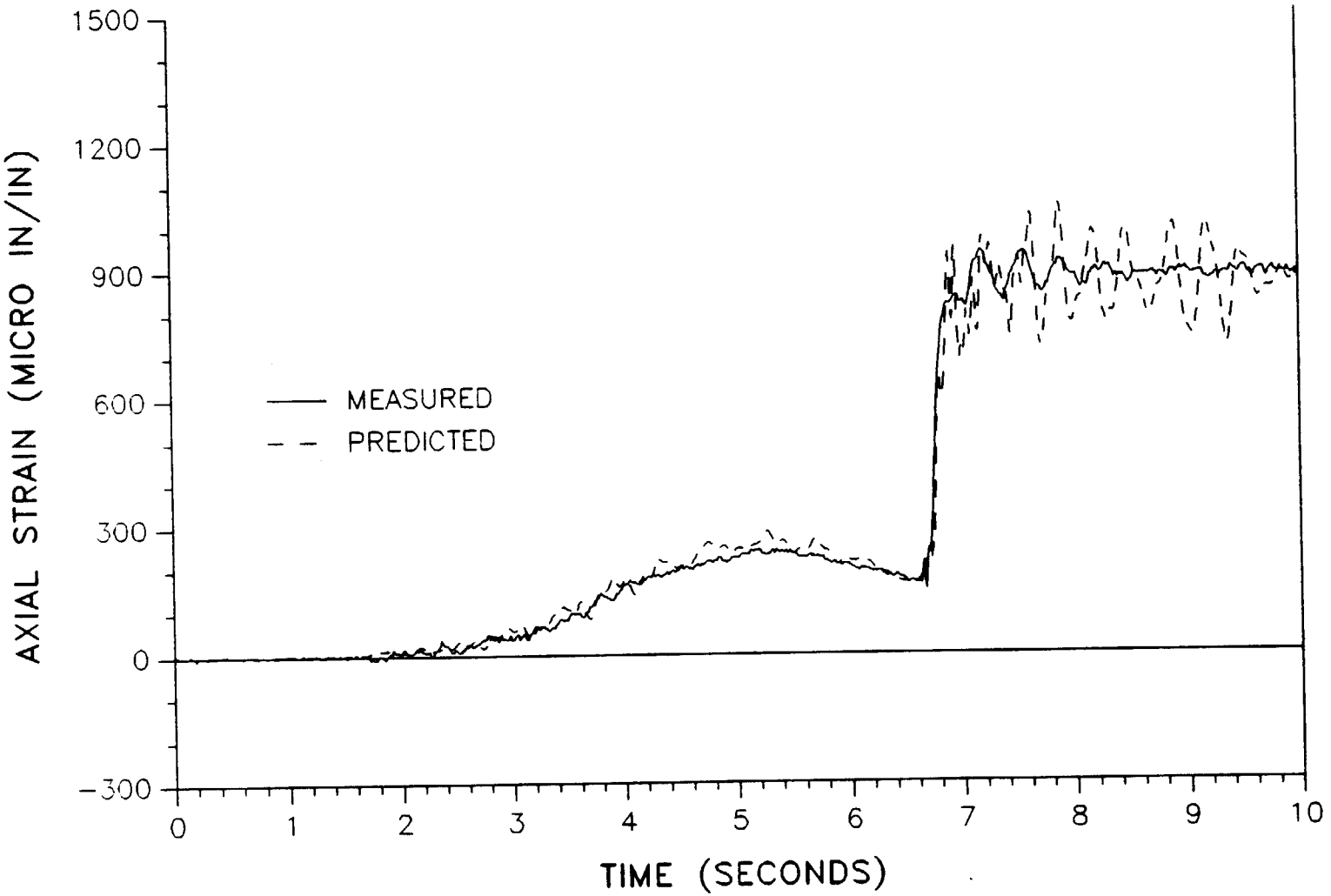

PREDICTED VS MEASURED AXIAL STRAIN

360L001 STRAIN GAGE B08G8398A – STATION 1501.0 AT 270 DEGREES

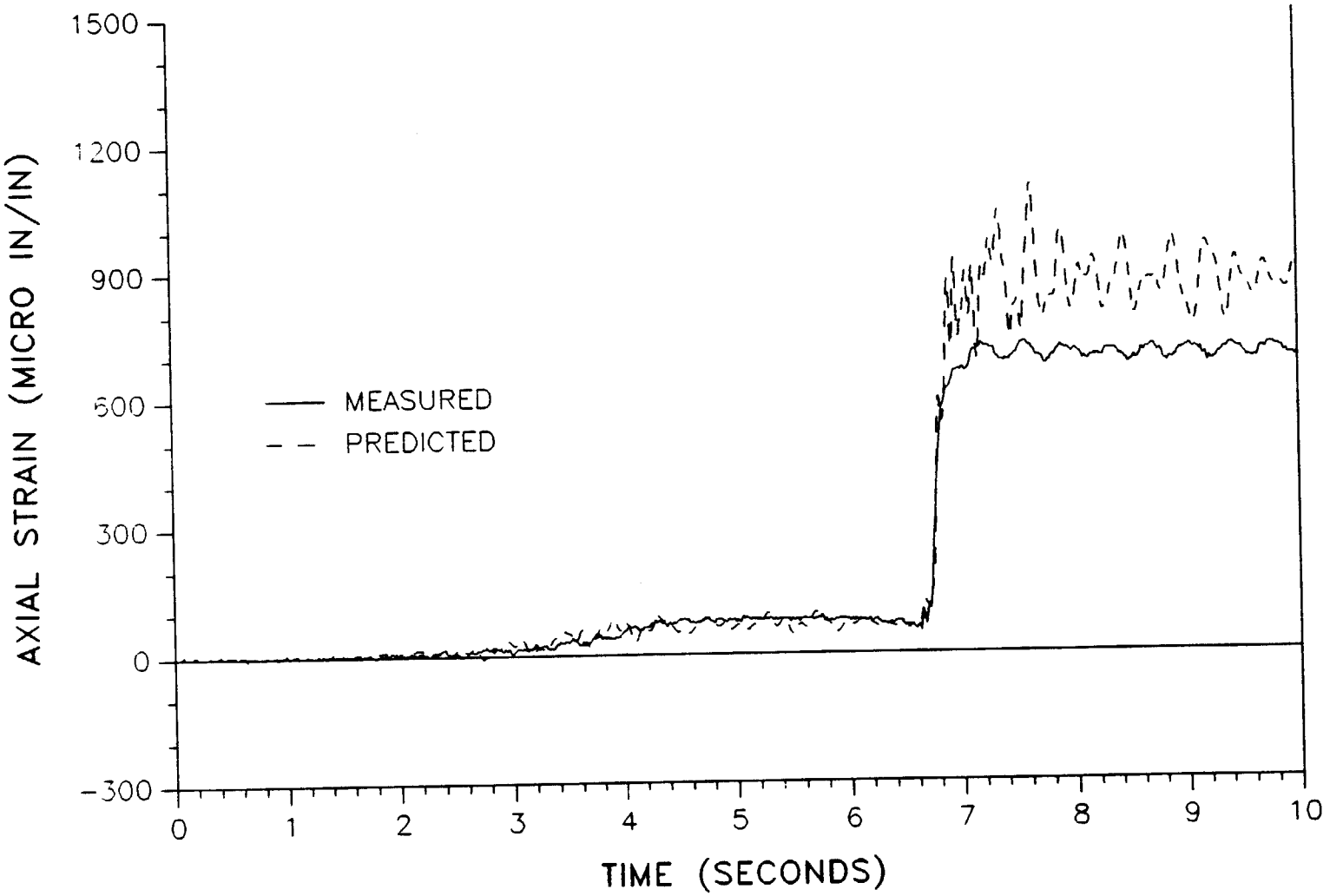

PREDICTED VS MEASURED AXIAL STRAIN

360L001 STRAIN GAGE B08G8400A – STATION 1501.0 AT 285 DEGREES

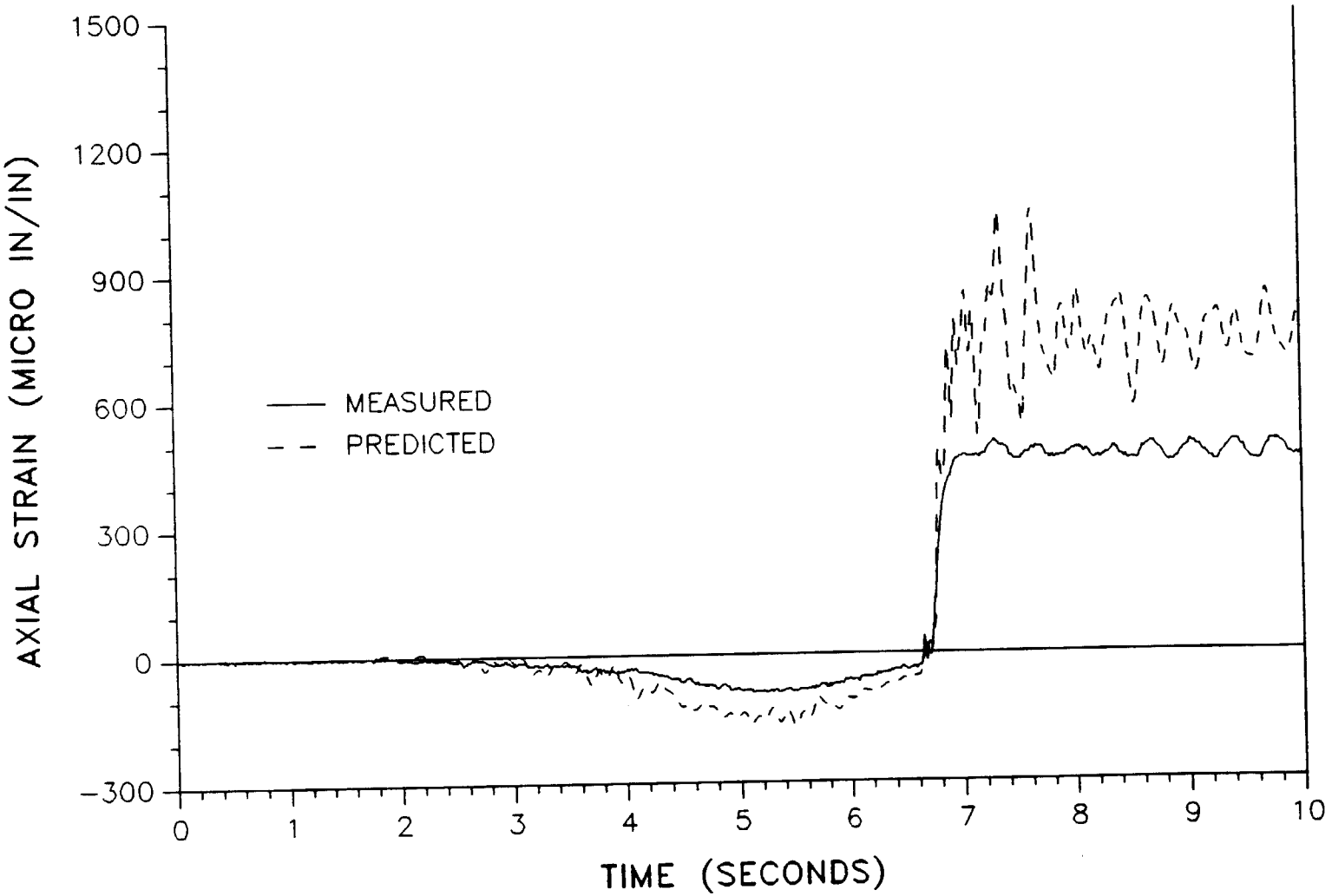

PREDICTED VS MEASURED AXIAL STRAIN

360L001 STRAIN GAGE B08G8402A – STATION 1501.0 AT 320 DEGREES

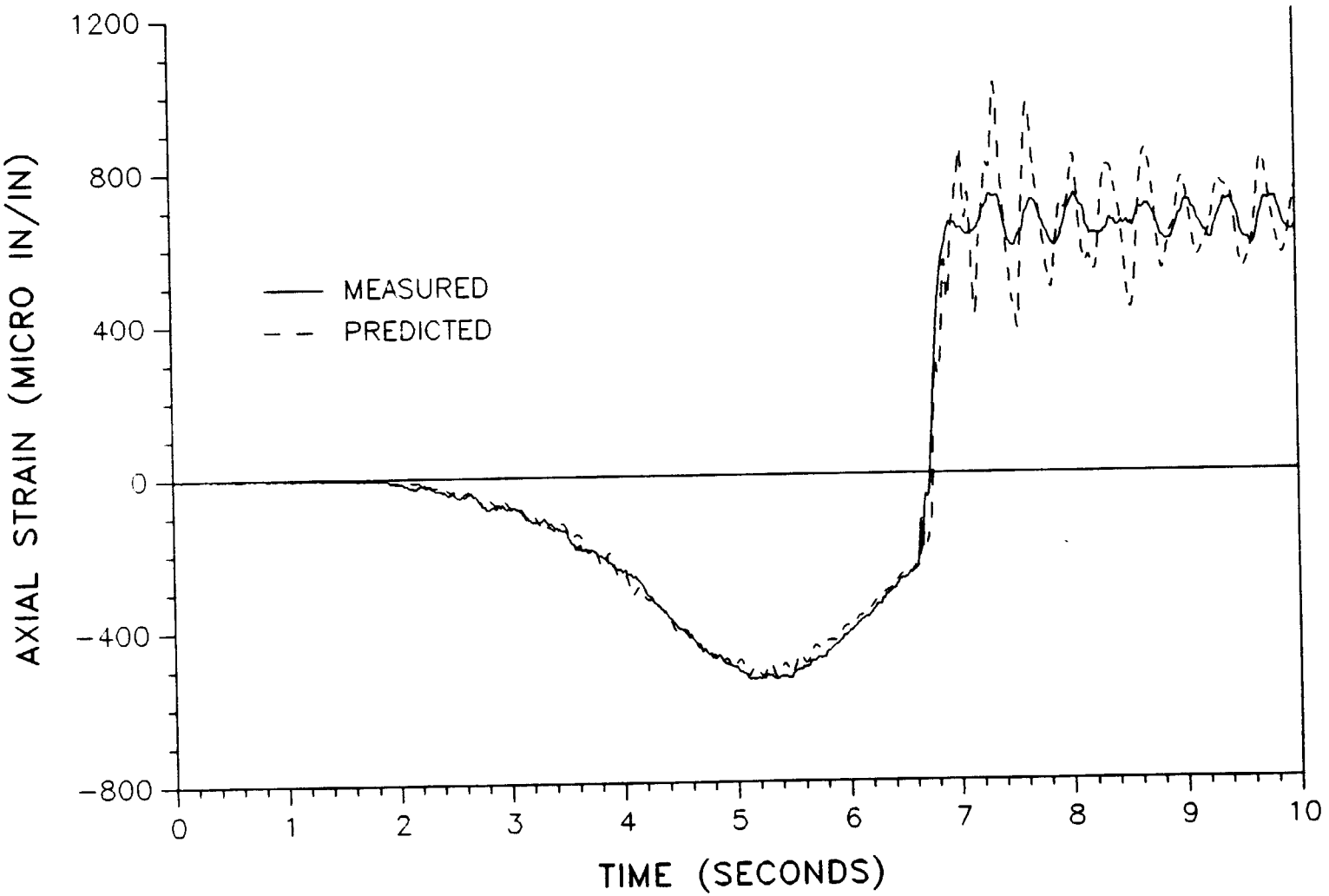

PREDICTED VS MEASURED AXIAL STRAIN

360L001 STRAIN GAGE B08G8404A – STATION 1797.0 AT 0 DEGREES

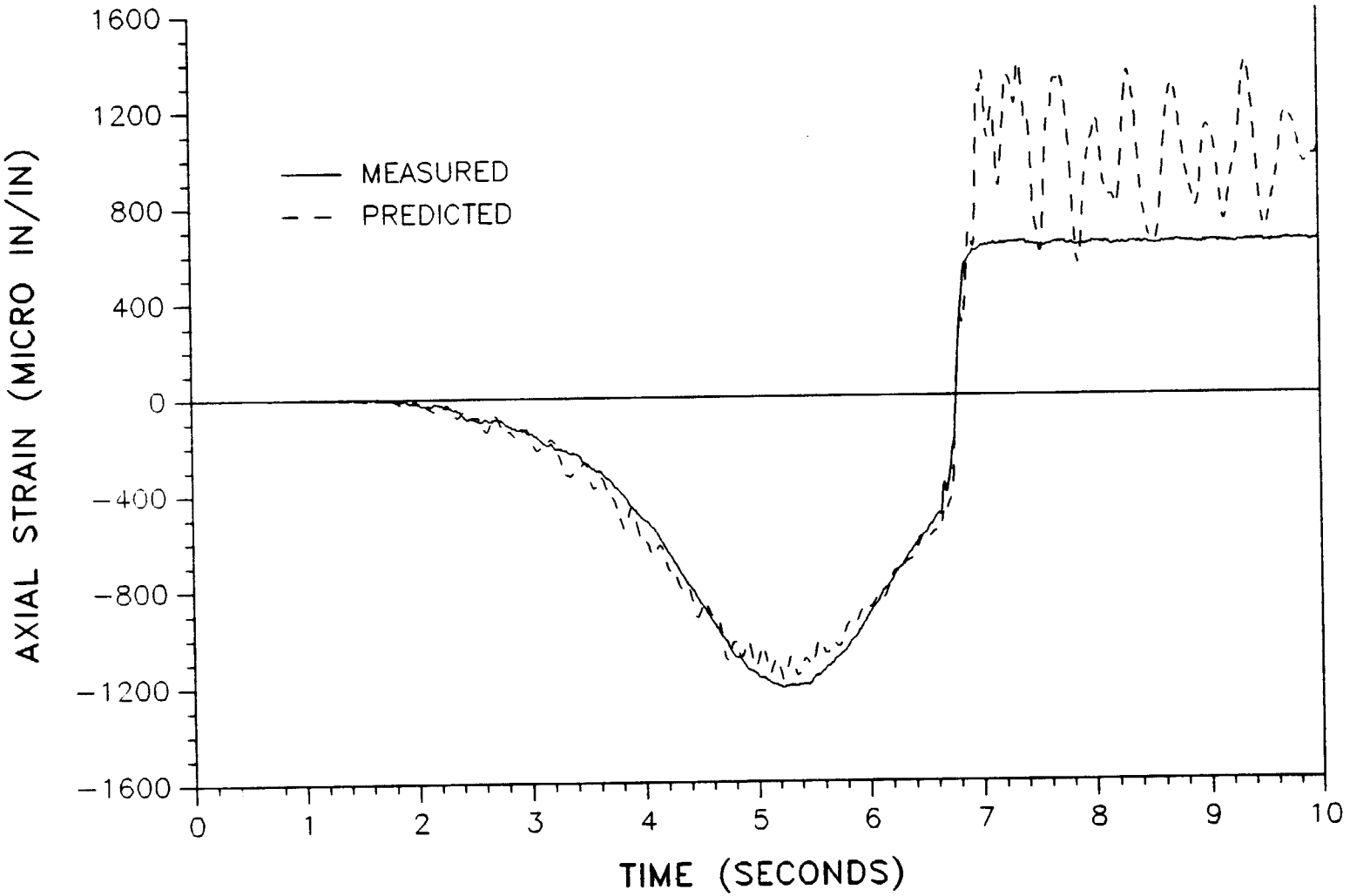

PREDICTED VS MEASURED AXIAL STRAIN

360L001 STRAIN GAGE B08G8406A – STATION 1797.0 AT 82 DEGREES

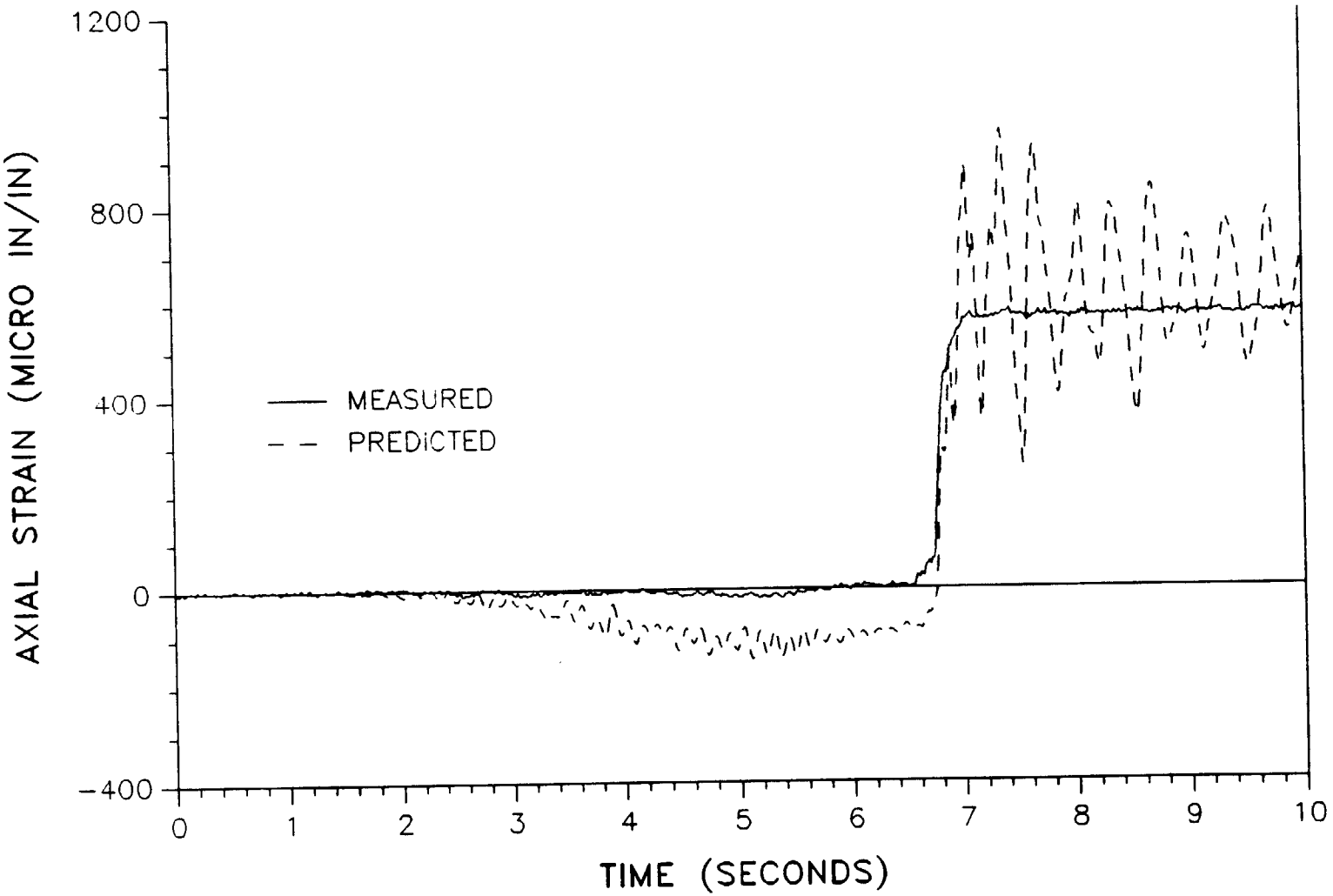

PREDICTED VS MEASURED AXIAL STRAIN

360L001 STRAIN GAGE B08G8404A – STATION 1797.0 AT 180 DEGREES

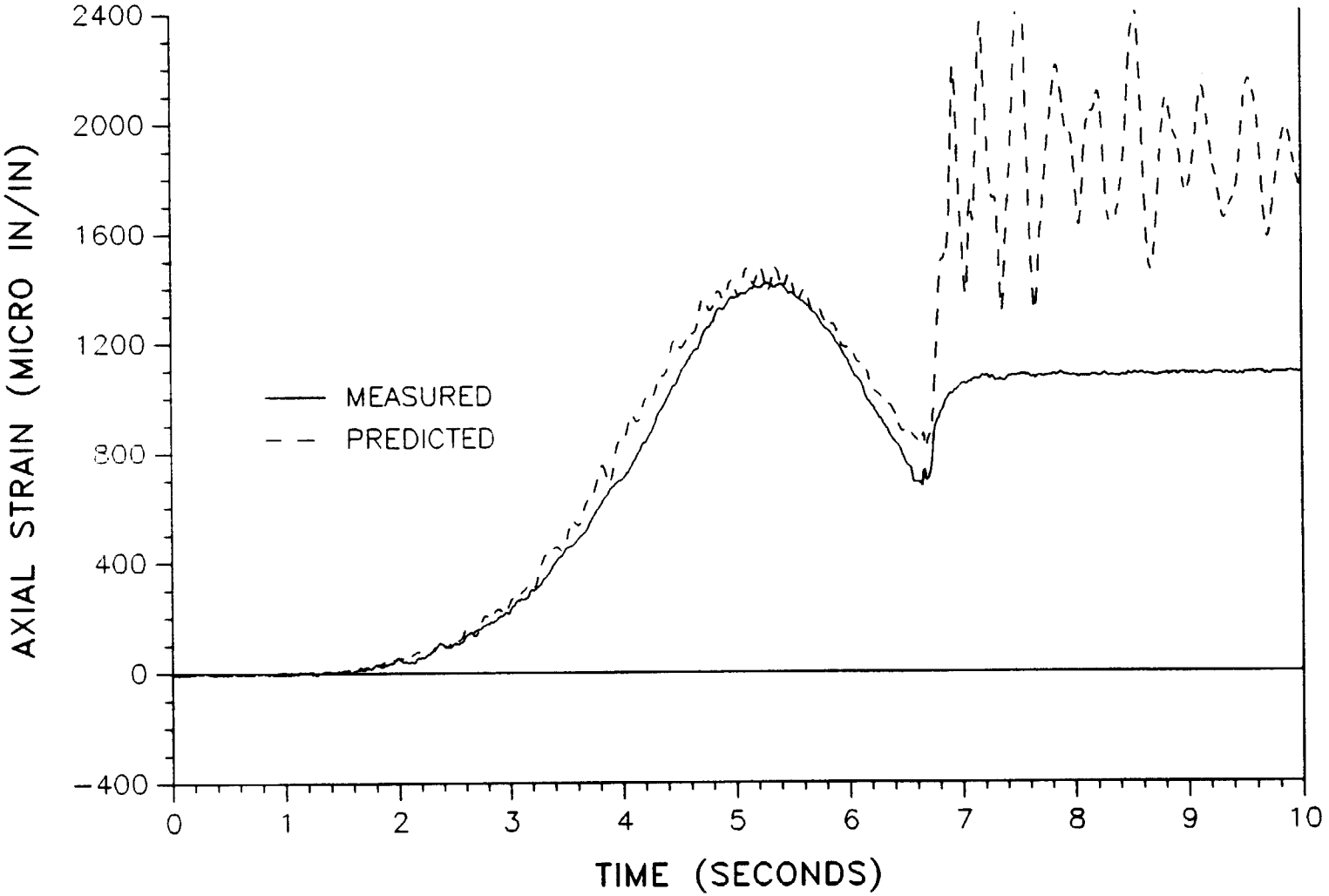

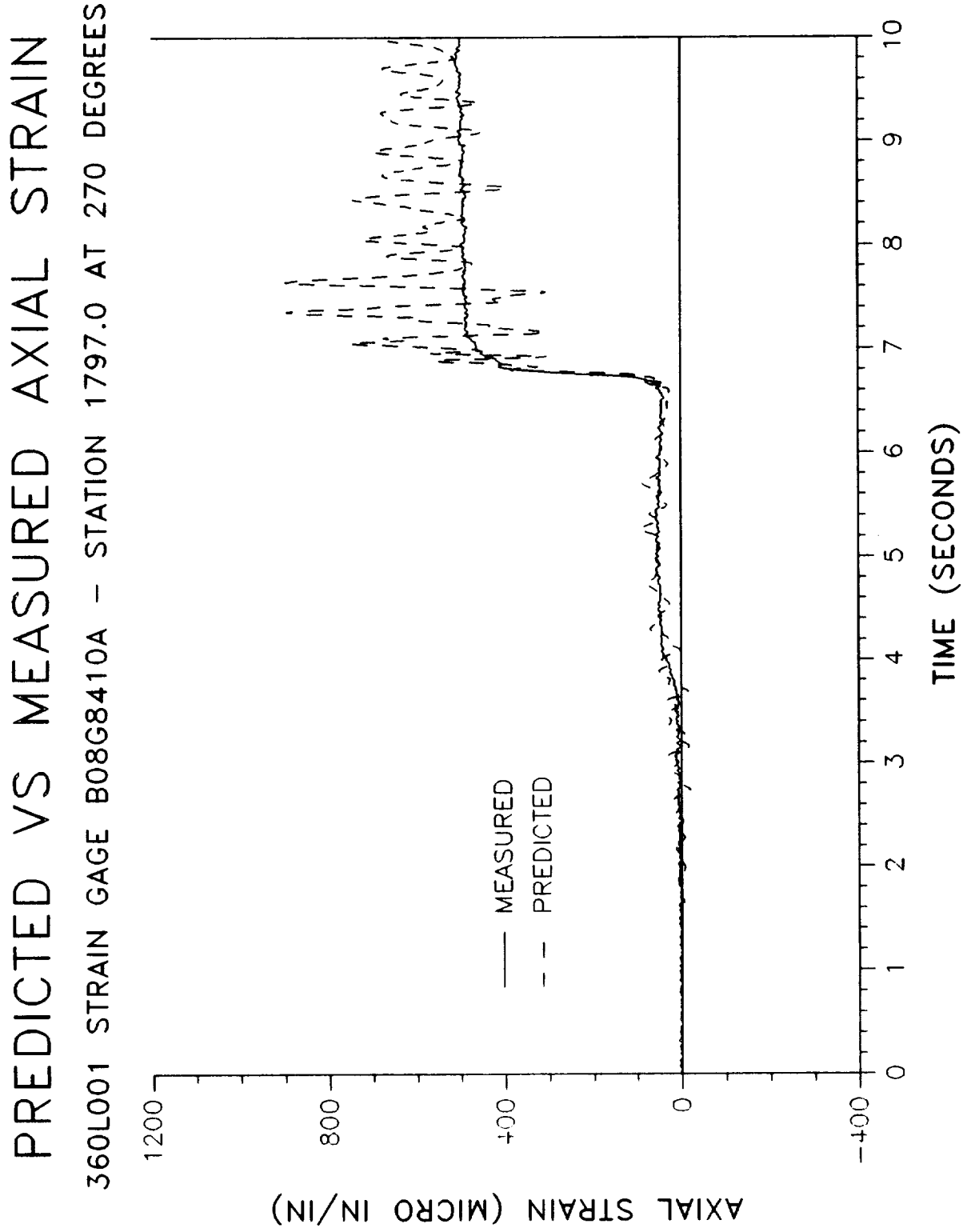
PREDICTED VS MEASURED AXIAL STRAIN
360L001 STRAIN GAGE B08G8410A - STATION 1797.0 AT 270 DEGREES
AXIAL STRAIN (MICRO IN/IN)
1200
800
400
0
-400
MEASURED
PREDICTED
0
1
2
3
4
5
6
7
8
9
10
TIME (SECONDS)

APPENDIX G

Acceleration Plots

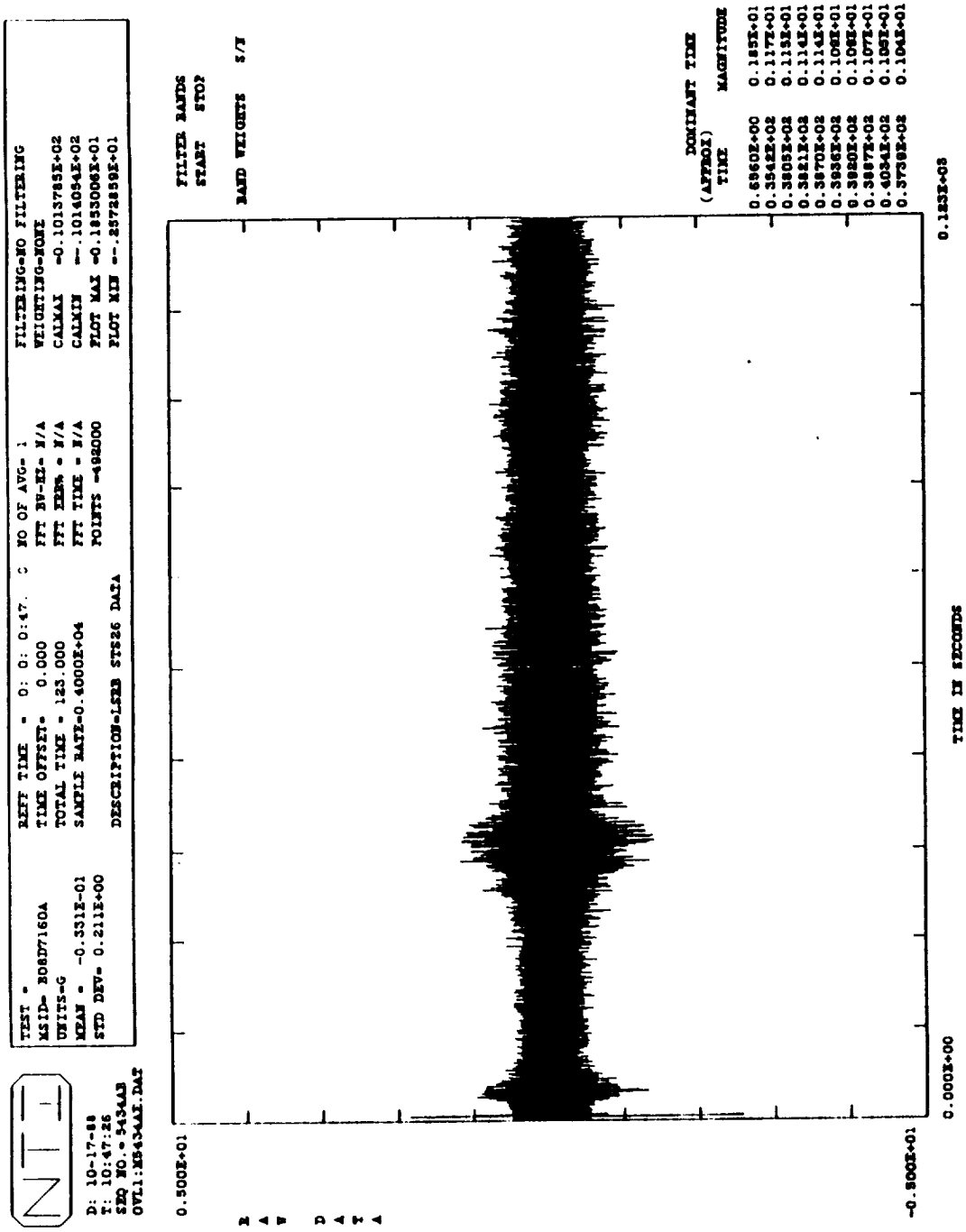

Time History of B08D7160

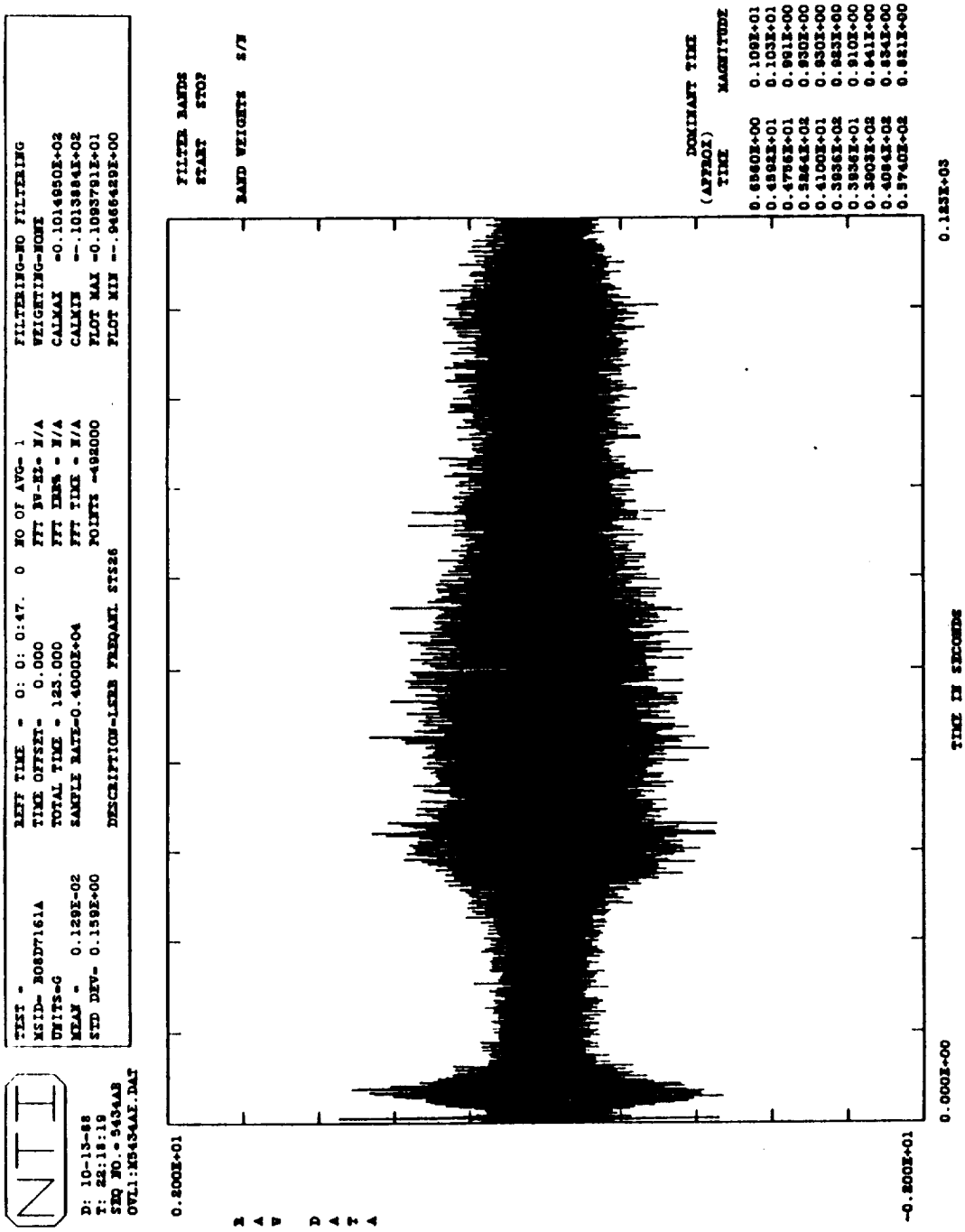

Time History of B08D7161

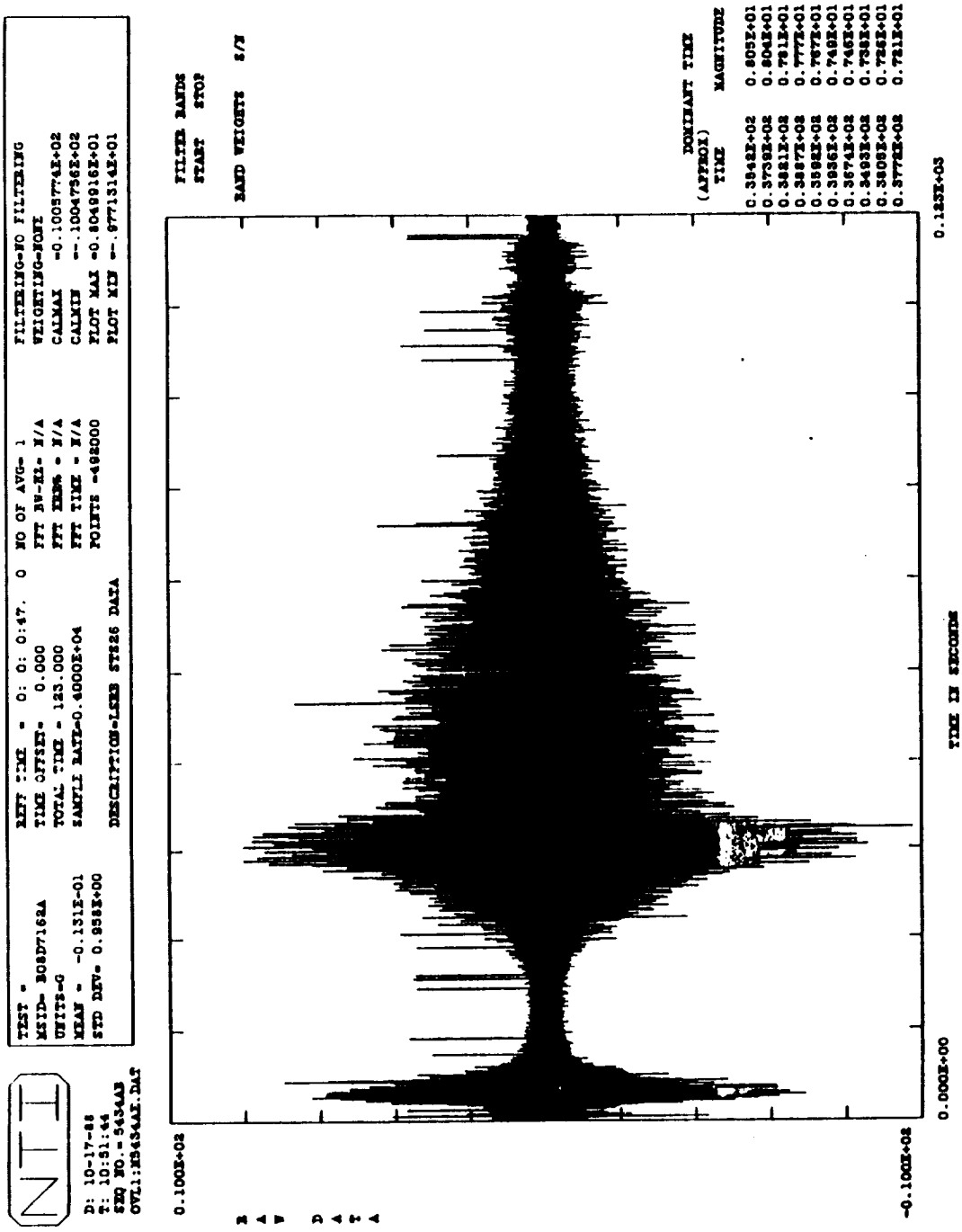

Time History of BO8D7162

ORIGINAL PAGE IS
OF POOR QUALITY

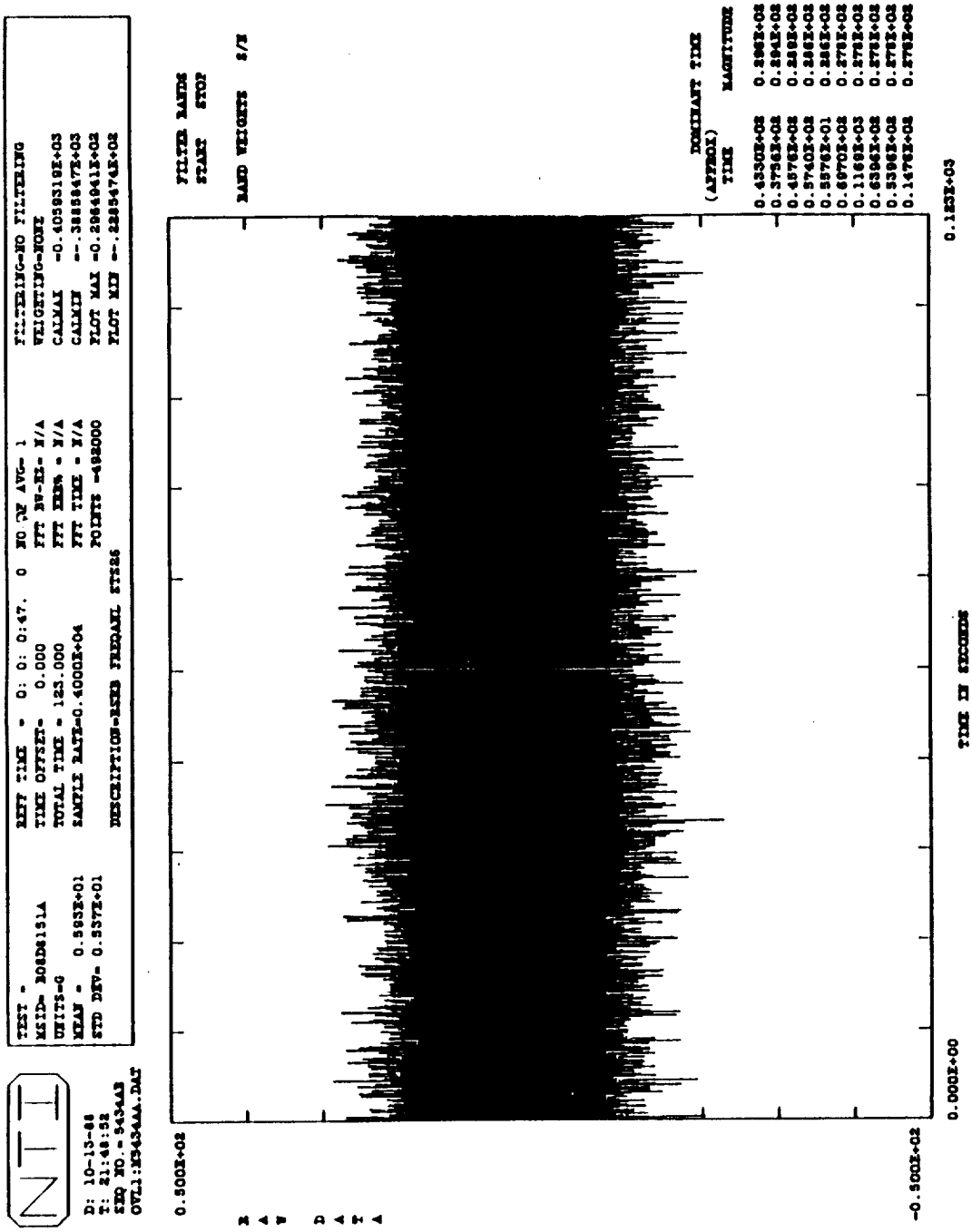

Time History of B08D8151

ORIGINAL PAGE IS
OF POOR QUALITY

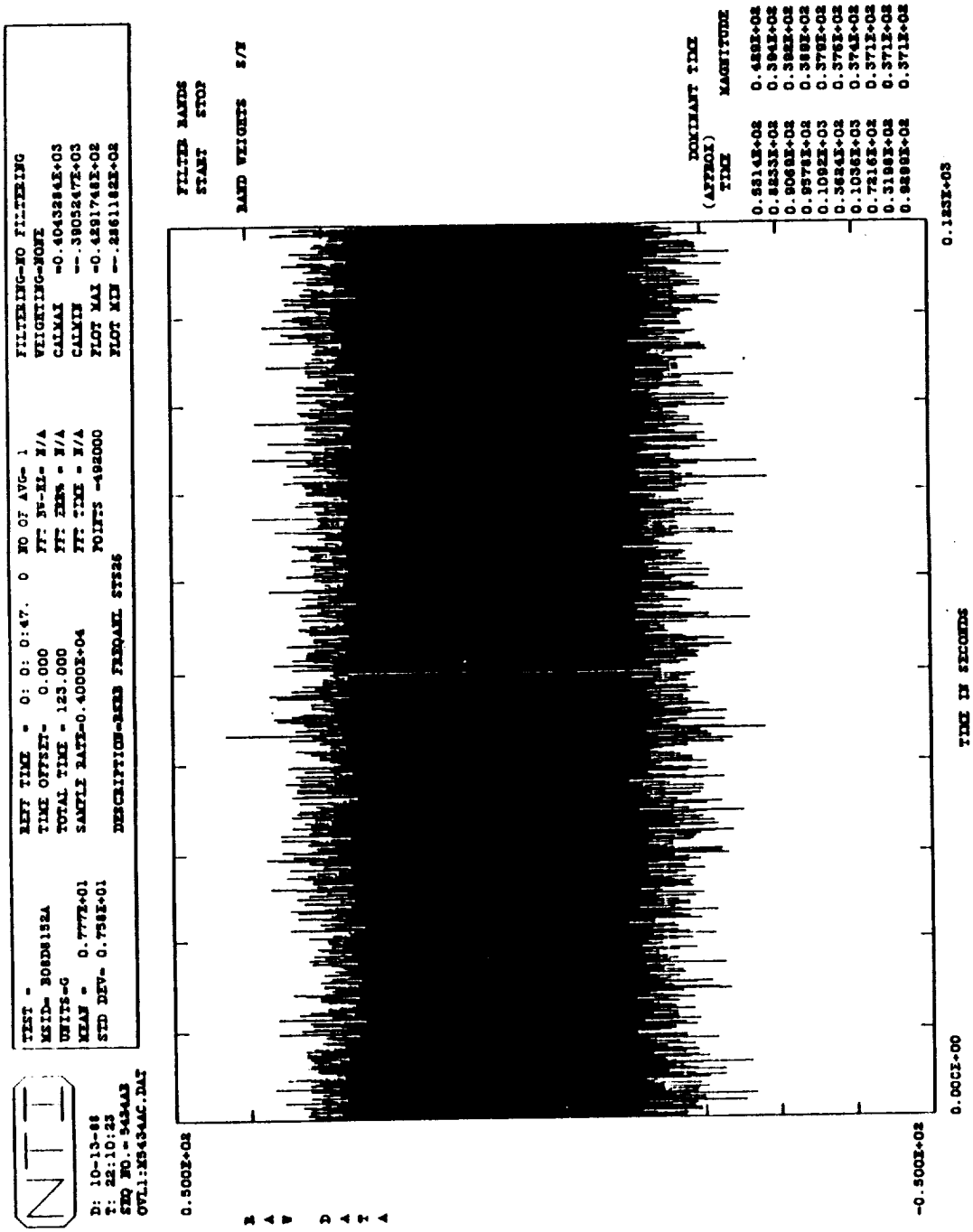

Time History of B08D8152

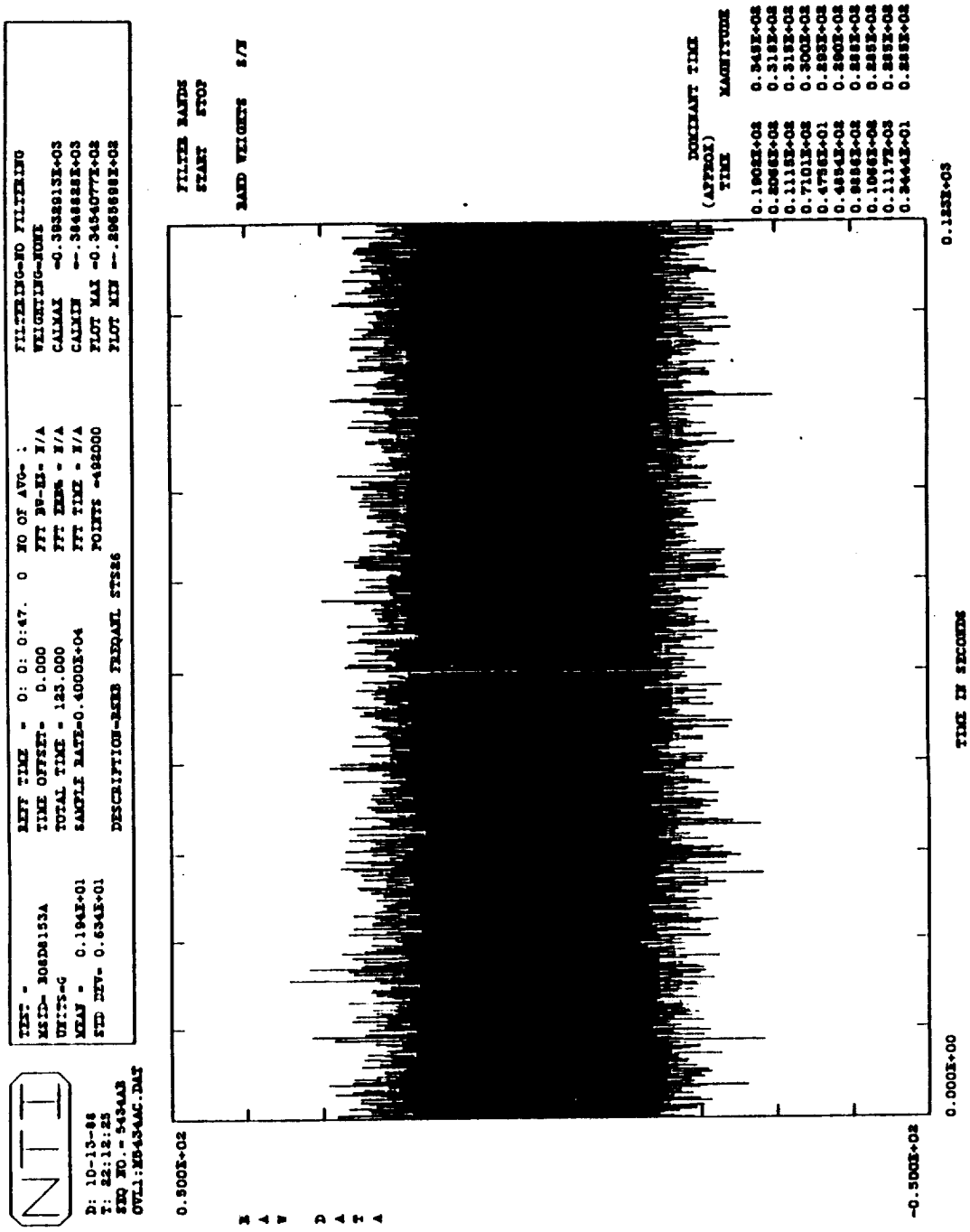

Time History of B08D8153

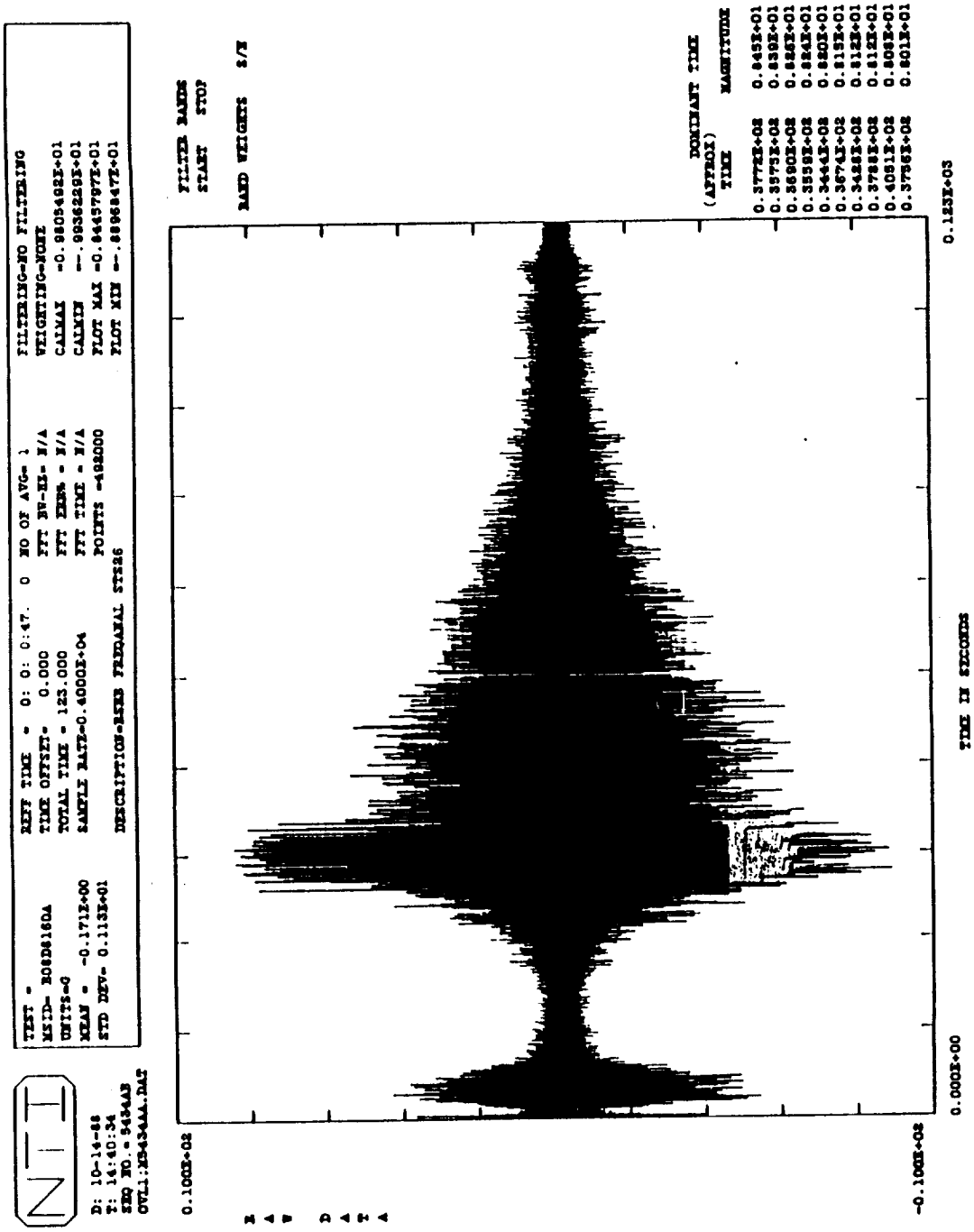

Time History of B08D8160

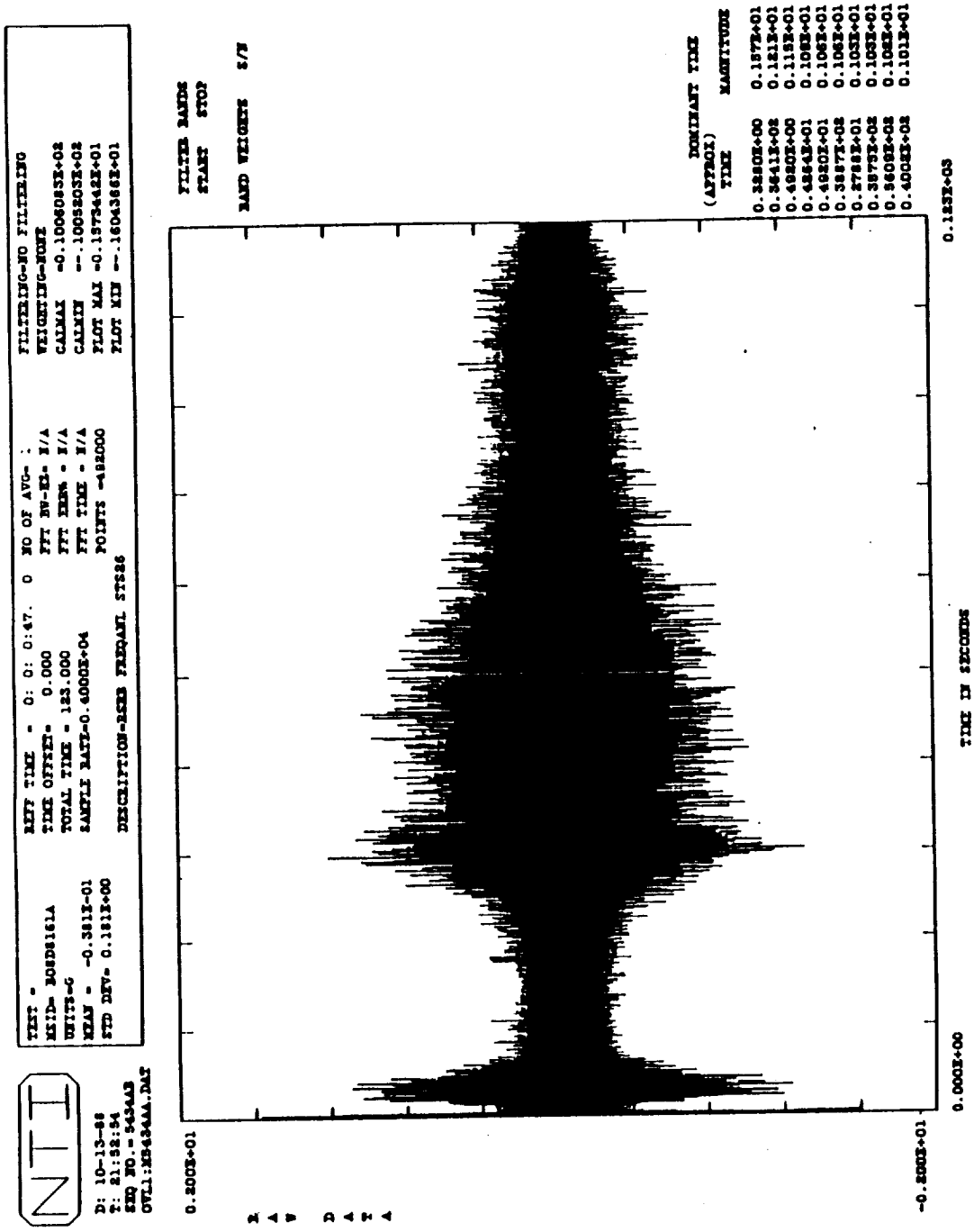

Time History of B08D8161

ORIGINAL PAGE IS
OF POOR QUALITY

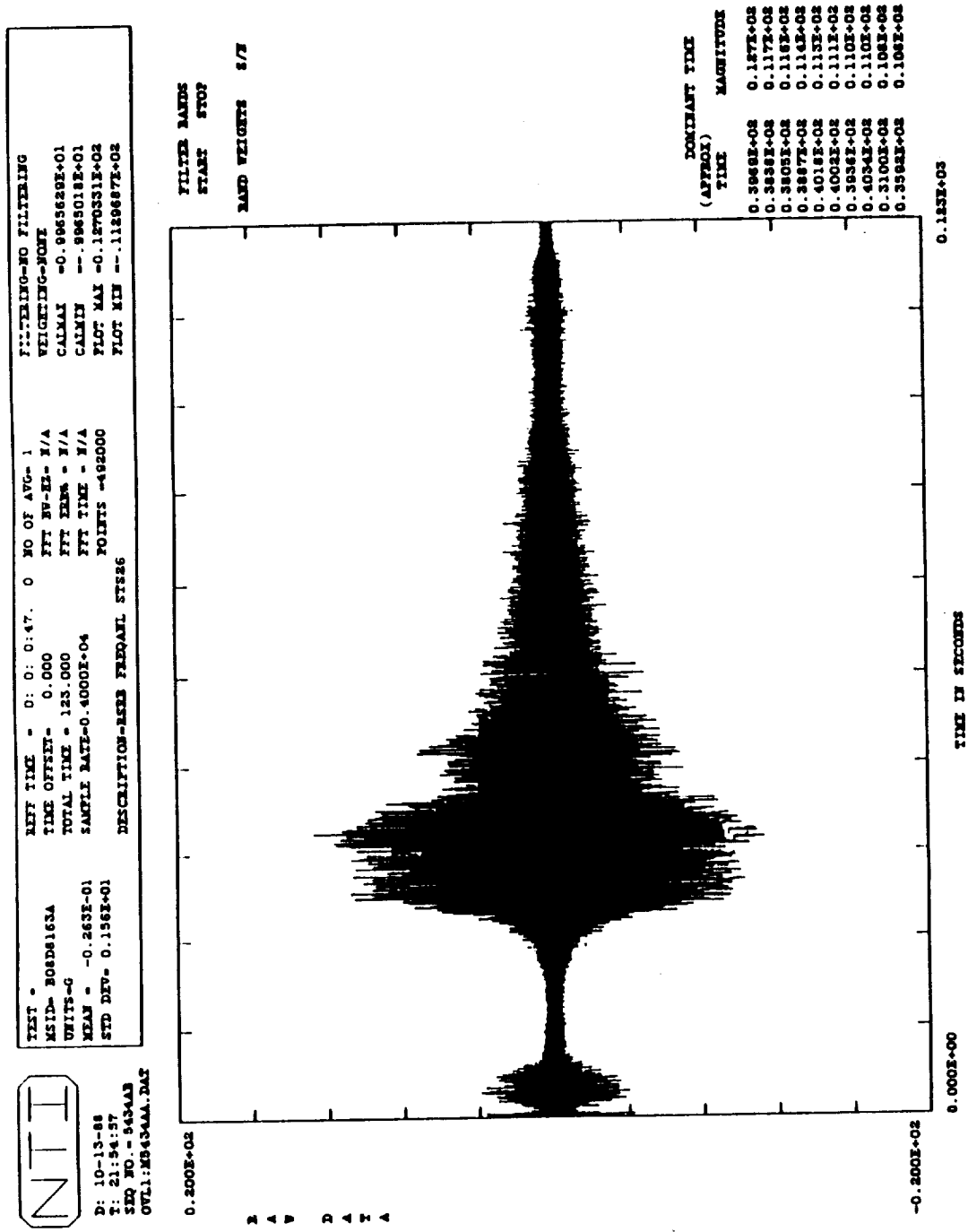

Time History of B08D8163

TIME HISTORY OF STS-26 ACCELEROMETER B08D7160A

DATA FILTERED TO 40 HZ

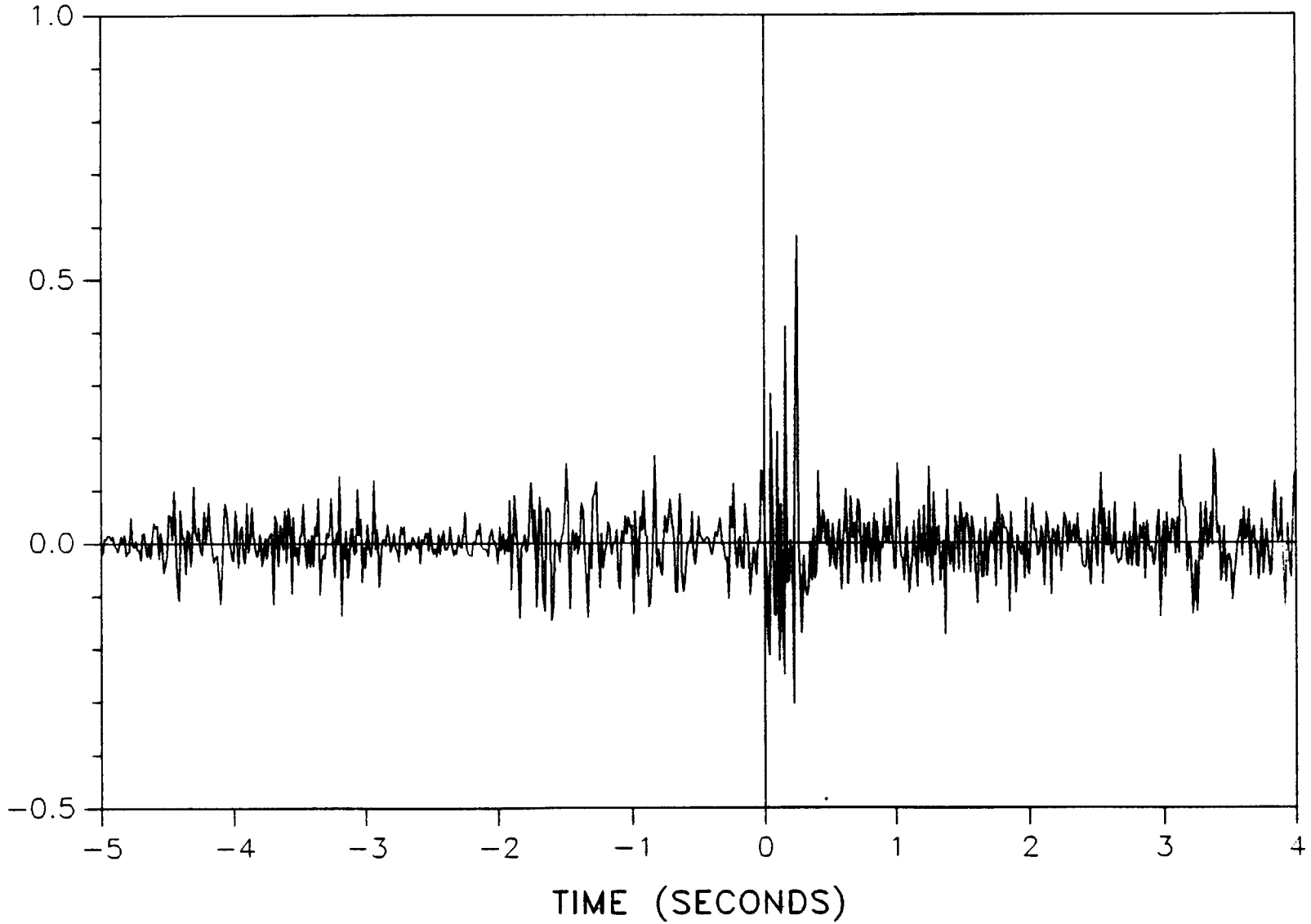

TIME HISTORY OF STS-26 ACCELEROMETER B08D7161A

DATA FILTERED TO 40 HZ

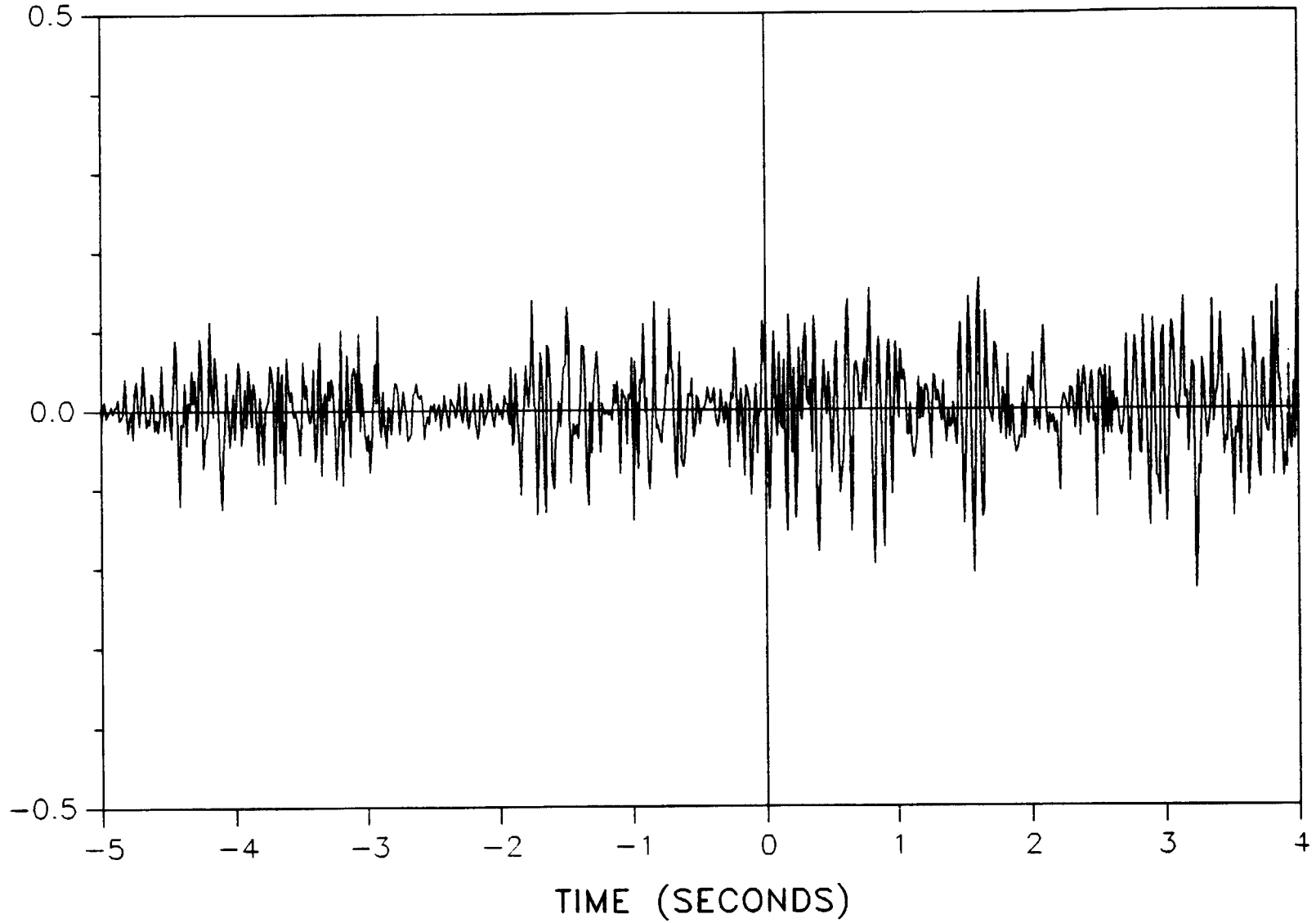

TIME HISTORY OF STS-26 ACCELEROMETER B08D7162A

DATA FILTERED TO 40 HZ

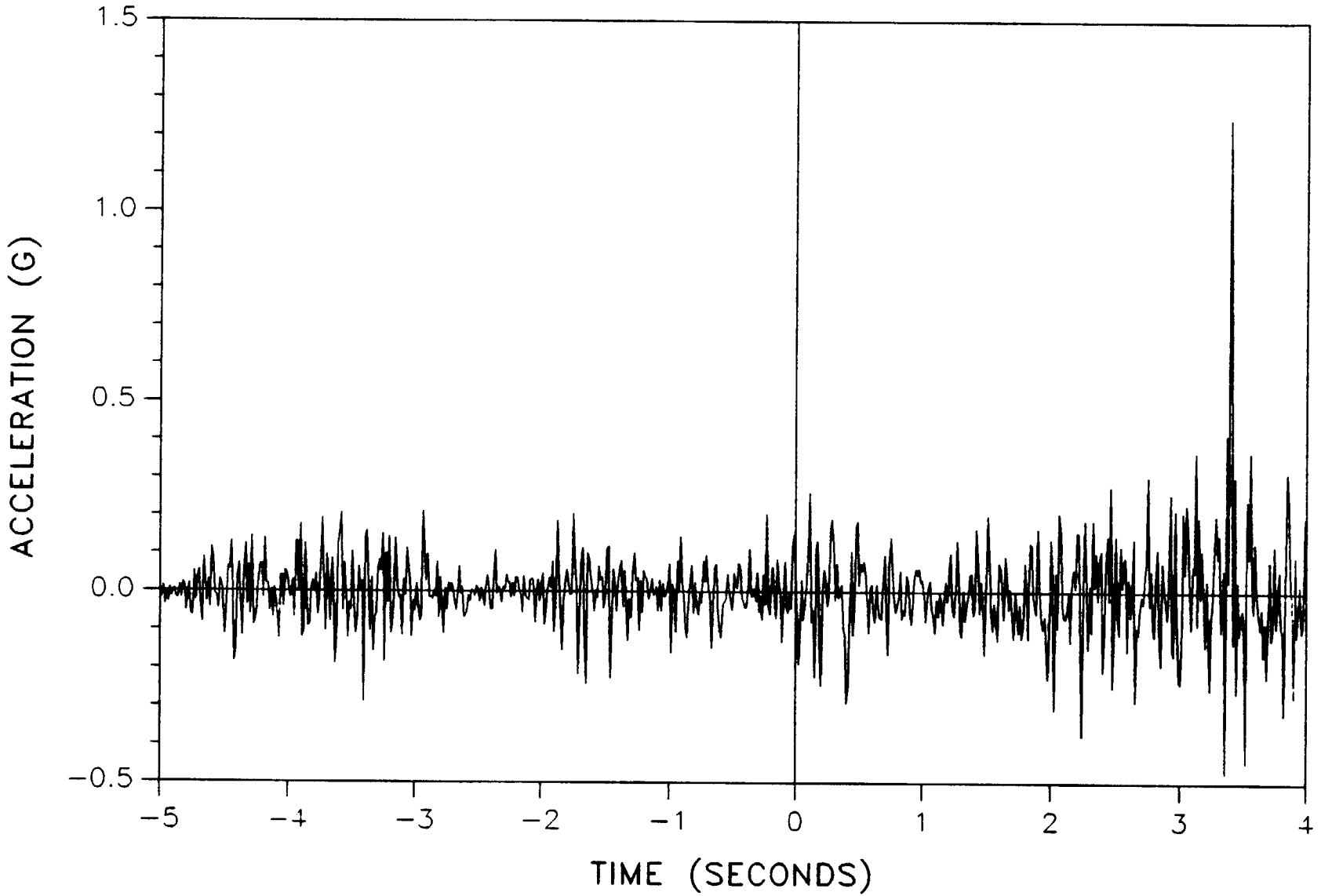

TIME HISTORY OF STS-26 ACCELEROMETER B08D8160A

DATA FILTERED TO 40 HZ

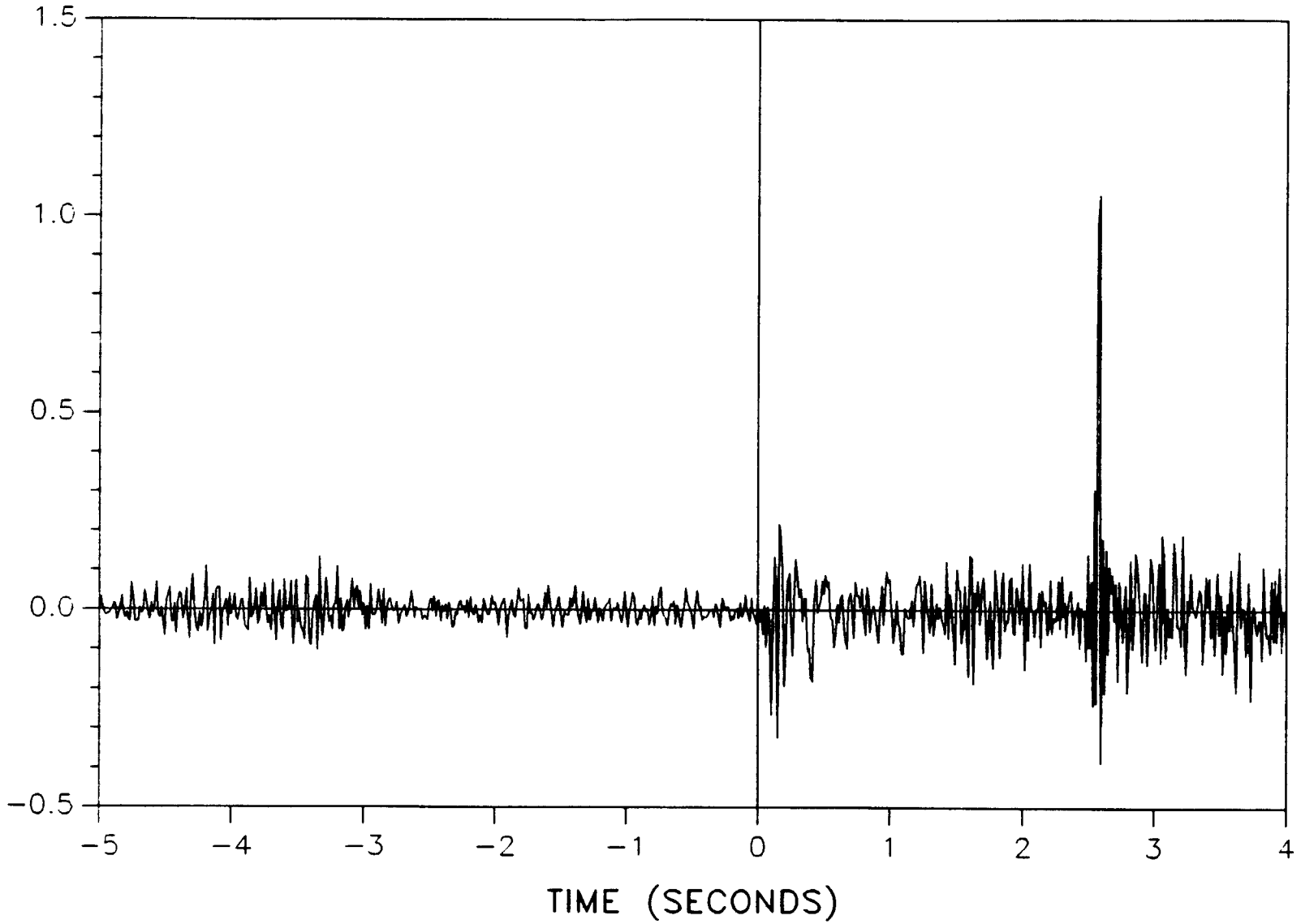

TIME HISTORY OF STS-26 ACCELEROMETER B08D8161A

DATA FILTERED TO 40 HZ

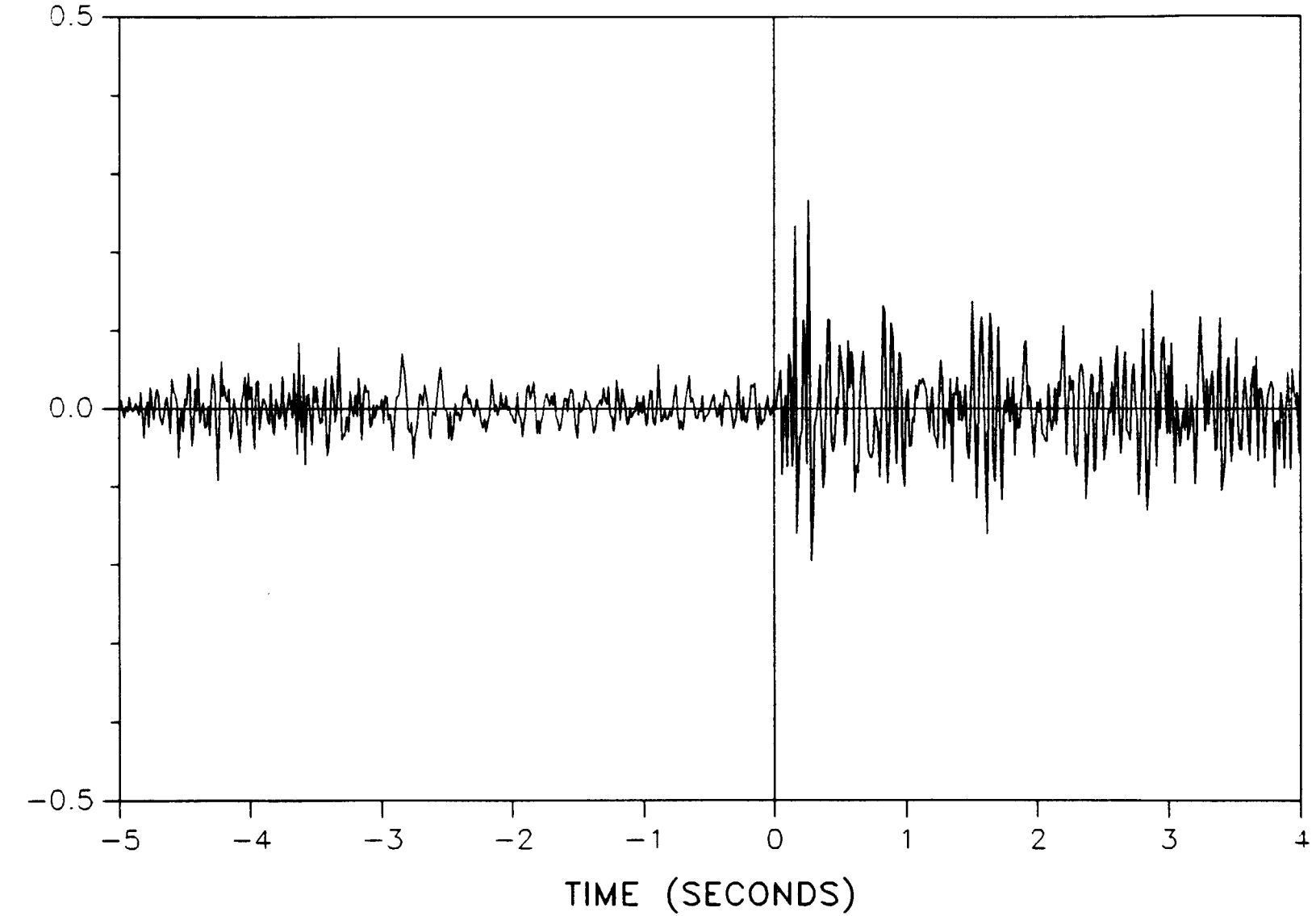

TIME HISTORY OF STS-26 ACCELEROMETER B08D8163A

DATA FILTERED TO 40 HZ

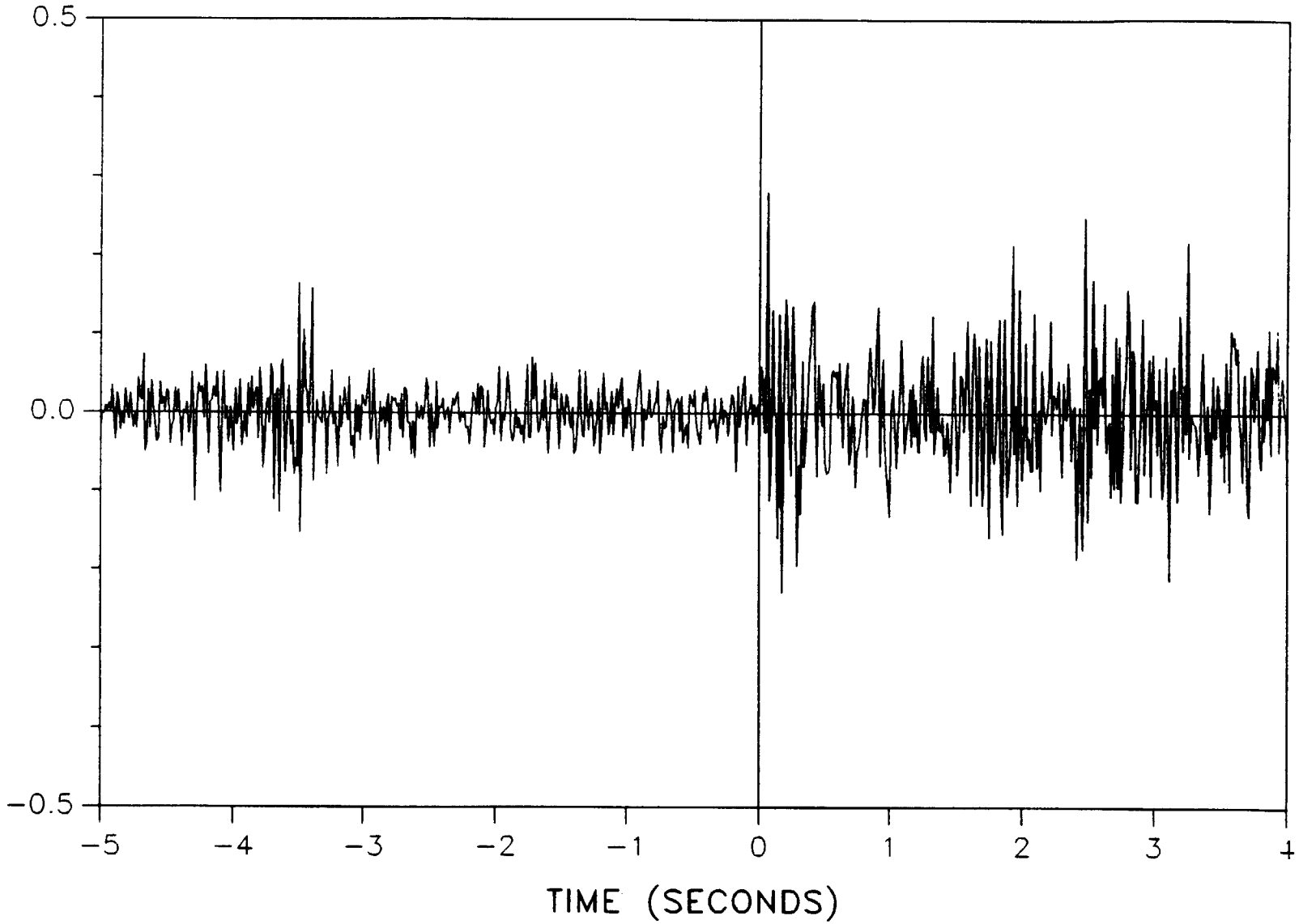

PREDICTED STS-26 RADIAL ACCELERATION - GAGE B08D7162A

STATION 500.0 AT 0 DEGREES

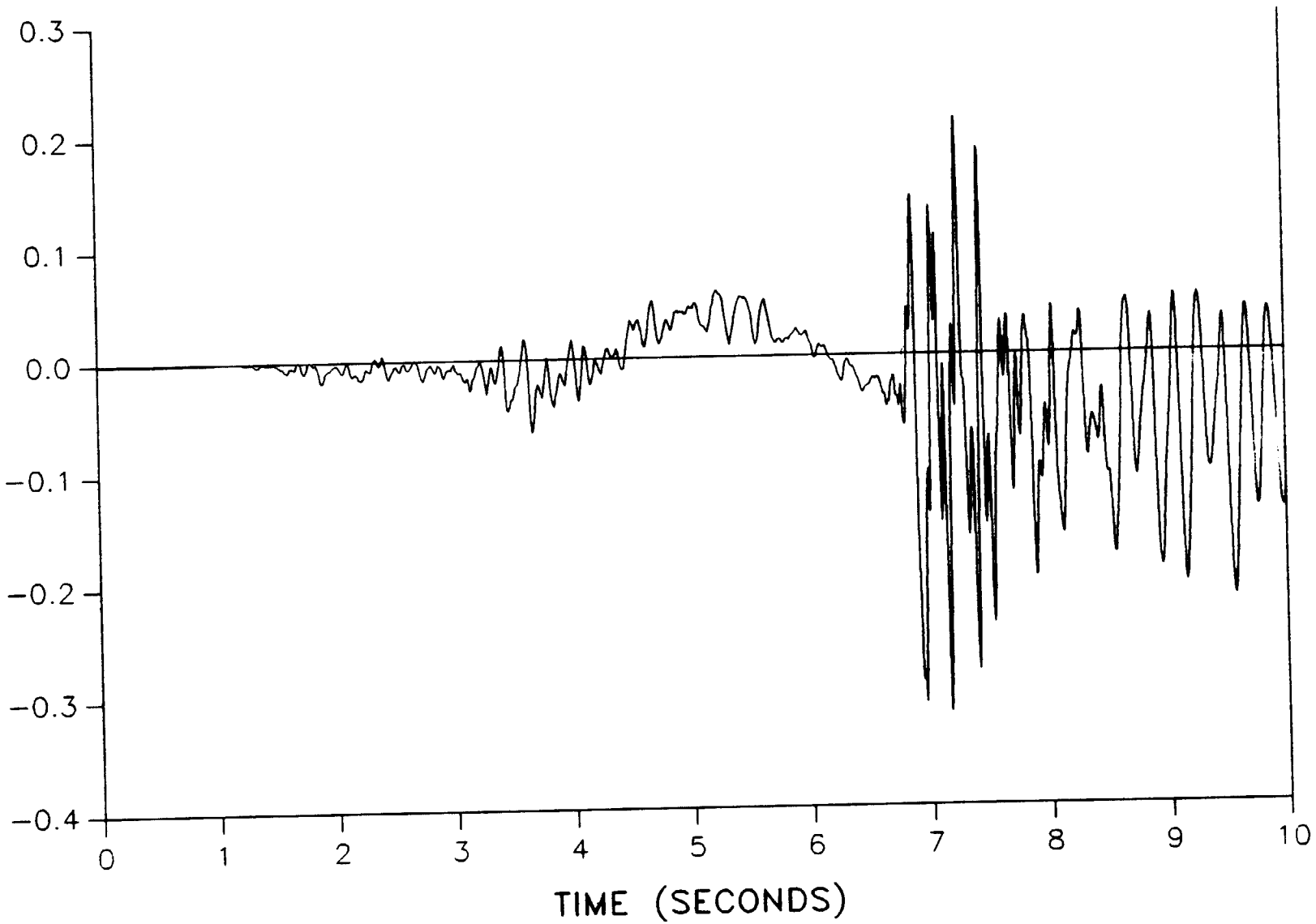

PREDICTED STS-26 TANG ACCELERATION - GAGE B08D7161A

STATION 500.0 AT 0 DEGREES

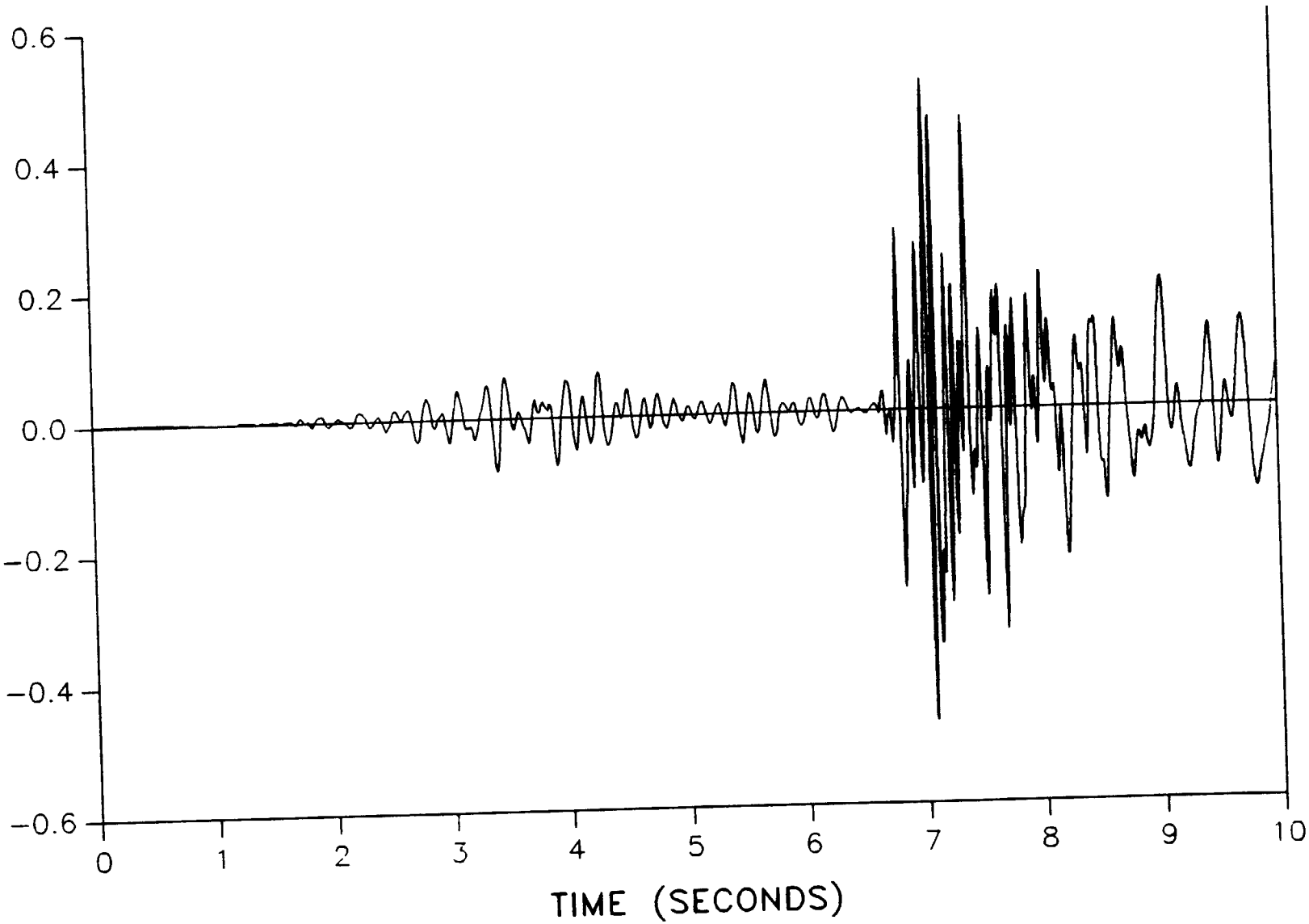

PREDICTED STS-26 AXIAL ACCELERATION – GAGE B08D7160A

STATION 500.0 AT 0 DEGREES

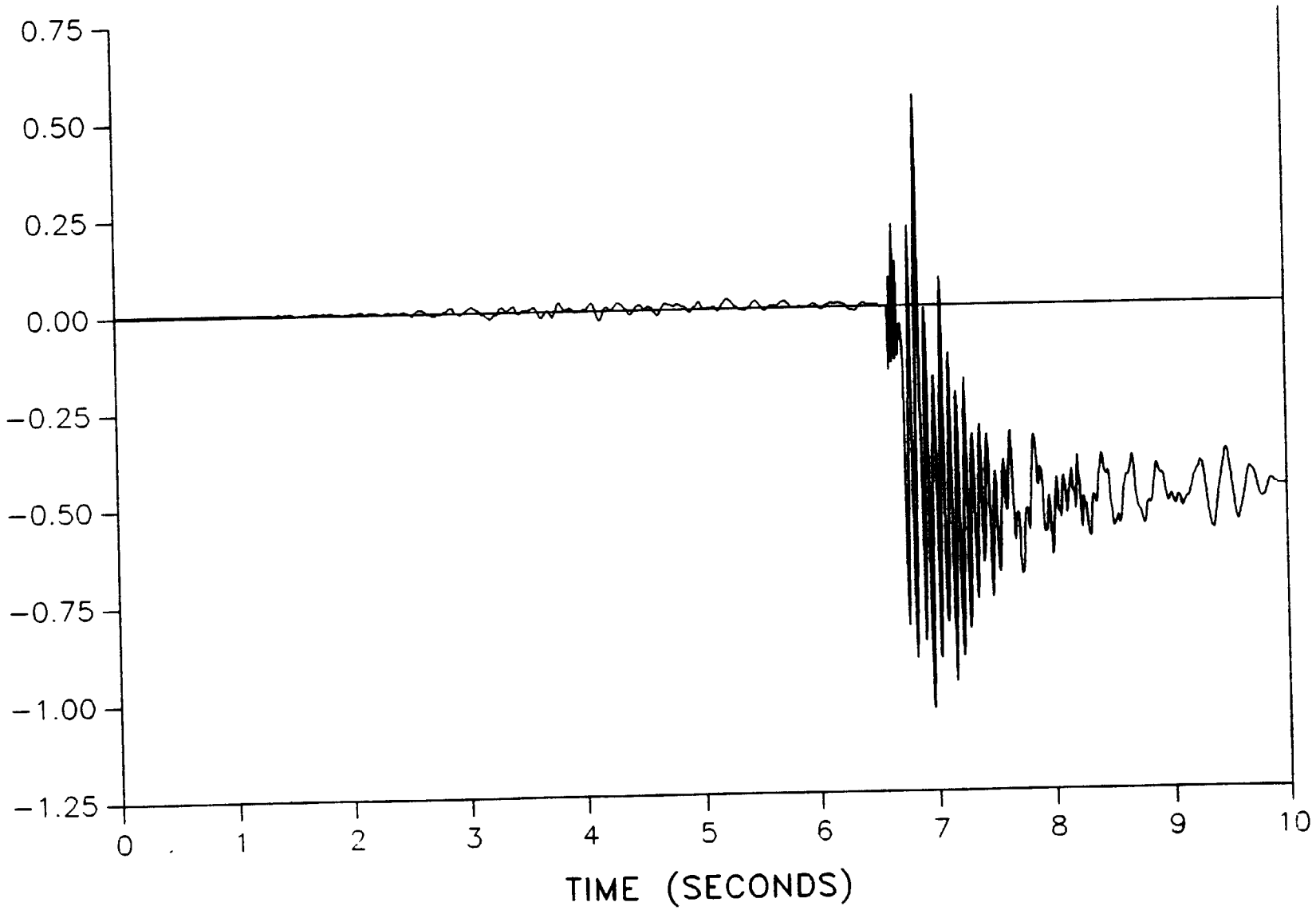

PREDICTED STS-26 AXIAL ACCELERATION - APPROX STA. 500.

GAGES B08D8151A AND B08D8160A - 180 DEGREES

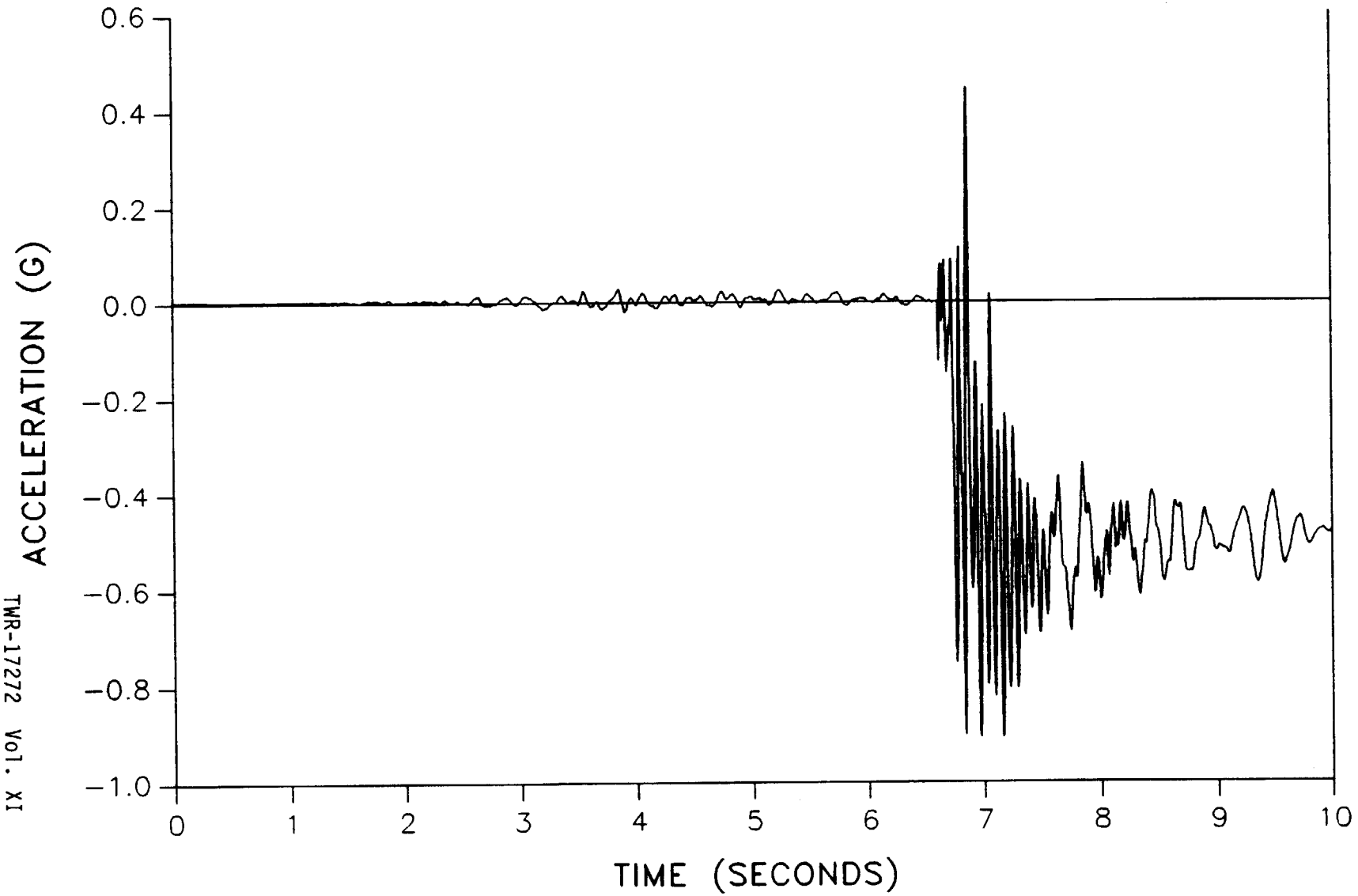

PREDICTED STS-26 RADIAL ACCELERATION – GAGE B08D8152A

STATION 487.0 AT 180 DEGREES

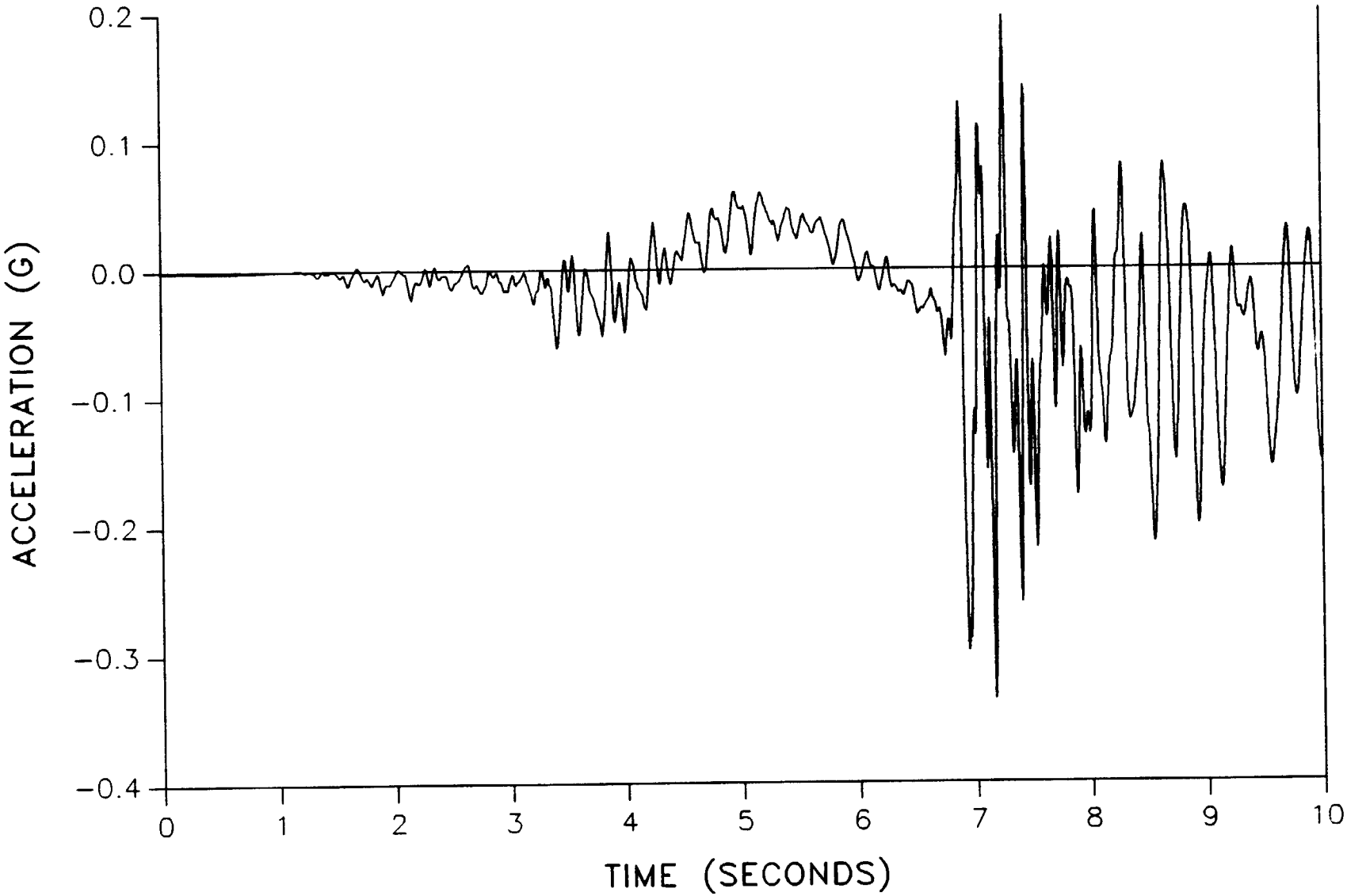

PREDICTED STS-26 TANG ACCELERATION - APPROX STA. 500

GAGES B08D153A AND B08D161A - 180 DEGREES

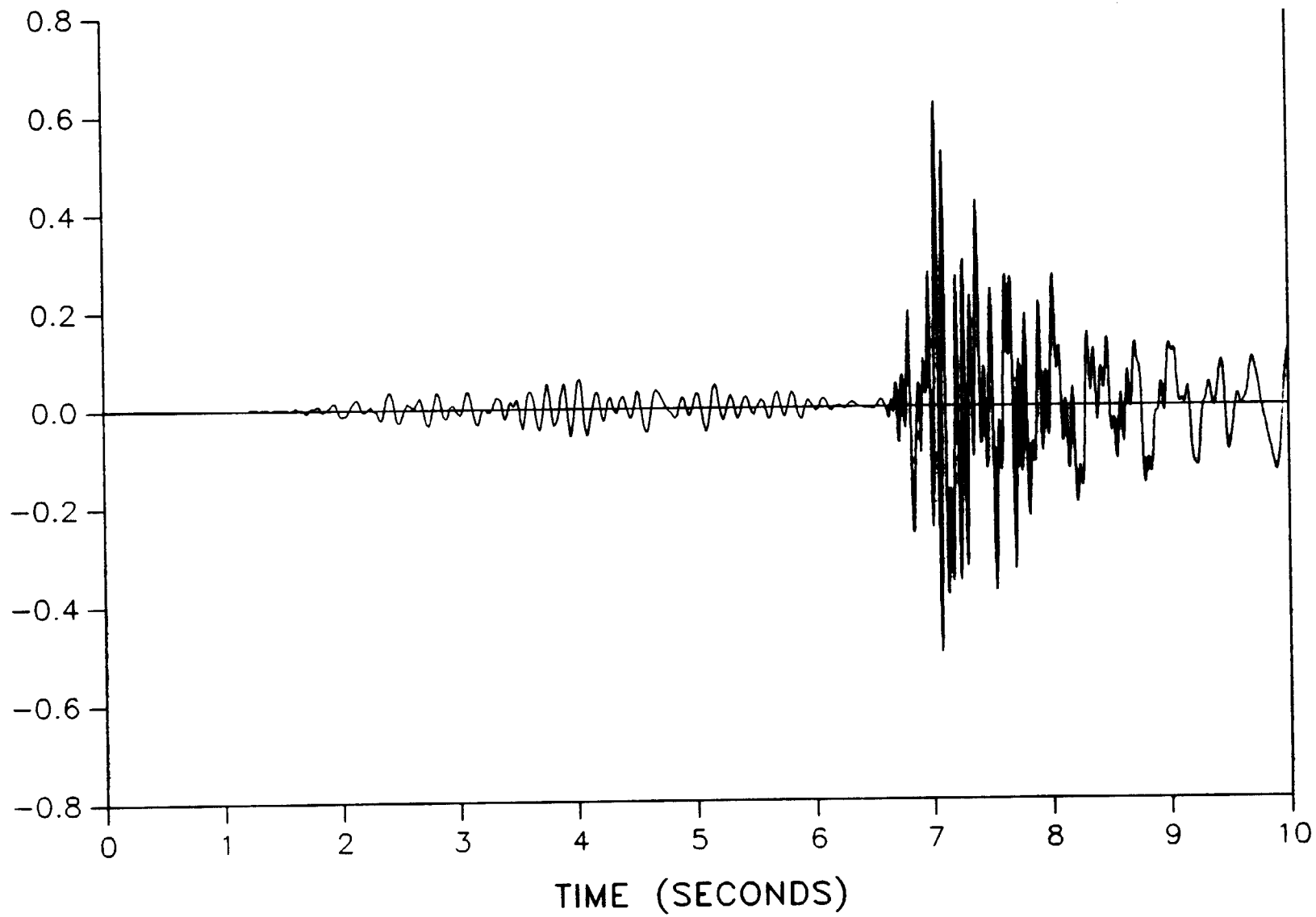

PREDICTED STS-26 TANG ACCELERATION - GAGE B08D8163A

STATION 500.0 - 0 DEGREES

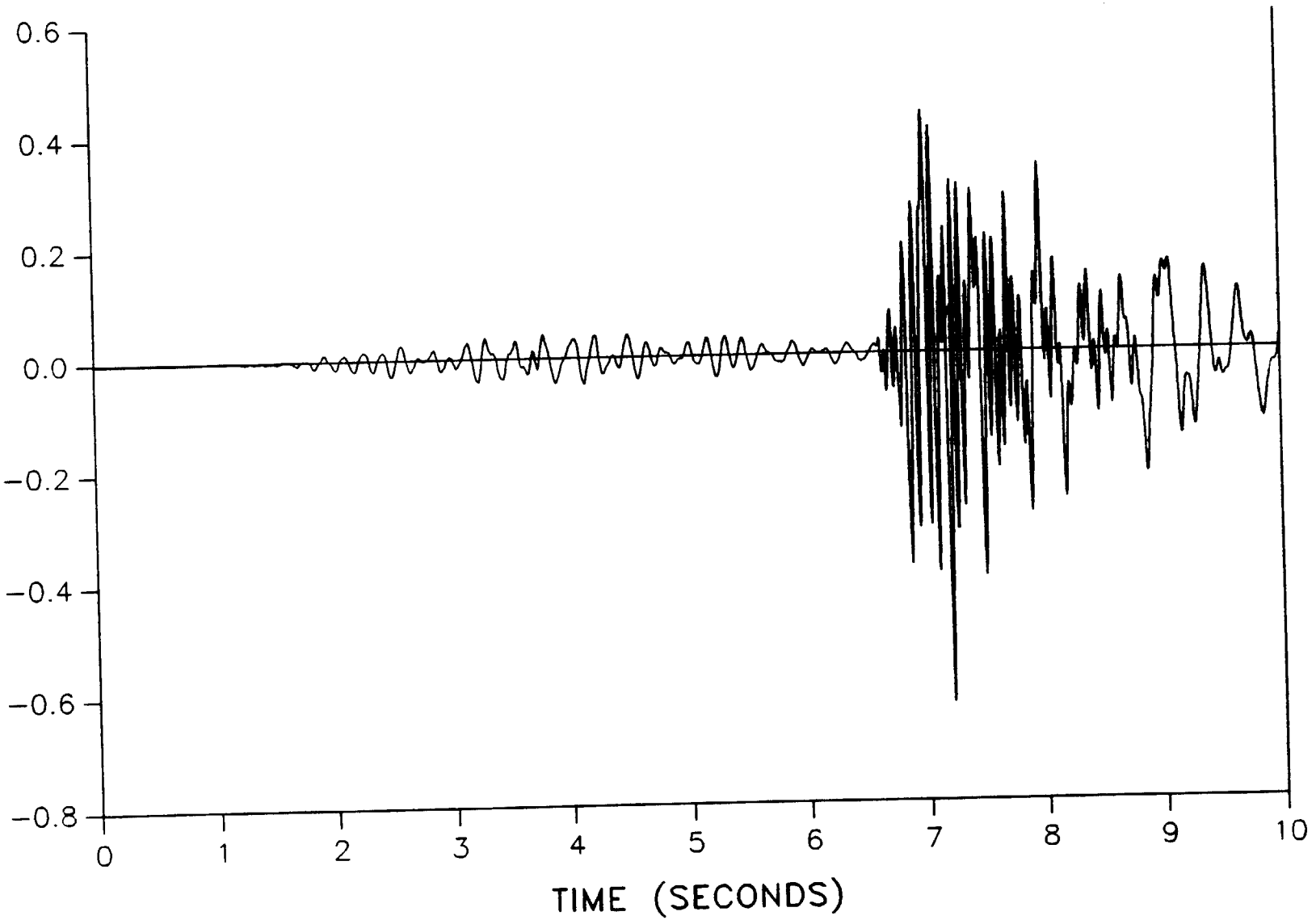

E HISTORY OF STS-26 ACCELEROMETER B08D7160A

DATA FILTERED TO 40 HZ

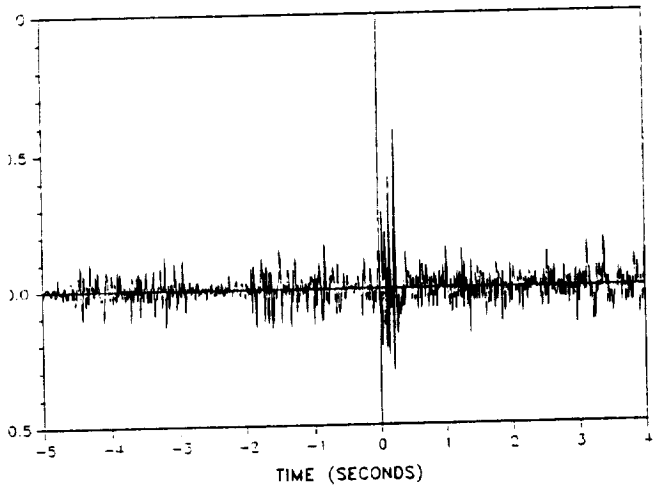

PREDICTED STS-26 AXIAL ACCELERATION - GAGE B08D7160A

STATION 500.0 AT 0 DEGREES

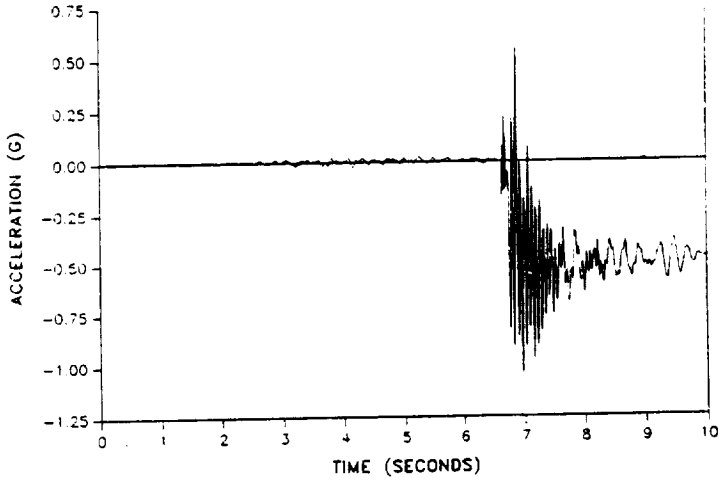

FFT OF ACCELEROMETER B08D7160A

TIME RANGE = -5. - 0. SECONDS

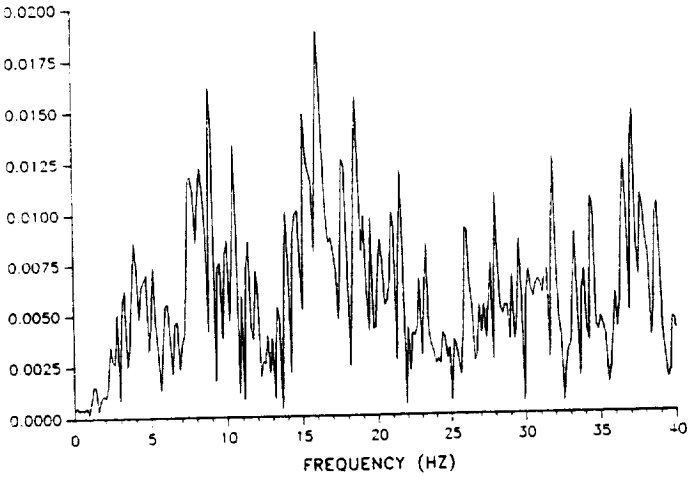

FFT OF ACCELEROMETER B08D7160A PREDICTION

TIME RANGE = 0. - 6.5 SECONDS

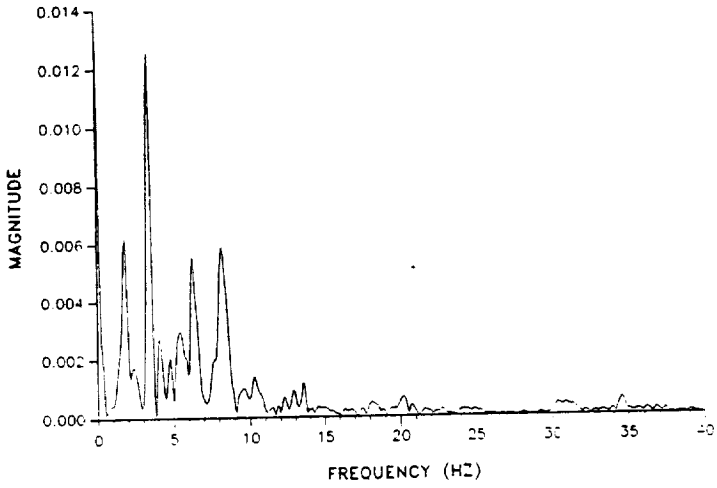

FFT OF ACCELEROMETER B08G7160A

TIME RANGE = 0. - 4. SECONDS

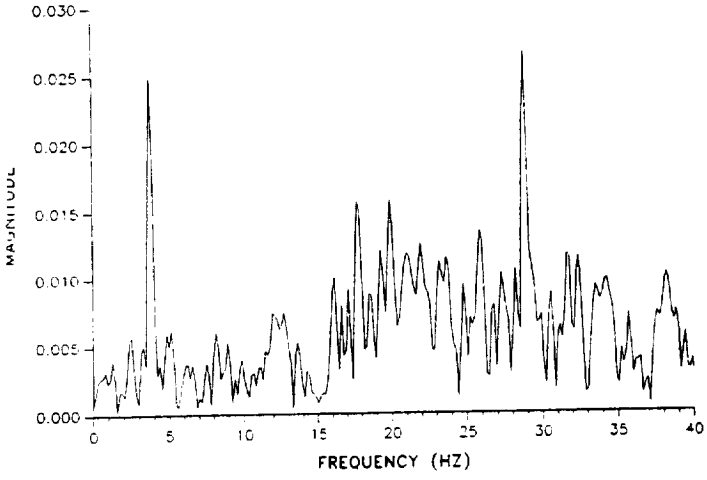

FFT OF ACCELEROMETER B08D7160A PREDICTION

TIME RANGE = 6.5 - 10. SECONDS

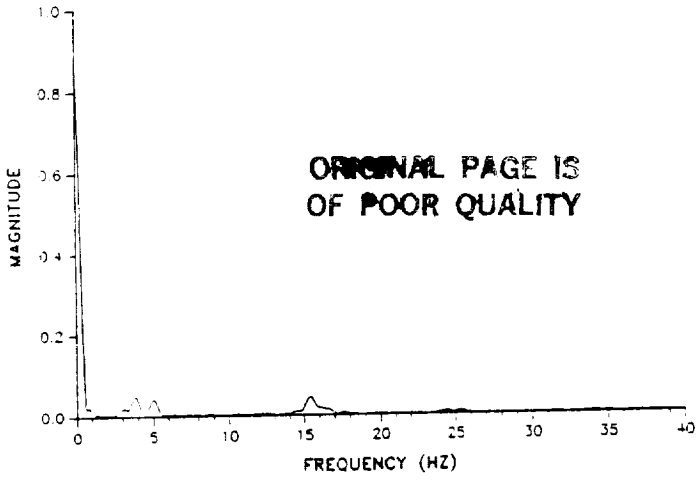

Comparison of Measured to Predicted Data for B08D7160A

HISTORY OF STS-26 ACCELEROMETER B08D7161A

DATA FILTERED TO 40 HZ

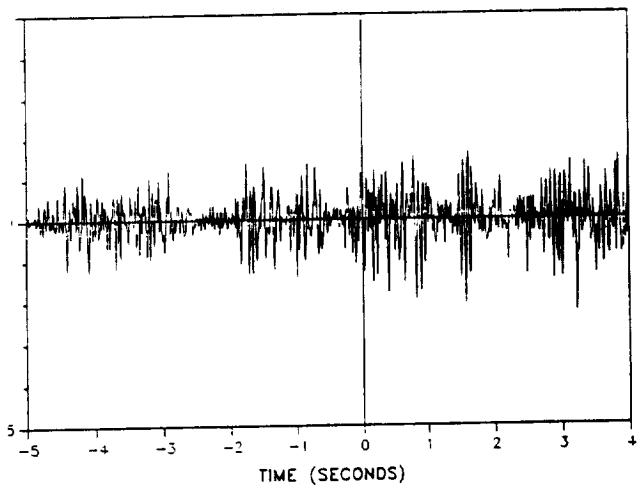

PREDICTED STS-26 TANG ACCELERATION - GAGE B08D7161A

STATION 500.0 AT 0 DEGREES

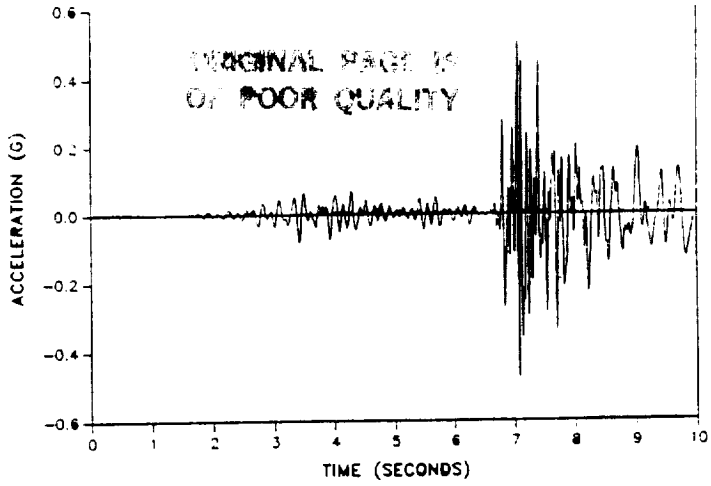

'T OF ACCELEROMETER B08D7161A

TIME RANGE = -5. - 0. SECONDS

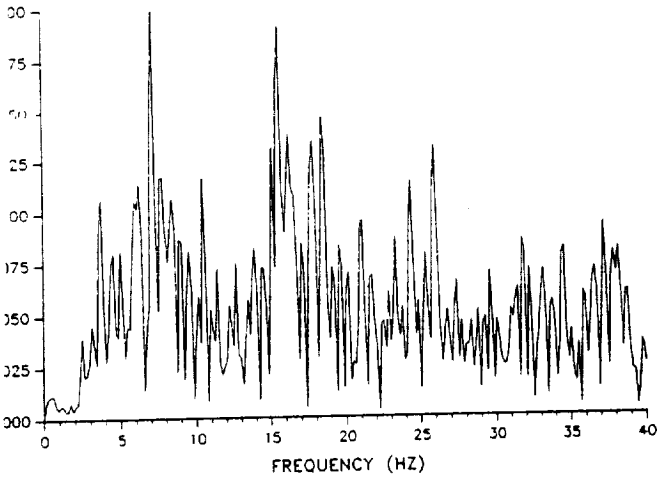

FFT OF ACCELEROMETER B08D7161A PREDICTION

TIME RANGE = 0. - 6.5 SECONDS

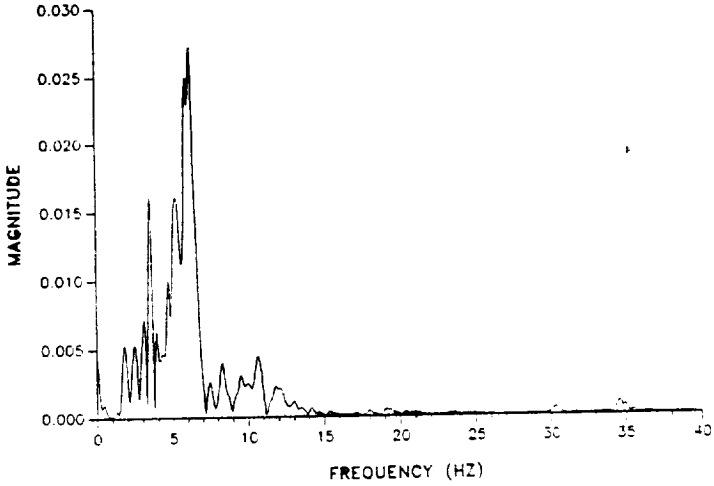

FT OF ACCELEROMETER B08D7161A

TIME RANGE = 0. - 4. SECONDS

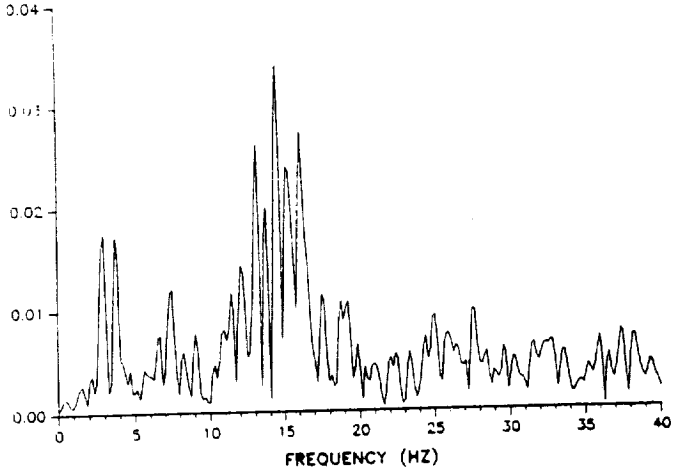

FFT OF ACCELEROMETER B08D7161A PREDICTION

TIME RANGE = 6.5 - 10. SECONDS

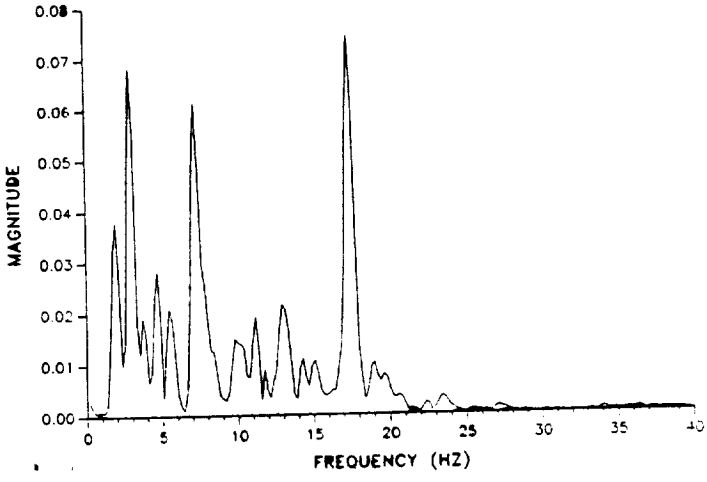

Comparison of Measured to Predicted Data for B08D7161A

ME HISTORY OF STS-26 ACCELEROMETER B08D7162A

DATA FILTERED TO 40 HZ

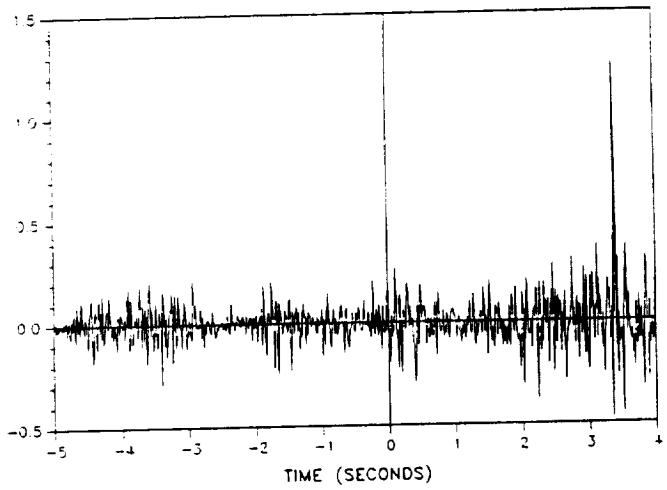

PREDICTED STS-26 RADIAL ACCELERATION - GAGE B08D7162A

STATION 500.0 AT 0 DEGREES

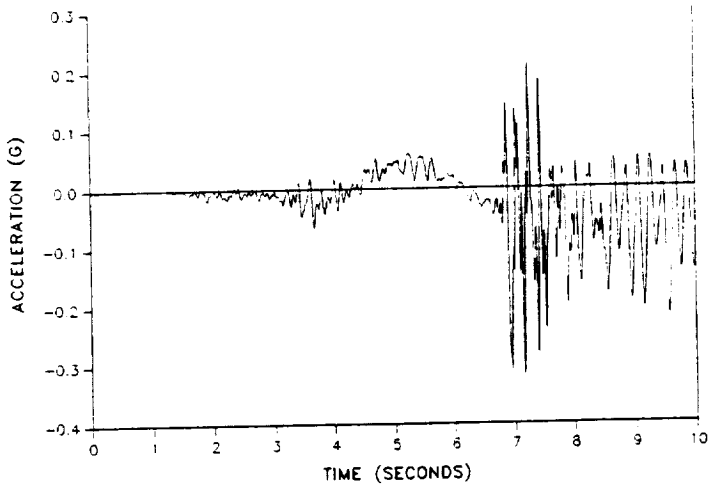

FT OF ACCELEROMETER B08D7162A

TIME RANGE = -5. - 0. SECONDS

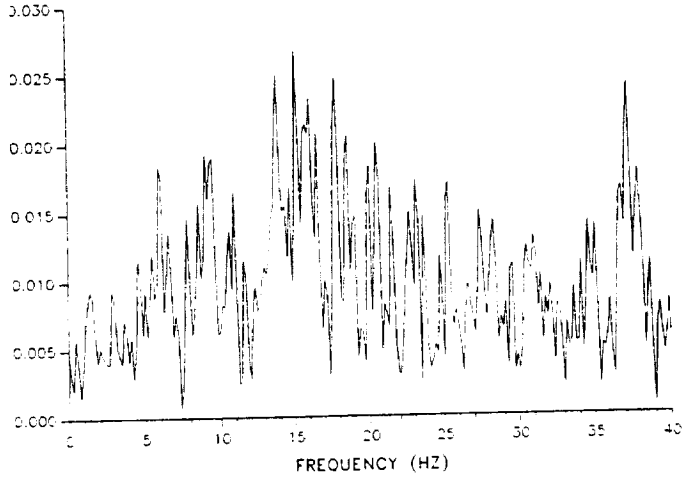

FFT OF ACCELEROMETER B08D7162A PREDICTION

TIME RANGE = 0. - 6.5 SECONDS

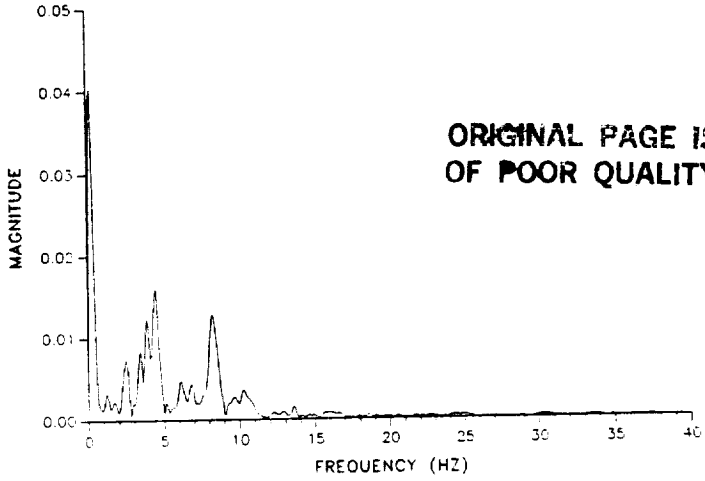

ORIGINAL PAGE IS
OF POOR QUALITY

FT OF ACCELEROMETER B08D7162A

TIME RANGE = 0. - 4. SECONDS

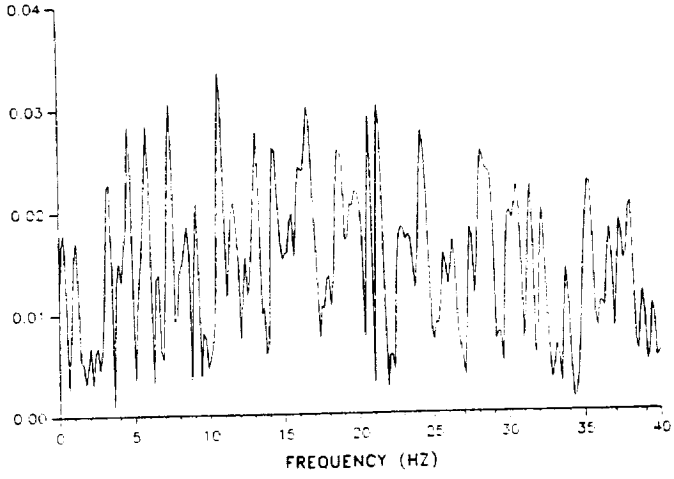

FFT OF ACCELEROMETER B08D7162A PREDICTION

TIME RANGE = 6.5 - 10. SECONDS

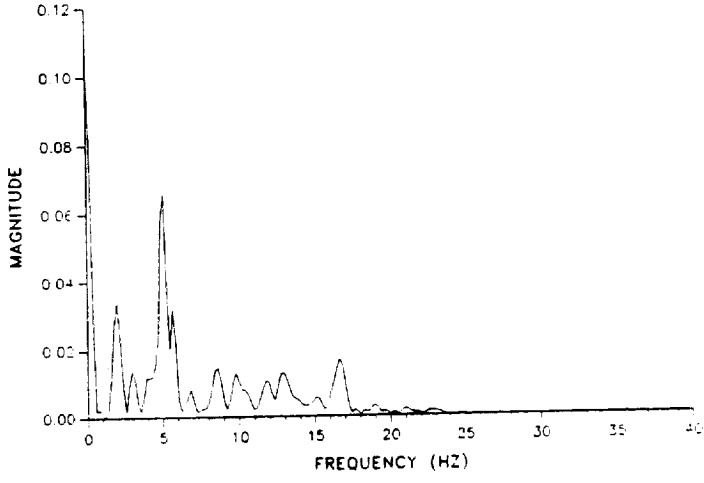

IME HISTORY OF STS-26 ACCELEROMETER B08D8160A

DATA FILTERED TO 40 HZ

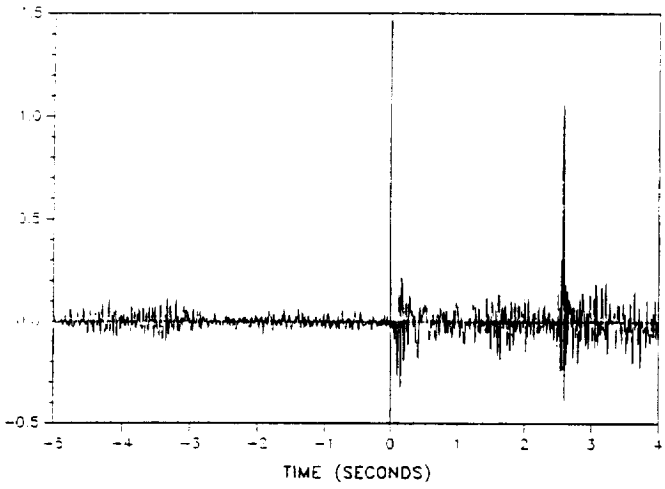

PREDICTED STS-26 AXIAL ACCELERATION - APPROX STA. 500.

GAGES B08D8151A AND B08D8160A - 180 DEGREES

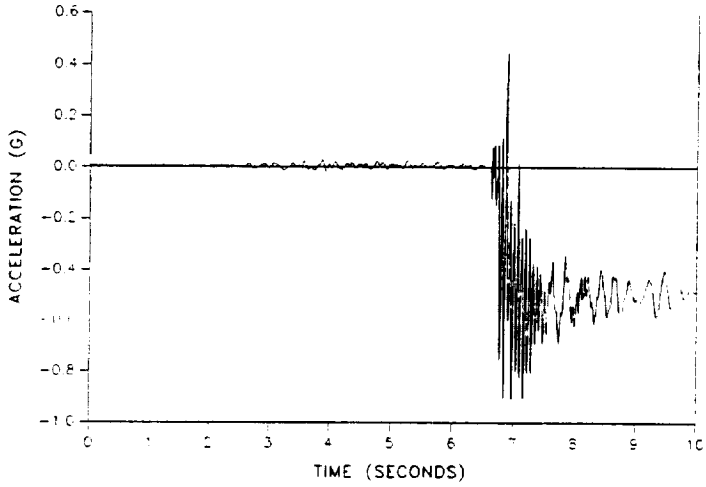

FFT OF ACCELEROMETER B08D8160A

TIME RANGE = -5. - 0. SECONDS

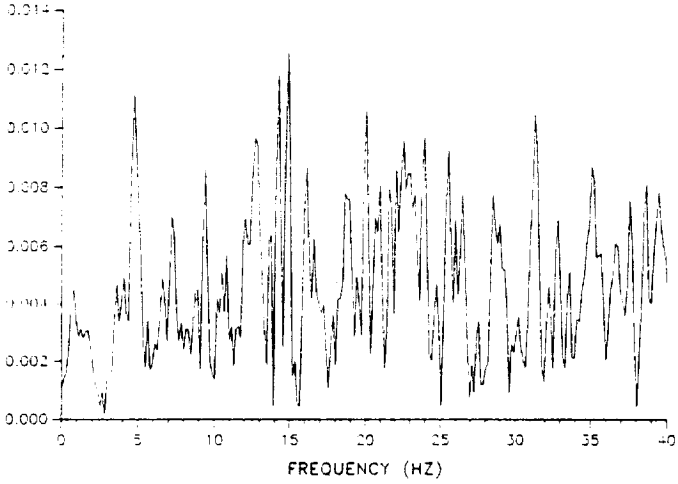

FFT OF ACCELEROMETER B08D8151A AND B08D8160A PREDICTIONS

TIME RANGE = 0 - 6.5 SECONDS

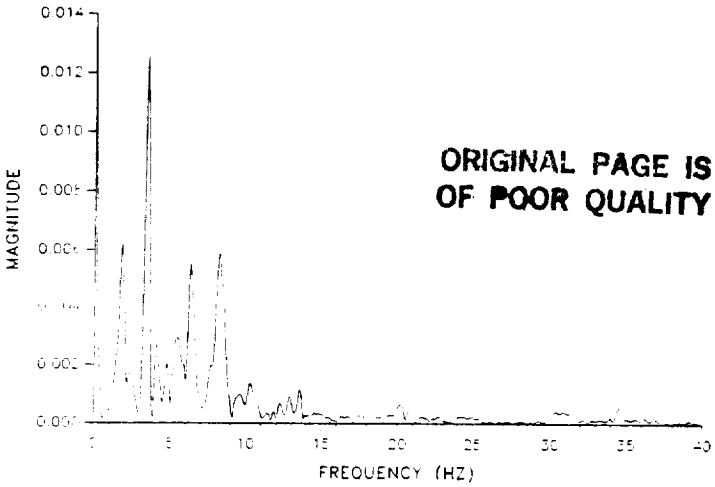

ORIGINAL PAGE IS
OF POOR QUALITY

FFT OF ACCELEROMETER B08D8160A

TIME RANGE = 0. - 4. SECONDS

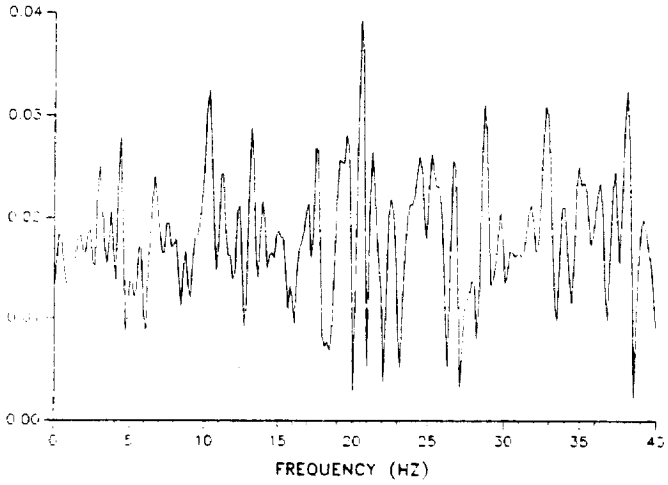

FFT OF ACCELEROMETER B08D8151A AND B08D8160A PREDICTIONS

TIME RANGE = 6.5 - 10. SECONDS

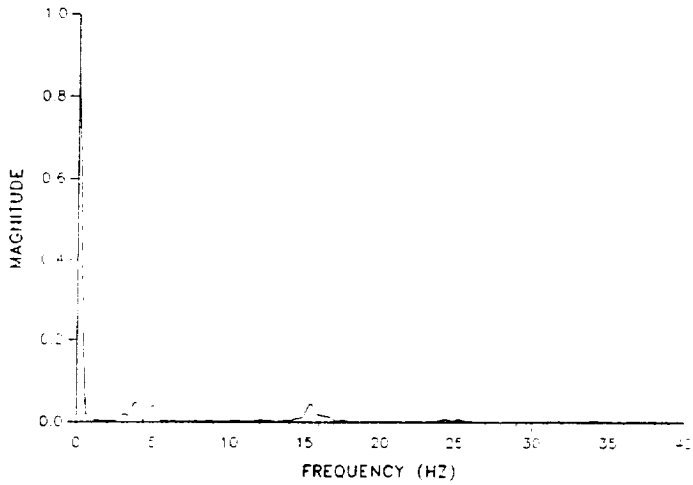

Comparison of Measured to Predicted Data for B08D8160A

'ME HISTORY OF STS-26 ACCELEROMETER B08D8161A

DATA FILTERED TO 40 HZ

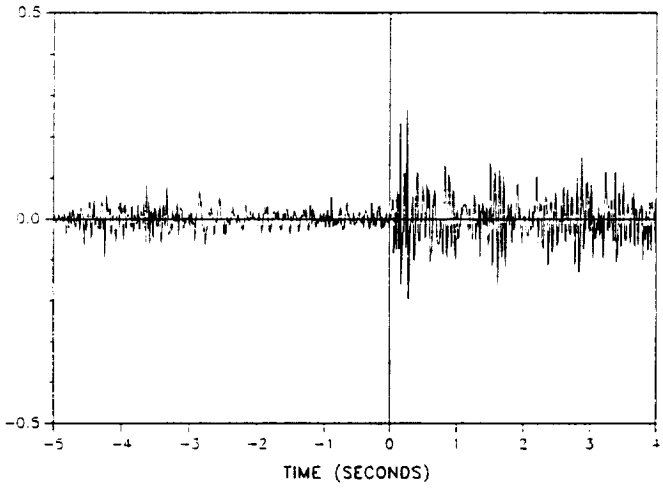

PREDICTED STS-26 TANG ACCELERATION - APPROX STA. 500

GAGES B08D153A AND B08D161A - 180 DEGREES

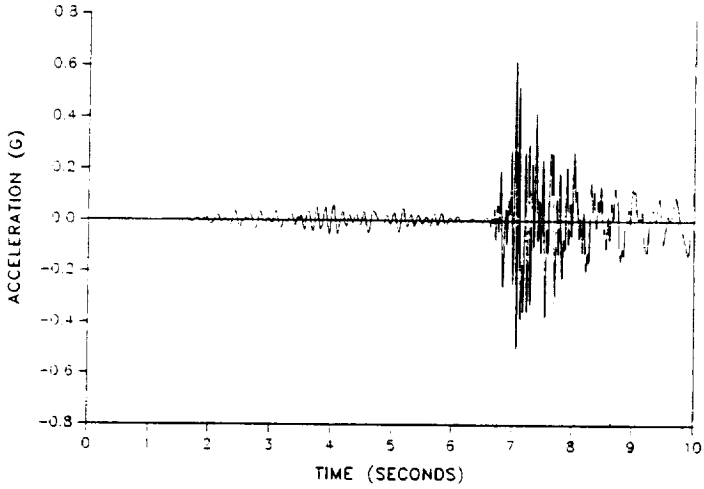

FFT OF ACCELEROMETER B08D8161A

TIME RANGE = -5. - 0. SECONDS

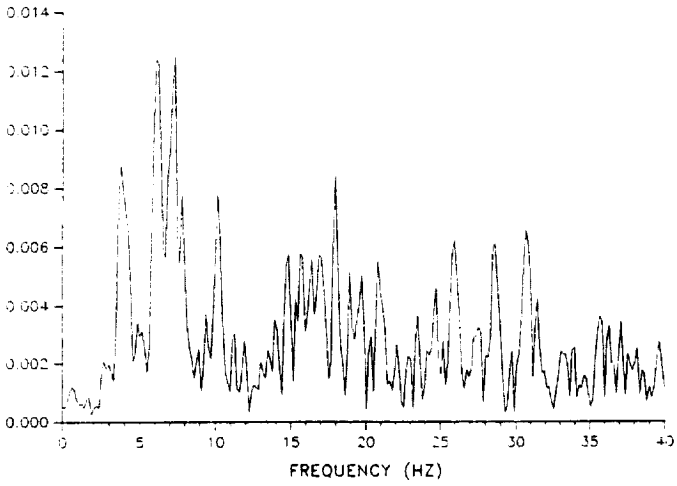

FFT OF ACCELEROMETER B08D8153A AND B08D8161A PREDICTIONS

TIME RANGE = 0. - 6.5 SECONDS

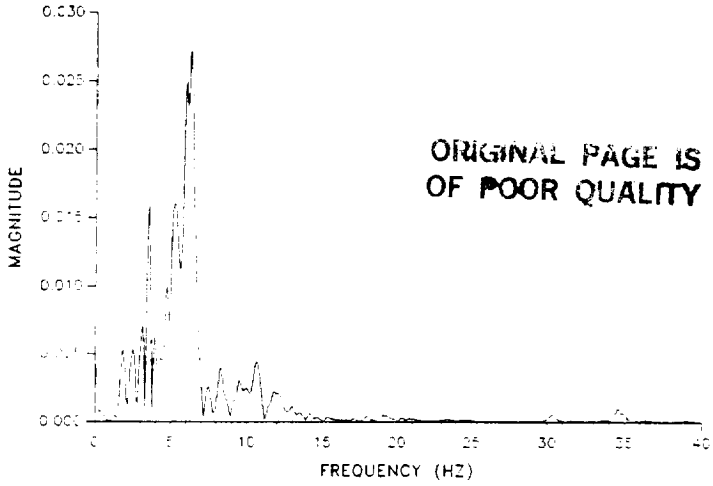

ORIGINAL PAGE IS
OF POOR QUALITY

FFT OF ACCELEROMETER B08D8161A

TIME RANGE = 0. - 4. SECONDS

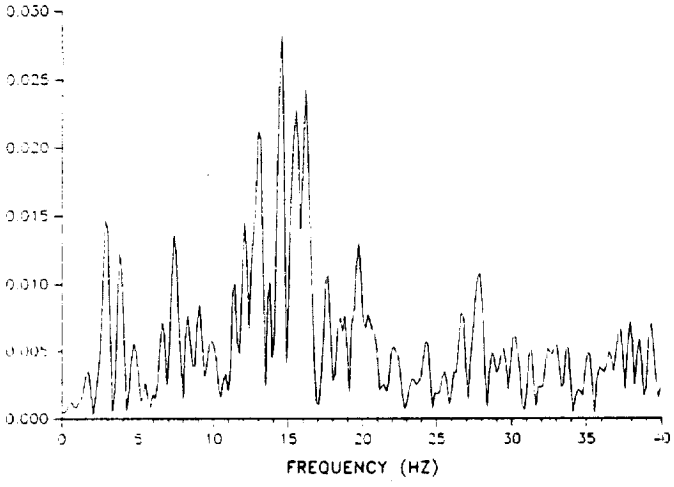

FFT OF ACCELEROMETER B08D8153A AND B08D8161A PREDICTIONS

TIME RANGE = 6.5 - 10. SECONDS

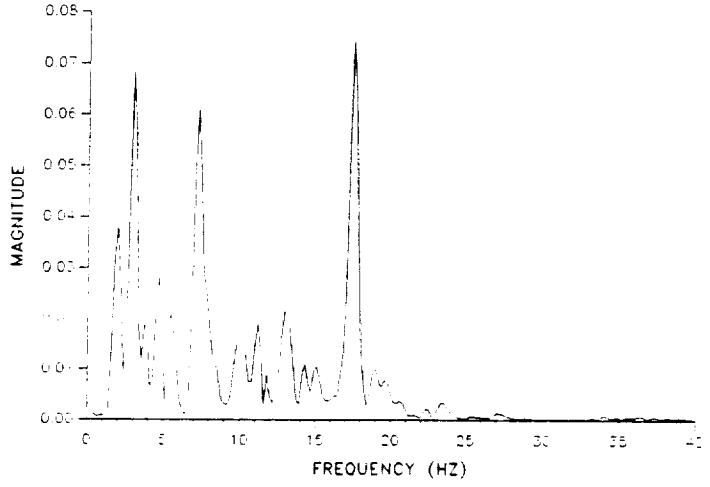

Comparison of Measured to Predicted Data for B08D8161A

TIME HISTORY OF STS-26 ACCELEROMETER B08D8163A

DATA FILTERED TO 40 HZ

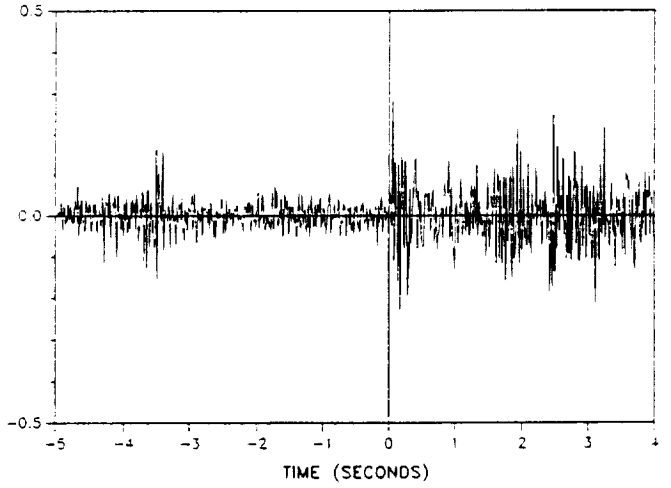

PREDICTED STS-26 TANG ACCELERATION - GAGE B08D8163A

STATION 500.0 - 0 DEGREES

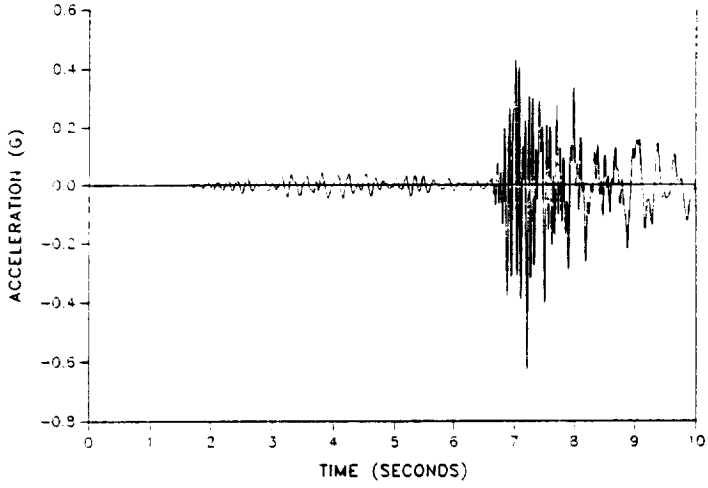

FFT OF ACCELEROMETER B08D8163A

TIME RANGE = -5. - 0. SECONDS

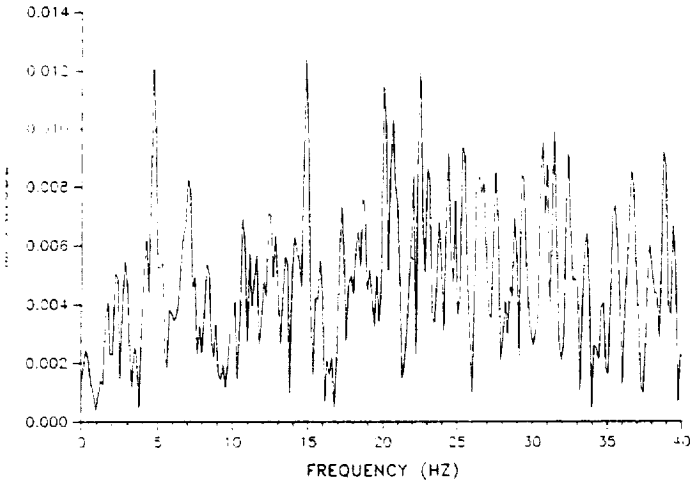

FFT OF ACCELEROMETER B08D8163A PREDICTION

TIME RANGE = 0. - 6.5 SECONDS

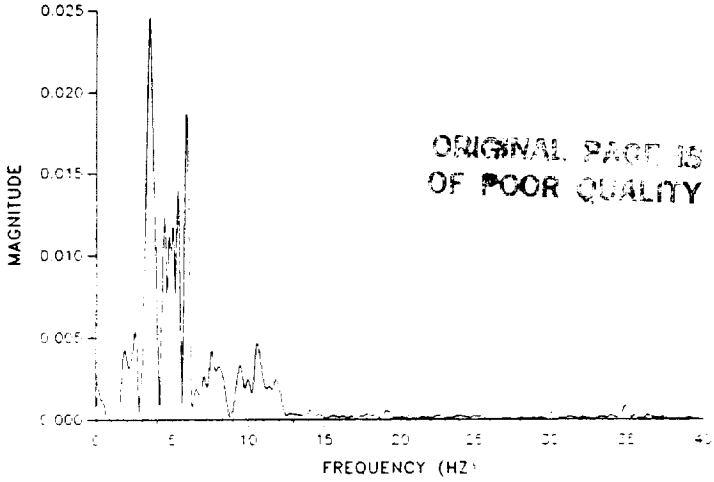

FFT OF ACCELEROMETER B08D8163A

TIME RANGE = 0. - 4. SECONDS

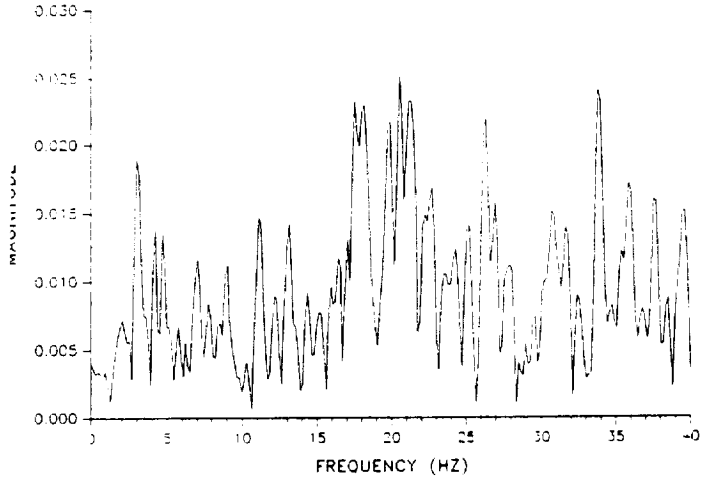

FFT OF ACCELEROMETER B08D8163A PREDICTION

TIME RANGE = 6.5 - 10. SECONDS

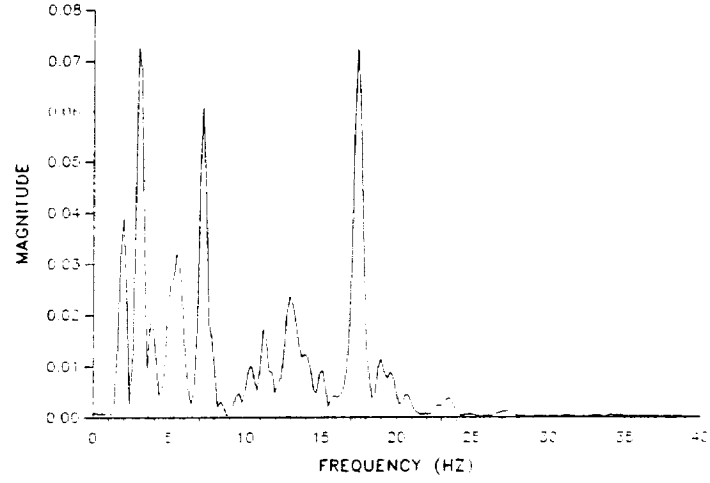

SDRC I-DEAS 4.0: Test Data Analysis 1-JUN-89 15:56:30

DATABASE: WATERFALL
VIEW : No stored VIEW

UNITS : IN
DISPLAY : No stored OPTION

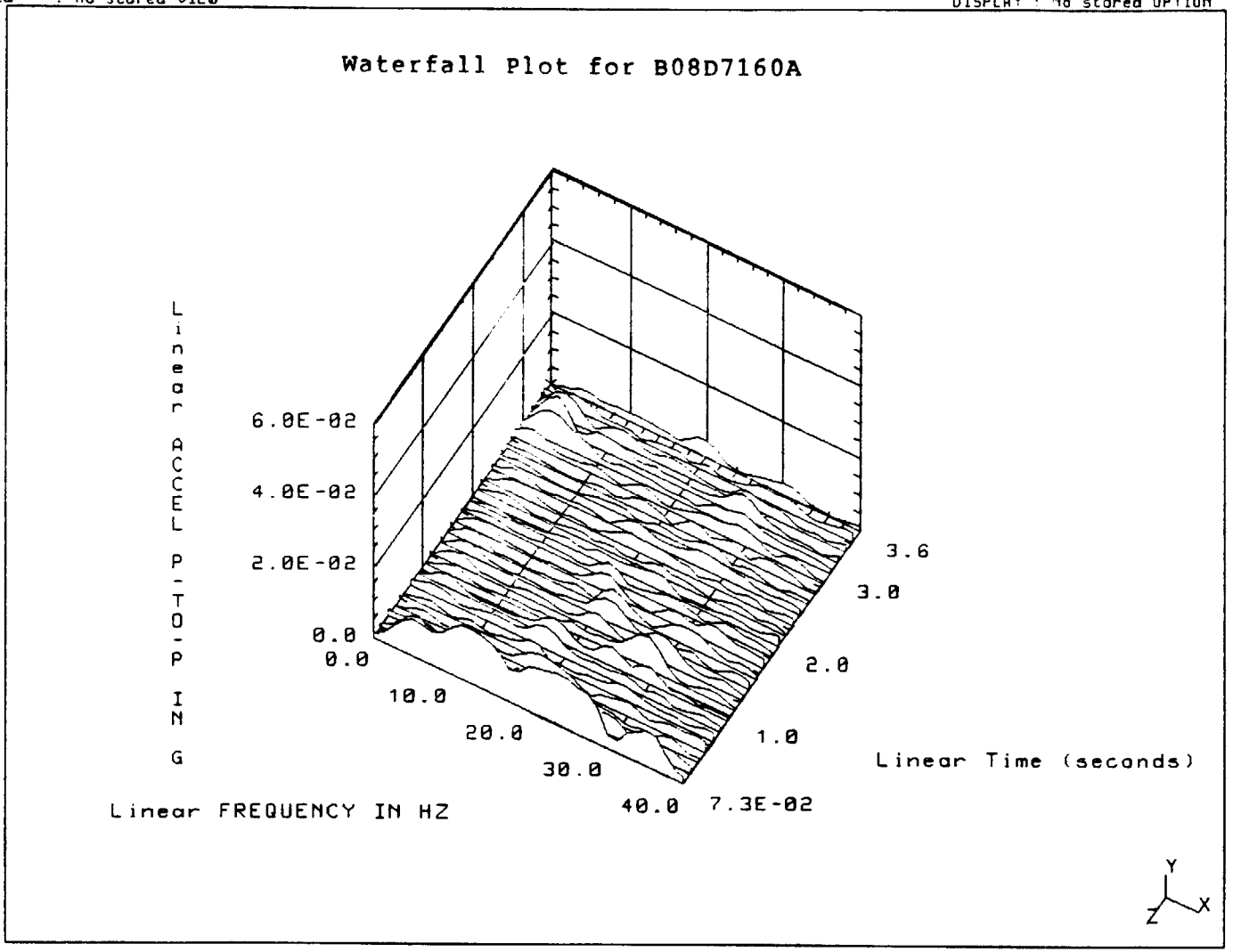

SDRC I-DEAS 4.0: Test Data Analysis 1-JUN-89 16:00:45

DATABASE: WATERFALL
VIEW : No stored VIEW

UNITS : IN
DISPLAY : No stored OPTION

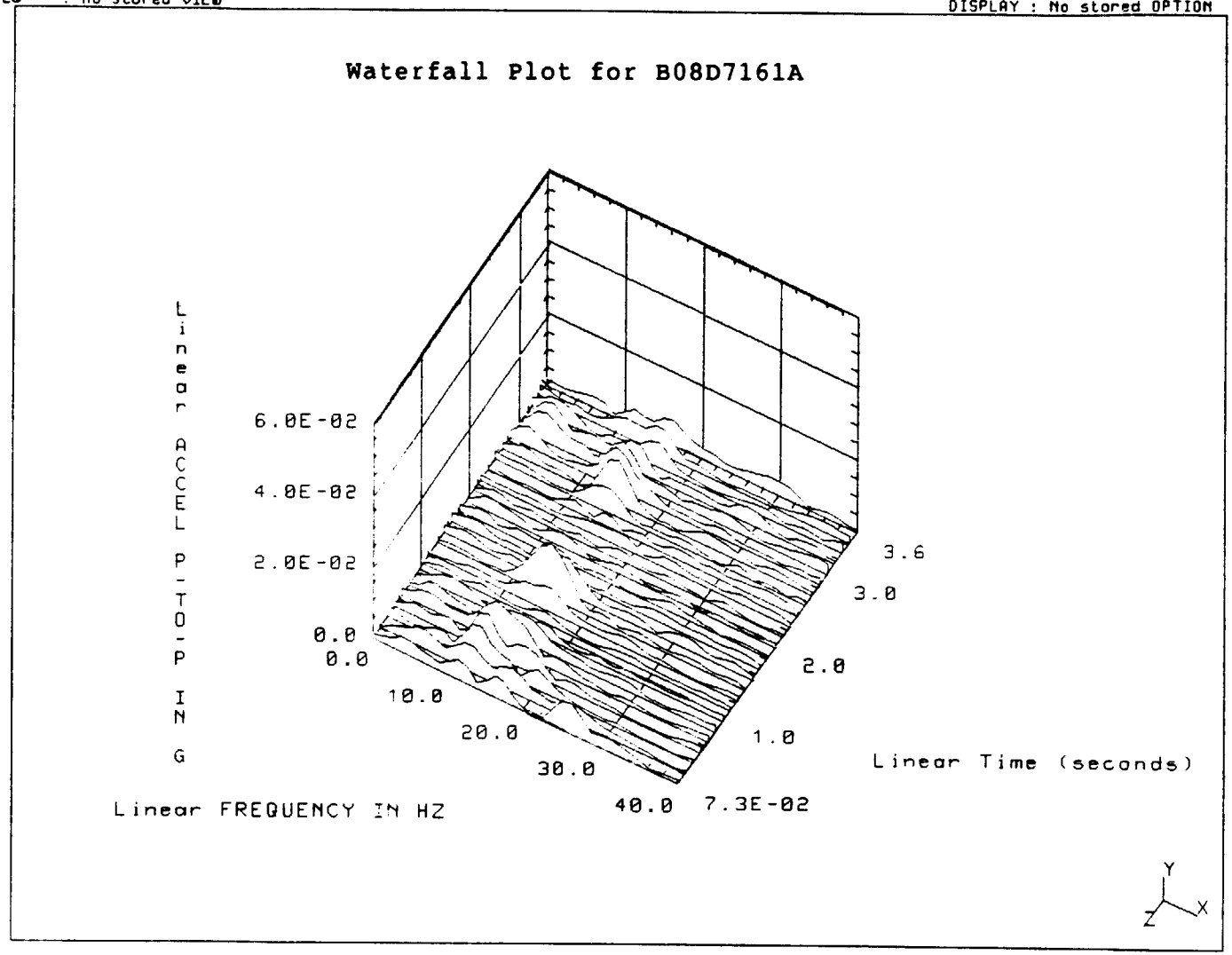

SDRC I-DEAS 4.0: Test Data Analysis 1-JUN-89 16:09:25

DATABASE: WATERFALL
VIEW : No stored VIEW

UNITS : IN
DISPLAY : No stored OPTION

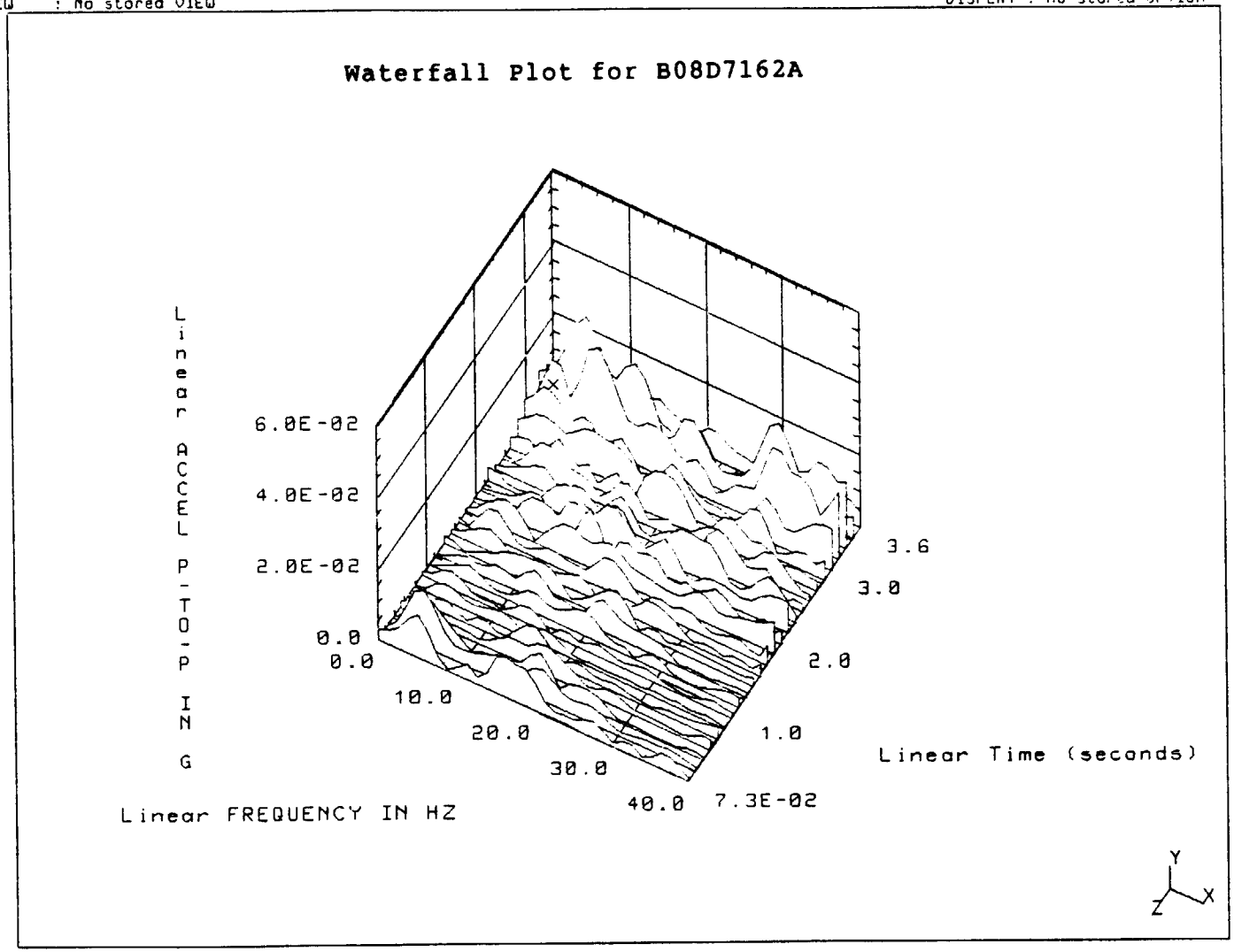

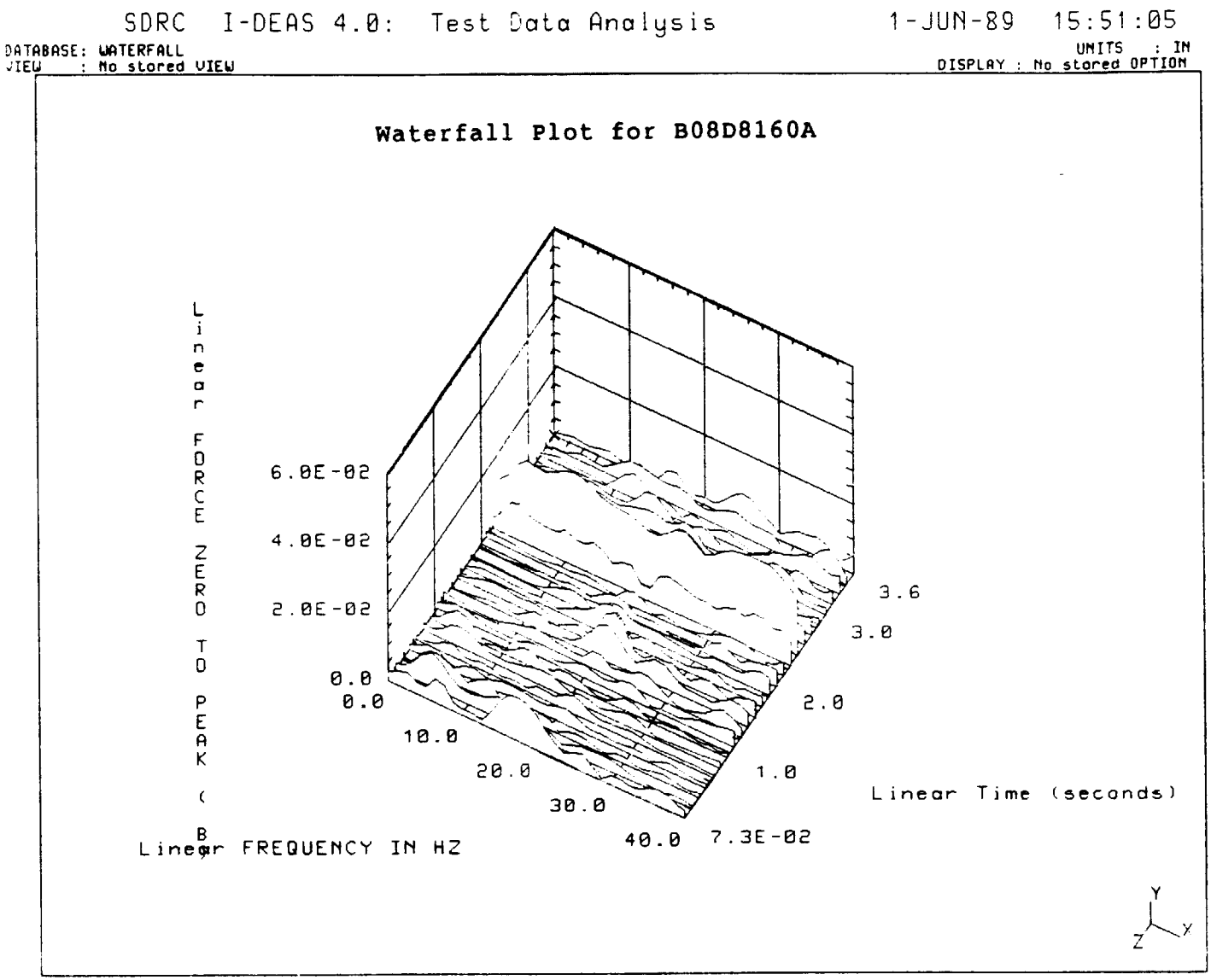
SDRC I-DEAS 4.0: Test Data Analysis
1-JUN-89 15:51:05
DATABASE: WATERFALL
VIEW : No stored VIEW
UNITS : IN
DISPLAY : No stored OPTION
Waterfall Plot for B08D8160A
Linear FORCE ZERO TO PEAK (
6.0E-02
4.0E-02
2.0E-02
0.0
0.0
10.0
20.0
30.0
40.0
Linear FREQUENCY IN HZ
3.6
3.0
2.0
1.0
7.3E-02
Linear Time (seconds)
Y
Z
X

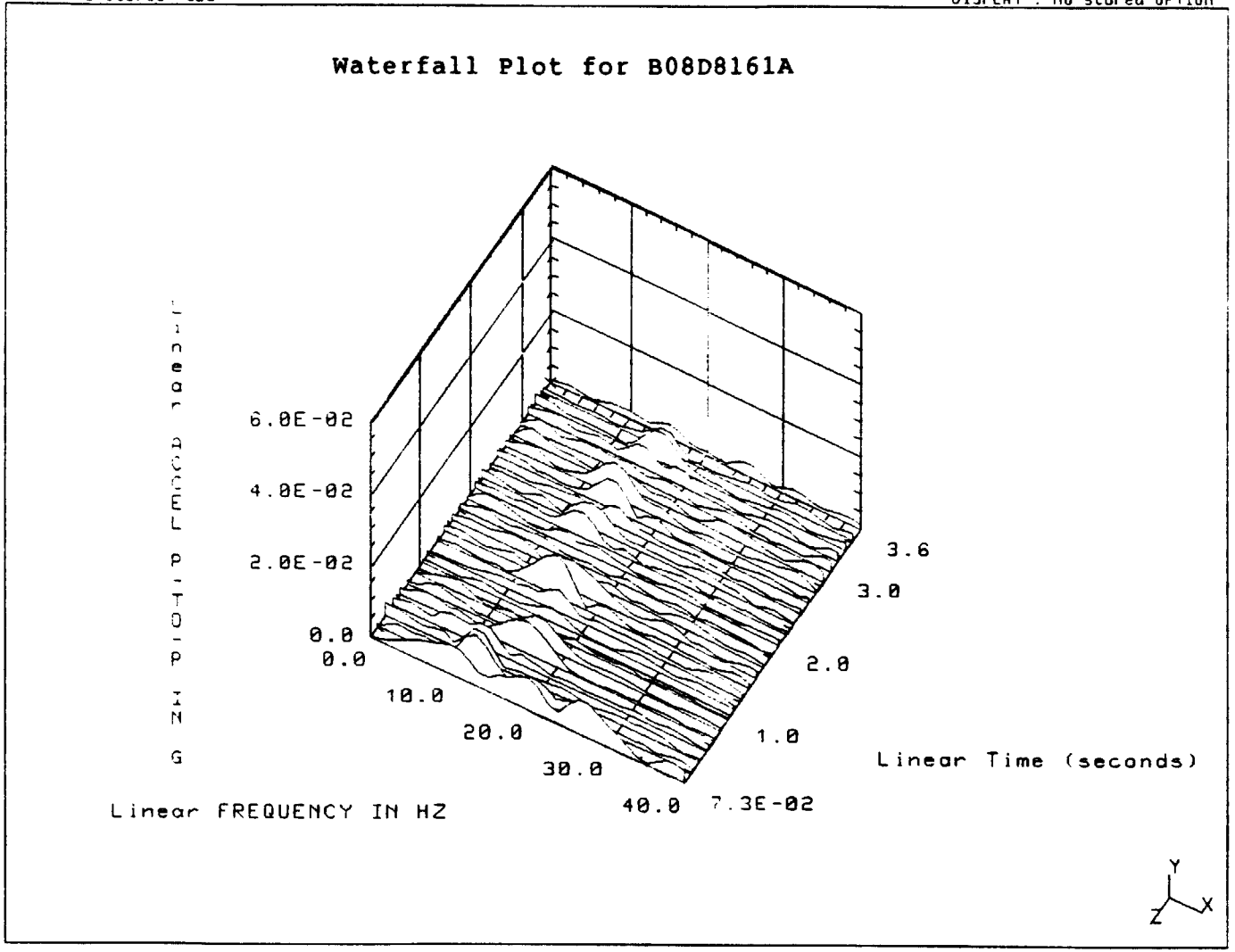
Waterfall Plot for B08D8161A
6.0E-02
4.0E-02
2.0E-02
0.0
0.0
10.0
20.0
30.0
40.0
7.3E-02
1.0
2.0
3.0
3.6
Linear Time (seconds)
Linear FREQUENCY IN HZ
Y
Z
X

SDRC I-DEAS 4.0: Test Data Analysis 1-JUN-89 15:48:14

DATABASE: WATERFALL
VIEW : No stored VIEW

UNITS : IN
DISPLAY : No stored OPTION

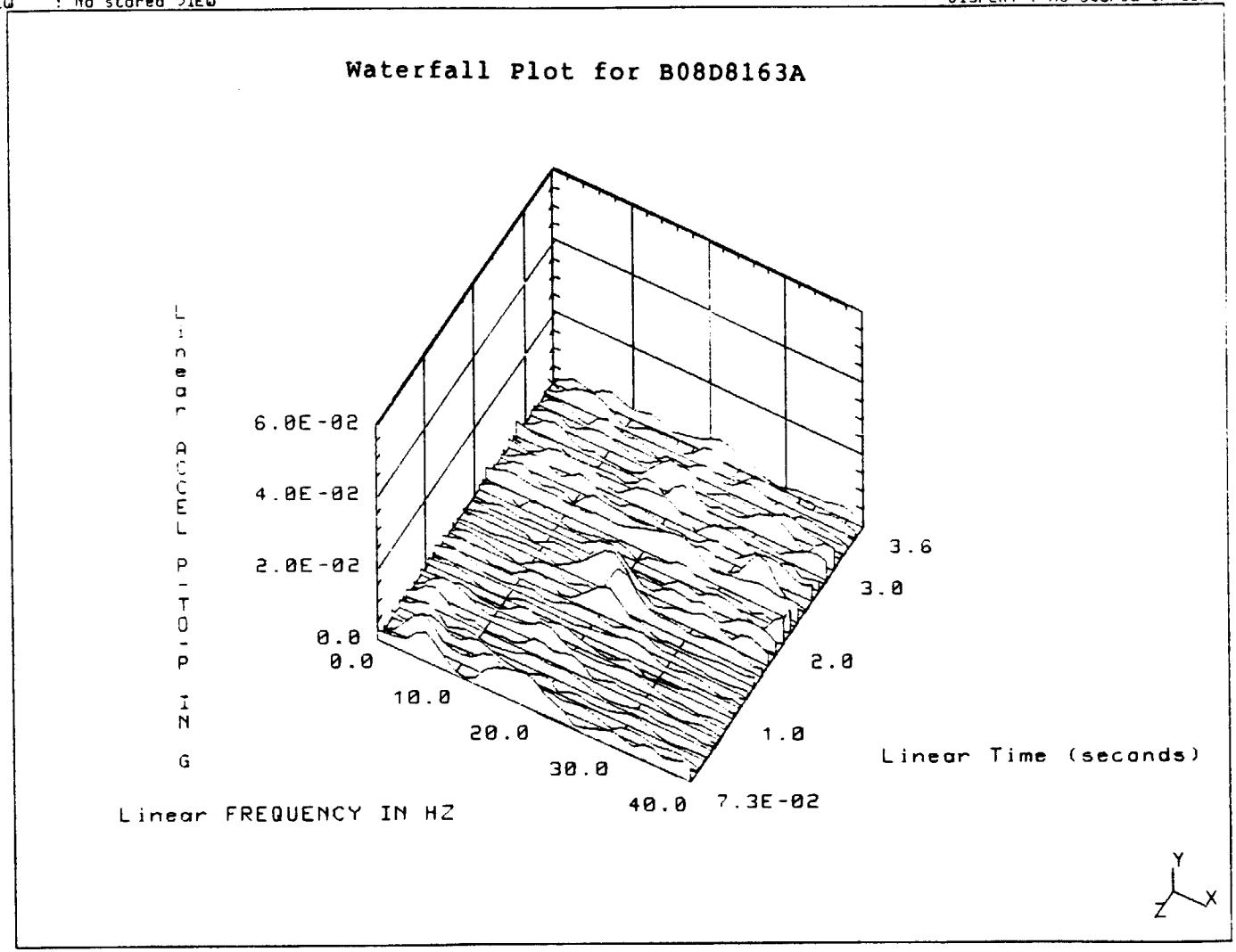

APPENDIX H

Field Joint Gap Opening Plots

MAXIMUM PRIMARY GAP OPENING – FWD FIELD JOINT

STS-26 RECONSTRUCTED ANALYSIS – LEFT MOTOR

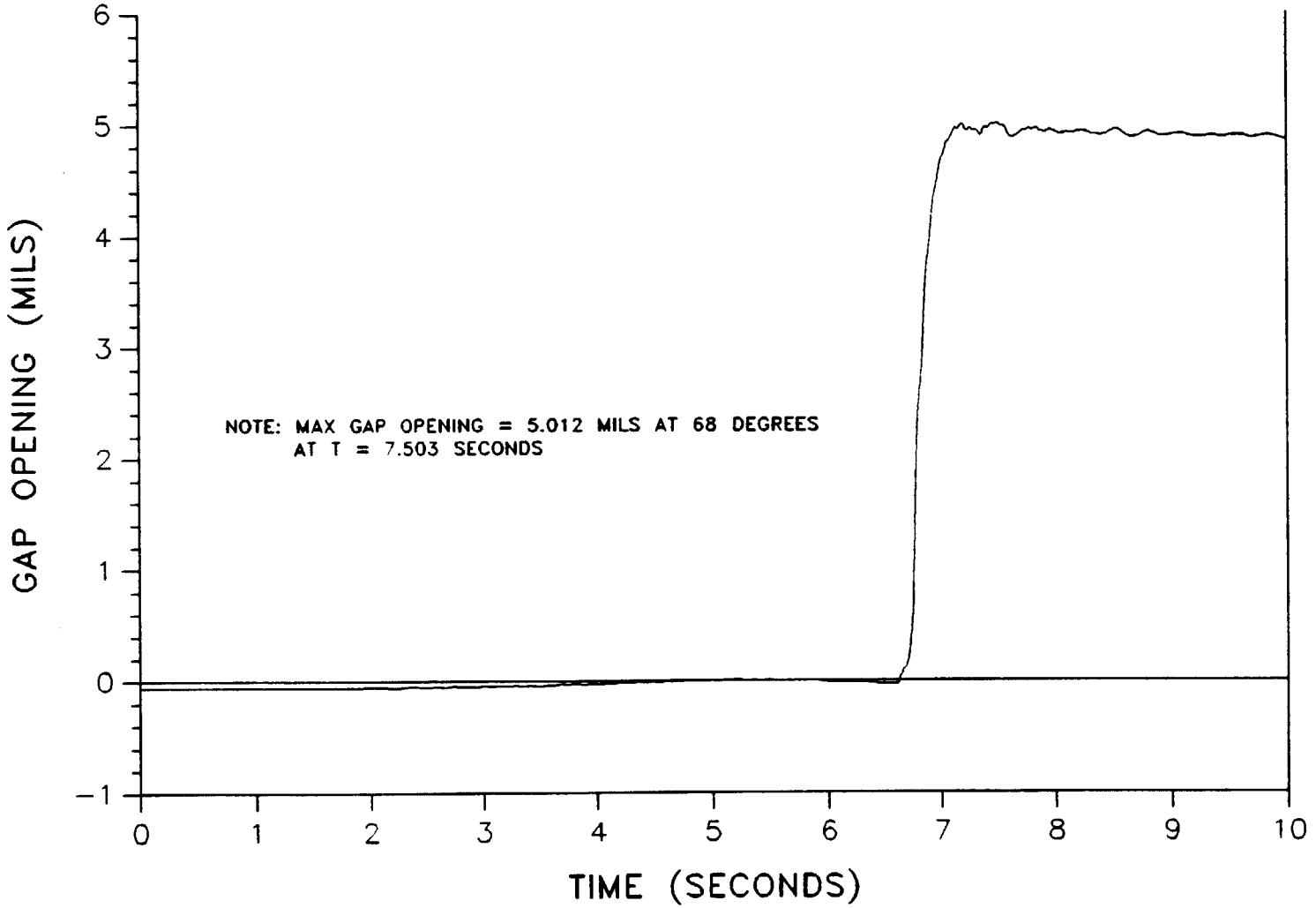

MAXIMUM SECONDARY GAP OPENING – FWD FIELD JOINT

STS-26 RECONSTRUCTED ANALYSIS – LEFT MOTOR

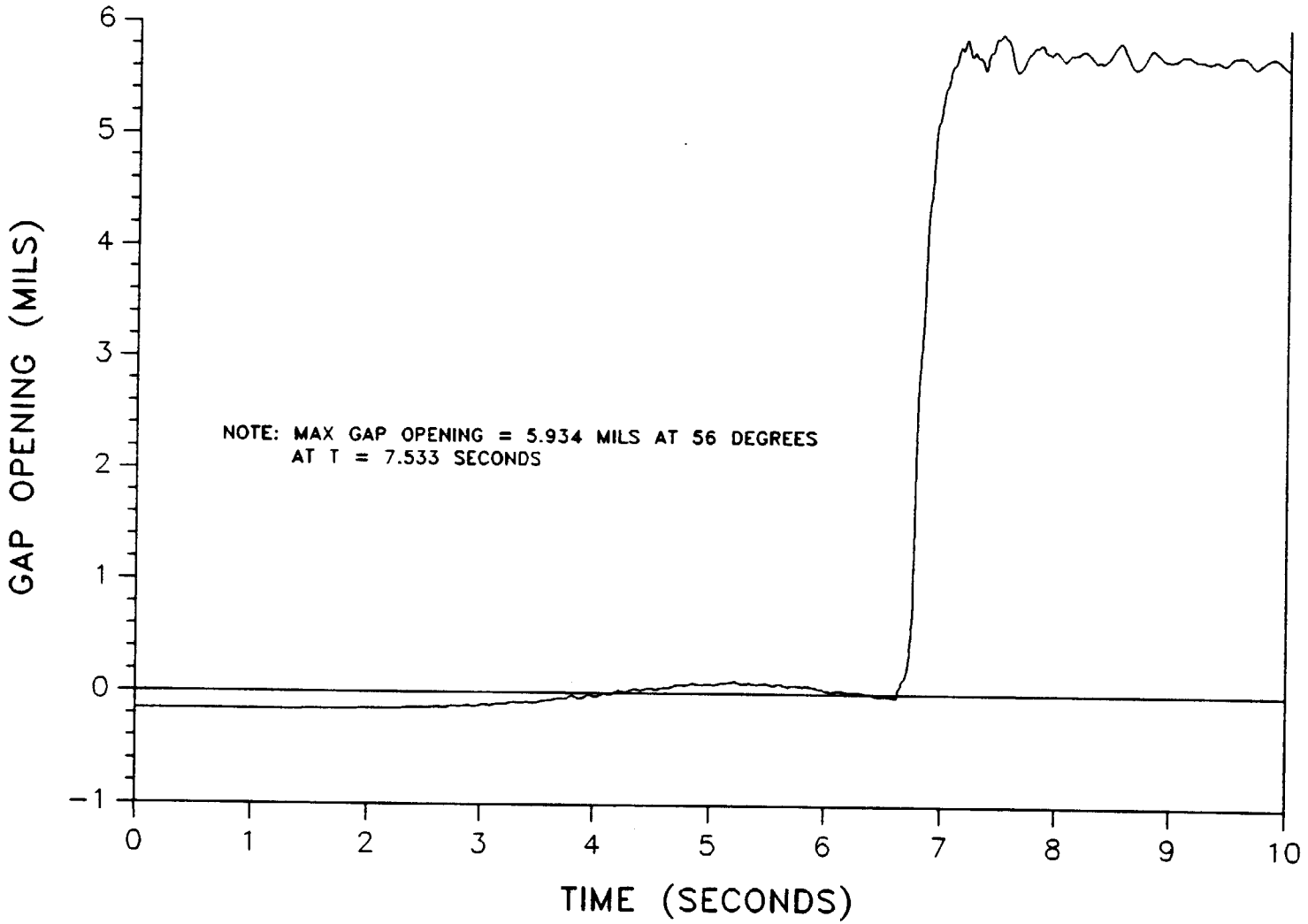

MAXIMUM PRIMARY GAP OPENING – CTR FIELD JOINT

STS-26 RECONSTRUCTED ANALYSIS – LEFT MOTOR

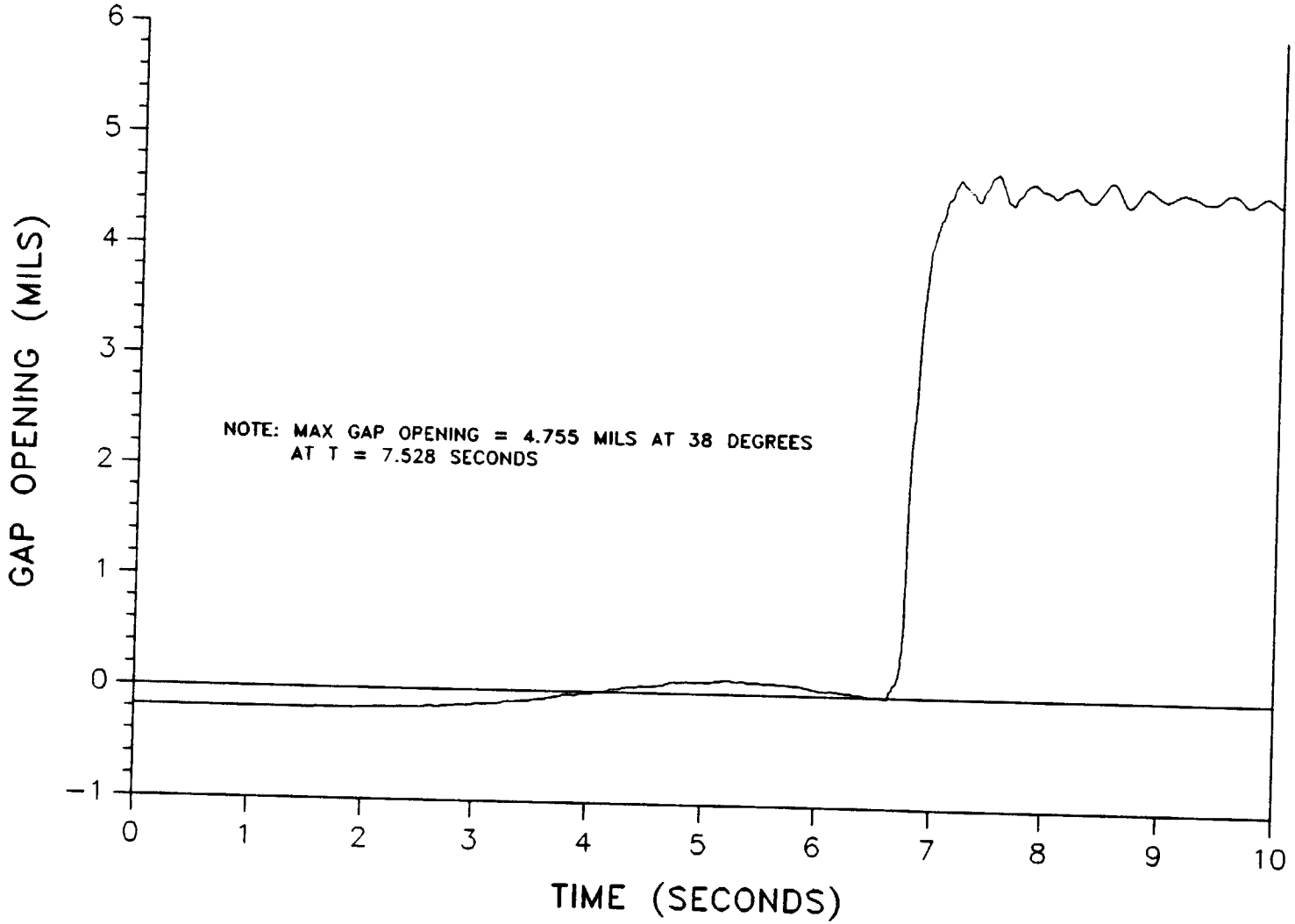

MAXIMUM SECONDARY GAP OPENING – CTR FIELD JOINT

STS-26 RECONSTRUCTED ANALYSIS – LEFT MOTOR

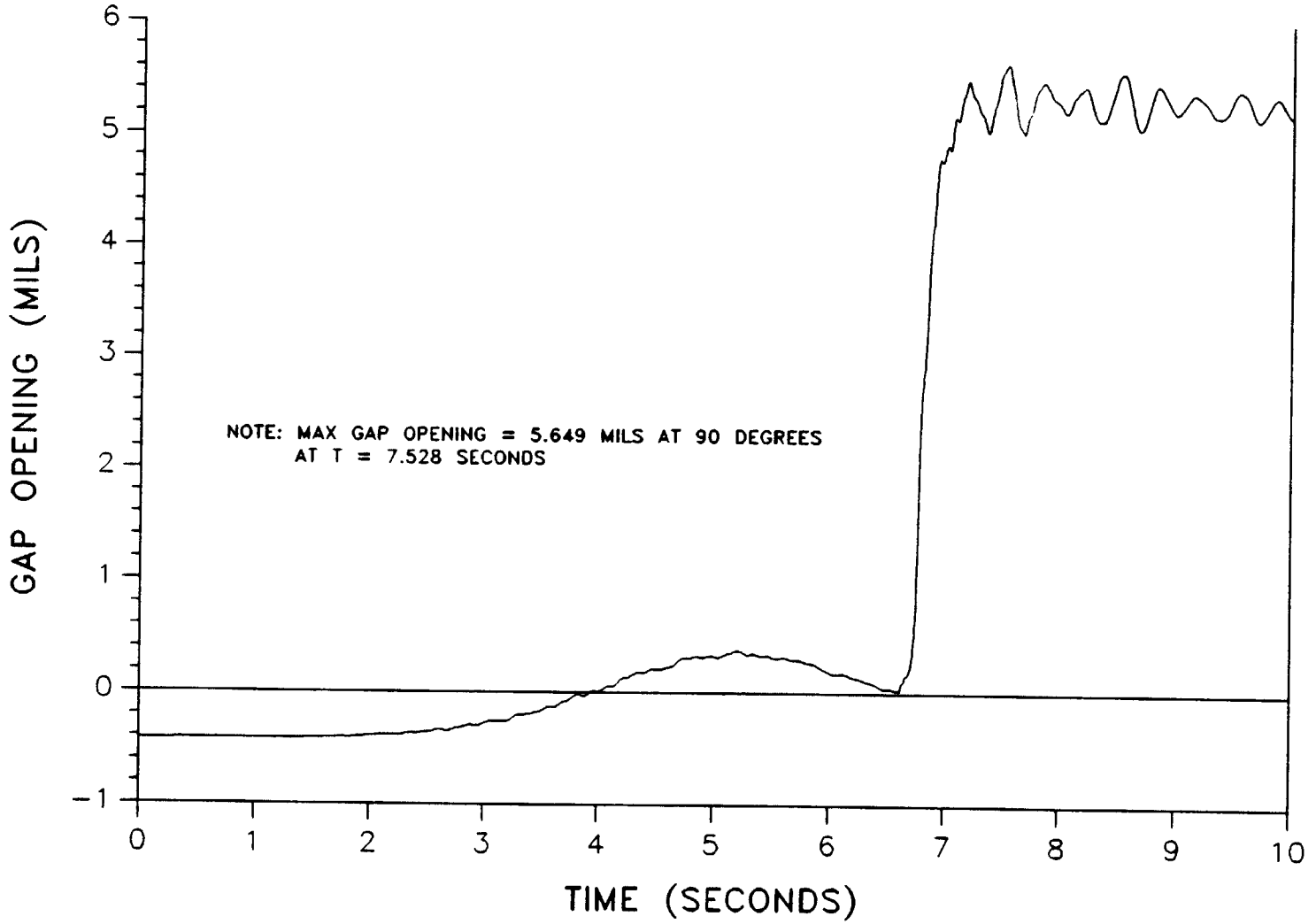

MAXIMUM PRIMARY GAP OPENING – AFT FIELD JOINT

STS-26 RECONSTRUCTED ANALYSIS – LEFT MOTOR

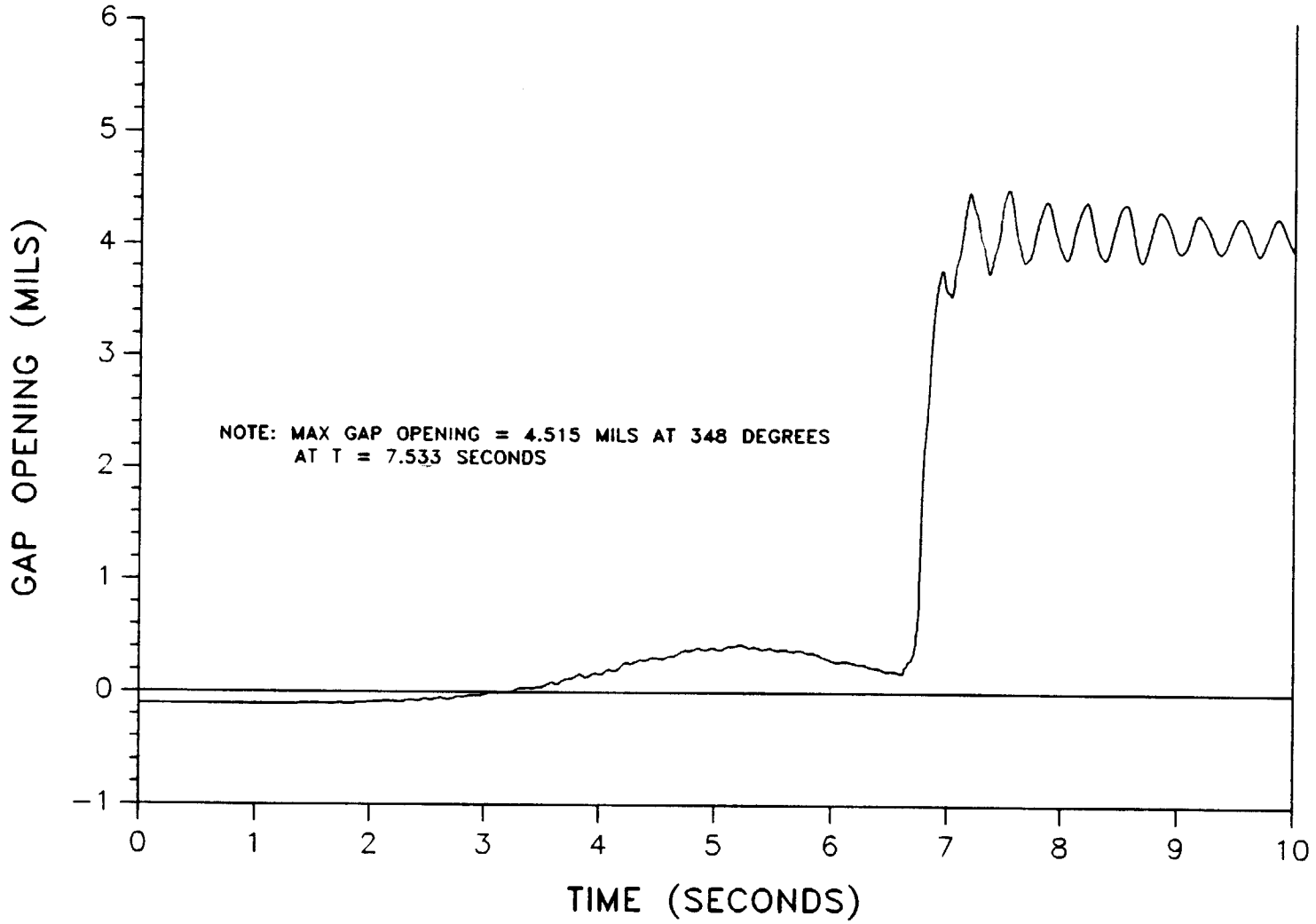

MAXIMUM SECONDARY GAP OPENING – AFT FIELD JOINT

STS–26 RECONSTRUCTED ANALYSIS – LEFT MOTOR

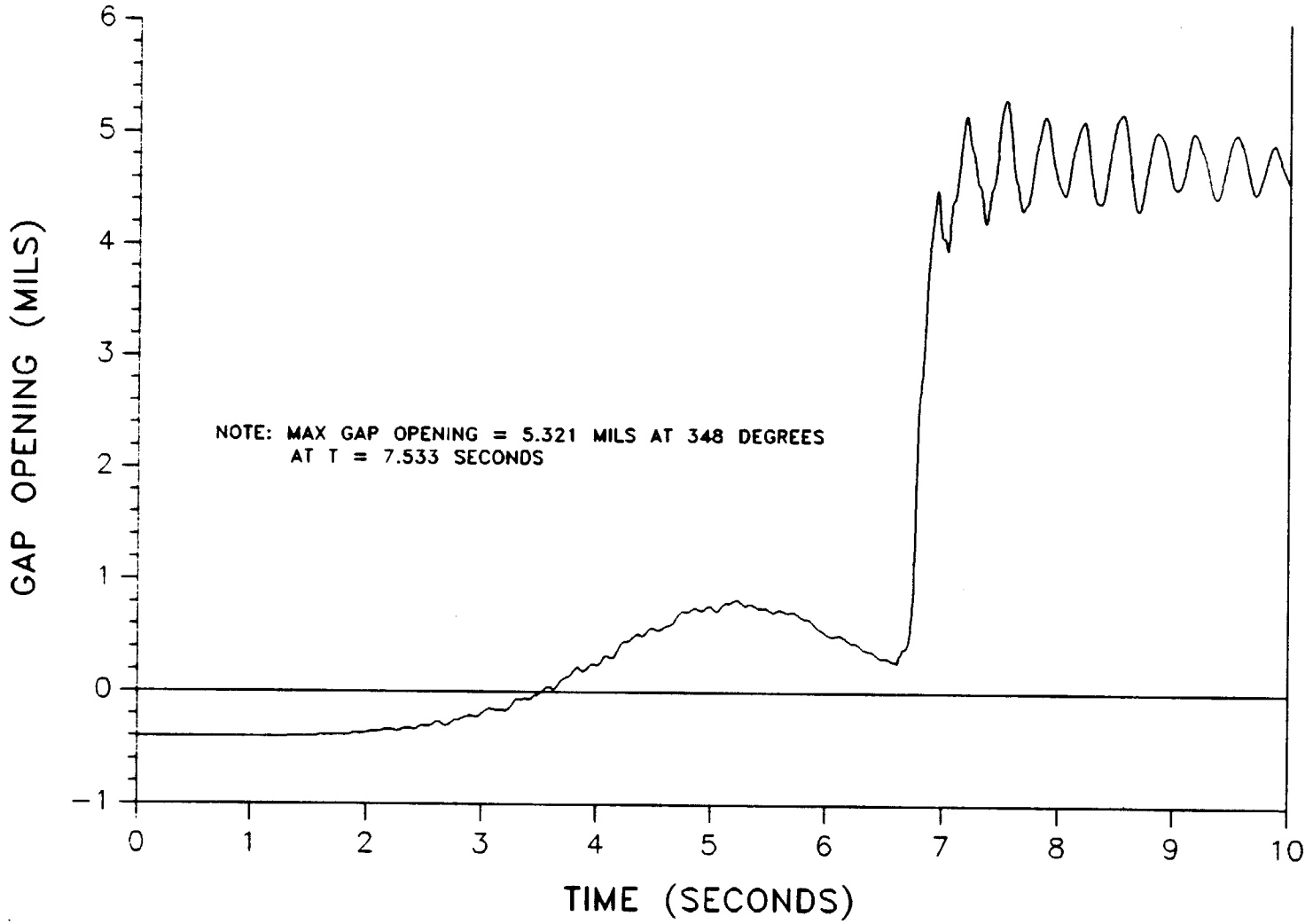

MAXIMUM PRIMARY GAP OPENING – FWD FIELD JOINT

STS-26 RECONSTRUCTED ANALYSIS – RIGHT MOTOR

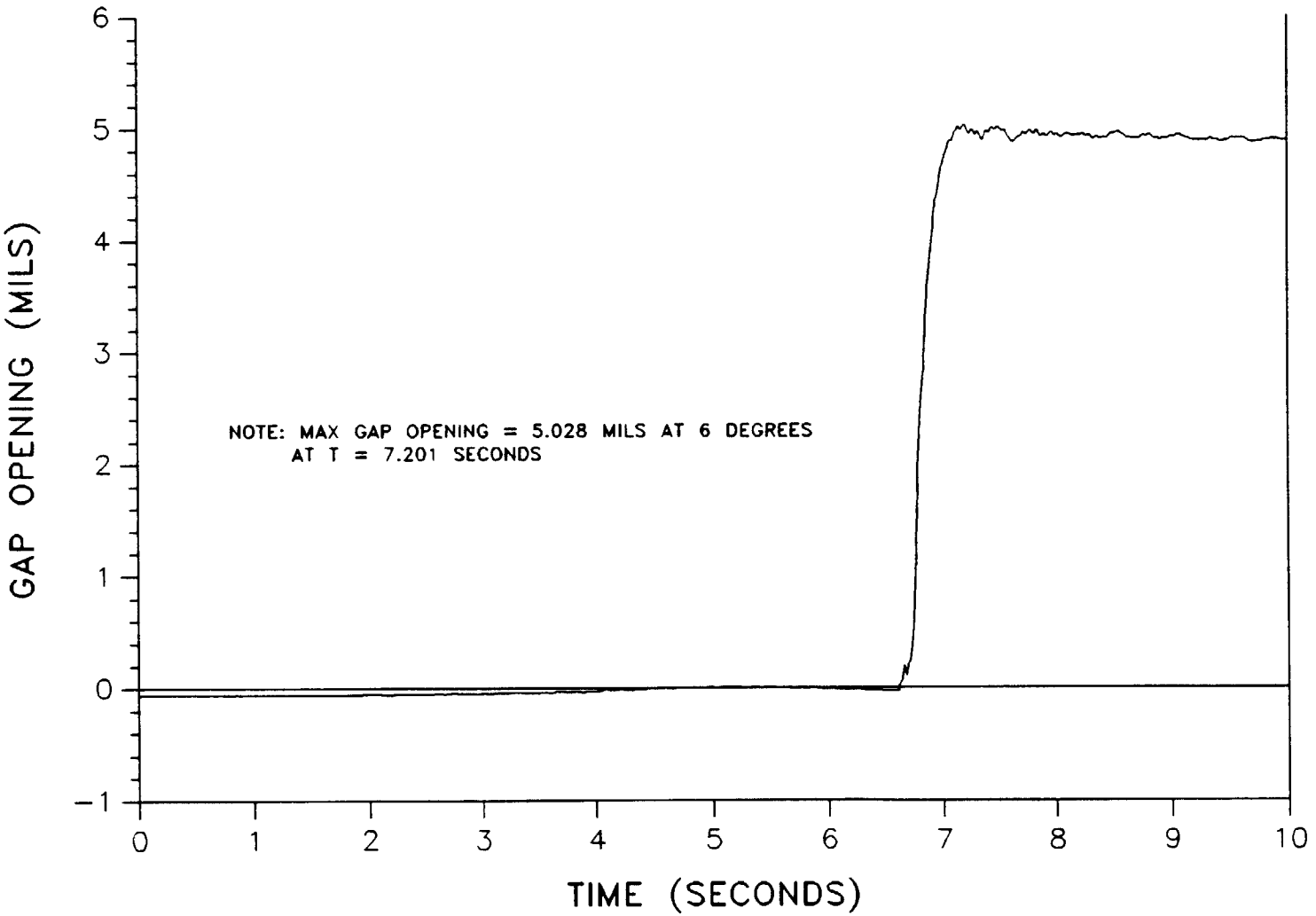

MAXIMUM SECONDARY GAP OPENING – FWD FIELD JOINT

STS-26 RECONSTRUCTED ANALYSIS – RIGHT MOTOR

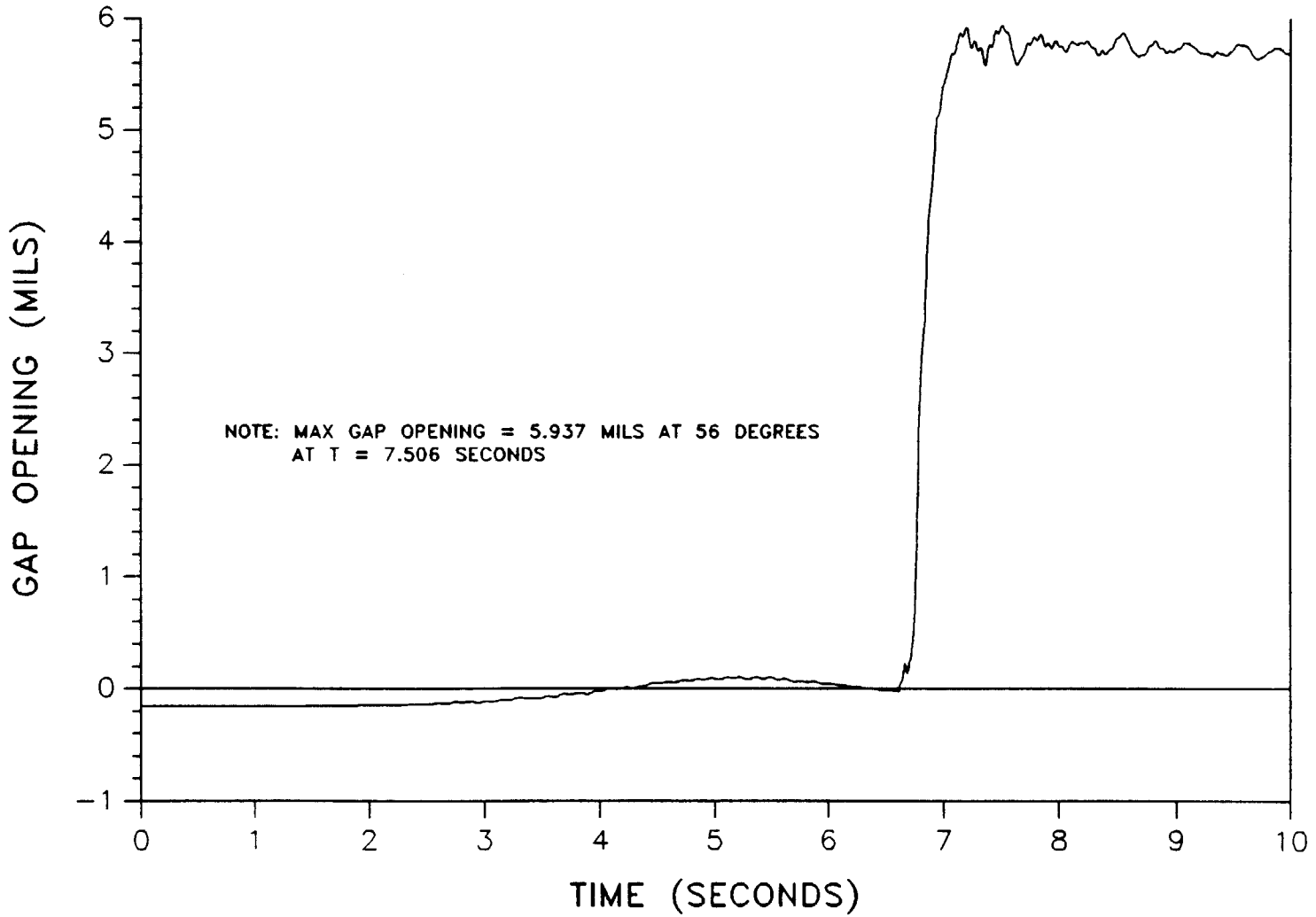

MAXIMUM PRIMARY GAP OPENING – CTR FIELD JOINT

STS-26 RECONSTRUCTED ANALYSIS – RIGHT MOTOR

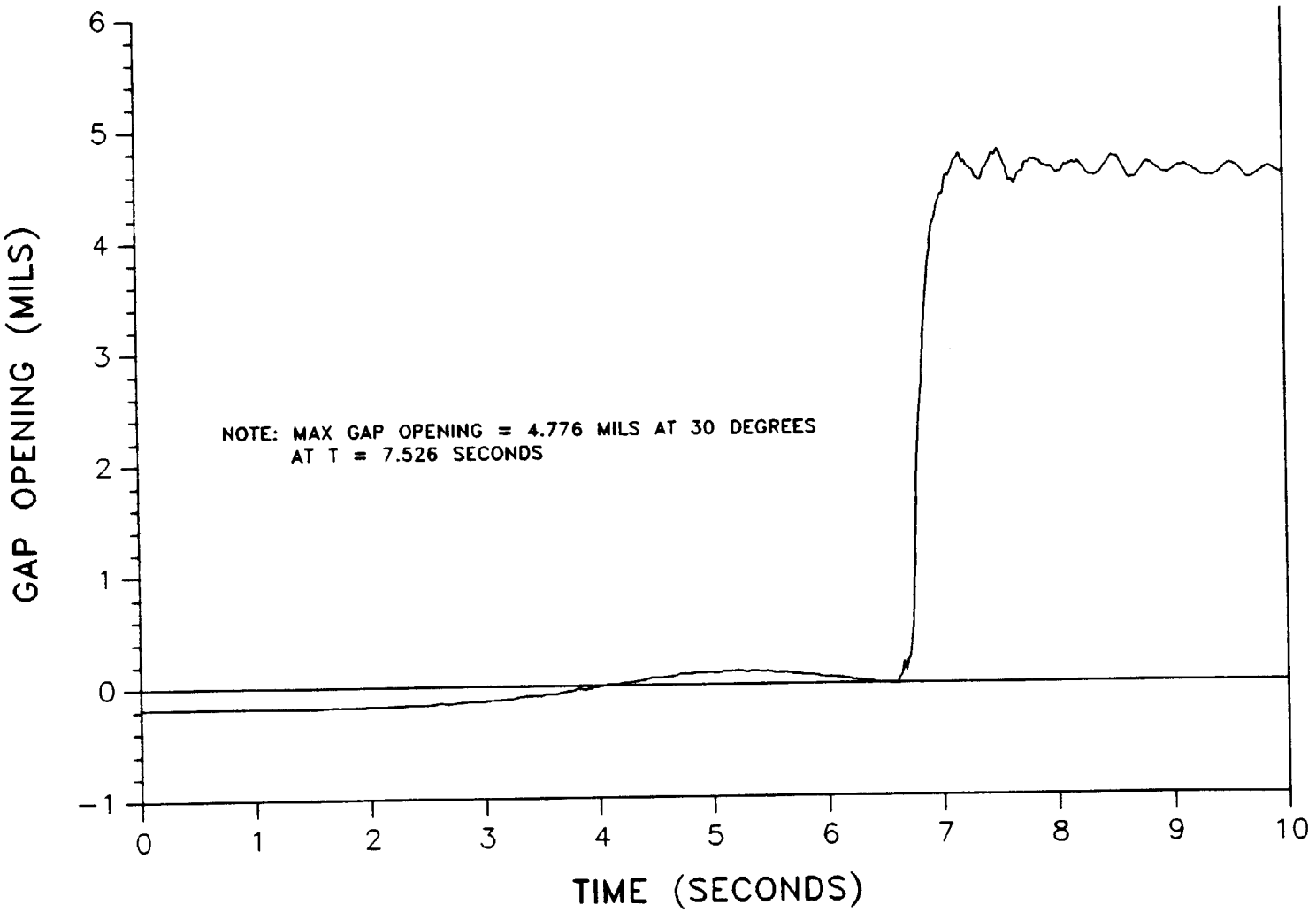

MAXIMUM SECONDARY GAP OPENING – CTR FIELD JOINT

STS-26 RECONSTRUCTED ANALYSIS – RIGHT MOTOR

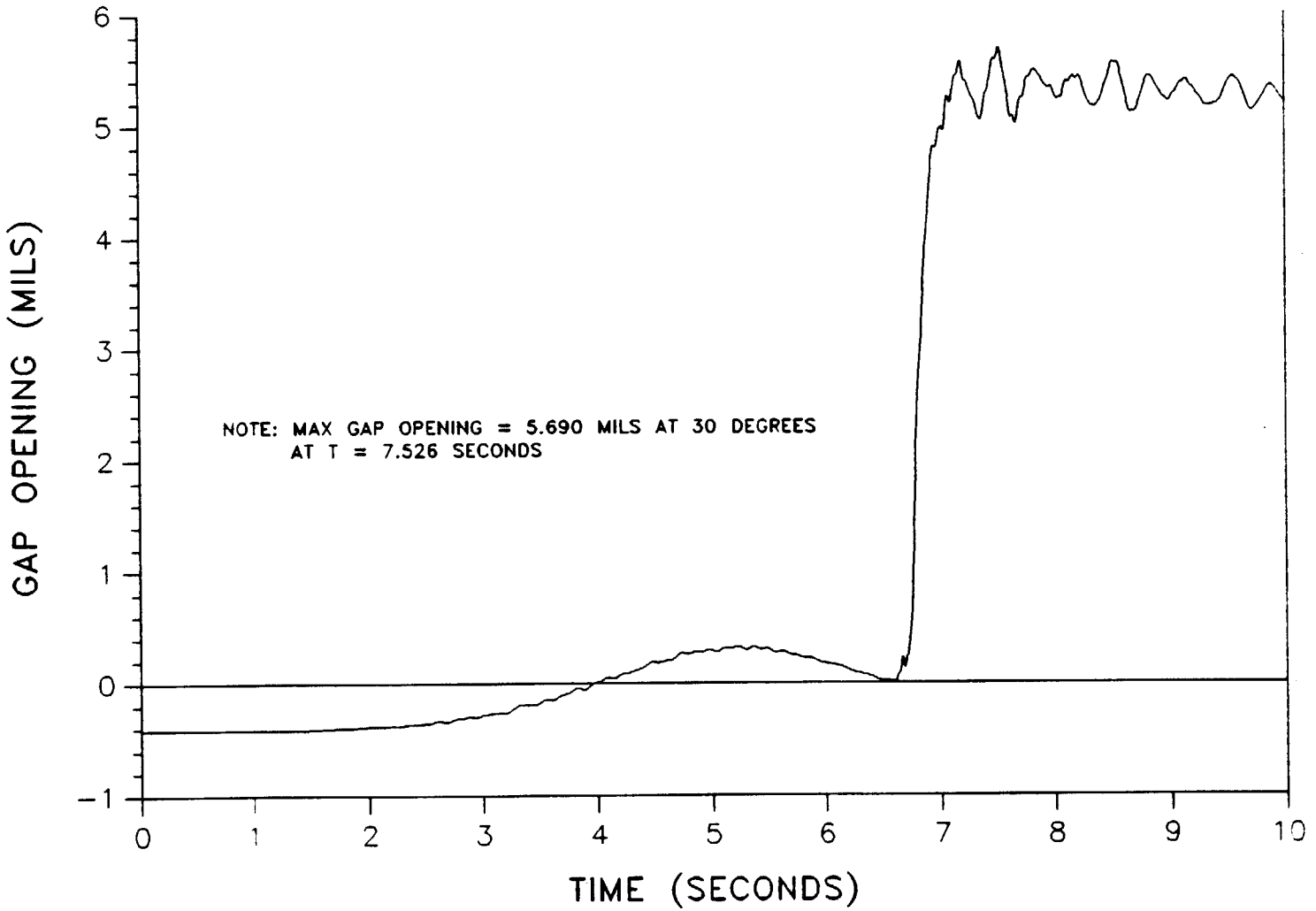

MAXIMUM PRIMARY GAP OPENING – AFT FIELD JOINT

STS-26 RECONSTRUCTED ANALYSIS – RIGHT MOTOR

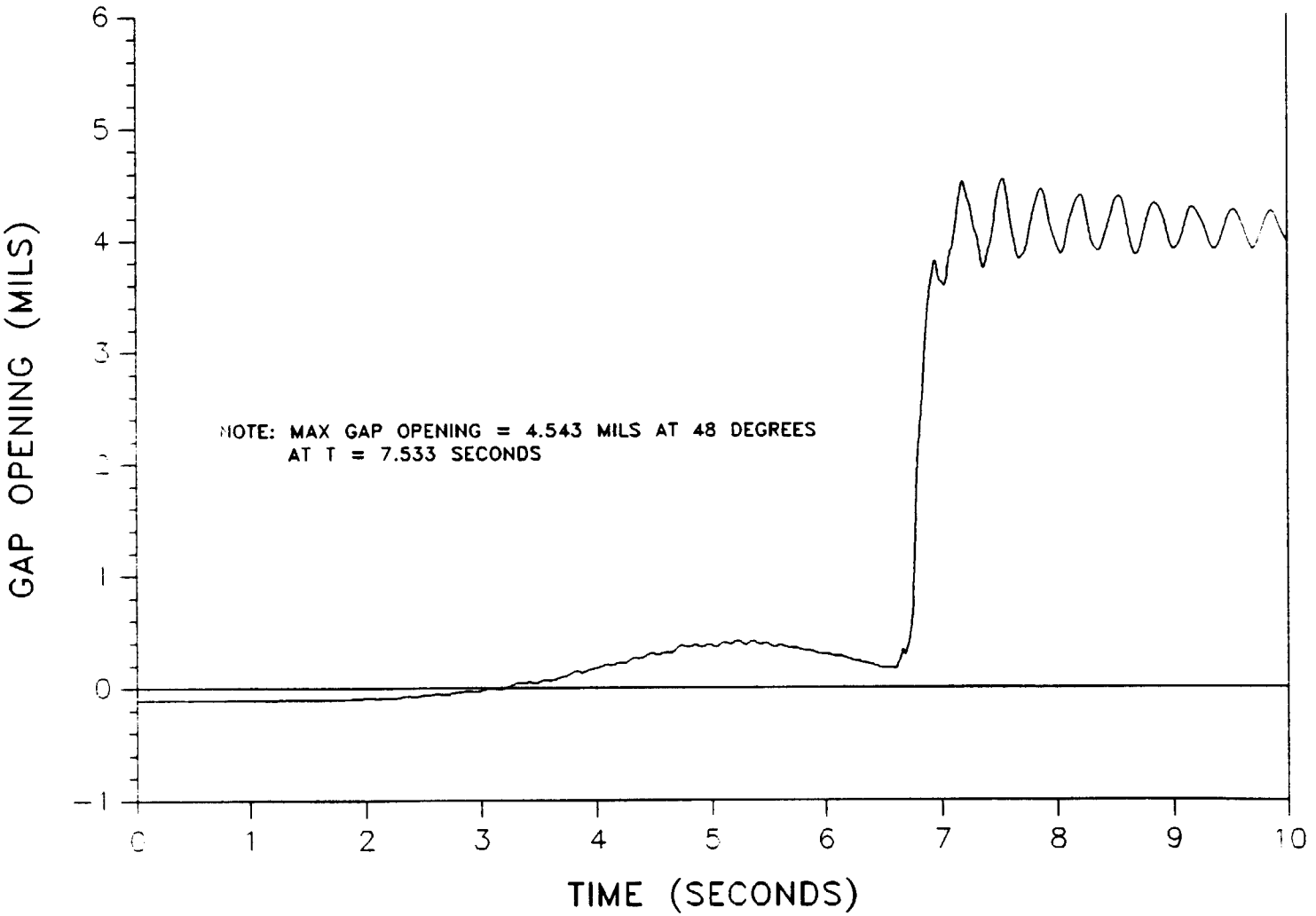

MAXIMUM SECONDARY GAP OPENING – AFT FIELD JOINT

STS-26 RECONSTRUCTED ANALYSIS – RIGHT MOTOR

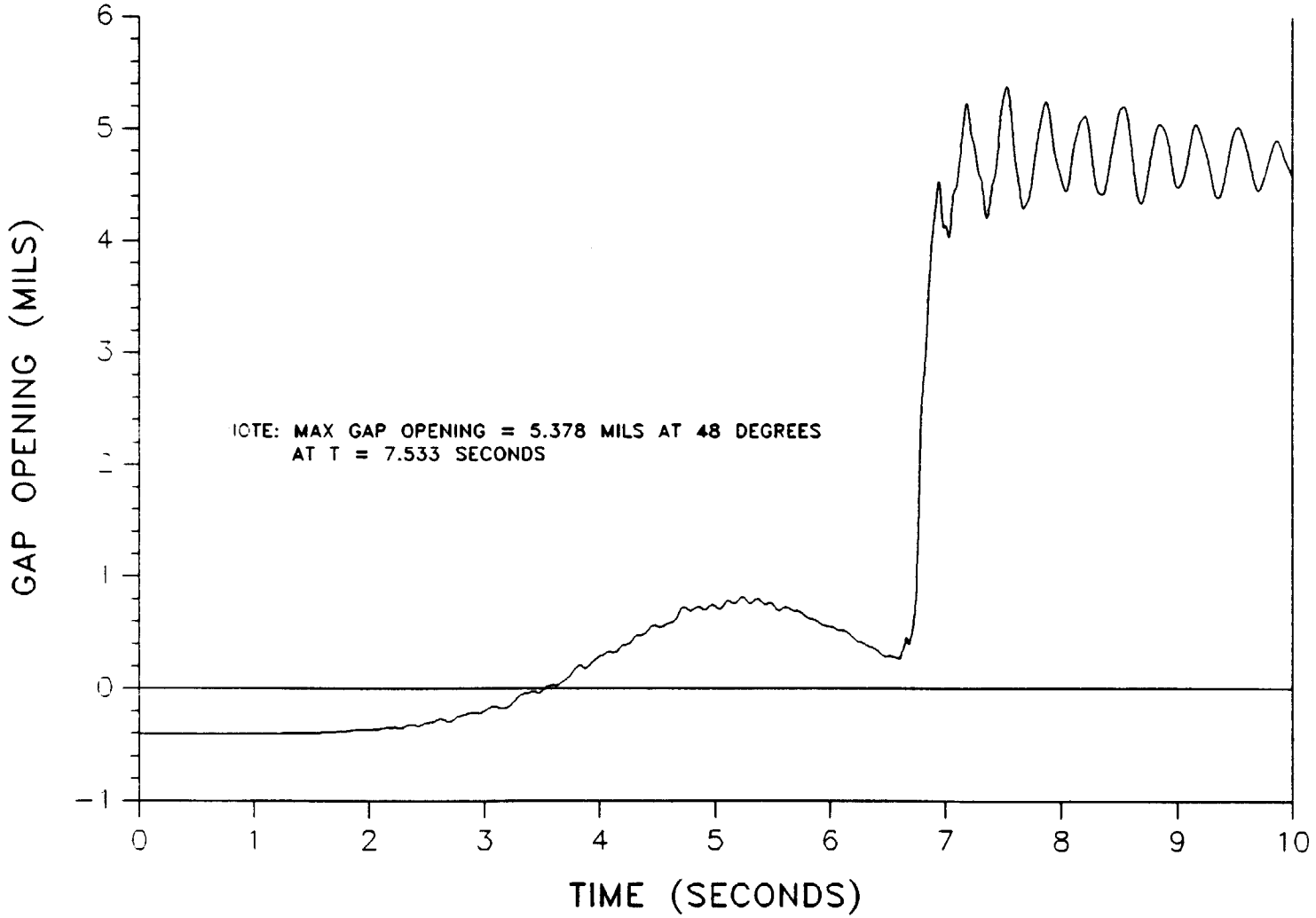

DISTRIBUTION

Recipient	No. of Copies	Mail Stop
S. B. Kulkarni	1*	L00
B. Jurewicz	1*	E05
C. A. Saderholm	1*	E11
J. R. Lavery	1*	L35
D. R. Mason	1	L22
V. B. Call	1	L22
C. T. Wiese	1	L35
B. R. McQuivey	1	L10
S. B. Medrano	1	L10
G. A. Ricks	1	L36
NASA	3	K68A
Technical Library	1	004A
Data Management	1	282
Print Crib	5	282

*Without Appendices